Technical Report
TR-23-01
March 2023

Post-closure safety for SFR, the final repository for short-lived radioactive waste at Forsmark

Main report, PSAR version

SVENSK KÄRNBRÄNSLEHANTERING AB

SWEDISH NUCLEAR FUEL
AND WASTE MANAGEMENT CO

Box 3091, SE-169 03 Solna
Phone +46 8 459 84 00
skb.se

ISSN 1404-0344
SKB TR-23-01
ID 1978000
March 2023

Post-closure safety for SFR, the final repository for short-lived radioactive waste at Forsmark

Main report, PSAR version

Svensk Kärnbränslehantering AB

Keywords: Post-closure safety, SFR, Final repository, Low- and intermediate-level radioactive waste, Forsmark, Safety assessment, Geological disposal, Nuclear waste, Radiological risk, Dose.

This report is published on www.skb.se

Contents

Executive summary

S1 Purpose and general prerequisites

S1.1 Purpose

This report constitutes the main report for the post-closure safety assessment that contributes to the preliminary safety analysis report (PSAR) for SFR, the repository for short-lived radioactive waste at Forsmark in Östhammar municipality, Sweden. Chapter 9 of the general part of the PSAR addresses post-closure safety and the present report is the main reference to Chapter 9. The contents of that chapter and this summary are essentially the same.

The main role of the post-closure safety assessment is to demonstrate that SFR is radiologically safe for humans and the environment after closure. This is done by evaluating compliance with respect to SSM's regulations concerning post-closure safety and the protection of human health and the environment.

The post-closure safety assessment evaluates the capability of the barrier system to protect human health and the environment after closure by containing, preventing or retarding the dispersion of radionuclides, based on a set of relevant scenarios for the evolution of the repository and its environs. The assessment considers the ability of the barrier system to withstand features, events and processes (FEPs) that can affect the post-closure performance of the barriers. The assessment relates to a period of 100 000 years after repository closure.

The post-closure safety assessment represented in this summary includes a description of the identification, documentation and handling of FEPs in the assessment. The initial state of the system, i.e. the expected state at closure, and the expected evolution of the repository and its environs are also described. Furthermore, it is presented how these are used as a basis for the selection of scenarios for which radionuclide transport and dose calculations are then performed. It is demonstrated how the requirements on the safety assessment methodology are met. Moreover, it is demonstrated how the requirements regarding the results of the assessment are fulfilled, including an evaluation against the regulatory risk criterion for the protection of human health, and evaluation of protection of the environment, as well as the barrier system robustness.

S1.2 Prerequisites

Necessary prerequisites include system boundaries and timescales for the assessment, the reference inventory, the reference design and status of SFR1, as well as the site descriptive model. Moreover, important inputs are results from previous assessments and RD&D related to SFR, and expected conditions in the repository and its environs at the time of repository closure.

Repository system and system boundaries

In the post-closure safety assessment, the repository system comprising the repository and its environs is evaluated. The repository includes the disposed waste forms (waste in its physical and chemical form, after treatment and/or conditioning where applicable), waste packaging, engineered barriers, and other components. The repository environs include the bedrock surrounding the repository stretching up to the surface (geosphere), and the part of the surface area that can be affected by radionuclide releases from the repository (biosphere or surface system).

The repository system evolves over time. The future state of SFR will depend on:

- the initial state, i.e. the expected state of the repository system at closure,
- internal processes that can affect the repository system over time,
- external conditions that can affect the evolution of the repository system after closure.

It can be noted that inspections will be carried out during construction, operation and before closure to ensure an adequate knowledge of the achieved initial state of the waste vaults.

Reference inventory

The requirements on the repository design and construction regarding post-closure safety are largely based on the characteristics of the disposed waste. The description of the waste inventory is based on the waste type descriptions, decommissioning studies and decommissioning plans as well as information regarding disposed waste and forecasts of waste volumes, materials and radioactive substances. Forecasts of the waste that is planned to be disposed and information on the waste that has already been disposed of in SFR is regularly updated. PSAR is based on the latest comprehensive forecast of, and information on, disposed waste delivered in 2016. This reference inventory is based on the assumption of closure of SFR in 2075 and includes an estimation of uncertainties in the forecast and data regarding the disposed waste. A more detailed account of radioactive substances in SFR is given in Chapter 4.

An indication of the radiological hazard of the waste can be obtained by calculating the radiotoxicity of the waste as the product of the activity of the relevant radionuclides and their corresponding ingestion dose coefficients. At repository closure the radiotoxicity is dominated by short-lived radionuclides such as Cs-137 and Ni-63. The largest part (88 %) of the radiotoxicity at closure is present in SFR1. A hundred years after closure the radiotoxicity in the repository has decreased to less than 20 % and after thousand years it has further decreased to about 2.5 % of its initial value (Figure S-1).

Reference design

The reference design constitutes a design of the repository that is valid from a defined point in time until further notice. The reference design of SFR, including the components constituting post-closure barriers and their functions is a prerequisite for the assessment. It is described in Chapter 4 and in detail in the **Initial state report**.

Site descriptive model

The site descriptive model (SDM) for the SFR area is documented in the site descriptive model report (SKB TR-11-04) and details regarding the surface systems are also described in the **Biosphere synthesis report**. The site descriptive model is a synthesis of qualitative and quantitative information on the present-day conditions in the bedrock and surface system at the repository site.

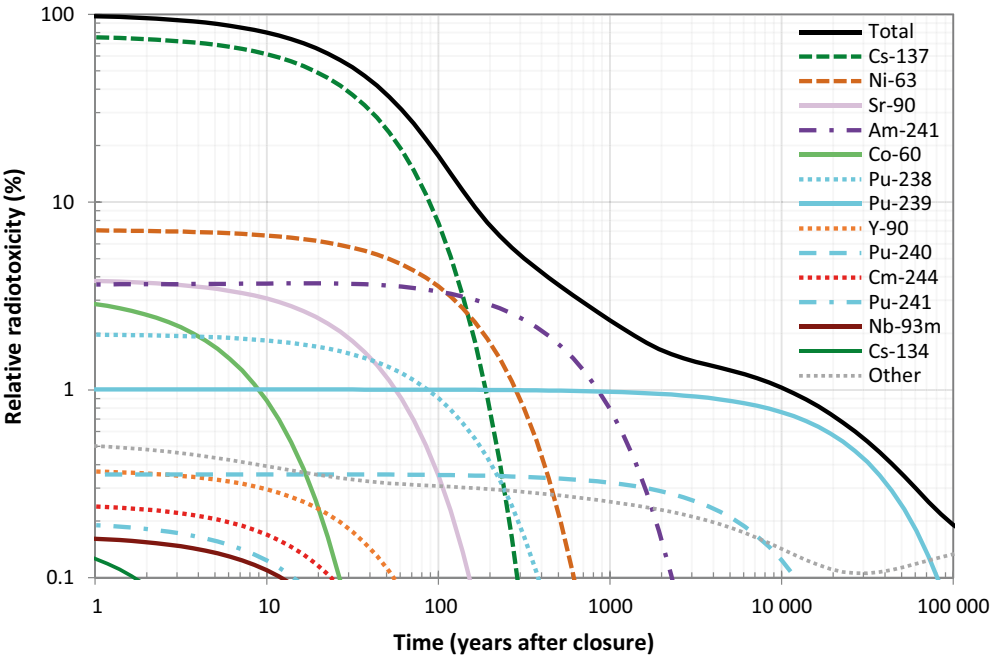

Figure S-1. *Contributions from radionuclides to total radiotoxicity (sum over all radionuclides) as a function of time after closure of the repository. Other (grey dotted line) include contributions from all radionuclides not explicitly shown in the figure.*

Management of uncertainties

The management of uncertainties is a fundamental aspect of a safety assessment. In the safety assessment methodology in ten steps, that is described in the next section, the management of uncertainties is an integral part. In the assessment uncertainties are categorised as scenario, system, modelling, and data uncertainties.

Uncertainties are managed in several ways in the assessment. A scenario analysis is performed to handle scenario uncertainty (Chapters 7–9). System uncertainties which concern comprehensiveness issues, i.e. the question of whether all aspects important for the safety evaluation have been identified is addressed by a systematic handling of FEPs that can affect the barrier system after closure. Modelling uncertainties are handled by analysing process uncertainties by means of mathematical models. Data uncertainties are managed by a structured approach to data selection and evaluation of data uncertainties. This includes probabilistic methods, e.g. used in the forecast of the radionuclide inventory as well as calculations of radionuclide transport and dos to humans. A commonly used way to handle uncertainties is to make cautious or pessimistic assumptions in the calculations to ensure that the risk from the repository is not underestimated. In Section 2.6 it is described how uncertainties are managed in each step in the safety assessment methodology.

S2 Safety assessment methodology

The methodology for the post-closure safety assessment for SFR consists of ten main steps that are briefly described in the following and in more detail in Section 2.6. The steps are partly carried out concurrently and partly consecutively. A graphical illustration of the steps in the methodology is shown in Figure S-2. In this summary, the implementation of the methodology is described in Sections S3–S9).

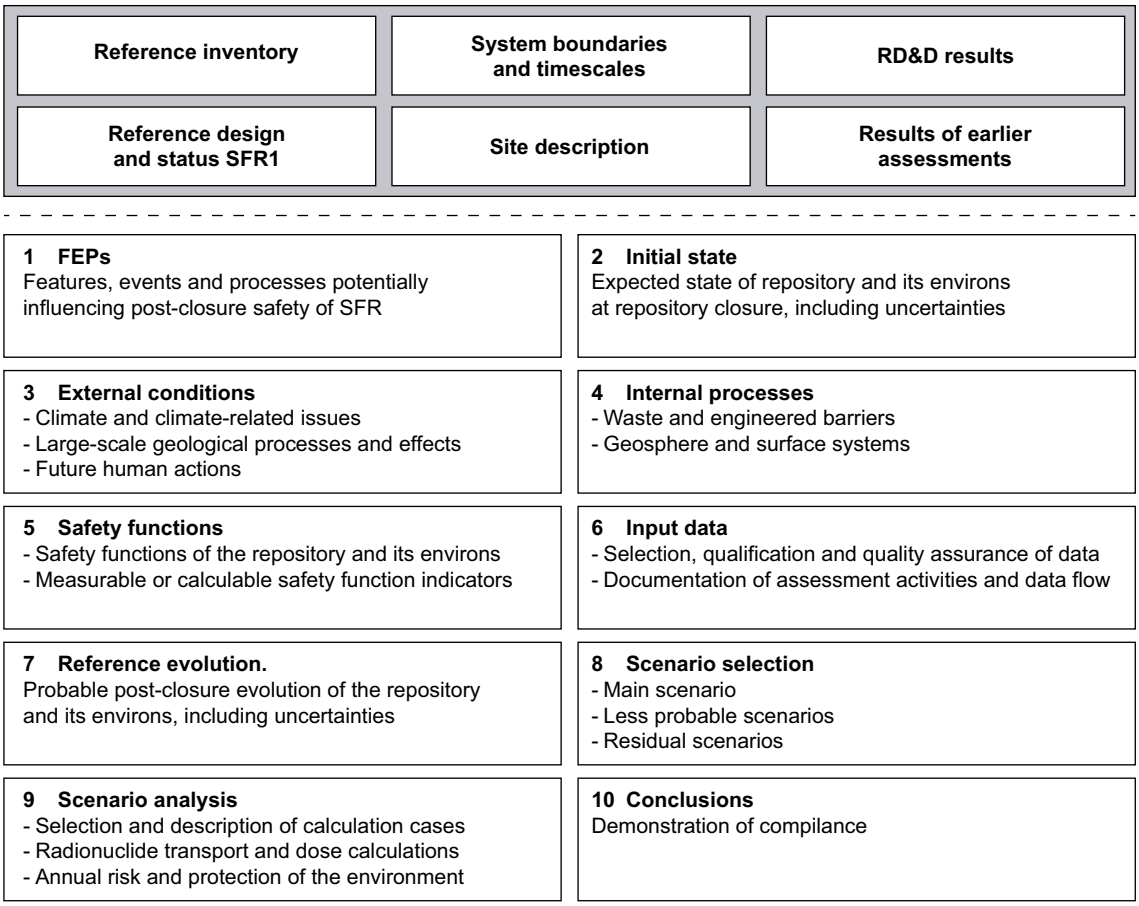

Figure S-2. *An outline of the ten main steps of the present post-closure safety assessment. The boxes above the dashed line are prerequisites for the methodology and its implementation.*

Step 1: Identification, selection and documentation of the handling of FEPs potentially relevant for the post-closure safety.

Step 2: Description of the expected state of the repository and its environs at closure, including uncertainties that can affect the capability of the repository to protect human health and the environment. This initial state is the starting point for the assessment of post-closure safety.

Step 3: Description of the external conditions identified in step 1. External conditions include climate and climate related issues, large-scale geological processes and effects such as earthquakes, as well as future human actions that can affect the protective capability of the repository. The step includes the selection and description of external reference conditions for the assessment and selection of less probable evolutions of external conditions. As the evolution of external conditions over the next 100 000 years is associated with considerable uncertainty, the reference external conditions are represented by several developments that span the range of the probable evolution of external conditions at Forsmark (Section S6).

Step 4: Description of the internal conditions identified in step 1, including the waste form and packaging, engineered barriers and other repository components, geosphere and surface system.

Step 5: Definition of safety functions and safety function indicators based on the safety principles *limitation of the activity of long-lived radionuclides* and *retention of radionuclides*. A safety function is defined as a role through which a repository component contributes to safety. The evolution of the safety functions over time is evaluated with the aid of a set of safety function indicators. These consist of measurable or calculable properties of respective repository system component.

Step 6: Compilation of input data is a structured procedure for selecting all data to be used in the quantification of the evolution of the repository and its environs, and in radionuclide transport and dose calculations.

Step 7: Description of the probable post-closure evolution of the repository and its environs, including uncertainties in the evolution that may affect the protective capability of the repository. This *reference evolution* starts from the time for the initial state (step 2), and then follows the reference external conditions (step 3). The reference evolution supports the selection (step 8) and analysis (step 9) of the main scenario and less probable scenarios.

Step 8: Selection of a set of scenarios that together illustrate the most important potential courses of development of the repository and its environs. The set consists of a main scenario, less probable scenarios and residual scenarios. The main scenario takes into account the most probable changes in the repository and its environment and is based on the initial state (step 2), the reference external conditions (step 3) and the reference evolution (step 7). The aim of less probable scenarios is to evaluate scenario uncertainties and other uncertainties that are not evaluated within the framework of the main scenario. Residual scenarios are selected to illustrate the significance of individual barriers and barrier functions, the effect of future human actions that potentially may affect the conditions of the repository, the health detriment to humans intruding into the repository, and the consequences of an unsealed repository that is not monitored.

Step 9: Analysis of selected scenarios including uncertainties to assess the protective capability of the barrier system. The scenarios are described together with the calculation cases which evaluate the uncertainties for each scenario. The cases are analysed with respect to radionuclide transport and appropriate calculational endpoints, typically annual effective dose to humans and dose rates to non-human biota. The risk of harmful effects of ionising radiation for a representative individual in the group exposed to the greatest risk is calculated for the relevant scenarios. The risk contributions from the main and less probable scenarios are then summed to a total annual risk considering the probabilities of the different scenarios to occur and compared to SSM's risk criterion. Furthermore, dose rates to non-human biota are compared to international screening values. Collective dose is also calculated.

Step 10: Conclusions of the performed assessment regarding compliance with SSM's regulations on barrier system robustness and protection of human health and the environment.

S3 Identification and handling of features, events and processes

S3.1 Identification and selection of features, events and processes

The analysis of FEPs that may influence post-closure safety is an important part of the safety assessment. The FEP analysis includes:

- Identification of all factors that may influence post-closure safety of the repository.
- Deciding whether each FEP identified needs to be addressed further in the safety assessment. The motivations for excluding FEPs are documented in the SKB FEP database.
- Documentation of each included FEP in a FEP-catalogue for SFR.

The main part of the FEP-analysis is described in the **FEP report**, with a summary and minor updates given in Chapter 3.

The bases for the identification of all relevant factors are international FEP databases and experience from preceding safety assessments. FEPs are then selected from this information that are important for the evolution of the repository system and/or that may influence post-closure safety. These are sorted in one of following classes:

- Factors influencing the state of the repository at closure, i.e. the initial state.
- Processes in the repository system of importance for post-closure safety and the variables needed to describe the state of the system at every given point in time.
- External conditions of importance for post-closure safety.

S3.2 Handling of FEPs

The handling of the processes in the repository system that are judged to be of importance for post-closure safety is described in the process reports, i.e. the **Waste process report**, the **Barrier process report**, and the **Geosphere process report.** Processes in the biosphere are described in the **Biosphere synthesis report** and climate-related processes in the **Climate report**.

S4 Initial state

The expected state of the repository and its environs at closure, including uncertainties in the state that may affect the protective capability of the repository is the starting point for the assessment. The description of this *initial state* is based on the prerequisites of the present assessment, including the reference waste inventory, repository reference design and the site descriptive model. A description of the initial state is given in Chapter 4. A detailed account is given in the **Initial state report**, the SDM (SKB TR-11-04) and in the **Biosphere synthesis report**.

The description of the waste and repository represents the estimated state at the time of closure of the repository, whereas the description of the environs, including the climate and climate-related conditions, assume that they are similar to present-day conditions.

During the operational phase the facility is drained and at closure it will be re-saturated from the surrounding rock. The time for resaturation depends on the occurrence of rock fractures and the characteristics of the repository materials but is sufficiently short to be neglected for most processes. Therefore, the repository is in the assessment assumed to be re-saturated at closure.

The initial state is important for the outcome of the post-closure safety assessment. To ensure that the state of the disposed waste and the barrier system corresponds to assumed initial state at closure requirements are defined for the waste and the engineered barriers (Chapter 2).

S5 Safety functions and safety function indicators

The overall post-closure safety principles for SFR are *limitation of the activity of long-lived radionuclides* and *retention of radionuclides*. Based on these principles, safety functions are defined for repository components that are of vital importance for post-closure safety. A safety function is defined as a role through which a repository component contributes to safety. Safety functions include barrier functions as well as other aspects important for post-closure safety that are not coupled to the function of a barrier (Section 5.1). The set of safety functions is an aid in the description of the repository functions after closure and for identification and selection of relevant scenarios. Uncertainties related to the safety functions are thereby evaluated in a structured manner.

The evolution of the safety functions over time is evaluated with the aid of a set of safety function indicators. These consist of measurable or calculable properties of respective repository system component. For these properties qualitative criteria are given that are coupled to the specified function.

An example of a safety function is *limit advective transport* through relevant engineered barriers. The related indicator is *hydraulic conductivity* of bentonite in the silo and plugs as well as outer concrete structures in 1–2BMA. The qualitative criterion specified is that the hydraulic conductivity shall be low.

The use of safety functions and indicators is an aid in the evaluation of post-closure safety but is not sufficient to demonstrate that an acceptable level of safety has been achieved. Nor is safety necessarily compromised if a safety function is poorly upheld, this is rather an indication that more in-depth analyses are needed to evaluate the safety. Quantitative calculations are required to show compliance with the regulatory requirements, such as the risk criterion, irrespective of whether none, one or several safety functions are poorly upheld. The safety functions and indicators are summarised in Table S-1.

The safety functions and indicators define aspects of the repository system important for post-closure safety and they can be used to assess, and in some cases infer, requirements for the waste and the barriers to be met at closure of the repository.

S6 Reference evolution

The reference evolution describes the probable post-closure evolution of the repository and its environs, including uncertainties in the evolution that may affect the protective capability of the repository. This *reference evolution* starts from the initial state and then follows the reference external conditions for the next 100 000 years, accounting for FEPs that are likely to influence the evolution. The description builds on the knowledge gained in the previous steps of the assessment methodology, as well as dedicated studies performed to assess the post-closure evolution of the repository and its environs. The reference evolution supports the selection and analysis of the main scenario and less probable scenarios.

Three *variants* of the reference external conditions are considered (see below). These represent the range of probable evolution of the external conditions at Forsmark over the next 100 000 years.

- The *present-day climate variant* represents a future development where present-day climate conditions prevail for the complete assessment period and the initial shoreline displacement is dominated by isostatic rebound following the last glaciation. This development results in 1 000 years of initial submerged conditions above the repository.
- The *warm climate variant* represents a likely future development where similar-to-present levels of anthropogenic greenhouse-gas emissions continue for the next few decades, after which they gradually decline to net-zero emissions in the beginning of the next century. This development results in 100 000 years of temperate climate conditions and an increased sea level, which leads to a prolonged initial period during which the area above the repository remains submerged beneath the sea.
- The *cold climate variant* represents a future development characterised by substantial reductions in anthropogenic greenhouse-gas emissions and/or removal of atmospheric CO_2 by technological measures. This development results in gradually colder climate conditions and two periods of periglacial conditions (i.e. permafrost development) at Forsmark during the latter half of the assessment period.

The evolution of climate conditions in these variants, illustrated in terms of climate domains, are shown in Figure S-3.

Table S-1. Safety functions and safety function indicators.

Safety function	Safety function indicator	Repository system (sub-)component
Waste form and waste packaging		
Limit quantity of activity	Activity of each radionuclide in each waste vault: limited	Waste form in silo, 1–2BMA, 1BRT, 1–2BTF, 1–5BLA
Limit gas formation	Amount of gas-forming materials: low	Waste form and waste packaging in silo, 1–2BMA, 1BRT and 1–2BTF
Limit advective transport	Hydraulic conductivity: low	Waste packaging (concrete tanks) in 1–2BTF
Limit corrosion	pH in porewater: high Redox potential E_h: low	Waste form with induced activity in 1BRT
Sorb radionuclides	Amount of cementitious material: high pH in porewater: high Redox potential: low (reducing) Concentration of complexing agents: low	Waste form and waste packaging in silo, 1–2BMA, 1BRT and 1–2BTF
Engineered barriers		
Limit advective transport	Hydraulic conductivity in concrete and bentonite: low	Bentonite in silo and plugs Outer concrete structures in 1–2BMA
	Hydraulic conductivity in backfill (including crushed rock foundation): high	Backfill (including crushed rock foundation) in 1–2BMA and 1–2BTF
Allow gas passage	Permeability: sufficient to allow gas passage	Gas evacuation system in silo and 2BMA Cementitious materials in 1BMA and 1–2BTF
Sorb radionuclides	Amount of cementitious material: high pH in porewater: high Redox potential: low (reducing) Concentration of complexing agents: low	Cementitious materials in silo, 1–2BMA, 1BRT, and 1–2BTF
Repository environs		
Provide favourable hydraulic conditions	Hydraulic conductivity: low Hydraulic gradient: low	Geosphere
Provide chemically favourable conditions	Redox potential: low (reducing)	Geosphere
Avoid boreholes in the direct vicinity of the repository	Intrusion boreholes: few/absent Boreholes downstream of the repository: few	Biosphere, geosphere

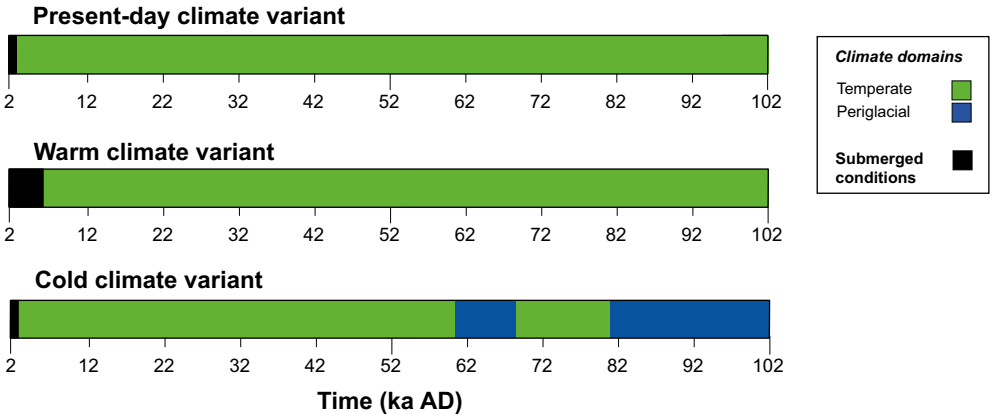

Figure S-3. *Succession of climate domains in the variants of reference external conditions.*

S6.1 Conditions in the repository environs

The evolution of the conditions in the repository environs that affect the assessment of the protective capability of the repository is described in the following based on the safety functions related to the repository environs (Table S-1).

Evolution of surface systems

Doses to humans are affected by transport and accumulation in the surface system of the radionuclides released from the geosphere to the biosphere.

The ecosystem development is strongly affected by the shoreline displacement that turns the seabed into terrestrial areas. Relatively enclosed sea bays may become isolated and gradually turn into lakes. After isolation from the sea, sedimentation and ingrowth gradually transform the lake into a mire system. More open bays can turn directly into mires, without intermediate lake stages and more exposed bottoms often become forested. Forests are the most common terrestrial ecosystem type in Forsmark, but fen mires have been identified as the terrestrial ecosystem where deep groundwater (e.g. from a repository) most likely will discharge. Such mires could after drainage be used as agricultural areas that potentially could lead to exposure and dose through ingestion if the groundwater contains radionuclides from the repository.

The Forsmark region is rich in calcite and calcite-bearing till deposits that have a marked influence on the hydrochemistry in the area. When new areas of the present seafloor are raised above the sea level, weathering of the calcite is initiated. This process increases the alkalinity and pH in the shallow groundwater, streams, lakes and soils. This influences the sorption and transport of many elements, including radionuclides. In the long-term, calcite is expected to be consumed leading to decreased alkalinity and pH.

Mechanical evolution

The fracture network in the bedrock surrounding SFR is expected to remain unaltered during the analysis period in the *present-day climate variant*. Rock fallout will occur, but predictions show that the pillar between the BMA and BLA vaults is stable and the backfill in 1–2BMA, 1BRT and 1–2BTF protects the concrete structures from potential damage from rock fallout.

Earthquakes can affect the stability of the bedrock as well as the stability of the repository. The seismic activity in the Fennoscandian shield is currently very low. However, it cannot be excluded that an earthquake of significant magnitude takes place during the 100 000 year assessment period.

Hydrogeological evolution

The safety function *provide favourable hydraulic conditions* relates to the groundwater flow through the repository being mainly controlled by the flow conditions in the bedrock. Low groundwater flow through the waste vaults supports slow advective transport and release of radionuclides out of

SFR and also slow inward transport of reactive substances such as oxidants as well as slow degradation of engineered barriers.

The groundwater flow in the bedrock surrounding SFR is expected to be very low during submerged conditions and to successively increase during the transition period to terrestrial conditions. Stationary values are expected by about 5000 AD.

During the submerged period the groundwater passing through the repository is expected to discharge at the sea bottom above the repository. During the transition to terrestrial conditions above the repository the discharge areas are diverted to the deformation zones north of the repository. When terrestrial conditions prevail the main part of the groundwater from the repository is expected to discharge in a topographical low point close to the deformation zones north of the repository (Figure S-4). The other parts of the groundwater are expected to discharge into lakes and water courses farther away from SFR.

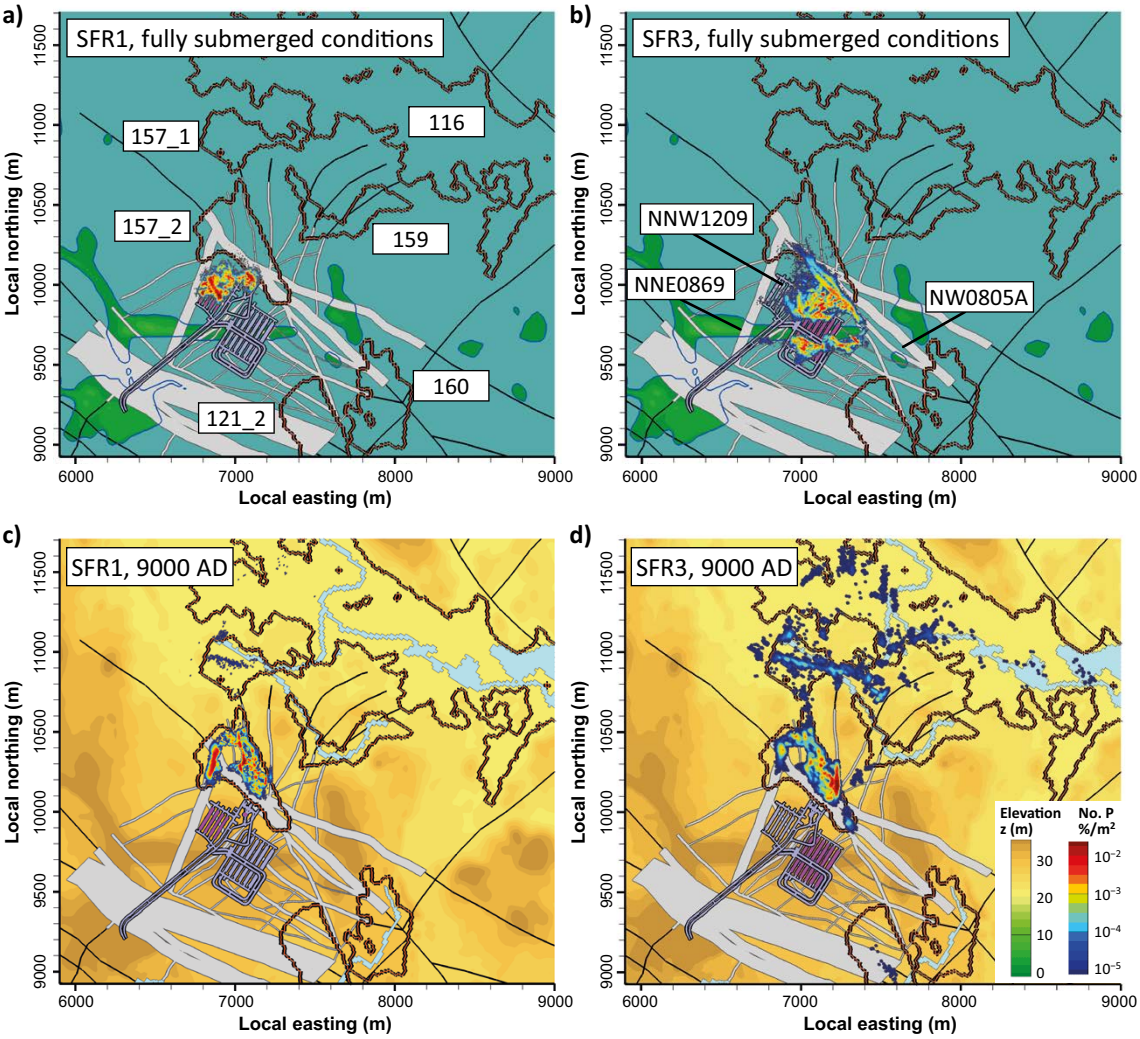

Figure S-4. *Distribution of groundwater discharge to the surface systems from the SFR1 waste vaults (a and c) and the SFR3 waste vaults (b and d) for fully submerged conditions (a and b) and terrestrial conditions (c and d). The colour scale shading from red to blue shows the density of particle exit locations (%/m²) and the colour scale shading from green to brown shows the surface elevation above sea level (m) during terrestrial conditions (c and d). The orange contours and associated labels in (a) outline biosphere objects. The black lines represent the location of deformation zones outside the SFR Regional domain. The straight black lines and the text within the black rectangles in (b) indicate the location of the deformation zones. The blue-grey colour indicates marine environment (a and b). The grey areas indicate the thickness at ground surface of deformation zones that are represented in the SFR Regional domain of the hydrogeological model. The waste vaults in SFR1 (a and c) and SFR3 (b and d) are indicated in magenta. The light blue colour represents surface waters (c and d). The figure is modified from Öhman and Odén (2018).*

Geochemical evolution

The safety function *provide chemically favourable conditions* relates to the redox conditions in the repository being influenced by the composition of the groundwater flowing into the repository. The redox conditions in the repository influence the sorption properties of many radionuclides and thus their retention in the repository.

During the initial period of submerged conditions, the groundwater composition in the bedrock surrounding SFR is not expected to change much. During the transition to terrestrial conditions, the brackish groundwater in the bedrock surrounding SFR will slowly change with time and be influenced by the introduction of meteoric water into the uppermost part of the bedrock. Reducing conditions are expected to prevail at repository depth during the entire analysis period. The dissolution of cement minerals in the repository may affect the pH of the groundwater in the vicinity and downstream of the repository. The groundwater from the repository is, however, expected to be substantially diluted at short distance from the repository along the bedrock flow paths.

Submerged conditions

The location of SFR beneath the Baltic Sea affects the safety function *avoid boreholes in the direct vicinity of the repository*.

The location of the repository also prevents humans locating boreholes above or downstream of the repository for the purpose of water extraction. However, it cannot be completely ruled out that drilling under water may be conducted for purposes other than water extraction. During terrestrial conditions above the repository, wells for drinking water or agricultural purposes could be drilled, which may affect radionuclide transport to the biosphere and doses to humans. The use and location of drilled wells therefore influences the safety and are considered in the safety assessment.

S6.2 Conditions in the repository

The evolution of the conditions in the repository that are of importance for the assessment of the capability of the repository to protect human health and the environment is in the following described based on relevant safety functions (Table S-1).

Near-field hydrological evolution

The safety functions *limit advective transport* and *allow gas passage* are related to the hydraulic conditions in the repository.

The initial evolution of the near-field hydrological system largely follows the evolution of the regional hydrogeological system driven by shoreline displacement. The degradation of the barriers is expected to have a minor influence on changes in the groundwater flow during the transition period. When the shoreline regresses past the repository, the main flow direction gradually changes from vertically upwards to horizontal. The hydraulic gradient increases, which leads to increased flow rates in the repository. The groundwater flow, however, still is expected to be fairly low due to the flat topography in the area.

The bentonite in the silo and plugs contribute to the prevention of release of radionuclides by limiting the groundwater flow through the vaults and the waste. The swelling capacity of the bentonite, caused by montmorillonite minerals, gives the material low hydraulic conductivity and also enables the clay to self-heal if channels or other forms of voids occur. Chemical processes affecting the bentonite are slow and are not expected to have a pronounced effect on the flow-limiting properties during the assessment period. In the silo and 2BMA, the barriers will have engineered gas-evacuation systems that will minimise the gas-pressure build-up and thus ensure that barriers are not affected adversely.

The outer concrete structures in 1–2BMA and the concrete tanks in 1–2BTF contribute to the prevention of release of radionuclides by limiting the groundwater flow through the waste. The flow-limiting properties relate to the combination of a dense concrete with a low porosity and no or only a few small cracks. In 1–2BMA and 1BRT a hydraulic contrast is created between the concrete structures with low hydraulic conductivity and the backfill with high hydraulic conductivity, which leads to preferential flow through the backfill and thus reduces the flow through the waste.

The properties of the concrete barriers will evolve over time due to internal processes, with leaching and crack formation having the largest effect. Formation of cracks occurs due to rebar corrosion in the concrete. The leaching of cement minerals is caused by the interactions between concrete and the groundwater. General dissolution of the cement minerals and leaching affects the composition of the hydrated cement, its porosity as well as the composition and pH of the cement pore water. The hydraulic conductivity as well as the loadbearing capability may be affected leading to crack formation. Together this leads to a larger part of the groundwater flow being directed through the waste. This is illustrated in Figure S-5 for the waste vaults that contain concrete barriers and for four concrete degradation steps, affecting the hydraulic conductivity, from intact to completely degraded.

The expected evolution of the hydraulic conductivity due to leaching and crack formation is illustrated by the four steps in the evolution shown in Figure S-6. Given pessimistic assumptions regarding the concrete properties at closure and its evolution, the hydraulic conductivity increases six orders of magnitude from intact to completely degraded (Figure S-6). The temporal evolution differs for the different waste vaults. The bentonite in the silo contributes to a slow degradation of the concrete structure. The outer concrete structures in 1–2BMA degrade slower than the existing structure in 1BMA.

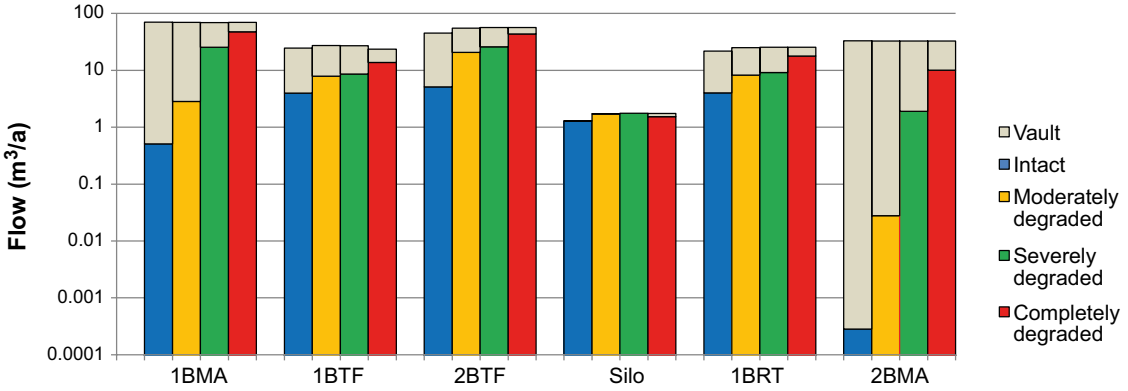

Figure S-5. *Modelled flow rates (m^3/a) in the waste vault (grey bars) and waste domains (coloured bars) for different concrete degradation states for terrestrial conditions above the repository (shoreline position corresponding to 5000 AD). Modified from Abarca et al. (2020).*

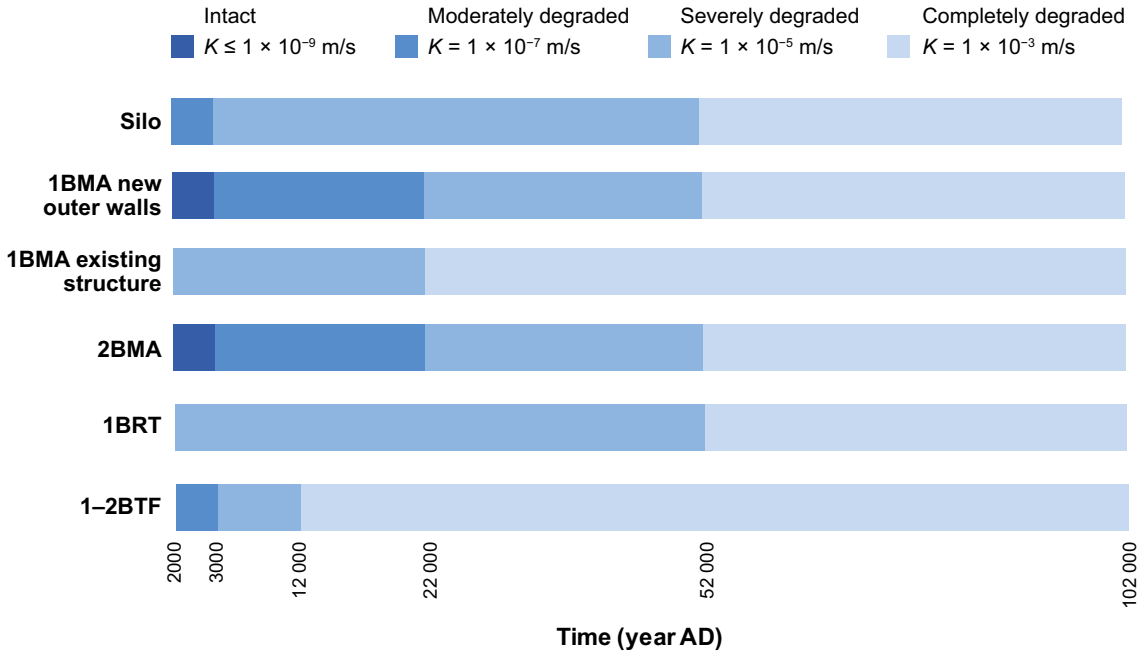

Figure S-6. *Succession of the hydraulic conductivity of concrete in the waste vaults that include concrete barriers, given pessimistic assumptions regarding the condition of the concrete at closure and its evolution.*

The main reason for this is that existing cracks in 1BMA are expected to widen, and new cracks may form due to corrosion of tie rods or reinforcement bars in the concrete. The relatively thin concrete of the tanks in 1–2BTF is the reason why the complete physical degradation in that vault occurs earlier than in the existing 1BMA structures.

Evolution of chemical conditions

The safety functions *limit corrosion*, *limit gas formation*, and *sorb radionuclides* are related to the chemical conditions in the repository.

The chemical conditions in the repository after closure are mainly controlled by the repository materials and to a lesser degree by the inflowing groundwater. Post-closure safety is affected by materials that are radionuclide-sorbing, affect pH, cement-degrading, gas producing, affect redox conditions, or complex forming. Cementitious materials have the greatest effect as they occur in large quantities and ensure high pH and high ionic strength, especially from calcium ions which leads to high sorption of many radionuclides and low corrosion rates. The pH value follows the mineralogical evolution of the cement and starts at pH > 13 and then decreases successively with the leaching of different cement minerals. The leaching process is determined by the groundwater flow through the vault and the amount of cement and is therefore different for the different vaults. The pH evolution in the vaults that include concrete barriers is illustrated in Figure S-7, given pessimistic assumptions that imply a faster evolution than expected.

Steel is also a material that affects the evolution of chemical conditions. The corrosion of steel results in very low redox potential until all steel is corroded, which is expected to take more than 100 000 years in all vaults except 1–5BLA in which the corrosion rates increase significantly when the pH value decreases below 9 about 9 000 years after closure. Thereafter the redox potential in 1–5BLA is controlled by the inflowing groundwater that is weakly reducing. The redox potential together with the pH affect the chemical form (speciation) of the radionuclides and determines the corrosion rates of steel and other base (non-noble) metals. The reducing conditions that prevail throughout the assessment period are thus important for limited corrosion and limited gas formation. Limited corrosion also ensures slow release of induced activity from the steel waste disposed in 1BRT.

The main processes for gas formation in the repository are corrosion of metals in the waste, the waste packaging and the rebar in the concrete structures, as well as microbial degradation of organic material in the waste. Radiation from the radioactive waste can also generate gas by radiolysis of water and of organic materials. Microbial gas formation is expected to be negligibly low due the high pH conditions. Corrosion of aluminium is fast at high pH and dominates the gas formation until all metallic aluminium is completely corroded, which is expected to be the case after a few years after resaturation of the repository, depending on the material thickness. After that gas formation due to steel corrosion is expected to dominate. If gas is formed faster than it is transported away the gas pressure will increase. A low pressure is either ensured by a sufficiently high permeability for allowing gas passage through the barrier materials or through a gas evacuation system. Thus, groundwater containing radionuclides is not expelled and the integrity of the barriers is not affected due to the effects of gas formation.

Many radionuclides are expected to sorb onto different materials in the repository, and in particular onto concrete that is a good sorbent that is present in large quantities. This significantly delays the release of these radionuclides, however it needs to be considered that the sorption properties are expected to change over time due to the mineralogical evolution of the cement. The bentonite in the silo also contributes to sorption. Other materials that sorb radionuclides are expected to have a smaller effect on radionuclide transport since they have weaker sorption properties (macadam) or they expect to interact with fewer radionuclides (metals and corrosion products).

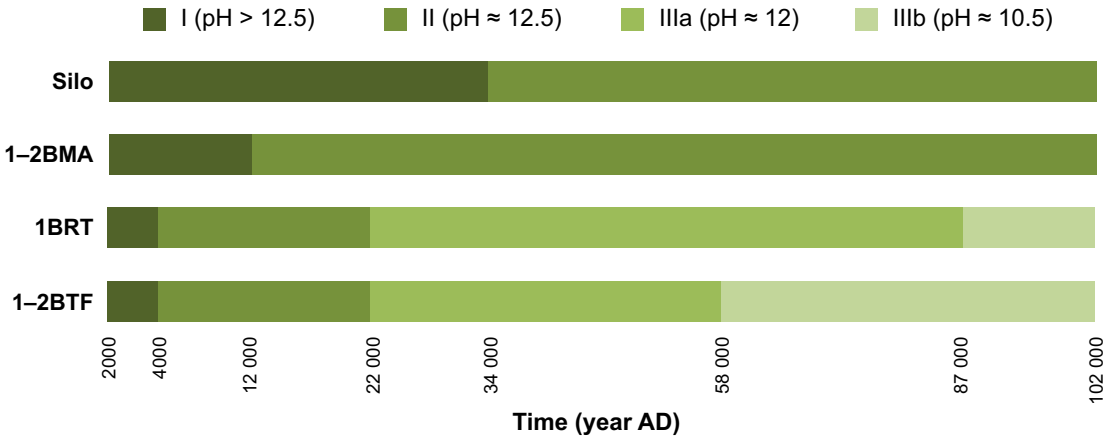

Figure S-7. *Succession of the four chemical concrete degradation states (I–IIIb) in the waste vaults that include concrete barriers, given pessimistic assumptions regarding the condition of the concrete at closure and its evolution.*

Complexing agents are organic molecules that chemically bind with certain radionuclides, in particular, positively charged metal ions. They form soluble metal complexes and thereby decrease their sorption. Complexing agents occur mainly in waste with contents from the use of certain detergents at the waste producers. Other organic materials in the repository can degrade to complexing agents. Some of these have a small effect (e.g. cement additives) and others a larger effect such as cellulose which degrades to isosaccharinate that sorbs onto cement and thus is retained in the repository for long times. Highly soluble complexing agents are expected to be transported out of the vaults within a few thousand years, depending on the groundwater flow through the vaults, and this decreases the effect of complexing agents over time. The concentrations of complexing agents and the amounts of materials degrading to complexing agents are regulated in the waste acceptance criteria to ensure good sorption of radionuclides.

S6.3 Warm climate variant

Conditions in the repository environs

In the *warm climate variant*, the evolution of the repository environs is expected to be similar to the *present-day variant*, albeit with a of 3 500 years delay in the effects caused by the transition to terrestrial conditions (Figure S-3).

Higher mean annual air temperature and changes in precipitation in the *warm climate variant* are expected to mainly affect surface hydrology and ecosystems. The changes can lead to a higher water deficit at or close to the surface and thus to an increased crop irrigation need compared with the *present-day climate variant*. The conditions in lakes and streams are affected by the warmer climate, but it has a limited effect on radionuclide transport in the surface system. A warmer climate is expected to yield higher production and biomass in terrestrial ecosystems, including a higher production of crops.

The changes in mean annual air temperature and precipitation are not expected to significantly affect hydraulic, chemical or mechanical conditions in the bedrock surrounding the repository.

Conditions in the repository

The evolution of hydraulic conditions in the repository follows the evolution in the surrounding bedrock. The chemical conditions in the repository are mainly controlled by dissolution of, and sorption onto, repository materials. These processes are not sensitive to the small temperature differences expected at repository depth in the *warm climate variant*. Thus, the same evolution as in the *present-day climate variant* is expected.

S6.4 Cold climate variant

Conditions in the repository environs

The evolution of the conditions in the repository environs in the *cold climate variant* does not differ from the evolution in the *present-day climate variant* over the first 50 000 years after closure (Figure S-3). During the periglacial periods that occur thereafter the groundwater flow is expected to halt around the repository. The freezing can occur in the entire area, but there could also be areas in the landscape in which the groundwater is not frozen and radionuclide transport to the surface could continue. A colder climate mainly affects hydrology and usually yields a lower production and biomass in terrestrial ecosystems, including lower crop production.

Conditions in the repository

The evolution of hydraulic conditions in the repository follows the evolution in the surrounding bedrock. During periglacial periods, the groundwater in the repository is expected to freeze and all relevant chemical processes and radionuclide transport are expected to halt. After thawing the chemical processes are expected to resume as before the permafrost. The water in the bentonite in the silo and the plugs will freeze to some degree, depending on how low the temperatures get. When the temperature rises after the periglacial period the bentonite is expected to regain its beneficial properties.

At the time of the first periglacial period, the concrete barriers are expected to have lost their flow limiting functions. Additional degradation of the concrete due to freezing of the pore water in the concrete is therefore expected to have a limited effect.

S7 Identification and selection of scenarios

The assessment of post-closure safety and the protection of human health and the environment is based on a scenario analysis. A scenario in the safety analysis comprises a description of how a given combination of external and internal conditions affects repository performance. Each scenario describes a sequence of events and conditions of the repository and its environs and how they affect the protective capability of the repository. Three categories of scenarios are included in the safety assessment. These are the main scenario, less probable scenarios and residual scenarios.

S7.1 Main scenario

The main scenario is based on the probable evolution of external conditions and realistic, or where justified, cautious assumptions with respect to the internal conditions. The description of the main scenario is based on the initial state, the reference external conditions and the reference evolution. The main scenario and its analysis are described in Section S8.

S7.2 Less probable scenarios

The aim of less probable scenarios is to evaluate scenario uncertainties and other uncertainties that are not evaluated within the framework of the main scenario. The selection is based on the safety functions and the FEPs identified as potentially affecting the safety function indicators. For each safety function, uncertainties in how the initial state, internal processes and external conditions are specified in the main scenario are evaluated to determine if there is a possibility that the status of the safety function deviates from that in the main scenario in such a way that post-closure safety may be impaired. It can be noted that the status of the safety functions evolves in the main scenario and that some safety functions are not upheld for the entire assessment period in the main scenario. If uncertainties are identified that lead to a deviation of the evolution of the status of a safety function in comparison with the main scenario a less probable scenario is defined to account for the uncertainty in the assessment of the risk from the repository.

The analysis of uncertainties coupled to the status of the safety functions resulted in the finding that deviations from their status in the main scenario could possibly occur for the safety functions *limit advective transport* and *sorb radionuclides* which relate to the waste form and packaging as well as the concrete barriers. Furthermore, deviations could possibly occur for the safety functions *provide favourable hydraulic conditions* and *provide favourable chemical conditions* that relate to the geosphere. The deviations have different causes, i.e. relate to different FEPs. Table S-2 shows the selected less probable scenarios and associated safety functions that deviate from their status in the main scenario.

Glacial conditions are judged to be less probable during the assessment period and therefore the main scenario does not include any period with glacial conditions. Several safety functions could be affected by a glaciation. A glaciation can lead to a pronounced increase in groundwater flow and thus affects the safety function *provide favourable hydraulic conditions*. The safety function *provide favourable chemical conditions* could be affected since high groundwater flows could lead to intrusion of oxygenated water to repository depth. It could also affect sorption properties for certain radionuclides and the safety function *sorb radionuclides* that relates to the waste form and packaging as well as the engineered barriers. Intruding groundwater could also have a low salinity and could thus affect the bentonite in the silo, which in turn affects the safety function *limit advective transport*. The flow-limiting properties of the concrete barriers in 1–2BMA already have degraded at about 60 000 AD when a glaciation occurs in the glaciation scenario (Figure S-6). Thus, a glaciation would not lead to a significant further impairment of the hydraulic barrier function. To consider the uncertainties connected to glacial conditions in the risk assessment a *glaciation scenario* is defined.

It cannot be excluded that higher concentrations of complexing agents compared with those in the main scenario could affect the transport out of the repository, even if this is judged to be unlikely. This would imply that the safety functions *sorb radionuclides* in the waste form and waste packaging as well as in the cementitious materials in the engineered barriers in the silo, 1–2BMA, 1BRT and 1–2BTF would deviate from the evolution in the main scenario. Therefore, the less probable scenario *high concentrations of complexing agents* is defined.

Table S-2. Less probable scenarios and associated safety functions that deviate from the status in the main scenario.

Less probable scenario	Safety function										
	Waste form and waste packaging					Engineered barriers			Repository environs		
	Limit quantity of activity	Limit gas formation	Limit advective transport	Limit corrosion	Sorb radionuclides	Limit advective transport	Allow gas passage	Sorb radionuclides	Provide favourable hydraulic conditions	Provide chemically favourable conditions	Avoid boreholes in the direct vicinity of the repository
Glaciation scenario					X	X		X	X	X	
High concentrations of complexing agents scenario					X			X			
Alternative concrete evolution scenario			X			X		X			
Earthquake scenario			X			X		X	X		

The concrete evolution is handled with cautious assumptions in the main scenario. In the analysis it can, however, not be excluded that the initial state of the barriers could be affected by fully penetrating initial cracks caused by mishaps together with deficiencies in quality control during construction that imply that the cracks are not detected in the inspections before closure, or due to repair measures for detected cracks that would be less effective than expected. Such fully penetrating cracks could affect the initial state and the evolution of the safety function *limit advective transport*. Crack formation in the engineered barriers of 1–2BMA could lead to smaller accessible amounts of cement for sorption along advection dominated transport paths through the cracks. The safety function *sorb radionuclides* could thus also deviate from its evolution in the main scenario. To account for these uncertainties in the risk assessment, a scenario with *alternative concrete evolution* is defined. Earthquakes have a low probability of occurrence in the area around SFR and are therefore not included in the main scenario. A sufficiently strong earthquake could affect the repository adversely. Earthquakes may cause displacement along fractures in the geosphere, which alter the hydraulic conditions of the geosphere. Furthermore, the hydraulic properties of the concrete structures as well as the waste form and packaging may be affected. If cracks are formed the groundwater flow is affected, but also sorption might be affected since accessible sorption surfaces along the radionuclide transport paths through the concrete barriers decrease in comparison to diffusive or advective transport through intact concrete. The bentonite in the silo could also be adversely affected. To account for these uncertainties the less probable *earthquake scenario* is selected.

It can be noted that a given scenario can arise due to deviations of the status of several safety functions in comparison to the main scenario. A deviation from the status in the main scenario of a safety function can also lead to the selection of several scenarios. This has been accounted for in the assumptions underlying the calculation cases for the less probable scenarios.

In principle, the uncertainties that lead to the definition of the less probable scenarios could occur in different combinations in a single scenario. The probability of the scenario combinations is the product of the probabilities of the less probable scenarios assuming their independence. Thus, the contribution to the total risk becomes very small unless the combinations yield significantly higher doses than the individual less probable scenarios. The identified possible scenario combinations shows that no combination of less probable scenarios would lead to significant contributions to the total annual risk. Scenario combinations are therefore not considered in the risk summation.

S7.3 Residual scenarios

Primarily, residual scenarios aim to illustrate the significance of individual barriers and barrier functions and how they contribute to the protective capability of the repository. They are also selected to contribute to the discussion of the robustness of the repository regarding the protection of human health. The residual scenarios are studied independently of probabilities and are not accounted for in the risk summation. The selection of the residual scenarios is based partly on the safety functions and partly from the assessment of future human actions, for instance intrusion. Furthermore, residual scenarios relating to an unsealed repository and unrepaired 1BMA are evaluated.

S8 Analysis of selected scenarios

S8.1 Description of calculation cases

The selected scenarios are evaluated with the aid of calculation cases. For each calculation case descriptions are given of the most important assumptions for the calculations, data used in the modelling, and the FEPs on which the calculation case focuses. Most scenarios are evaluated by only a single calculation case. For some scenarios, however, several calculation cases are considered necessary in order to evaluate all uncertainties identified by the scenario description. An overview of the scenarios and calculation cases included in the present safety assessment is given in Table S-3.

Table S-3. Scenarios and calculation cases analysed in the PSAR.

Scenario		Calculation case	
Main scenario		Present-day climate (base case) Warm climate Cold climate	
		Supporting calculation cases	Timing of shoreline regression Delayed release from repository Subhorizontal fracture Alternative landscape configurations Ecosystem properties [a)] Alternative delineation [a)] Mire object properties [a)] Calcite depletion [a)]
Less probable scenarios	**Glaciation**	Glaciation	
	High concentrations of complexing agents	High concentrations of complexing agents	
	Alternative concrete evolution	Alternative concrete evolution	
	Earthquake	Earthquake	
Residual scenarios	**Hypothetical early permafrost**	No effect on engineered barriers [b)] Effect on engineered barriers	
	Loss of engineered barrier function	No sorption in the repository No hydraulic barriers in the repository	
	Loss of geosphere barrier function	No sorption in the geosphere No transport retention in the geosphere	
	Alternative radionuclide inventory	Extended operation of reactors Increased fuel damage frequency Extended use of molybdenum-alloy fuel spacers	
	Oxidising conditions	Oxidising conditions	
	Initial concrete cracks	Initial concrete cracks	
	Unrepaired 1BMA	Unrepaired 1BMA	
	Unsealed repository	Unsealed repository	
	Drilling into the repository [c)]	Drilling event Construction on drilling detritus landfill Cultivation on drilling detritus landfill	
	Intrusion well [c)]	Intrusion well	
	Water management [c)]	Construction of a water impoundment	
	Underground constructions [c)]	Rock cavern in the close vicinity of the repository Mine in the vicinity of the repository	

Included in the risk assessment.
[a)] Described in the **Biosphere synthesis report**.
[b)] Described in the **Radionuclide transport report**.
[c)] FHA scenarios.

Three calculation cases are selected for the main scenario based on the reference external conditions. The *present-day climate calculation case* is selected as *base case* in the present safety assessment. The *base case* constitutes the basis for the evaluation of uncertainties in the other calculation cases. The descriptions for all other calculation cases are based on differences from the *base case* regarding initial state, internal and external conditions. The results from these cases are compared with the results from the *base case*.

The *warm climate calculation case* and *cold climate calculation case* of the main scenario represent the range of probable evolution of the external conditions.

The main scenario also includes a set of supporting calculations (Table S-3), providing support for the selection of assumptions in the calculation cases for the main scenario. They are defined to provide a sensitivity analysis of specific uncertainties in external conditions and internal processes potentially important to radionuclide transport through the repository. The calculations are used as input for the selection of assumptions in the *base case* and, thereby, ensure that the evaluated uncertainties do not lead to underestimating the dose in the main scenario. Therefore, the resulting doses in the supporting calculations are similar, or lower, than the dose of the *base case* and, thus, it is not necessary to propagate the calculations to the risk assessment in Chapter 10. It can be noted that in order to support the selection of assumptions the supporting cases are evaluated before the assumptions in the *base case* are set. The reason for evaluating these uncertainties in the main scenario, in contrast to the less probable scenarios, is that a low probability of occurrence may not be justifiable or that they do not relate to uncertainties in any safety functions of the repository system.

S8.2 Modelling radionuclide transport and dose

Background

For each calculation case, the radionuclide transport through the repository (near-field) and through the bedrock (geosphere) to the surface system (biosphere) is quantified by means of mathematical models. The calculations are performed using a sequential chain of models, where output data from one model, in the form of annual activity releases for each radionuclide, is used as input data for the subsequent model. As part of the management of uncertainties in the safety assessment, calculations are performed both deterministically and probabilistically for most calculation cases. In this report, results from probabilistic calculations are presented unless otherwise noted. Each calculation case is stochastically evaluated by Monte Carlo simulations with 1 000 iterations based on pre-defined statistical distributions of the input data. The models used in the radionuclide transport calculations are described in the **Radionuclide transport report** and the **Biosphere synthesis report**, and the process for selecting data and the selected parameter values are documented in the **Data report** and in selected parts of the **Radionuclide transport report**, Appendix A, and the **Biosphere synthesis report**, Chapter 8.

Repository

The models for the repository describe the transport and retention of radionuclides in the waste domain and the surrounding engineered barriers, and the release of radionuclides to the geosphere. The engineered barriers limit the release of radionuclides from the repository by reducing the groundwater flow and provide sorption capacity. The steel in the reactor pressure vessels in 1BRT also constitutes a barrier in that the slow corrosion rate limits the release of activity induced in the steel.

Separate models have been developed for each waste vault to account for different barrier designs and waste types as well as different groundwater flows. The vault models have been developed to consider the main retaining properties of the barriers in the vaults but, depending on the vault, some retaining abilities are neglected. Most importantly, sorption is pessimistically not considered in the 1–5BLA vault models, despite the presence of significant amounts of cement and other sorbents. Further simplifications in the modelling of the repository include, among other things, that (i) solubility limits for radionuclides are neglected, meaning radionuclides are assumed to be fully dissolved in the waste porewater, with the exception of the fractions sorbed on the barrier material or induced in the reactor pressure vessels disposed in 1BRT, (ii) sorbent properties of metals and their corrosion products are pessimistically disregarded, and (iii) the potential transport-limiting effect of waste matrices and steel packaging is neglected. Potential influence on the radiological consequences of these simplifications are evaluated in the *delayed release from the repository calculation case*.

Geosphere

The geosphere model describes the transport of radionuclides released from the repository through the bedrock towards the surface. The model includes retention of radionuclides in the rock matrix. Discharge areas for groundwater from the geosphere to the surface system (Figure S-4) occur in so called *biosphere objects*. A biosphere object is an area in the modelled landscape that is predicted to receive a substantial portion of the radionuclides following release from the geosphere. Seven biosphere objects have been identified based on the modelled discharge areas for groundwater and the local topography of the landscape (for more information, see the **Biosphere synthesis report**, Chapter 5).

During periglacial conditions, radionuclide releases from the geosphere are presumed to occur only via so called through taliks, that is unfrozen areas in the landscape.

Biosphere

Radionuclides are released from the geosphere to the deepest regolith layer represented in the biosphere transport and exposure model. During temperate climate conditions, all radionuclides released from the geosphere are presumed to be discharged into the same biosphere object located north of the repository (object 157_2), which is the object with the highest density of discharge locations for groundwater from the repository (Figure S-4). From this biosphere object the releases are further transported to other biosphere objects. Uncertainties with respect to radionuclide transport to and between biosphere objects are assessed in the supporting calculations *subhorizontal fracture calculation case* and the *alternative landscape configurations calculation case*. Uncertainties with respect to properties and delineation of biosphere object 157_2 are assessed in the *mire object properties calculation case* and the *alternative delineation calculation case*.

The biosphere transport and exposure model describes radionuclide transport, retention and accumulation of radionuclides in aquatic ecosystems (including sea basins, lakes and streams) and terrestrial ecosystems (including mires and agricultural land). Moreover, it calculates potential doses to humans and dose rates to non-human biota. Two different types of water wells are also included in the assessment, as water pumped from these wells may contain radionuclides from SFR. Both wells dug in the regolith and drilled in the bedrock downstream (north) of the repository are evaluated. Drilled wells that penetrate the repository are evaluated in the residual scenario *drilling into the repository*. Uncertainties in the input data to, and processes in, the biosphere transport and exposure model are assessed in the **Biosphere synthesis report**. As part of the management of uncertainties, a number of supporting calculation cases have been identified and evaluated (Table S-3). These calculations evaluate, among other things, uncertainties in how ecosystems are handled in the modelling (*ecosystem properties calculation case*) and the effect of calcite depletion on sorption in the regolith (*calcite depletion calculation case*).

The primary assessment endpoints from the modelling are annual effective dose to humans and absorbed dose rates to non-human biota. Doses to humans are calculated for representative individuals of four potentially exposed groups, describing different variants of land use. The potentially exposed groups in the assessment are hunter-gatherers, infield–outland farmers, drained mire farmers and garden-plot households. As basis for the risk calculation, the dose to an individual in the potentially exposed group receiving the highest annual dose, obtained at each point in time, is used. Dose rates to non-human biota are evaluated in relation to international screening values.

S8.3 Results of radionuclide transport and dose calculations for the main scenario

Base case

In the *base case*, chemical and physical degradation of cementitious materials occur in the waste form and packaging as well as in the engineered barriers. The degradation leads to a gradual decline of the material's capability to retard the transport of radionuclides via sorption and to preserve low groundwater flows. The temporal evolution of the hydraulic conductivity and pH of concrete have been simplified to a number of stages corresponding to different degradation states for the concrete (Figures S-6 and S-7). The presence of complexing agents in certain waste vaults is handled by

applying sorption reduction factors for the radionuclides that are affected. The steel in the reactor pressure vessels in 1BRT is expected to corrode during the entire assessment period. However, it is in the *base case* pessimistically assumed that release of the entire induced activity from the reactor pressure vessels occurs within the first 30 000 years.

The groundwater flow through the repository and its environs is initially very low but increases gradually over the first 1 000 years of the assessment period due to shoreline regression. The discharge areas are still submerged during this period (Figure S-4), which results in low doses (Figure S-8). At just after 3000 AD, the land has risen sufficiently high above sea level that it is feasible to drain and cultivate mires in object 157_2, resulting in increased doses compared with the submerged period and the group *drained mire farmers* receives the highest dose. The maximum annual dose during the assessment period, 5.6 µSv, occurs around 7000 AD. Thus, the dose in the *base case* remains below the dose corresponding to the regulatory risk criterion (14 µSv) throughout the entire assessment period.

Most radionuclides have a limited impact on the total dose in the *base case* (Figure S-9). Of the 53 radionuclides included in the analysis only 11 contribute with a dose exceeding 0.1 µSv (about 1 % of the dose corresponding to the regulatory risk criterion). A contributing factor to the small dose contributions from most radionuclides is the high retention in the repository. For 41 of the 53 radionuclides considered in the analysis, especially those with the highest radiotoxicity, more than 90 % of the initial or produced radiotoxicity remains or decays within the waste vaults during the assessment period. The radionuclides contributing most to the total dose are in the *base case* C-14 in the beginning of the assessment period, Mo-93 at the time of maximum dose, Ca-41 in the middle of the assessment period, and Ni-59 at the end of the assessment period. The relatively high dose from Mo-93 is caused, among other things, by weak sorption on cement and rock matrix in combination with high accumulation in the upper regolith layers cultivated by the group *drained mire farmers*.

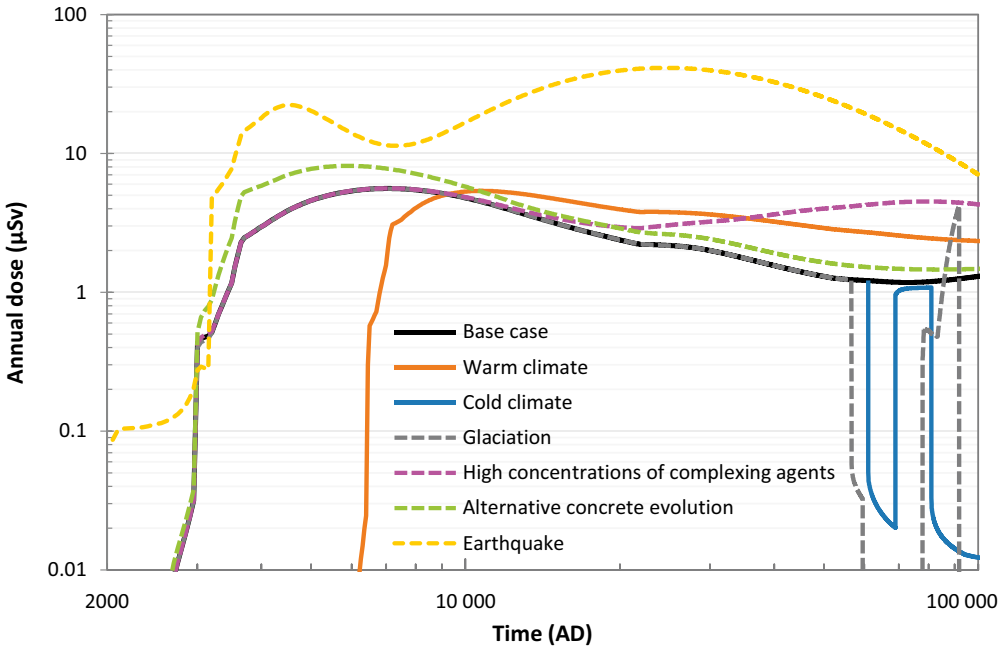

Figure S-8. *Annual dose to a representative individual in the calculation cases that are evaluated in the main scenario (solid lines) and in less probable scenarios (dashed lines). The doses represent the mean of the probabilistic calculations for each case and only the doses of the exposed group receiving the highest dose at each time point are shown. For the earthquake calculation case, only the calculation that gives the highest dose maximum is displayed, i.e. the calculation in which the earthquake occurs at closure. Note that the probabilities of the different scenarios have not been accounted for in this figure.*

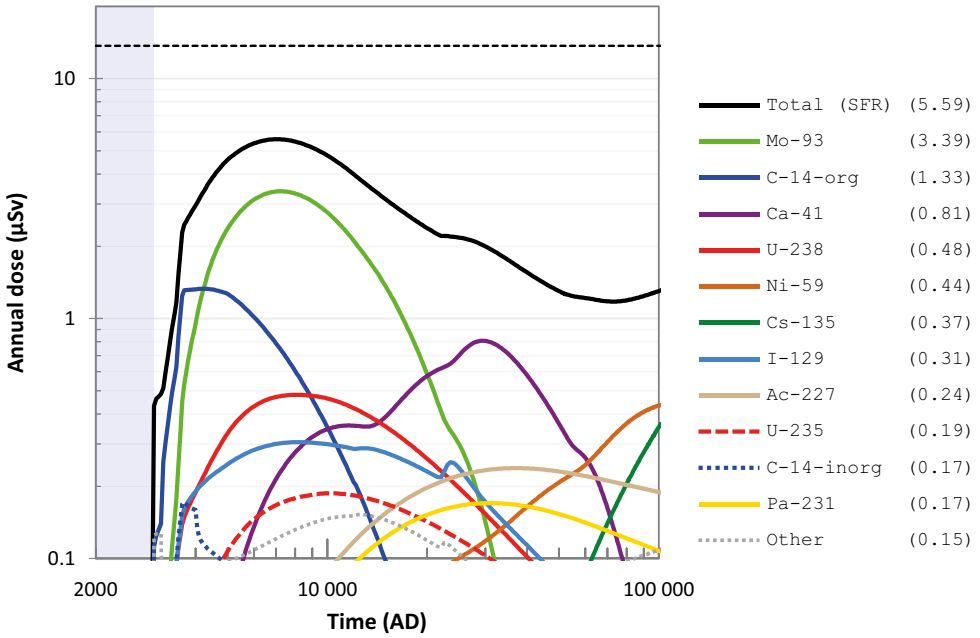

Figure S-9. *Annual dose (µSv) to a representative individual in the base case (black line) and for the radionuclides contributing most to the total dose (coloured lines). The doses represent the mean of the probabilistic calculations and only the doses of the exposed group receiving the highest dose at each time point are shown. The total dose contribution from the remaining radionuclides is illustrated by the grey dotted line. The maximum doses during the assessment period (µSv) are shown in parentheses in the legend. The dose corresponding to the regulatory risk criterion (14 µSv) is indicated by the black dashed line. The blue shading indicates the period with submerged conditions above the repository.*

Another key result from the analysis of the *base case* is that the dose contributions from different waste vaults are relatively similar. There is only one order of magnitude difference in maximum dose between the waste vault that gives the highest dose (silo) and one that gives the lowest dose (1BTF), despite the difference in initial radiotoxicity being approximately two orders of magnitude between the waste vaults. This result indicates that the initial radiotoxicity of the waste is adequately distributed between the individual waste vaults with their different barrier systems. It can be mentioned that the contribution from SFR1 at the time of the maximum dose in the *base case* is 74 % and thus SFR3 contributes with 26 %.

Warm climate calculation case

In the *warm climate calculation case*, a longer submerged period compared with the *base case* is assumed (Figure S-3), which means that it takes longer before new land areas emerge from the sea. It also means low groundwater flow in the repository and surrounding bedrock for a longer period at the beginning of the assessment period. The length of the submerged period is associated with large uncertainty, which is evaluated in the supporting calculation case *timing of shoreline regression*. In addition to a longer submerged period, an average drier climate is assumed, leading to an increased water demand for cultivating crops and lower water flows through the regolith compared with the *base case*.

The maximum dose throughout the assessment period is slightly lower in the *warm climate calculation case* than in the *base case* (Figure S-8). This is primarily due to the consideration that the main contributing radionuclide Mo-93 (Figure S-9), decays to a greater extent in the repository during the longer submerged period in this calculation case. On the other hand, the dose is slightly higher than in the *base case* after about 10 000 AD (Figure S-8). This increase is mainly due to the fact that the water flows through the regolith are assumed to be lower than in the *base case*, which leads to lower dilution with groundwater and thus greater accumulation in the regolith of certain radionuclides with a long half-life (e.g. Ca-41 and Ni-59).

Cold climate calculation case

In the *cold climate calculation case*, two periods of periglacial conditions occur during the last 50 000 years of the assessment period (Figure S-3). During the initial period of temperate climate, conditions in the repository and its environs are assumed to be identical to the *base case*. Releases and doses are evaluated for both continuous permafrost, which results in a complete cessation of radionuclide releases, and for discontinuous permafrost, which enables the releases to occur via a talik. Since cultivation and water abstraction from wells is prevented by the frozen landscape, it is assumed that *hunter-gatherers* is the only exposed group during periods of permafrost. At the time of permafrost, the engineered concrete barriers are so severely degraded that freezing would not lead to a significant further impairment of the hydraulic barrier function. The effect of earlier freezing is illustrated in the residual scenario *hypothetical early permafrost*.

The analysis of the *cold climate calculation case* shows that the presence of permafrost does not lead to higher doses than in the *base case* (Figure S-8). The reason is that the only identified exposure pathway during periglacial periods is hunting and gathering food, which gives more than an order of magnitude lower doses than cultivation and well water usage.

Supporting calculation cases

The supporting calculation cases provide support for the selection of assumptions in the calculation cases for the main scenario. Specifically, they assess uncertainties in future sea level rise (*timing of shoreline regression calculation case*), uncertainties in the initial retention capacity of the repository (*delayed release from repository calculation case*), and uncertainties in the biosphere analysis. These relate to the spatial dispersion of the release (*subhorizontal fracture calculation case*), transport pathways within the landscape (*alternative landscape configurations calculation case*), and delineation of biosphere object 157_2 (*alternative delineation calculation case*).

The *timing of shoreline regression calculation case* shows that the maximum dose gradually decreases with the length of the submerged period; for the longest conceivable submerged period (20 000 years), the decrease is more than 50 %. Thus, the assumption of a relatively short submerged period in the *base case* and the *cold climate calculation case* is cautious since a longer, more realistic, submerged period results in lower doses. In the *alternative delineation calculation case* the entire radionuclide release is assumed to occur pessimistically to the part of biosphere object 157_2 that is most suitable for cultivation, which corresponds to one fifth of its total area. The assumption is considered hypothetical, because it is not in line with the modeling of discharge areas in the landscape (Figure S-4). Despite this, the doses in the calculation case are only about a factor of two higher than in the *base case*, showing that the resulting dose is not very sensitive to the object delineation. In the remaining supporting calculation cases, the maximum doses are slightly lower than in the *base case*. In summary, the supporting calculation cases confirm that the assumptions in the main scenario are well chosen and that the uncertainties evaluated in them are unlikely to result in a significantly higher maximum dose than in the *base case*.

S8.4 Results of radionuclide transport and dose calculations for the less probable scenarios

Glaciation calculation case

In the *glaciation calculation case* radiological consequences of an ice-sheet (glaciation) above the repository are evaluated. The underpinning assumption is that the next glaciation of the Forsmark area will occur around 60 000 AD, as a result of a substantial insolation minimum around 56 000 AD. Such a climate evolution is considered to be significantly less probable than the development towards periglacial climatic conditions during the end of the assessment period that is included in the main scenario. Should the repository area be glaciated after about 60 000 AD, both geological data and modelling of future climates indicate that further glaciation will occur towards the end of the assessment period; thus, a further glaciation is assumed during the last approximately 10 000 years of the assessment period in the calculation case.

At the time of the first ice sheet's advance over the area, the concrete barriers in the waste vaults are already completely degraded. The glaciation is expected to lead to a complete degradation of the bentonite's hydraulic barrier function, altered sorption properties for certain radionuclides due to penetration of oxygen-rich glacial meltwater and increased groundwater flows in the repository and geosphere in connection with the retreat of the ice-sheet from the area.[1] All these effects are considered in this calculation case.

After a glaciation, the Forsmark area is expected to have a temperate climate and submerged conditions. The highest doses occur when draining and cultivation of the mire in object 157_2 becomes possible again, i.e. when the object has become terrestrial after the submerged period, which is assumed to occur between about 80 000 and 90 000 AD. However, the dose during this period is lower than the maximum dose in the main scenario (Figure S-8; note that the probabilities of the less probable scenarios are not taken into account in the figure).

Since the glaciation occurs so long after closure, only releases and doses of long-lived radionuclides and their potential decay products are affected. Ni-59 is the radionuclide that contributes most to the dose after a glaciation. The primary reason is the impaired function of the bentonite around the silo.

High concentrations of complexing agents calculation case

Complexing agents from chemical products used in the operation of the nuclear facilities are present in part of the waste. Complexing agents can also be produced in the repository by degradation of waste components such as cellulose and superplasticizers in concrete. The effect of complexing agents is handled in the main scenario by reducing the sorption of certain radionuclides by applying sorption reduction factors.

There are essentially four sources of uncertainty that could affect the concentrations of complexing agents in the waste:

(i) degradation of superplasticisers,

(ii) dissolved complexing agents that may potentially travel with the groundwater from 1BLA to 1BMA,

(iii) possible yet unidentified amounts of complexing materials, and

(iv) polyamines in paint and their interaction with nickel.

These uncertainties are handled in the calculation case by applying a tenfold increase in the sorption reduction factors compared with the main scenario. In addition, a tenfold decrease in sorption is applied for nickel due to its interaction with polyamines, which is not accounted for in the main scenario.

Higher concentrations of complexing agents have only a limited effect on the maximum dose, as the radionuclides that contribute most at the time of maximum dose in the *base case* (Mo-93 and C-14, see Figure S-9) are not affected by complexing agents. On the other hand, the dose from Ni-59 increases noticeably, resulting in an increase in the total dose especially at the end of the analysis period (Figure S-8). However, the dose during that period does not exceed the maximum dose that occurs around 7000 AD.

Alternative concrete evolution calculation case

Uncertainties related to the hydraulic properties of the concrete in the repository are mainly related to the existence of cracks in the concrete, the degradation rate of the concrete, and the hydraulic properties of the degraded concrete. However, these aspects are judged to be handled cautiously in the main scenario. Despite this, it is assumed that the hydraulic conductivity of the concrete in this calculation case is initially higher and increases earlier (degrades faster) during the first 50 000 years than in the main scenario, which leads to higher groundwater flow through the waste. In addition, it is assumed that the effective diffusivity of the radionuclides in concrete and the porosity of the

[1] During the advance of the ice-sheet, the pore water in the geosphere and repository is assumed to be frozen due to permafrost, whereby the impact of the ice on the groundwater flow is not considered.

concrete increase earlier than in the main scenario and that cracks in the concrete are formed earlier. After 52 000 AD, the concrete is assumed to be completely degraded in all waste vaults, as in the main scenario (Figure S-6).

These assumptions result in the total dose being higher than in the *base case* during the entire assessment period (Figure S-8). The maximum dose is almost 50 % higher than in the *base case*. The difference in dose compared with the *base case* is explained by higher releases of all radionuclides from the repository except those present mainly in the BLA-vaults, where the concrete has no flow-limiting or sorbing function in the analysis.

Earthquake calculation case

Radiological consequences of an earthquake are evaluated in the *earthquake calculation case*. Potential consequences are only evaluated for the silo, where a pessimistic handling has been selected. The pessimistic handling is judged to adequately compensate for the potential consequences of an earthquake for other waste vaults. The earthquake is pessimistically assumed to lead to insignificant retention in the geosphere and to damage of the concrete structure in the silo as well as a loss of its sorption capacity.

The evaluation includes calculations with earthquakes assumed to occur at different times. The highest maximum dose is obtained when the earthquake occurs at closure. The maximum dose from this calculation is almost 20 times higher than the corresponding dose from the silo in the *base case* (Figure S-8), which is due to the fact that the entire activity of Ni-59 is transported out of the silo.[2] It should be pointed out, however, that this result is a direct consequence of the pessimistic assumptions that have been made, in particular the assumed lack of sorption in the silo. The *earthquake calculation case* is therefore considered to provide an upper-bound estimate with respect to radiological consequences resulting from an earthquake rather than a realistic assessment.

S8.5 Results of radionuclide transport and dose calculations for the residual scenarios

The set of residual scenarios (Table S-3) illustrate, among other things, the significance of individual barriers and barrier functions and are not included in the assessment of risk.

Overall, the evaluation of the residual scenarios shows that both sorption and the hydraulic properties of the engineered barriers are important to achieve a dose in the main scenario that is lower than the dose corresponding to the risk criterion. Radionuclide sorption and travel time in the geosphere are less important for the dose than in the engineered barriers. When interpreting the results, it should be noted that the conditions used in the calculation cases in the main scenario are already cautious for both the repository and the geosphere.

The residual scenarios also cover a wide range of credible future human activities, which are based on the premise that the actions cannot be performed if there was knowledge of the repository and/or its nature (the location of the repository, its purpose and the consequences of the actions). These scenarios are evaluated against criteria set out by the IAEA for when efforts to reduce the probability of intrusion or to limit its consequences are warranted. The conclusion from such a comparison is that no further efforts are warranted.

Finally, the analysis of the residual scenarios shows the importance of an adequate closure of the repository.

[2] In comparison, more than 99 % of Ni-59 activity is retained or decayed in the silo in the *base case*.

S8.6 Annual risk and dose rates to non-human biota

Based on the annual doses for the main scenario and the less probable scenarios (Figure S-8), the annual risk of harmful effects from ionizing radiation is calculated for a representative individual in the group exposed to the greatest risk. The annual doses are multiplied with the coefficient for conversion of effective dose to risk 7.3 percent per Sievert in accordance with SSMFS 2008:37. The main scenario is assigned a probability of 1 and the probabilities for the less probable scenarios have been estimated using expert judgments. The probability of the *earthquake scenario* has been calculated based on, among other things, earthquake statistics and that the accumulated probability that an earthquake has occurred by the end of the assessment period is 0.1. The estimations for the other less probable scenarios have resulted in a probability of 0.1 being assumed for these in the calculations, however, the probabilities are judged to be lower than that. The results for annual risk in the calculation cases in the main scenario and in the less probable scenarios are shown in Figure S-10.

The total annual risk is summed up taking into account that the main scenario and the less probable scenarios are mutually exclusive. Hence, when less probable scenarios contribute to the total annual risk at a given time, the probability of the main scenario is reduced by the probabilities of the contributing less probable scenarios. Combinations of less probable scenarios have not been considered in the risk summation.

To avoid underestimating the risk, the less probable scenarios are only included in the summation of the total risk for time points when they give a higher dose than the main scenario.

The maximum total annual risk is 4.4×10^{-7} (Figure S-11, Section S9.1), occurs at 6900 AD, and is obtained assuming present-day climate for the main scenario and the less probable scenarios, except for the *glaciation scenario*. An evaluation based on the development of cold and warm climate conditions gives a lower maximum total annual risk. The total annual risk is thus below SSM's risk criterion of 10^{-6}. The contribution of the main scenario dominates the total annual risk, except towards the end of the assessment period when the contribution from the *earthquake scenario* is greatest. The other less probable scenarios also contribute to the total annual risk.

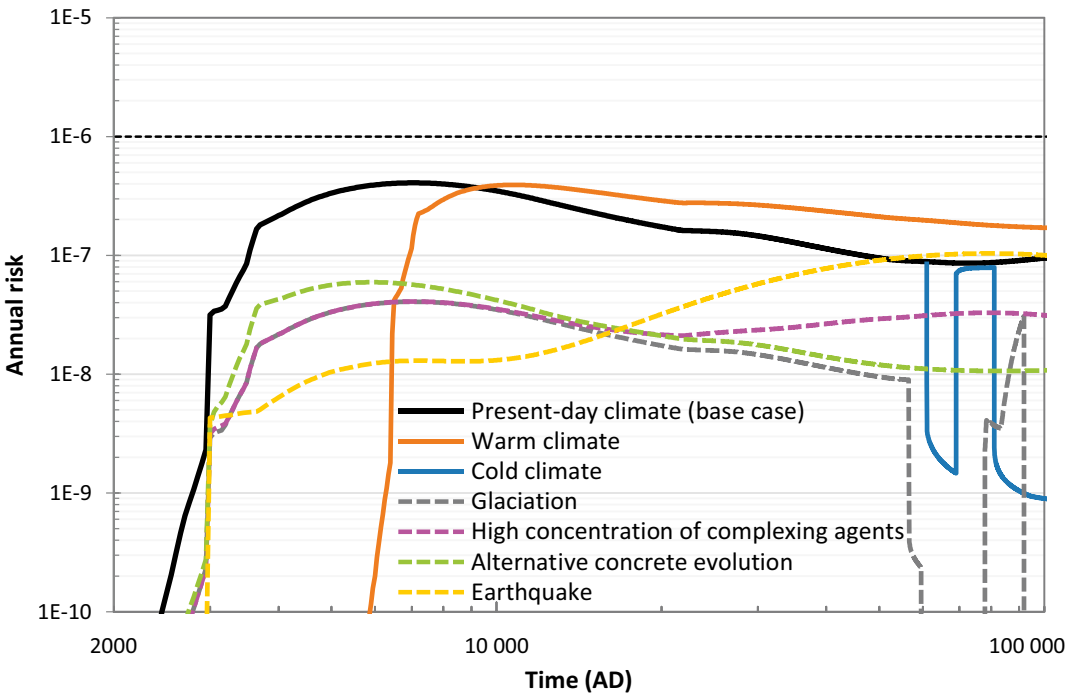

Figure S-10. *Annual risk as a function of time, for the calculation cases in the main scenario (solid lines) and the less probable scenarios (dashed lines). The annual risk from the less probable scenarios is calculated with respect to the base case (present-day) climate. The dashed black line represents the regulatory risk criterion.*

The contributions to the risk from different waste vaults depend on several factors such as the initial radiotoxicity of the radionuclides, the flow-limiting and retention capacities of the barrier system, accumulation and plant uptake of different radionuclides in the surface system, and the relative importance of different exposure pathways. The silo contributes most to the total annual risk at the time of maximum risk, while 1BMA dominates in the beginning of the assessment period. Similar to the calculated dose in the *base case*, the contributions from Mo-93 and C-14 dominate the total annual risk when the maximum occurs, while the very long-lived radionuclides Ca-41 and Ni-59 contribute most to the total annual risk after about 20 000 years. Risk dilution has been evaluated and is deemed to have a limited impact on the calculated total annual risk.

Furthermore, additional safety indicators are used to support the assessment of the protective capacity of the repository. Calculated activity concentrations in environmental media for U-238 and Ra-226 from SFR have been compared with measured background concentrations in Forsmark. In addition, the calculated concentrations of these radionuclides in water from a drilled well have been compared with measured concentrations in Swedish wells. Both comparisons show that the calculated concentrations from SFR are below background concentrations and thus that SFR does not make any significant contribution to the concentrations of these radionuclides in the environment.

In order to show that biological diversity and the sustainable use of biological resources are protected against the harmful effects of ionizing radiation, potential dose rates to non-human biota in affected habitats and ecosystems have been evaluated. The evaluation has been done using the ERICA code and is carried out for the *base case*, *warm climate calculation case*, *cold climate calculation case*, as well as the supporting *alternative delineation calculation case*. In all calculation cases, the maximum dose rates are three orders of magnitude below the international ERICA screening dose rate (10 μGy h^{-1}). Furthermore, all dose rates are significantly lower than the lower limit of the most restrictive screening value from the ICRP (4 μGy h^{-1}; which only applies to some vertebrates and coniferous trees). Thus, populations of non-human biota are not expected to be affected by radionuclides from the repository.

S9 Conclusions of the safety assessment

The main objective of the post-closure safety assessment is to demonstrate that SFR is radiologically safe for humans and the environment after closure. Compliance with regulations regarding the protection of human health and the environment, as well as the robustness of the barrier system, are demonstrated.

S9.1 Protection of human health and the environment

The results from the calculation of the risk of harmful effects after closure show that the risk over the entire assessment period of 100 000 years is below 10^{-6} for a representative individual in the group exposed to the greatest risk (Figure S-11). The risk calculation is based on present-day climate (*base case*), which gives the highest maximum total annual risk among the variants of climate conditions.

Collective doses have been calculated for a global population (for C-14 releases) and a regional population around the Baltic Sea (for all radionuclide releases) for relevant calculation cases in the main scenario and the less probable scenarios. The calculated collective doses for the selected calculation cases are 1.6–2.0 man Sv for the global population and 0.12–0.14 man Sv for the regional population around the Baltic Sea.

The assessment of the biological effects of ionising radiation on the habitats and ecosystems concerned shows that biodiversity and sustainable use of biological resources are protected against harmful effects of ionising radiation from SFR.

S9.2 Robustness of the barrier system

The requirements from SSM concerning safety in connection with the disposal of nuclear material and nuclear waste means that the repository must be robust, in the sense that regulatory requirements related to the barrier system and barrier functions as well as the design and construction of the barrier system are met. The post-closure safety of SFR is maintained through a system of passive barriers.

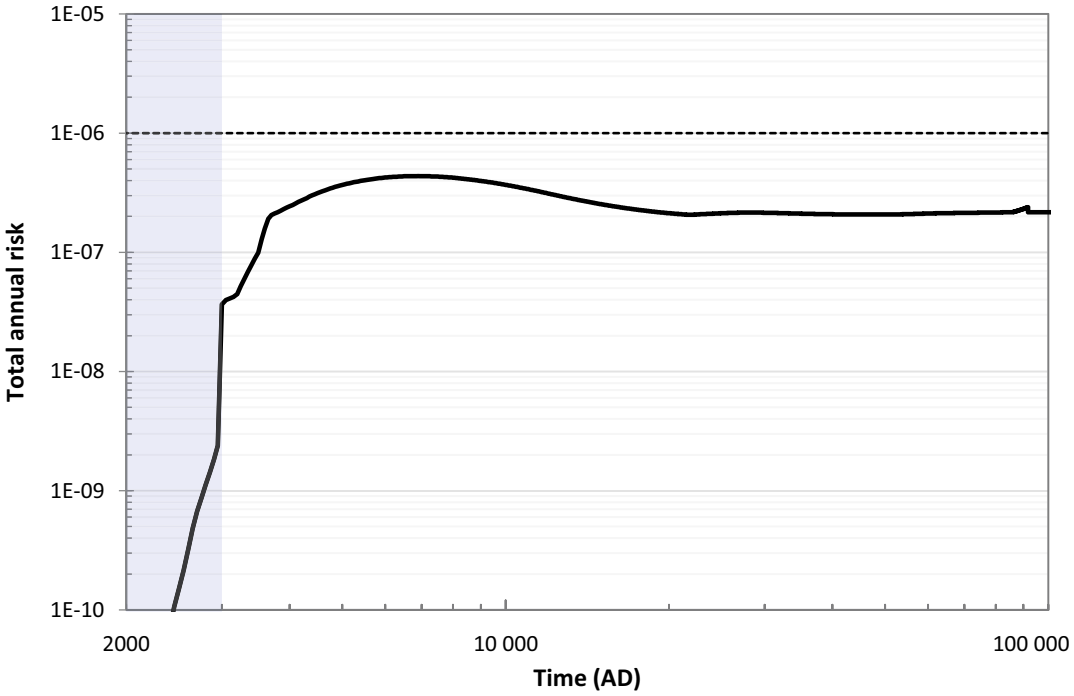

Figure S-11. *Total annual risk as a function of time, obtained from the weighted summation of the main scenario and all less probable scenarios using the base case (present-day) climate. The blue shaded area shows the period of submerged conditions. The dashed black line represents the regulatory risk criterion.*

The passive barrier system consists of engineered barriers and natural barriers and is described in detail in the initial state of SFR. The post-closure safety assessment shows that the barriers contribute to the containment and prevention or retention of dispersion of radionuclides, either directly or indirectly by protecting other barriers in the barrier system. This can be illustrated by the results of the risk calculations that show that none of the radionuclides that contribute most to the total radiotoxicity at closure give any significant contribution to the total annual risk after closure.

The post-closure safety assessment is based on all features, events and processes (FEPs) potentially relevant for the post-closure performance of the barriers. Relevant FEPs are addressed in the safety assessment and the results show that SFR can withstand such FEPs. This conclusion is strengthened by the analysis of the residual scenarios that aim to illustrate the significance of individual barriers and barrier functions. These scenarios include cases with hypothetical defects that strongly affect the barrier functions and includes unrealistic assumptions. Despite this, they result in annual doses in the same order of magnitude as the dose corresponding to the risk criterion, which in turn is approximately two orders of magnitude below the annual natural background radiation in Sweden of approximately 1–2 mSv.

Best available technique has been considered in the design of the barrier system, which generally also leads to optimisation of the repository with respect to risk. Within the framework of the operation of the existing SFR, waste acceptance criteria have been developed, among other things based on the results of previous post-closure safety assessments. The revision of the acceptance criteria contributes to reduced uncertainties in the actual initial state and thus the optimisation of the repository.

The importance of single deficiencies in individual barriers has been analysed in the less probable scenarios and residual scenarios, and the results show that post-closure safety is not unduly dependent on a single barrier or barrier function.

S9.3 Confidence in post-closure safety conclusions

There are several aspects of the post-closure safety assessment that strengthen confidence in the compliance regarding the protection of human health and the environment and the robustness of the repository.

The safety assessment methodology is systematically structured and takes into account the regulatory requirements regarding the methodology and includes the aspects relevant for assessing post-closure safety and protection of human health and the environment. The methodology is thus adequate to be able to draw firm conclusions from the results of the post-closure safety assessment regarding regulatory compliance.

The post-closure safety assessment is based on a well-defined initial state. The site of the extension of the repository has been characterised in detail and was selected based on requirements on post-closure safety. The barrier design is coupled to the overall post-closure safety principles *limitation of the activity of long-lived radionuclides* and *retention of radionuclides*. The waste form and packaging as well as the different characteristics and the radiotoxicity of the radionuclides have been the basis for barrier design of the different waste vaults. The waste with the main part of the radiotoxicity is disposed in the silo and 1–2BMA that have the engineered barrier systems with the highest retention capabilities. For low radiotoxicity wastes, a simpler barrier design is accordingly adapted. During construction, operation and before closure, the barriers are inspected to ensure a well-defined initial state. The waste acceptance criteria ensure that the properties of the disposed waste are appropriate in relation to post-closure safety.

The assessment of post-closure safety is based on an adequate understanding of the evolution of the repository and its environs. The site of the SFR has been thoroughly investigated and characterised in the site descriptive model, and the latest investigations in five core-drilled boreholes confirm the understanding of the site. The reference evolution is based on a scientifically founded process understanding regarding processes affecting the barrier system and the surrounding environs, as described in the FEP analysis and associated process reports. The reference evolution is the foundation for the main scenario, which is based on probable evolutions of external conditions and realistic or, where justified, cautious assumptions with respect to internal conditions. Scenario uncertainties are evaluated with a set of less probable scenarios and also in supporting calculations to the main scenario. The results from the scenario analysis and associated radionuclide transport and dose calculations have been interpreted in detail and the sensitivity of the results to various uncertainties has been evaluated.

As long as the area above the repository is submerged beneath the Baltic Sea, groundwater flow through the waste is very low due to low hydraulic gradients and that the barrier system is limiting the flow. Human intrusion is restricted by the subsea location. The uncertainties regarding the protective capability of the repository during this period are low and a large part of the initial radiotoxicity decays. As the shoreline moves away from the repository, the groundwater flow through the waste increases until about 5000 AD, when the flow stabilises at a low level due to the flat topography and the barrier system. The flow-limiting concrete barriers in 1–2BMA degrade slowly and, in the main scenario, it is not until 22 000 AD that the flow-limiting capabilities are expected to be lost (Figure S-6). For the radionuclides that dominate the dose in the first 20 000 years post-closure, retention in the repository is important. For the time after 22 000 AD, only very long-lived radionuclides have any significant effect on releases and doses from SFR. The flow-limiting properties of the bentonite are upheld throughout the entire assessment period. The favourable sorption properties of concrete provide an effective retention capacity throughout the assessment period for most of these long-lived radionuclides. Long-lived radionuclides that are weakly or non-sorbing on concrete are primarily handled with limitation of the inventory in SFR.

The management of uncertainties has been given great attention in the assessment. In SKB's safety assessment methodology, management of uncertainties is an integral part. The uncertainties have been classified as scenario uncertainties, system uncertainties, modelling uncertainties and data uncertainties and all these types of uncertainties have been taken into account in the safety assessment. A set of residual scenarios aims to create an understanding of the importance of different barrier functions and can be seen as bounding cases for the impact of uncertainties.

In summary, the understanding of the initial state and the evolution of the repository system, together with credible or pessimistic assumptions in the radionuclide transport and dose calculations, and thoroughly interpreted results, lend confidence in the conclusion that human health and the environment are protected after closure of the repository.

1 Introduction

This document is the main report for the post-closure safety assessment that contributes to the preliminary safety analysis report (PSAR) for SFR, the repository for short-lived radioactive waste at Forsmark in Östhammar municipality, Sweden (Figure 1-1). The main role of the post-closure safety assessment is to demonstrate that SFR is radiologically safe for humans and the environment after closure.

This chapter gives a brief overview of the PSAR post-closure safety assessment undertaken as part of the construction license application for the extension of SFR, the waste disposed in SFR, the repository layout and relevant regulations. In addition, the purpose and content of this report are described.

1.1 Licensing of SFR

The safety assessment documented in the present report evaluates post-closure safety for SFR, which consists of the existing part, SFR1 (Figure 1-2, top right, grey part), and the extension, SFR3 (Figure 1-2, top right, blue part). SFR1 is designed for disposal of short-lived low- and intermediate-level waste produced during operation of the Swedish nuclear power reactors, as well as waste generated during the application of radioisotopes in medicine, industry, and research. This part became operational in 1988. SFR3 is designed primarily for disposal of short-lived low- and intermediate-level waste from decommissioning of nuclear facilities in Sweden. The extension is called SFR3 since the name SFR2 was used in a previous plan to build vaults adjacent to SFR1.

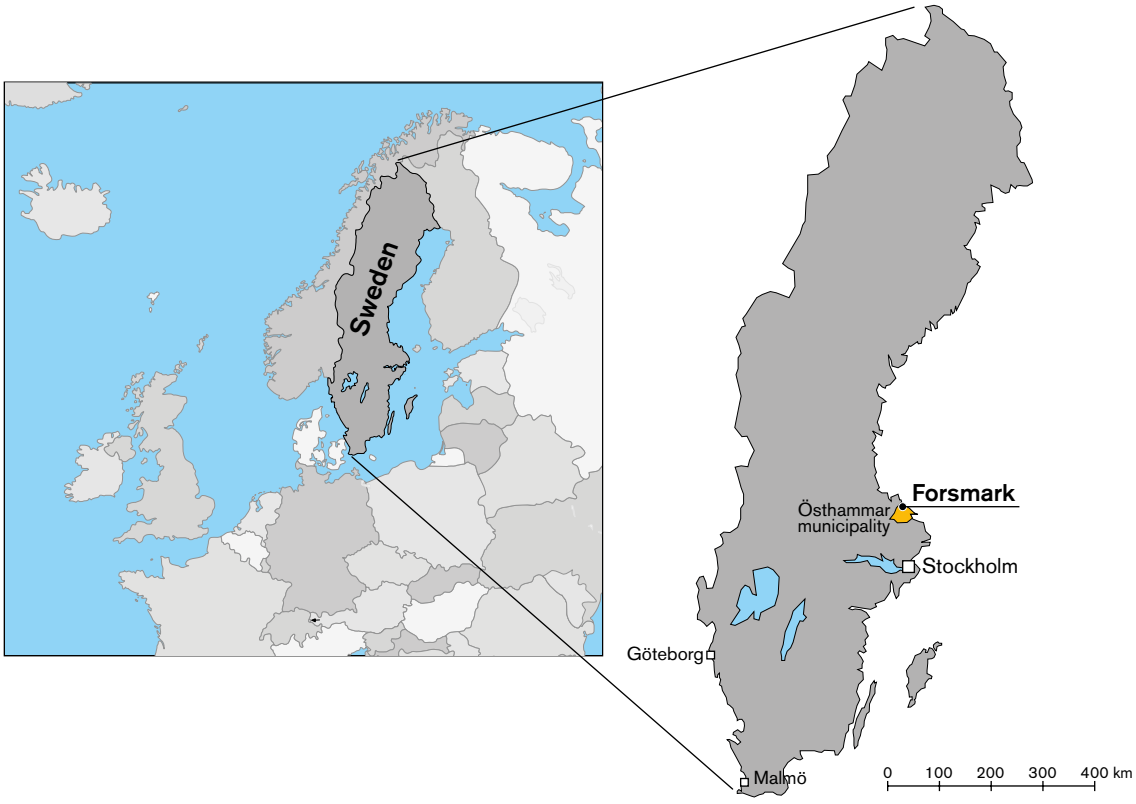

Figure 1-1. *Map showing the location of Forsmark. Forsmark is situated in Östhammar municipality, which belongs to the County of Uppsala.*

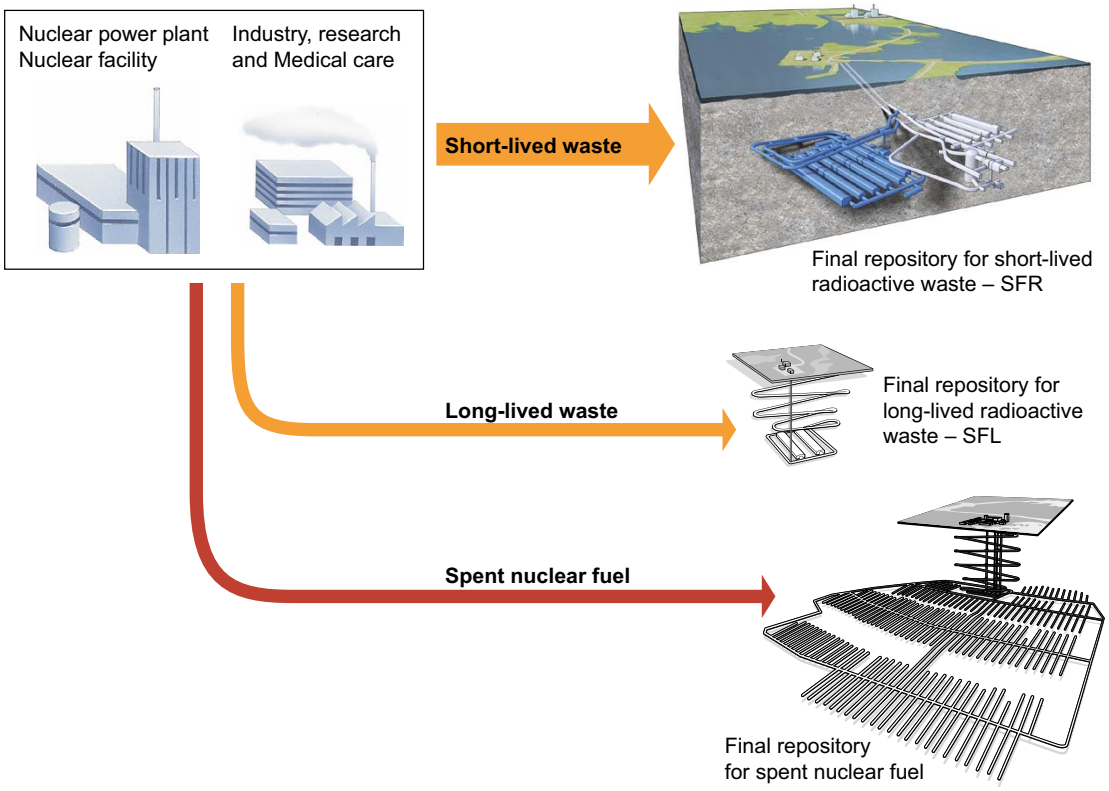

Figure 1-2. *SKB's existing and planned final repositories. The existing part of SFR (SFR1) is illustrated in grey and the extension (SFR3) is illustrated in blue.*

SFR is operated by the Swedish Nuclear Fuel and Waste Management Company, SKB, and is part of the Swedish system for management of waste from nuclear power plants, other nuclear activities, industry, research and medical care. In addition to SFR, the Swedish nuclear waste management system also includes the repository for spent nuclear fuel and the repository for long-lived radioactive waste (SFL; Figure 1-2, middle right). A detailed description of the Swedish nuclear waste management system is given in SKB's research, development and demonstration (RD&D) programme (SKB TR-22-11).

A prerequisite for the extension of SFR is the licensing of the extended facility, SFR3. The licensing follows a stepwise procedure. In December 2014, SKB submitted two licence applications to extend and continue the operation of SFR, one to the Swedish Radiation Safety Authority (SSM) for permission under the Act on Nuclear Activities (SFS 1984:3) and one to the Land and Environment Court for permissibility under the Environmental Code (SFS 1998:808).

The applications included a post-closure safety assessment (SKB TR-14-01[3]) that was a part of the first preliminary safety analysis report (F-PSAR) for the extended SFR. The applications were complemented with additional information requested by SSM and the Land and Environmental Court. SSM served as a statutory referral body for the Court's review, and the authority submitted a consultation response to the Court recommending approval of SKB's licence application in January 2019. During two weeks in autumn 2019, SKB's application was examined by the Land and Environmental Court in a main hearing. In October 2019 SSM submitted their pronouncement to the Swedish Government and recommended approval of the permission sought by SKB. In November 2019 the Court submitted its statement to the Swedish Government and recommended approval of the licence application. The Swedish Government granted permit and permissibility in December 2021.

The current step in the licensing of the extended SFR is the processing of the construction license application, submitted by SKB to SSM for review under the Act on Nuclear Activities. The licence documentation consists of an application document and a set of supporting documents. A central

[3] For SKB reports without named authors, the report number is used instead of publication year when referring to them in the text.

supporting document is the preliminary safety analysis report (PSAR), with a general part consisting of 10 chapters. Chapter 9 of the general part of that report addresses post-closure safety and the present report is the main reference to Chapter 9.

The next step will be an updated safety analysis report (SAR) that reflects the construction of the facility. The updated SAR needs to be approved by SSM before trial operation of the facility may commence. The SAR shall then be supplemented, taking the experience of such trial operation into account, which needs to be approved by SSM before the facility can be taken into regular operation. The repository is currently estimated to be closed by year 2075.

The main role of the post-closure safety assessment is to demonstrate that SFR is radiologically safe for humans and the environment after closure. This is done by evaluating compliance with respect to SSM's regulations concerning post-closure safety and the protection of human health and the environment. The post-closure safety of the existing SFR, and subsequently the extended SFR, has been assessed on several occasions. The preliminary safety report that served as a basis for the government licence to construct the facility was submitted in 1982, and the supplemented safety report that was required for the operating licence was finished in 1987. The safety report was then supplemented in 1991 regarding the silo and updated in 1993. The safety assessment SAFE (SKB 2001) was reported to the regulatory authorities in 2001 and supplements to this were produced in response to the regulator review comments in 2005 and in the safety assessment SAR-08 (SKB R-08-130). The licence application for the extended SFR included the first post-closure safety assessment of both the facility in operation and the extension (SKB TR-14-01).

1.2 SFR – waste

1.2.1 Waste origin, characteristics, packaging and volumes

Short-lived low- and intermediate-level waste is disposed in SFR. According to the definitions used by SKB[4], which are based on operational considerations, intermediate-level waste requires shielding, but no cooling, during handling and storage. In contrast, low-level waste can be handled without special shielding. The waste can be divided into short-lived[5] and long-lived, with the activity content in the short-lived waste being dominated by short-lived radionuclides.[6]

The physical and radiological properties of the various types of waste disposed in SFR differ and the waste is packaged, handled and disposed accordingly. The waste disposed in SFR1 has mainly been produced during operation of the Swedish nuclear power reactors, such as spent ion-exchange resins from cleaning reactor water, scrap metal from refurbishment and contaminated consumable items such as protective clothing and equipment. The contamination derives from leakage of radionuclides from the fuel, or from neutron activation of particles in the reactor water and components of the reactors. Low- and intermediate-level waste from other Swedish nuclear facilities, including the decommissioned nuclear reactor Ågesta, the decommissioned nuclear research reactors in Studsvik, as well as from the interim storage facility for spent fuel (Clab) is also disposed in SFR. In addition, legacy waste from AB SVAFO (a company managing radioactive waste and facilities from early Swedish nuclear research), Studsvik Nuclear AB (a company treating radioactive waste from hospitals, research and industry) and Cyclife Sweden AB (a company treating low- and intermediate-level waste from the nuclear industry and other industries using radiation) is disposed in SFR.

Most of the waste to be disposed in SFR3 originates from the dismantling of the nuclear power plants and other nuclear facilities. This waste is mainly activated or contaminated reactor components, scrap metal, concrete and other building materials.

---

[4] SKB, 2022. PSAR SFR – Allmän del kapitel 3 – Krav och konstruktionsförutsättningar. SKBdoc 1702855 ver 3.0, Svensk Kärnbränslehantering AB. (In Swedish.) (Internal document.)

[5] Short-lived waste is defined according to the IAEA Safety Glossary (IAEA 2018) as "*radioactive waste that does not contain significant levels of radionuclides with a half-life greater than 30 years*". SKB uses a similar definition, but with 31 years to include cesium-137, which is used as a key radionuclide to estimate the content of other radionuclides. Waste that is not short-lived is consequently considered long-lived.

[6] In the safety assessment context, radionuclides with a half-life shorter than 31 years.

The types of waste packaging used in SFR are ISO-containers, concrete tanks, steel drums and concrete or steel moulds. In the waste vaults 1–2BMA and silo (see Figure 1-6), wastes (e.g. ion-exchange resins, concentrates and sludge) are either solidified with cement or bitumen or embedded in concrete (solid waste e.g. trash and scrap metal). This can be preceded by, for example, incineration, compaction, segmentation or even melting of the wastes. All waste disposed in SFR must conform to approved waste acceptance criteria (WAC).

The information on waste produced up until the end of 2016 and the future forecast from the inventory report (SKB R-18-07) show that the volume of decommissioning wastes is expected to be greater than that of operational wastes (Figure 1-3), but their activity content at closure is generally lower. SFR will have a capacity of about 180 000 m^3 in total, and the current forecast for the waste volume allocated to SFR1 is about 54 000 m^3 and about 100 000 m^3 for SFR3.

1.2.2 Activity and radiotoxicity of the waste

At the time of disposal, the activity of radionuclides in the waste in SFR is dominated by short-lived radionuclides, e.g. Fe-55 and Co-60. This means that a large fraction of the activity disposed in SFR will decay substantially before year 2075, when the repository is estimated to be closed. The total activity 100 years after closure is about 40 % of its initial value at closure and about 1.5 % remains after 1 000 years (Figure 1-4). Initially, Ni-63 dominates the total activity, with Cs-137 as the second most contributing radionuclide. Then, from about 600 years after closure, Ni-59 dominates the total activity until the end of the assessment period.

Ingestion radiotoxicity, below denoted ‘radiotoxicity’, serves to quantify the radiological hazard from individual radionuclides in a simple way, here defined as the product of the activity of a radionuclide and its corresponding ingestion dose coefficient. The radiotoxicity of a radionuclide is dependent on factors such as the type and energy of the radiation it emits and its biokinetic behaviour in the body. The radionuclides with the highest activity are not necessarily those that contribute the most to the radiotoxicity of the waste. Initially, the radiotoxicity is dominated by Cs-137, with Ni-63 as the second most contributing radionuclide (Figure 1-5). SFR1 contains 88 % of the total radiotoxicity at closure. The total radiotoxicity 100 years after closure is less than 20 % of its initial value and decreases to about 2.5 % after 1 000 years dropping to about 1 % after 10 000 years. By the end of the assessment period, after 100 000 years, less than 0.2 % of the initial radiotoxicity remains.

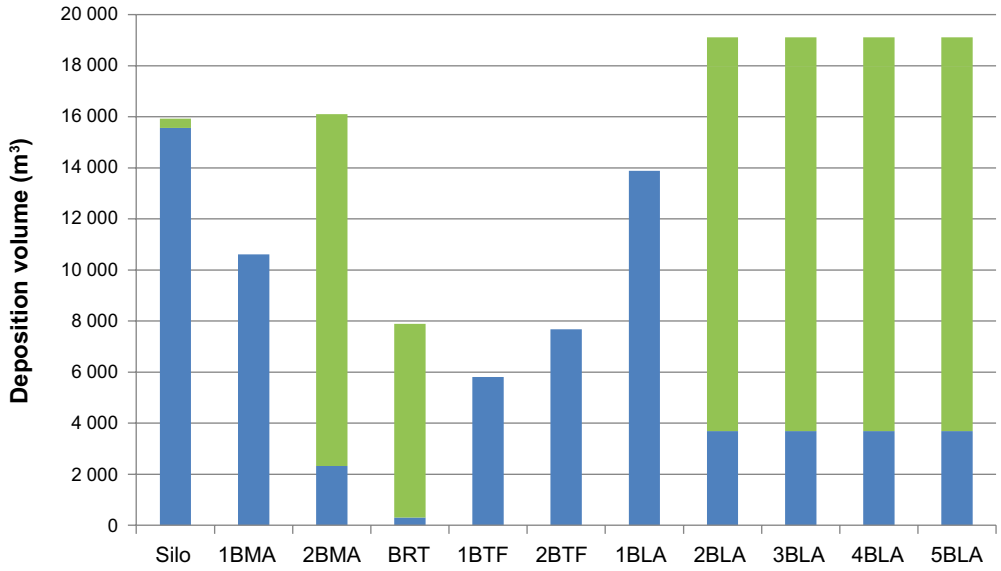

Figure 1-3. *Volume of waste allocated to different waste vaults in SFR (see Section 1.3 and Figure 1-6). Operational waste is shown in blue and decommissioning waste in green.*

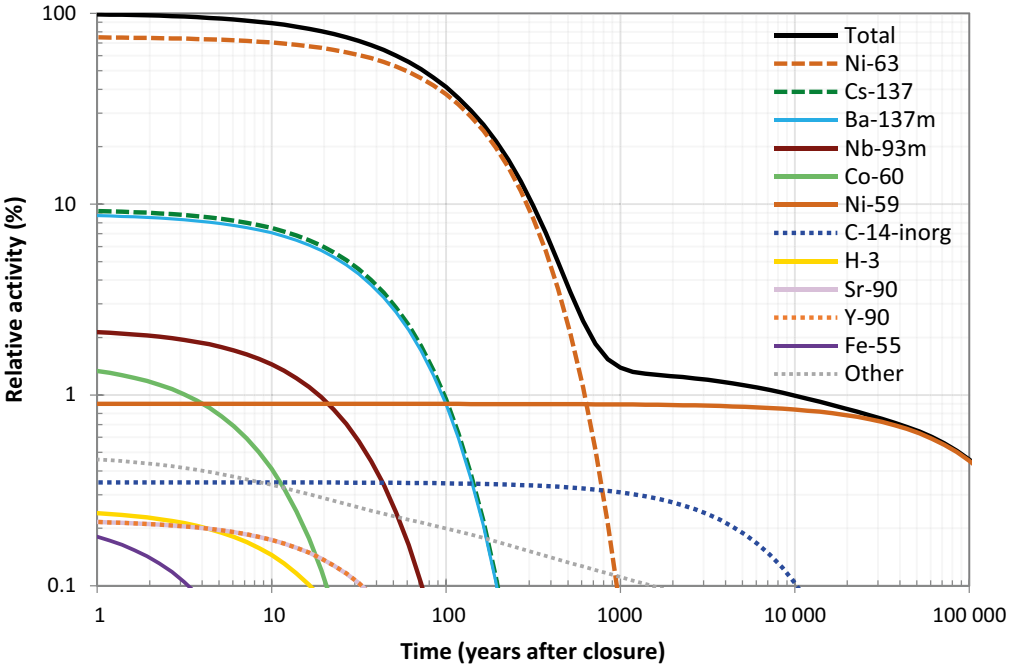

Figure 1-4. *Contributions from radionuclides to total activity (sum over all radionuclides) as a function of time after closure of the repository. Other (grey dotted line) includes contributions from all radionuclides not explicitly shown in the figure. Note that the C-14 activity shown relates only to inorganic C-14 (84 % of disposed C-14 is in this form). Due to different transport properties of carbon in organic form, inorganic form and irradiation-induced C-14, these are treated separately in the assessment. The relative activity of organic and irradiation-induced C-14 is less than 0.1 % of the total initial activity and thus included in the 'other' values.*

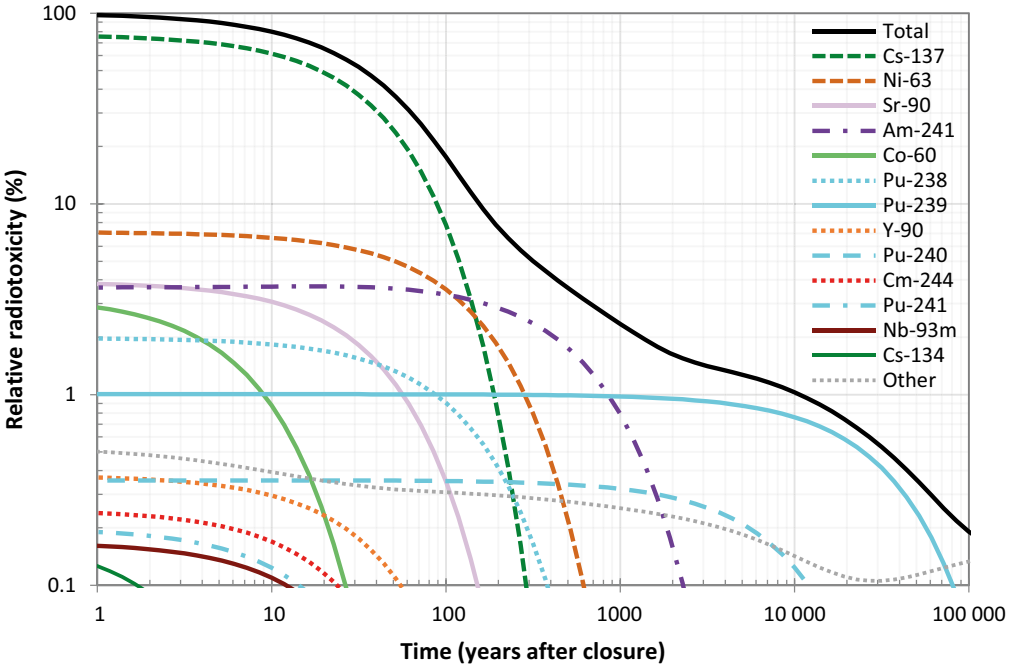

Figure 1-5. *Contributions from radionuclides to total ingestion radiotoxicity (sum over all radionuclides) as a function of time after closure of the repository. Other (grey dotted line) include contributions from all radionuclides not explicitly shown in the figure.*

1.3 SFR – layout

SFR is sited and designed with the aim to ensure that the disposal of the nuclear waste included in the SFR inventory is radiologically safe for humans and the environment.

The SFR waste vaults are located below the Baltic Sea and are connected to the ground surface via two access tunnels. SFR1 consists of one 70-metre-high waste vault (silo) and four 160-metre-long waste vaults (1BMA, 1–2BTF and 1BLA), see Figure 1-6. The waste vaults are covered by about 60 metres of bedrock.

SFR3 consists of six waste vaults, varying in length from 255 to 275 m: one waste vault for intermediate-level waste (2BMA), one waste vault for segmented reactor pressure vessels (1BRT) and four waste vaults for low-level waste (2–5BLA), see Figure 1-6. The waste vaults are covered by about 120 metres of bedrock.

The barrier design is adapted to the waste form and the characteristics and radiotoxicity of the radionuclides in the waste. The waste that constitutes the main part of the radiotoxicity is deposited in the silo and 1–2BMA that have the barrier systems with the highest protective capability. For waste that contributes with less relative radiotoxicity, the barriers are adapted accordingly with a simpler design.

1.4 Regulations relating to post-closure safety assessments

The criteria to be used to assess the post-closure safety of the repository are defined in regulations issued by SSM and they are based on various pertinent components of framework legislation, the most important being the Nuclear Activities Act (SFS 1984:3) and the Radiation Protection Act (SFS 2018:396). Guidance on radiation protection matters is provided by several international bodies and national legislation is often, as is the case of Sweden, influenced by international recommendations, such as the IAEA (International Atomic Energy Agency) safety standards.

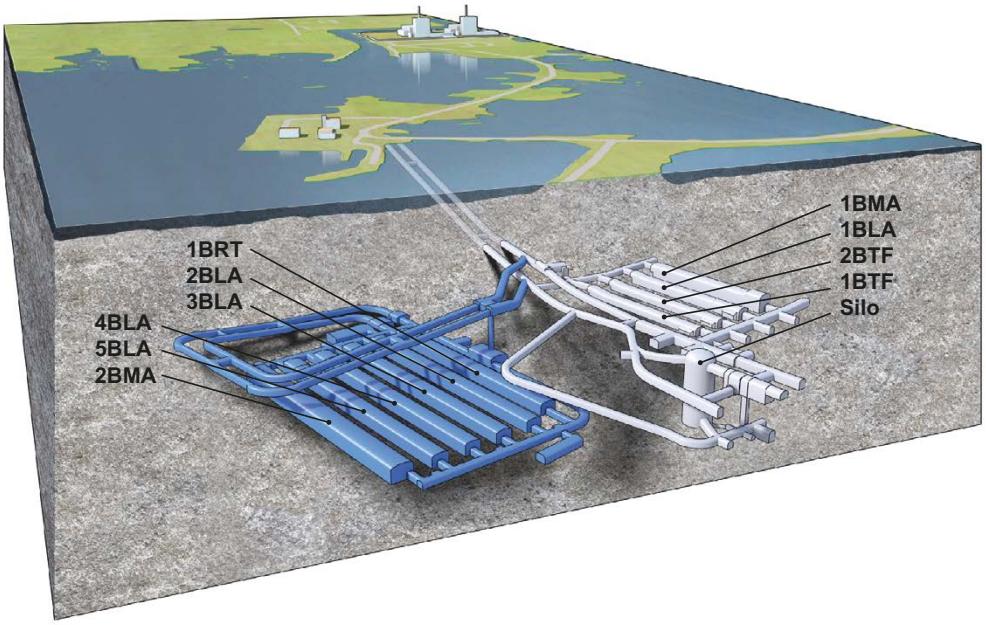

Figure 1-6. *Schematic illustration of SFR. The grey part is the existing repository (SFR1) and the blue part is the extension (SFR3). The waste vaults in the figure are the silo for intermediate-level waste, 1–2BMA vaults for intermediate-level waste, 1BRT vault for segmented reactor pressure vessels, 1–2BTF vaults for concrete tanks and 1–5BLA vaults for low-level waste.*

Regarding the post-closure safety of nuclear waste repositories, there are two more detailed regulations of particular importance, issued under the Nuclear Activities Act and the Radiation Protection Act respectively:

- "The Swedish Radiation Safety Authority's Regulations concerning safety in connection with the disposal of nuclear material and nuclear waste" (SSMFS 2008:21). The document also contains general advice on the application of the regulations.
- "The Swedish Radiation Safety Authority's Regulations concerning the protection of Human Health and the Environment in connection with the Final Management of Spent Nuclear Fuel and Nuclear Waste" (SSMFS 2008:37). The same document contains general advice on the application of the regulations.

In PSAR general part Chapter 3[7], all relevant regulatory criteria in relation to post-closure safety are described together with other regulatory requirements relating to the PSAR. Potential risks to human health and the environment due to chemotoxic materials in the repository are addressed in the environmental impact assessment (SKB 2014).

1.5 Post-closure safety assessment

1.5.1 Overview

Demonstrating that SFR is radiologically safe for humans and the environment after closure is done by evaluating compliance with respect to SSM's regulations concerning post-closure safety and the protection of human health and the environment. Furthermore, the post-closure safety assessment is being successively developed in the stepwise licensing process for the extended SFR and thus the results from the PSAR assessment[8] provide input to the forthcoming updated assessment to be carried out before trial operation of the facility.

The basis for evaluating compliance is a safety assessment methodology that conforms to the regulatory requirements regarding methodology, and that supports the demonstration of regulatory compliance regarding post-closure safety and the protection of human health and the environment. The overall ten step safety assessment methodology applied has been developed and refined throughout the latest post-closure safety assessments performed by SKB for SFR as well as for the spent nuclear fuel repository.

1.5.2 Main developments since the SR-PSU

The PSAR post-closure safety assessment is an update and development of the safety assessment SR-PSU that was part of the licence application to extend and continue the operation of SFR submitted in 2014. The updates and developments relate to several aspects. The amendments that were submitted to SSM during SSM's license application review are incorporated into the PSAR assessment. SSM's findings in their license application review, included in the authority's statement to the government, are also considered. Since the SR-PSU assessment, SKB's RD&D programme has continued with efforts that are related to the safety assessment (SKB TR-19-24, SKB TR-22-11). These developments are, for instance, related to the radionuclide inventory, initial state of the concrete barriers and refinements of the safety assessment and underlying data. In the work with the update of the reporting in the PSAR assessment, the ambition has been to improve the implementation and description of the methodology and to clarify the arguments presented to facilitate regulatory review.

These amendments are accounted for in the PSAR and examples include the modifications of 1BRT, exclusion of a planned third access tunnel as a consequence of the decision to segment the reactor pressure vessels, and the development of the design of 2BMA with increased thickness of the outer concrete walls and lids of the caissons and inner walls instead of grouting around the waste packages.

[7] PSAR SFR – Allmän del kapitel 3 – Krav och konstruktionsförutsättningar. SKBdoc 1702855, ver 3.0, Svensk Kärnbränslehantering AB. (In Swedish). (Internal document.)

[8] For brevity, the PSAR post-closure safety assessment for SFR is also referred to as "the PSAR assessment" or "the PSAR" in the present report.

A gas venting system was added to 2BMA. The update of the reference inventory with new information on materials and activities is an additional important development in the PSAR from SR-PSU. Smoke detectors that were part of the SR-PSU inventory have now been reallocated to SFL, lowering the radiotoxicity of the waste significantly. The layout of the tunnels and vaults in the extension of SFR has been updated and refined. New information gained from RD&D ensures an adequate initial state for the concrete caissons of 2BMA and the repair measures for 1BMA. New information used to refine the assessment relates to, for example, sorption on cementitious materials of very long-lived radionuclides of importance for post-closure safety, sorption reduction due to various complexing agents, future shoreline displacement and data on metal corrosion. New data have also been gathered for the surface ecosystems on chlorine content in terrestrial vegetation and organic soils, for example.

The description of the safety assessment methodology is improved. This includes a more thorough description of the management of uncertainties, an update of the set of safety functions (defined as a role by means of which a repository component contributes to safety) along with improved descriptions of the initial state FEPs (features, events and processes) and their coupling to safety functions and the selection of less probable scenarios. The set of scenarios and calculation cases is updated to include updated information on external conditions and internal processes; and supporting calculation cases are identified to support the selection of a base case and increase confidence in the results of the main scenario. The management of uncertainties is also improved by probabilistic handling of data uncertainties in, for example, the estimation of the inventory, estimation of concentrations of complexing agents, calculation of corrosion in 1BRT and groundwater flow in the radionuclide transport calculations. The calculation of exposure of non-human biota is updated to include developments in the method applied to derive dose rates and updates in the underlying data.

Part of the development work for SFR is carried out in relation to the operation of SFR1. This includes the investigations of the 1BMA repair measures or updates of the inventory or WAC. In general, the safety assessment is based on the layout, design and data that were available at the point in time when the assessment was carried out, i.e. a data freeze is applied. The present post-closure safety assessment that is part of PSAR thus constitutes a base line for subsequent developments carried out in relation to the operation of the existing SFR. In the results and reporting of such work, the differences from the present post-closure safety assessment will be discussed. For instance, this can apply to potential future changes of the details of the inventory. When the developments are finalised, the results will be incorporated in the work with the subsequent safety assessment that is to be reported as part of the renewed SAR (FSAR).

1.5.3 Report hierarchy

The construction license application for the extension of SFR consists of an application document and a set of supporting documents. A central supporting document is the general part of the preliminary safety analysis report, that consists of ten chapters.[9] Chapter 9 of that report addresses post-closure safety, for which the present report constitutes the main basis.

The present report, the **Post-closure safety report**, is supported by eleven main references for the post-closure safety assessment. These are listed in Table 1-1 with a brief description of their content and the abbreviated titles (in bold) by which they are identified in the text. Furthermore, there are numerous additional references that include documents compiled either by SKB or other organisations, or that are available in the scientific literature, as indicated in Figure 1-7.

[9] PSAR SFR – Allmän del kapitel 1 – Introduktion. SKBdoc 1702853, ver 3.0, Svensk Kärnbränslehantering AB. (In Swedish.) (Internal document.)

Table 1-1. Post-closure safety report and main references for the post-closure safety assessment. The reports are available at www.skb.se

Abbreviated title by which the reports are identified in this report and in the main references Report number	Content
Post-closure safety report SKB TR-23-01 (this report)	The main report of the PSAR post-closure safety assessment for SFR.
Initial state report SKB TR-23-02	Description of the expected conditions (state) of the repository at closure. The initial state is based on verified and documented properties of the repository and an assessment of its evolution during the period up to closure.
Waste process report SKB TR-23-03	Description of the current scientific understanding of the processes in the waste form and in the packaging that have been identified in the FEP processing as potentially relevant for the post-closure safety of the repository. Reasons are given as to why each process is handled in a particular way in the safety assessment.
Barrier process report SKB TR-23-04	Description of the current scientific understanding of the processes in the engineered barriers that have been identified in the FEP processing as potentially relevant for the post-closure safety of the repository. Reasons are given as to why each process is handled in a particular way in the safety assessment.
Geosphere process report SKB TR-14-05	Description of the current scientific understanding of the processes in the geosphere that have been identified in the FEP processing as potentially relevant for the post-closure safety of the repository. Reasons are given as to why each process is handled in a particular way in the safety assessment.
Climate report SKB TR-23-05	Description of the current scientific understanding of climate and climate-related issues that have been identified in the FEP processing as potentially relevant for the post-closure safety of the repository. Description of the current scientific understanding of the future evolution of climate and climate-related issues.
Biosphere synthesis report SKB TR-23-06	Description of the present-day conditions of the surface systems at Forsmark, and natural and anthropogenic processes driving the future development of those systems. Description of the modelling performed for landscape development, radionuclide transport in the biosphere and potential exposure of humans and non-human biota.
FEP report SKB TR-14-07	Description of the establishment of a catalogue of features, events and processes (FEPs) that are potentially relevant for the post-closure safety of the repository.
FHA report SKB TR-23-08	Description of the handling of inadvertent future human actions (FHA) that are defined as actions potentially resulting in changes to the barrier system, affecting, directly or indirectly, the rate of release of radionuclides, and/or contributing to radioactive waste being brought to the surface. Description of radiological consequences of FHAs that are analysed separately from the main scenario.
Radionuclide transport report SKB TR-23-09	Description of the radionuclide transport and dose calculations carried out for the purpose of demonstrating compliance with the radiological risk criterion.
Data report SKB TR-23-10	Description of how essential data for the post-closure safety assessment are selected, justified and qualified through traceable standardised procedures.
Model tools report SKB TR-23-11	Description of the model tool codes used in the safety assessment.

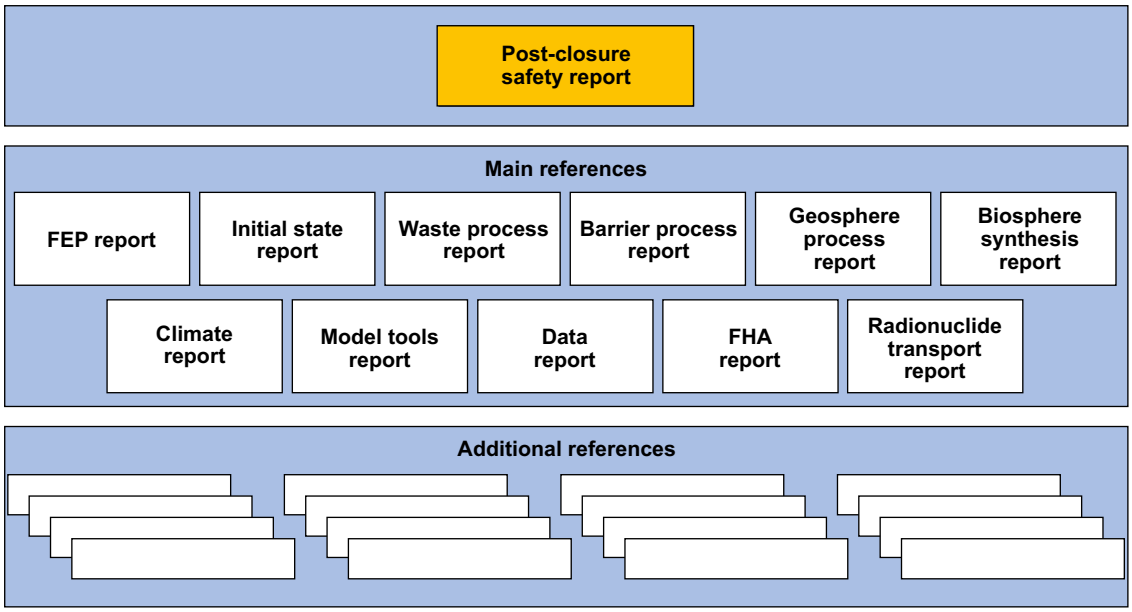

Figure 1-7. *The hierarchy of the* ***Post-closure safety report****, main references and additional references in the post-closure safety assessment.*

1.6 This report

1.6.1 Structure of this report

The present **Post-closure safety report** comprises a description of the assessment and includes conclusions of importance and arguments for compliance with applicable requirements. It consists of eleven chapters and eight appendices. The following is a brief description of the contents.

Chapter 1 – Introduction. This chapter describes the background to and the role of the post-closure safety assessment. In addition, it provides an overview of the radioactive waste, the SFR repository and its functioning, relevant regulations and the post-closure safety assessment.

Chapter 2 – Methodology. This chapter provides an overall description of the ten-step methodology used in the safety assessment. This includes the prerequisites for the safety assessment methodology and its implementation. The management of uncertainties is described at a general level and the documentation and quality assurance are described.

Chapter 3 – FEPs. This chapter describes the analysis of FEPs potentially influencing the post-closure safety of SFR. The FEP analysis includes identification of all factors that may influence post-closure safety of the repository, deciding whether each FEP identified needs to be included in the analysis or not and documentation of each included FEP.

Chapter 4 – Initial state. This chapter describes the expected state of the repository and its environs at closure, including uncertainties in the state that may affect the protective capability of the repository. The description of this *initial state* is based on the prerequisites of the present assessment, including the reference waste inventory, repository reference design and the site descriptive model. The chapter also includes descriptions of the barrier's contributions to post-closure safety.

Chapter 5 – Safety functions. This chapter describes the method for identifying safety functions and describes the identified safety functions and safety function indicators.

Chapter 6 – Reference evolution. This chapter describes the probable post-closure evolution of the repository and its environs, including uncertainties in the evolution that may affect the protective capability of the repository. This *reference evolution* starts from the initial state (Chapter 4) and then follows reference external conditions for the next 100 000 years, accounting for FEPs that are likely to influence the evolution (Chapter 3). First, the evolution is described for the initial period after

closure when the area above SFR is submerged beneath the Baltic Sea, then the evolution during the remaining time of the safety assessment, i.e. from the end of the initial, submerged period to 100 000 years after closure.

Chapter 7 – Main scenario. The post-closure safety assessment is based on a set of scenarios that together illustrate the most important courses of development of the repository and its environs. This chapter describes the main scenario, which takes into account the most probable changes within the repository and its environs, accounting also for identified uncertainties. The evolution described is based on the initial state (Chapter 4), the reference external conditions and the reference evolution (Chapter 6). The main scenario includes three calculation cases to analyse the three considered variants of external conditions, and a set of supporting calculation cases to provide a sensitivity analysis of specific uncertainties in external conditions and internal processes important for radionuclide transport through the repository system. The chapter also includes a description of the radionuclide transport and dose calculation methodology and a presentation and discussion of the results.

Chapter 8 – Less probable scenarios. Less probable scenarios evaluate scenario uncertainties related to alternative evolutions of the repository, or variations in the specified initial state or external conditions that are not evaluated within the framework of the main scenario. This chapter first presents the selection of less probable scenarios based on a systematic assessment of scenario uncertainties related to each safety function (Chapter 5). Then the scenarios are described, including an assessment of the probability of the occurrence of the scenario, and analysed.

Chapter 9 – Residual scenarios. Primarily, residual scenarios aim to illustrate the significance of individual barriers and barrier functions and how they contribute to the protective capability of the repository. The residual scenarios comprise sequences of events and conditions that are selected and studied independently of the probabilities of the occurrences of the scenarios. The results for the residual scenarios are used as a basis for discussing the robustness of the repository system regarding the protection of human health and the environment. This chapter presents the selection of the residual scenarios which are then described and analysed.

Chapter 10 – Annual risk and protection of the environment. This chapter presents the assessment of the results from the analysis of the scenarios in Chapters 7 and 8 with respect to the radiological safety for humans and the environment. The methodology for estimating the annual radiological risk to humans is presented, together with the results for the main scenario, the less probable scenarios and the sum of the risk from these scenarios. Furthermore, the evaluation of the protection of the environment is presented. Alternative safety indicators as well as risk dilution are also addressed in the chapter.

Chapter 11 – Conclusions. This chapter presents the demonstration of compliance with respect to the protection of human health and the environment as well as the robustness of the barrier system. The aspects of the assessment that strengthen confidence in the compliance statement are discussed. Furthermore, the development of the safety assessment and feedback to subsequent steps of the repository programme are described.

Appendix A – Terms and abbreviations. This appendix comprises terms, acronyms and abbreviations used in the report.

Appendix B – Handling of requirements from SSMFS 2008:21. This appendix describes how the regulations in SSMFS 2008:21, “The Swedish Radiation Safety Authority’s regulations and general advice concerning safety in connection with the disposal of nuclear material and nuclear waste” have been complied with in the assessment.

Appendix C – Handling of requirements from SSMFS 2008:37. This appendix describes how the regulations in SSMFS 2008:37, “The Swedish Radiation Safety Authority’s regulations and general advice concerning the protection of human health and the environment in connection with the disposal of spent nuclear fuel and nuclear waste” have been complied with in the assessment.

Appendix D – FEPs in the SFR FEP catalogue.

Appendix E – Radionuclide and materials inventory.

Appendix F – Approach to estimate dose from barrier failure in the silo following an earthquake.

Appendix G – Map of the Forsmark area.

Appendix H – Post-closure safety assessment flowchart. This appendix provides an overview of the various assessment activities used in the evaluation of repository evolution and radionuclide transport, as well as the connection between them in the form of data flow.

1.6.2 Contributing experts

Project leader for the PSAR safety assessment has been Jenny Brandefelt. A large number of people from various fields of expertise have been involved in documenting the post-closure safety assessment. Contributing experts are listed in each of the main references (see Table 1–1).

Main authors for this report, SKB employees unless otherwise noted, have been Georg Lindgren, Johan Liakka, Maria Lindgren (Kemakta Konsult AB), Niko Marsic, Per-Gustav Åstrand and Thomas Hjerpe (Kemakta Konsult AB). In addition, the following experts, in alphabetical order, have significantly contributed to this report: Katrin Ahlford, Patrick Bruines, Per-Anders Ekström (Kvot AB), Svante Hedström, Olle Hjerne, Birgitta Kalinowski, Klas Källström, Diego Mas Ivars, Teresita Morales, Per Mårtensson, Karin Pers, Maria Rasmusson, Jan Rosdahl, Peter Saetre, Patrik Sellin, Frederic Wagner and Ola Wessely.

This report has been significantly improved at different stages by adjustments in accordance with comments provided by informal and factual reviewers. Many of the experts listed above have also contributed as informal reviewers. Further informal reviewers have been; Abel Sánchez Juncal, Fredrik Vahlund, Jens-Ove Näslund, Jesper Petersson, Johan Öhman (GeoSigma), Johannes Johansson, Kent Werner, Lino Nilsson, Magnus Odén, Olli Nummi (Fortum), Peter Hultgren, Rikard Svenman, Robert Earon, Russell Alexander (Bedrock geosciences). Factual reviewers have been; Allan Hedin, Mike Thorne (Mike Thorne and Associates Ltd.) and Jordi Bruno (Amphos 21 Consulting).

2 Methodology

2.1 Introduction

This chapter presents the methodology used in this post-closure safety assessment. The methodology was developed in SR-PSU (SKB TR-14-01) based on SKB's previous safety assessment for SFR1 (SAR-08, SKB R-08-130). Further, it is consistent with the methodology used for the post-closure safety assessment for the final repository for spent nuclear fuel to the extent appropriate, given the differences of the two repositories. The methodology used in PSAR is essentially the same as in SR-PSU with some refinements based on the experience from SR-PSU and regulatory review comments. The *description* of the methodology has, however, been revised in response to review comments, for instance regarding the descriptions of the management of uncertainties.

The core of this chapter is the description of the methodology in ten steps (Section 2.6). Sections 2.2 to 2.5 present some background information and prerequisites for the methodology and its implementation. These include descriptions of post-closure safety principles for the extended SFR and regulatory requirements regarding the methodology. Necessary prerequisites include system boundaries and timescales for the assessment, the reference inventory, the reference design and status of SFR1, as well as the site descriptive model. Moreover, important inputs are results from previous assessments and RD&D related to SFR. An account of how uncertainties are managed in the context of the methodology and its implementation is also given. The present safety assessment is carried out in the context of the stepwise licensing process and the handling of feedback to subsequent steps in the SFR repository programme is described in Section 2.7. In the last section of this chapter, 2.8, a description of documentation and quality assurance within the safety assessment work is given.

2.2 Post-closure safety and safety principles

The overall aim in developing a geological repository for nuclear waste is to ensure that the amounts of radionuclides reaching the accessible biosphere are such that possible radiological consequences are acceptably low at all times. SSM has in its post-closure safety regulations (SSMFS 2008:21 and 2008:37) stipulated what level of safety and protection of human health and the environment from harmful effects of ionising radiation[10] (*protective capability*) shall be achieved and detailed the means by which this shall be realised. Furthermore, there are requirements on the approach to assessment of safety and reporting. Important aspects of the regulations are that safety after closure shall be maintained through a system of passive barriers. Moreover, the function of each barrier shall be to, in one or several ways, contribute to the containment and prevention or retention of dispersion of radioactive substances, either directly or indirectly, by protecting other barriers in the barrier system. These aspects underly the post-closure safety principles set out below.

[10] In this context, *harmful effects* comprise cancer (fatal and non-fatal) as well as hereditary effects in humans caused by ionising radiation, in accordance with ICRP (1991, paragraphs 47–51).

Post-closure safety principles

The post-closure safety for SFR is based on two safety principles:[11]

- *Limitation of the activity of long-lived*[12] *radionuclides* is a prerequisite for the post-closure safety of the repository. The WAC (Section 4.3) and the waste type descriptions ensure that the waste disposed conforms to applicable requirements including those that relate to post-closure safety.
- *Retention of radionuclides* is achieved by the functions of the engineered and natural barriers. The properties of the waste, together with the properties of the waste packaging and of the engineered barriers in the waste vaults, contribute to safety by ensuring low water flow and a suitable geochemical environment to reduce the mobility of the radionuclides. The bedrock surrounding the repository provides stable geochemical and physical conditions and favourable low groundwater flow conditions.

Thus, while *retention of radionuclides* relates mainly to the siting and design of the repository, *limitation of the activity of long-lived radionuclides* relates to the waste. The two safety principles are interlinked and applied in parallel. The engineered barrier system is designed for an inventory that contains a limited amount of long-lived radionuclides, given the conditions at the selected site and the natural barriers.

The relative importance of the safety principles is determined by the characteristics of different radionuclides and the evolution of the barrier system and its functions during the assessment period. The design and siting of the repository provide a higher degree of retention at early times than for later times when groundwater flow increases due to the transition from submerged to terrestrial conditions and engineered barriers degradation. Especially for mobile radionuclides that contribute to doses to humans, the limitation of radionuclide activity concentration is of importance. Specifically, disposal of very long-lived radionuclides with weak or no sorption needs to be limited with respect to the inventory to be able to meet regulatory criteria related to the protection of human health and the environment.

2.3 Regulatory requirements regarding methodology

The format and scope of this post-closure safety assessment and, specifically, the criteria to be used to assess the safety of the repository are defined in regulations from SSM as described in Section 1.4.

The main regulations are SSMFS 2008:21 concerning *safety in connection with the disposal of nuclear material and nuclear waste* and SSMFS 2008:37 concerning *the protection of human health and the environment in connection with the disposal of spent nuclear fuel and nuclear waste*. Selected parts of these documents are reproduced in Appendices B and C. The appendices also indicate how the requirements in the regulations are handled in the post-closure safety assessment by reference to relevant sections or through a description directly in the appendices.

One part of these regulations that influences the scope of the post-closure assessment is Section 9 of SSMFS 2008:21 that states that the safety analysis shall comprise FEPs that can lead to dispersion of radioactive substances after closure (see Section 2.6.1). Further, as noted in Section 2.4.2, the timescale for the assessment is coupled to requirements in both SSMFS 2008:21, Section 10 and 2008:37, Sections 10–12. Appendix 1 in SSMFS 2008:21 is referred to in Section 9 in the same regulation and explicitly states requirements regarding reporting of analysis methods and post-closure conditions:

[11] It can be noted that the term safety principle is not uniquely defined. Here the term is used in the same way as in F-PSAR, i.e., to denote a basic idea underlying the repository concept. The term has, however, also been used in the post-closure safety assessment for the final repository for spent nuclear fuel to denote a starting point underlying the development of the KBS-3 concept including, for instance, the decision to use natural materials that show long-term stability in the repository environment. The term safety principle is also used in IAEA's Safety Fundamental SF-1 (IAEA 2006) to denote the ten safety principles that are associated with the fundamental safety objective to protect people and the environment from harmful effects of ionising radiation.

[12] In the safety assessment context, radionuclides with a half-life greater than 31 years (Section 1.2.1).

The following shall be reported with regard to analysis methods:

- *How one or several methods have been used to describe the passive system of barriers in the repository, its performance and evolution over time; the method or methods shall contribute to providing a clear understanding of the features, events and processes that can affect the performance of the barriers and the links between these features, events and processes.*
- *How one or several methods have been used to identify and describe relevant scenarios for sequences of events and conditions that can affect the future evolution of the repository; the scenarios shall include a main scenario that takes into account the most probable changes in the repository and its environment.*
- *The applicability of models, parameter values and other assumptions used for the description and quantification of repository performance as far as reasonably achievable.*
- *How uncertainties in the description of the barrier system's functions, scenarios, calculation models and calculation parameters as well as variations in barrier properties have been dealt with in the safety analysis, including the reporting of a sensitivity analysis showing how the uncertainties affect the description of the evolution of barrier performance and the analysis of the impact on human health and the environment.*

The following shall be reported with respect to the analysis of post-closure conditions:

- *The safety analysis in accordance with Section 9 comprising descriptions of the evolution in the biosphere, geosphere and repository for selected scenarios; the environmental impact of the repository for selected scenarios, including the main scenario, thereby considering defects in engineered barriers and other identified uncertainties.*

The regulations also include detailed requirements that relate to the scope of the safety assessment. Specifically, SSMFS 2008:37 states in what way the collective dose shall be reported (Section 4), how the probability of harmful effects shall be calculated that underlie the compliance with the risk criterion (Section 5), how biological effects of ionising radiation in the habitats and ecosystems concerned shall be described (Section 7) and that consequences of intrusion into a repository shall be reported for different time periods (Section 9).

The management of uncertainties is an important aspect of a safety assessment, and the regulations state several requirements. How these are addressed in this assessment is described on a general level in Section 2.5 and more in detail in Section 2.6. According to the general advice to SSMFS 2008:37, the reporting should include an account of how quality assurance has been used in the work with the repository and associated risk analyses and this is described in Section 2.8.

2.4 Assessment prerequisites

In addition to the safety principles and regulatory requirements described in the previous sections, other necessary prerequisites for the post-closure safety assessment are described in this section.

2.4.1 System boundaries

The spatial boundaries for the assessment are established by the definition of the *repository system*, consisting of the repository and its environs. The repository consists of the disposed waste forms, waste packaging, engineered barriers and other repository structures. The repository environs consist of the bedrock surrounding the repository (geosphere) and the surface systems (biosphere) above the repository that can be affected by radionuclide releases from the repository.

In general, a strict boundary definition is neither necessary nor possible and the same boundaries are not necessarily relevant to all parts of the safety assessment. Roughly the portions of the surface systems and bedrock considered in the site descriptive model (SDM, SKB TR-11-04) are regarded as part of the repository system. The analysis of the surface systems extends downward to the surface of the bedrock and the analysis of the bedrock extends down to a depth of about 1 000 m. Depending on the analysis context, these definitions may be somewhat modified.

Future human actions (FHAs) on a local scale are internal to the system, but not issues related to the characteristics and behaviour of future society at large.

Local effects of climate are internal, but not the climate system on a larger scale. These definitions relating to system boundaries are used as a basis for the FEP handling to be able to distinguish between FEPs belonging to the repository system and external FEPs acting from outside the system (**FEP report,** Section 2.1.1). These definitions are also used here to delineate the repository system description.

2.4.2 Timescale for the assessment

The timescale for the assessment is established based on regulatory requirements which requires knowledge on timescales relevant to the evolution of the repository and its environs.

Regulatory requirements regarding timescale for the assessment

The requirements on the assessment period are described in SSMFS 2008:21 and SSMFS 2008:37. *A safety analysis shall comprise the requisite duration of barrier functions, though a minimum of ten thousand years* (SSMFS 2008:21, Section 10). *For the first 1 000 years following repository closure, the assessment of the repository's protective capability shall be based on quantitative analyses of the impact on human health and the environment* (SSMFS 2008:37, Section 11). *For the period after the first thousand years following repository closure, the assessment of the repository's protective capability shall be based on various possible sequences for the development of the repository's properties, its environment and the biosphere* (SSMFS 2008:37, Section 12). Both regulations give recommendations in the form of general advice. For instance, it is recommended that the assessment should extend at least to the time until the expected maximum consequences regarding risk and environmental impact have occurred, but no longer than 100 000 years. In the present assessment, the safety of the repository is evaluated over a period of 100 000 years.

Time periods relevant for evolution of conditions in the repository environs

During the assessment period, the external conditions will change. The position of the shoreline will change due to a combination of eustatic changes, i.e. changes in sea level and isostatic changes in the form of vertical movement of the Earth's crust which, at Forsmark, is dominated by post-glacial rebound. The shoreline position will affect the flow and chemistry of groundwater around the repository and the potential for inadvertent intrusion. Hence, for the evolution of the repository, the following time periods related to the shoreline position are relevant:

- The initial period, of 1 000 years or more, when the area above the repository is submerged beneath the sea. During this period a low hydraulic gradient, and hence low groundwater flow, in the bedrock and a limited potential for inadvertent intrusion is expected.
- The period when the repository and its environs is affected by the movement in the position of the shoreline.
- The period when the repository is located so far inland of the shoreline that steady-state conditions prevail at repository depth.

In addition, the climate will change during the assessment period. For the evolution of the repository, the following time periods related to climate are relevant (see further Section 2.6.3 for handling of climate and climate-related issues):

- Periods when temperate climate conditions prevail. During these periods, the area above the repository may be submerged under the sea, as today, or alternatively, terrestrial.
- Periods when periglacial climate conditions prevail with presence of permafrost at the surface and within the bedrock. During these periods, the area above the repository is terrestrial.
- A period of glacial climate conditions followed by a post-glacial period. During the post-glacial period the area above the repository is first submerged and subsequently terrestrial.

In summary, the various processes and events occurring during the periods outlined above provide a well-defined basis for the description of the thermal, hydrological, mechanical and geochemical evolution of the repository system over the time periods considered in the safety assessment.

Timescales relevant for the radionuclide inventory

As noted in Section 1.2.2, as a result of radioactive decay, less than 2.5 % of the radiotoxicity in the waste disposed in SFR remains 1 000 years after closure. After 100 000 years, less than 0.2 % of the radiotoxicity remains. The radionuclide content disposed in SFR can be divided into short-lived and long-lived (Section 1.2.1). Only a limited amount of long-lived radionuclides is accepted in the wastes already disposed or to be disposed in SFR, which is reflected in the WAC and waste type descriptions. These radionuclides may contribute to the radiological risk at longer times. For the discussions in this report, a categorisation of radionuclides, based on their half-lives, is used:

- Short-lived radionuclides with a half-life of less than 10 years. These radionuclides are generally not included in the radionuclide transport calculations, as they will decay during the operational and resaturation period. To show compliance to the risk criterion, the radiological consequence of these very short-lived (from the perspective of geological disposal) radionuclides must, however, be considered. For radionuclides with a half-life less than 10 years Co-60 dominates the radiotoxicity in the initial inventory (Section 1.2.2). Therefore Co-60 is included in the radionuclide transport calculations for illustrative purposes.
- Short-lived radionuclides with a half-life longer than 10 years but less than 31 years are included in the radionuclide transport calculations. These radionuclides will decay to insignificant levels within a relatively short time. About 10 half-lives of these short-lived radionuclides coincides with the 300 year period for which institutional control, in an international context (e.g. IAEA 2009), is foreseen to contribute to safety. Examples of radionuclides belonging to this category are Sr-90 and Cs-137.
- Long-lived radionuclides with a half-life short enough to decay substantially during time periods assessed. Times of relevance are, for instance, that when the shoreline passes over the repository, the period up until a well for drinking water may be drilled in the vicinity of the repository, the period until the concrete barriers totally degrade and lose their function and the period until the point permafrost reaches repository depth. Examples of radionuclides belonging to this category are Ni-63, Am-241, C-14 and Mo-93.
- Long-lived radionuclides with half-lives so long that they will not decay substantially during the 100 000-year period of the assessment. Examples of such radionuclides are Ni-59, Ca-41, I-129 and U-238.

2.4.3 Input for determining conditions at repository closure

The expected conditions (state) of the repository and its environs at closure of the repository are established based on the assumed repository closure in 2075 AD and prerequisites regarding the disposed waste, repository design and repository site. These are needed as input to the description of the initial state that constitutes the point of departure for the assessment of the protective capability of the repository. Necessary information is the reference waste inventory (SKB R-18-07), the reference design (**Initial state report**), the status of SFR1, and information from the site investigations conducted on the site for SFR and documented in the site descriptive model (SDM; SKB TR-11-04), and the **Biosphere synthesis report**.

2.5 Management of uncertainties

The management of uncertainties is a fundamental aspect of any safety assessment. This is reflected in SSM's regulations in which requirements regarding the handling and reporting of uncertainties related to post-closure safety are stated. It shall be reported *how uncertainties in the description of the barrier system's functions, scenarios, calculation models and calculation parameters as well as variations in barrier properties have been dealt with in the safety analysis* (SSMFS 2008:21,

Section 10 and appendix 1). The appendix also states that in the reporting of the analysis of post-closure conditions, identified uncertainties shall be considered in relation to the descriptions of the evolution of the repository system for selected scenarios. It can be noted that the requirements in SSMFS 2008:21 also cover the more general requirement in SSMFS 2008:1 with Chapter 4, Section 1 stating that uncertainties in models, methods and data that are used for safety analyses shall be taken into account. According to SSMFS 2008:37, Section 10, *uncertainties in the assumptions made shall be described and taken into account when assessing the protective capability of the repository*. In the general advice to SSMFS 2008:21 and 2008:37, recommendations are given on which types of uncertainties should be considered and how they can be addressed in a safety assessment.

The safety assessment methodology in ten steps, which is described in Section 2.6, has been developed accounting for the stated requirements on management of uncertainties. Hence, the management of uncertainties is an integral part of the methodology. In Section 2.6, the handling of uncertainties in the steps of the safety analysis is described and some general aspects of uncertainties are discussed here. These include the classification of uncertainties used in PSAR, the relation between the approaches to management of uncertainties and the importance of the uncertainties for the results of the safety assessment, and temporal aspects of uncertainties.

There is no unique way in which to classify uncertainties in a safety assessment. Here the classification is adopted and described that is suggested in the general advice to SSMFS 2008:21. It captures relevant aspects that also relate to the recommendations described in the general advice to SSMFS 2008:37 as well as international practice in this type of analysis (e.g. NEA 2012, IAEA 2012). The following broad definitions are used:

- *Scenario uncertainty* refers to uncertainty with respect to external conditions and internal processes in terms of the type, degree and time sequence, resulting in an uncertainty in the future states of the repository system. It includes uncertainty in, for example, the evolution of the repository system and climatic and other long-term processes.
- *System uncertainty* concerns comprehensiveness issues, i.e. the question of whether all aspects important for the safety evaluation have been identified and whether the assessment is capturing the identified aspects in a qualitatively correct manner. In short, have all FEPs been identified and included in a satisfactory manner or has their exclusion been appropriately justified?
- *Modelling uncertainty* arises from a necessarily imperfect understanding of the nature of processes involved in repository evolution which leads to imperfect conceptual models. The mathematical representation of conceptual models involves some simplification, also contributing to modelling uncertainty. Imprecision in the numerical solution of mathematical models is another source of uncertainty that fall into this category.
- *Data uncertainty* concerns all quantitative input data, i.e. parameter values, used in the assessment. There are several aspects to consider in the management of data uncertainty. These include correlations between data, the distinction between uncertainty due to lack of knowledge (epistemic uncertainty) and due to natural variability (aleatoric uncertainty) and situations where modelling uncertainty is treated by broadening the range of input data. The input data required by a particular model is in part a consequence of the conceptualisation of the modelled process, meaning that modelling uncertainty and data uncertainty are to some extent intertwined.

Different aspects of the safety assessment have different impacts on the results that underpin the compliance discussion. Therefore, a part of the management of uncertainties is to identify the most important aspects to be able to focus on them. In general, potential measures are to avoid, reduce and assess uncertainties. The successive enhancement in the identification and evaluation of the importance of uncertainties is a part of the iterative process of safety assessments. In this case, this includes the experience from previous safety assessments for the present SFR (i.e. SAFE, Andersson et al. 1998 and SAR-08, SKB R-08-130) and the update of the safety assessment that was part of the license application for the extension of SFR (F-PSAR).

Temporal aspects are important for a post-closure safety assessment in general and the management of uncertainties in particular. This is, for instance, reflected in SSMFS 2008:37 where different requirements are placed on the assessment for the first thousand years and the time thereafter (see Section 2.4.2 for details). In general, the uncertainties increase with time due to the need

for projections of, for instance, external conditions. However, the effect of such uncertainties with respect to compliance with the risk criterion generally decreases with time due to the decrease of the radiotoxicity of the inventory.

The strategy for managing uncertainties in the present safety assessment includes several elements. One element, primarily addressing data uncertainties, is the implementation of a probabilistic approach to radionuclide transport and dose calculations using input data in the form of probability distributions (**Radionuclide transport report**, Section 2.5.4). System and scenario uncertainties are primarily managed by applying systematic approaches to FEP handling and scenario selection, respectively. Another element, addressing particularly modelling and data uncertainties, is to opt for *cautious* or *pessimistic* choices to ensure that calculation results, with a high degree of certainty, do not underestimate any potential radiological consequences. In the present safety assessment (and, in particular, in this present report, the **Radionuclide transport report** and the **Biosphere synthesis report**), these two terms are used as follows:

- *Cautious* indicates an expected overestimate of annual effective dose that follows from assumptions made, or models and parameter values selected, *within* the reasonably expected range of possibilities.
- *Pessimistic* indicates an expected overestimate of annual effective dose that follows from assumptions made, or models and parameter values selected, *beyond* the reasonably expected range of possibilities.

Calculations that serve as input to the radiological risk assessment are, when possible, based on cautious rather than pessimistic assumptions, models or parameter values. Deliberately pessimistic assumptions, models or parameter values may be used in e.g. calculations that are intended to illustrate and/or bound the effect of a certain process or hypothetical event, but that are not included in the radiological risk assessment. The choice of cautious or pessimistic approaches may also indicate availability of data, or lack thereof.

2.6 Methodology in ten steps

Prerequisites for the methodology and its implementation in the present post-closure safety assessment have been described in the sections above, e.g. system boundaries, timescales, reference inventory, reference design and the status of SFR1, and information from the site investigations conducted on the site for SFR. Given these inputs, the safety assessment is carried out in ten main steps. These steps are partly carried out concurrently and partly consecutively. A graphical illustration of the steps in the methodology is shown in Figure 2-1. The methodology, and the implementation in subsequent chapters, is described in the following subsections. Further details of the methodology are sometimes provided in connection with the implementation, as appropriate. This applies, e.g., to the methodology applied in the radionuclide transport calculations. Management of uncertainties is an integral part of the methodology and, in the following subsections, aspects of uncertainty that relate to the steps are described. It can also be noted that the work carried out in previous assessments is a basis for the current assessment and that some parts of the present assessment are only updated to a limited extent. A summary of main developments since the SR-PSU are summarised in Section 1.5.2.

2.6.1 Step 1: FEPs

A FEP is a feature, an event or a process that is potentially relevant for the post-closure safety and hence needs to be addressed in the assessment. The first step in the methodology is thus to obtain a comprehensive FEP catalogue in the sense that it covers all these factors. An extensive effort was undertaken in the previous safety assessment SR-PSU (**FEP report**) to establish the FEP catalogue for the assessment of post-closure safety of SFR, based on international and national databases as well as SKB's previous safety assessments. The FEP catalogue in the present safety assessment has been established by performing a validity check of the SFR FEP catalogue from SR-PSU, accounting for new knowledge, and a check against new international FEP lists (Section 3.3.2). This review did not lead to any change in the set of FEPs included in the catalogue. The SFR FEP catalogue for PSAR thus contains the same FEPs as the SR-PSU catalogue and covers all identified factors that may influence post-closure safety.

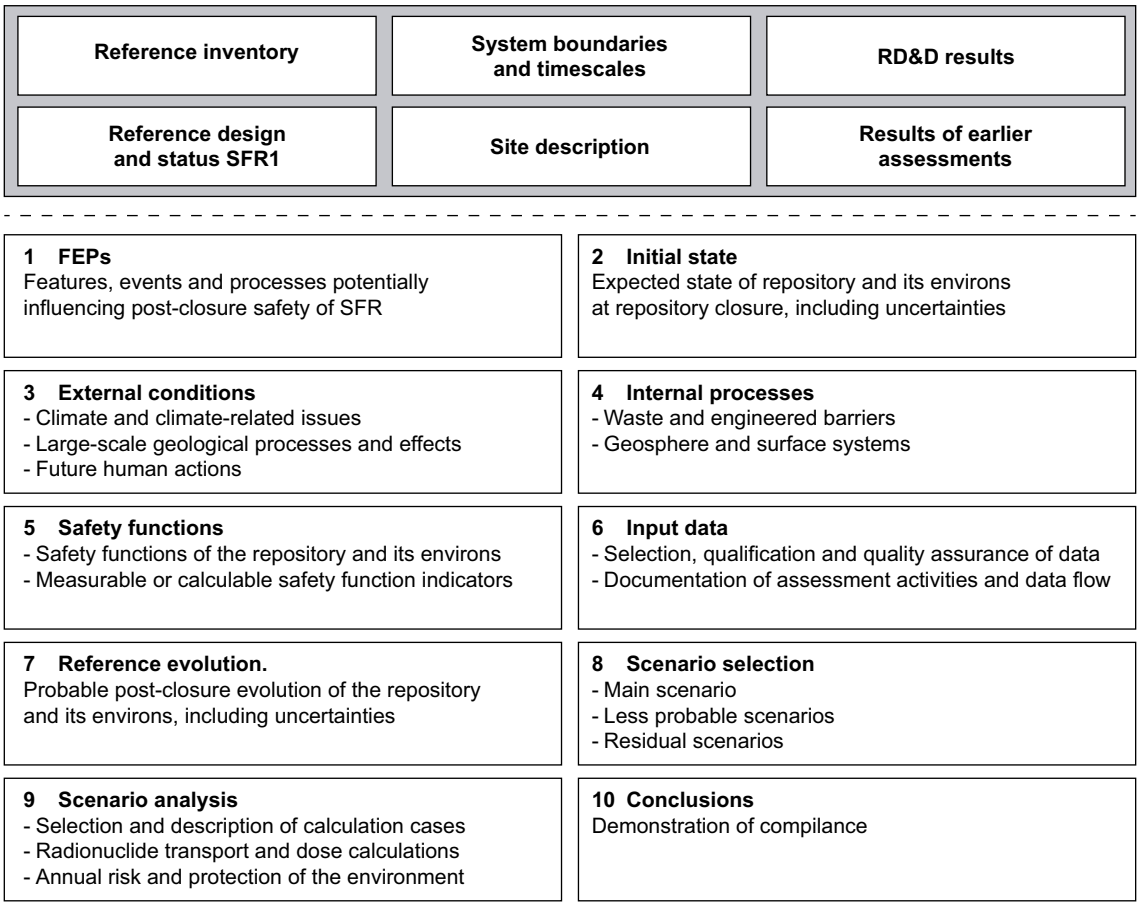

Figure 2-1. *An outline of the ten main steps of the present post-closure safety assessment. The boxes above the dashed line are prerequisites for the methodology and its implementation. The contents of each step are described in detail in Sections 2.6.1–2.6.10.*

The objective of the FEP analysis in the PSAR is two-fold; to make sure that all factors that may influence post-closure safety are identified and to document the handling of each FEP in the SFR FEP catalogue for PSAR. In this sense the FEP catalogue constitutes a "look-up-table" with a brief description of the handling of each FEP and references to relevant reports that detail the handling further.

The FEPs in the database are classified as i) initial state FEPs, ii) internal processes or iii) external FEPs (Chapter 3). The remaining FEPs are either related to the assessment methodology in general or have been found to be irrelevant to SFR. A detailed description of the handling of FEPs and the different tools that have been used to ensure a systematic and thorough treatment is given in Chapter 3 and in the **FEP report**. Furthermore, Appendix D provides tables of the complete set of FEPs included in the SFR FEP catalogue (PSAR version), including a reference to the corresponding description in various reports.

Management of uncertainties

The handling of FEPs is an important part of the management of system uncertainties. That is, this step ensures that all aspects important for post-closure safety have been identified and properly addressed in the safety assessment. This includes, for instance, handling of FEPs that relate to uncertainties in the repository evolution and to uncertainties due to defects in engineered barriers and the initial state of the repository.

2.6.2 Step 2: Description of initial state

The initial state is defined as the expected state of the repository and its environs at closure. The initial state is fundamental to the safety assessment and requires thorough substantiation. The initial state of SFR1 is based on verified and documented properties of the wastes and the repository and an assessment of how these will change up to the time of closure, whereas the initial state of SFR3 is mainly based on the reference design and present waste prognosis, see the **Initial state report**. The WAC and the waste type descriptions ensure that the waste disposed conforms to applicable requirements including those that relate to post-closure safety. The initial state of the repository environs is assumed to be similar to present-day conditions, as described in the site descriptive model, SDM-PSU, see SKB TR-11-04 and the **Biosphere synthesis report**. The SDM-PSU is based on the result of the site characterisation work performed during site investigations and includes data from the bedrock and the near-surface systems. The resaturation period for the repository occurs after the point in time when the initial state is defined but is sufficiently short to be neglected for most processes. A summary of the initial state of the repository and its environs is given in Chapter 4.

Management of uncertainties

Uncertainties in the initial state of the barriers are a central aspect of the safety assessment. The FEP processing performed in Step 1 resulted in identification of several relevant FEPs related to the initial state. In the **Initial state report** uncertainties relating to the different existing waste vaults are described. Some of the initial state FEPs relate to uncertainties such as potential deviations from the initial state, which require separate assessment (Section 3.2). Deviations from the expected initial state may occur for example through undetected mishaps leading to design deviations, incomplete closure of the repository, etc. The initial state FEPs are considered in the scenario selection described in Chapter 7 and 8. To limit uncertainties in the initial state, quality control measures are carried out before closure of the repository (**Initial state report**). Research and development in relation to the engineered barriers is carried out to ensure a robust initial state. For instance, tests have been carried out at Äspö Hard Rock Laboratory to evaluate material and production methods for the concrete caissons for 2BMA (Mårtensson and Vogt 2019, 2020) which can also form the basis for production methods for other concrete structures in SFR3. Furthermore, uncertainties in the inventory of radionuclides and other materials relevant to post-closure safety are also included in the description of the initial state. Regarding the description of bedrock and surface systems, management of uncertainties regarding the conceptualisation and parameterisation is an integral part of SDM-PSU and the **Biosphere synthesis report**. The confidence in the description and remaining uncertainties have been assessed and the remaining key uncertainties are discussed elsewhere (SKB TR-11-04, Section 9.8).

2.6.3 Step 3: Description of external conditions

Step 3 in the methodology concerns the description of external conditions. FEPs related to external conditions identified in step 1 are handled in the three categories climate and climate-related issues, large-scale geological processes and effects and FHAs. These external conditions and the handling of related FEPs are described in the **Climate report**, the **Geosphere process report** and the **FHA report**, respectively.

A key point in the handling of external conditions in SKB's post-closure safety assessments is the establishment of reference external conditions for the subsequent analysis. These serve as a basis for the analysis of the reference evolution (defined in step 7, Section 2.6.7), which in turn supports definition of the main scenario (step 8, Section 2.6.8). As the evolution of external conditions over the next 100 000 years is associated with considerable uncertainty, for example with regard to future anthropogenic greenhouse-gas emissions and sea level rise, it is not possible to assign a single development as probable. Therefore, the reference external conditions are represented by several developments that span the range of the probable evolution of external conditions at Forsmark.

In addition to the reference external conditions, less probable future evolutions of external conditions are identified and included in the analysis of scenario uncertainty (Section 2.6.8). Finally, highly unlikely developments of external conditions that would have a more severe influence on individual barriers and barrier functions are identified in support of the analysis of residual scenarios (Section 2.6.8).

Most long-term processes that are relevant to post-closure safety that occur in the surface systems and bedrock are affected by climate change and climate-related changes. Thus, a central part of the description of external conditions is the formulation of a well-founded future evolution of the climate and climate-related processes as described in the following subsection.

The large-scale geological processes that are included in the FEP handling are mechanical evolution of the Baltic Shield and earthquakes. These processes are in common with the final repository for spent nuclear fuel since the latter is planned to be located close to SFR. The processes are included in the **Geosphere process report**, Section 1.4, with references to the descriptions in the geosphere process report for the post-closure safety assessment for the final repository for spent nuclear fuel (SR-Site, SKB TR-10-48).

FHAs may potentially affect the safety functions of the SFR repository and other factors important for the overall post-closure safety. FHAs are not included in the reference external conditions but are treated separately as residual scenarios (step 8, Section 2.6.8 and Chapter 9). This follows the recommendations in the general advice to SSMFS 2008:37 by including several residual scenarios for inadvertent human impact on the repository's protective capability. These scenarios are stylised in the way suggested in the general advice.

Methodology for handling climate and climate-related issues

The methodology for handling the future evolution of climate and climate-related issues is described in the **Climate report**, Sections 1.4.2–1.4.3. In summary, the methodology consists of the following steps.

- Identifying and describing a range within which future climatic conditions and climate-related processes may vary at the repository site. Within these limits, characteristic climate-related conditions of importance for repository safety can be identified. The conceivable climate-related conditions can be represented as climate-driven process domains (Boulton et al. 2001), where such a domain is defined as "a climatically determined environment in which a set of characteristic processes of importance for repository safety appear". In the following parts of this report, these climate-driven process domains are referred to as *climate domains*. At a Swedish Baltic Sea coastal site such as Forsmark, characteristic climate-related conditions can be represented by the temperate, periglacial and glacial climate domains (**Climate report**, Section 1.4.3). In short, the temperate climate domain is defined as a region without the presence of permafrost or ice sheets, whereas the periglacial and glacial climate domains are defined as regions that contain permafrost and ice sheets, respectively.
- Identifying and describing a few possible representative climate developments, so-called *climate cases*, as a basis for assessing repository safety and the repository's protective capabilities. These climate cases are selected so that they together illustrate the most important and reasonably foreseeable sequences of future climate states and their impact on the protective capability of the repository and their environmental consequences. The set of climate cases for a specific safety assessment is chosen to represent conditions covering the range of possible future climate development at the repository site that may influence post-closure safety for the specific repository, see Näslund et al. (2013). The selection of climate cases is based on the (i) identified range within which future climatic conditions and climate-related processes may vary at the repository site (see bullet point above) and (ii) knowledge of which processes are of importance for the functioning of the repository concept under consideration (Step 1). The latter has been obtained from the iterative process of having performed several safety assessments for a specific repository concept.
- In the PSAR, the selection of climate cases is further developed from previous safety assessments to support the definition of scenarios in accordance with the regulations (SSMFS 2008:37 general advice Sections 5–7). The main objective is to define climate cases in support of a main scenario, less probable scenarios and residual scenarios (Step 8). For this purpose, a likelihood assessment of the future climate evolution is conducted (**Climate report**, Chapter 4).

Based on these steps, five climate cases are selected for further analysis in the safety assessment.

The *present-day climate case* represents a simplified development where present-day climate conditions prevail for the complete assessment period and the initial shoreline displacement is dominated by isostatic rebound following the last glaciation. These assumptions result in 100 000 years of continued temperate climate conditions at Forsmark, consistent with a likely future climate evolution during this time (see below). This climate case also fulfils the regulatory requirement that the description should include a case where the biosphere conditions prevailing at the time of the application will not change (SSMFS 2008:37, Section 10 and general advice Sections 10–12).

The *warm climate case* represents a likely future development where similar-to-present levels of anthropogenic greenhouse-gas emissions continue for the next few decades, after which they gradually decline to net-zero emissions at the beginning of the next century. This development results in 100 000 years of temperate climate conditions and a prolonged initial period during which the repository area remains submerged beneath the sea.

The *cold climate case* represents a future development characterised by substantial reductions in anthropogenic greenhouse-gas emissions and/or removal of atmospheric CO_2 by technological measures. This development results in gradually colder conditions and two periods of periglacial climate conditions at Forsmark within the latter half of the assessment period.

The *glaciation climate case* represents an unlikely future development towards colder climate conditions that result in the succession of periglacial, glacial, submerged and temperate climate conditions at Forsmark within the latter half of the assessment period. This climate case is included to evaluate scenario uncertainty.

The *hypothetical early permafrost climate case* represents a highly unlikely future development characterised by the development of permafrost and periglacial conditions at Forsmark within the next 50 000 years. This climate case is included to facilitate illustration of the significance of individual barriers and barrier functions independently of probabilities, under hypothetical assumptions of early permafrost development.

A more detailed description of the climate cases used in the present assessment is provided in the **Climate report**, Chapter 5.

Selection of reference external conditions

The *present-day climate case*, *warm climate case* and *cold climate case* are chosen as *variants* of the reference external conditions, representing the range of probable evolution of the external conditions at Forsmark over the next 100 000 years. Future events related to large-scale geological processes that affect the post-closure repository safety such as earthquakes are considered unlikely and are therefore not included as part of the reference external conditions. The external conditions of the reference evolution are described in Chapter 6 and in the **Climate report**, Section 5.2. The external FHA FEPs are not part of the reference external conditions, because the FHAs are not part of the reference evolution of the repository. The handling of FHAs is described in Chapter 9.

Management of uncertainties

The large-scale geological processes are discussed in SDM-PSU and the uncertainties are assessed within the SDM (SKB TR-11-04, Section 5.5.2). The confidence level regarding the deformation history and broad tectonic framework of the region is judged to be high. The uncertainties regarding climate and climate-related issues can be classified as scenario uncertainty. The management of these uncertainties follows SSM's recommendations in the general advice to SSMFS 2008:21 and is handled by introduction of several variants and calculation cases in the reference evolution and main scenario. This is also in line with the general advice to SSMFS 2008:37 that states that given the great uncertainties associated with climate evolution in a remote future and to facilitate interpretation of the risk to be calculated, the risk analysis should be simplified to include a few possible climate evolutions. In addition, the handling of FHA follows the recommendations in the general advice to SSMFS 2008:37 by including several residual scenarios for inadvertent human impact on the repository's protective capability.

2.6.4 Step 4: Description of internal processes

The FEP processing (Step 1) identifies all internal processes considered to be of potential importance for the post-closure safety of the repository system. The scientific knowledge and handling of each of these processes in the post-closure safety assessment are described in detail in the **Waste process report**, the **Barrier process report**, the **Geosphere process report**, and the **Biosphere synthesis report** and underlying reports (SKB R-13-43, SKB R-14-02). The handling in the safety assessment is the key outcome of these descriptions. The number of biosphere FEPs is large and detailed descriptions of each FEP (within each ecosystem) are provided in underlying reports (SKB R-13-43, SKB R-14-02). Several of the processes are handled through quantitative modelling, where each model, in general, includes several interacting processes. The **Model tools report** provides an overview of the computer codes used in these modelling activities, as well as computer codes used in other steps of the methodology. To provide an overview of the various assessment activities and models used in the evaluation of repository evolution and radionuclide transport, as well as the connection between them in the form of data flow, a flowchart is provided in Appendix H.

Management of uncertainties

The internal processes are identified in the FEP handling and are described in the process reports for the waste, the barriers and the geosphere as well as the **Biosphere synthesis report** including underlying reports (SKB R-13-43, SKB R-14-02). For each process that is described in the process reports, the handling of uncertainties is described in a separate subsection. This includes, for instance, modelling and data uncertainties. In the **Biosphere synthesis report** and underlying reports (SKB R-13-43, SKB R-14-02) different document structures are applied, which include the handling of uncertainties. Many of the processes are handled with quantitative modelling. This modelling effort relates to many different disciplines and the management of the uncertainties is adapted to the needs and the importance of the modelling within the safety assessment. For instance, the combined effects of bedrock heterogeneity, parameterisation uncertainty and the transient flow regime on the hydrogeological calculation results are assessed in a sensitivity analysis (Öhman and Odén 2018). In response to a review comment on SR-PSU by SSM (SSM 2019, Section 2.8), SKB has analysed conceptual uncertainties (modelling uncertainties) in the near-field radionuclide transport modelling for the silo and 1–2BMA by using simplified models, see Appendix C in the report describing the radionuclide transport models for the near- field (Åstrand et al. 2022).

In addition, uncertainties relating to internal processes may be handled by defining relevant scenarios (Section 2.6.8). For instance, the high concentration of complexing agents scenario assesses the effects of uncertainties in the transport of complexing agents between 1BLA and 1BMA. The uncertainties may include system uncertainty, scenario uncertainty, modelling uncertainty and data uncertainty.

2.6.5 Step 5: Definition of safety functions

A safety function is a role through which a repository component contributes to safety. The set of safety functions is an aid for describing the post-closure functioning of the repository and its components. In addition, they are used for identification of scenarios.

This step consists of identifying and describing the repository system's safety functions and how they can be evaluated with the aid of a set of safety function indicators. These consist of measurable or calculable properties of the waste, engineered barriers, geosphere and surface system. The safety functions and indicators defined in this assessment are an update of the safety functions and indicators identified in SR-PSU, accounting for experiences from SR-PSU and regulatory review comments (Chapter 5).

In SR-PSU, the set of safety functions was based on knowledge of the expected future evolution of the repository described in terms of the three areas 1) Initial state, 2) Internal processes and 3) External conditions. In the identification process, the potentially important FEPs were screened and a list of all potential safety aspects that need to be considered for relevant sub-components was used as input, based on the description of the initial state in SR-PSU (SKB TR-14-01, SKB TR-14-02). The two overall safety principles for SFR – *limitation of the activity of long-lived radionuclides* and *retention of radionuclides* (Section 2.2) are in this way broken down and described in terms of several specified safety functions and safety function indicators (Chapter 5).

In subsequent steps, the safety functions are used to describe the post-closure functioning of the repository. More specifically, the status of the safety functions related to the different repository components is described in Section 8.2. In this context it is noted that a poorly upheld safety function does not necessarily mean that safety is compromised, but rather that more in-depth analyses are needed to evaluate safety. The selection of less probable scenarios is based on the evaluation of the status of the safety functions in the main scenario (Section 2.6.8).

Management of uncertainties

The definition of safety functions is not directly coupled to the management of uncertainties. The safety functions define the principles of the repository functioning and these definitions are, by their nature, not subject to uncertainty. However, uncertainties regarding the evolution of the status of the safety functions are handled within other steps of the safety analysis methodology, most notably in the selection of less probable scenarios (Section 2.6.8).

2.6.6 Step 6: Compilation of input data

In this step, all data to be used in the quantification of the evolution of the repository and its environs, and in radionuclide transport and dose calculations, are selected using a structured procedure.

The selection of data is determined by the conditions that exist over the period of relevance, as well as the identified safety functions and their longevity of applicability, as reported in the **Data report,** the **Radionuclide transport report**, the **Biosphere synthesis report** and Grolander (2013). These reports describe how essential data for post-closure safety assessment of the SFR repository are selected, justified and qualified through traceable standardised procedures. Additionally, the flowchart in Appendix H describes the flow of input data between the different assessment activities that are related to steps in the methodology described in this chapter. The flowchart is based on a database that documents data flows and assessment activities.

Management of uncertainties

In the **Data report,** Section 2.1, the structured process is described in detail for data that relate to the safety functions of the repository. A central aspect of the data supply is the data qualification, based on, among other things, a discussion of modelling uncertainty and data uncertainty due to limited precision, bias and issues of representativity. Moreover, the spatial and temporal variability of the data are discussed. The so-called data customer that requests the data (the SKB assessment team), then judges the adequacy and recommends the data that should be used in the modelling, considering the uncertainties discussed by the data supplier. The structured process for selection, justification and qualification of parameters used in radionuclide transport and dose calculations is described in the **Radionuclide transport report**, Appendix A, the **Data report**, the **Biosphere synthesis report**, Chapter 8, and Grolander (2013).

2.6.7 Step 7: Reference evolution

In this step, the probable post-closure evolution of the repository and its environs, including uncertainties in the evolution that may affect the protective capability of the repository, is described (Chapter 6). This *reference evolution* starts from the time for the initial state (step 2, Chapter 4), and then follows the reference external conditions for the next 100 000 years (step 3, Section 2.6.3), accounting for FEPs that are likely to influence the evolution (step 1, Chapter 3). The description builds on the knowledge gained in the previous steps of the assessment methodology (Section 2.6.1 to 2.6.6), as well as dedicated studies performed to assess the post-closure evolution of the repository and its environs. The reference evolution supports the selection (step 8) and analysis (step 9) of the main scenario (Chapter 7) and less probable scenarios (Chapter 8).

Three *variants* of the reference external conditions (the *present-day variant*, *warm climate variant* and *cold climate variant*) are considered. These represent the range of probable evolution of the external conditions at Forsmark during the next 100 000 years (Section 2.6.3). The effect of the variants of the external conditions on the internal processes and the evolution of the repository system is described in Chapter 6.

The description of the reference evolution is divided into two parts. The first part is the evolution of the repository and its environs during the initial period when the area above SFR is submerged beneath the sea, including the transition to terrestrial conditions (Section 6.2). The duration of this period may range from one thousand to several thousands of years depending on the future relative sea level change at Forsmark, which is represented in the variants of the external reference conditions. This part includes a detailed description of the evolution of the repository during the first 1 000 years as required in the regulations (Section 2.2, SSMFS 2008:37, Section 11 and general advice).

The second part of the reference evolution includes the evolution of the repository and its environs during the remaining time of the safety assessment, i.e. from the end of the initial submerged period to 100 000 years after closure for the three variants of external reference conditions (Sections 6.3–6.5).

The post-closure evolution of the repository and its environs under these external conditions is described for the following:

- Surface systems.
- Bedrock; thermal, mechanical, hydrogeological and groundwater chemistry.
- Repository including waste and engineered barriers; thermal, mechanical, hydrology and chemistry.

Management of uncertainties

The reference evolution is based on the previous steps in the methodology and therefore the treatment of uncertainties in these steps is propagated into the reference evolution. The reference evolution concerns many different disciplines that make use of different methods, models and data. The treatment of uncertainties is thus related to the approaches within the different disciplines in the reference evolution. This includes uncertainties related to all different steps as described in this chapter (Sections 2.6.1–2.6.6). For instance, a range of probable external conditions is accounted for in the reference evolution by considering the three different climate variants described in Section 2.6.3. Potential further uncertainties that are not captured by the reference evolution, e.g. since they are judged unlikely to occur or that may impair post-closure safety, are evaluated as part of the selection of less probable scenarios (Section 2.6.8).

2.6.8 Step 8: Selection of scenarios

The assessment of the capability to protect human health and the environment is based on a set of scenarios that together illustrate the most important courses of development of the repository and its environs.

The requirements in Section 11 and Appendix 1 of SSMFS 2008:21 stipulate that it shall be reported how one or several methods have been used to identify and to describe relevant scenarios for sequences of events and conditions that can affect the future evolution of the repository. The scenarios shall include a main scenario that takes into account the most probable changes in the repository and its environment. For the scenarios, description of the evolution in the biosphere, geosphere and repository shall be included and the environmental impact of the repository shall be reported thereby considering defects in engineered barriers and other identified uncertainties. In the general advice of the regulation, it is further detailed how scenarios should be classified and selected. The general advice on how to show compliance with the risk criterion given in SSMFS 2008:37 also elaborates on scenarios. It is stated that an assessment of the protective capability of the repository and the environmental consequences should be based on a set of scenarios that together illustrate the most important courses of development of the repository, its surroundings and the biosphere (SSMFS 2008:37, general advice to Sections 5–7). Furthermore, the different scenarios should describe how a given combination of external and internal conditions affects repository performance, given an initial state of the repository and specified conditions in the environment.

The scenarios in the present assessment thus include a main scenario that takes into account the most probable changes in the repository and its environment and based on the general advice in the regulations, also include less probable and residual scenarios.

The main scenario

The main scenario takes into account the most probable changes within the repository and its environs based on the initial state (step 2), the reference external conditions (step 3) and the reference evolution (step 7). It is used as the starting point for the analysis of the impact of uncertainties, particularly a base case is defined that is used as a starting point for this analysis (step 9), in line with the general advice to SSMFS 2008:21, Section 9 and Appendix 1. The main scenario includes several calculation cases (step 9) evaluating uncertainties in external conditions and internal processes potentially important for the radionuclide transport through the repository system. The main scenario is described in Chapter 7.

Less probable scenarios

The aim of less probable scenarios is to evaluate scenario uncertainties and other uncertainties that are not evaluated within the framework of the main scenario, as recommended in SSM general advice to SSMFS 2008:21. The selection of less probable scenarios is based on the safety functions (step 5) and the FEPs (step 1) identified to potentially affect the safety function indicators. For each safety function, uncertainties in how the initial state, internal processes and external conditions are specified in the main scenario are evaluated to determine if there is a possibility that the status of the safety function deviates from that in the main scenario in such a way that post-closure safety may be impaired. The safety functions are evaluated primarily with respect to the key scenario uncertainties affecting the safety function indicators, but also considering relevant system, modelling and data uncertainties (Section 8.2). The evaluation systematically addresses uncertainties in the state of the safety function indicators relating to the initial state, internal processes, and external conditions. These uncertainties are discussed based on information given in the reference evolution (Chapter 6), the **Initial state report**, the **Waste process report**, the **Barrier process report**, the **Geosphere process report** and the **Climate report**.

The probabilities of each less probable scenario are assessed in connection to the scenario descriptions (Sections 8.3–8.6). In general, the estimation of probabilities is based on expert judgement. Where data are available, the estimation of probabilities is based on quantitative analyses.

In principle, each less probable scenario could be examined in each variant of reference external conditions. In practise, however, it is deemed sufficient to evaluate less probable scenarios with the present-day climate variant. For each less probable scenario, the possible effects of implementing one of the other variants of reference external conditions is discussed (Section 8.7). If the result for another variant are judged to give rise to higher dose consequences, this is explored further.

Residual scenarios

In line with the general advice to SSMFS 2008:21 and 2008:37, residual scenarios are selected to illustrate the significance of individual barriers and barrier functions, the effect of future human actions that potentially may affect the conditions of the repository, detriment to humans intruding into the repository, and the consequences of an unsealed repository that is not monitored. The approach for selecting residual scenarios that illustrate the significance of individual barriers and barrier functions is based on the safety functions (step 5). Furthermore, the scenarios are selected to contribute to the discussion of the robustness of the repository regarding the protection of human health. To this end, the residual scenarios may include hypothetical assumptions that are associated with a low realism or events with exceptionally low likelihood of occurrence. They comprise sequences of events and conditions that are selected and studied independently of probabilities and the results from the residual scenarios are thus not considered in the calculation of risk. Residual scenarios are described in Chapter 9.

Combinations of scenarios

The different less probable scenarios explore uncertainties that are not handled in the main scenario. The scenarios are defined based on different assumptions regarding the initial state, internal processes or external conditions. In principle, the assumptions in the less probable scenarios that differ from

the main scenario could be combined to form combinations of scenarios. Some assumptions might be mutually exclusive, while others could be combined in a single scenario. As the scenarios are less probable, a combination of two or more rather unlikely scenarios will be even more unlikely. Combinations of scenarios therefore only give significant contributions to the risk if the consequences of the combined scenario are significantly higher than the individual scenarios that are combined. It is therefore foreseen that, at most, only a few, if any, of the many possible combinations need to be explored. It can be noted that the increased use of probabilistic approaches, e.g. in the estimation of the inventory and groundwater flow in the radionuclide transport calculations, implies that uncertainties are combined to a greater extent in the main and less probable scenarios compared to SR-PSU. The need for selection of combinations of scenarios is analysed in Section 8.7.2.

Management of uncertainties

The safety assessment methodology includes scenarios in line with the regulations and the objective of the selection of scenarios is to handle scenario uncertainties, but other types of uncertainties, such as modelling uncertainties, may also be relevant. The uncertainties are handled primarily in the main scenario and the less probable scenarios. A set of supporting calculation cases in the main scenario evaluate uncertainties for which a low probability of occurrence may not be justifiable or that do not relate to uncertainties in any safety functions of the repository system. The primary objective of residual scenarios is to illustrate the significance of individual barriers and barrier functions rather than evaluating plausible scenario or modelling uncertainties. However, some of the residual scenarios can be interpreted as bounding cases, thus also bounding the effects of the uncertainties related to the scenario in question. For instance, the effect of uncertainties in the process of sorption is bounded by analysing a residual scenario neglecting sorption in the repository entirely.

2.6.9 Step 9: Analysis of selected scenarios

In this step, the scenarios selected in step 8 are first described together with the calculation cases which evaluate the uncertainties for each scenario. Thereafter, these cases are analysed with respect to appropriate calculational endpoints, typically annual effective dose to humans and dose rates to non-human biota.

Description of scenarios

In general, each scenario describes a sequence of events and conditions of the repository and its environs and how they affect the protective capability of the repository and dose consequences. This is in line with requirements in SSMFS 2008:21, Section 11 relating to the reporting of a method for description of relevant scenarios. The main scenario is based on the initial state (step 2), the reference external conditions (step 3) and the reference evolution (step 7). The scope of the main scenario, including the management of uncertainties in the scenario, is described in Section 7.2.

The descriptions of the less probable (Chapter 8) and residual scenarios (Chapter 9) focus on the aspects that differ from the main scenario with regard to the initial state, external and internal conditions and the evolution of the repository system.

Description of calculation cases

To estimate radiological consequences, the scenarios are evaluated with the aid of calculation cases that are analysed with mathematical models. For each scenario, calculation cases are identified and described with respect to the most important assumptions for the calculations, data used in the modelling and description of the FEPs on which the calculation cases focus. Often, only a single calculation case is selected per scenario. For some scenarios, however, several calculation cases are considered necessary in order to evaluate all uncertainties identified by the scenario description. A calculation case may also include variants selected to evaluate the impact of alternative assumptions within the framework of the calculation case description. An overview of the calculation cases included in the present safety assessment is given in Table 2-1.

Table 2-1. Scenarios and calculation cases analysed in the PSAR (Chapters 7–9).

Scenario		Calculation case	
Main scenario		Present-day climate (base case) Warm climate Cold climate	
		Supporting calculation cases	Timing of shoreline regression Delayed release from repository Subhorizontal fracture Alternative landscape configurations Ecosystem properties [a)] Alternative delineation [a)] Mire object properties [a)] Calcite depletion [a)]
Less probable scenarios	**Glaciation**	Glaciation	
	High concentrations of complexing agents	High concentrations of complexing agents	
	Alternative concrete evolution	Alternative concrete evolution	
	Earthquake	Earthquake	
Residual scenarios	**Hypothetical early permafrost**	No effect on engineered barriers [b)] Effect on engineered barriers	
	Loss of engineered barrier function	No sorption in the repository No hydraulic barriers in the repository	
	Loss of geosphere barrier function	No sorption in the geosphere No transport retention in the geosphere	
	Alternative radionuclide inventory	Extended operation of reactors Increased fuel damage frequency Extended use of molybdenum-alloy fuel spacers	
	Oxidising conditions	Oxidising conditions	
	Initial concrete cracks	Initial concrete cracks	
	Unrepaired 1BMA	Unrepaired 1BMA	
	Unsealed repository	Unsealed repository	
	Drilling into the repository [c)]	Drilling event Construction on drilling detritus landfill Cultivation on drilling detritus landfill	
	Intrusion well [c)]	Intrusion well	
	Water management [c)]	Construction of a water impoundment	
	Underground constructions [c)]	Rock cavern in the close vicinity of the repository Mine in the vicinity of the repository	

Included in the risk assessment.
[a)] Described in the **Biosphere synthesis report**.
[b)] Described in the **Radionuclide transport report**.
[c)] FHA scenarios.

Three calculation cases are selected for the main scenario based on the reference external conditions (step 3). The *present-day climate calculation case* is selected as *base case* in the present safety assessment. The descriptions for all other calculation cases are based on differences from the *base case* regarding external conditions as well as the handling of FEPs for the repository (near-field), the bedrock surrounding the repository (geosphere) and the surface systems above the repository (biosphere). The *warm climate calculation case* and *cold climate calculation case* of the main scenario represent the range of probable evolution of the external conditions.

The main scenario is complemented with a set of supporting calculations (Table 2-1), providing sensitivity analysis of specific aspects coupled to external conditions and internal processes potentially important for radionuclide transport through the repository system. The objective of these calculations is to support the selection of assumptions in the base case and improve the confidence in the results of the main scenario. Given this objective and noting that the supporting calculations are evaluated before the choice of assumptions in the base case and thus generally result in similar or lower mean annual doses than the base case, these are not propagated to the summation of radiological risk. The reason for evaluating these uncertainties in the main scenario, in contrast to the less probable scenarios, is that a low probability of occurrence may not be justifiable or that they do not relate to uncertainties in any safety functions of the repository system.

Radionuclide transport and dose calculations

For each calculation case, the radionuclide transport from the repository (near-field) through the bedrock (geosphere) to the surface system (biosphere) is quantified. The endpoints of the calculations are the *annual effective doses* to humans and *absorbed dose rates* to non-human biota. The term *annual dose* is defined as the effective dose from external exposure in a year, plus the committed effective dose from intakes of radionuclides in that year. It is calculated as the annual effective dose for an adult, which is considered to provide a sufficiently good approximation of the average exposure during a lifetime. Further details regarding the definition and calculation of annual effective doses are given in the **Biosphere synthesis report**, Section 2.3.5. In the present assessment, *dose* refers to annual effective dose and *dose rates* refer to absorbed dose rates unless otherwise noted. All exposure pathways deemed to be relevant have been taken into account in the dose calculations.

The resulting effective doses that humans can incur, and for some calculation cases dose rates to biota, from exposure to repository-derived radionuclides are then evaluated. The details of the calculations are given in the **Radionuclide transport report** and summarised for each calculation case in this report (Chapters 7–9).

As required in SSMFS 2008:37, Section 4, the collective dose is calculated as a result of the expected release of radioactive substances over a period of 1 000 years after closure of SFR. The collective dose is estimated by summing the annual collective dose over 10 000 years. Collective dose is calculated for the *base case* and for calculation cases in the main scenario and less probable scenarios with altered repository-derived releases during the first 1 000 years compared to the *base case*. The *earthquake calculation case* is however excluded, even though releases could be substantially altered if an earthquake were to occur within the first 1 000 years. The reason is that the annual probability of an earthquake powerful enough to damage the barriers and to significantly alter radionuclide release is only 10^{-6} (Section 8.6.1). Hence, the cumulative probability for at least one earthquake to occur is significant considering the entire assessment period but is two orders of magnitude lower if it is postulated that the earthquake occurs during the first 1 000 years. The calculation cases for which collective doses are calculated are the *base case*, the *warm climate calculation case*, the *alternative concrete evolution calculation case*, and the *high concentrations of complexing agents calculation case*. The calculation of collective dose is documented in the **Radionuclide transport report**, Chapter 9.

Annual risk – protection of human health

The estimation of annual risk based on the results from the dose calculations of the main and less probable scenarios is described in detail in Section 10.2. SSM has established criteria against which the results of risk calculations should be evaluated to ascertain whether the repository can be considered safe. SSMFS 2008:37, Section 5 stipulates that the annual risk of harmful effects may not exceed 10^{-6} for a representative individual in the group exposed to the highest risk from the repository (the most

exposed group). This corresponds to an annual effective dose of 14 μSv, where the conversion to dose uses a risk factor of 7.3 percent per Sv (as given in the regulation). This criterion applies if the exposed group is relatively large. If the exposed group consists of a few individuals, the annual risk to the most exposed individual can be evaluated against a risk criterion[13] of 10^{-5} which is equivalent to an annual effective dose of 140 μSv.

For each of the scenarios defined, radiological consequences have been calculated. The main scenario and the less probable scenarios are the basis for the risk calculation. The approach taken in the risk evaluation is described in detail in Section 10.2 and can be summarised as being to:

1. Calculate the conditional risk for each relevant calculation case of the included scenarios, i.e. multiply the arithmetic mean dose for calculation cases with the dose to risk conversion factor given in the regulations. This is called a conditional risk, since it assumes that the scenario in question has occurred.
2. Sum the results from the different calculation cases considering their probability of occurrence to obtain a total annual risk estimate as a function of time, accounting for some scenarios being mutually exclusive. The less probable scenarios are only considered for a given point in time if they yield a larger conditional risk than the main scenario. The probability of occurrence of the main scenario is lowered by the probability of occurrence of the less probable scenarios that contribute to the total annual risk such that the total probability is 1.

The estimated time-dependent total annual risk is the basis for the comparison with the risk criteria in the regulations. The general advice to SSM's regulations also recommends that the issue of risk dilution is addressed. Risk dilution in its broadest sense refers to a situation in which an increase in the uncertainty of the values of input parameters, or in the assumptions with respect to the timing of an event, leads to a decrease in calculated dose or risk. Risk dilution and its handling are addressed in Section 10.6.

Protection of the environment

The regulations require that a repository shall be implemented so that biodiversity and the sustainable use of biological resources are protected against the harmful effects of ionising radiation (SSMFS 2008:37, Section 6). The biological effects of ionising radiation in the habitats and ecosystems concerned shall furthermore be described (SSMFS 2008:37, Section 7). However, there is no limiting value for exposure of animals and plants stipulated in SSM's regulations, nor is there any international consensus on values that should be used (see further discussion in the **Biosphere synthesis report**, Chapter 12). Rather, the consensus is to apply an approach whereby a screening value (or range) is applied; if dose rates are predicted or calculated to be above such a value or range, it is assumed that there is the possibility of negative effects to a population of organisms and further assessment is thus warranted.

The results of the calculations are interpreted with respect to the ERICA screening dose rate (Andersson et al. 2009, Garnier-Laplace et al. 2010). Consideration is also given to relevant screening benchmarks recommended by UNSCEAR (2011) and ICRP (2008), where these are more restrictive than the generic ERICA screening value. The ERICA approach utilises a single screening dose rate of 10 μGy h^{-1} across all organism types. Given that there are no quantitative regulatory criteria for protection of the environment with regard to ionising radiation, these values are considered to be relevant for the assessment of regulatory compliance, noting that the methodology is in line with the general guidance in ICRP (2003) that SSM recommends in the general guidance to SSMFS 2008:37. The protection of the environment is discussed in Section 10.8.

[13] In the present analysis, only the exposure from a drilled well in the well interaction area is considered to be relevant for a small group (**Radionuclide transport report**, Section 4.4). To account for this, the calculated dose to this exposed group is divided by 10 to be comparable to the dose to other exposed populations, instead of applying the 10^{-5} criterion directly. In all other cases the 10^{-6} criterion is applied.

Management of uncertainties

In accordance with SSM's general advice, the main scenario includes several calculation cases that relate to uncertainties with respect to external and internal conditions, e.g. several climate variants are part of the main scenario. Moreover, the supporting calculation cases address scenario and modelling uncertainties that are not necessarily associated with a low probability or do not affect the status of any safety function.

Data uncertainties are accounted for by performing probabilistic simulations. An exception among the scenarios is the *unsealed repository scenario* (Section 9.10); as this scenario is highly simplified and pessimistic, it is considered appropriate to apply only deterministic calculations. Another exception is the *earthquake scenario* for which a deterministic simulation was carried out for all radionuclides except the key radionuclide Ni-59 (Section 8.6). The methodology used for the *earthquake scenario* implies that the available computational capacity cannot handle probabilistic simulations for all radionuclides and thus only probabilistic calculations for the key radionuclide Ni-59 were considered merited.

The impact of data uncertainty on the annual dose is analysed specifically for the *base case* (Section 7.4.6). The treatment of uncertainty in the radionuclide transport and dose calculations is further described in the **Radionuclide transport report**, Section 2.5. This includes discussions of parameter uncertainties and variation as well as numerical uncertainties and code variations. In relation to dose calculation, human exposure to radionuclides dispersed in the environment is modelled for representative individuals of four distinct potentially most exposed groups reflecting diverse sets of relevant exposure pathways as described in Section 7.3.6. This is in line with the general advice to SSMFS 2008:37.

As suggested in the general advice to SSMFS 2008:21 and 2008:37 alternative safety indicators have been considered. The estimated activity concentrations in the environment for the main scenario *base case* are compared with activity concentrations of naturally occurring radionuclides (Section 10.7).

In the risk calculations, the consideration of uncertainty is inherent, with the included scenarios being weighted by their estimated probabilities. The uncertainties of the preceding radionuclide transport and dose calculations are propagated into the risk calculations.

2.6.10 Step 10: Conclusions

The tenth and last step in the safety assessment methodology demonstrates compliance with regard to the protection of human health and the environment as well as the robustness of the barrier system (Chapter 11). These aspects are considered to be the central parts of SSM's post-closure regulations SSMFS 2008:37 and 2008:21. The robustness of the barrier system relates to barriers and their functions as well as design and construction utilising best available techniques. This also couples to requirements on optimisation. A discussion of compliance for each section of the regulations, together with the handling of the recommendations in the general advice, is presented in Appendices B and C. The compliance demonstration is based on the results and discussions in the preceding safety assessment methodology steps, and the most important aspects that strengthen the confidence in the compliance statement are discussed. Moreover, important developments of the safety assessment since SR-PSU that consider the comments that SSM highlighted in its review of SR-PSU are described. Finally, the handling of feedback to subsequent steps in the SFR repository programme is described.

Management of uncertainties

In Chapter 11 the confidence in the compliance statement is discussed and, the role of the management of uncertainties is highlighted. Furthermore, the feedback to the subsequent steps in the SFR repository programme *inter alia* aims at efforts to manage uncertainties, for instance regarding the initial state of the post-closure safety assessment.

2.7 Feedback to subsequent steps in the repository programme

The main contribution of the post-closure safety assessment to the preliminary safety analysis report is to demonstrate that SFR is radiologically safe for humans and the environment after closure. The assessment is a basis for SSM to evaluate regulatory compliance and to approve the start of facility construction. However, the safety assessment is also used by SKB as an important input for the detailed design of the facility, including the barrier system, for defining future RD&D needs, and for the further development of the safety assessment in future steps. For instance, further development applies to the estimated conditions in the repository and its environs at repository closure, as well as the post-closure evolution and WAC, which are important prerequisites for subsequent safety assessments in the future steps in the SFR repository programme and associated licensing steps. The stepwise licensing of SFR is briefly described in Section 1.5 and the feedback to subsequent steps in the repository programme in Section 11.3.2.

2.8 Documentation and quality assurance

The present safety assessment has been conducted in accordance with SKB's integrated quality management system that is certified according to ISO 9001:2015 (quality management), ISO 14001:2015 (environmental management) and ISO 45001:2018 (occupational health and safety). Several processes of the management system relate to the safety assessment work and reporting. This includes the main process *construct, develop, and optimise repository systems* and in particular the subprocess *license for nuclear facility* that relates to the stepwise licensing process. Moreover, several support processes are relevant, including *performing programs, projects and assignments*; *organisation, personnel and competence*; *management of requirements for repository systems and repositories*; and *management of information*. A list of the steering documents relevant for the description in this section is given in Table 2-2.

Based on these overarching processes and related steering documents the *program management plan PSU – stage 1* has been established, which defines the programme-specific steering documents including the *quality plan for the SFR extension programme*. The quality plan states that overall quality objectives are that the preparation of the products within the programme follows SKB's quality management system, and to ensure that all finalised products comply with the requirements that are specified in the *programme charter*.

For the quality assurance of the safety assessment reports the SKB quality management system process instructions regarding *formal review* and *preparation of public reports* that relate to the process *management of information* are important. At a detailed level, procedures for the qualification and handling of data have been implemented in line with the process *management of information*. These are described in the related reports. For instance, the procedure for qualification of input data is described in detail in the **Data report**, Section 2.3. The procedure aims *inter alia* at ensuring scientific adequacy and traceability of the data. Quality assurance aspects of the FEP-analysis and the FEP-database are described in detail in the **FEP report,** Section 2.3 and the quality assurance principles for the computer codes are described in the **Model tools report**, Chapter 2. In the process reports, the structure for establishing the process descriptions is described, e.g. the **Waste process report**, Section 1.5. In the **Radionuclide transport report**, Appendix A, quality assurance aspects of the data handling relating to the modelling are described.

It is important that the requirements that the post-closure safety puts on the design and construction of the SFR extension are propagated in an adequate way to other relevant processes and roles. The process instructions in SKB's management system concerning *management of requirements for repository systems and repositories* and *change control management of requirements and design premises* are refined for the SFR repository programme in the programme-specific *plan for requirement management, verification and validation within PSU*.

An important overarching aspect of the quality management is the competence of the persons involved in the work. The SKB's management system process instructions on *organisation, personnel and competence* give support to ensuring adequate competence and staffing with the aim to develop the organisation to maintain a high level of safety and to reach the objectives of existing and new activities.

Table 2-2. Processes, process instructions, and PSU programme specific steering documents relevant for post-closure safety assessment work and reporting.

Title of process (main process HP, support process SP), process instruction or programme specific steering document	Steering document title (in Swedish)	Document number[14]
HP 1 Construct, develop, and optimise repository systems	Processbeskrivning HP1 Uppföra, utveckla och optimera slutförvarssystem	SKBdoc 1609269, ver 5.0
HP1.4 License for nuclear facility	Tillstånd för kärnteknisk anläggning	SKBdoc 1938653, ver 2.0
SP1 Performing programs, projects and assignments	Processbeskrivning SP1 Genomföra program, projekt och uppdrag	SKBdoc 1609284, ver 2.0
SP2.2 Organisation, personnel and competence	Processbeskrivning SP2 Säkra personal och kompetensförsörjning	SKBdoc 1908377, ver 3.0
Process instruction:		
• Organisation, personnel and competence	• Säkra organisation, kompetens och bemanning	• SKBdoc 1051846, ver 23.0
SP16 Management of requirements for repository systems and repositories	Processbeskrivning SP16 Hantera krav på slutförvarssystem och slutförvar	SKBdoc 1886606, ver 6.0
Process instructions:		
• Management of requirements for repository systems and repositories	• Hantera krav på slutförvarssystem och slutförvar	• SKBdoc 1699400, ver 4.0
• Change control management of requirements and design premises	• Ändringshantering av krav och Konstruktionsförutsättningar	• SKBdoc 1701954, ver 4.0
SP6.2 Management of information	Hantering av dokument	SKBdoc 1039085, ver 17.0
Process instructions:		
• Formal review	• Sakgranskning	• SKBdoc 1050857, ver 19.0
• Preparation of public reports	• Framtagning av publika rapporter	• SKBdoc 1066520, ver 13.0
PSU – Programme-specific steering documents		
Program management plan PSU – stage 1	Program Management Plan PSU – Etapp 1	SKBdoc 1948878, ver 1.0
Quality plan for the SFR extension programme	Kvalitetsplan program SFR-Utbyggnad	SKBdoc 1480982, ver 4.0
Programme charter	Project Charter för Projekt SFR-utbyggnad	SKBdoc 1375964, ver 7.0
Plan for requirement management, verification and validation within PSU	Plan för kravhantering och VoV – PSU	SKBdoc 1479880, ver 3.0

[14] Internal document. In Swedish.

3 FEPs

3.1 Introduction

This chapter describes the analysis of features, events and processes (FEPs) potentially influencing post-closure safety of SFR. The FEP analysis is one of the main steps in the safety assessment methodology, as described in Section 2.6.

The FEP analysis includes:

- Identification of all factors that may influence post-closure safety of the repository, by screening potentially important FEPs that are contained in international and national databases and SKB's previous safety assessments.
- Deciding whether each FEP identified needs to be included in the analysis or not. The motivations for excluding FEPs are documented in the SKB FEP database.
- Documentation of each included FEP.

In Table 3-1, a description of the terminology used in the FEP analysis and within the SKB FEP database is given.

An extensive effort to establish the FEP catalogue for the assessment of post-closure safety of SFR was undertaken in the previous safety assessment SR-PSU (**FEP report**). The resulting SFR FEP catalogue (SR-PSU version) contains all identified factors that may influence post-closure safety. The FEP catalogue in the present safety assessment has been established by performing a validity check of the SFR FEP catalogue (SR-PSU version), accounting for new knowledge, and a check against new international FEP lists. As explained in Section 3.4, this review did not lead to any change in the set of FEPs included in the catalogue.

The objective of the FEP analysis in the PSAR is two-fold; to make sure that all factors that may influence post-closure safety are identified and to document the handling of each FEP in the SFR FEP catalogue (PSAR version). In this sense, the FEP catalogue constitutes a "look-up-table" with a brief description of the handling of each FEP and references to relevant reports that detail the handling further.

The PSAR FEP analysis procedure is described in Section 3.2. The selection of sources used to identify relevant FEPs for the PSAR is described in Section 3.3. The FEP audit, comprising review and update of the FEP catalogue, is described in Section 3.4. The different steps and results from the FEP processing work are further described in Section 3.5 with separate subsections for each of the main categories of FEPs. Since only minor changes have been made to the process descriptions and handling of the FEPs, the SR-PSU FEP report has not been updated and the short name **FEP report** refers to the SR-PSU FEP report.

Table 3-1. Terminology used in the FEP analysis and within the SKB FEP database.

Term	Description
SKB FEP database	The SKB FEP database comprises separate FEP catalogues for all three of SKB's final repositories, i.e. SFK, SFR and SFL.
FEP catalogue	Each FEP catalogue contains a list of all FEPs (in the form of FEP records) included in the safety assessment. In addition, the FEP catalogue may include information such as Couplings (i.e. Influence tables and diagrams, Process tables and diagrams), Mapping (i.e. NEA mapping and Matrix mapping), FEP charts, Assessment model flow charts (AMF), Interaction matrices and references to associated reports (e.g. process reports). The different FEP catalogues for each performed safety assessment are referred to as *versions* of the respective FEP catalogue. A FEP catalogue is denoted by prefixing the name of the repository and suffixing the version in question, e.g. "The SFR FEP catalogue (PSAR version)".
FEP list	A list of FEPs. The term is commonly used for FEP catalogues, or a part of these, in other national programmes.
FEP record	Each FEP is represented by a FEP record specifying the FEP id, FEP name, main category, system component and/or subcategory, description, handling, reference and revision.
NEA FEP database	The NEA International FEP database comprises two main components: • the International FEP (IFEP) list, and • project-specific FEP (PFEP) lists. Every NEA PFEP is mapped to at least one IFEP.
IFEP	The NEA IFEP list contains FEPs relevant to the post-closure safety assessment of solid radioactive waste repositories that attempts to be comprehensive at a given level of detail and within defined bounds. This forms a master list and classification scheme by which to examine project-specific database entries.
PFEP	The NEA PFEP list are a collection of several national FEP lists and databases, with references, compiled during various repository safety assessments and scenario development studies for geological disposal programmes.
FEP analysis	FEP analysis is used to denote the entire procedure where FEPs are analysed (identified, processed and documented) within a safety assessment.
Audit	The systematic review of selected FEP sources, performed to ensure that all relevant factors influencing post-closure safety are identified. The result of the FEP audit is further treated in the FEP processing procedure.
Processing	The procedure applied to the FEPs identified in the FEP audit, performed to ensure that all relevant aspects of a process are addressed in the process description and handled within the safety assessment. The result of the FEP processing is documented in the SKB FEP database and in associated reports for the safety assessment.
Handling	The description of the way FEPs are taken into account within the safety assessment.
Mapping	The operation whereby FEPs in the SKB FEP database are mapped to either NEA PFEPs (i.e. NEA mapping) or to the Interaction matrices (i.e. Matrix mapping).
Coupling	Couplings are used to define the mutual influences between processes and variables. The couplings within a system component are described using Influence tables, Process diagrams and Interaction matrices, which are also included in the SKB FEP database.

3.2 FEP analysis procedure

The FEP analysis procedure in the PSAR is based on a review of the FEP catalogue developed for the SR-PSU. The establishment of the SR-PSU catalogue is documented in the **FEP report**. The FEP analysis procedure, schematically illustrated in Figure 3-1, comprises several steps for the SR-PSU and the PSAR respectively, as explained below. Steps denoted *a)* to *d)* relate to work conducted in the SR-PSU (see the **FEP report**, Section 2.2), while steps *e)* to *h)* relate to the PSAR.

SR-PSU FEP analysis procedure

a) **FEP sources**. Selection of sources for the FEP processing comprises the SFR1 Interaction matrices, including associated reports from the previous safety assessments for SFR, SAFE and SAR-08 (SKB R-01-13, SKB R-08-12); the SFK FEP catalogue (SR-Site version) and associated SR-Site process reports; and the PFEP lists in the NEA International FEP database, version 2.1 (NEA 2006). In addition, two FEP lists from other low- and intermediate-level waste disposal projects, Olkiluoto LILW (Hjerpe et al. 2021) in Finland and Rokkasho 3 in Japan (unpublished version), were included.

b) **FEP audit**. A preliminary FEP catalogue was established based on the contents of the selected FEP sources to ensure that all factors relevant to the SR-PSU were identified. The FEPs were divided into the following seven main categories: *initial state, internal processes, system variables, biosphere, external factors, methodology* and *site-specific factors*. Some of the main categories are also divided into system components or subcategories, see Section 3.4.1. The SR-PSU FEP audit is described in more detail in the **FEP report**, Chapter 3.

c) **FEP processing**. The preliminary FEP catalogue was further processed to ensure that all relevant aspects of the FEPs were addressed in the description and appropriately handled in the SR-PSU. The processing and handling of FEPs in the SR-PSU were documented in several reports, see Section 3.3.3, and are described in more detail in the **FEP report**, Chapter 4.

d) **Establishment of the SFR FEP catalogue (SR-PSU version)**. Based on the FEP processing, the SFR FEP catalogue (SR-PSU version) was established. The set of FEPs handled in the reports listed in Section 3.3.3 comprised the FEP catalogue for the SR-PSU. This FEP catalogue contained all FEPs that needed to be included in the SR-PSU. The contents of the FEP catalogue are described in more detail in the **FEP report**, Chapter 5.

PSAR FEP analysis procedure

e) **FEP sources**. The PSAR uses the SFR FEP catalogue (SR-PSU version) together with the associated reports produced for the SR-PSU, as a basis for the FEP processing (Sections 3.3.1 and 3.3.3). In addition, the following relevant FEP lists from other radioactive waste disposal projects that became available after the establishment of the SR-PSU are included (Section 3.3.2)
   - NEA International FEP list version 3.0 (NEA 2019)
   - Posiva's SNF and LILW repositories (Hjerpe et al. 2021)
   - Posiva's LILW repository (Nummi et al. 2012)
   - Ontario Power Generation's (OPG) LILW repository (NWMO 2011).

f) **FEP audit**. This step comprised a simplified audit including a check of the validity of the outcomes (i.e. the lists of component-specific processes and variables, Interaction matrices, and handling of FEPs in the assessment) of the SR-PSU FEP analysis (Section 3.3.3). This check comprised two tasks:
   1. Validity check of the SFR FEP catalogue (SR-PSU version) (Section 3.4.1).
   2. Check against international and national FEP lists that became available after establishing the SFR FEP catalogue (SR-PSU version) (Section 3.4.3).

g) **FEP processing**. The FEP catalogue was further processed to ensure that all relevant aspects of the FEPs were addressed in the description and appropriately handled in the PSAR. The processing and handling of FEPs in the PSAR are documented in several updated SR-PSU reports (Section 3.5.1).

h) **Establishment of the SFR FEP catalogue (PSAR version)** (Section 3.6).

The steps in the PSAR FEP analysis procedure are summarised in the following sections.

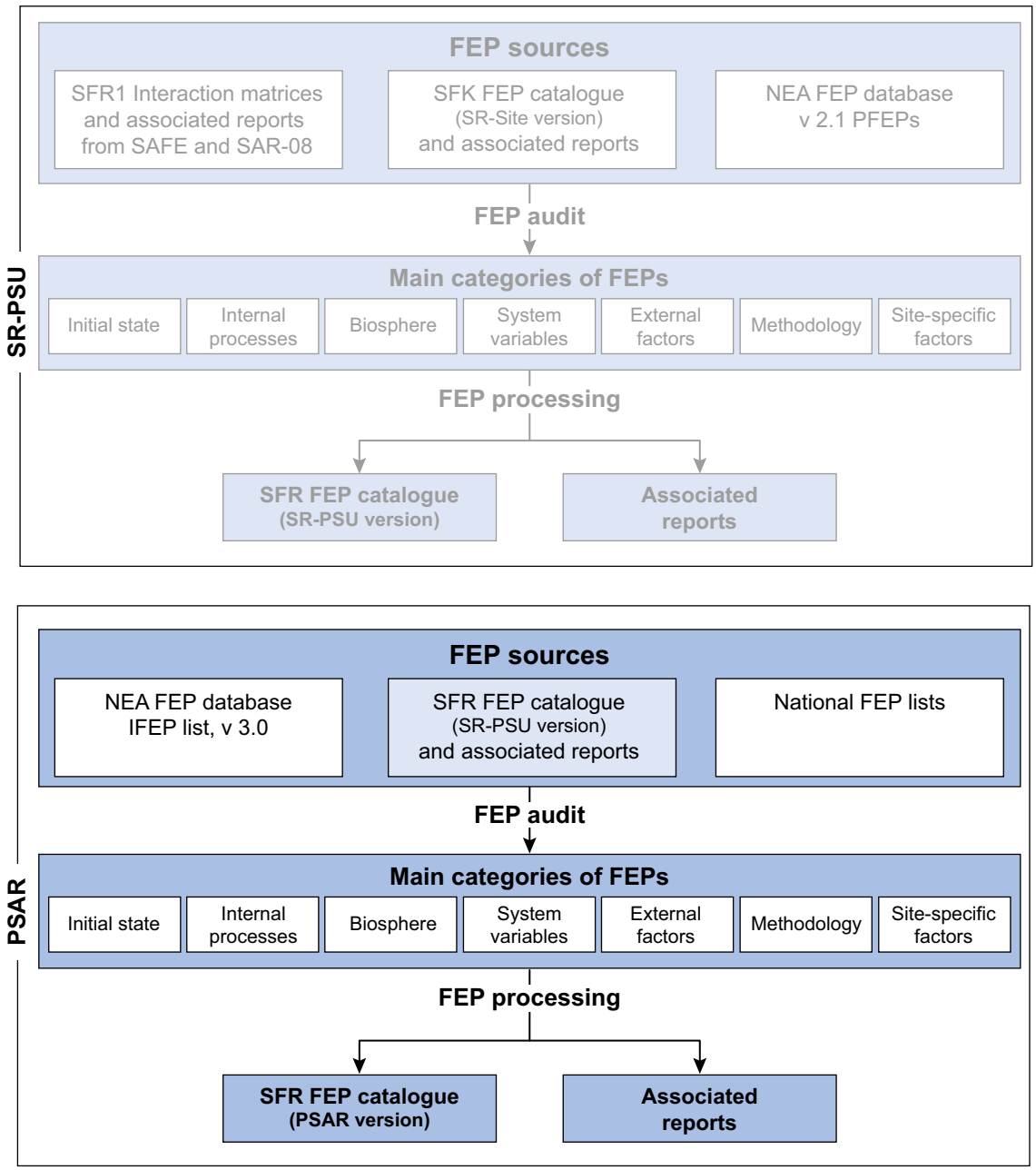

Figure 3-1. *Schematic illustration of the FEP analysis procedure applied in the SR-PSU and the PSAR.*

3.3 FEP sources

3.3.1 The SKB FEP database

The SKB FEP database is used as a tool for documentation of the outcome of the different steps in the FEP analysis procedure carried out within safety assessments conducted at SKB. Thus, the FEP database is regarded as a quality assurance instrument. A schematic overview of the two versions of the FEP catalogue for the SFR repository is shown in Figure 3-2. In addition, the sources included in the PSAR are shown.

For clarity, the different parts of the SKB FEP database are defined in Table 3-1. The SKB FEP database comprises FEP catalogues for all three of SKB's final repositories (i.e. SFK, SFR and SFL). It also includes the complete list of NEA PFEPs included in the NEA International FEP database

version 2.1 (NEA 2006). Each NEA PFEP belongs to one of the categories relevant or irrelevant to the specific safety assessment. The NEA PFEPs considered to be relevant to the specific safety assessment are mapped to FEPs defined and included in the FEP database for that specific assessment. The NEA PFEPs considered to be irrelevant to the specific assessment, are included in a list of assessment-specific irrelevant NEA PFEPs. Thus, each of SKB FEP catalogues constitutes a complete set of currently known factors that can influence post-closure safety for the repository in question.

The SFR FEP catalogue (SR-PSU version) used the SR-Site version as input together with the SFR1 Interaction matrices. The approach adopted for FEP analysis and the structure of the FEP database for SFR1, developed using interaction matrices, are documented for the previous safety assessments, SAFE and SAR-08 (SKB R-01-13, SKB R-08-12). The database for SFR1, with Interaction matrices, was superseded and relevant information from it was transferred via Matrix mapping into the SFR FEP catalogue (SR-PSU version) (**FEP report**).

The PSAR uses the SFR FEP catalogue (SR-PSU version) together with the associated reports produced for the SR-PSU, as a basis for the FEP audit and processing. A more detailed description of the SKB FEP database can be found in the **FEP report**.

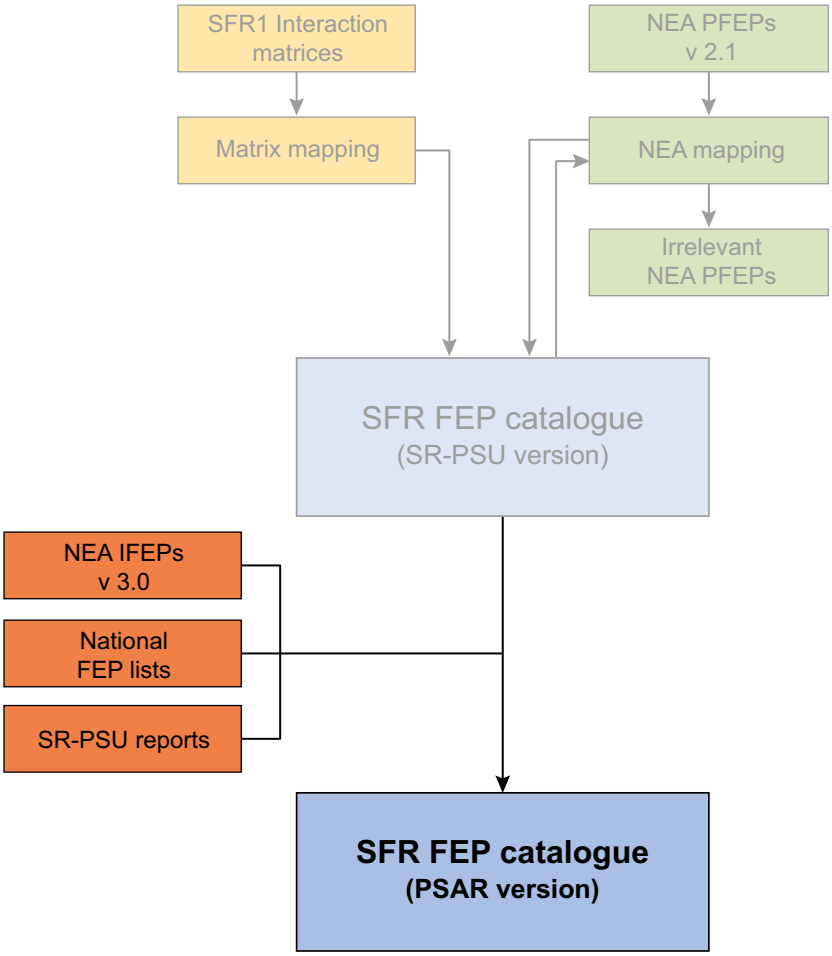

Figure 3-2. *Schematic overview of the two versions of the FEP catalogue for the SFR repository. The sources included in the PSAR are also shown. The lighter colours refer to earlier safety assessments, while the darker colours refer to the current safety assessment.*

3.3.2 Other international and national FEP lists

Since the SR-PSU, FEP lists from other relevant radioactive waste disposal projects have become available. In the PSAR, the following FEP lists were included in the analysis and checked against the content of the SFR FEP catalogue (SR-PSU version) (see Section 3.4.3):

- *NEA International FEP list version 3.0* (NEA 2019), which the NEA released together with a new web-based FEP database (version 2.0). The IFEP list has been revised both in terms of its structure and its content in comparison with the 2000 IFEP list (NEA 2000). Consistent with many of the more recent PFEP lists (e.g. those from Sweden, Finland and Japan), the new IFEP list is structured around a classification scheme based on external factors and disposal components (waste package, repository, geosphere and biosphere), rather than on the 2000 IFEP list scheme that used external, environment and contaminant factors. Each FEP contains a description, category, commentary on its relevance to performance and safety and mapping to related FEP(s) in the previous public version of the IFEP list. In total, 268 IFEPs (including FEP groups and subgroups) are contained within version 3.0 of the NEA IFEP list.
- *Posiva's SNF and LILW repositories* (Hjerpe et al. 2021). A preliminary version of the FEP list for SC-OLA, which is Posiva's safety case in support of the operating licence application for a geologic disposal facility situated at Olkiluoto. This facility comprises a repository for disposal of spent nuclear fuel based on the KBS-3V design and a repository for the low- and intermediate-level waste arising from the operation and decommissioning of the encapsulation plant for the spent nuclear fuel.
- *Posiva's LILW repository* (Nummi et al. 2012). FEP list for Posiva's safety case in support of the construction licence application for a geologic disposal facility situated at Olkiluoto, limited to the repository for low- and intermediate-level waste.
- *OPG's LILW repository* (NWMO 2011). FEP list for the post-closure safety assessment for Ontario Power Generation's proposed deep geologic repository for low- and intermediate-level waste at the Bruce nuclear site in Canada. It should be noted that the geological environment at the Bruce site differs significantly from the Forsmark site. The OPG repository was planned to be located in Ordovician sediments overlaid by Silurian sediments. This important difference was kept in mind when comparing the FEP lists.

3.3.3 The SR-PSU reports

PSAR uses the SFR FEP catalogue (SR-PSU version), together with the associated reports produced for the SR-PSU, as a basis for the FEP audit and processing (Sections 3.4 and 3.5). The reports where processing and handling of FEPs was documented in the SR-PSU are listed below.

The processing and handling of *initial state* FEPs were documented in:

- Initial state report for the safety assessment SR-PSU (SKB TR-14-02, Chapter 12).
- Main report for the safety assessment for SR-PSU (SKB TR-14-01, Section 3.3, Initial state deviations).

The processing and handling of *internal process* FEPs were documented in several process reports:

- Waste form and packaging process report for the safety assessment SR-PSU (SKB TR-14-03).
- Engineered barrier process report for the safety assessment SR-PSU (SKB TR-14-04).
- Geosphere process report for the safety assessment SR-PSU (**Geosphere process report**).

The processing and handling of *system variable* FEPs were documented in:

- Initial state report for the safety assessment SR-PSU (SKB TR-14-02).
- Waste form and packaging process report for the safety assessment SR-PSU (SKB TR-14-03).
- Engineered barrier process report for the safety assessment SR-PSU (SKB TR-14-04).
- Geosphere process report for the safety assessment SR-PSU (**Geosphere process report**).

The processing and handling of *biosphere* FEPs were documented in:

- Biosphere synthesis report for the safety assessment SR-PSU (SKB TR-14-06).
- Components, features, processes and interactions in the biosphere (SKB R-13-43).
- Handling of biosphere FEPs and recommendations for model development in SR-PSU (SKB R-14-02).

The processing and handling of *external factor* FEPs concerning *climatic processes and effects* were documented in:

- Main report for the safety assessment for SR-PSU (SKB TR-14-01, Sections 2.4.3 and 6.2).
- Climate and climate related issues for the safety assessment SR-PSU (SKB TR-13-05).

The processing and handling of *external factor* FEPs concerning *large-scale geological processes and effects* were documented in:

- Geosphere process report for the safety assessment SR-PSU (**Geosphere process report**).

The processing and handling of *external factor* FEPs concerning *future human actions (FHA)* were documented in:

- Handling of future human actions in the safety assessment SR-PSU (SKB TR-14-08).

The processing and handling of *methodology* FEPs were documented in:

- Main report for the safety assessment SR-PSU (SKB TR-14-01, Chapters 2 and 3).

The processing and handling of *site-specific factor* FEPs and *other* FEPs were documented in:

- Main report for the safety assessment SR-PSU (SKB TR-14-01, Chapter 3).
- Handling of future human actions in the safety assessment SR-PSU (SKB TR-14-08).
- FEP report for the safety assessment SR-PSU (**FEP report**, Section 4.3.4).

3.4 FEP audit

The purpose of the FEP audit is to ensure that all relevant factors influencing post-closure safety are identified. For the PSAR, the audit is simplified to a review of previous work including a validity check (Section 3.4.2) and a check against other FEP lists (Section 3.4.3).

As described in Section 3.2, the SFR FEP catalogue (SR-PSU version) was used as a basis for the audit. The classification of FEPs used in the SR-PSU is also used in the PSAR, see Section 3.4.1 and the **FEP report**, Section 2.1.2. The classification was set up to facilitate the auditing procedure and the development of the SR-PSU catalogue and it is also a valuable tool used throughout the post-closure safety assessment.

3.4.1 Classification of the PSAR FEPs

FEPs are classified using the same main categories as were used in the FEP processing for the SR-PSU (**FEP report**). Consequently, the PSAR FEPs are divided into the following seven main categories: *initial state, internal processes, system variables, biosphere, external factors, methodology* and *site-specific factors*. The categories are listed in Table 3-2.

The system analysed in the PSAR, i.e. the repository and its environs, comprises the disposed radioactive waste and packaging, the engineered barriers surrounding the waste packages, the geosphere and the biosphere in the proximity of the repository. For the main categories *internal processes* and *system variables* in the FEP catalogue, the system is divided into the following system components: *waste form*, *concrete and steel packaging*, *silo barriers*, *BMA barriers*, *BRT barriers*, *BTF barriers*, *BLA barriers*, *plugs and other closure components* and *geosphere*. The main category *biosphere* comprises the subcategories: *biosphere processes*, *biosphere subsystem components* and *biosphere variables*. Based on the nature of the *biosphere processes* they are subdivided into six subcategories: *biological processes*, *processes related to human behaviour*, *chemical, mechanical and physical processes*, *transport processes*, *radiological and thermal processes* and *landscape development processes*.

The main category *external factors*, comprises the subcategories: *climatic processes and effects, large-scale geological processes and effects, future human actions* and *other*.

Table 3-2. Classification of FEPs.

Main category	System component or Subcategory
Initial state	
Internal processes	Waste form Concrete and steel packaging Silo barriers BMA barriers BRT barriers BTF barriers BLA barriers Plugs and other closure components Geosphere
System variables	Waste form Concrete and steel packaging Silo barriers BMA barriers BRT barriers BTF barriers BLA barriers Plugs and other closure components Geosphere
Biosphere	Biosphere processes Biosphere subsystem components Biosphere variables
External factors	Climatic processes and effects Large-scale geological processes Future human actions Other
Methodology	
Site-specific factors	

3.4.2 Validity check of the SFR FEP catalogue (SR-PSU version)

The lists of component-specific processes and variables, and Interaction matrices established for the SFR FEP catalogue (SR-PSU version) were examined to check if they were still valid. The validity check, including suggested adjustments, was conducted by the person responsible for the FEPs and the manager of the post-closure safety assessment in co-operation with the editors of the reports where processing of FEPs was documented.

It was found in the validity check that there was no need to change the lists of component-specific processes and variables. Updates were made, but only in process descriptions, which are addressed in the process reports. In the validity check of the Interaction matrices there was only one change made, it is now identified that the variable ‘Radiation intensity’ may influence the process ‘Colloid formation and transport’ (**Waste process report**, Table 3-13).

3.4.3 Check against other international and national FEP lists

The resulting FEP lists from the validity check were checked against relevant FEP lists from other radioactive waste disposal projects that became available since establishing the SFR FEP catalogue (SR-PSU version) (Section 3.3.2). The following FEP lists were included: NEA International FEP

list version 3.0 (NEA 2019), Posiva's SNF and LILW repositories (Hjerpe et al. 2021), Posiva's LILW repository (Nummi et al. 2012) and OPG's LILW repository (NWMO 2011). Checking against international[15] and national FEP lists[16] did not result in any changes made to the FEP catalogue and no formal documentation of the outcome of the review was added to the SKB FEP database. The validity checks are available in two unpublished internal SKB documents.[15,16]

3.5 FEP processing

The overall conclusion from the FEP audit described above, is that the SFR FEP catalogue (SR-PSU version) is still valid for the PSAR. However, during the update of the process reports, modifications have been made to the handling of internal processes included in the safety assessment. The handling of each FEP in the PSAR was examined, accounting for new models and approaches applied, compared with how they were handled in the SR-PSU. This task was typically performed after the assessment was done or, at earliest, when the handling of a FEP had been decided. The processing, and especially the handling of the PSAR FEPs, is briefly described for each of the main categories in the following sections.

3.5.1 The PSAR processing documentation

The reports where processing, including the handling of FEPs, was documented in the SR-PSU are listed in Section 3.3.3. In the PSAR, updated versions of the following reports have been produced:

- **Initial state report**
- **Waste process report**
- **Barrier process report**
- **Climate report**
- **Biosphere synthesis report**
- **FHA report**.

In addition, the following three SR-PSU reports are used in the PSAR, but not updated:

- **FEP report**
- Components, features, processes and interactions in the biosphere (SKB R-13-43)
- Handling of biosphere FEPs and recommendations for model development in SR-PSU (SKB R-14-02)
- **Geosphere process report**.

It should be noted that the FEP audit and processing were implemented as an iterative process, since the final contents of the updated reports in the list above may be dependent on the outcome of both steps.

The process reports[17] document all internal processes that have been found to be potentially relevant to post-closure safety of SFR in the waste, the engineered barriers and in the geosphere. The processes in the biosphere are briefly described in the **Biosphere synthesis report**; full definitions of the processes and a detailed description of the handling of the biosphere FEPs in the safety assessment are given in two supporting biosphere reports for SR-PSU (SKB R-13-43, SKB R-14-02). The documentation of the processes related to external conditions are addressed in the **Climate report,** the **Geosphere process report** and the **FHA report** as detailed in Section 3.5.7.

[15] Hjerpe T, 2022. Avstämning mot NEA IFEP 3.0. SKBdoc 1860518, ver 1.0, Svensk Kärnbränslehantering AB. (In Swedish.) (Internal document.)

[16] Hjerpe T, 2022. Avstämning mot internationella FEP-listor. SKBdoc 1860515, ver 1.0, Svensk Kärnbränslehantering AB. (In Swedish.) (Internal document.)

[17] Process reports comprise the **Waste process report**, **Barrier process report** and **Geosphere process report**.

The purpose of the process reports is to document scientific knowledge regarding the processes to the extent required to deal with them in an adequate manner in the safety assessment. For this reason, the documentation is not completely exhaustive or detailed from a scientific perspective, because this is neither necessary for the purposes of the safety assessment nor feasible within the framework of an assessment. In general, all arguments, along with background data relating to decisions and supporting references, are given in the process description under relevant headings. Furthermore, the process reports provide documentation on which expert(s) compiled the fundamental information for each process. All processes addressed in the process reports are documented according to a common template comprising the following headings:

- Overview/general description.
- Dependencies between process and variables.
- Boundary conditions.
- Model studies/experimental studies.
- Natural analogues/observations from nature.
- Time perspective.
- Handling in the safety assessment.
- Handling of uncertainties in the safety assessment.
- Adequacy of references supporting the handling in the safety assessment.

The descriptions of the processes in the biosphere do not strictly follow this template. The main reason for this is that the biosphere is a complex system consisting of many different subcomponents with numerous interactions between them, making it impractical to discuss each process in detail separately.

3.5.2 Summary of FEPs and handling

In Appendix D, a compilation of all FEPs in the SFR FEP catalogue (PSAR version) is provided. For each FEP, the FEP ID, FEP name and a reference to the corresponding description in various reports, is given. The full descriptions and handling are very extensive for some FEPs therefore, for practical reasons, these fields were omitted in Appendix D.

3.5.3 Initial state

The *initial state* FEPs are either related to an initial state in conformity to the specification given for the repository design or to deviations from the expected initial state. The former are handled in the category of system variables, see Section 3.5.5. There are five FEPs included in the main category *initial state.* These *initial state* FEPs that are related to deviations from the expected initial state are listed in Appendix D, Table D-1, with references given to the corresponding descriptions in the **FEP report** and this report.

It was decided to exclude three of the *initial state* FEPs related to deviations from scenario selection. One of them is related to severe perturbations like fire, explosions, sabotage and severe flooding (ISGen01). The reasons for excluding this FEP are *i)* the probabilities for such events are low and *ii)* if they occur, they shall be reported to SSM, their consequences assessed and correcting or mitigating actions made accordingly. The second FEP excluded concerns effects of phased operation (ISGen02). Since phased operation is in accordance with the plans, but the whole repository will be closed at the same time, potential effects of phased operation are not considered to be a deviation from the initial state. The third FEP excluded is related to effects detrimental to safety after repository closure caused by monitoring activities (ISGen04). This FEP was excluded from further analysis because this type of monitoring will not be accepted.

One of the two remaining *initial state* FEPs concerns the effects of an abandoned, not completely sealed repository or open monitoring boreholes (ISGen03). This FEP is handled by the residual scenario *unsealed repository* (Section 9.10).

The last *initial state* FEP concerns undetected design deviations and mishaps during manufacturing, transportation, deposition and repository operations etc (ISGen05). Measures to avoid or mitigate such deviations during excavation, manufacturing, handling deposition etc are described in the **Initial state report**. To the extent that such deviations may still occur, these issues are handled in the scenario selection in Sections 8.2.3 and 8.2.6 and included in the less probable scenario *alternative concrete evolution* (Section 8.5) and in the residual scenario *initial concrete cracks* (Section 9.8).

3.5.4 Internal processes

An in-depth understanding and handling of the processes that take place over time in the repository system is fundamental to the safety assessment. The primary sources of information for this are the results of decades of research and development work carried out by SKB and other organisations which has led to the identification and understanding of the main processes relevant to post-closure safety that are likely to occur in the repository and its environs.

There are 178 FEPs included in the main category internal processes. These are subdivided into the SFR system components waste form, concrete and steel packaging, silo barriers, BMA barriers, BRT barriers, BTF barriers, BLA barriers, plugs and other closure components and geosphere. Each FEP in this category describes a process relevant to one or more of the SFR system components, excluding the biosphere. The biosphere FEPs are handled as a separate category in the FEP catalogue, see Section 3.5.6. The various system components are also characterised by several system variables, see Section 3.5.5. Within a system component, each process is influenced by one or several of the system variables describing the state of the component, and the process, in turn, influences one or several of the system variables. The internal process FEPs are further described in the **Waste process report**, the **Barrier process report** and the **Geosphere process report**.

All *internal process* FEPs are listed in Appendix D, Tables D-2 to D-4, with references given to the corresponding descriptions in the respective process report.

3.5.5 System variables

There are 71 FEPs included in the main category *system variables.* In the same way as for *internal processes*, these FEPs are subdivided into the SFR system components *waste form*, *concrete and steel packaging*, *silo barriers*, *BMA barriers*, *BRT barriers*, *BTF barriers*, *BLA barriers*, *plugs and other closure components* and *geosphere*. Within a system component, each process is influenced by one or several of the *system variables* describing the state of the component, and the process, in turn, influences one or several of the *system variables*. The FEPs are used to characterise the system components, both in terms of the initial state of these variables and their states during repository evolution. The *biosphere* FEPs are excluded from the main category *system variables* in the same way as they are from the *internal processes*. Instead, the *biosphere* FEPs are handled as a separate main category in the FEP catalogue with their own processes and variables, see Section 3.5.6.

The following *system variables* are defined for each of the eight system components in the repository

- Gas variables.
- Geometry.
- Hydrological variables.
- Material composition.
- Mechanical stresses.
- Temperature.
- Water composition.

For the *waste form*, two additional *system variables* are defined

- Radionuclide inventory.
- Radiation intensity.

This adds up to a total of 58 *system variables* for the system components in the repository. For the geosphere, there are 13 FEPs defined with slightly different and more detailed definitions, but they essentially cover the same topics.

For all system variable FEPs defined for the system components waste form, concrete and steel packaging, silo barriers, BMA barriers, BRT barriers, BTF barriers, BLA barriers and plugs and other closure components, the FEP description and handling are identical to that in the SR-PSU.

The *system variables* are documented in the **Waste process report**, the **Barrier process report**, the **Biosphere synthesis report**, and the **Geosphere process report.** The initial state of the system components in the repository is described in the **Initial state report**, Chapter 12. A description of the initial state of the *geosphere* and the *biosphere* is provided in Chapter 4 of this report. Each *system variable* in these reports is also associated with a FEP record in the FEP catalogue.

All *system variable* FEPs are listed in Appendix D, Tables D-5 to D-7, with references given to the corresponding descriptions in the respective process report, the **Initial state report** and this report.

3.5.6 Biosphere

The *biosphere* FEPs describe variables or processes relevant to one or several of the *biosphere subsystem components*. There are 68 FEPs included in the main category *biosphere*, identified as 12 *biosphere subsystem components* (divided into 10 *physical components* and 2 *boundary components)*, 6 *biosphere variables* and 50 *biosphere processes*. These are treated separately in the FEP catalogue, i.e. they are not included in the main categories *internal processes* or *system variables*. The biosphere system components and variables are given in the **Biosphere synthesis report** and the biosphere FEPs are documented in the SR-PSU FEP report for the biosphere (SKB R-13-43).

A major effort was directed to the formulation of the *biosphere* FEPs in the SR-PSU (SKB R-14-02, **FEP report**), building on work done for the SR-Site (SKB TR-10-45) and previous safety assessments for SFR. This work also served as a basis for the analysis of biosphere FEPs in the PSAR. SKB (R-13-43) contains general descriptions of the processes considered to be of importance for the safety assessment. In addition, it contains definitions of subsystems of the biosphere and variables needed to describe the evolution of the biosphere in relation to those aspects that are of importance for radionuclide accumulation and transport. For each *biosphere process, biosphere subsystem component* and *biosphere variable* defined in SKB (R-13-43), a *biosphere* FEP has been included in the FEP catalogue.

Based on the nature of biosphere processes, six subcategories of processes can be defined (biological processes, processes related to human behaviour, chemical, mechanical and physical processes, transport processes, radiological and thermal processes and landscape development processes). In the **Biosphere synthesis report**, these process categories are defined and key processes are briefly described, pointing out mainly the changes compared with the SR-PSU. In addition, features of the physical components are briefly described.

Not all identified *biosphere processes* are expected to be quantitatively important for transport and accumulation of radionuclides. Of the 50 *biosphere processes* identified, 45 were considered sufficiently relevant to consider. However, to incorporate all 45 relevant FEPs into the biosphere transport end exposure model would result in a very complex model. Instead, many of the FEPs are included in supporting modelling used to derive parameter values for the biosphere transport and exposure model. All processes, considered and not considered, have a record in the FEP catalogue. All PSAR *biosphere* FEPs are identical to those in the SR-PSU and are listed in Appendix D, Table D-8, with references given to the corresponding descriptions in the two supporting biosphere reports for the SR-PSU (SKB R-13-43, SKB R-14-02).

3.5.7 External factors

External conditions at the disposal site may change significantly during the period addressed in the safety assessment. External conditions and the way in which they change with time are described within the main category *external factor* FEPs.

There are 27 FEPs included in the main category *external factor* in the FEP catalogue, divided into the subcategories *climatic processes and effects*, *large-scale geological processes and effects*, *future human actions* and *other*, see sections below. The results from the FEP processing of the *external factors* are described separately for each subcategory in the following.

All *external factor* FEPs are listed in Appendix D, Tables D-9 to D-12, with references given to the corresponding descriptions in the respective report.

Climatic processes and effects

Variations in climate and climate-related issues, such as the ongoing relative sea level change, are the most important external conditions that influence the conditions in the repository environs and thus may affect the repository in a time perspective up to a hundred thousand years. Most processes that are relevant to post-closure safety and that occur in the biosphere or the geosphere are affected by variations in climate and climate-related issues. The safety assessment must therefore treat the potential influence of all plausible climate-related changes on the post-closure safety of the repository.

There are seven *climatic processes and effects* FEPs included in the FEP catalogue. These represent climate and climate-related issues relevant for the repository site and have been identified to potentially influence the post-closure safety of SFR. These include climate forcing and climate evolution. Further, the following climate-related issues of relevance for the repository site in South-Central Sweden are included: development of permafrost, ice-sheet dynamics and hydrology, glacial isostatic adjustment, shore-level changes and denudation. The handling of the *climatic processes and effects* FEPs resulted in the different climate evolutions considered in the safety assessment (Section 2.6.3).

All *climatic processes and effects* FEPs are identical to those in the SR-PSU and are documented in the **Climate report** and listed in Appendix D, Table D-9.

Large-scale geological processes and effects

The large-scale geological processes are related to the mechanical evolution of the Baltic Shield and earthquakes, including uplift due to tectonic activity.

The causes of mechanical processes in the geosphere may be of quite different origin, from natural large-scale processes, such as tectonic plate movements, to fast small-scale events, such as rock fall in a tunnel. Rock mechanical processes take place in the bedrock due to changes in load or due to changes in material properties. Irrespective of the nature of the cause, the response in the rock mass will consist of some displacement and maybe fracturing. Hence, large-scale geological processes are implicit in the descriptions of intrinsic processes and interactions in the **Geosphere process report**. The large-scale mechanical evolution of the Baltic Shield as well as earthquakes are further described in the SR-Site **Geosphere process report** (SKB TR-10-48, Sections 4.1.2 and 4.1.3 respectively). These descriptions also apply to the post-closure safety assessment for SFR.

There are two *large-scale geological processes and effects* FEPs included in the FEP catalogue and these are listed in Appendix D, Table D-10.

Future human actions (FHA)

Issues related to FHA include potential human actions that are conducted at, or near, the repository site and that may affect, either directly or indirectly, the conditions of the repository. The PSAR addresses inadvertent FHA potentially resulting in changes to the barrier system affecting, directly or indirectly, the rate of the release of radionuclides from SFR, and radioactive waste being brought to the surface giving rise to exposure of people at the surface. Inadvertent future human actions are defined as actions carried out without knowledge of the repository and/or its nature (the location of the repository, its purpose and the consequences of the actions).

The methodology has been developed so that the technical aspects of *FHA* FEPs are closely tied to the safety functions of the repository system and other factors relevant from the perspective of post-closure safety, such as disposal depth and potential for natural resources. The *FHA* FEPs have

been checked against the safety functions and other factors identified as relevant in the context of assessing FHA for SFR. When identified as important to consider, they have been included in one of the four FHA scenarios assessed in the PSAR.

There are 17 *FHA* FEPs defined in the FEP catalogue. These FEPs are documented in the **FHA report** and listed in Appendix D, Table D-11.

Other

There is only one FEP defined in the subcategory *other* in the FEP catalogue and it deals with meteorite impact. This FEP has been excluded from further handling in the safety assessment. The motivation for this is that there is very little likelihood over the assessment period that a meteorite big enough to damage the repository will impact the Earth. The probability that the impact will occur on the repository site is very low. Moreover, such an impact would cause great damage to the local and regional biosphere, humans included (Collins et al. 2005). These direct effects of a meteorite impact are judged to be far more serious than any possible radiological consequences. This is discussed in the **FHA report** and the FEP is listed in Appendix D, Table D-12.

3.5.8 Methodology

The *methodology* FEPs address aspects relevant to the basic assumptions for the assessment and to the methodology used in it. There are two *methodology* FEPs (Assessment basis and Assessment methodology) included in the FEP catalogue. The *methodology* applied in the safety assessment is described in Chapter 2.

NEA PFEPs associated with the Assessment basis relate to:

- Biological evolution that might lead to different effects of radiation in the future compared with today
- Changes in society's ability to treat cancer or its view on radiation hazards
- Aspects that are addressed in the environmental impact assessment, which is part of the licence application submitted to the Land and Environment Court for permission under the Environmental Code (SFS 1998:808), rather than in the post-closure safety assessment.
- Technological advances in food production.

NEA PFEPs associated with the Assessment methodology relate to:

- Data and modelling issues such as correlations and uncertainties
- Design issues
- Implementation of various features in the modelling.

These NEA PFEPs are all mapped to the corresponding *methodology* FEP in the FEP catalogue. The *methodology* FEPs are listed in Appendix D, Table D-13.

3.5.9 Site-specific factors

The *site-specific factor* FEPs represent issues that are specifically relevant to the Forsmark site. Two site-specific factors are included in the FEP catalogue. One is related to the construction of nearby rock facilities and the other to the nearby nuclear power plant.

Construction of nearby rock facilities concerns the impact of future construction of rock facilities like the planned spent fuel repository at Forsmark or other underground constructions. Impacts of the spent fuel repository are not considered in the assessment, since no effects on a closed SFR are expected except possibly for a small hydraulic impact from the repository during its operational period (SKB TR-11-01, Section 10.2.5). Other such potential future events have been considered in the selection and analysis of scenarios related to future human actions, which is reported in the SR-PSU FHA report (SKB TR-14-08, Section 5.4).

Issues related to the nearby nuclear power plant concern the potential impact of the Fenno-Skan cable which is a submarine high voltage direct current power cable between Sweden and Finland. Corrosion has been observed in down-hole sampling equipment in boreholes at Forsmark and the effect has been attributed to the influence of electric power cables. Earth currents is one of the processes included in the **Geosphere process report** and the impact of earth currents on corrosion rates is addressed in the **Waste process report** and the **Data report**.

The *site-specific factor* FEPs are listed in Appendix D, Table D-14.

3.6 Establishment of the SFR FEP catalogue (PSAR version)

Based on the FEP analysis described above, the SFR FEP catalogue (PSAR version) was established and included in the SKB FEP database. The FEP catalogue contains all FEPs that need to be handled in the PSAR. Each FEP is represented by a FEP record specifying the FEP ID, FEP name, main category, system component and/or subcategory, description, handling, reference and revision. Table 3-2 summarises the classification of FEPs in the FEP catalogue, which comprises in total **353 FEP records**.

In Appendix D, a compilation of all FEPs in the FEP catalogue is provided together with updated references. The complete information for each FEP is present in the FEP catalogue, including updated references to the PSAR reports, and in the associated reports, see Section 3.5.1.

4 Initial state

4.1 Introduction

This chapter describes the expected state of the repository and its environs at closure, including uncertainties in the state that may affect the protective capability of the repository. The description of this *initial state* is based on the prerequisites of the present assessment (Section 2.4.3), including the year of repository closure expected to be in 2075, the reference waste inventory, the repository reference design and the site descriptive model. The initial state is the starting point for the description of the reference evolution (Chapter 6) and thus for the selection and analysis of the main scenario (Chapter 7) and less probable scenarios (Chapter 8).

This chapter begins with a description of the barriers contributing to post-closure safety (Section 4.2). Thereafter, the description of the initial state is divided into two major parts; the first part describes the waste and the repository (Sections 4.3 and 4.4) and the second part describes the conditions in the environs (Sections 4.5–4.7). The description of the waste and repository represents the estimated state at the time of closure of the repository, whereas the description of the environs, including the climate and climate-related conditions, assume that they are similar to present-day conditions.

4.2 Barriers contributing to post-closure safety

The description of the initial state focuses on, but is not limited to, the barrier system of SFR, which comprises engineered and natural barriers (Table 4-1). The function of each barrier is to, in one or more ways, contribute to the containment or retention of radioactive substances, either directly or indirectly by protecting other barriers in the barrier system (Section 2.2). Depending on the waste vault under consideration, barrier functions may be connected to the waste form (i.e. the waste in its physical and chemical form after treatment and/or conditioning), waste packaging, grouting, concrete structures, bentonite, backfill material and plugs. The barrier functions of the geosphere and the sub-sea location are related to low groundwater flow that limits concrete degradation and the radionuclide release from the repository, and to avoiding boreholes in the direct vicinity of the repository. Moreover, the geosphere provides a stable geochemical environment around the repository with reducing conditions that are favourable for slow steel corrosion and results in effective sorption on material surfaces in the repository for many elements. The geosphere and the sub-sea location are also barriers to human intrusion. All vaults will be sealed with plugs (see Section 4.4.8). These plugs have hydraulic barrier function which reduces the groundwater flow through the vaults. The description of the barrier functions is an important basis for the definition of *safety functions* (Chapter 5).

The barrier functions of the various components are described for each vault in Section 4.4. The components with the most important barrier functions (Table 4-1) are also assigned a safety function; these are selected in Chapter 5, which also provides additional descriptions complementing those in Section 4.4. Components with indirect contributions to post-closure safety are still considered barriers. These include, for example, components providing mechanical stability, which are also included in Table 4-1 even though they are not assigned a safety function.

Table 4-1. Barriers essential to the post-closure safety of the SFR repository and its different vaults, as described under the subsections *Barriers contributing to post-closure safety* in Section 4.4.

Silo	1–2BMA	1BRT	1–2BTF	1–5BLA
Waste form	Waste form	Waste form	Waste form[1]	-
Concrete moulds	Concrete moulds		Concrete packaging[2]	-
Concrete structures[3], grout[4]	Concrete structures[5]	Concrete structures[6]	Concrete structures[7], grout[4], cementitious backfill[8]	-
Bentonite[9]	-	-	-	-
Gas evacuation system	Gas evacuation system[10]	-	-	-
Backfill (top)	Backfill[11]	Backfill[11]	Backfill[11]	-
Plugs[12]	Plugs[12]	Plugs[12]	Plugs[12]	Plugs[12]
Geosphere	Geosphere	Geosphere	Geosphere	Geosphere
Sub-sea location	Sub-sea location	Sub-sea location	Sub-sea location	Sub-sea location

[1)] Ash-filled drums (concrete between outer and inner drums).
[2)] Concrete tanks and concrete moulds.
[3)] Slab, outer wall, inner walls and lid.
[4)] Grout around waste packages.
[5)] 1BMA: slab, existing and new outer walls, inner walls and lid.
2BMA: slab below caissons, caissons including slabs, outer and inner walls and lids.
[6)] Slab, walls, inner walls between waste packages and lid.
[7)] Slab and lid.
[8)] At sides between waste packages and rock.
[9)] Side bentonite layer, bottom and top sand-bentonite layers.
[10)] Applies to 2BMA only.
[11)] Backfill material in waste vaults and in tunnels adjacent to plugs and foundation material on which the structures rest.
[12)] Bentonite in plugs in connection with waste vaults and bentonite in plugs in tunnels.

4.3 Waste

This section describes the waste in terms of a reference waste inventory and summarises the information contained in the **Initial state report**. Waste in its physical and chemical form, after treatment and/or conditioning where applicable, is here denominated waste form. The waste form together with its waste packaging constitutes a waste package.

4.3.1 Origin of the waste

Operational waste

A large part of the waste in SFR comes from the operation of the Swedish nuclear power plants. Radioactive waste stems from radioactive materials produced when neutrons from nuclear fission in the reactor core react with atoms in surrounding materials, the reactor water or material deposited on the core surfaces (so called *crud*) to produce radionuclides. Furthermore, radionuclides are also formed in the fission process itself and by neutron capture in the fuel material. These radionuclides are typically contained within the fuel rods but can be released to contaminate the reactor water and surfaces of the reactor in the case of fuel damage.

The reactor water undergoes clean-up to remove the radionuclides and other impurities. The reactor water is purified in the reactor's clean-up circuits by means of ion-exchange resins that retain ionic radionuclides in the reactor water. The ion-exchange resins serve also as filters to remove contamination in the form of dispersed particles.

Even though most of the radionuclides are removed from the reactor water by the clean-up system, all surfaces that come in contact with the reactor water or steam (in the case of a BWR) will be contaminated to some degree. Hence, even the ion-exchange resins used to purify the water from the condensers in BWR plants will be radioactive.

Waste consisting of such ion-exchange resins, as well as mechanical filter resins, evaporator concentrates and precipitation sludges arises during the operational period.

Some radionuclides are released from the spent fuel stored in storage pools at the nuclear power plants and at the interim storage Clab. The pools also have clean-up systems with ion-exchange resins that are used in roughly the same way as in the reactor water clean-up systems.

Solid waste is also generated. Some solid waste consists of components of the primary system or other active systems at the nuclear facilities, but most consists of material that has been brought into a controlled area and contaminated and then discarded.

In addition to the waste from the nuclear power plants and Clab/Clink, operational waste is produced by the activities at Studsvik Nuclear AB, AB SVAFO and Cyclife AB. Operational waste has also arisen from the Ågesta nuclear reactor. Radioactive wastes also arise in other industrial activities, research and medical care.

Decommissioning waste

Large quantities of contaminated scrap metal and concrete are generated during decommissioning of nuclear power plants. Most of the decommissioning waste is conventional or is released as conventional waste if the level of radioactivity is shown to be below the regulatory limits for clearance or after approval from SSM. For the very low-level waste, near-surface repositories are planned to be used when available. The remaining volumes of short-lived low- and intermediate-level waste are to be disposed in SFR. Materials that have been close to or within the reactor core, such as control rods and other core components, are classified as long-lived and are planned to be disposed in the repository for long-lived low- and intermediate-level waste, SFL.

The reactor pressure vessels (RPVs) of the BWR have sufficiently low levels of activation in the material to qualify as short-lived waste suitable for disposal in SFR. To limit exposure during decommissioning, the RPVs and other surfaces of the primary circuits will be decontaminated. Decontamination will also likely be performed for less active surfaces to achieve activity levels below the clearance limits. Ion-exchange resins will be used to process the liquid waste from decontamination and the spent resins are to be disposed in SFR. Secondary waste is also expected from decommissioning when equipment and material, brought into a controlled area, is contaminated and then discarded.

4.3.2 Materials in the waste

A large part of the radioactivity in the operational waste originates from different water clean-up systems. This waste consists of bead resin, powdered resin, mechanical filter aids, evaporator concentrate and precipitation sludge. The ion-exchange resins consist of organic polymers with acidic or basic groups, making them capable of cation or anion exchange.

A relatively large fraction of the operational waste consists of metals, mostly carbon steel and stainless steel. Scrap metal arises mainly during maintenance outages when plant systems are modified, renovated or dismantled.

The largest volume of raw waste consists of combustible solid waste. However, incineration or disposal in near-surface repositories, means that the volume remaining for disposal in SFR is comparatively small. The waste consists mainly of plastics (including PVC, polyamine, polystyrene, polyethylene and polypropylene) and cellulose-based materials (paper, cotton and wood), although cellulosic waste has in recent years decreased due to concerns about complexing agents (Section 6.2.8). Ashes from incineration of this type of waste are also disposed in SFR.

In addition to these materials, operational waste also includes mineral wool, brick and concrete, as well as small quantities of other materials.

Management of radioactive material that does not come from nuclear-power activities takes place at the facilities in Studsvik before final disposal. Examples of such waste are spent radiation sources, equipment containing radiation sources, waste from radiotherapy units, radioactively contaminated

material and radioactive chemicals. This handling gives rise to scrap metal in the form of iron, stainless steel and aluminium, and trash in the form of residual products such as ashes and soot from incineration of combustible waste such as clothing and rags.

The radioactive waste from decommissioning of the nuclear power reactors primarily consists of iron, steel and concrete. Large quantities of concrete come from the so-called biological shields surrounding the reactor pressure vessels. In addition to these materials, there are also other metals, sand from sand beds in the off-gas treatment system and some secondary waste (metals, plastic and cellulose-based materials).

4.3.3 Waste packaging

Nearly all waste disposed in SFR is contained in some kind of packaging. The different types of waste packaging in use or planned to be used in SFR are described below and shown in Figure 4-1.

Steel packaging such as containers, steel moulds and drums, will start corroding already during (and even before) the operational period. However, this corrosion is not expected to be extensive and not significantly affect their integrity. Corrosion of rebars, in concrete tanks and moulds, that cause small cracks in the concrete during the operational period cannot be ruled out. This is not expected to be of importance for the properties of the concrete packages as sorption barriers for radionuclides but may lead to increased hydraulic conductivity compared with fully intact concrete.

ISO container

ISO containers of steel are used for low-level solid waste from both operation and decommissioning, which is disposed in the BLA vaults. Inside the containers, the waste is packed in boxes, bales, drums or directly in the container. The containers are made of carbon steel and consist of 20-foot full- and half-height containers and 10-foot full- and half-height containers. A 20-foot full-height container has outside dimensions of 6.1 m × 2.5 m × 2.6 m (L × W × H).

Steel mould

Steel moulds are used primarily for cement- or bitumen-solidified waste (ion-exchange resins, filter aids, evaporator concentrates) or concrete-embedded solid waste, which is disposed in the silo and 1–2BMA. The steel moulds are made of carbon steel. The outside dimensions of the steel moulds are 1.2 m × 1.2 m × 1.2 m.

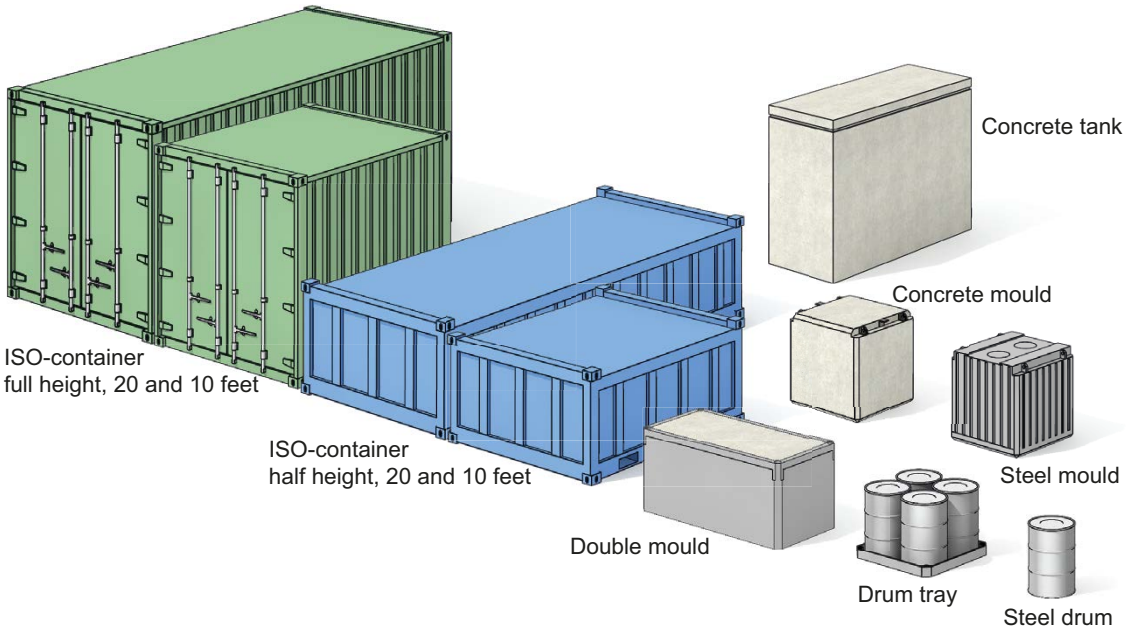

Figure 4-1. *Schematic illustration of waste packaging used or intended to be used in SFR.*

Double mould

SKB plans to use steel double moulds for intermediate-level decommissioning waste that will be disposed in 2BMA or 1BRT. The waste in double moulds primarily consists of concrete and steel, but also sand. Among other things, the segmented reactor pressure vessels from BWR are planned to be disposed in this type of container. The waste is embedded in concrete. The double moulds are made of carbon steel. A double mould is twice as big as a steel mould. The outside dimensions of the double mould are 2.4 m × 1.2 m × 1.2 m (L × W × H).

Steel drum, drum tray

Steel drums are used primarily for cement- and bitumen-solidified waste, which is disposed in the silo and 1BMA, as well as for ashes, which are disposed in 1BTF. Furthermore, steel drums are used as inner packaging in some containers and moulds. The standard outer dimensions of the steel drums are: diameter 0.6 m and height 0.9 m.

Steel drums assigned to the silo and 1BMA are usually handled on a drum tray, normally made of carbon steel, but some are made of stainless steel. Using a drum tray enables four drums to be handled at the same time with outside dimensions of 1.2 m × 1.2 m × 0.9 m (L × W × H).

Concrete tank

Concrete tanks are used for dewatered ion-exchange resins, filter aids and sludges, which are disposed in 1–2BTF. The concrete tanks are made of 15-cm-thick reinforced concrete. The outside dimensions of a concrete tank are 3.3 m × 1.3 m × 2.3 m (L × W × H).

Concrete mould

Concrete moulds are used primarily for solidified waste (ion-exchange resins, filter aids, evaporator concentrates and sludges) or concrete-embedded solid waste that is disposed in the silo, 1–2BMA and to a lesser extent (used as supporting walls) in 1BTF. Concrete moulds are made of reinforced concrete, normally with a wall thickness of 10 cm, but sometimes thicker. The outside dimensions of the concrete mould are 1.2 m × 1.2 m × 1.2 m.

4.3.4 Waste acceptance criteria (WAC)

The main tool used to ensure that the waste is properly managed and emplaced in the correct waste vault in SFR is the set of WAC. WAC are quantitative or qualitative requirements given in the safety analysis report (SAR) for the existing repository and address post-closure safety but also aspects related to waste handling during the operational period that must be fulfilled for the waste to be accepted for final disposal. The WAC include general requirements on geometry, dimensions, weight, labelling and conditioning, as well as radiological, chemical, physical and mechanical requirements.

SFR1 have had a complete, standalone set of WAC since 2012. It has been updated successively and version 5.0 was approved in 2021.[18] When the WAC is updated, existing waste types undergo a compliance control with respect to the new requirements. If not fully compliant, SKB judges whether the non-compliance has an insignificant impact on the safety of SFR in which case no action is needed. On the other hand, if measures are warranted, these could for example be updates to the safety assessment including increased conservatism, or practical measures within SFR.

As of now and until taken into operation, SFR3 has only preliminary WAC, largely based on the SFR1 WAC.

To systematically classify the wastes, different waste types have been defined. All waste that is disposed in SFR must satisfy an approved waste type description that covers the whole handling sequence from production to final disposal for each specific waste type. The waste type descriptions contain

[18] Södergren K, Snis K, Reitti M, 2021. Acceptanskriterier för avfall i SFR. SKBdoc 1336074 ver 5.0, Svensk Kärnbränslehantering AB. (In Swedish.) (Internal document.)

information on how the WAC, relevant for the specific waste type, are to be fulfilled and verified. More information on WAC, waste handling and quality controls is found in the **Initial state report**, Chapter 3**.**

4.3.5 Waste volumes and material quantities

Waste volumes, material quantities and radionuclide inventories for the waste vaults are presented in this section. The waste volume allocated to SFR1 according to the current prognosis is about 54 000 m^3 of operational waste and less than 400 m^3 of decommissioning waste to be disposed in the silo. The waste volume allocated to SFR3 according to the current prognosis is 100 000 m^3, whereof more than 80 % is decommissioning waste.

The waste volumes allocated to different waste vaults are shown in Figure 1-3. The waste volumes, material quantities and inventory of radionuclides are based on the current prognosis given in the inventory report (SKB R-18-07) where the number of packages of the different waste types allocated to the respective waste vaults are also reported. Characteristics of the waste in the respective vaults are summarised in Appendix E, Table E-3, including material quantities and corrosion surface areas in the waste form and the packaging, the voids and pore volumes in the packaging along with the outer volume and disposal volume of waste packages.

Uncertainties in the waste volume and uncertainties related to unforeseen changes in operational conditions at the waste producers have not been considered. Uncertainties in material composition with regard to gas-forming materials, ion-exchange resin, cellulose as well as aluminium and zinc have been calculated (SKB R-18-07, Section 3.3 and Table C-3). The uncertainty in ion-exchange-resin quantity affects C-14 and Cl-36, for which the accumulated activity is distributed to the packages in proportion to the quantity of ion-exchange resin per package.

The waste type S.14 (concrete-embedded trash and scrap metal) has been included with the information regarding activity and material available in the waste register and earlier estimates of the material composition. This is assumed to be representative since the deviating waste suspected to be present in some S.14 packages is assumed to be removed from 1BLA (SSM 2020) prior to closure of the facility. The removed waste will be further characterised, and disposed according to the results, where SFL could be an option if SFR is found not suitable.

4.3.6 Waste allocation to different vaults

The distribution of waste packages between vaults in SFR is given in the inventory report (SKB R-18-07). The characteristics of waste assigned to each vault are described in the subsequent sections.

Waste in silo

The silo is intended for intermediate-level waste. The waste form consists of bitumen- or cement-solidified ion-exchange resins and smaller quantities of concrete-embedded trash and scrap metal. A limited amount of cement-solidified sludge is also included. The waste is disposed in concrete- and steel moulds or in steel drums on a drum tray.

Waste in 1–2BMA

The 1–2BMA vaults are intended for intermediate-level waste. The waste form in 1BMA consists primarily of bitumen- or cement-solidified ion-exchange resins and concrete-embedded trash and scrap metal. A small quantity of evaporator concentrates and sludge is also disposed here. The waste in 1BMA is packaged either in concrete and steel moulds, in steel drums on drum trays or in steel boxes. 2BMA is designed primarily for intermediate-level waste such as trash, scrap metal, sand and concrete. The waste in 2BMA will normally be disposed in concrete or steel moulds and in steel double moulds. Steel drums placed on drum trays can also be used as packaging.

Waste in 1BRT

The 1BRT vault is intended for decommissioning waste which primarily consists of segmented reactor pressure vessels (RPVs). The waste in 1BRT includes the ten BWR pressure vessels from Barsebäck

(B1, B2), Forsmark (F1, F2, F3), Oskarshamn (O1, O2, O3), Ringhals (R1) and Ågesta. In addition, the non-activated but contaminated parts from the segmented PWR pressure vessels, Ringhals (R2, R3, R4), are also included in the 1BRT waste inventory. The waste from the pressure vessels, which consists exclusively of iron and steel, is placed in steel double moulds and embedded in concrete. The exchanged reactor pressure vessel lid from R2 and the two exchanged reactor pressure vessel lids from R3 and R4, will also be disposed in 1BRT.

Waste in 1–2BTF

The waste form in 1–2BTF is primarily dewatered ion-exchange resins. Ashes and some cement-solidified ion-exchange resins are also disposed in 1BTF.

Waste in 1–5BLA

1–5BLA are all intended for low-level waste. Operational waste that consists primarily of trash and scrap metal but also bitumen- or cement-solidified waste (ion-exchange resins, evaporator concentrates and sludge), is disposed in 1BLA. The waste form in 2–5BLA includes a small fraction of operational waste in the form of trash and scrap metal, while most of it is decommissioning waste consisting of concrete, metals, sand etc.

4.3.7 Radionuclide inventory

The radionuclide inventory for SFR, including uncertainties, is calculated from the best-estimate inventory and uncertainties for different wastes (SKB R-18-07).

The main difference in the present inventory compared with the inventory calculated for the SR-PSU is that the radionuclide inventory in the decommissioning waste from the nuclear facilities at the Studsvik site is now included.

Furthermore, some components that were previously excluded from the reported short-lived decommissioning waste, have now been included. Non-activated parts (with only surface contamination) from the Swedish PWR reactor pressure vessels, for example, are now disposed in 1BRT. The estimated activity of these parts includes activity for some radionuclides that were not present in the previous 1BRT inventory. Isotopes of uranium, which were previously excluded from the decommissioning waste from the NPPs, are now included. Hence this additional information could appear as a significant difference compared with the inventory in SR-PSU, but the absolute activity levels for these radionuclides are quite modest.

Another significant difference in the PSAR is that some operational waste is allocated to 2BMA, which results in an overall activity increase for this particular waste vault whereas the corresponding decrease can be observed in 1BMA.

The Swedish inventory of discarded industrial smoke detectors that previously was planned for disposal in the silo is now allocated to SFL. The activity levels of the radionuclides Am-241 and its decay product Np-237 are therefore substantially lower in the silo as compared with those adopted in SR-PSU.

There are also some differences with respect to the methodology. The method for estimating the activity levels of Ni-59 and Ni-63 in low- and intermediate-level waste from Clab has been updated since SR-PSU. The method is now based on measurements of Ni-63 and subsequent correlation of Ni-59 instead of the previous correlation of these two radionuclides with the Co-60 activity. The result of this change is a somewhat higher inventory of Ni-63 and Ni-59 in the silo.

The distribution of non-package-bound data has been improved for the radionuclide C-14, where the distribution now is based on the actual ion-exchange resin weight in the waste package rather than the weight of the whole waste form. This change results in a redistribution of C-14 activity for waste packages containing waste of common origin but having different waste forms. Moreover, C-14 from the PWRs is now distributed to all waste packages containing ion-exchange resins from Ringhals NPP. Previously, this activity was thought to be confined to waste in the silo, but there is not enough evidence to support this assumption. In general, the so-called difficult-to-measure radionuclides for the operational waste forecast are now estimated from a forecast of non-package-bound activity based on a statistical analysis of yearly reported activity levels for disposed activity.

Finally, the present inventory is compiled from all disposed and forecast packages individually whereas the previous inventory was compiled from package type average activities. The previous approach led to short-lived radionuclides being overestimated in vaults dominated by already disposed waste and underestimated in vaults that primarily will contain forecast operational and decommissioning waste.

The reference inventory for 2075, the estimated year of repository closure, is shown in Figure 4-2. The uncertainties are handled in a probabilistic manner and include measurement uncertainties, uncertainties in correlation factors and uncertainties in other methods used to calculate the best estimate of the radionuclide inventory (see more details in the **Initial state report** and SKB R-18-07). Uncertainties in material composition applicable to ion-exchange resin, cellulose as well as aluminium and zinc have also been calculated. The uncertainty in ion-exchange resin quantity affects C-14 and Cl-36, for which the accumulated activity is distributed to the packages in proportion to the quantity of ion-exchange resin per package.

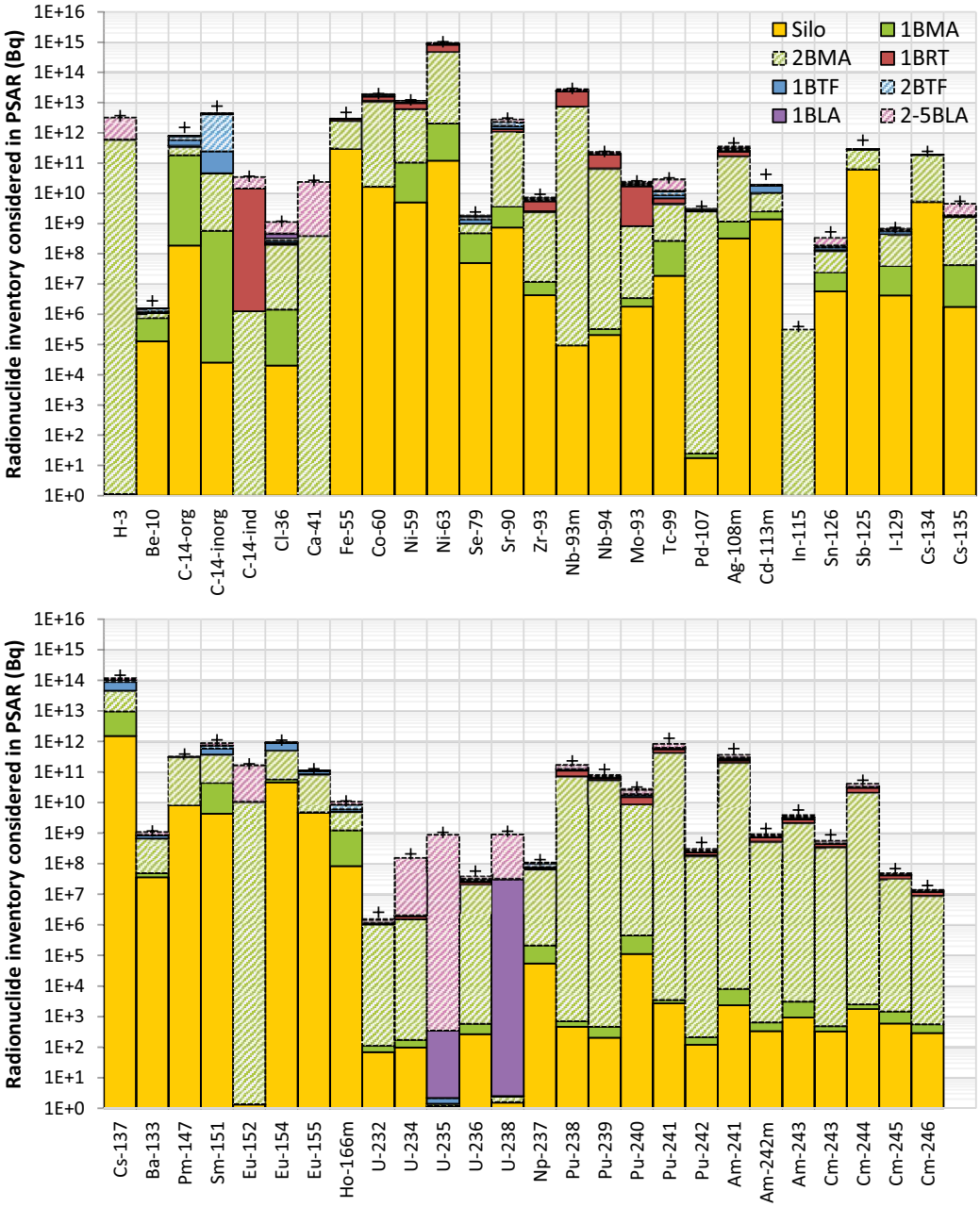

Figure 4-2. *Radionuclide inventory considered in the PSAR. The top of each bar shows the best estimate of total disposed activity in SFR (Bq, left vertical axis) and the black plus shows the uncertainty (95th percentile). Also, the fraction of disposed radioactivity in each waste vault is indicated by the colours (on a linear scale) for each radionuclide with shading according to the legend. (Based on Table E-1 and Table E-2 in Appendix E.)*

Uncertainty in waste volume and uncertainties related to unforeseen changes in operational conditions at the waste producers have not been considered in the uncertainty compilation presented in Figure 4-2. However, such changes have been considered by three alternative inventories that are used as the basis for a residual scenario. The alternative inventories include extended operation of the remaining reactors from 60 years to 80 years, extensive fuel damage during the remaining operation, and extended use of fuel spacers with a high molybdenum content. The input data for these calculation cases is described in the **Data report**, Chapter 4.

4.4 Repository

This section describes the repository in terms of a reference design and summarizes the information contained in the **Initial state report**. The respective vaults are presented in Sections 4.4.1–4.4.7.

SFR is a subsea hard rock repository that is reached via two access tunnels from a surface facility. SFR1 comprises a silo and four waste vaults for different waste categories. The waste vaults are located about 60 m down in the bedrock. The bottom of the silo is located much deeper, however, about 130 m down in the bedrock. When SFR3 is built it will comprise six waste vaults located about 120 m down in the bedrock, which means that they are approximately at the same level as the bottom of the silo, see Figure 4-3.

The reference design of SFR3 has been developed since SR-PSU was submitted to SSM and repair measures are planned for 1BMA in SFR1. The main design features that have changed are:

- In 1BMA, concrete walls will be erected outside the existing structure and a concrete lid will be cast on top to ensure an adequate initial state.
- The height and width of both the rock cavity and caissons have increased in 2BMA and the number of caissons has decreased by one.
- There will be no grouting of 1–2BMA.
- Inner walls will be constructed within the caissons of 2BMA.
- The reactor pressure vessels will be segmented and packaged rather than disposed whole. 1BRT will contain a concrete structure with compartments for embedded waste packages. The waste packages are surrounded by grout. On top of the radiation shielding lids a reinforced concrete lid will be cast.
- The dimensions of the 1BRT waste vault have increased.
- The geometry of the 2–5BLA waste vaults has been slightly modified.

The reference design for the extension of SFR, except for that used in the post-closure safety assessment, is based on the design Layout 2021 (**Initial state report**). The post-closure safety assessment for the SFR repository (PSAR), including this report, is instead based on the repository extension design from Layout 2020. Since the preparation of a licence application is a relatively long process, the hydrogeological models for the PSAR are based on an earlier design than described in this report (Abarca et al. 2020, Section 3.1, Öhman and Odén 2018), these discrepancies are very small and will not have a significant effect on the conclusions from the safety assessment. All other parts of the post-closure safety assessment are, however, based on the design described in present report. An overall picture of the closed repository is shown in Figure 4-4.

Inspection and control of the repository during construction and operation

Handling of uncertainties in the initial state of the barriers is a central aspect of the safety assessment. To limit the uncertainties in the initial state of the vaults, inspections and controls are to be carried out (**Initial state report**). SKB has a quality management system that includes procedures for e.g. project management and safety audit. These procedures have served as a basis for framing the control documents, or quality assurance systems, that have governed the work with both SFR1 and SFR3. The quality management system meets the requirements in ISO 9001:2015.

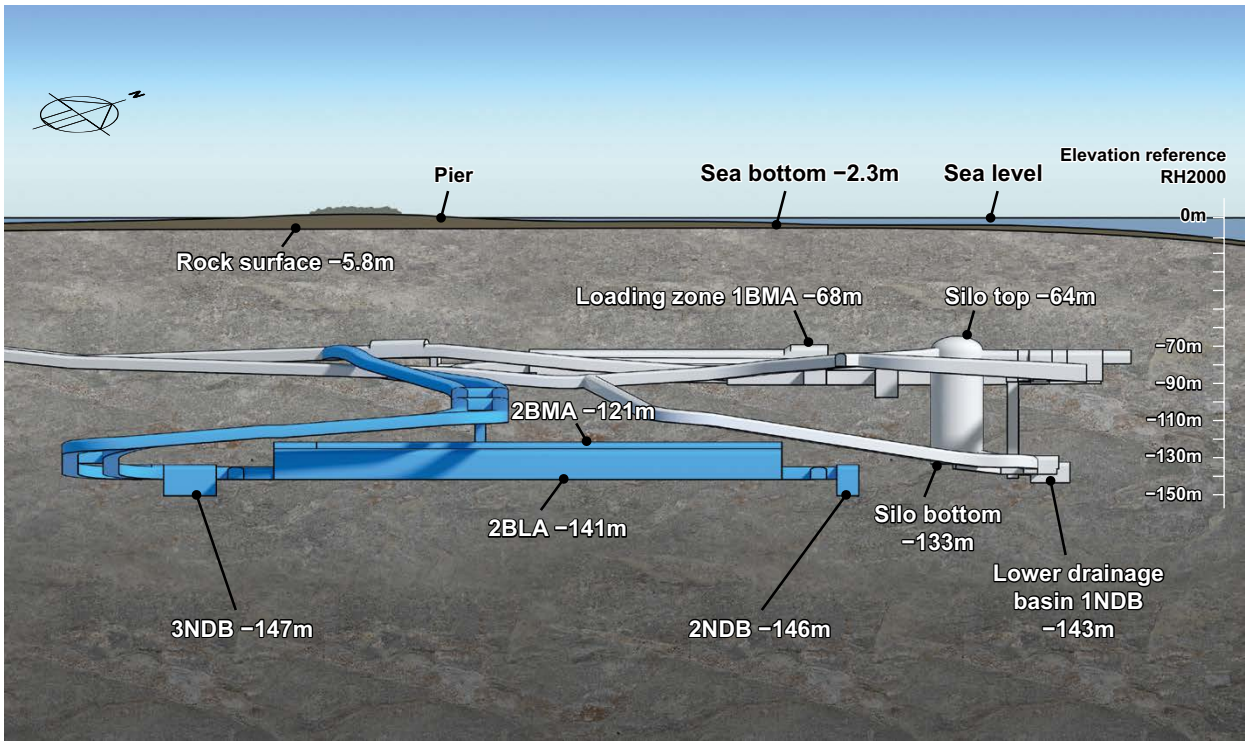

Figure 4-3. *View of SFR with designated levels in RH2000 (the Swedish national reference height system). View is towards the NW, approximately perpendicular to the waste vaults. The grey part is SFR1 and the blue part is SFR3.*

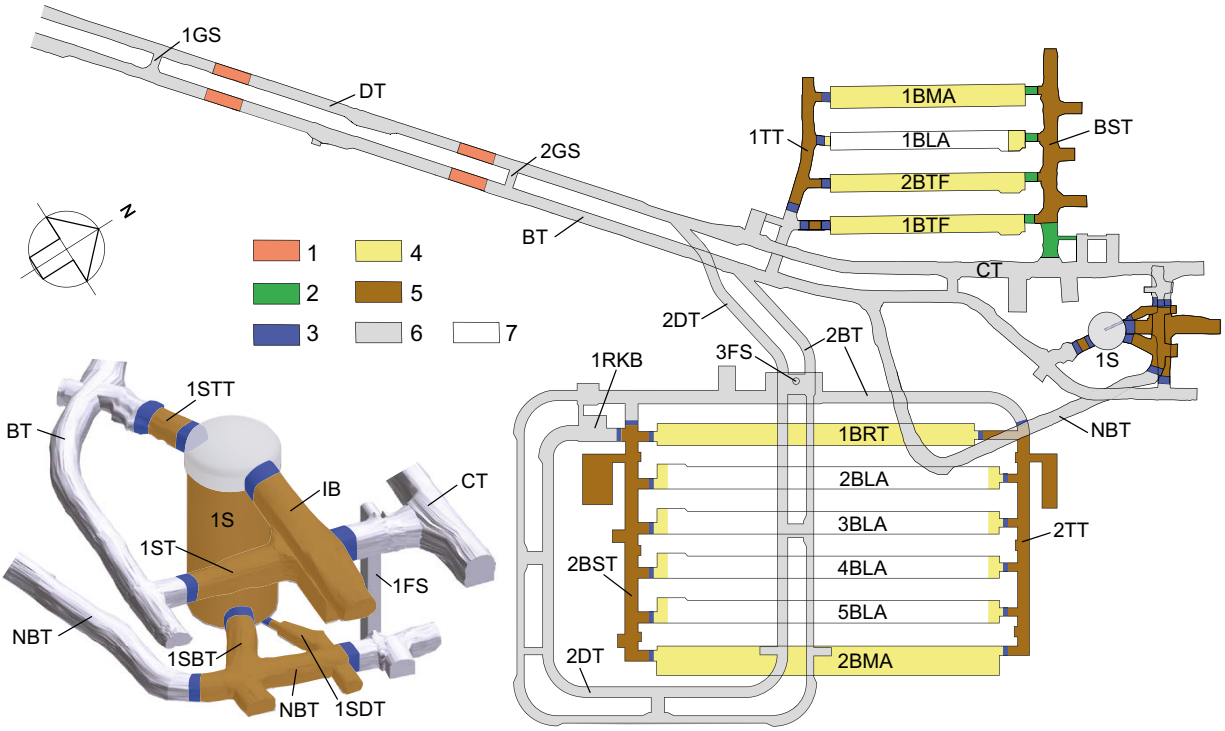

Figure 4-4. *Schematic plan of the closed SFR with a detailed view of the silo. Key to numbering: 1) Plugs in access tunnels 2) Transition material 3) Mechanical plug of concrete 4) Backfill material of macadam 5) Hydraulically tight section of bentonite 6) Backfill material in access tunnels and the central area of the tunnel system 7) Non-backfilled openings. Note that the figure shows the Layout 2021 while Layout 2020 is used as basis for the modelling in the PSAR (except for hydrogeology that uses an earlier layout).*

In particular, there is a focus on the system uncertainties related to the initial state of 1BMA after the planned measures to repair and strengthen the concrete structure. For the 1BMA repairs and the vaults in SFR3, controls and inspections are to be undertaken during construction to ensure that requirements are met. During the emplacement of the waste, the conditions in each waste vault will be inspected and controlled.

Before closure, final inspections and controls are to be carried out in all vaults, including planned backfilling and plugs. The inspections and controls are to ensure an adequate knowledge of the achieved initial state of the waste vaults, which reduces the overall assessment uncertainties.

4.4.1 Silo

The silo is a cylindrical vault with a free-standing concrete cylinder, see Figure 4-5. The silo vault is about 70 m high with a diameter of about 30 m. The concrete cylinder is made of *in situ* cast concrete and the concrete bottom is founded on a bed of 90 % sand and 10 % bentonite. The concrete cylinder is divided into several vertical shafts, and the gap between the concrete cylinder and the rock is filled with Na-bentonite. The material composition of the bentonite is given in the **Initial state report**, Section 12.3.5. The rock walls are lined with shotcrete and a rock drainage system is installed between the bentonite and the rock.

Conditioned intermediate-level waste is disposed in the silo in concrete and steel moulds as well as in steel drums, see Figure 4-5. Grouting of waste packages in the shafts is done progressively. During operation, each shaft is provided with a radiation shielding lid that will be removed before closure.

Figure 4-5. *The silo, a vault for intermediate-level waste in SFR1, during the operational period.*

Description of the closure of the vault

The closure plan for SFR (Mårtensson et al. 2022) describes the planned measures for closure of the silo. In an initial step of the closure, the shafts are to be covered with cement grout up to the top rim of the concrete silo. This provides a radiation shield on top of the concrete silo, which simplifies the work of reinforcing and casting a concrete lid. The concrete lid is cast on a thin layer of sand and provided with gas venting in the form of pipes filled with sand that penetrate the lid, see Figures 4-6 and 4-7.

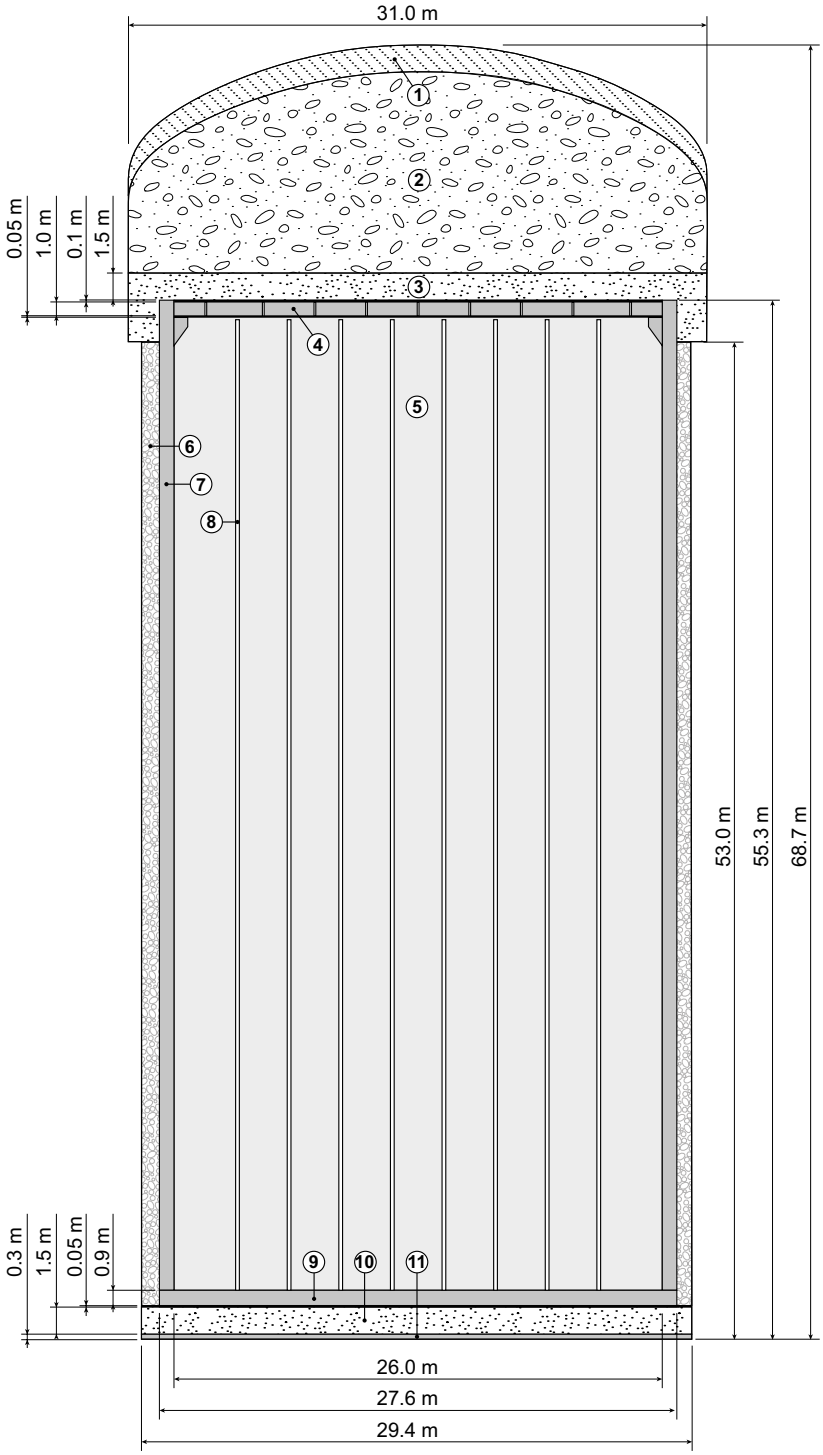

Figure 4-6. *Schematic vertical cross-section of the silo at closure. The waste packages are surrounded by grout in this waste vault. Key to numbering 1) Cement-stabilised sand 2) Crushed rock backfill 3) Compacted fill with a mixture of 10 % bentonite and 90 % sand 4) Reinforced concrete slab with sand layer and gas evacuation channels 5) Waste 6) Side bentonite layer 7) Outer concrete wall 8) Inner (shaft) walls of concrete 9) Concrete slab 10) Bottom sand-bentonite layer 11) Bottom drainage system.*

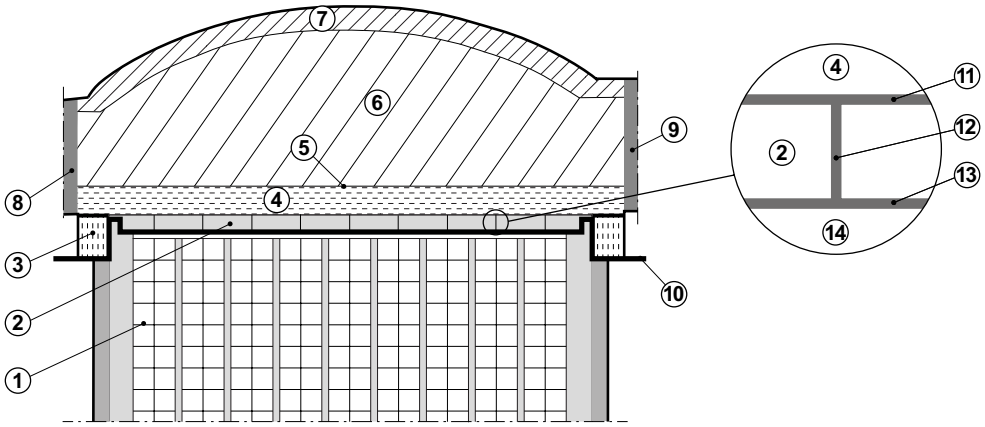

Figure 4-7. *Schematic cross-section of silo top at closure. Key to numbering: 1) Waste 2) Reinforced concrete slab with sand layer and gas evacuation channels 3) Compacted fill with a mixture of 30 % bentonite and 70 % sand 4) Compacted fill with a mixture of 10 % bentonite and 90 % sand 5) Unreinforced concrete slab 6) Compacted fill of friction material 7) Cement-stabilised sand 8) Constraining wall of concrete against silo roof tunnel (1STT) 9) Constraining wall of concrete against loading-in building (IB) 10) Boundary between works associated with grouting and backfilling 11) Sand layer 100 mm 12) Gas evacuation channel Ø 0.1 m 13) Sand layer 50 mm 14) Grout (permeable).*

The top bentonite layer in the gap between the rock and the concrete silo may have been affected during the operational period and is planned to be replaced and complemented with new bentonite. The silo top above the concrete lid is to be backfilled with different layers of backfill material. The backfill materials intended to be used in the silo top are shown in Figure 4-7. A mixture of sand and bentonite is placed on top of a thin layer of sand and protected by a thin unreinforced concrete slab. The space above it is filled with crushed rock or macadam and, at the very top, with cement-stabilised sand.

Finally, a plug is installed at the bottom of the silo and two at the top to seal the silo, see Section 4.4.8.

Barriers contributing to post-closure safety

The entire concrete silo and its interior including shaft walls, grout, concrete moulds and waste form serve as mechanical elements that withstand the swelling pressure from water-saturated bentonite, the pressure from gas formation and the load from self-weight. All these cementitious materials also have chemical barrier functions by ensuring good sorption properties for many radionuclides on the surface of the material, thus limiting their release. Cementitious materials also set a high pH value, which limits corrosion of steel and gas production caused by microbial activity.

Concrete moulds, concrete structures and grout also contribute to limit the groundwater flow through the waste and thus the release of radionuclides.

The side bentonite layer mainly constitutes hydraulic barrier, which limits the groundwater flow through the waste. The top and bottom sand-bentonite layers also have hydraulic barrier function. The bottom layer also contributes mechanically stable foundation for the concrete structure. The bentonite also contributes to good sorption properties for many radionuclides.

The gas evacuation system in the silo top has a barrier function to allow gas to escape to avoid high gas pressure which can result in gas-driven advective transport of dissolved radionuclides.

The top backfill of crushed rock protects the engineered barriers against rock fallout.

Condition of the subcomponents at initial state

The waste packages in the silo are embedded in grout as they are emplaced. This means that the condition of the waste packages cannot be inspected afterwards. Steel packaging will probably start to corrode during the operational period. The possibility of small cracks, more than 0.1 mm wide, forming in the concrete packaging during the operational period cannot be ruled out.

The silo concrete barrier is anticipated to be intact (i.e. non-cracked) at closure of the repository. Due to the bentonite barrier outside the concrete barrier in the silo, continuous inspection of the concrete barrier is difficult to perform and inspection has therefore only been done during construction. The condition of this barrier at closure is thus somewhat uncertain.

4.4.2 1BMA, vault for intermediate-level waste

The 1BMA waste vault is approximately 20 m wide, 17 m high and 160 m long. The waste is disposed in an approximately 140 m long concrete structure divided into 13 large compartments and two smaller compartments. The load-bearing parts of the concrete structure are founded on solid rock and the slab on a base of crushed rock levelled with gravel. The slab and walls structures are made of *in situ* cast reinforced concrete. To keep the forms in place during casting, penetrating form rods made of steel were used. The walls and roof in the vault are lined with shotcrete.

In the compartments, concrete and steel moulds, as well as steel drums (on a drum tray or in a drum box) are disposed by a remote-controlled overhead crane that runs on the top edge of the walls of the concrete structure, see Figure 4-8. The waste is disposed in an appropriate compartment as it arrives at SFR; moulds are stacked six high and drums eight high. As the compartments are filled, they are temporarily closed with thick radiation-shielding prefabricated concrete elements. At least two rows of concrete moulds are installed in each compartment to support the prefabricated concrete elements.

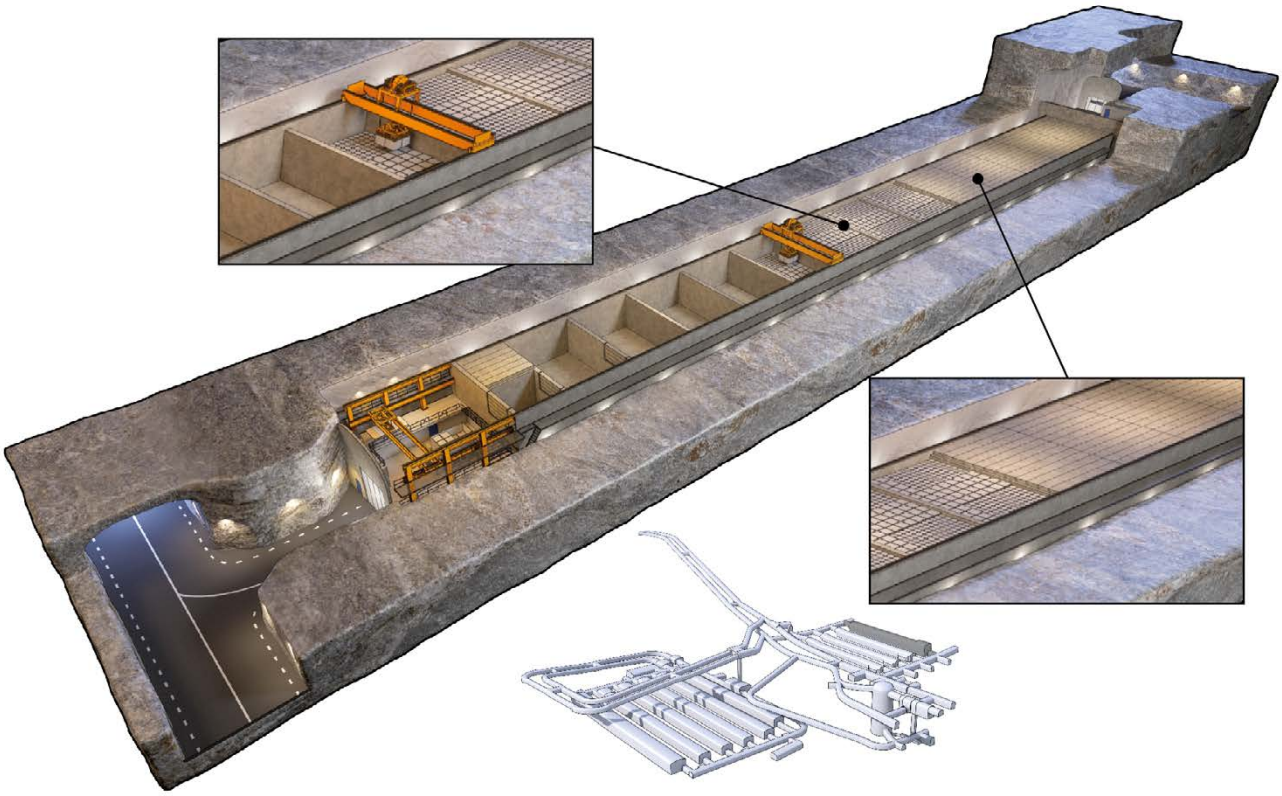

Figure 4-8. *Vault for intermediate-level waste, 1BMA, in SFR1 during the operational period. The upper detail shows the emplacement of waste packages, the lower detail shows the concrete lid. In addition, there is a view of SFR with the position of 1BMA in darker grey.*

Description of the closure of the vault

The closure plan for SFR (Mårtensson et al. 2022) describes the planned measures for closure of 1BMA. An extensive programme for investigation of the concrete structure has been carried out and has revealed that extensive repair and strengthening measures need to be adopted to achieve the desired hydraulic and mechanical properties at closure. The repair and strengthening measures are planned to take place when the operational period is complete (Elfwing et al. 2018). The measures include that new reinforced external concrete walls are erected on the outside of the existing ones, see Figure 4-9. This will limit groundwater flow through the waste and will compensate for the cracking that has been observed in the existing structure. The external concrete walls replace the existing ones as the main hydraulic barrier of the concrete structure and ensure that the desired initial state is obtained. A thick reinforced concrete lid that can carry the load of the backfill material is cast on top of the prefabricated concrete elements that provide radiation shielding during the operational period, Figure 4-9. It should be noted that the base slab in 1BMA is not being repaired by injecting cement into cracks or by introducing a new hydraulic barrier. The slab is thus considered to be highly conductive in this assessment.

When the operations are concluded, but before closure, the equipment and installations in the vault are removed and the space between the concrete structure and the rock wall is backfilled with macadam, see Figure 4-9.

At the end of the waste vault that connects to the transverse tunnel (1TT), a concrete plug is installed as a mechanical constraint for the bentonite in the tunnel. It is not possible to install a concrete plug in the connection to the waste vault tunnel (BST); instead, here the mechanical constraint for the bentonite consists of a section with transition material and backfill material in the waste vault, see Figure 4-4.

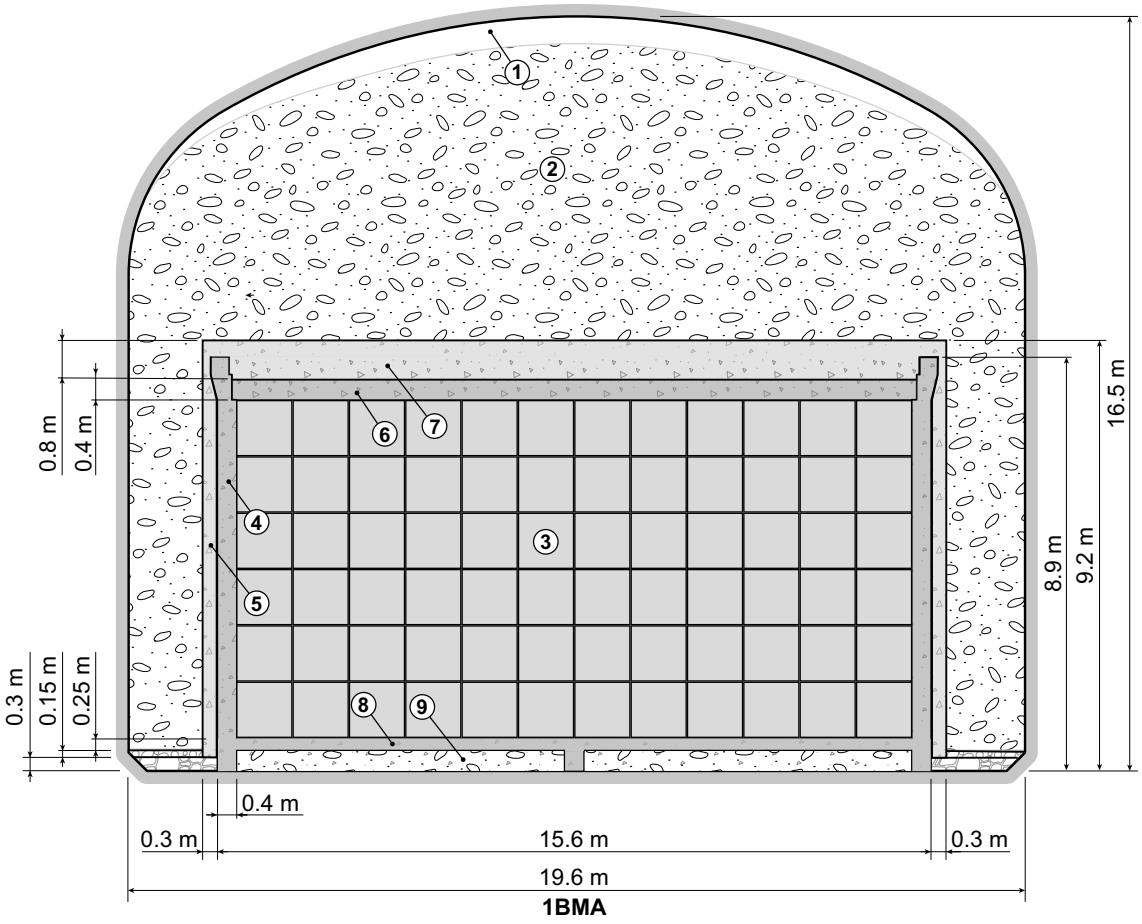

Figure 4-9. *Schematic cross-section of 1BMA at closure. Key to numbering: 1) Void 2) Macadam backfill 3) Waste domain 4) Existing outer wall 5) New outer wall 6) Pre-fabricated concrete element 7) New concrete lid 8) Slab 9) Crushed rock.*

Barriers contributing to post-closure safety

The new outer walls and lid constitute the main hydraulic barriers, limiting the groundwater flow through the waste. The remaining parts of the concrete structure and the concrete moulds also contribute to limit the groundwater flow through the waste.

In addition, the new outer walls and lid maintain the mechanical integrity of the concrete structure against the load from the backfill and water pressure that may occur during saturation at repository closure. The macadam backfill protects the engineered barriers against rock fallout and constitutes support for the plugs. Moreover, the high hydraulic conductivity of the macadam backfill and the crushed rock foundation provide a hydraulic barrier function as they lead the groundwater flow around the waste.

All the cementitious materials (waste form, concrete moulds and concrete structures) have chemical barrier functions. The choice of cementitious materials ensures good sorption properties for many radionuclides on the surface of the material, thus limiting their release. Cementitious materials also set a high pH value, which limits corrosion of steel and gas production caused by microbial activity.

Condition of the subcomponents at initial state

The waste packaging in 1BMA is made of reinforced concrete or steel. Steel waste packaging will probably start to corrode during the operational period. The possibility of small cracks, of more than 0.1 mm wide, forming in the concrete packaging during the operational period cannot be ruled out.

Steel reinforcement (rebar) in the original concrete structure will corrode during the operational period and this assessment therefore focuses on uncertainties related to the initial state of 1BMA and the planned measures to repair the concrete structure (Elfwing et al. 2018). Inspections show that the original concrete structure is cracked to an extent that will significantly affect the hydraulic conductivity (Hejll et al. 2012). The inspections have been performed in empty compartments in 1BMA, corresponding to one quarter of the entire concrete structure. Extrapolating the results from the mapping of cracks to the entire concrete structure introduces further uncertainties. A new outer hydraulic barrier will therefore be built outside the walls and roof of the existing concrete structure. The situation is similar for the 1BMA slab, where extrapolating the crack distribution from inspected compartments to the rest of the concrete foundation also is uncertain. The 1BMA slab will however remain unrepaired. In this assessment, it is assumed that the concrete foundation has penetrating cracks and is therefore highly conductive.

For the 1BMA repairs, controls and inspections are to be undertaken during construction to ensure that requirements are met. The inspections and controls are to ensure an adequate knowledge of the achieved initial state of the waste vaults, which reduces overall assessment uncertainties.

A recent compilation of available information (see the **Data report**, Chapter 7) for the existing 1BMA concrete structure shows furthermore that the cement content is lower than was reported as the initial state in the previous assessment, which contributes to an uncertainty in the material composition and other parameters (e.g. diffusivity) describing the initial state properties of the concrete structure.

4.4.3 2BMA, vault for intermediate-level waste

The 2BMA waste vault in SFR3 is an approximately 23.5 m wide, 18.6 m high and 275 m long vault for intermediate-level waste (Figure 4-10). Experience from the construction of 1BMA has been utilised in the design of 2BMA. Specifically, the use of reinforced concrete is reduced to a minimum to avoid adverse effects of steel rebar corrosion on post-closure barrier performance. Therefore, 2BMA has 13 free-standing unreinforced concrete caissons with a base of 18.1 m × 18.1 m and a height of 9 m.

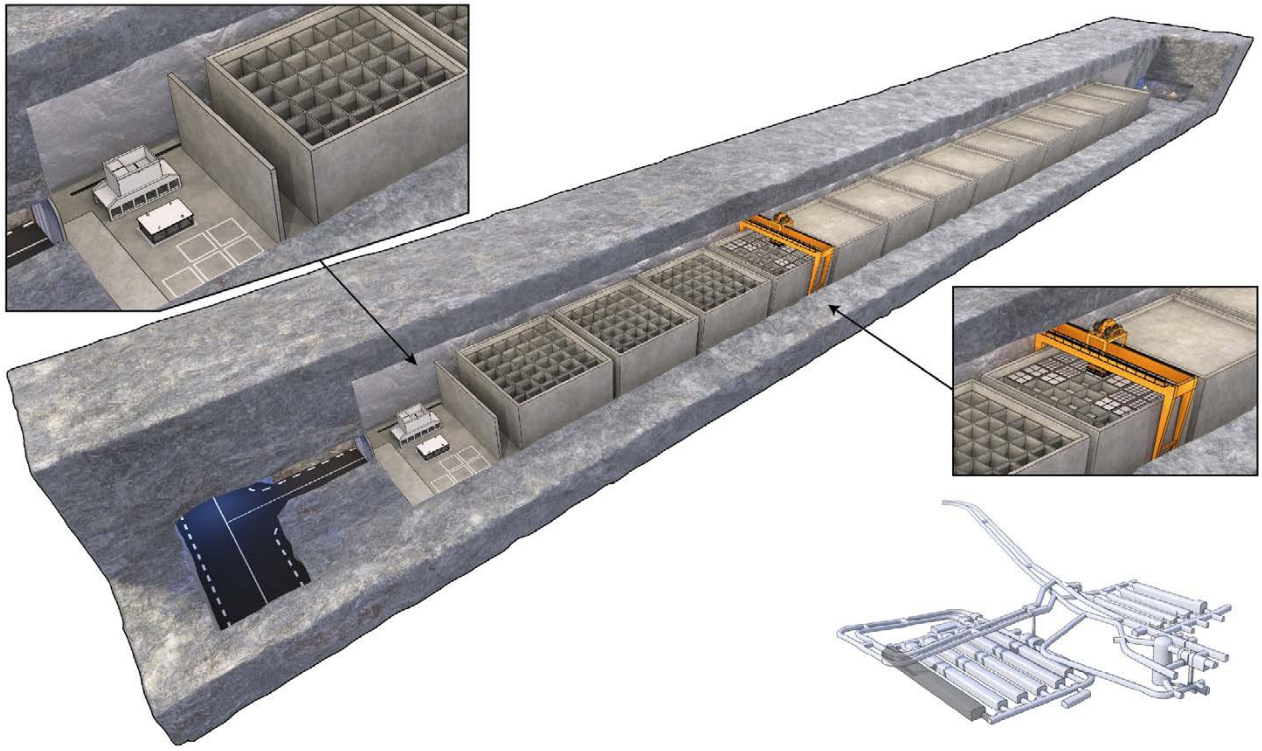

Figure 4-10. *Vault for intermediate-level waste, 2BMA, in SFR3 during the operational period. The lower detail shows a view of SFR with the position of 2BMA in SFR3 in darker grey.*

The bottom slabs of the concrete caissons are 0.60 m thick and the outer walls are 0.68 m thick. The thickness of the outer walls is slightly reduced at the top to act as support for pre-fabricated concrete elements. The inner walls are built of pre-fabricated reinforced concrete.

The concrete caissons are founded on a concrete slab cast on top of the of crushed rock and the vault walls and roof are lined with shotcrete.

Waste packages in the form of steel moulds, concrete moulds and drums are to be disposed in each caisson by a remote-controlled gantry crane. The gantry crane moves on tracks being cast firmly into the vault floor, implying that it does not rest on the caissons. Prefabricated concrete elements, emplaced on top of the caissons, provide radiation shielding during the operational period.

Description of the closure of the vault

The closure plan for SFR (Mårtensson et al. 2022) describes the planned measures for closure of 2BMA. The radiation shielding lids are left in place and act as support for the covering concrete (0.6 m) which is cast at repository closure at the latest. The radiation shielding lids (pre-fabricated concrete elements) and the overcast concrete together make up the lid of the concrete structure. A gas evacuation system is installed during closure (see Figure 4-11), which consists of:

1. Horizontal (empty) discharge channels running along the border between the pre-fabricated concrete elements and the more compact overcast.
2. Vertical gas discharge channels filled with porous cement mortar emplaced along an outer wall (and which penetrate the cast lid). In the present design, six vertical gas discharge channels for each caisson will be built with the cross section of 0.20 m × 0.25 m. The gas evacuation system is designed so that the structural integrity of the concrete structure is not affected.

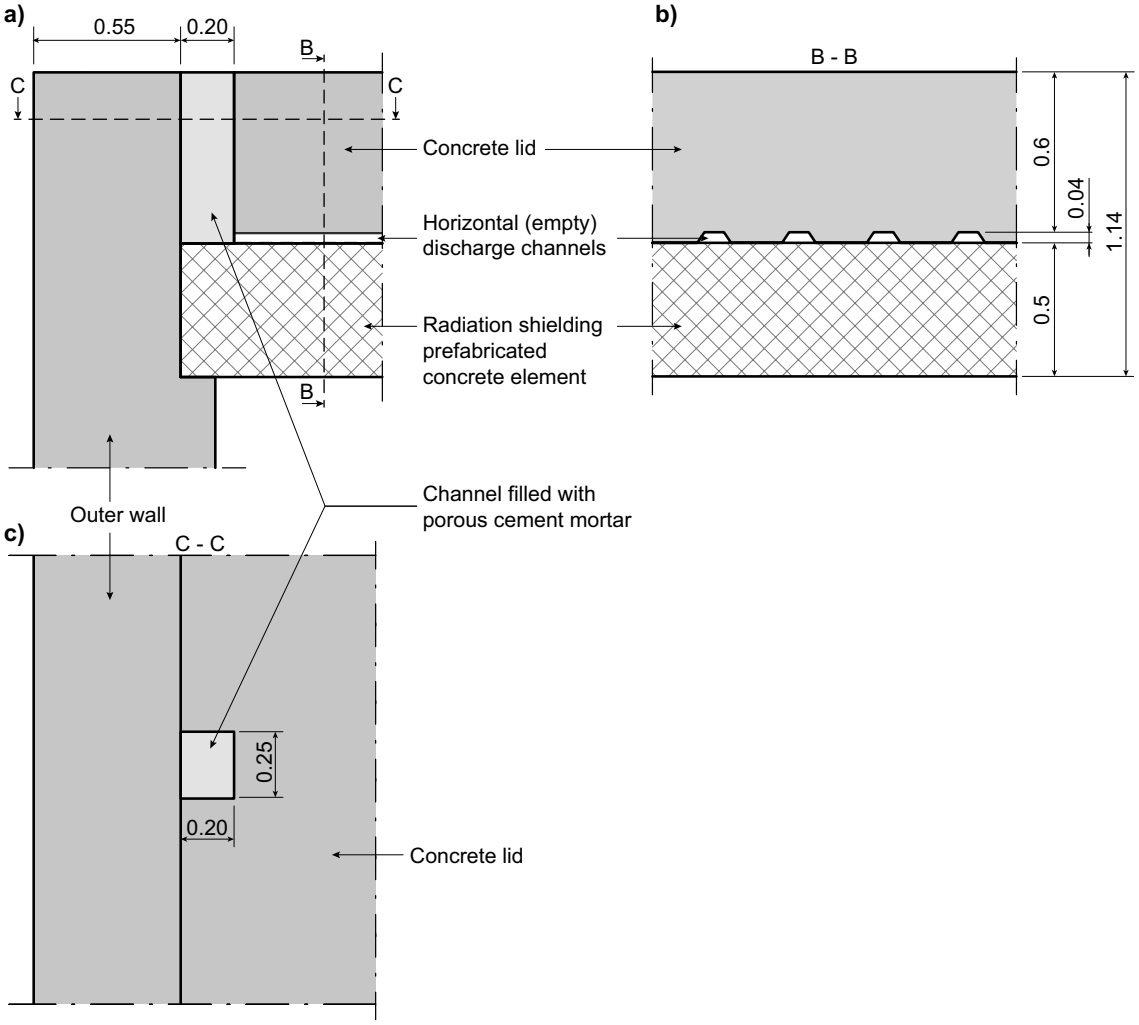

Figure 4-11. *Schematic illustration of the planned gas evacuation system in 2BMA (units in metre). a) Cross section of the whole system. b) Cross section showing horizontal (empty) discharge channels. c) Vertical discharge channels filled with porous cement mortar, seen from above.*

Equipment and installations in the waste vault are removed and the space between caissons, as well as between caissons and the rock wall, is backfilled with macadam, see Figure 4-12. The geometry of the waste vault is such that concrete plugs can be installed at both ends of the waste vault as mechanical constraints for the bentonite in connecting tunnels.

Barriers contributing to post-closure safety

The concrete caissons constitute the main hydraulic barriers, limiting the groundwater flow through the waste. The remaining parts of the concrete structure and the concrete moulds also contribute to limit the groundwater flow through the waste.

In addition, the caissons including the inner concrete walls maintain the mechanical integrity of the structure against the load from the backfill and water pressure that may occur during saturation at repository closure. The macadam backfill protects the engineered barriers against rock fallout and constitutes support for the plugs. Moreover, the high hydraulic conductivity of the macadam backfill and the crushed rock foundation provide hydraulic barrier function as they lead the groundwater flow around the waste.

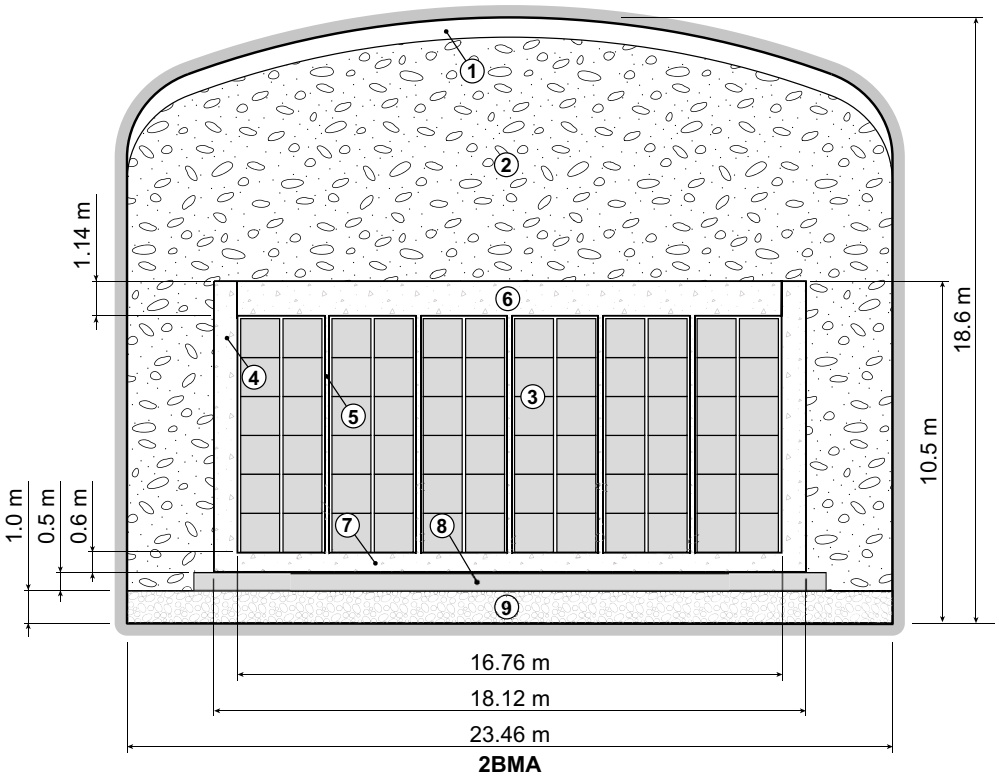

Figure 4-12. *Schematic cross-section of 2BMA at closure. Key to numbering: 1) Void 2) Macadam backfill 3) Waste domain 4) Outer wall 5) Inner wall 6) Lid 7) Caisson slab 8) Slab 9) Crushed rock.*

All the cementitious materials (waste form, concrete moulds and concrete structures) have chemical barrier functions. The choice of cementitious materials ensures good sorption properties for many radionuclides on the surface of the material, thus limiting their release. Cementitious materials also set a high pH value, which limits corrosion of steel and gas production caused by microbial activity.

The gas evacuation system in the caissons has a barrier function to allow gas to escape to avoid high gas pressure which can result in gas-driven advective transport of dissolved radionuclides.

Condition of the subcomponents at initial state

Steel waste packaging will probably start to corrode during the operational period. The possibility of small cracks, more than 0.1 mm wide, forming in the concrete packaging during the operational period cannot be ruled out.

Since 2BMA has not yet been built, there is uncertainty regarding the properties of the barrier after construction. However, SKB has built similar concrete structures in the Äspö Hard Rock laboratory (Mårtensson and Vogt 2019, 2020) and this experience suggests they can be constructed appropriately.

The foundation is an important factor that could affect the flow-limiting properties of the concrete barrier. If the laying of the foundation is not done satisfactorily, it could result in uneven load distribution and subsequent crack propagation in the concrete structures.

4.4.4 1BRT, vault for segmented reactor pressure vessels

The 1BRT waste vault for segmented reactor pressure vessels from BWRs in SFR3 is about 17.5 m wide, 15.2 m high and 255 m long. The walls and roof of the vault are lined with shotcrete and a concrete slab is cast on a layer of crushed rock. The vault has a cast reinforced concrete structure which is divided into compartments by inner walls, see Figure 4-13.

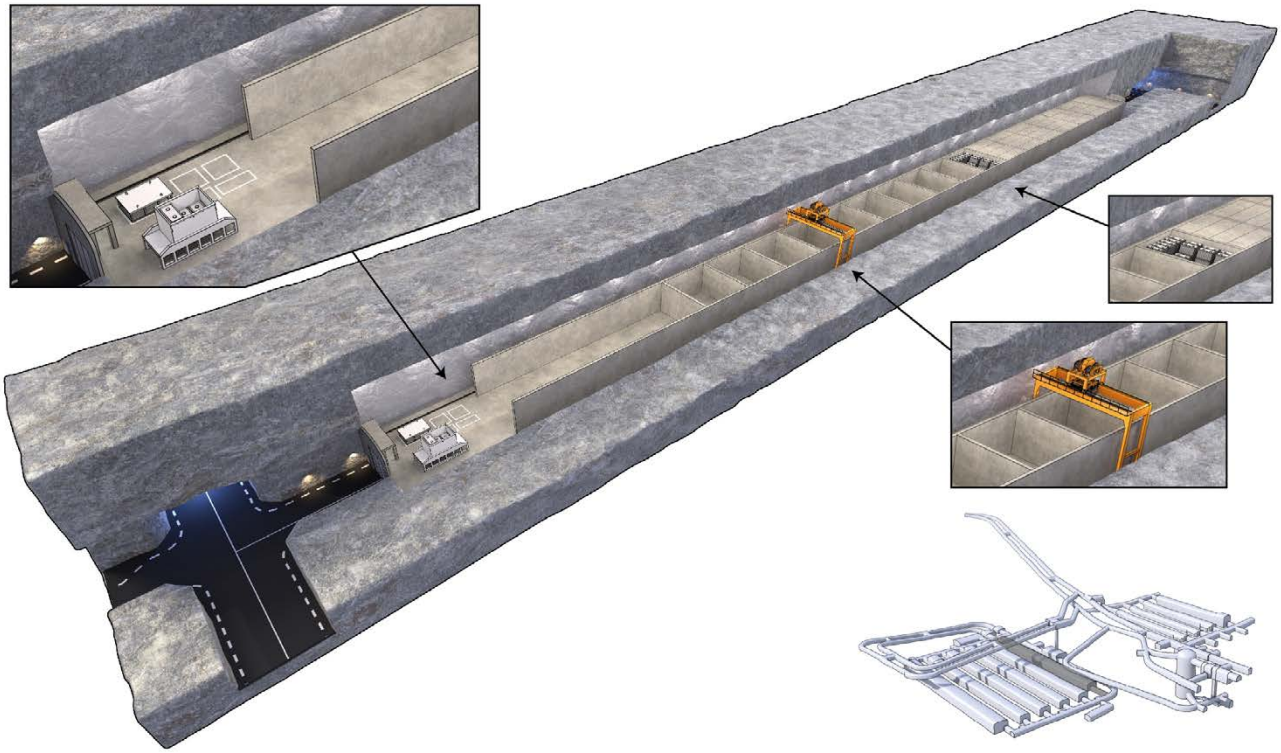

Figure 4-13. *Vault for reactor pressure vessels, 1BRT, in SFR3 during the operational period. The lower detail shows SFR with the position of 1BRT in darker grey.*

One part of the concrete structure is intended for disposal of the double moulds and is divided into compartments by inner walls. The other part is for disposal of waste packages of different dimensions and the inner walls are added between the waste packages as the space is filled.

The double moulds are positioned in the compartments using a remote-controlled overhead or gantry crane that is supported outside the concrete structure. Other waste is transported into the vault by truck. Pre-fabricated concrete elements are placed over full compartments.

Description of the closure of the vault

The planned measures at closure of 1BRT are described in the closure plan for SFR (Mårtensson et al. 2022). At closure of the vault, the space between the waste packages will be filled with self-compacting concrete so that a network of load-bearing structures is formed and a low corrosion rate is ensured. A reinforced concrete lid will be cast on top of the pre-fabricated concrete elements.

The space outside the concrete structure will be backfilled with macadam and concrete plugs will be installed at the ends towards the waste vault tunnel (2BST) and the transverse tunnel (2TT), see Figure 4-4. Figure 4-14 shows a schematic illustration of 1BRT at closure.

Barriers contributing to post-closure safety

The waste form in itself contributes to slow release of radionuclides since a significant portion of the radioactivity is induced in slowly corroding steel.

All cementitious materials (waste form and concrete structures) have chemical barrier functions. The choice of cementitious materials ensures a high pH value, which limits corrosion of steel and thus the release of induced radioactivity. Further, it limits the gas production and ensures good sorption properties for many radionuclides on the surface of the material, thus limiting their release.

The concrete structures contribute to limit the groundwater flow through the waste. Moreover, the high hydraulic conductivity of the backfill and the base of crushed rock provide hydraulic barrier function as they lead the groundwater flow around the waste.

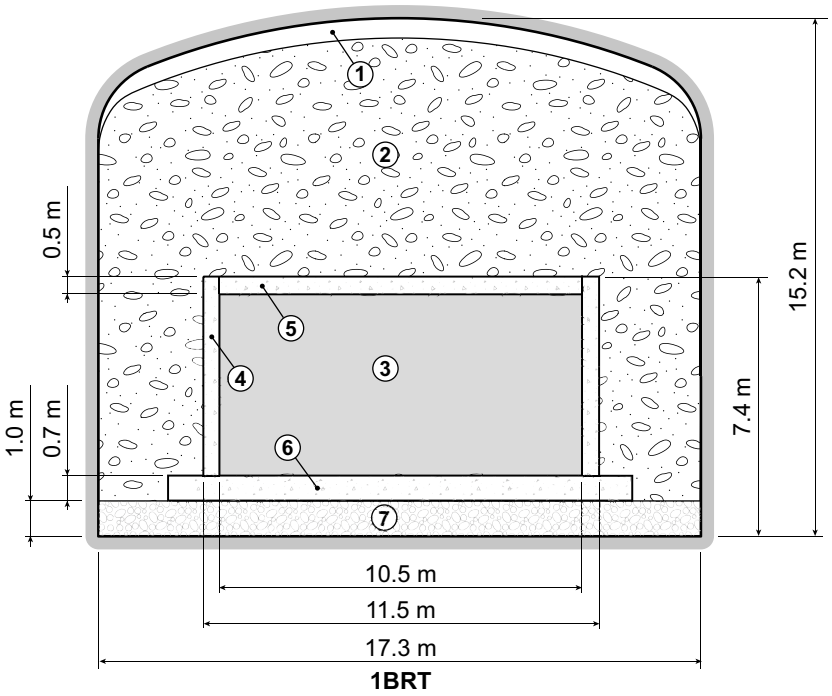

Figure 4-14. *Schematic cross-section of 1BRT at closure. Key to numbering: 1) Void 2) Macadam backfill 3) Waste domain 4) Outer wall 5) Lid 6) Slab 7) Crushed rock.*

In addition, the concrete structures maintain the mechanical integrity of the whole structure against the load from the backfill and water pressure that may occur during saturation at repository closure.

The macadam backfill protects the concrete structures against rock fallout and constitutes support for the plugs.

Condition of the subcomponents at initial state

Steel waste packaging will probably start to corrode during the operational period.

1BRT is not yet built and there are presently no approved waste type descriptions or acceptance criteria. This introduces uncertainties regarding the amount of concrete that will be disposed in the waste vault, but note that the requirement states at least 12 000 m^3 concrete which is assumed in the safety assessment.

4.4.5 1BTF and 2BTF, vaults for concrete tanks

The two waste vaults 1BTF and 2BTF in SFR1 are approximately 15 m wide, 9.5 m high and 160 m long. The vaults are primarily designed for disposal of dewatered ion-exchange resins in concrete tanks. The walls and roof of the vaults are lined with shotcrete. The concrete slab is cast on a foundation of crushed rock and surrounded by a 1 m high moulded skirting along the rock wall to divert possible groundwater leaks from the host rock. To facilitate the planned grouting around the concrete tanks, several concrete pillars are cast on the skirting; see the illustration at the bottom of Figure 4-15 and Figure 4-16.

Besides concrete tanks, drums containing ash from incineration at the facilities in Studsvik are also disposed in 1BTF. To provide support for the ash-filled drums in 1BTF, concrete tanks are positioned along the tunnel long axis and partition walls are built up of concrete moulds with low activity contents and low surface dose rates; see the illustration at the top of Figure 4-15. Grouting around the ash-filled drums is done progressively during operations.

2BTF predominantly contains concrete tanks which are positioned four abreast and two high, after which prefabricated concrete elements are placed on top to provide radiation shielding during operation, see Figure 4-16.

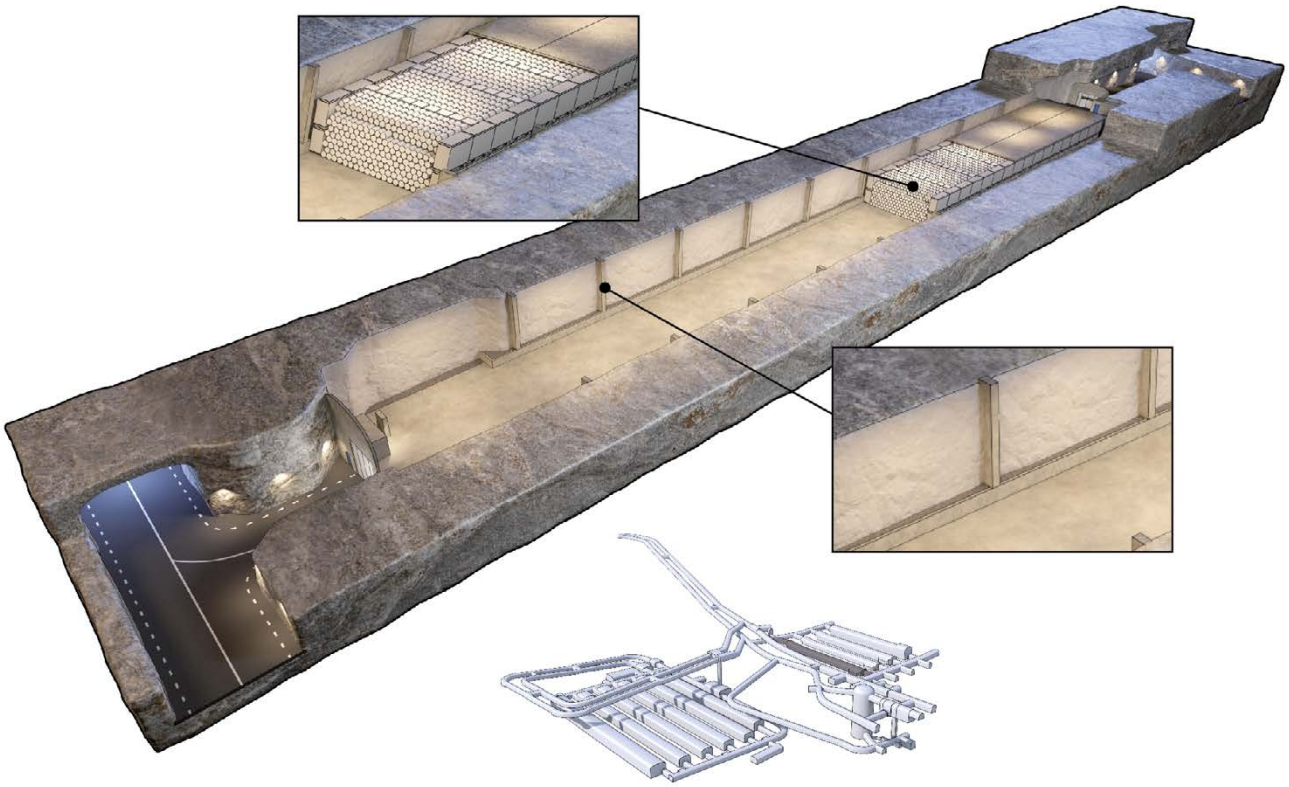

Figure 4-15. *Vault for concrete tanks, 1BTF, in SFR1 during the operational period. The upper detail shows the emplacement of ash-filled drums, the lower detail shows the skirting and concrete pillars. In addition, there is a view of SFR with the position of 1BTF in darker grey.*

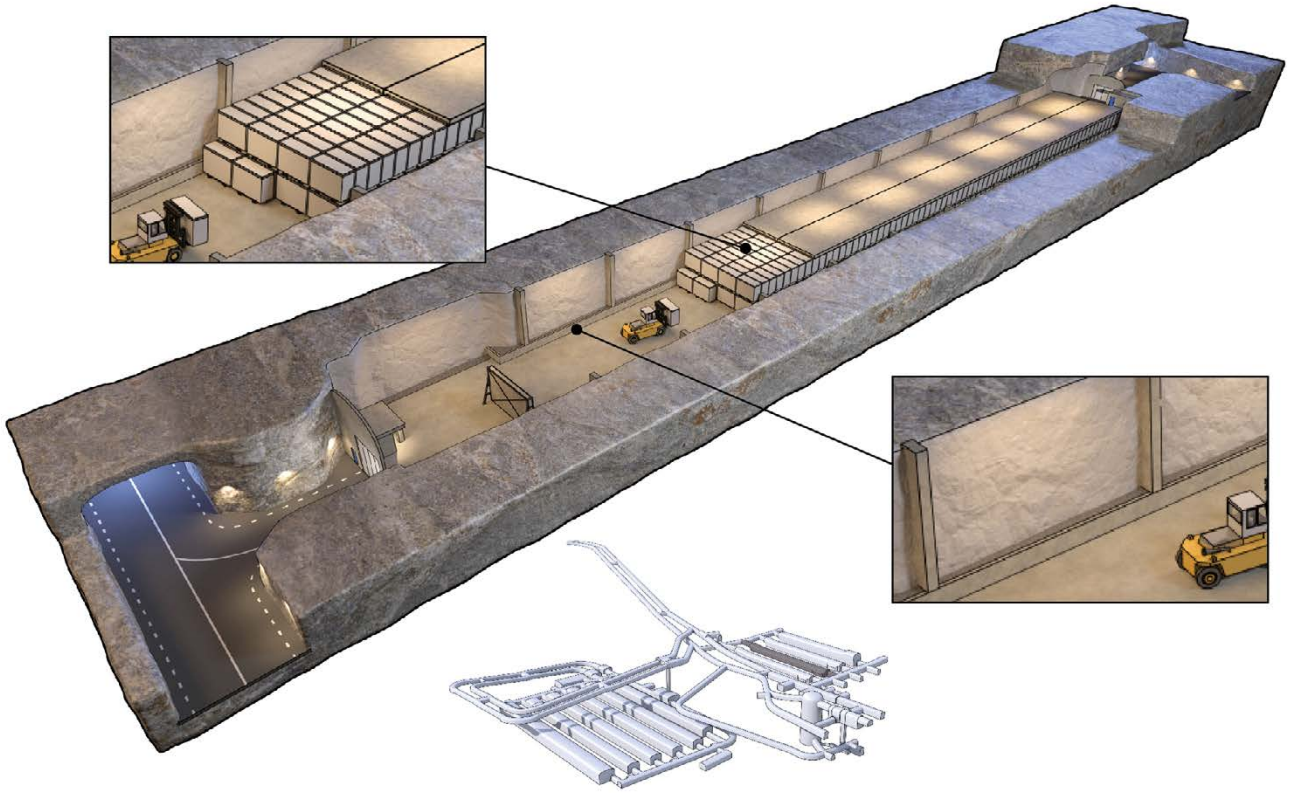

Figure 4-16. *Vault for concrete tanks, 2BTF, in SFR1 during the operational period. The upper detail shows the emplacement of concrete tanks, the lower detail shows the skirting and concrete pillars. In addition, there is a view of SFR with the position of 2BTF in darker grey.*

Description of the closure of the vaults

The closure plan for SFR (Mårtensson et al. 2022) describes the planned measures for closure of 1BTF and 2BTF. The space between concrete tanks and rock wall is filled with cementitious backfill as the first step in closure of the waste vaults. In 2BTF, which contains only concrete tanks, the spaces between the concrete tanks are filled with grout in the next step and, on top of the prefabricated concrete elements, a concrete slab is cast to bear the weight of the macadam. In 1BTF, the ash-filled drums in the inner part of the waste vault are already grouted and the outer part with only concrete tanks is, at closure, grouted in the same way as in 2BTF. Finally, the space above the concrete lid is filled with macadam up to the roof and the waste vaults are plugged in the same way as 1BMA, see Section 4.4.2.

Figure 4-17 shows a schematic illustration of 1BTF and 2BTF at closure.

Barriers contributing to post-closure safety

For the concrete tank section, the tank walls are the main hydraulic barriers. For the sections containing the ash-filled drums, the concrete between inner and outer steel drums, the grout and the concrete packaging surrounding them contribute to limit the groundwater flow through the waste.

The macadam backfill protects the engineered barriers against rock fallout and constitutes support for the plugs. Moreover, the high hydraulic conductivity of the macadam backfill and the crushed rock foundation provide hydraulic barrier function as they lead the groundwater flow around the waste.

All the cementitious materials (waste form, waste packaging, grout, cementitious backfill and concrete structures) have chemical barrier functions. The choice of cementitious materials ensures good sorption properties for many radionuclides on the surface of the material, thus limiting their release. Cementitious materials also set a high pH value, which limits corrosion of steel and gas production caused by microbial activity.

Condition of the subcomponents in 1BTF and 2BTF at initial state

The waste packages (ash-filled drums) in 1BTF are embedded in grout as they are emplaced. This means that the condition of the waste packages cannot be inspected afterwards, although it is likely that the steel waste packaging will start to corrode during the operational period.

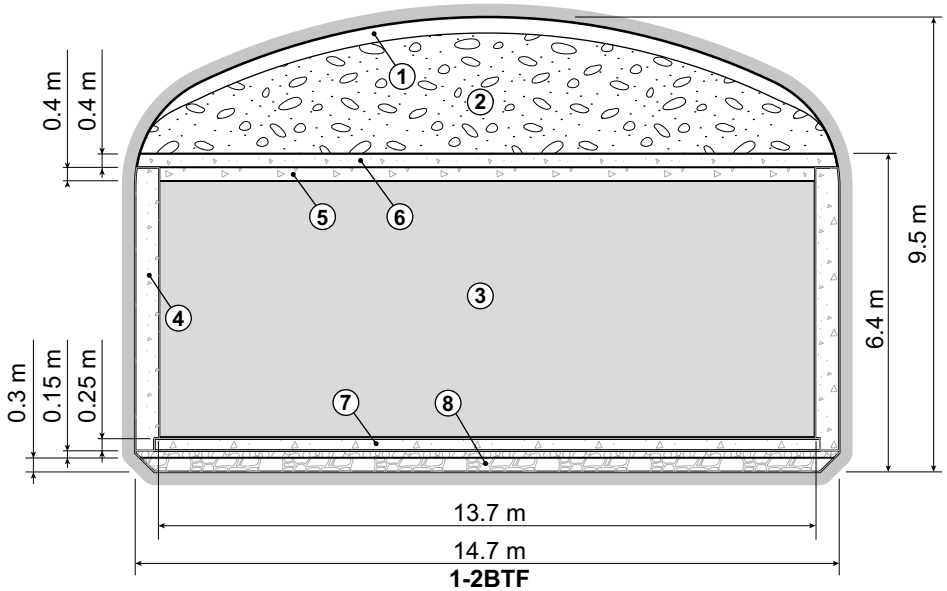

Figure 4-17. *Schematic cross-section of 1BTF and 2BTF at closure. Key to numbering: 1) Void 2) Macadam backfill 3) Waste domain 4) Cementitious backfill 5) Pre-fabricated concrete elements 6) Cast concrete lid 7) Slab 8) Crushed rock (0.3 + 0.15 m).*

The main hydraulic barrier in 1–2BTF consists of painted concrete tanks in which the waste is being stored. These tanks are successively disposed in the waste vaults during the operational period. The fact that the concrete tanks have painted surfaces makes their initial state difficult to evaluate and this introduces uncertainties regarding the flow-limiting properties that the concrete tanks have at initial state.

The possibility of small cracks, more than 0.1 mm wide, forming in the concrete packaging as well as in the concrete grout during the operational period cannot be ruled out.

4.4.6 1BLA, vault for low-level waste

The 1BLA waste vault in SFR1 for ISO containers with low-level waste is about 15 m wide, 13 m high and 160 m long. The waste is disposed in ISO containers stacked two abreast and three to six high, depending on their size, see Figure 4-18. The vault has a concrete slab cast on a foundation of crushed rock, and the rock walls and roof are lined with shotcrete.

Description of the closure of the vault

The closure plan for SFR (Mårtensson et al. 2022) describes the planned measures for closure of 1BLA. A concrete wall is installed at the end towards the transverse tunnel (1TT) and approximately 4 m is backfilled with macadam, after which a concrete plug is cast. A mechanical constraint consisting of backfill material is needed at the end towards the waste vault tunnel (BST) to hold the transition material in the earth dam plug in place, see Figure 4-4. This mechanical constraint is made by back-filling 10 m of the waste vault with macadam against a retaining wall and filling the space above the backfill and above the level of the connecting tunnel with concrete. Figure 4-19 shows a schematic illustration of 1BLA at closure.

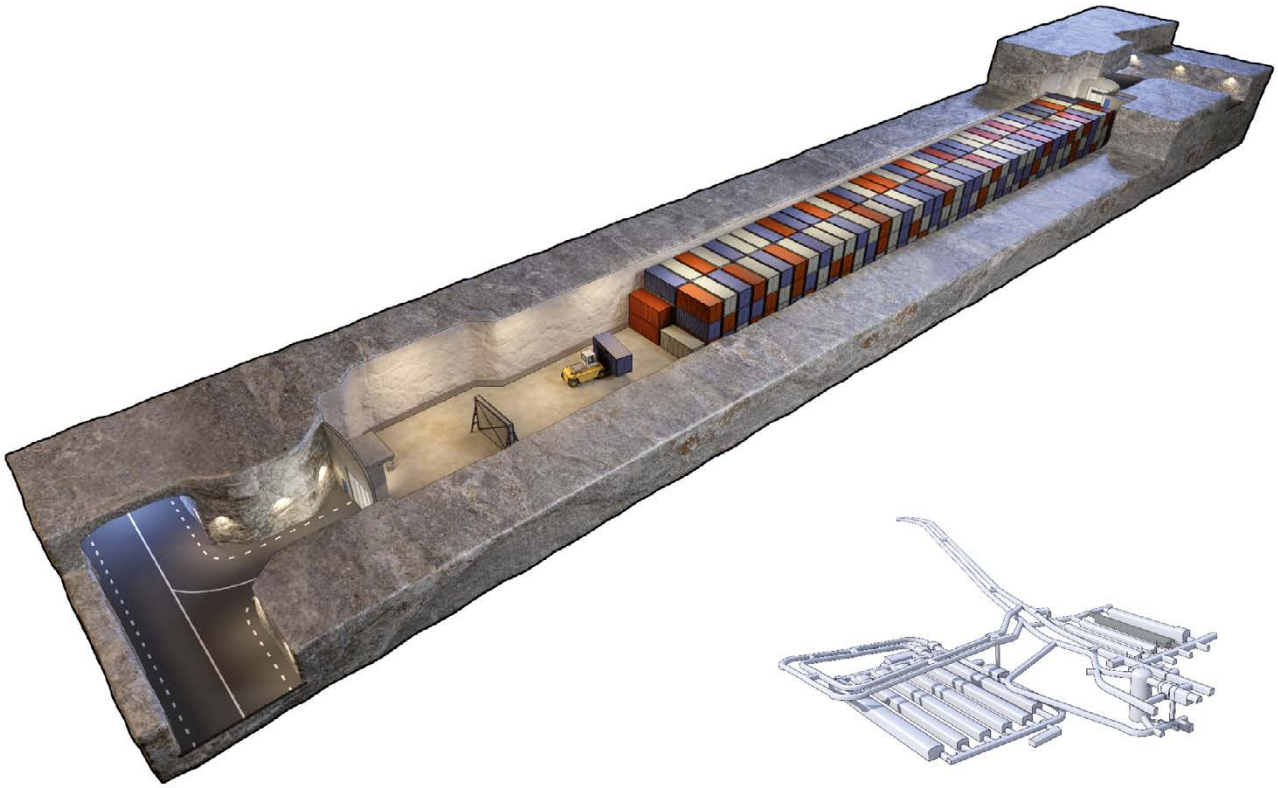

Figure 4-18. *Vault for low-level waste, 1BLA, in SFR1 during the operational period. The lower detail shows SFR1 with the position of 1BLA in darker grey.*

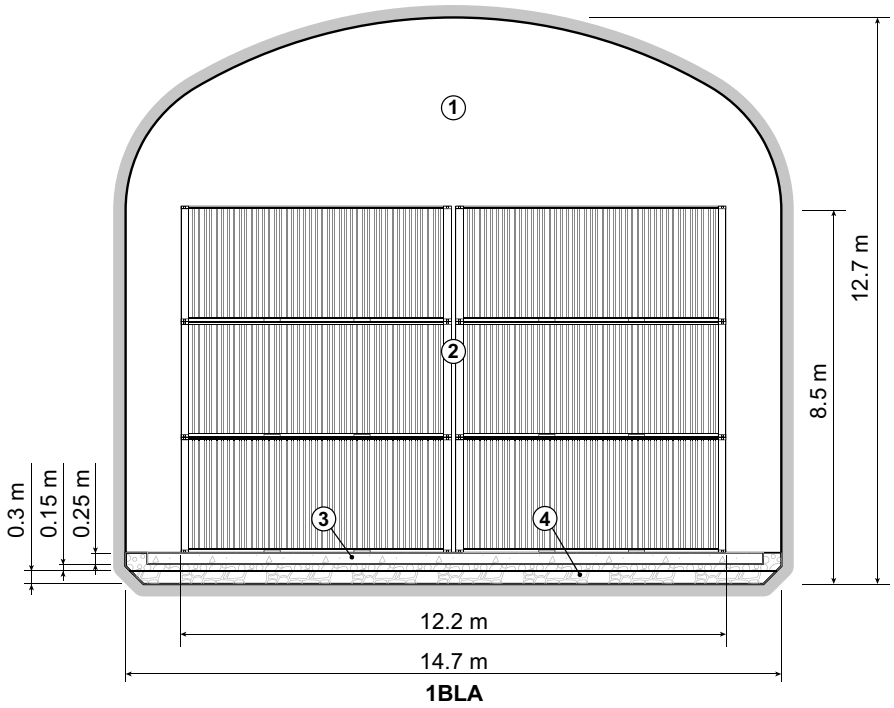

Figure 4-19. *Schematic cross-section of 1BLA at closure, exemplified with full-height containers. Key to numbering: 1) Void 2) Waste domain 3) Slab 4) Crushed rock (0.3 + 0.15m).*

Barriers contributing to post-closure safety

There are no engineered barriers in 1BLA other than the plugs, see Section 4.4.8.

Condition of the subcomponents at initial state

No grouting of the waste packages is planned, nor will the vault be backfilled. The ISO-containers are expected to corrode somewhat during the operational period.

4.4.7 2–5BLA, vaults for low-level waste

The four vaults, 2–5BLA, for low-level waste in SFR3 are approximately 17.5 m wide, 12.4 m high and 275 m long. The waste is disposed in ISO containers stacked two abreast and three to six high, depending on their size, see Figure 4-20. The vault has a concrete slab on top of a crushed rock layer and the rock walls and roof are lined with shotcrete.

Description of the closure of the vaults

The closure plan for SFR (Mårtensson et al. 2022) describes the planned measures for closure of 2–5BLA. Concrete plugs are to be installed at the ends towards the waste vault tunnel (2BST) and the transverse tunnel (2TT) along with mechanical constraints intended to serve as support when the concrete plugs are no longer intact. The constraint is made by backfilling 10 m of the waste vault with macadam against a retaining wall and filling the space above the backfill and above the level of the connecting tunnel with concrete. Figure 4-21 shows a schematic illustration of 2–5BLA at closure.

Figure 4-20. *Vaults for low-level waste, 2–5BLA, in SFR3 during the operational period. The lower detail shows SFR with the position of the four waste vaults in darker grey.*

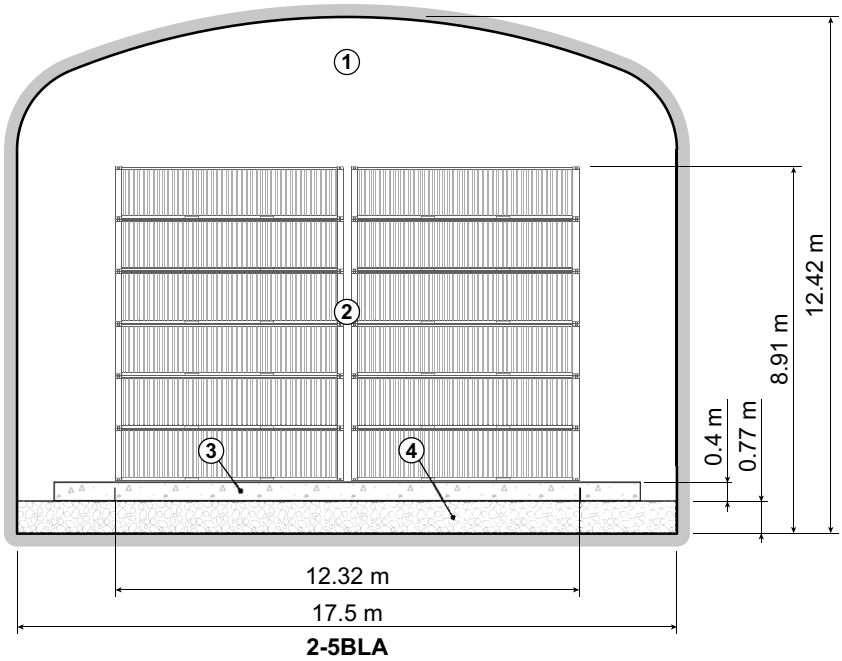

Figure 4-21. *Schematic cross-section of 2–5BLA at closure, exemplified with half-height containers. Key to numbering: 1) Void 2) Waste domain 3) Slab 4) Crushed rock.*

Barriers contributing to post-closure safety

There are no engineered barriers in 2–5BLA other than the plugs, see Section 4.4.8.

Condition of the subcomponents at initial state

No grouting of the waste packages is planned, nor will the vaults be backfilled. Steel waste packaging will probably start to corrode during the operational period.

4.4.8 Plugs and other closure components

The closure plan for SFR (Mårtensson et al. 2022) describes the planned measures for closure of SFR. Plugs for waste vaults plus closure of tunnels, the tunnel system and boreholes are described in the following.

The upper part of the access tunnels is to be filled with stone blocks and sealed with concrete plugs. Finally, the ground surface will be restored to blend in with the surrounding landscape. In addition, all boreholes at SFR will be sealed so that the water flow in the surrounding rock is not affected by them.

The plug sections are hydraulically tight sections with bentonite that is held in place by mechanical constraints. Wherever warranted by the geometry of the tunnels and the properties of the rock, concrete plugs are installed as mechanical constraints. Where this is not suitable, a mechanical constraint consisting of backfill and transition material is installed instead. The role of the transition material is to hinder bentonite transport out from the hydraulically tight section, to take up the load from bentonite swelling and transfer it to the backfill material. The backfill material consists of macadam and the transition material of 30 % bentonite and 70 % crushed rock. A mechanical constraint of backfill and transition material together with a tight section of bentonite is called an earth dam plug.

Plugs for waste vaults

A total of five plug sections (P1TT, P1BTF, P1BST, P2TT and P2BST) are to be installed to seal the waste vaults in SFR1 and SFR3, see Figure 4-22. All plugs consist of a hydraulically tight section and mechanical constraints that hold it in place. In most positions, concrete plugs are planned for mechanical support. In the sections adjacent to the connecting tunnel BST where the geometry and the local geological conditions make it difficult to construct concrete plugs, earth dam plugs (Mårtensson et al. 2022) are planned as they do not require local mechanical support from the rock walls. The function of the bentonite-filled sections (Figure 4-4) is to act as hydraulic seals and the function of the plugs is as mechanical constraints for the bentonite sections.

Plugs to silo

Three plug sections: lower silo plug (NSP), upper silo plug (ÖSP) and silo roof plug (STP) are installed to seal the silo, see Figure 4-23. An important factor in designing the plugs has been to find suitable tunnel geometries to install the mechanical constraints that hold the hydraulically tight sections with bentonite in place.

Sealing of access tunnels and tunnel system

Plugs of concrete and bentonite, see Figure 4-4, will be installed in the access tunnels to minimise the water flow along these tunnels. The design of the plugs is shown in Figure 4-24. The tight section of bentonite is 10 m long. The remaining part of the access tunnels and tunnel system will be backfilled with macadam. The motive for choosing macadam is that it should constitute mechanical support for the plugs and impede human intrusion into the repository. In addition, vertical shafts connecting different parts of the repository are planned to be sealed and plugged.

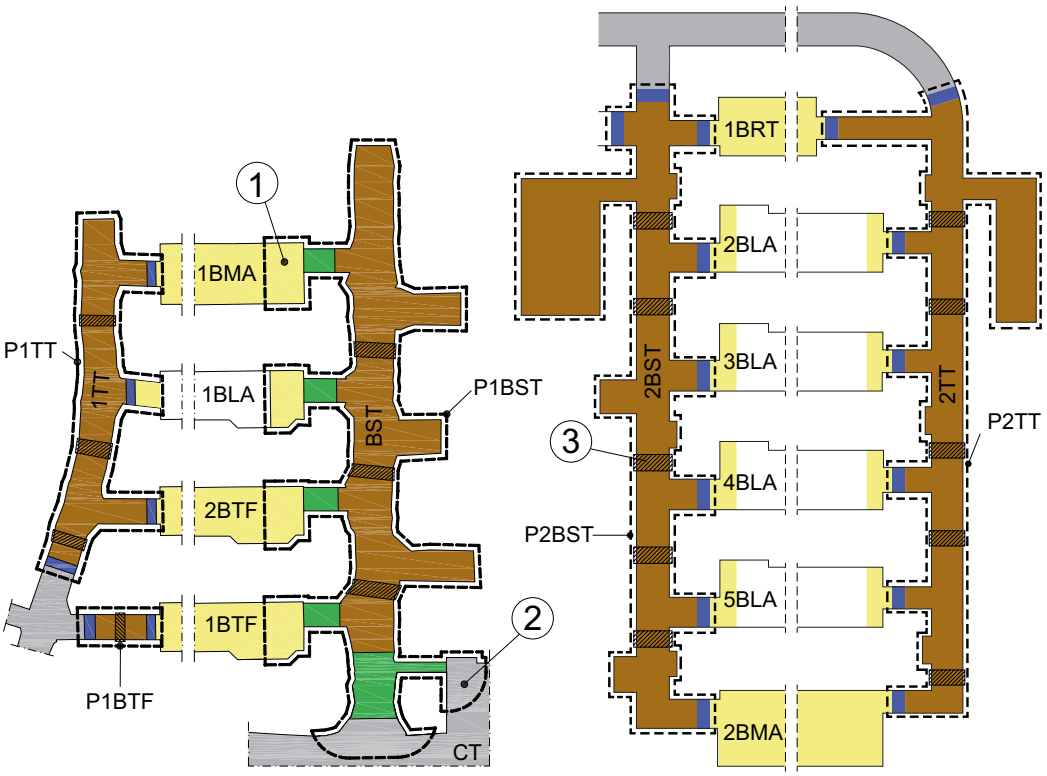

Figure 4-22. *Plugs adjacent to waste vaults are marked with a dashed line. Key to numbering: 1) Yellow colour within borderline for plug sections shows parts of crushed rock backfill that are active parts of the earth dam plug, green colour shows transition material (a mix of bentonite and crushed rock) and brown colour shows hydraulically tight material 2) Grey colour within borderline for plug shows parts of backfill in tunnel system that are active parts of the earth dam plug 3) Hatched areas indicate where the damaged zone should be removed by controlled methods. Blue colour represents concrete sections.*

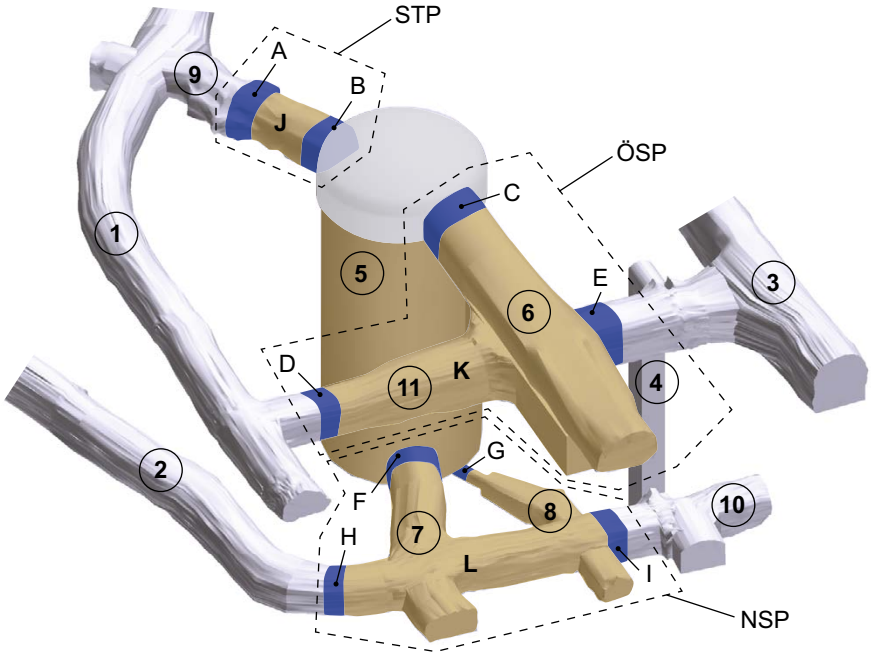

Figure 4-23. *Illustration of closed silo with three plug sections (NSP, ÖSP and STP). Blue colour shows concrete plugs (A-I) and brown colour shows hydraulically tight sections (J, K, L). Key to numbering: 1) Construction tunnel, BT 2) Lower construction tunnel, NBT 3) Central tunnel, CT 4) Connecting shaft 5) Silo 6) Loading-in building, IB 7) Silo bottom tunnel, 8) Drainage tunnel 9) Silo roof tunnel, 1STT 10) Terminal part of lower construction tunnel 11) Silo tunnel. Tunnel parts 1, 2, 3, 4 and 10 belong to the tunnel system.*

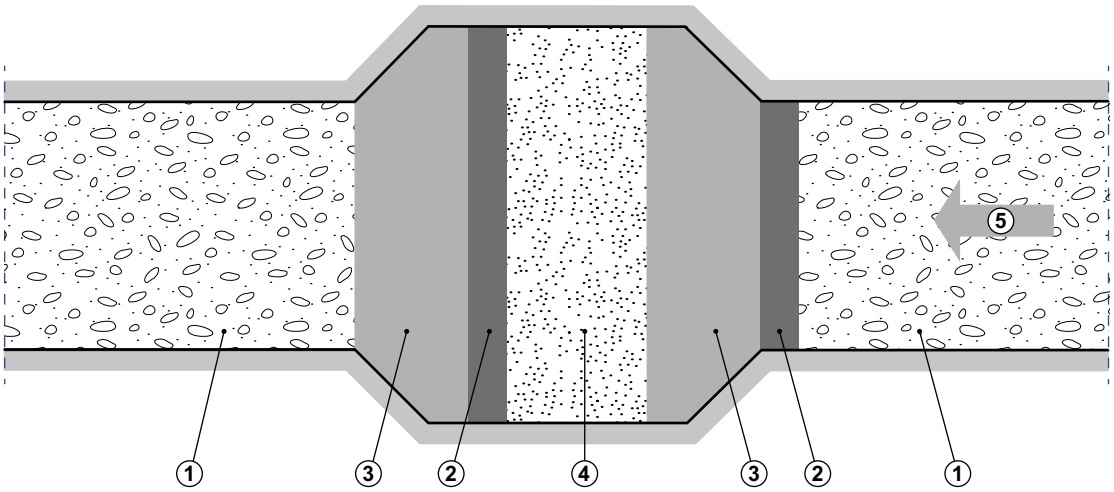

Figure 4-24. *Schematic reference design of the access tunnel plug. Key to numbering: 1) Macadam backfill 2) Constraining concrete wall 3) Concrete 4) Bentonite 5) Working direction.*

Sealing of boreholes

The boreholes that were included in the preliminary investigations and those that intersect or are located very close to the underground facility have been or will be sealed prior to the start of construction of SFR3 and the remaining boreholes will be sealed after the repository operational period.

Barriers contributing to post-closure safety

All repository parts will be sealed with plugs. These barriers limit groundwater flow through the repository vaults.

Condition of the system components at initial state

Plugs and other closure components are installed near the time of closure and are expected to be in good condition at initial state.

4.4.9 Decommissioning and closure

The SFR facility will be decommissioned when all waste has been disposed in the facility. When the decision to end operations has been taken and appropriate permits have been granted, decommissioning of the facility will begin and continue until the repository has been closed and sealed. The PSAR-version of the closure plan (Mårtensson et al. 2022) describes the presently planned closure sequence and this plan will be updated before the closure works begin. Demolition and dismantling of existing systems will then be coordinated with the execution of closure. After decommissioning and closure, the repository is a passive system that can be left without having to take any further measures to maintain proper function. Facilities above ground will be demolished during clearance of the site.

Closure of SFR includes installation of backfill material and plugs at selected locations in the underground facility (Section 4.4.8).

Directly after sealing and the cessation of drainage pumping, water will start to re-saturate the repository. Numerical calculations (Börgesson et al. 2015) have shown that it will take 13 to 53 years for water to fully saturate the silo vault, which is surrounded by bentonite. Full resaturation of the other waste vaults has been calculated to take a few years (Holmén and Stigsson 2001) and the cement-conditioned waste will become saturated shortly after repository closure, whereas the bitumen-conditioned waste will take a considerably longer time due to the hydrophobic character of bitumen. In the perspective of the long duration of the safety assessment period, the resaturation process is assumed to be instantaneous, and the repository is considered saturated at initial state.

4.5 Climate

This section describes climate and climate-related conditions relevant to the initial state of the repository environs and summarises information from the **Climate report**.

4.5.1 Temperature, precipitation and potential evapotranspiration

The initial-state climate is represented by locally measured meteorological data during the full year between October 2003 and September 2004, defined here as the normal year (Bosson et al. 2010). During that year, the average air temperature was 6.4 °C and the accumulated precipitation was 583 mm. The annual potential evapotranspiration of that year is estimated to have been 421 mm. These values are similar to the average annual air temperature and precipitation during the 1986–2005 reference period used by the IPCC (**Climate report**, Section 3.3) as well as the 2004–2010 period when the site investigations were carried out (Bosson et al. 2010, Werner et al. 2013). The average air temperature of the normal year is however nearly 1 °C higher than that for the 1961–1990 AD reference period used in the SR-PSU, and thus is consistent with the overall warming trend observed in the Forsmark region.

Due to current and future greenhouse-gas emissions, the average annual surface air temperature, precipitation and potential evapotranspiration in Forsmark are expected to increase up until the time of closure (see the **Climate report**, Section 3.4.3). Based on the fifth assessment report from the IPCC and regional modelling of the future climate in Sweden (IPCC 2013, Sjökvist et al. 2015), the increases in air temperature and precipitation, respectively, are projected to be within the range of 0.5–4 °C and 0–20 % up until the time of closure, depending e.g. on the amount of future greenhouse gas emissions (see the **Climate report**, Section 3.4.3). Based on an analysis of future projections from global hydrological models, the annual potential evapotranspiration in Forsmark is estimated to increase by 3–6 percentage points per degree of air temperature increase (**Climate report**, Appendix D), thus resulting in an increase within the range of 0–25 % up until closure.

Due to the uncertainty in the magnitude of these increases, the initial state is, for simplicity, defined with reference to the normal year. The uncertainty in the future increase in air temperature, precipitation and potential evapotranspiration is captured by the span of future climate evolutions described by the reference external conditions (Chapter 6).

4.5.2 Shoreline displacement

Changes in the shoreline displacement, i.e. the relative sea level, in the Forsmark area are determined by the opposing contributions of eustasy and isostasy. SFR is situated within an area with considerable isostasy, which amounts to 6.7 mm per year (Vestøl et al. 2019). The isostatic component is partly compensated by the eustatic contribution in the area today which amounts to 2.6 mm per year. This means that the relative sea level is currently decreasing by 4.1 mm per year (see the **Climate report,** Section 3.5.1).

At closure of the repository, the shoreline is assumed to be in the same position as today. This is a reasonable assumption given the large uncertainty associated with future changes in sea level (see the **Climate report,** Section 3.5). According to the study of Pellikka et al. (2020), the median projection of the Forsmark relative sea level change, from 2000 to 2080 AD, is −0.29 m for weak global warming, −0.19 m for moderate global warming and −0.04 m for strong global warming. However, when considering the 5 to 95 % percentile range of the projections, the equivalent changes are −0.40 to −0.10 m for weak global warming, −0.35 to +0.21 m for moderate global warming and −0.25 to +0.66 m for strong global warming (Pellikka et al. 2020).

4.6 Surface systems

This section describes the initial state of the surface systems and summarizes information from the site investigations that were conducted for the SR-PSU and documented in the site descriptive model (SDM-PSU; SKB TR-11-04), and the **Biosphere synthesis report**.

For the surface system, the initial state is assumed to be similar to the present-day conditions at Forsmark. This is presented below for the topography and the regolith composition (Section 4.6.1), the hydrology and near-surface hydrogeology (Section 4.6.2), the chemical conditions (Section 4.6.3), the ecosystems (Sections 4.6.4), the human population and land use (Section 4.6.5) and wells and water resource management (Section 4.6.6). The information is here summarised from the **Biosphere synthesis report**, Chapter 3 and mainly originates from the site descriptive model (SDM) for SR-PSU (SKB TR-11-04) which, in turn, is largely based on SDM-Site (SKB TR-08-05), i.e. the site description for the repository for spent nuclear fuel at Forsmark.

4.6.1 Topography and regolith

The Forsmark region has a comparatively flat bedrock surface with a gentle slope towards the north-east. The existing fracture zones and the small-scale variations in bedrock topography are partly evened out by variations in thickness of the regolith, i.e. unconsolidated deposits above the bedrock, resulting in a relatively flat topography (Figure 4-25).

A digital elevation model (DEM; Strömgren and Brydsten 2013) was developed in the SR-PSU project to describe the topography and bathymetry of the Forsmark area (Figure 4-26) The DEM has a resolution of 20 m and is a central data source for the site characterisation. It is also used as input to most of the descriptions and models of the surface system.

Figure 4-25. *The Forsmark area seen from the southeast with the only larger arable land area, Storskäret, in the foreground and the Forsmark nuclear power plant in the background.*

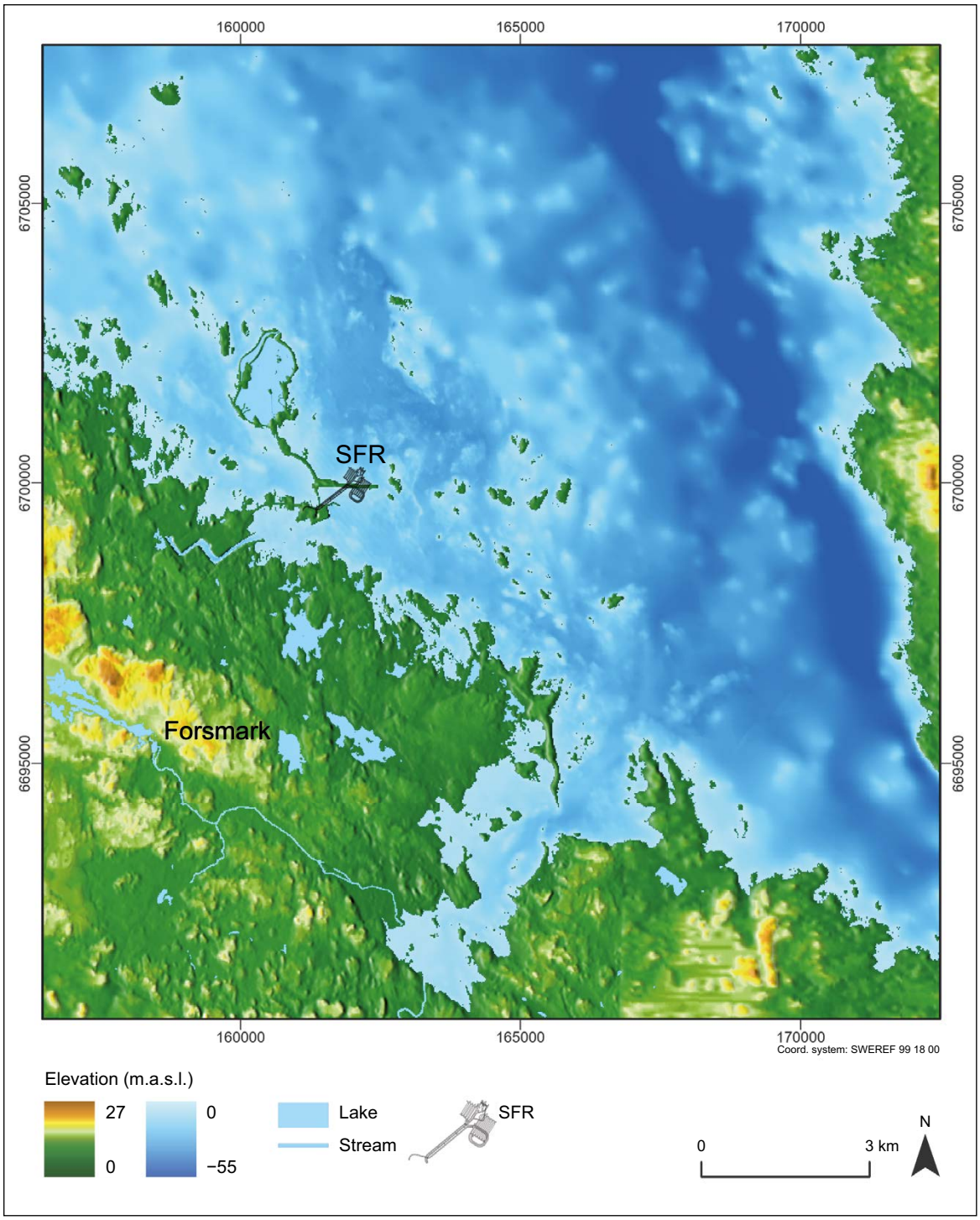

Figure 4-26. *The digital elevation model (DEM) of the Forsmark area, including the bathymetry (bottom level) of the sea (Strömgren and Brydsten 2013). The map shows the location of the existing and planned extension of SFR.*

The elevation differences are small in the terrestrial parts of the Forsmark area, especially near the coastline, and in the marine areas in the vicinity of SFR. Prominent topographical features of the landscape are the relatively small glacial landforms such as eskers. The most elevated areas are in the southwestern part of the area and the deepest area (about 55 m below sea level) is a trough (Gräsörännan) that runs in a NNW–SSE direction in the eastern part of the bay Öregrundsgrepen (for a map of the area including the geographical positions mentioned in the report, see Figure G-1).

In the Forsmark area, most regolith was formed during, or after, the final phase of the latest glaciation. Data describing regolith properties are an important input for modelling of hydrology and transport of elements within the biosphere. Soil, i.e. the upper part of the regolith in terrestrial systems, properties are also strongly associated with vegetation types and land use in terrestrial ecosystems. The description of the spatial distribution of regolith and its properties is based on primary data obtained from extensive field mapping, investigations in the form of drilling, excavations and geophysics and physical and chemical laboratory tests (for further details, see Sohlenius et al. 2013b and references therein).

The distribution of surface regolith in Forsmark (Figure 4-27) is typical for areas located below the highest coastline since the last glaciation. Exposed bedrock occurs in locally high topographical areas, mainly along the shoreline and in terrestrial areas. Till is the dominant type of regolith in the most elevated areas and occupies about 65 % of the surface in terrestrial areas and 30 % of the sea floor outside Forsmark (exemplified by Figure 4-27). A glaciofluvial deposit, Börstilåsen, has N–S and NW–SE orientations along the coast of the mainland and continues on the sea floor east of SFR. Glacial clay primarily occurs below present lakes and in depressions on the sea floor. Postglacial sand often covers the glacial clay. Postglacial clay gyttja, rich in organic material, is predominantly found and is currently being deposited in shallow bays and in the deepest parts of the sea floor. Gyttja mainly consists of organic material and is currently being deposited in lakes. Peat accumulates in fens and along the lake shores. The sea floor close to the location of SFR is dominated by till and in the lower topographical areas by glacial clay covered with sand.

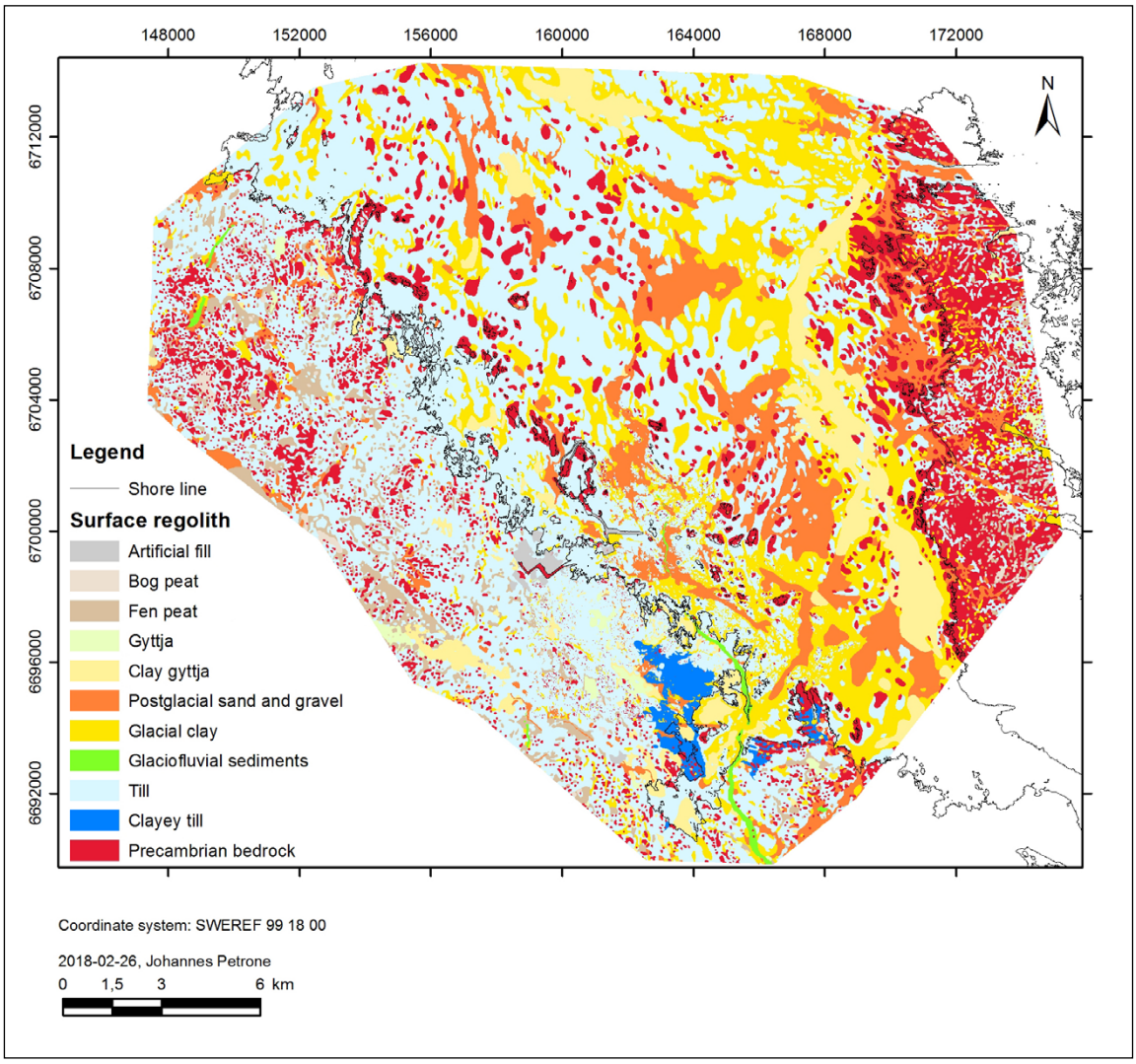

Figure 4-27. *Surface distribution of regolith layers with a minimum thickness of 0.5 m and areas with exposed rock in the Forsmark area. Note that lakes and the sea are shown without surface water. Modified from Petrone et al. (2020).*

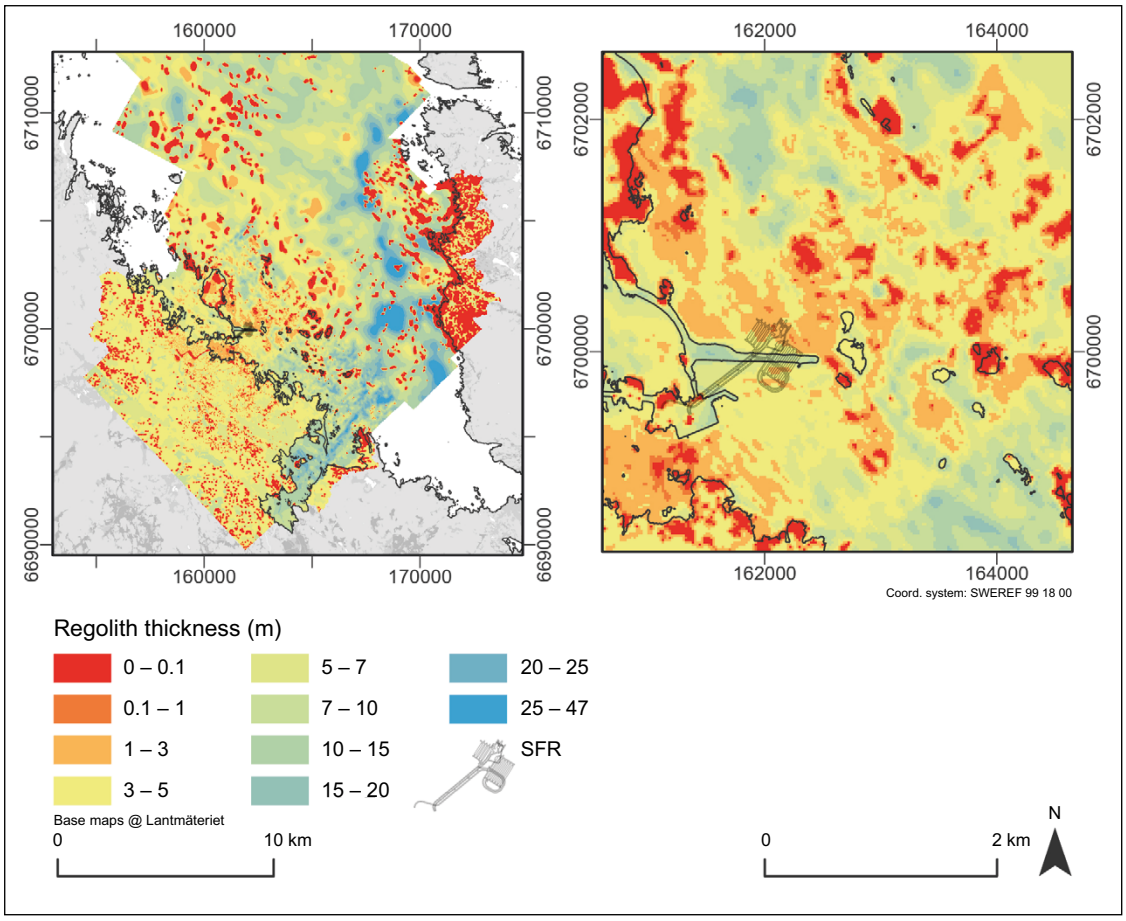

Figure 4-28. *Modelled total regolith thickness, left) in the Forsmark area and right) closest to SFR (Sohlenius et al. 2013b). Bedrock outcrops are shown as areas with regolith depth 0–0.1 m.*

A regolith depth and stratigraphy model (RDM) has been constructed to provide a geometric model of the thickness and distribution of regolith layers. The RDM is based on the general top-down stratigraphy of the Forsmark area, consisting of peat, gyttja and clay gyttja, postglacial sand/gravel, glacial clay, glaciofluvial sediments and till (Sohlenius et al. 2013b).

The total regolith depth ranges from negligible up to 47 m. The coastal zone and the islands (including the coastal zone of the island of Gräsö) are characterised by thin regolith layers and frequent rock outcrops. Generally, the regolith is deeper in the sea, with an average thickness of about 8 m, whereas the average thickness in the terrestrial area is about 4 m. The regolith thickness on the sea floor around the SFR pier is mostly 1–5 m (Figure 4-28).

4.6.2 Hydrological and near-surface hydrological conditions

The marine area at Forsmark consists of the open bay Öregrundsgrepen, with a wide and deep boundary towards the north and a narrow and shallower strait towards the south. Most of this coastal area is shallow (sea depth less than 10 m), except for Gräsörännan (down to >50 m). Local freshwater runoff produces a slightly lower salinity than in the Gulf of Bothnia as a whole and the salinity stratification in Öregrundsgrepen is generally weak (Aquilonius 2010). The direction of seawater flow through Öregrundsgrepen varies with time but, on an annual basis, there is a net flow directed from north to south (Karlsson et al. 2010).

Based on the sea bathymetry according to the DEM (Strömgren and Brydsten 2013), the present-day marine area outside Forsmark was divided into 38 basins. The water retention time (average age in the 38 basins) was calculated to vary between 13 and 29 days (average 19; Werner et al. 2014). Water exchange is more rapid in the deeper areas close to the open Bothnian Sea, whereas it is slower in the partly isolated shallow coastal basins.

The area above SFR is currently mainly sea covered, but the lakes, streams and hydrological conditions of the present landscape can give valuable information about the future hydrology and element transport pathways in the release area from SFR. A total of 25 present and future (currently sea-covered) lake catchments and sub-catchment areas, ranging from 0.03 to 8.67 km^2 have been delineated within the Forsmark area (Brunberg et al. 2004, Andersson 2010). Lake Fiskarfjärden, Lake Bolundsfjärden and Lake Eckarfjärden (Figure 4-30a) are the largest present lakes in the area (Figure 4-29), but they all have a surface area less than 1 km^2 and their average depth is about 1 m. The streams in Forsmark are small (Figure 4-30b) with highly seasonal flows and many stretches are often dry in the summer. Wetlands are common and cover 10–20 % of the Forsmark area (Löfgren 2010).

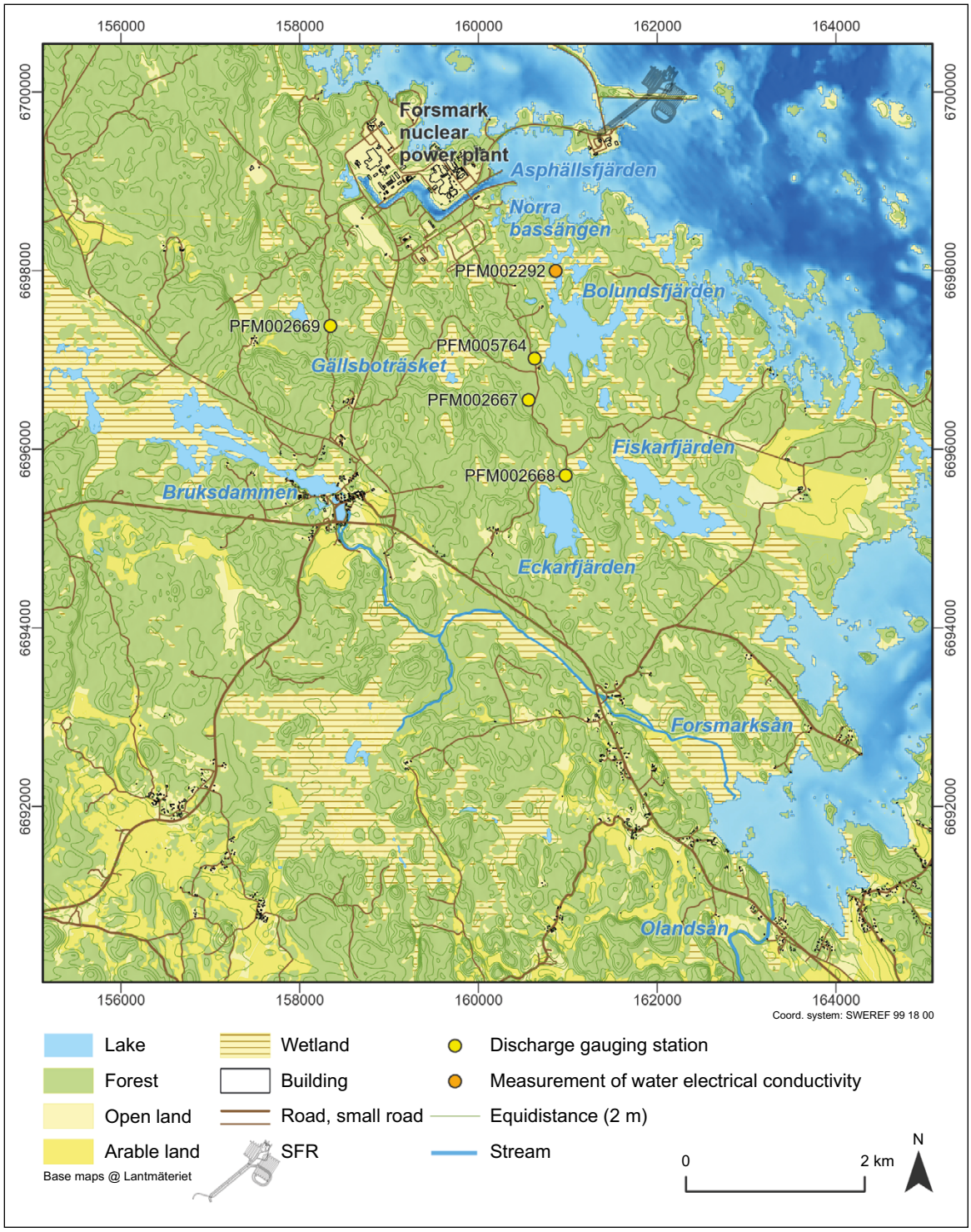

Figure 4-29. *Overview map of lakes, streams and some monitoring stations.*

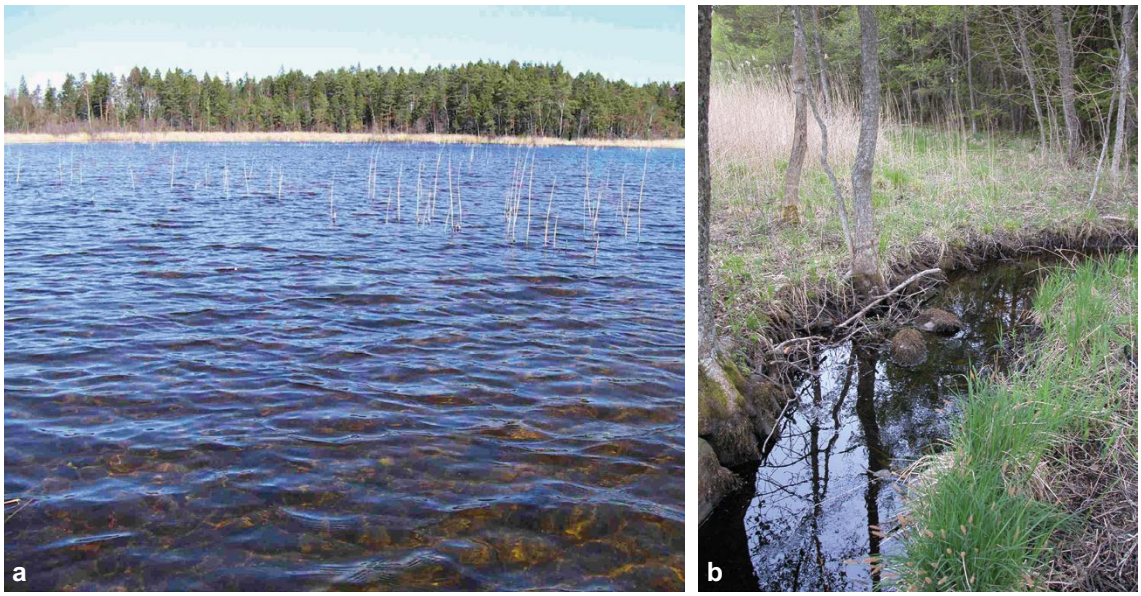

Figure 4-30. *a) Lake Eckarfjärden, one of the larger lakes in the Forsmark area. Like other lakes in the area, Eckarfjärden is a shallow oligotrophic hard water lake surrounded by reed. b) The third largest stream in Forsmark, near the inlet to the second largest lake in the Forsmark area (Lake Bolundsfjärden).*

The groundwater pressure gradients at Forsmark generally follow the elevation gradients of the surface topography when examining the yearly average groundwater pressure data. Groundwater divides in the regolith are therefore assumed to coincide with topographical surface-water divides. The close correlation between the ground-surface topography and near-surface groundwater levels results in a small-scale near-surface groundwater flow system that overlie more large-scale groundwater flow systems at greater depths.

4.6.3 Chemical conditions

The mobility and retention of chemical elements in the landscape are the basis for the radionuclide transport modelling of the biosphere. Knowledge about the distribution of elements and how this is determined by the chemical conditions of the surface system at Forsmark is based on extensive site investigations and modelling of limnic, marine and terrestrial systems including surface water, ground water, regolith, soils, sediments and biota (**Biosphere synthesis report,** Section 3.4 and references therein). Since 2002 there has been an ongoing long-term chemical monitoring programme at the site, comprising surface water and groundwater from regolith and bedrock (SKB R-07-34, Berglund and Lindborg 2017). The distribution of different elements in biotic and abiotic pools, together with estimates of element fluxes into and out of the pools, shows the major sources and sinks of elements in the landscape (Tröjbom and Grolander 2010). The results indicate that by far the largest fraction of most elements in both terrestrial and limnic ecosystems is found in soils and sediments, but significant pools of nutrients and essential trace elements are also found in organisms in terrestrial ecosystems. Recent studies have shown that a significant fraction of the Cl is bound in the biomass of the terrestrial system and that this pool has a high turnover rate (Svensson et al. 2021).

Till and glacial clay in Forsmark have a high content of calcite which originates from Palaeozoic calcite containing limestone that outcrops on the sea floor north of the Forsmark area (**Biosphere synthesis report**, Section 3.4). The high calcite content strongly affects chemical properties of the regolith, including sorption and element transport. The surface water and shallow groundwater generally become slightly alkaline (pH 7–8) from calcite weathering processes and have high concentrations of major constituents from marine relics after the recent emergence from the sea. Calcite also influences the development of terrestrial and limnic ecosystems at the site. For instance, secondary calcite precipitation and co-precipitation of phosphate contribute to the development of the nutrient-poor oligotrophic hard water lakes that are characteristic of the Forsmark area (Section 4.6.4 and Andersson 2010). The rich supply of calcium also influences soil formation and the development and structure of the terrestrial ecosystems (Löfgren 2010).

4.6.4 Ecosystems

One use of the description of the present-day surface ecosystems, together with scientific knowledge, is to identify processes potentially affecting transport, accumulation and uptake of elements to account for in the radionuclide transport modelling and safety assessment. This is done in a systematic manner by developing an interaction matrix for the surface system and FEP identification (**Biosphere synthesis report**, Chapter 6). The most important such processes in aquatic and terrestrial ecosystems, respectively, are summarised below (Figure 4-31 and Figure 4-32).

Marine ecosystems

The marine ecosystems at Forsmark are characterised by brackish conditions (salinity between freshwater and saltwater), resulting in low species diversity as few organisms are adapted to the brackish environment. Shallow waters, subdued bathymetry, restricted light penetration and upwelling along the coast result in a relatively high primary production of primarily benthic vegetation in the near-shore zone, in a region of otherwise fairly low production (Aquilonius 2010). The primary producers are dominated by benthic organisms such as microalgae, vascular plants and benthic macroalgae. The fauna is dominated by detrivores (i.e. snails and mussels feeding on dead organic material) on both hard and soft bottom substrates. The fish community is dominated by the marine species herring (*Clupea harengus*) in the pelagic zone, whereas limnic species (especially Eurasian perch, *Perca fluviatilis*) and three-spined sticklebacks (*Gasterosteus aculea*) dominate in near-shore areas.

Both abiotic and biotic processes influence transport and accumulation of elements in marine ecosystems (Figure 4-31). However, carbon budgets show that advective flux (water exchange) rather than biotic fluxes (e.g. primary production and consumption) often regulate transport and accumulation of elements (particular in open and offshore basins).

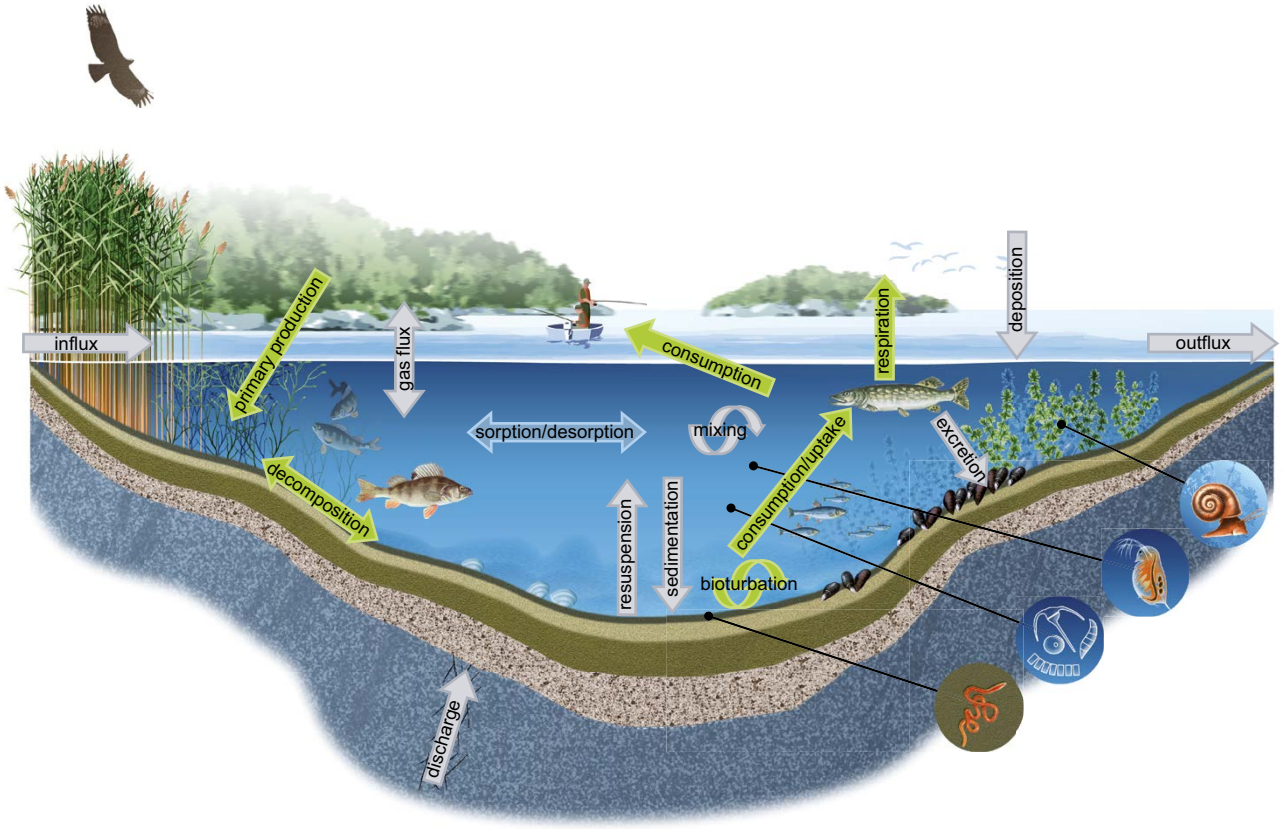

Figure 4-31. *Conceptual model of functional groups and important fluxes affecting transport and accumulation of elements in aquatic, i.e. limnic (Andersson 2010) and marine (Aquilonius 2010) ecosystems. Green arrows are fluxes mediated by biota (including consumption of fish by humans), grey arrows are fluxes of water, particles and gas, and the blue arrow represents sorption/desorption processes. The symbols on the right are examples of smaller-bodied flora and fauna in aquatic ecosystems.*

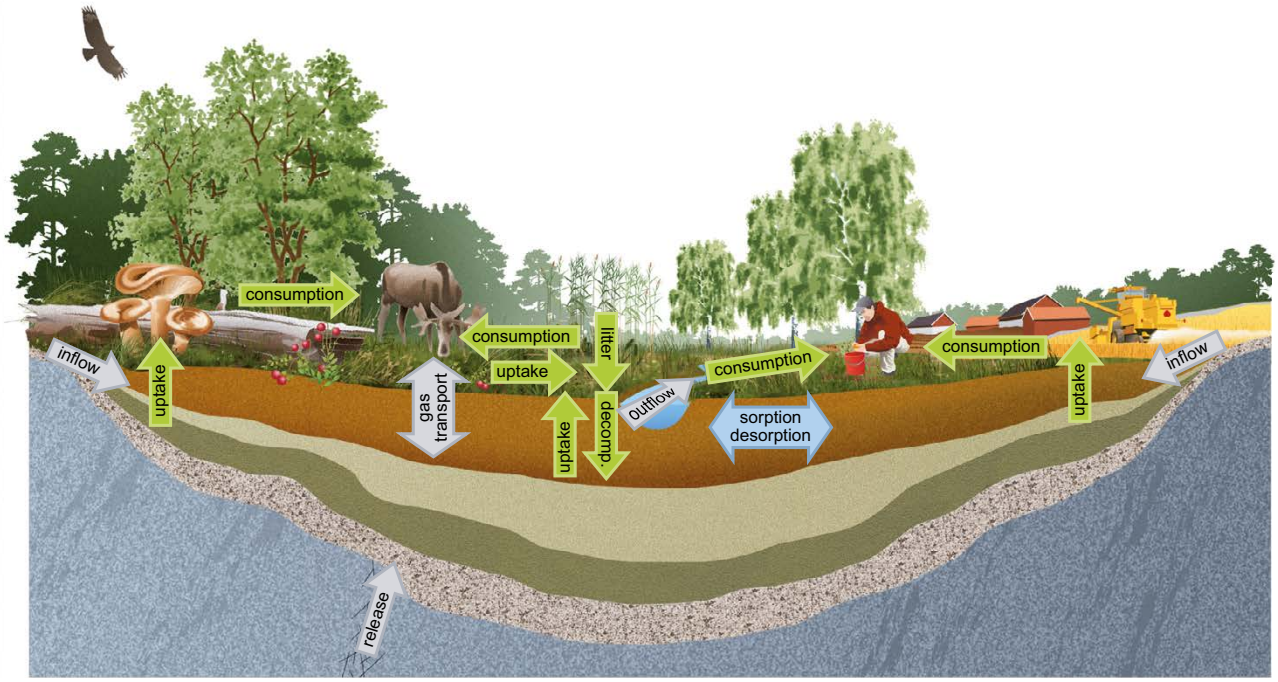

Figure 4-32. *Conceptual model of important fluxes affecting transport and accumulation of elements in a wetland ecosystem and arable land on a drained part of a mire (Löfgren 2010). Green arrows are fluxes mediated by biota (the uptake includes water for drinking), grey arrows are water and gas fluxes, and the blue arrow represents sorption/desorption processes. "Release" indicates a hypothetical release of groundwater from the bedrock containing repository-derived radionuclides. The mire was preceded by a lake stage and a marine stage, in which gyttja/clay and postglacial clay (shown as greenish regolith layers) were disposed prior to the peat (uppermost, brown layer).*

Limnic ecosystems

Present-day lakes in the Forsmark area are small and shallow (Figure 4-29 and Figure 4-30a). They are characterised as oligotrophic hardwater lakes, with high calcium and low nutrient levels (Andersson 2010). This lake-type is common along the coast of northern Uppland but is rare in the rest of Sweden (Brunberg et al. 2002, Hamrén and Collinder 2010).

Shallow depths and relatively clear waters allow photosynthesis in the entire benthic habitat and the lake bottoms are covered by dense stands of macrovegetation and a thick layer of microphytobenthos (microscopic algae and bacteria). The benthic primary producers dominate the biomass and primary production. The shorelines are dominated by reed belts, which are extensive especially around the smaller lakes. The fish community is dominated by perch (*Perca fluviatilis*), roach (*Rutilus rutilus*), tench (*Tinca tinca*) and crucian carp (*Carassius carassius*), of which the two latter species are resistant to low oxygen concentrations that could occur during winter under the ice.

Modelling of carbon dynamics in limnic ecosystems shows that, in some of the largest lakes in the area (e.g. Bolundsfjärden and Eckarfjärden), the primary production involves large amounts of carbon compared with the amounts that are transported from the surrounding catchment area. Consequently, there is a large potential for inorganic carbon entering the lakes, e.g. with deep groundwater, to be incorporated in the food web via primary producers. In the larger lakes, there is a relatively high degree of accumulation in sediments, which can be a permanent sink for radionuclides and other compounds. In the smaller lakes, the primary production is less important, and they function more as through-flow systems (Andersson 2010).

The small streams in the Forsmark area (see Figure 4-30b) are often dry in summer and the vegetation coverage is highly variable. However, some streams close to the coast carry water for most of the year that allow for fish migration and extensive spawning migration has been observed between the sea and Lake Bolundsfjärden (Andersson et al. 2011).

Terrestrial ecosystems

The terrestrial vegetation is strongly affected by topography, regolith characteristics and human land use. Some three quarters of the land area in Forsmark is covered by forests, dominated by Scots pine (*Pinus sylvestris*) and Norway spruce (*Picea abies*). Due to the calcareous regolith, the field layer is characterised by herbs, broad-leaved grasses and many orchid species. The area has a long history of forestry, with a high percentage of younger and older clear-cuts in different succession stages. Most of the frequent wetlands are coniferous forest swamps or open mires (Figure 4-33). Less mature wetlands consist of rich fens due to the high calcareous content of the regolith. Agricultural land (arable land and grassland) covers only a minor part of the land area of Forsmark today.

The most common larger mammal species in the Forsmark area are roe deer (*Capreolus capreolus*) and moose (*Alces alces*). In total, 139 bird species have been found in the Forsmark area (Green 2019). The most common species in Forsmark are, as in comparable regions of Sweden, chaffinch (*Fringilla coelebs*) and willow warbler (*Phylloscopus trochilus*) (Löfgren 2010). The conservational aspects are primarily associated with wetlands and forests containing red-listed and/or legally protected species (Hamrén and Collinder 2010). Two such rare species are the fen orchid (*Liparis loeselii*) and the pool frog (*Rana lessonae*).

Earlier safety analyses showed that wetlands are the natural terrestrial ecosystems most likely to receive and accumulate radionuclides directly from a geological repository via deep groundwater transport (SKB TR-10-09 and SKB TR-14-06). An extensive description of wetlands and other terrestrial ecosystems, including availability of primary data, evaluations of data and terrestrial models for the Forsmark area, is provided in Löfgren (2010).

Figure 4-33. *A wetland in the Forsmark area dominated by reed, Phragmites australis (Figure 4-2 in Löfgren 2010).*

4.6.5 Human population and land use

At the site, the Forsmark nuclear power plant is a large industrial activity in an otherwise relatively undisturbed area. There are a few holiday homes and permanent residents within a 5 km radius from SFR and one farm (Storskäret about 5 km from SFR, Figure 4-25 and Figure G-1). The area is used for hunting and fishing, but only occasionally used for other recreational activities due to the small local population, the relative inaccessibility of the area and the distance from major urban areas. Land use has previously been dominated by commercial forestry and timber extraction has been the only significant anthropogenic outflow of biomass from the area.

Despite the lack of farming close to SFR, present agricultural activities in the areas around Forsmark are described due to the importance of cultivated land for potential future radionuclide exposure. Currently, most arable land in the region around Forsmark, as generally in the county of Uppsala, is situated in areas with water-deposited clays (glacial and postglacial) and other fine-grained deposits, formed in topographical depressions when the area was covered by the Baltic Sea (Lindborg 2010). These deposits are, however, almost lacking in the terrestrial areas close to SFR and the proportion of arable land is therefore low. That can, however, change in the future when the fine-grained deposits situated at shallow water depths around SFR become available for cultivation through the shoreline displacement (further described in Section 6.3.2). A smaller fraction of the arable land is situated in areas with till and peat. The till in most areas has a high content of boulders and stones and is therefore not suitable for cultivation. The proportion of organic deposits used for cultivation has generally decreased significantly in Sweden during the last 60 years and the proportion of cultivated peat deposits in the County of Uppsala (5 %) is close to the Swedish average (Berglund et al. 2009). Today, creating new ditches in areas unaffected by ditches is generally forbidden and peat-covered wetlands (i.e. mires) are at present not converted to arable land in Sweden. However, a larger proportion of the Swedish peatland could potentially be used for cultivation in the future.

4.6.6 Wells and water resources management

All public water supply in the Municipality of Östhammar is based on groundwater (Werner et al. 2010). The public water supply closest to SFR is located at the Börstilåsen esker, about ten kilometres southeast of SFR.

At present, c. 30 % of the inhabitants in Östhammar obtain their drinking water from private wells (Werner et al. 2010). Today, there are some private wells (dug in regolith or drilled in bedrock) in land areas along the coast. Analyses of the well water show that the water quality varies from potable to non-potable. Some wells are not used as drinking water supplies, but instead for other purposes, e.g. irrigation of garden plots.

The current well density (both dug and drilled wells) varies between 0.5 and 2 wells per km^2 in different sub-areas within northern Uppland (size 3 300 km^2). According to an analysis of data from the Geological Survey of Sweden (SGU) Well Archive for more than 5 000 private wells drilled in bedrock in northern Uppland, the depth ranges from a few tens of metres up to about 200–250 metres (Werner et al. 2013, Figure 6-2). Generally, the deeper wells have been drilled for the purpose of geo-energy production. A typical depth for a water-supply well in bedrock is about 60 m (Werner et al. 2013, Section 6.2).

Current water management in Forsmark includes pumping out groundwater from SFR, a cooling-water channel from the sea to the Forsmark nuclear power plant, the use of Lake Bruksdammen (about 4 km southwest from Forsmark) as a water supply, and a groundwater drainage system at the nuclear power plant. There are no land improvement or drainage activities registered in public records. However, there are shallow (drainage) ditches in the forests and the level of Lake Eckarfjärden has previously been artificially lowered.

In Sweden today, the proportion of arable land that is irrigated is small, 3–4 % (Bergström and Barkefors 2004) and is primarily located in the county of Skåne (southern Sweden). In Uppsala County, the total irrigated area was estimated to be below 100 ha in 2006 and irrigated areas thus make up less than 0.1 percent of the total arable land in the county (Brundell et al. 2008, see also Löfgren 2010 for a discussion). Irrigation of land for cereals and fodder is very rare and, instead, it is primarily potatoes and horticultural products that are cultivated on irrigated land.

4.7 Geosphere

This section describes the initial state of the geosphere and summarizes information from the site investigations that were conducted on the site for SFR. The SFR3 site investigations included seven new core drilled boreholes and four percussion drilled boreholes. The site investigation is documented in the site descriptive model (SDM-PSU; SKB TR-11-04).

Supplementary investigations (Earon et al. 2022) have been performed in five cored boreholes as a part of the preparations for construction of the extension and they confirm the understanding of the site presented in the SDM-PSU. However, this section focuses on data collected up to the end of the site investigation for PSU.

4.7.1 Bedrock temperature

For consistency with the definition of the initial-state air temperature (Section 4.5.1), the temperature in the repository and the bedrock at repository depth is assumed to be the same as the present-day bedrock temperature at initial state, i.e. about 5–7 °C (Sundberg et al. 2009, Väisäsvaara 2009).

4.7.2 Rock types and rock domains

The area at SFR has been divided into four domains (RFR01–RFR04) with similar conditions with regard to rock types. Domain RFR01 is dominated by pegmatite to pegmatitic granite (SKB rock type code 101061). Domain RFR02 has a much more heterogeneous composition than RFR01 and locally consists of fine- to medium-grained metagranite–granodiorite (101057), which is the most common rock type in this domain (Curtis et al. 2011). The domain also contains a considerable amount of pegmatite and pegmatitic granite. Both SFR1 and SFR3 are situated for the most part in domain RFR02, whereas the access tunnels are situated in RFR01, see Figure 4-34.

There are no data from drill cores or tunnels for domain RFR03, but the interpretation of magnetic measurements indicates that the domain is dominated by pegmatite and pegmatitic granite. Data are also lacking for RFR04, but the assessment is that the rock type composition is similar to that in RFR02. The rock type composition in RFR03 and RFR04 is uncertain, but due to the peripheral location of these domains to SFR, the uncertainty is not important.

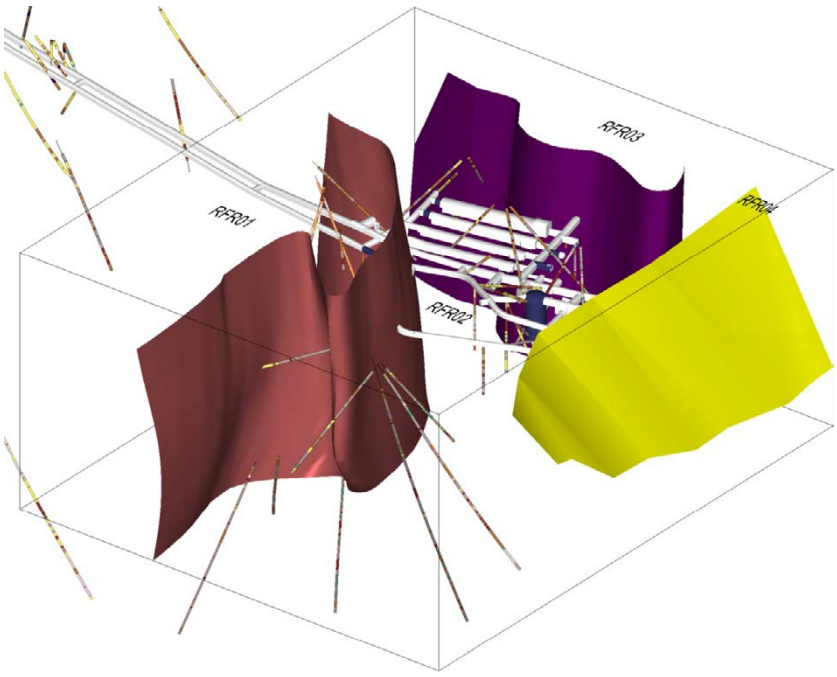

Figure 4-34. *3D view of SFR1 towards the west. The coloured areas show the boundaries between the different rock domains. The area for SFR3 is located for the most part in domain RFR02, on the side towards the viewer (SKB TR-11-04).*

4.7.3 Deformation zones and subhorizontal superficial structures

A local and a regional model have been constructed that show the interpreted deformation zones in the area based on available information (see Figure 4-35 and Figure 4-36). The latter figure contains a combined model with both deformation zones and rock domains shown in a 3D view. This figure also shows the location of SFR1. SFR3 will be on a level with the deepest parts of SFR1, in the Central Block to the southeast of SFR1 (see Figure 4-3).

The local model contains all modelled deformation zones that have a size corresponding to a trace length on the ground surface of ≥ 300 m. The regional model contains only local major and larger zones, i.e. zones with a trace length on the ground surface of ≥ 1 000 m. The regional-scale volume is referred to as the SFR Regional domain.

The conceptual understanding of the deformation zones and the bedrock structure at Forsmark, described in Stephens et al. (2007) and presented in Curtis et al. (2011), Section 2.3 was adopted in the SFR study. Further details on fracture domains and fracture properties such as fracture mineralogy are discussed in Curtis et al. (2011), Section 4.5.

The deformation zones are divided into different groups, namely:

1) Vertical to steeply dipping zones with a WNW to NW strike. Six zones in the Central Block belong to this group and some of them are expected to intersect the planned rock volume for SFR3.
2) Vertical to steeply dipping zones with a NNE to ENE strike. These zones are shorter compared with zones in group 1. The group consists of a total of seven zones, one of which lies within the Central Block.
3) Vertical to steeply dipping zones with a NS to NNW strike. These end at zones belonging to the preceding two groups. This group includes two zones that intersect the Central Block.
4) Moderately to gently dipping (≤ 45 °) zones. The group consists of a total of three zones, one of which lies within the Central Block.

There are also water-bearing subhorizontal structures observed above all in the near-surface bedrock, these were probably formed due to destressing and they are interconnected to differing degrees to other horizontal fractures and to the deformation zones (see also Section 4.7.5).

Information on uncertainties in the geological understanding at SFR are discussed in SKB (TR-11-04) and Curtis et al. (2011, Section 5.6).

4.7.4 Rock mechanical characterisation

The expected range of common rock mechanical parameters of intact rock is given in Table 4-2. It should be noted that the rocks in average can be classified as R5 (very strong) to R6 (extremely strong) using the ISRM Strength Classification (Brown 1981).

Table 4-3 provides estimated values of mechanical parameters for single fractures. When it comes to assessment of mechanical properties for single fractures, subhorizontal shallow fractures (0–50 m) have been described in a category of their own, since their properties are expected to differ from all the other fractures. Observations in televiewer logging images support this separate description and difference in character of the subhorizontal shallow fractures (SKB TR-11-04).

A common way to characterise the properties of a rock mass is to model the strength with a Mohr–Coulomb failure criterion and deformation properties with elastic parameters. Table 4-4 gives typical values of these rock mechanical parameters for the rock mass in SFR, both in the rock domains and in the deformation zones. The properties in the deformation zones are expected to differ between the core and the outer parts (transition zone towards the less damaged rock mass), although many of the minor zones are not expected to have any pronounced core. See further details in Stephens et al. (2007, Section 5.2).

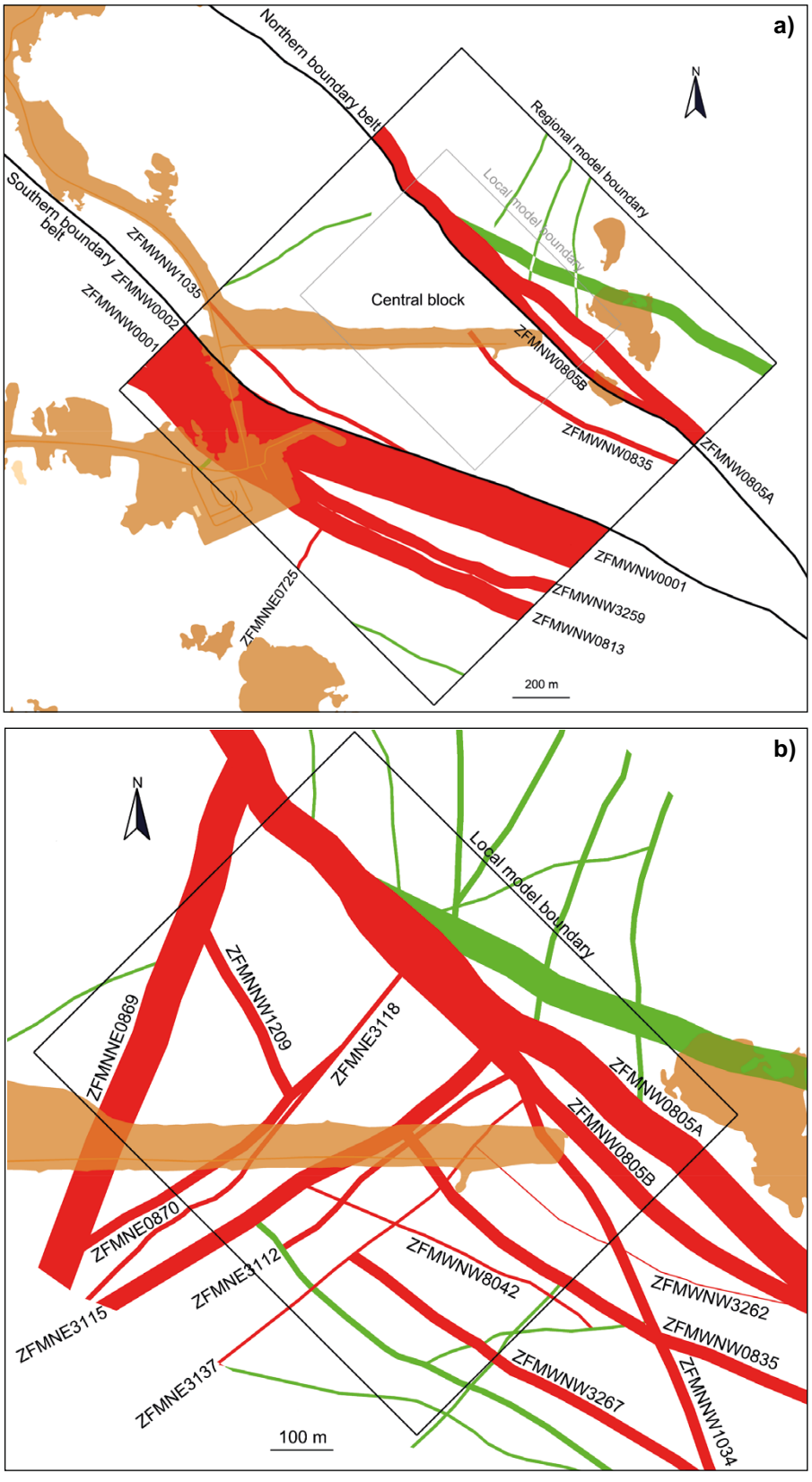

Figure 4-35. *Intersection of deformation zones with the ground surface. a) Regional model area. The large regional zones ZFMWNW0001 and ZFMNW0805A comprise, along with their splays, the boundaries of the central tectonic block in which both SFR1 and SFR3 are situated. The colours indicate confidence in the model with regard to the existence of the zones: high = red, medium = green. The brown area indicates what is currently terrestrial. b) Local model area (SKB TR-11-04, modified from Figure 5-16).*

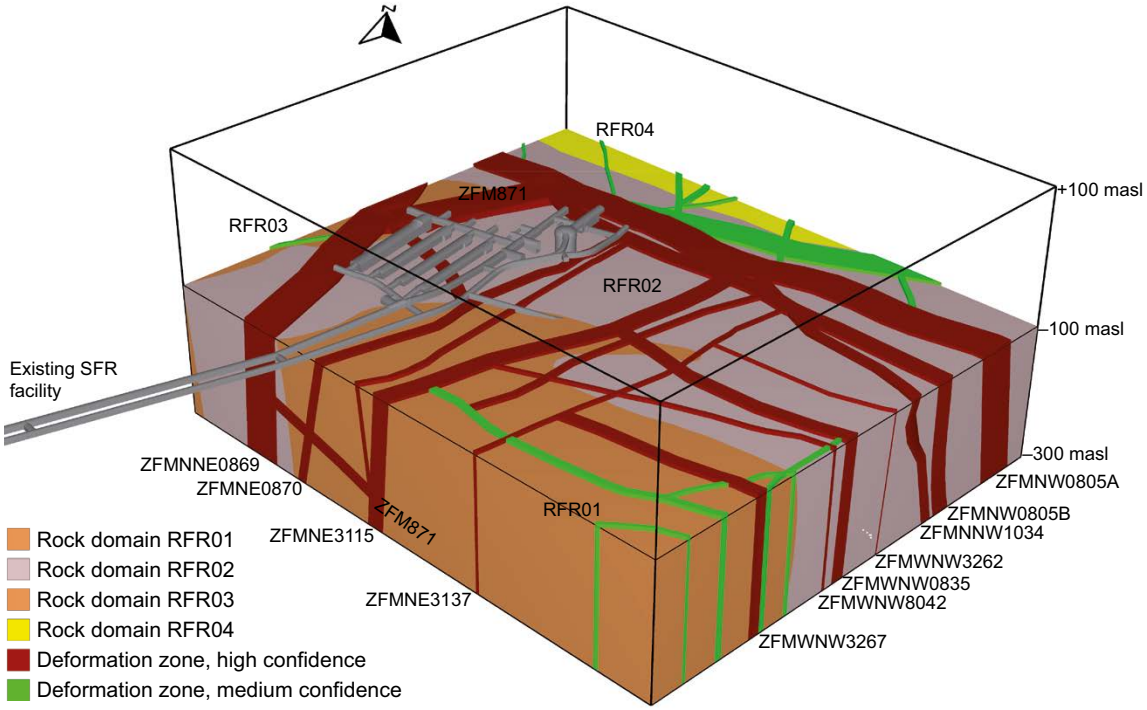

Figure 4-36. *Rock domains (the colours indicate rock type composition) and deformation zones in the SFR local model volume, version 1.0 viewed obliquely downwards towards the north. The block location is shown in Figure 4-35.*

Table 4-2. Rock mechanical parameters of intact rock in the SFR area (Given in the form of a truncated normal distribution: mean/standard deviation and min–max). SKB (TR-11-04, Table 6-3).

Parameter	101057 – Granite to granodiorite	101061 – Pegmatite, pegmatitic granite	111058 – Fine- to medium-grained granite	103076 – Felsic to intermediate metavolcanic rock	102017 – Amphibolite
Uniaxial compressive strength (MPa)	226/50 126–326	183/45 90–270	280/45 210–350	139/45 100–200	142/45 60–230
Crack initiation stress (MPa)	116/26 64–168	114/22 64–166	148/22 104–192	--	--
Indirect tensile strength (Brazilian test) (MPa)	13/2 10–18	12/3 8–16	16/2 12–20	9/2 5–13	9/2 5–13
Young's modulus (GPa)	75/3 69–81	74/4 66–82	74/2.5 70–79	99/3 93–105	81/4 73–89
Poisson's ratio	0.23/0.04 0.14–0.30	0.30/0.03 0.26–0.35	0.28/0.03 0.22–0.32	0.35/0.03 0.29–0.41	0.22/0.04

Table 4-3. Estimated mechanical properties of single fractures in the SFR area. SKB (TR-11-04, Table 6-6).

Parameter	Subhorizontal (dip 0–20°) fractures at a depth z = 0–50 m, σ_n' = effective normal stress	Other fractures at a depth z = 0–150 m and Subhorizontal fractures where z > 50 m, σ_n' = effective normal stress
Normal stiffness, K_n [MPa/mm]	$K_n = 10 \times \sigma_n$'	$K_n = 10 \times \sigma_n$'
Shear stiffness, K_s [MPa/mm]	$K_s = K_n/3$	$K_s = K_n/20$
Friction angle, φ_1 [°] for normal stress range 0–0.5 MPa	66°	48°
Friction angle, φ_2 [°] for normal stress range 0.5–1.5 MPa	32°	35°
Apparent cohesion for normal stress range 0.5–1.5 MPa	0.4	0.4
Dilatancy	15°	15°

Table 4-4. Rock mass values of strength and deformation properties in rock domains and deformation zones. The Mohr–Coulomb constitutive model has been assumed. Data for depth of 20–150 metres. SKB (TR-11-04, Tables 6-8 and 6-9).

	Friction angle, M-C (0–5 MPa)	Cohesion, M-C (0–5 MPa)	Deformation modulus for the rock mass, Em	Poisson's ratio
Rock domain	50–60°	13 MPa	50 GPa	0.34
Outer part of deformation zone	51°	2 MPa	13 GPa	0.35
Core of deformation zone	37°	2 MPa	2.6 GPa	0.46

No direct measurements of the rock stress have been made in the area where SFR3 is planned to be located, but there are several stress measurements conducted in the SFR area close to the SFR3 location (SKB TR-11-04, Section 6.4), however there is a large spread in the measurements. Furthermore, a greater variation in rock stresses can be expected in the shallowest rock. The estimate that has been made (Table 4-5), based on measurements made in the SFR area, must therefore be regarded as uncertain. The stress magnitudes will, however, be relatively low at repository level, and are not expected to be a significant factor for constructability or safety. The dominant orientation of the principal stress is judged to be relatively well known.

Adjacent to the excavated tunnels and waste vaults, the stresses will be redistributed so that they differ from the *in situ* stress given in Table 4-5. There is expected to be an excavation-damaged zone (EDZ) in the rock mass along the tunnel walls, caused by the blasting. The fracture frequency in the EDZ is expected to be higher than in the surrounding rock but limited to the close vicinity of the vaults (**Geosphere process report**).

Table 4-5. Rock stresses with depth dependence in the SFR area from the rock surface down to a depth of 250 metres (z is the depth in metres). SKB (TR-11-04, Table 6-11).

All rock domains	Major horizontal stress	Minor horizontal stress	Vertical stress
Magnitude (MPa)	$\sigma_H = 5+0.07z$	$\sigma_n = 0.07z$	$\sigma_v = 0.027z$
Orientation (trend from north)	142°	52°	Vertical

4.7.5 Bedrock hydrogeology

The SFR3 site investigations included fracture mapping surveys and hydraulic tests. A detailed description of the investigations and analysis of the geometric and hydraulic properties of the fractures is provided in the Site Descriptive Model of the SFR area, SDM-PSU (SKB TR-11-04, Chapter 7). An account is given there of the occurrence of transmissive fractures in deterministically modelled deformation zones (larger than 300 m) and between them in the rock mass, consisting of stochastically modelled fractures (smaller than 300 m). One of the observations in SDM-PSU is that the most transmissive fractures down to 200 m have been encountered in the rock mass between deterministically modelled deformation zones. Another observation is that gently dipping fractures are the most transmissive, even inside the steeply dipping deformation zones. Among the steeply dipping fracture sets, it is the NW-SE set that is the most transmissive. In the area planned for SFR3, the frequency of transmissive gently dipping fractures is lower in the interval −100 to −150 m than it is above or below this depth interval, see Figure 4-37.

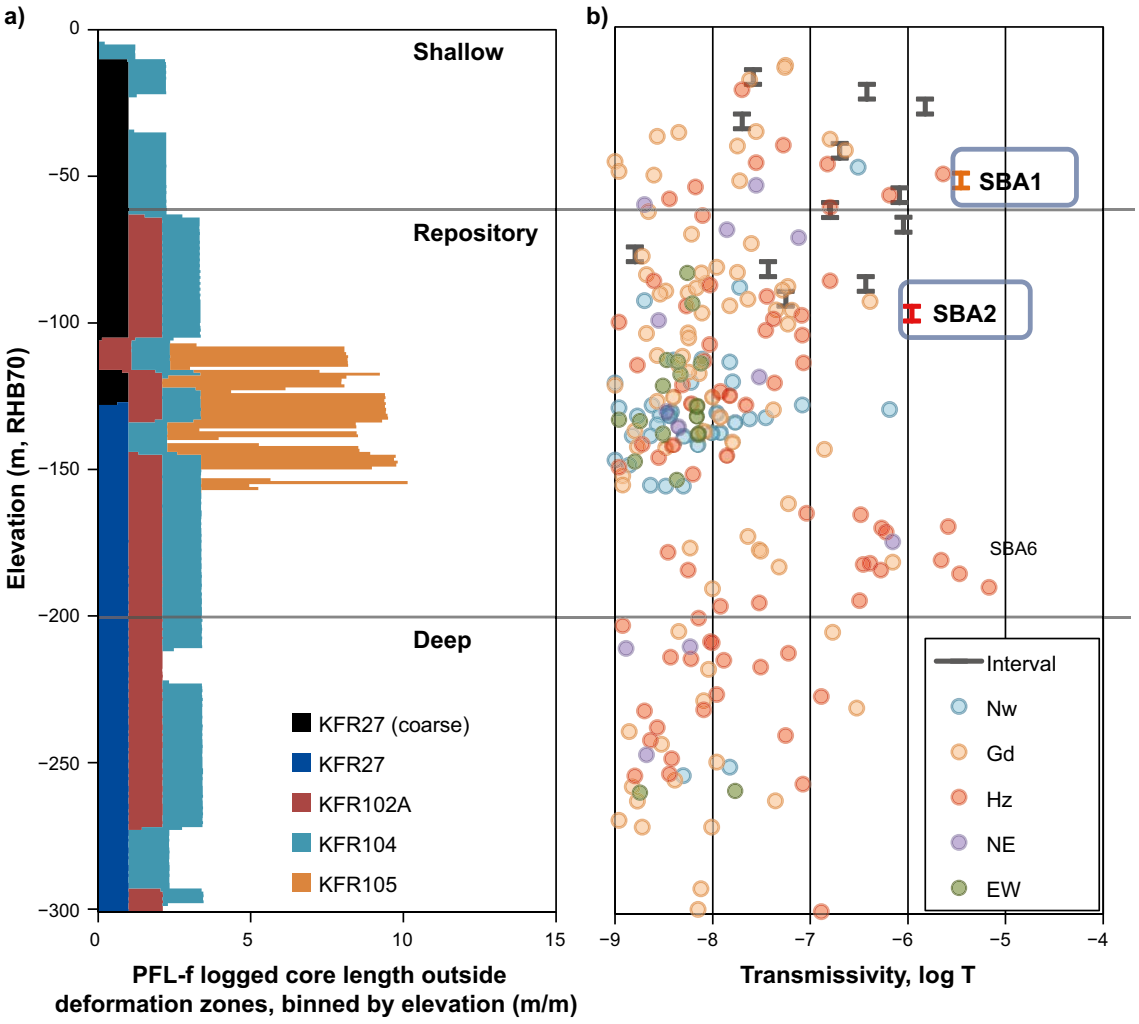

Figure 4-37. *a) Borehole coverage (total borehole length) in the area closest to SFR3, and b) PFL-f[19] and PSS[20] transmissivity data (in interval) outside deformation zones divided into fracture sets (NW, Gd = Gently dipping, Hz = Horizontal, NE and EW). SBA = shallow bedrock aquifer (for explanation, see text). The depth interval 100–150 m contains fewer highly transmissive fractures than the interval 50–100 m (SKB TR-11-04, Figure 9-14).*

[19] Flowing fractures detected by the Posiva Flow Log (PFL), known as PFL-f data (Follin et al. 2007).

[20] Single-hole Pipe String System (PSS) injection tests (Follin et al. 2007)

In SDM-PSU, a total of eight shallow bedrock aquifers (SBA) structures (SBA1-SBA8) have been modelled (Figure 4-38). Three of these subhorizontal structures are shown in Figure 4-37: SBA1, SBA2 and SBA6. The SBAs are deterministic representations of hydrogeological data interpretations (PFL-fs, hydraulic interferences and borehole radar), and they are represented as planar structures in the conceptual and numerical flow models. The SBA structures are linked together into a persistent fracture network by steeply dipping fractures (see Öhman et al. 2012, Appendix B).

4.7.6 Present groundwater composition and origin

The hydrochemical conditions in the bedrock are described in the SDM-PSU (SKB TR-11-04) and in Nilsson et al. (2011). The SFR groundwaters show some characteristic features. The chloride concentration range is within 1 500 to 5 500 mg/L. The $\delta^{18}O$ values varies within–15.5 to –7.5 ‰ V-SMOW. Marine indicators, such as Mg/Cl, K/Cl, SO_4/Cl and Br/Cl ratios show relatively large variations, especially considering the limited salinity range. This suggests the presence of groundwaters with different origins.

From measured Eh values – and in accordance with the redox chemistry for iron, manganese, sulfur and uranium – it can be concluded that weakly reducing conditions (−140 to −190 mV) prevail generally in the investigated groundwaters. The redox-buffering capacity is provided by fracture-filling iron(II) minerals (mainly chlorite, clay minerals and pyrite) present in the conductive fractures in addition to biotite in the bedrock (Sandström and Tullborg 2011, Sandström et al. 2014).

Of great importance for the understanding of the present-day groundwater chemistry at SFR is the evolution of today's "Baltic Sea" area during Weichselian and Holocene times (Westman et al. 1999, SKB TR-08-05). This is further discussed in SKB (TR-11-04, Chapter 8).

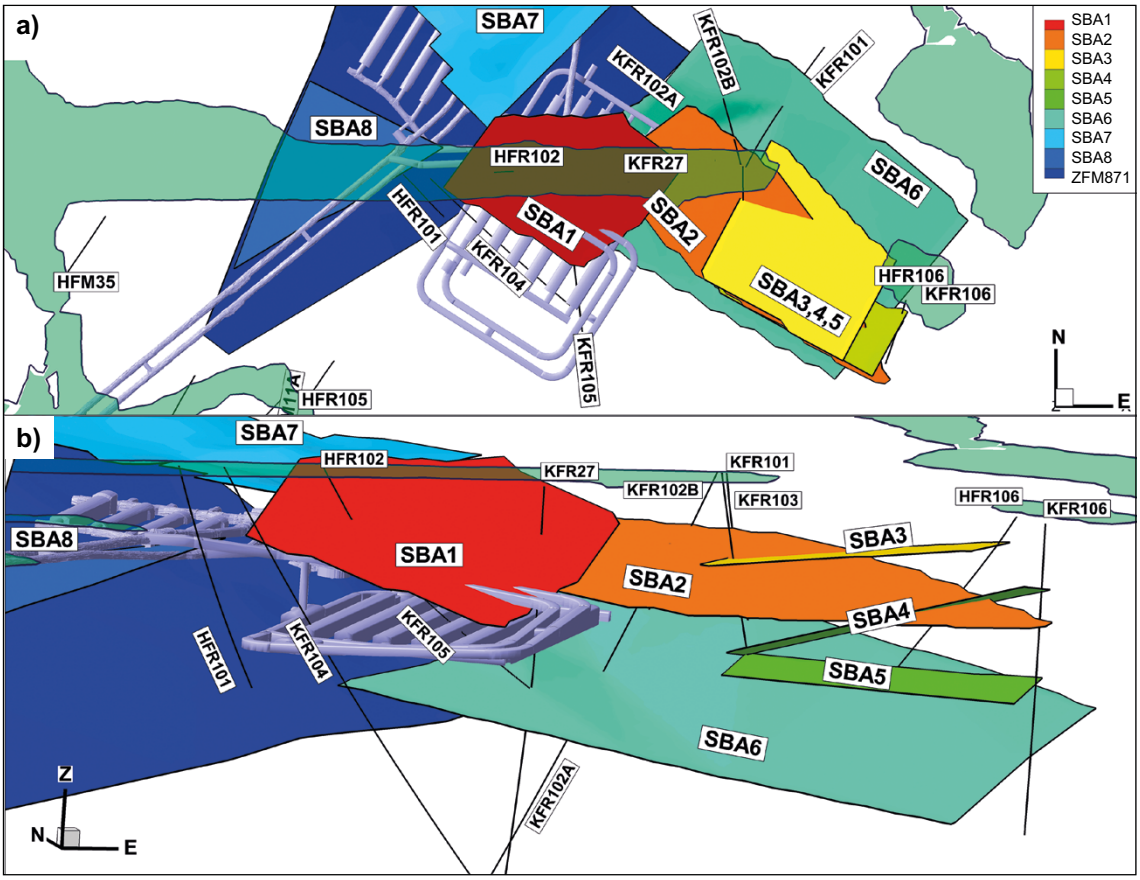

Figure 4-38. *Visualisation of eight SBA structures a) view from above and b) view towards the northeast. The relevant boreholes are designated by their KFR (cored boreholes) and HFR (percussion boreholes) numbers.*

Groundwater types identified in SFR1

Four different types of groundwaters have been defined considering the climatic history of the Holocene (Westman et al. 1999): Local Baltic, Littorina Sea with a glacial component, Brackish-glacial and Mixed-brackish (transition type). These groundwater types reflect the main origin of the groundwater but also changes due to mixing and reaction that occurred after the intrusion into the bedrock. The subdivision into these characteristic types of groundwater has been based on the chemical variables, chloride, magnesium and $\delta^{18}O$.

The composition of the present groundwater types, as well as reactions and processes that have influenced their chemistry, are presented in Table 4-6.

Table 4-6. Groundwater types in SFR – composition, reactions/processes and origin (SKB TR-11-04, modified from Table 8-1).

Groundwater type	Composition/ characteristics	Dominant reactions and processes	Origin
Local Baltic Sea	Chloride 2 500–3 500 mg/L $\delta^{18}O$ −9 to −7.5 ‰ V-SMOW Na-(Ca)-(Mg)-Cl-SO_4 type Cl/Mg weight ratio < 27	Ion exchange and micro-biological reactions in the bedrock have resulted in decreased concentrations of Mg, K, Na and SO_4 as well as enrichment of Ca and HCO_3 compared with Baltic Sea water.	It is unclear whether the Baltic Sea water was present at all in the deformation zones before the construction of the tunnels in SFR. It is more probably a modern component that has been introduced due to the drawdown caused by tunnels as indicated by the tritium content.
Littorina Sea with a glacial component	Chloride 3 500–6 000 mg/L $\delta^{18}O$ −9.5 to −7.5 ‰ V-SMOW Na-Ca-(Mg)-Cl-SO_4 type Cl/Mg weight ratio < 27	The Na/Ca ratio is lower than the marine ratio. These changes are caused by ion exchange, but also by dilution with glacial meltwater.	Compared with the original Littorina Sea water, it has been diluted (lower Cl and $\delta^{18}O$ values) with glacial meltwater.
Brackish-glacial	Chloride 1 500–5 000 mg/L $\delta^{18}O$ < −12.0 ‰ V-SMOW Na-Ca-Cl type Cl/Mg weight ratio > 32	An old mixture of different, mainly non-marine groundwaters.	This is the oldest groundwater type at SFR and the amounts of post-glacial components are very small. It is a mixture of primarily glacial meltwater (last deglaciation or older) and brackish non-marine water (pre-glacial). It probably contains components of old meteoric water prior to the last deglaciation as well.
Mixed-brackish (transition type)	Chloride 2 500–6 000 mg/L $\delta^{18}O$ −12.0 to −9.5 ‰ V-SMOW Na-Ca-(Mg)-Cl-(SO_4) type	Natural or artificial mixing of the three different groundwater types above.	Significant mixing of the brackish-glacial and the two brackish marine groundwater types (mostly the Littorina Sea type) has caused this ground water of transition type. It is more common during the last two decades, according to data from long time series sampling, which suggests artificial mixing due to the presence of the repository.

Figure 4-39 displays a 3D presentation of the SFR site, the boreholes, the groundwater types and the deformation zones. The hydrostructural properties of the SFR site determine the distribution and the degree of mixing of the different groundwater types. The Littorina Sea type is observed primarily along vertical deformation zones with high hydraulic conductivity, with the propagation of the Local Baltic Sea type expanding downwards in basically the same zones. The oldest groundwater type at the SFR site (Brackish-glacial) is present in bedrock with low conductivity located above and below subhorizontal, highly conductive structures/zones. Processes of mixing, resulting in the so-called Mixed-brackish (transition type) of groundwater, are occurring mainly along, and in the vicinity of, these conductive structures, for example in and close to subhorizontal zone ZFM871.

Groundwater types in the area for SFR3

The hydrochemical sampling carried out in SDM-PSU has yielded data from a total of fifteen borehole sections in five cored boreholes and three percussion boreholes. Furthermore, the SICADA database contains data from two percussion boreholes from the site investigation in Forsmark for the spent fuel repository (Laaksoharju et al. 2008) and from a total of 45 borehole sections in 18 older cored boreholes drilled from the existing tunnels in SFR1 (Nilsson et al. 2011).

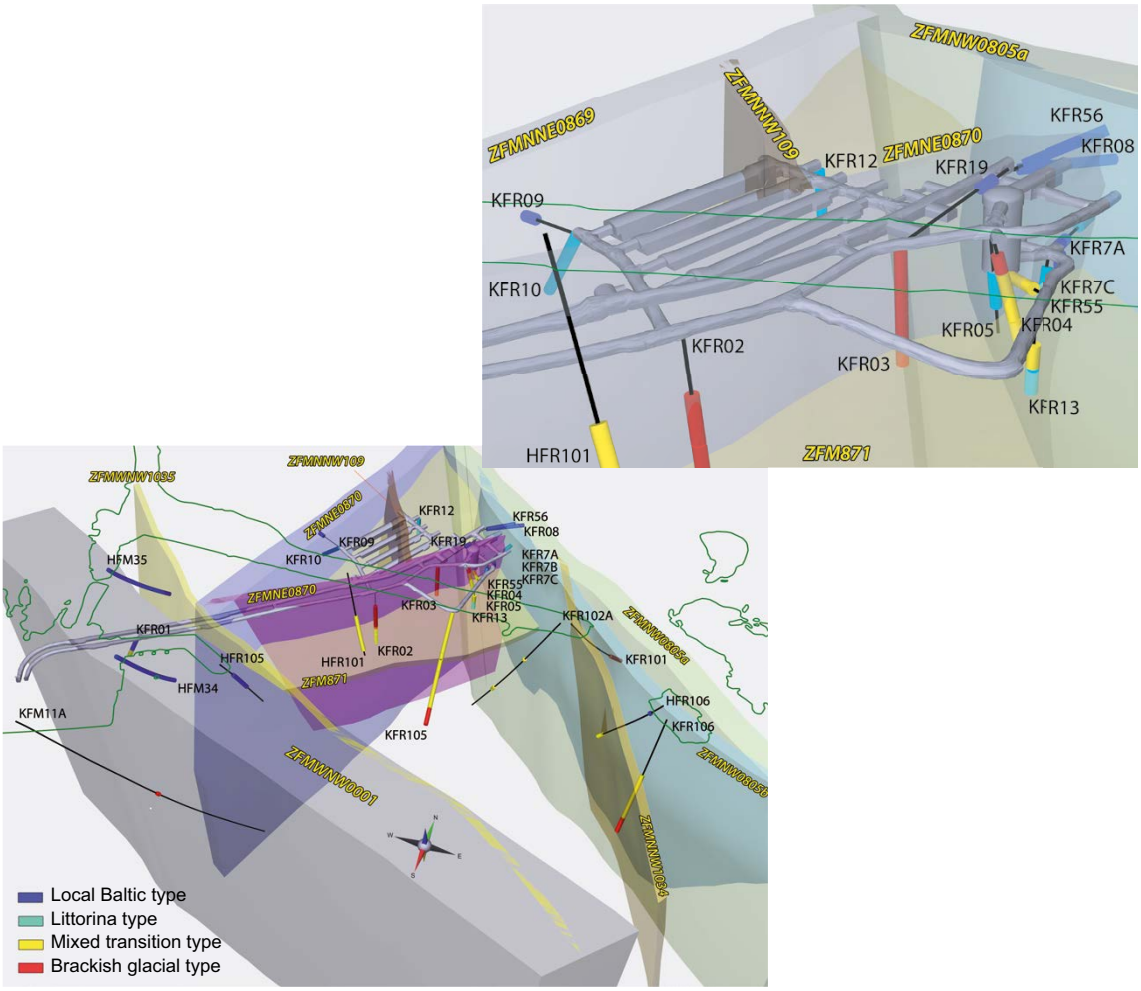

Figure 4-39. *3D presentation, viewed from above and from the southeast, of the groundwater type distribution in the regional model volume. The SFR boreholes are enlarged in the upper figure. The green outline at the surface demarcates the shoreline with the pier and small islet.*

Fewer data are available from the area for SFR3 than from the SFR1 area and data from the central part of SFR3 are entirely lacking. In general, most of the deeper sections in the investigated boreholes are characterised by various proportions of glacial meltwater (brackish-glacial groundwater type), whereas the groundwater type Mixed-brackish (transition type) is mostly prevalent at shallower levels (see Figure 4-39; borehole KFR105). It can be noted that no waters of the Littorina Sea type and only a few waters of Local Baltic Sea type have been encountered in the investigated borehole sections. The Local Baltic Sea type of water is present only at shallow depths.

4.7.7 Changes in water composition caused by drawdown in SFR

In general, mixing takes place mainly in and near the deformation zones – between Littorina Sea type and Local Baltic Sea type groundwater, and between Brackish-glacial type and Littorina Sea type groundwater, the latter forming the Mixed-brackish (transition type) groundwater. The distribution of the different groundwater types shows that the major deformation zones have acted as flow paths for groundwater during long geological periods and still act as efficient pathways, whereas fractures in less conductive bedrock between these zones generally retain old, more isolated groundwaters.

Measurement series in boreholes and tunnel systems show that the Cl content declined between years 1986 and 2000, followed by a nearly stable period up to year 2010 (SKB TR-11-04). This is as expected because the greatest changes with regard to groundwater pressure and inflows to the boreholes and the tunnel system occurred soon after construction. During the construction and operation of SFR3, the same pattern in groundwater chemistry can be expected as in SFR1, with an increasing occurrence of the local Baltic Sea and Mixed transition groundwater types. However, no Littorina Sea type groundwater has been encountered, which would indicate a lack of flow paths. Therefore, intrusion of modern Baltic Sea water will probably be less pronounced in SFR3 compared with the existing part of SFR. This may imply that the rate of changes will be slower in SFR3.

However, the observed changes in SFR1 indicate that the future impact of SFR3 on the groundwater chemistry may occur in a relatively short time. A few positive Eh values have been measured, most of them in year 2000. It is possible that they may be linked to the presence of amorphous Fe(III) oxyhydroxides (Gimeno et al. 2011), but it is more probable that they are due to the influence of an open repository (and/or that the time required for making adequate redox measurements was not allocated). More recent and repeated measurements show reducing conditions. Furthermore, in a supplementary study (Sandström et al. 2014), minerals interpreted as Fe(III) oxyhydroxides were re-evaluated and with the exception of two samples found to be iron-rich layered clay minerals, uranium-minerals, hematite-stained adularia and albite or even rust-coloured metallic iron from the drilling process.

Although it has not been proven, it is quite possible that the groundwater flow path from the mainland Forsmark may supply shallow groundwater. Potentially, this groundwater can contribute to a mixing between groundwater of meteoric origin and water originating from the Littorina Sea. However, the composition of this mixture cannot, at present, be distinguished from that of Baltic Sea/Littorina Sea water mixtures.

4.7.8 Water composition in the initial state

The composition of penetrating groundwater (used as reference groundwater composition in the PSAR) is given in Auqué et al. (2013), see Table 4-7. The composition is based on weighted values for all groundwater types occurring in SFR with broad intervals. The redox potential (E_h) is based on modelled values and on the measured values reported in Section 4.7.9. It is likely that the E_h will stay at today's value or even decline, since the dissolved oxygen in the groundwater will be rapidly consumed as the tunnels are filled with water.

When the repository resaturates, reactions will also occur with the concrete in the structures in SFR. The pH in the pore water in the concrete is around 13 and, when the repository has become water-saturated, hydroxide ions from the concrete's pore water will contribute to an increase of the pH in the water in the repository. During the sampling period 1986 to 2010, a slightly rising trend in the groundwater pH can be seen, but the range of measured values is large.

Table 4-7. Composition of penetrating water and range of variation of the relevant parameters during the temperate climate domain when the area above the repository is submerged beneath the sea. Concentrations in mg/L (Auqué et al. 2013, Tables 4.1 and 4.2). Data from the earlier safety assessment SAFE are shown for comparison (Höglund 2001).

Quantity	Reference value	Range Samples from SFR down to –200 m	SAFE reference value and (range)
pH	7.3	6.6–8.0	7.3 (6.5–7.8)
E_h	–225	–100 to –350	Red. (–100 to –400)
Cl	3 500	2 590–5 380	5 000 (3 000–6 000)
SO_4^{2-}	350	74–557.2	500 (20–600)
HCO_3^-	90	40–157	100 (40–110)
Na	1 500	850–1 920	2 500 (1 000–2 600)
K	20	3.8–60	20 (6–30)
Ca	600	87–1 220	430 (200–1 600)
Mg	150	79–290	270 (100–300)
SiO_2	11	2.6–17.2	5.66

Uncertainties

A large amount of data on the groundwater composition is available, which minimises the significance of errors in single points and, as far as temporal uncertainties are concerned, there are enough data to see trends. The spatial distribution, however, is uneven since there are many sampling points in SFR1, whereas there are fewer in the area for SFR3 and none in the central part of SFR3.

The undisturbed hydrochemical conditions prevailing before the construction of SFR1 are not known since there are no groundwater chemistry data available before the construction of SFR1, and this adds to the uncertainty.

Site-specific aspects of the groundwater regarding pore water, microbes and gases were not studied in the site investigations for SDM-PSU (SKB TR-11-04). SFR data on organic matter (dissolved or total organic carbon) are also relatively few. Some interpretations and knowledge from the Forsmark site, SDM-Site Forsmark (Laaksoharju et al. 2008, SKB TR-08-05) are considered applicable and also relevant for SFR.

5 Safety functions

5.1 Introduction

The post-closure safety of SFR is achieved by limiting the activity of long-lived radionuclides disposed in the repository and ensuring that the transport of radionuclides from the waste, through the engineered barriers and through the geosphere and biosphere is sufficiently retarded. The overall post-closure safety principles for SFR are therefore formulated as *limitation of the activity of long-lived radionuclides* and *retention of radionuclides* (Section 2.2). The content of long-lived radionuclides in the waste is limited by only accepting waste that conforms to approved waste type descriptions. Slow outward transport of radionuclides is achieved by ensuring a low groundwater-flow rate through the waste and the engineered barriers, through each waste vault, and by retarding radionuclide transport relative to this groundwater flow. This retardation is achieved mainly by ensuring effective sorption. The barriers contributing to the post-closure safety of the SFR repository are listed in Table 4-1 and a description of the barrier functions is given in Chapter 4.

A detailed and quantitative understanding and evaluation of repository safety requires a description of how the main safety principles, limitation of the activity of long-lived radionuclides and retention, relate to the components of the repository. Based on the understanding of the properties of the components and the long-term evolution of the system, several safety functions connected to the safety principles can be identified. In this context, a safety function is defined as how a repository component contributes to post-closure safety. Safety functions include barrier functions as well as other aspects important for post-closure safety that are not coupled to the function of a barrier. For instance, a safety function regarding the safety principle limitation of long-lived radionuclides in the repository is coupled to the waste, which is a component of the repository, but not coupled to a function of the barriers. There are also cases in which a barrier has a function in retaining radionuclides, but that this is not defined as a safety function that the analysis relies on, for instance sorption onto the macadam backfill is not accounted for in the calculations. The safety functions are an important input for defining requirements on the barriers and the waste (WAC).

To evaluate the extent to which the safety function is upheld over time, each safety function is associated with one or several safety function indicators. A safety function indicator is defined as a measurable or calculable property of a repository component.

The evaluation of safety functions and indicators is an aid in the evaluation of post-closure safety but is not sufficient to demonstrate that an acceptable level of safety has been achieved. Nor is safety necessarily compromised if a safety function is poorly upheld, this is rather an indication that more in-depth analyses are needed to evaluate the safety. Quantitative calculations are required to show compliance with the regulatory requirements, such as the risk criterion, irrespective of whether none, one or several safety functions are poorly upheld.

An important use of the safety functions and indicators is in the selection of scenarios. The methodology is described in Section 2.6.8. The selection of the less probable scenarios is entirely based on the safety functions and indicators, whereas the residual scenarios partly are derived based on safety functions and partly on other considerations. The implementation with respect to the less probable scenarios is given in Chapter 8 and for the residual scenarios in Chapter 9.

Less probable scenarios are selected to evaluate uncertainties that are not evaluated within the framework of the main scenario. In principle, less probable scenarios are identified when there is a probability that safety function indicators deviate significantly from the conditions in the main scenario, such that post-closure safety may be impaired. The approach for the identification of the less probable scenarios is based on an evaluation of uncertainties related to the initial state, internal processes and external conditions. To facilitate this evaluation of uncertainties, FEPs potentially affecting the safety function indicators for each safety function were identified (Section 5.6).

5.2 Method for identification of safety functions and update after SR-PSU

Safety functions were first introduced in the post-closure safety assessment for the existing SFR in SAR-08 (SKB R-08-130) and were also used in SR-PSU including safety functions for the extension part of SFR (SKB TR-14-01). The safety functions defined in this assessment are based on the safety functions and indicators identified in those previous assessments, taking into account the results and regulatory review comments. These developments are part of the general iterative process of an evolving safety assessment.

A safety assessment depends on an assessment of the future evolution of the repository and is described in the following three areas; 1) Initial state, 2) Internal processes and 3) External conditions (Section 2.6). From these areas of knowledge, including the screening of potentially important FEPs, a set of safety functions was defined in previous analyses that described how the repository system components contribute to the post-closure safety. In this identification process, a list of all potential safety aspects that need to be considered for relevant sub-components was used as an input, given the description of the initial state in SR-PSU (SKB TR-14-01, SKB TR-14-02).

As a result of the experience from SR-PSU and review comments from SSM (SSM 2019), several changes were introduced in this assessment. In summary, the safety function indicator hydraulic contrast in the 1–2 BMA and 1–2 BTF waste vaults has been substituted by the two indicators hydraulic conductivity in the concrete barrier and in the surrounding macadam backfill. A safety function relating to gas formation has been introduced for the waste packages in the silo (previously safety function indicator gas pressure), 1–2BMA, 1BRT and 1–2BTF. Furthermore, limit corrosion has been introduced as a safety function for 1BRT. Finally, a safety function relating to allowing gas passage has been defined for the engineered barriers in the silo, 1–2BMA and 1–2BTF. SSM suggested separate safety functions for the engineered barriers and the geosphere, which has also been introduced in the present assessment.

SSM suggested in the review of SR-PSU that it would be adequate to consider mechanical stability of the waste packaging and barriers in the waste vaults as a safety function (SSM 2019). The mechanical stability of the repository is taken into account in the design to ensure that the concrete structures can withstand the loads from resaturation, macadam and rock fallout. For instance, the mechanical stability of 1–2BMA for 20 000 years after closure has been evaluated (Mårtensson 2017). The mechanical stability of the waste packages is ensured by the waste acceptance criteria and waste type descriptions (Section 4.3.4). Since SR-PSU, SKB has carried out further work on mechanical stability of the concrete barriers in 1BMA and anticipated measures including the construction of concrete walls outside the existing structure and casting a concrete lid on top of the concrete structure as described in the closure plan (Mårtensson et al. 2022). There is also ongoing work relating to the concrete tanks in 1–2BTF in connection with an injunction from SSM. In the present assessment, it is judged that even though no safety function for mechanical stability is introduced, the possible post-closure effects of mechanical degradation are handled in an appropriate way by the analysis of the temporal evolution of post-closure mechanical stability of 1–2BMA. Furthermore, the safety functions coupled to hydraulic conductivity of the concrete barriers and sorption represent the effects of mechanical degradation, for instance by considering fracturing of the concrete due to various post-closure processes. The handling of the effects of mechanical stability of the BTF tanks awaits further results from the ongoing analysis and possible future actions.

SSM furthermore commented that SKB should consider defining quantitative criteria for the safety function indicators (Part III Section 2.7 in SSM 2019). The use of criteria for the safety function indicators has been revisited in this assessment with the result that it is still judged to be appropriate not to define such quantitative criteria. The reason for this decision is explained in the following.

The performance of the repository components does not generally change in discrete steps. The repository performance will change continuously with time and there is no clear distinction between an acceptable and an unacceptable performance for the individual components and their safety functions. As explained in the introduction to this chapter, the scenario selection is coupled to the deviation of the safety function indicators from their developments in the main scenario. Thus, uncertainties not handled within the main scenario are analysed in the less probable scenarios, as described in the definitions of the respective calculation cases. Including quantitative criteria would not necessarily

simplify the understanding of which uncertainties are handled in the main scenario in contrast to the less probable scenarios. Even in the main scenario, the status of the safety functions slowly degrades over time and the criteria may not be met at some point in time during the assessment period. For example, the flow-limiting function of the concrete barriers in 2BMA is assumed to completely degrade during the assessment period, even in the main scenario. Thus defining a safety function indicator criterion is not an aid to define which uncertainties are evaluated in the main scenario and the less probable scenarios. The key issue as regards the role of safety functions in the evaluation of less probable scenarios is not whether a function indicator fulfils a quantitative criterion or not, but whether the performance of the function, as probed by the development of its associated indicator, is significantly impaired compared to the situation in the main scenario. An indication of the magnitude of uncertainty handled within the main scenario is given by the probabilities of the less probable scenarios, they handle evolutions that are judged to have a probability of 10 % or less to occur.

In Sections 5.3 and 5.4 the safety functions and indicators relating to the two safety principles for SFR are described and, in Section 5.5, they are summarised in a table.

5.3 Safety functions for limitation of the activity of long-lived radionuclides

The overall safety principle: *limitation of the activity of long-lived radionuclides* entails that only certain kinds of waste are accepted for disposal. This safety principle takes account of the general SKB mission and is therefore to be seen in a wider perspective, including the roles of other facilities in the waste management programme.

Waste is allocated to the extended SFR and distributed within the repository in accordance with certain criteria (SKB R-18-07). In the license for the extended SFR, conditions are given for the inventory of activity relating to the entire repository and to the different waste vaults (Regeringen 2021).

The waste that is considered suitable for disposal in the extended SFR is presented in an inventory report (SKB R-18-07). This is based on data on already disposed operational wastes and estimates of future operational and decommissioning wastes.

In recognition of the safety principle: *limitation of the activity of long-lived radionuclides,* the safety function ***limit quantity of activity*** is defined. In this respect the waste is a component of the repository system and the radionuclide-specific inventory has an important role in contributing to the post-closure safety of the repository. Thus, a relevant safety function indicator is the *activity of each radionuclide in each waste vault*.

5.4 Safety functions for retention of radionuclides

The overall safety principle *retention of radionuclides* applies to waste form and packaging, barriers in waste vaults, plugs and other closure components, the geosphere and surface system. Retention is achieved mainly by limiting advective transport and ensuring effective sorption. Thus, the waste is contained in such a way as to only allow for a slow release and transport of radionuclides.

Within the context of the disposal strategy discussed in Section 5.3, WAC are fundamental and the specific properties of the waste packages are selected to limit radionuclide release. Thus, the following discussion focuses first on requirements placed on the waste and waste packaging, before considering the engineered barriers, geosphere and biosphere.

5.4.1 Waste form and packaging

In the **Initial state report,** the waste form and the packaging are defined separately. In the context of a safety function, the waste form and packaging are considered together and described as waste packages. In the following, the safety functions defined for the waste packages and related indicators are described.

Limit gas formation. The materials in the waste must be limited so that possible negative effects on the hydraulic function of the surrounding barriers are avoided. The most relevant gas-forming materials that the waste in the different waste vaults may contain are metallic aluminium, metallic zinc, easily degradable organic waste such as paper and metal parts with high specific surface area, e.g. metal swarf.

The defined safety function is ***limit gas formation*** with the safety function indicator *amount of gas-forming materials*.

Limit advective transport. For waste packages made of materials with low hydraulic conductivity, their hydraulic resistance, in combination with the surrounding barrier's hydraulic resistance, will limit the groundwater flow. The limited flow of water through the waste packages should, in turn, ensure a slow advective transport of radionuclides through them. In 1BRT, 1–2BMA, 1–5BLA and the silo, low groundwater flow through the waste packages is, however, not relied upon in the safety assessment. In 1–2BMA and the silo the surrounding technical barriers ensure favourable flow conditions through the waste and 1BRT relies upon slow release of induced activity and sorption in the surrounding concrete barrier. In the case of 1–5BLA, there are no requirements regarding the hydraulic properties of the waste packages and the safety assessment does not take credit for the hydraulic resistance that can be attributed to the waste packages. Thus, the advective transport in 1–5BLA is limited by the favourable low groundwater flow conditions provided by the surrounding geosphere and the plugs in the repository.

The hydraulic influence of the waste packaging in 1–2BTF has a role in contributing to safety and the safety function ***limit advective transport*** is defined with the safety function indicator *hydraulic conductivity*.

Limit corrosion. The induced activity content that is present in the reactor pressure vessels and possibly also in other metal wastes in 1BRT is released because of corrosion and the rate of release is controlled by the corrosion rate. The corrosion is limited by high pH and low redox potential in the porewater surrounding the metal surfaces. This is described in detail in the **Waste process report.**

Limited release of induced radionuclides has a role in contributing to safety and thus the safety function ***limit corrosion*** is defined with *pH in porewater* and *redox potential* as safety function indicators.

If the concentration of a certain element is sufficiently high, it reaches equilibrium with a solubility limiting phase and the element will not dissolve further. This means that the solubility limit is reached. The solubility limit is dependent on the water chemistry. Examples of radionuclides whose concentration might be limited by solubility are C-14, Ni-59 and Ni-63 (see the **Waste process report**). Solubility limitations are, however, not considered in the present safety assessment and no safety function is defined. Excluding solubility limitation is generally a cautious approach; the effect of it for SFR has been briefly investigated separately (SKB TR-14-09, Appendix B).

Sorb radionuclides. Many radionuclides sorb to solid materials in the waste package, where the sorption capacity varies depending on the solid material and the porewater chemistry. This sorption limits the concentration of dissolved radionuclides in the porewater (see the **Waste process report)** and this contributes to slow release from the waste, regardless of whether the transport is diffusive or advective. In principle, radionuclides can sorb not only onto the concrete or cement in the waste form, but also to ion-exchange resins, ash, corrosion products, etc, as well as to waste packaging. The sorption properties of waste destined for disposal in the silo, 1–2BMA, 1BRT and 1–2BTF are determined by how the waste is conditioned. However, the safety assessment only takes credit for sorption onto cementitious materials in the waste packages. According to Appendix E, Table E-3, the quantity of cementitious materials is limited in 1BLA (about 3 % of the total waste weight). For 2–5BLA about 26 % of the waste material consists of concrete, see Appendix E, Table E-3. However, no credit is taken for sorption in 1BLA or 2–5BLA, even though sorption is likely to contribute to the retardation in 2–5BLA to some extent.

Sorption takes place on solid surfaces. Cement has a relatively large porosity, which favours sorption. The large amount of cement in the silo, 1–2BMA, 1BRT, and 1–2BTF ensures that there are available sites for sorption in the repository vaults. The availability of sorption sites along the radionuclide transport paths is considered in the radionuclide transport calculations.

As long as the cementitious materials are not significantly chemically altered, the pH in the porewater will be higher than 10.5. This generally guarantees favourable sorption conditions for important cations. Anions are assumed to sorb poorly to cementitious materials in the entire relevant pH range. This is described in detail in the **Waste process report.**

The redox potential is an important parameter for sorption, where low redox potential leads to increased sorption of some important radionuclides. A low redox potential is ensured by the presence of a large amount of oxidizable materials, mainly metallic iron in the form of steel.

The waste contains complexing agents (e.g. NTA and citric acid) and, moreover, degradation of some organic matter in the waste (particularly cellulose) can give rise to complexing agents. These agents can impact sorption by complexing with certain radionuclides in solution and reducing the degree of radionuclide sorption due to this change of chemical form. In dissolved form, complexing agents could also conceivably compete for radionuclide uptake via sorption onto solid surfaces. Furthermore, complexing agents can bind and dissolve radionuclides that are otherwise solubility limited. Therefore, the amounts and, more specifically, the concentrations of dissolved complexing agents in the waste needs to be kept low.

Hence a safety function ***sorb radionuclides*** is defined with the safety function indicators *amount of cementitious materials, pH in porewater, redox potential* and *concentration of complexing agents.*

5.4.2 Engineered barriers

The engineered barriers in the waste vaults are concrete structures, macadam backfill, bentonite and top backfill in the silo, grout and shotcrete (Chapter 4). The plugs and other closure components are also part of the engineered barrier system.

In the following, the safety functions for the engineered barriers are described.

Limit advective transport. Water flow in the interior of the waste vaults and through the waste packages should be limited. Two different approaches are used to achieve this: 1) the hydraulic contrast between the permeable macadam backfill (including crushed rock foundation) surrounding the concrete structures and the less permeable concrete structures enclosing the waste packages (only the concrete tanks in 1–2BTF) diverts water flow away from the concrete structures to the more permeable surrounding materials and 2) the bentonite buffer surrounding the silo has a low hydraulic conductivity and will limit groundwater flow through the silo.

The hydraulic conductivity of both the macadam backfill and the concrete barriers is of importance for 1–2BMA and 1–2BTF (concrete tanks), whilst the hydraulic conductivity of bentonite is of main importance for the silo and the bentonite-filled sections of the plugs that act as hydraulic seals to the waste vaults.

The hydraulic barrier function has a role in contributing to safety and the safety function defined is ***limit advective transport*** with the safety function indicators *hydraulic conductivity in concrete and bentonite* and *hydraulic conductivity in backfill* (including crushed rock foundation).

Allow gas passage. In the silo, a permeable grout is used and the lid will be provided with evacuation pipes in order to allow gas to escape. However, there is a slight possibility that gas formed inside the silo will create an over-pressure that might expel water. Gas formed in 1–2BMA and 1–2BTF might also influence the advective transport of radionuclides. The possible influence is governed by the amount of gas-forming materials and the permeability of the barrier, i.e. the ability of the barrier to release gas. The calculated gas quantities are discussed in Section 6.2.8 and it can be noted that little gas formation is expected in 1–2BTF. The permeability is either sufficient to allow gas passage within the barrier material itself or a technical solution is necessary to ensure passage. Such a technical solution will be implemented for 2BMA.

Hence, the safety function ***allow gas passage*** is defined with the safety function indicator *permeability* for the silo, 1–2BMA and 1–2BTF.

Allow gas passage has not been defined as a safety function for 1BRT even though the waste comprises scrap metals. A permeable grout will be used to grout the waste packages, allowing for gas to be transported through the grout. The formed gas might lead to fracturing of the outer concrete structures in 1BRT allowing gas and water to be transported through the fractures. Since *limit advective transport* has not been defined as a safety function in 1BRT the safety function *allow gas passage* is not of concern for 1BRT either.

Sorb radionuclides. The radionuclides released from the waste packages are retarded by sorption in the grout surrounding the waste packages, the concrete structures and the macadam outside the concrete structures as well as in the bentonite surrounding the concrete in the silo.

The highest sorption capacity for radionuclides is found in cementitious materials (concrete walls, grout, etc) that have large specific surface areas, which favours sorption. It should, however, be noted that the safety assessment also takes credit for sorption in bentonite and crushed rock in the radionuclide transport calculations. Sorption in the plugs is not considered in the safety assessment, even though sorption is expected to occur within the material of the plugs.

As long as the cementitious materials are not significantly chemically altered, the pH in the pores will be higher than 10.5. The gradual leaching of minerals from cementitious materials will lead to changes in the sorption capacity for different radionuclides, but many cationic radionuclides sorb well during all stages of cement chemical degradation. Anions are assumed to sorb poorly to cementitious materials in the entire relevant pH range.

The redox potential is an important parameter for sorption. For a repository such as SFR, a low redox potential implies a slower release of some important radionuclides.

The waste is the main source for complexing agents. However, complexing agents in the waste also influence the sorption in the barriers.

Sorption in the engineered barriers contributes to the safety and the safety function ***sorb radionuclides*** is defined with the safety function indicators *amount of cementitious materials*, *pH in porewater*, *redox potential* and *concentration of complexing agents*.

5.4.3 Repository environs

The geosphere has several functions from a post-closure perspective. The main functions of the geosphere concern its role as a boundary condition for the waste vaults and are described below. In addition, the geosphere retards radionuclides, however no safety function has been identified for retardation in the geosphere, since its contribution to post-closure safety is not vital. The geosphere also ensures the isolation of the repository from the biosphere.

Provide favourable hydraulic conditions. Low groundwater flow through the waste vaults is a prerequisite for slow advective transport of radionuclides out of SFR. This applies in particular to slightly or non-sorbing radionuclides. Low groundwater flow through the waste vaults is also a prerequisite for slow inward transport of reactive substances such as oxidants and slow barrier degradation.

Groundwater flow through the waste vaults is mainly determined by the groundwater flow in the geosphere, considering the role of the plugs and the bentonite surrounding the silo that hinders advective flow. The flow through the geosphere is determined by the hydraulic gradient and the hydraulic conductivity of the bedrock. The hydraulic conductivity relates to the flowing fracture network characteristics. These quantities can be changed by e.g. an earthquake (see the **Geosphere process report**).

The site for SFR was chosen in part for the low hydraulic gradient of the geosphere. At present, the area above SFR is located beneath the sea where the general hydraulic gradient is very low. The direction and magnitude of the hydraulic gradient will change due to shoreline displacement. After a few millennia, when the ground surface above the repository is expected to be above sea level, the hydraulic gradient in the geosphere will be higher. Deviations from the general gradient are then expected to be controlled more by the local, rather than the regional, topography.

The safety function ***provide favourable hydraulic conditions*** is defined given that the geosphere provides the boundary conditions for groundwater flow through the waste vaults. The relevant safety function indicators are *hydraulic gradient* and *hydraulic conductivity*.

Provide chemically favourable conditions. Sorption of many elements – such as Tc, Pu, Np and Se – is sensitive to the redox conditions in the repository. Sorption of these elements under oxidising conditions can differ considerably from sorption under reducing conditions. The redox conditions in the repository are determined by the composition of inflowing groundwater and oxidation reactions inside the repository, mainly corrosion of iron.

The safety function ***provide chemically favourable conditions*** is defined as the inflowing groundwater is a boundary condition influencing the redox potential and has a role in contributing to the safety through its effect on sorption in the waste vaults. The relevant safety function indicator is the groundwater *redox potential*.

Avoid boreholes in the direct vicinity of the repository. An important safety aspect of SFR is its location beneath the Baltic Sea where it is expected to remain for at least 1 000 years after closure. In addition to the beneficial hydraulic features, the external condition of the sub-sea location of the repository also prevents humans locating boreholes above or downstream of the repository for the purpose of water extraction. However, it cannot be completely ruled out that drilling under water may be conducted for purposes other than water extraction.

Due to shoreline displacement, the surface component will change over time, which is accounted for in the safety assessment.

Drilled wells intended for drinking water or agricultural purposes may affect radionuclide transport to the biosphere. The use and location of drilled wells therefore influences the safety and this must be considered in the safety assessment.

The location of the repository in relation to the shoreline is considered of crucial importance for the possibility of boreholes in the repository area or immediately downstream of the repository.

In recognition of the safety principle *retention of radionuclides* the safety function ***avoid boreholes in the direct vicinity of the repository*** is defined. The relevant safety function indicators are *intrusion boreholes*, and *boreholes downstream of the repository*.

5.5 Summary of defined safety functions for the assessment

The safety functions and safety function indicators that have been defined in this chapter are summarised in Table 5-1.

As stated above, the following definitions are used:

- A safety function is defined as a role by means of which a repository component contributes to safety.
- A safety function indicator is a measurable or calculable property of a repository component that is used to indicate the extent to which the safety function is upheld.

Table 5-1. Safety functions and safety function indicators.

Safety function	Safety function indicator	Repository system (sub-)component
Waste form and waste packaging		
Limit quantity of activity	Activity of each radionuclide in each waste vault: limited	Waste form in silo, 1–2BMA, 1BRT, 1–2BTF, 1–5BLA
Limit gas formation	Amount of gas-forming materials: low	Waste form and waste packaging in silo, 1–2BMA, 1BRT and 1–2BTF
Limit advective transport	Hydraulic conductivity: low	Waste packaging (concrete tanks) in 1–2BTF
Limit corrosion	pH in porewater: high Redox potential E_h: low	Waste form with induced activity in 1BRT
Sorb radionuclides	Amount of cementitious material: high pH in porewater: high Redox potential: low (reducing) Concentration of complexing agents: low	Waste form and waste packaging in silo, 1–2BMA, 1BRT and 1–2BTF
Engineered barriers		
Limit advective transport	Hydraulic conductivity in concrete and bentonite: low	Bentonite in silo and plugs Outer concrete structures in 1–2BMA
	Hydraulic conductivity in backfill (including crushed rock foundation): high	Backfill (including crushed rock foundation) in 1–2BMA and 1–2BTF
Allow gas passage	Permeability: sufficient to allow gas passage	Gas evacuation system in silo and 2BMA Cementitious materials in 1BMA and 1–2BTF
Sorb radionuclides	Amount of cementitious material: high pH in porewater: high Redox potential: low (reducing) Concentration of complexing agents: low	Cementitious materials in silo, 1–2BMA, 1BRT, and 1–2BTF
Repository environs		
Provide favourable hydraulic conditions	Hydraulic conductivity: low Hydraulic gradient: low	Geosphere
Provide chemically favourable conditions	Redox potential: low (reducing)	Geosphere
Avoid boreholes in the direct vicinity of the repository	Intrusion boreholes: few/absent Boreholes downstream of the repository: few	Biosphere, geosphere

5.6 Identification of FEPs potentially affecting the safety functions

The safety functions are used as a tool for scenario selection (Section 2.6.8). The selection of the less probable scenarios is based on an evaluation of uncertainties related to the initial state, internal processes and external conditions causing deviations in safety functions and safety function indicators. To facilitate this evaluation of uncertainties, key FEPs potentially affecting the safety function indicators for each safety function were identified. This was done by the safety assessment team, consulting subject matter experts where needed. The results of this exercise, i.e. key FEPs potentially affecting safety function indicators, are presented in Tables 5-2 to 5-4.

Since safety function indicators are measurable, or calculable, properties of repository components, they are directly related to the variable FEPs which describes the properties and conditions of each system component. The first step was to identify which variable FEPs may affect the safety function indicators; this was done by expert judgement.

The second step was to identify key internal processes that may affect the identified variable FEPs in such a manner that the safety function indicators may be affected. FEPs that are judged to only have a negligible, or minor, influence on the variable are excluded. In this step, the influence tables in the process reports (**Waste process report, Barrier process report** and **Geosphere process reports**) were used, where, for each internal process, it is evaluated if it influences one or more of the variable FEPs. Hence, this identification of internal processes is based on expert judgement of possible influences made by the authors of the individual chapters of the process report. The selection of key internal processes was made by expert judgement.

The third step was to, by expert judgement, identify key external FEPs related to climate or large-scale geological processes or events that may affect the identified variables. Note, external FEPs related to future human actions (FHA FEPs) are not included in this exercise since identification of scenarios based on such FEPs is treated separately, as they are driven by specific regulatory guidelines (Chapter 9).

The fourth and final step was to identify, using expert judgement, if any initial state FEPs may affect the safety function indicators for each safety function.

Table 5-2. Safety functions for the waste form and waste packaging and FEPs that may directly affect the safety function indicators, limited to key FEPs to address in the selection of less probable scenarios. The codes for the FEP classification given in brackets are found in the FEP report, Chapter 5 and Appendix 2.

Safety function	Key FEPs	Repository system (sub-)component
Limit quantity of activity	Radionuclide inventory (VarWM06) Radioactive decay (WM01)	Waste in silo, 1–2BMA, 1BRT, 1–2BTF, 1–5BLA
Limit gas formation	Material composition (VarWM07, VarPa05) Gas variables (VarWM09, VarPa07) Degradation of organic materials (WM15), Microbial processes (WM17), Metal corrosion (WM18, Pa12), Gas formation and transport (WM19, Pa13)	Waste form and waste packaging in silo, 1–2BMA, 1BRT and 1–2BTF
Limit advective transport	Geometry (VarPa01), Hydrological variables (VarPa03) Phase changes/freezing (Pa02), Fracturing/deformation (Pa05), Dissolution, precipitation and recrystallisation (Pa10) Climate evolution (Cli03), Ice-sheet dynamics and hydrology (Cli06), Earthquakes (LSGe02) Design deviations – Mishaps (IsGen05)	Packaging (concrete tanks) in 1–2BTF
Limit corrosion	Water composition (VarWM08) Dissolution, precipitation and recrystallisation (WM14), Metal corrosion (WM18) Climate evolution (Cli03), Ice-sheet dynamics and hydrology (Cli06)	Waste form with induced activity in 1BRT
Sorb radionuclides	Material composition (VarWM07, VarPa05), Water composition (VarWM08, VarPa06) Dissolution, precipitation and recrystallisation (WM14, Pa10), Degradation of organic materials (WM15), Metal corrosion (WM18, Pa12), Diffusive transport of dissolved species (Pa07) Climate evolution (Cli03), Ice-sheet dynamics and hydrology (Cli06)	Waste form and waste packaging in silo, 1–2BMA, 1BRT and 1–2BTF

Table 5-3. Safety functions for the engineered barriers and FEPs that directly may affect the safety function indicators, limited to key FEPs to address in the selection of less probable scenarios.

Safety function	Key FEPs	Repository system (sub-)component
Limit advective transport	Geometry (VarSi01, VarBMA01, VarPg01), Hydrological variables (VarSi03, VarBMA03, VarPg03) Phase changes/freezing (SiBa02, BMABa02), Piping/erosion (SiBa06, Pg06), Mechanical processes (SiBa07, Pg07, BMABa06), Dissolution/precipitation (SiBa14), Montmorillonite transformation (SiBa17, Pg15), Concrete degradation (BMABa12), Metal corrosion (BMABa15) Climate evolution (Cli03), Ice-sheet dynamics and hydrology (Cli06), Earthquakes (LSGe02) Design deviations – Mishaps (IsGen05)	Bentonite in silo and plugs Outer concrete structures in 1–2BMA
	Geometry (VarBMA01, VarBTF01), Hydrological variables (VarBMA03, VarBTF03) Phase changes/freezing (BMABa02, BTFBa02), Mechanical processes (BMABa06, BTFBa06), Concrete degradation (BMABa12, BTFBa11) Design deviations – Mishaps (IsGen05)	Backfill in 1–2BMA and 1–2BTF
Allow gas passage	Geometry (VarSi01, VarBMA01, VarBTF01), Hydrological variables (VarSi03, VarBMA03, VarBTF03) Mechanical processes (SiBa07, BMABa06, BTFBa06), Concrete degradation (SiBa13, BMABa12, BTFBa11),	Gas evacuation system in silo and 2BMA Cementitious materials in 1BMA and 1–2BTF
Sorb radionuclides	Material composition (VarSi05, VarBMA05, VarBRT05, VarBTF05) Concrete degradation (SiBa14, BMABa12, BRTBa11, BTFBa11), Sorption (including ion exchange of major ions) (SiBa10), Aqueous speciation and reactions (SiBa15), Sorption on concrete/shotcrete (BMABa09), Sorption (BTFBa09, BRTBa09) Climate evolution (Cli03), Ice-sheet dynamics and hydrology (Cli06)	Cementitious materials in silo, 1–2BMA, 1BRT, and 1–2BTF

Table 5-4. Safety functions for the repository environs and FEPs that directly may affect the safety function indicators, limited to key FEPs to address in the selection of less probable scenarios.

Safety function	FEPs	Repository system component
Provide favourable hydraulic conditions	Temperature (VarGe01), Repository geometry (VarGe05), Fracture and pore geometry (VarGe06), Geometry (VarBio01) Freezing (Ge02), Displacements along existing fractures (Ge06), Sea level change (Bio49) Climate evolution (Cli03), Ice-sheet dynamics and hydrology (Cli06), Shore level changes (Cli09), Earthquakes (LSGe02)	Geosphere
Provide chemically favourable conditions	Groundwater composition (VarGe10) Freezing (Ge02), Diffusive transport in the rock mass (Ge11), Reactions groundwater/rock matrix (Ge13), Dissolution/ precipitation of fracture-filling minerals (Ge14) Climate evolution (Cli03), Ice-sheet dynamics and hydrology (Cli06)	Geosphere
Avoid boreholes in the direct vicinity of the repository	Matrix minerals (VarGe08), Stage of succession (VarBio04), Water composition (VarBio06) Intrusion (Bio09), Sea level change (Bio49) Shore-level changes (Cli09)	Biosphere, geosphere

6 Reference evolution

6.1 Introduction

This chapter describes the probable post-closure evolution of the repository and its environs, including uncertainties in the evolution that may affect the protective capability of the repository. This *reference evolution* starts from the initial state (Chapter 4) and then follows the reference external conditions for the next 100 000 years (Section 2.6.3), accounting for features, events and processes that are likely to influence the evolution (Chapter 3). The description builds on the knowledge gained in the previous steps of the assessment methodology (Sections 2.6.1–2.6.6), as well as dedicated studies performed to assess the post-closure evolution of the repository and its environs. The reference evolution supports the selection and analysis of the main scenario (Chapter 7) and less probable scenarios (Chapter 8).

Three *variants* of the reference external conditions are considered (see below). These represent the range of probable evolution of the external conditions at Forsmark over the next 100 000 years. The evolution of climate conditions in these variants, illustrated in terms of climate domains (Section 2.6.3), are shown in Figure 6-1.

- The *present-day climate variant* (Sections 6.2 and 6.3) represents a future development where present-day climate conditions prevail for the complete assessment period and the initial shoreline displacement is dominated by isostatic rebound following the last glaciation. The initial state climate conditions defined in Section 4.5 are assumed in this variant, resulting in 100 000 years of continued temperate climate conditions at Forsmark.
- The *warm climate variant* (Sections 6.2 and 6.4) represents a likely future development where similar-to-present levels of anthropogenic greenhouse-gas emissions continue for the next few decades, after which they gradually decline to net-zero emissions in the beginning of the next century. This is in line with the Intergovernmental Panel on Climate Change (IPCC) medium emissions scenarios RCP4.5 and RCP6.0[21] as well as recent "business-as-usual" projections of future emissions which assume that current policies to mitigate climate change are implemented, but no new policies are adopted in the future (**Climate report**, Section 4.2). This development results in 100 000 years of temperate climate conditions and an increased sea level, which leads to a prolonged initial period during which the area above the repository remains submerged beneath the sea.
- The *cold climate variant* (Sections 6.2 and 6.5) represents a future development characterised by substantial reductions in anthropogenic greenhouse-gas emissions and/or removal of atmospheric CO_2 by technological measures. This development results in gradually colder climate conditions and two periods of periglacial conditions at Forsmark during the latter half of the assessment period.

The description of the reference evolution is divided into two parts. The first part is the evolution of the repository and its environs during the initial period when the area above SFR is submerged beneath the sea including the transition to terrestrial conditions (Section 6.2). The duration of this period may range from one to several thousands of years depending on the future relative sea level change at Forsmark, which is represented in the variants of the external reference conditions (Figure 6-1) This part includes a detailed description of the evolution of the repository during the first 1 000 years as requested in the regulations (SSMFS 2008:37, Section 11 and General advice).

The second part of the reference evolution is the evolution of the repository and its environs during the remaining time of the safety assessment, i.e. from the end of initial submerged period to 100 000 years after closure for the three variants of external reference conditions (Sections 6.3–6.5).

[21] Nomenclature is adopted from IPCC's fifth assessment report (IPCC 2013). In the most recent, sixth, IPCC assessment report (IPCC 2021), emissions scenarios are denominated Shared Socioeconomic Pathways (SSPs) rather than Representative Concentration Pathways (RCPs), see further **Climate report**, Section 4.2.1.

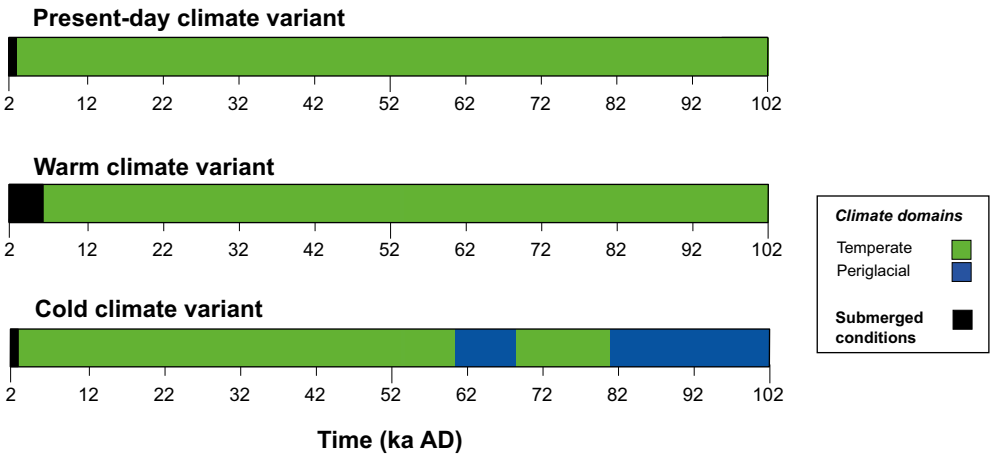

Figure 6-1. *Succession of climate domains in the variants of reference external conditions.*

The post-closure evolution of the repository and its environs under these external conditions is described under the following subsections:

- *Evolution of surface systems*
- *Thermal evolution*
- *Mechanical evolution*
- *Hydrogeological evolution*
- *Geochemical evolution*
- *Near-field hydrological evolution*
- *Evolution of the waste and of the repository chemical conditions*
- *Evolution of engineered barriers*

The subsections *Near-field hydrological evolution*, *Evolution of the waste and of the repository chemical conditions* and *Evolution of engineered barriers* specifically describe the reference evolution within the repository, whereas the subsections *Evolution of surface systems*, *Hydrogeological evolution* and *Geochemical evolution* mainly describe the evolution of its environs (i.e., the surface systems above the repository and the bedrock surrounding the repository). The remaining subsections, *Thermal evolution* and *Mechanical evolution*, describe the evolution both within the repository and in the bedrock surrounding the repository.

For part of the description, most notably *Mechanical evolution* and *Evolution of the waste and of the repository chemical conditions*, it is not always possible to separate the description of the reference evolution between the initial period of submerged conditions and the remaining assessment period. Most of these descriptions are therefore, for simplicity, included under the section about the initial period of submerged conditions (Section 6.2), even though they are often also relevant for the later stages of the reference evolution.

6.2 Initial period of submerged conditions

This section describes the evolution of the repository system during the initial period after closure when the area above SFR is still submerged beneath the sea, as well as the subsequent transition period to terrestrial conditions. As discussed and described in the **Climate report**, Section 1.4.3, the transition from submerged to terrestrial conditions above the repository is assumed to be completed when the relative sea level decreases by 5.8 m or more compared to the present level. At this level, between 75 % and 100 % of the surface above the repository is terrestrial. Furthermore, when the relative sea level decreases to approximately this level, the groundwater flow through the waste

vaults begins to converge towards stationary values and potential discharge areas of repository-derived radionuclides begin to rise above the sea (see further Section 6.2.5 and Figure 6-3, panels e and f). The duration of the initial submerged period is expected to be at least 1 000 years, but is likely to be longer, up to several thousands of years, due to anthropogenic global warming.

6.2.1 External conditions

During the initial period after closure when the area above the repository is submerged, the climate at Forsmark is expected to be warmer than at present due to continued anthropogenic warming. Thus, temperate climate conditions will prevail at Forsmark during this time.

The uncertainty in future global sea level rise over the next few thousand years is very large, ranging from a few metres to several tens of metres depending on the degree of global warming and how Earth's ice sheets and glaciers will respond to that warming (**Climate report**, Section 3.5.3). At Forsmark, this uncertainty translates into either a continued marine regression, resulting in the gradual exposure of more land above the repository over the next few thousand years, or a marine transgression, resulting in continued submerged conditions and an increased water depth above the repository. Due to the large uncertainty in future sea level rise, multiple variants of initial submerged conditions above SFR are described in the reference external conditions, see below.

Present-day climate variant

The *present-day climate variant* assumes that the contribution of future sea level rise is negligible and thus that the shoreline displacement at Forsmark is dominated by the post-glacial isostatic rebound (as described in e.g. Brydsten and Strömgren 2013). The same shoreline regression was used in the main scenario in the SR-PSU (SKB TR-14-01, Section 7.4.1). As noted previously, this development results in 1 000 years of initial submerged conditions above the repository.

Warm climate variant

The effect of a prolonged initial period of submerged conditions due to global warming is described in the *warm climate variant*. In the present safety assessment, the uncertainty in the relative sea level at Forsmark under business-as-usual anthropogenic greenhouse-gas emissions is described by two alternative developments, corresponding to either a marine transgression or a continued marine regression over the next millennia (**Climate report**, Section 3.5.3). Since it is not possible to deduce a most likely relative sea level change from this range, the mean of the uncertainty range is chosen for the *warm climate variant* (**Climate report**, Section 5.2.2). The resulting initial period of submerged conditions for SFR is 4 500 years (**Climate report**, Figure 5-2).

The *warm climate variant* can be compared to the extended global warming climate case of the reference evolution in the SR-PSU, which also included a prolonged initial period of submerged conditions for SFR (SKB TR-14-01, Section 6.2.2). The duration of this period in the SR-PSU extended global warming climate case was only 2 200 years, thus considerably shorter than the 4 500 years considered in the *warm climate variant*. This difference reflects a general tendency in the scientific literature since the SR-PSU towards more high-end projections of future sea level rise (**Climate report**, Section 3.5).

Cold climate variant

The relative sea level development at Forsmark in the *cold climate variant* is assumed to be identical to that of the *present-day climate variant*, i.e. it includes a negligible contribution of future sea level rise (see above). This is a reasonable assumption as a development towards colder climate conditions in the latter half of the 100-ka assessment period likely requires that the ongoing climate warming is strongly mitigated within the next few decades (**Climate report**, Section 4.3). Even if the consequences of the warming, such as global sea level rise, may continue for centuries after the emissions have been reduced, isostatic effects mean that the current shoreline regression will likely continue if the emissions are strongly reduced (**Climate report**, Section 3.5.3).

6.2.2 Evolution of surface systems

The development of the surface system will influence the conditions for radionuclide transport and exposure over the assessment period. The evolution of surface systems during the initial period of submerged conditions (this section) as well as for the *present-day climate variant*, *warm climate variant* and *cold climate variant* of the reference evolution (Sections 6.3.2, 6.4.2 and 6.5.2, respectively) are based on the descriptions of the site development in the **Biosphere synthesis report**, Chapter 4.

During the submerged period, all potential release areas of radionuclides from SFR will still be submerged. Changes of the surface ecosystem during this period mainly include the development of topography and regolith within the sea, the oceanography and the surface hydrology during the gradual change of the marine ecosystem towards shallower conditions with increasing terrestrial influence. The development of marine ecosystems is also briefly discussed here.

Development of regolith and topography

The initial state of the marine topography and the regolith stratigraphy is determined by the geological history, the accumulation of sediments (till, glacial clay and post-glacial clay-gyttja) since the last glaciation and submarine erosion of sediments (Section 4.6.1). The accumulation of clay-gyttja on deep or sheltered bottoms as well as the erosion of sediment on more exposed bottoms will continue during the submerged period. Vegetation ingrowth and peat accumulation along sheltered marine shores start before lake isolation or land emergence.

In the SR-PSU, a regolith-lake development model (RLDM) was used to describe the future landscape development in Forsmark (Brydsten and Strömgren 2013). No additional landscape modelling has been performed for the PSAR. The RLDM simulates the surface geology, stratigraphy and thickness of various regolith strata for the period considered in a safety assessment based on the assumed shoreline regression and natural processes like sedimentation, erosion and resuspension, vegetation ingrowth and peat accumulation. The model is divided into two modules: a marine module that simulates the sediment dynamics caused by wind-generated waves (briefly described below) and a lake module that simulates the lake infilling processes (Section 6.3.2).

The marine module starts at the time of deglaciation (8500 BC) in the area. The Forsmark area is then submerged and all regolith materials (till and glacial clay) are of glacial origin. A sediment dynamic sub-routine model in RLDM determines sedimentation and erosion based on the modelled wind-generated wave-driven currents (Brydsten 2009). For each time step of 500 years, the marine module outputs are raster maps of regolith layer thicknesses, bathymetry and the distribution of ecosystems in the landscape (examples are shown in Figure 6-2). These results were used as input to the hydrological modelling.

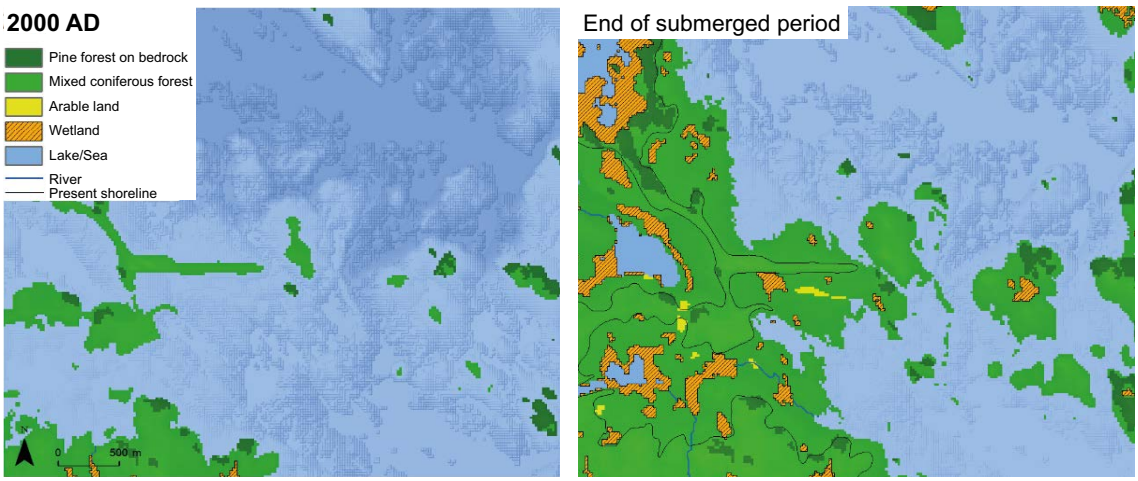

Figure 6-2. *Illustration of the simulated landscape at 2000 AD and at the end of the submerged period. The yellow colour represents land that could potentially be cultivated. Note that, in this projection, mires within lakes are not marked as potential arable land until the lake has been completely covered by mire vegetation (modified from Figure 4-6 in* ***Biosphere synthesis report****).*

Development of the oceanography and near-surface hydrology

The water exchange in the marine basins is mainly controlled by the interchange of seawater between Öregrundsgrepen and the Bothnian Sea (for a map of the area, see Figure G-1). In the future, surface-water exchanges across the strait outside Öregrund in the south, as well as inter-basin exchanges, will decrease as the shoreline recedes and the basins are isolated from the sea. At the end of the submerged period, the strait is expected to close and Öregrundsgrepen will turn into a bay and the only connection between the marine basins and the open water of the Baltic Sea will exist in the northern part of Öregrundsgrepen (Karlsson et al. 2010, Werner et al. 2013).

Conceptual and numerical models describing present and future hydrology were developed, based on SDM-Site (Bosson et al. 2008), SR-Site (Bosson et al. 2010) and SR-PSU (Werner et al. 2013). In general, near-surface groundwater flow is lower during submerged conditions and increases when land emerges from the sea. Based on the development of topography and regolith simulated by the RLDM, numerical hydrodynamic models were developed for present (2000 AD) and future conditions (e.g. the end of the submerged period, c.f. Figure 6-2). Werner et al. (2013) examined the water balance for several groundwater discharge areas in the landscape. Results confirmed that the annual groundwater discharge rate from the bedrock to the regolith increases over time as the hydraulic gradient between the terrestrial groundwater and open sea increases with the shoreline regression.

Ecosystem development

Future temperate marine ecosystems are expected to be similar to those at present, in particular if the future climate warming is limited (Aquilonius 2010, Lindborg 2010). However, with continued shoreline regression and shallower basins, as assumed in the *present-day variant* and *cold climate variant* and eventually also in the *warm climate variant*, a shift towards more benthic production and a gradual shift from a mix of freshwater and marine species towards higher dominance of freshwater species is expected. Nevertheless, the magnitude of the primary production in these altered habitats will likely be similar to that of the shallow coastal areas existing today. Under global warming conditions and increasing sea levels, pelagic and marine species might initially increase and warm-water species will extend their habitats at the expense of the cold-water species. Further information on the anticipated changes in marine ecosystems under a warmer climate is given the **Biosphere synthesis report**, Section 4.5.2.

6.2.3 Thermal evolution

The effect of the repository on the surrounding temperature is negligible, since there are no significant heat generating processes in SFR (**Barrier process report**). Thus, the temperature within the repository will be determined almost entirely by the exchange of heat with the surrounding bedrock and groundwater.

During the initial period of submerged conditions, the prevailing temperature on the seafloor above the repository will increase due to the warmer climate. However, these warmer conditions at the upper boundary of the bedrock will only have a very small effect on the temperature in the repository and the surrounding bedrock.

6.2.4 Mechanical evolution

Mechanical processes are the consequence of changing boundary conditions, such as the doming of the ground surface associated with glaciation cycles or the rapid stress redistribution that can occur during rock excavation. The most significant changes of the mechanical conditions of the rock mass take place during excavation of the repository (**Geosphere process report**, Section 4.1) and these are not further discussed in the reference evolution.

Mechanical processes/deformation of the rock might influence the hydraulic conductivity indirectly through changes in fracture and pore geometry. The rock stresses needed for this to occur are mainly related to glaciation (large rock loads) where increased pore pressures and propagation of fractures may change the hydraulic conductivity through changes in the fracture network. During the assessment period, this is not likely to happen and is of negligible significance compared with the overall uncertainties associated with the fracture network modelling (**Geosphere process report**, Section 4.2 and Chapter 3).

The installations and structures, such as rock reinforcement, concrete waste compartments, bentonite, backfill and plugs, will be in direct or indirect mechanical contact with the rock walls. Loads from the structures, for example from the tunnel plugs due to swelling pressures from bentonite (Section 4.4.8), will cause mechanical processes in the intact rock and the existing fractures close to these locations. During the initial period of submerged conditions, there will be an on-going degradation of the reinforcements. This degradation will to some extent alter the stress distribution locally around the reinforced rock caverns.

A detailed theoretical assessment of the long-term stability (with respect to processes assumed to occur within the 100 000-year assessment period) of SFR1 and SFR3 has been performed by means of numerical modelling (Mas Ivars et al. 2014, Lönnqvist 2019, 2022). This study includes the effect of deformation zones and the long-term degradation of the rock mass under pessimistic assumptions. In the long term, some rock blocks became detached in all models, but no systematic collapse of (or large displacements in) roof or pillars was observed for pessimistic long-term fracture friction angles (i.e. fracture friction angle $\geq 18°$). In the rigid block model cases, where the blocks were purposely allowed to fall into the vault by decreasing the fracture friction angle to unrealistically low values, a stable arch is formed and the cave-in does not in any analysed case continue up to the seafloor. This means that there should be no risk that a direct connection between the vaults and the seafloor will develop. The numerical analyses also predict that the pillar between the BMA and BLA vaults is stable. Even if the hydraulic conductivity of the rock mass near the waste vaults (i.e. pillar and roof) were to increase, this does not mean that groundwater flow through the waste vaults increases. It is still the fracture system and fracture zones in the surrounding rock (outside the affected rock mass) that control the total amount of groundwater that can flow through the repository volume.

A section of the rock wall may detach after a long time and collapse onto the filling of bentonite around the silo. This could potentially lead to the formation of an open void in the rock wall, under the circumstances that the bentonite is unable to keep the rock section in position (due to loss in swelling pressure). Additionally, the rock fallout may lead to a loss in bentonite compression, thereby making the barrier less effective. The consequences of such an event have been investigated with both analytical and numerical modelling (Börgesson et al. 2015). Results from finite element calculations of rock block fallout where the bentonite does not fulfil the swelling pressure requirements (Börgesson et al. 2015) show that there might be substantial displacement. However, they also show that the consequence is a consolidation of the bentonite and subsequent increase in the swelling pressure that ends in a stable situation with a remaining substantial thickness of the bentonite barrier. The backfill in 1–2BMA, 1BRT and 1–2BTF protects the concrete structures from potential damage from rock fallout.

Earthquakes can affect the stability of the bedrock as well as the stability of the repository. Large intraplate earthquakes cannot be ruled out in a 100 000-year perspective, as evidenced by the events in New Madrid (USA), Ungava (Canada), West Australia and elsewhere (e.g. Gangopadhyay and Talwani 2003). The seismic activity in the Fennoscandian shield is currently very low (e.g. Bödvarsson et al. 2006). However, it is not possible to predict when and where future earthquakes will occur and what magnitude they will have. Thus, it cannot be excluded that an earthquake of significant magnitude takes place during the initial period of submerged conditions.

6.2.5 Hydrogeological evolution

In fractured rock, groundwater flows predominantly in fractures. The groundwater flow in the bedrock surrounding the repository influences the groundwater flow in the waste vaults (Section 6.2.7). Further, for radionuclides potentially released from the repository, groundwater flow and retention processes in the bedrock control the rate at which the radionuclides are transported away from the repository and where they discharge to the surface systems (Section 6.2.2). Based on the site characterisation, regional hydrogeological models with different bedrock conceptualisations have been developed, the most recent of which are described in Odén et al. (2014) and Öhman and Odén (2018). An important aspect of these models is the distribution of the hydraulic conductivity of the bedrock, which is not expected to change significantly during the assessment period (**Geosphere process report,** Sections 3.2, 4.4, 4.5, 5.6). Thus, changes in flow magnitude and direction, as well as groundwater discharge points, are expected to be controlled by other factors. In the following, as well as in Section 6.3.5, the result from Öhman and Odén (2018) are presented and discussed foremost. However, these results largely confirm those by Odén et al. (2014).

The regional hydrogeological models have been used to assess the groundwater flow into and out of the repository and to describe how inert particles released from the repository will be transported along flow paths through the geosphere and exit to the surface systems. The position of discharge areas, i.e., the exit locations of particles identified by means of particle tracking, change with time, and are mainly determined by the relative sea level change (Section 6.2.1), leading to changes in the shoreline position. Further, the exit locations are determined by the topography and location of deformation zones.

The regional hydrogeological model takes the initial shoreline displacement into account and encompasses a regional area for which outer boundaries have been selected based on natural hydraulic boundary conditions (future groundwater divides). The results from the regional hydrogeological model are used as boundary conditions in the near-field hydrological model (Section 6.2.7), which includes a detailed description of the repository and the surrounding rock mass and fracture zones. The near-field hydrological model also includes the various structures inside the waste vaults.

The evolution of the hydrogeological system is driven by the net flux of precipitation and potential evapotranspiration (i.e. the climate conditions), and the shoreline displacement. During the transition from submerged to terrestrial conditions, groundwater flow is almost exclusively controlled by the position of the shoreline. During this period, the shoreline regression results in a gradually increasing hydraulic gradient in the bedrock located beneath areas emerging from the sea and, consequently, in gradually higher groundwater flow rates in these areas. The present situation in Forsmark, with annual precipitation exceeding annual evapotranspiration, is assumed to prevail during this period (see further Section 6.3.1), such that the groundwater recharge is adequate to sustain a water table that roughly follows the land topography (**Geosphere process report**, Chapter 3).

During the submerged period, groundwater that has passed through the waste vaults discharges on the seafloor (Öhman and Odén 2018). Hydrogeological modelling shows that the evolution of the shoreline gradually forces the discharge areas further away from the repository towards the deformation zones ZFMNNE0869 and ZFMNW0805A (Figure 6-3; note that the zones are denoted without the prefix ZFM in the figure).

Due to shoreline displacement, the predominate flow direction changes from upwards during present-day fully submerged conditions, to become more horizontal as the repository location becomes partially terrestrial (Öhman and Odén 2018). Particle tracking predicts the density of particle exit locations (particles/unit surface area) to be strongly correlated with the presence of deformation zones. During fully and partially submerged conditions (Figure 6-3a, c) the dominant flow path cutting through the rock vaults in SFR1 discharges into deformation zone ZFMNNW1209 (called Zone 6 in SKB R-08-130). For SFR3, the exit locations of particles change from north and south of the SFR pier (Figure 6-3b) at an early stage to further north, towards ZFMNW0805A (Figure 6-3d) as the predominant flow direction becomes horizontal.

When terrestrial conditions begin to dominate the area above the repository, the flow direction is almost completely determined by the topography (Öhman and Odén 2018). The particles still exit on the seafloor and the density of particle exit locations is strongly correlated to the presence of deformation zones. The main discharge area for flow paths released from SFR1 is located north-north-east and north-west of the repository (Figure 6-3e). For particles released from SFR3, exit locations are predicted both north and south of the SFR pier, but the exit locations are now more concentrated on ZFMNW0805A, see Figure 6-3f.

6.2.6 Geochemical evolution

The evolution of the groundwater composition is closely related to the groundwater flow evolution. Shoreline regression will result in changing flow paths and flow conditions (Sections 6.2.5 and 6.3.5), which in turn may affect geochemical processes through changes in water velocities, contact times and surface areas of the fractured rock. This section covers the geochemical evolution during the initial period of submerged conditions for all variants of reference external conditions, including the prolonged initial period of submerged conditions due to global warming, as given by the *warm climate variant*.

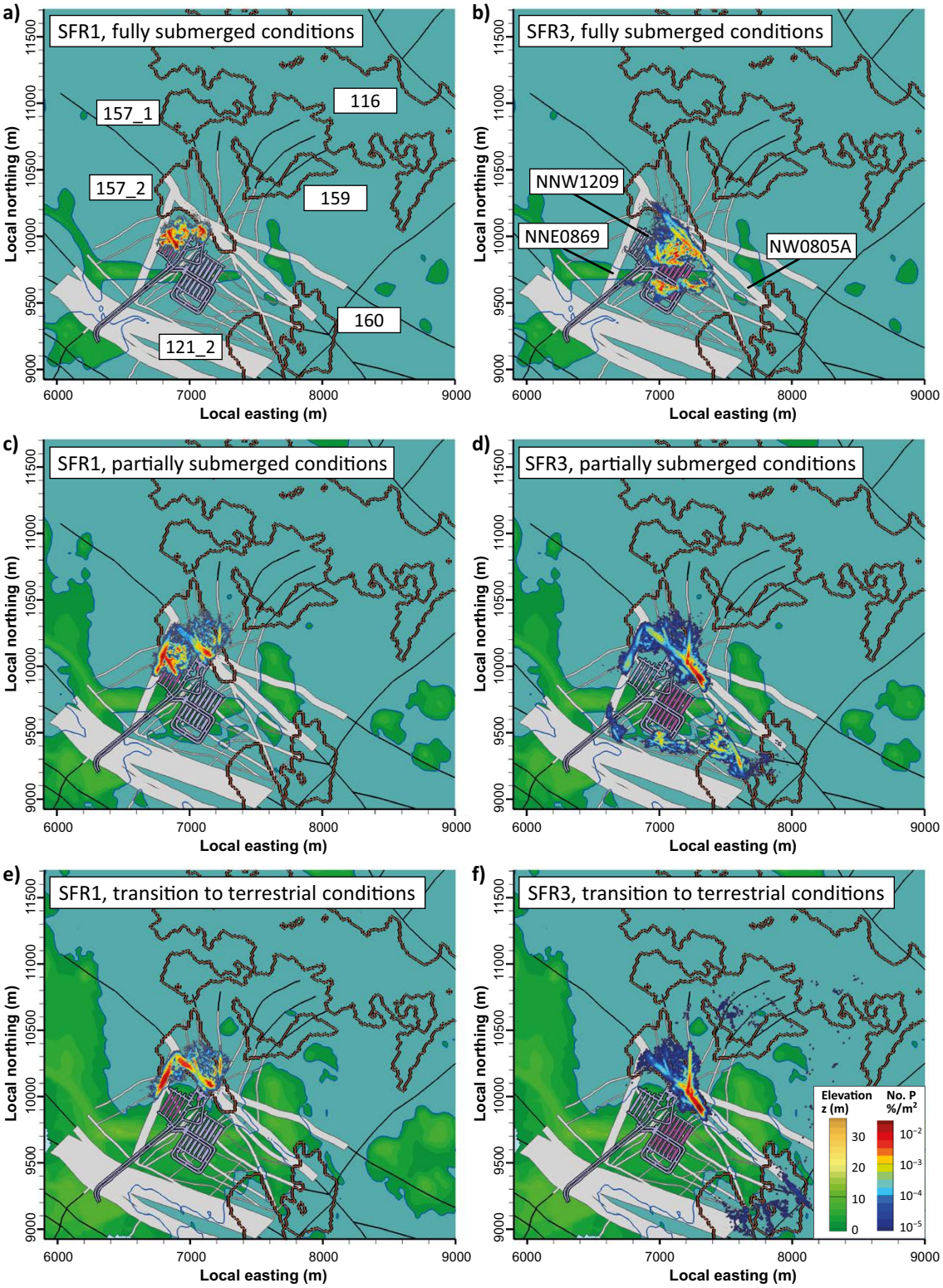

Figure 6-3. *Distribution of discharge to the surface systems from the SFR1 waste vaults (a, c and e) and the SFR3 waste vaults (b, d and f), based on density (shading from blue to red) of particle exit locations (fraction of released particles/surface unit) in the hydrogeological modelling. Results are shown for fully submerged conditions (a and b), partially submerged conditions (500 years before transition to terrestrial conditions; c and d) and during transition from submerged to terrestrial conditions (e and f). Waste vaults in SFR1 (panels a, c and e) and SFR3 (panels b, d and f) are indicated in magenta. Surface elevation above sea level is shown according to the elevation scale. The blue-grey colour indicates marine environment. The grey areas indicate the thickness at ground surface of deformation zones that are represented in the SFR Regional domain of the hydrogeological model (Section 4.7.3). The black lines represent the location of deformation zones outside the SFR Regional domain. The straight black lines and the text within the black rectangles in (b) indicate the location of the deformation zones discussed in the text. The orange contours and associated labels in (a) outline biosphere objects defined in Section 7.3.5. Figure is modified from Öhman and Odén (2018).*

The groundwater composition in the bedrock surrounding the repository influences the composition of the groundwater in the repository (Section 6.2.8). Further, for radionuclides potentially released from the repository, the geochemical evolution influences retention processes in the bedrock and thus the release of radionuclides to the surface systems. In addition to processes related to groundwater flow, several processes in the geosphere affect the geochemical evolution, including thermal gradients in the rock, erosion and sedimentation in fractures and chemical processes related to transport and concentrations of dissolved solids (advection, diffusion, sorption, dissolution and precipitation of fracture minerals, dissolution of organic matter, colloid transport and microbial activity). These processes are discussed in relation to different climates and their importance for the safety assessment in the **Geosphere process report**.

The description of the future evolution of the groundwater composition in the bedrock surrounding the repository is based on reference groundwater composition evolutions estimated for the three different climate domains: temperate, periglacial and glacial (Auqué et al. 2013, Román-Ross et al. 2014). The basis of this concept is a model that predicts different reference groundwater types evolving until the present day and that were identified at the site (Nilsson et al. 2011, Section 4.8), with the evolution occurring as a result of mixing waters from the past (Gimeno et al. 2009, see further subsection *Pre-conditions for the initial period of submerged conditions*). Of note is that the relative effects of water–rock interaction on the groundwater chemistry are small when compared with the effects of mixing of different groundwater types (Auqué et al. 2017, Auqué and Gimeno 2017, SKB 2017a).

Modelling the chemical evolution of the bedrock surrounding the repository is important to properly understand the hydrochemical conditions prevailing at repository depth with time (see further Section 6.2.8).

Pre-conditions for the initial period of submerged conditions

Before the intrusion of meltwater from the last deglaciation, brackish groundwater without a marine signature, but with components of old meteoric waters from both temperate and cold climate events, was present. This water was then mixed with glacial meltwater during the Weichselian glaciation due to the high hydrostatic pressure in the rock. Under such conditions, it is possible that a larger number of fractures become conductive or that the conductivity in existing fractures/fracture zones increased. This may explain the downward transport of dilute meltwater from previous glaciations, which can still be traced in the area.

During the subsequent Littorina Sea stage, brackish seawater with higher density entered some of the deformation zones and fractures previously infiltrated by meltwater. This brackish water mixed with or displaced the resident fresh groundwater. The maximum salinity during the Littorina Sea stage was between 10 and 15 ‰ (today c. 7 ‰) as indicated by fossil assemblages, ^{18}O analysis and trace-element content in sediments (Westman et al. 1999, Laaksoharju et al. 2008). Even though occasional findings of molluscs indicate a salinity of up to 20 ‰ (Westman et al. 1999), these waters seem to not have reached these depths because other fracture systems were probably closed at the time due to a changed pressure situation. This trapped the brackish non-marine groundwater with a significant glacial component in this less fractured bedrock where it currently remains. In the deeper matrix rock in Forsmark, for example, cold-climate porewaters seem to have been overprinted with a brackish marine-type signature closer to water-conducting fractures (Waber et al. 2009). The analogy for SFR is not conclusive with regards to porewater data, since no samples from SFR exist.

Groundwater composition during the initial period of submerged conditions

During the initial period of submerged conditions, the groundwater composition in SFR is not expected to change much and will exhibit a relatively limited salinity range (1 500 to 5 500 mg/L chloride concentration, Table 4.2 in Auqué et al. 2013). However, the $\delta^{18}O$ values, as an indicator for colder climate conditions, show larger variation (–15.5 to –7.5 ‰ V-SMOW (Vienna standard mean ocean water)), similar to that reported from the site investigations for the spent fuel repository (Laaksoharju et al. 2008). Low $\delta^{18}O$-levels, < –13 ‰ V-SMOW, are interpreted for the Forsmark area as indicative of a significant proportion of glacial meltwater in the groundwaters. Despite the limited salinity range, other marine indicators also show relatively large variations in the bedrock surrounding SFR. Hydrogeochemical observations together with palaeo-climatic considerations have been used to

classify the groundwaters into four major types, each of which has very different residence times in the bedrock. The groundwater types are: 1) local Baltic Sea water type, 2) Littorina water type, with a glacial component, 3) brackish glacial water type, and 4) mixed brackish water (transition type), as given in Nilsson et al. (2011).

The distribution of the different groundwater types shows that the major deformation zones must have served as important groundwater flow pathways over long time periods, whereas single fractures in rock volumes between zones generally contain older and more isolated groundwater. Due to the hydraulic situation around the present SFR, the mixed brackish groundwater type has become more and more frequent since the excavation and construction of the SFR (Nilsson et al. 2011). This may lead to homogenisation of different salt concentrations to a more uniform value of 3 000 mg/L. This is expected to happen also in the extension area of SFR, even though no geochemical borehole data from the extension area are available to confirm this. The steeply dipping structures have accentuated the drawdown of modern Baltic Sea water that has been observed where those structures are connected to the seabed.

The composition of penetrating brackish groundwater and ranges of the parameters of interest for the initial period of submerged conditions, when the area above the repository is mostly submerged beneath the Baltic Sea, follows that of the initial state composition (see Table 6-1). This reference composition is based mainly on the dataset compiled for the SFR extension Site descriptive model (Gimeno et al. 2011, Nilsson et al. 2011, Auqué et al. 2013), where updated site data for groundwaters down to a depth of 200 m are used. The dissolved organic content (DOC) in the groundwater of SFR is often quite low, in general between 1 and 2 mg/L, for depths between −20 and −400 m.a.s.l (Auqué et al. 2013). The pH ranges between 6.6 and 8.0, however no pH above 9.7 has been found considering the whole data set from the site (Appendix A in Auqué et al. 2013, Nilsson et al. 2011). Thus, for the geosphere, pH < 10 is considered during the initial period of submerged conditions.

Adjacent to and downstream of the repository, high pH conditions may evolve in the surrounding groundwaters, originating from dissolution of the cement minerals in the repository (Section 6.2.8). This is however not expected during the initial period of submerged conditions due to the low groundwater flow.

Table 6-1. Expected composition of penetrating brackish groundwater during the initial period of submerged conditions (based on Gimeno et al. 2011, Nilsson et al. 2011 and Auqué et al. 2013).

Parameter	Reference value	Range
pH	7.3	6.6–8.0
E_h (mV)	−225	−100 to −350
Cl^- (mg/L)	3 500	2 590–5 380
SO_4^{2-} (mg/L)	350	74–557.2
HCO_3^- (mg/L)	90	40–157
Na^+ (mg/L)	1 500	850–1 920
K^+ (mg/L)	20	3.8–60
Ca^{2+} (mg/L)	600	87–1 220
Mg^{2+} (mg/L)	150	79–290
SiO_2 (mg/L)	11	2.6–17.2
DOC (mg/L)	1.85	0.7–5.1

Reducing conditions prevail during the whole initial period of submerged conditions. Water interactions with the rock matrix, minerals in water-conductive fractures, and microbially mediated reactions may modify groundwater chemistry. However, this is not expected to be of major importance during the initial submerged period, but it may become more important with time (Section 6.3.6). With time it becomes more uncertain whether these reactive processes may alter for instance groundwater composition due to changes to terrestrial conditions and hence to what degree these changes in composition may interact with water chemistry in the waste vaults (Sections 6.3.6 and 6.3.8).

During the remaining period of submerged conditions, high partial pressures of CO_2 (and thus high HCO_3^- concentrations) are expected to prevail also in the groundwater due to infiltration of waters affected by the biological activity of seabed sediments (a generic term coupled indirectly to the carbonate system, and elevated concentrations of bicarbonate as an indication of organic biological activity) mixing with marine waters. Several microbial respiration processes depend on electron acceptors that are present also in some fracture minerals, for example Mn(IV) and Fe(III). However, variations in the fracture minerals are of minor importance to the overall microbial processes since on-going microbial processes in the bedrock are likely to contribute to only a minor extent, because cell concentrations and activity are very low and hence of minor importance for repository safety.

If the initial submerged period becomes extended due to future sea level rise, the groundwater composition in SFR is considered to be maintained since stable hydraulic conditions are expected. A relatively limited salinity range (defined by chloride concentration) is expected to prevail. However, this state is dependent on the development of the Baltic Sea. With increasing sea levels, an inflow via the strait of Öresund cannot be excluded and hence an increase of the salinity range, might be possible. Steeply dipping structures east of SFR (North of the extension of SFR) have accentuated the drawdown of the modern Baltic Sea water. It is uncertain whether or not this drawdown will result in more dilute groundwater in the adjacent bedrock.

Transition towards terrestrial conditions

The brackish groundwater in the bedrock surrounding SFR may start to change eventually, and become more and more diluted with time, as the shoreline becomes located further East. During this period, the groundwater composition will slowly change with time (Section 6.3.6), and be influenced by the introduction of meteoric water into the uppermost part of the bedrock, promoting dissolution of e.g. pyrite and precipitation of Fe(oxy)hydroxides promoting the maintenance of reducing conditions in the geosphere. Further uplift above the sea level will affect the groundwater flow pattern through dynamic changes in hydraulic properties and changes in the direction of groundwater flow, from being a discharge area to a situation with more horizontal groundwater flow (Section 6.2.5).

The extent and direction of solute transport by advection will hence change in response to the prevailing groundwater flow field. Liquid-phase diffusion in stagnant water may continue to be of importance for radionuclide retention and for the evolution of the groundwater composition in the longer term (**Geosphere process report**).

Organic complexing agents

Some wastes contain organic complexing agents which may form metal complexes with certain radionuclides (Section 6.2.8). Complexing agents dissolved in the repository cement-leachate water are gradually transported to the geosphere, where their impact on radionuclide sorption in the bedrock is tightly coupled to the high pH of the same water (Crawford 2017). The reason for this strong coupling is the significant pH sensitivity of the radionuclides' affinity both to the bedrock (i.e. sorption) and to the complexing agents. As such, the effect of complexing agents is strongest near the repository and then diminishes as the complexing-agent concentration and pH are gradually diluted along the bedrock flow paths.

Metal complexes formed in the repository are expected to mostly dissociate in the geosphere due to a lower complexing-agent concentration, as determined by the stability constants of the respective complexes. The kinetic stability of complexes is expected to be shorter than the travel time through the geosphere given the low flow-conditions of the initial submerged period.

6.2.7 Near-field hydrological evolution

The repository is considered to be fully saturated at the initial state (Section 4.4.9). The initial evolution of the near-field hydrological system largely follows the evolution of the regional hydrogeological system driven by shoreline displacement (Section 6.2.5). SFR is located in an area with a low hydraulic gradient during submerged conditions. The site for the repository was partly selected to ensure low groundwater flow rates through the waste vaults. The magnitude, direction and distribution of the groundwater flow within the repository also depends on the hydraulic properties of the engineered barriers.

The SFR repository has been designed to retain radionuclides through the use of barriers. The barriers aim to limit and delay the release of radionuclides from the waste vaults by sorption and by limiting the interior water flow (flow through the waste and barriers) and the flow through waste vaults. At sufficiently low interior flow velocities, diffusion becomes the dominating transport process, and the rate of radionuclide migration through the system is significantly reduced. Consequently, changes in the engineered barriers caused by physical and chemical degradation (Section 6.2.9), impact the near-field hydrology. In addition, multiphase-flow processes following chemical evolution of waste in the repository could also impact the near-field hydrology. Concrete and bentonite are the main construction materials used for the hydraulic barriers in SFR. These materials have much lower permeability compared to for example crushed rock used as backfill material. Permeability differences in structure and filling materials leads to preferential flow paths inside the vaults, and this is used to reduce the flow through the waste.

The silo, which will receive most of the disposed activity in SFR, has both bentonite and concrete barriers, where the bentonite barrier constitutes the main hydraulic barrier. The intermediate-level waste in 1BMA and 2BMA is emplaced in concrete compartments, where the walls, slab and lids of the structures reduce the groundwater flow through the waste. In these vaults, a highly permeable backfill of crushed rock will be installed at closure, creating a hydraulic contrast between the concrete structure and the backfill, and also between the backfill and the surrounding bedrock. Water entering the vaults will therefore preferentially flow through the backfill and the flow through the concrete barriers and waste will be reduced. In 1BTF and 2BTF, grouted concrete tanks constitute a hydraulic barrier. A highly permeable backfill will be installed on top of the concrete structures. In the 1BRT vault, reactor, pressure vessels will be emplaced in a concrete structure. Prior to emplacement, the reactor pressure vessels will be segmented, put in double moulds and embedded in grout. Crushed rock will be used to backfill the vault, creating a basis for preferential flow. The BLA vaults, containing low-level waste in ISO-containers, have no internal structures restricting the groundwater flow. However, the host rock surrounding the vaults limits the flow substantially. In addition to hydraulic barriers installed in the waste vaults, tunnel sections connecting them will be sealed with bentonite to further restrict groundwater flow. The initial state of the waste vaults and tunnel system is further described in Chapter 4.

The evolution of the regional hydrogeology, which constitutes the boundary conditions for the near-field hydrological evolution, is described in Section 6.2.5. Results from regional hydrogeology simulations have shown that the presence of SFR3 has only a modest effect on the groundwater flow in SFR1 (Öhman et al. 2014). The near-field hydrological models of SFR1 and SFR3 include the waste vaults and the tunnel system that connects them (Figure 6-4). The near-field models have more detailed representations of the engineered barriers and waste compared to the regional hydrogeological models. The near-field hydrological models and predicted near-field hydrological conditions are presented in detail in the modelling reports by Abarca et al. (2013, 2014, 2020).

The shoreline displacement impacts the near-field hydrology and therefore the boundary conditions used in the near-field hydrological model have been obtained from the regional hydrogeological model (Section 6.2.5) considering different shoreline positions. Initially, during fully submerged conditions above the repository, the general flow direction in the near-field, as in the surrounding bedrock (both for SFR1 and SFR3) is vertically upwards as illustrated for SFR1 in Figure 6-5.

Concrete hydraulic barrier degradation

Degradation processes start to influence the hydraulic properties of concrete structures and materials in the repository during the initial period of submerged conditions (Section 6.2.9). However, the resulting effect on groundwater flow through the repository is considered small compared to the increase in groundwater flow due to the retreating shoreline (Abarca et al. 2013, 2020). Section 6.3.7 outlines the effect of more developed concrete degradation on the flow in the near-field.

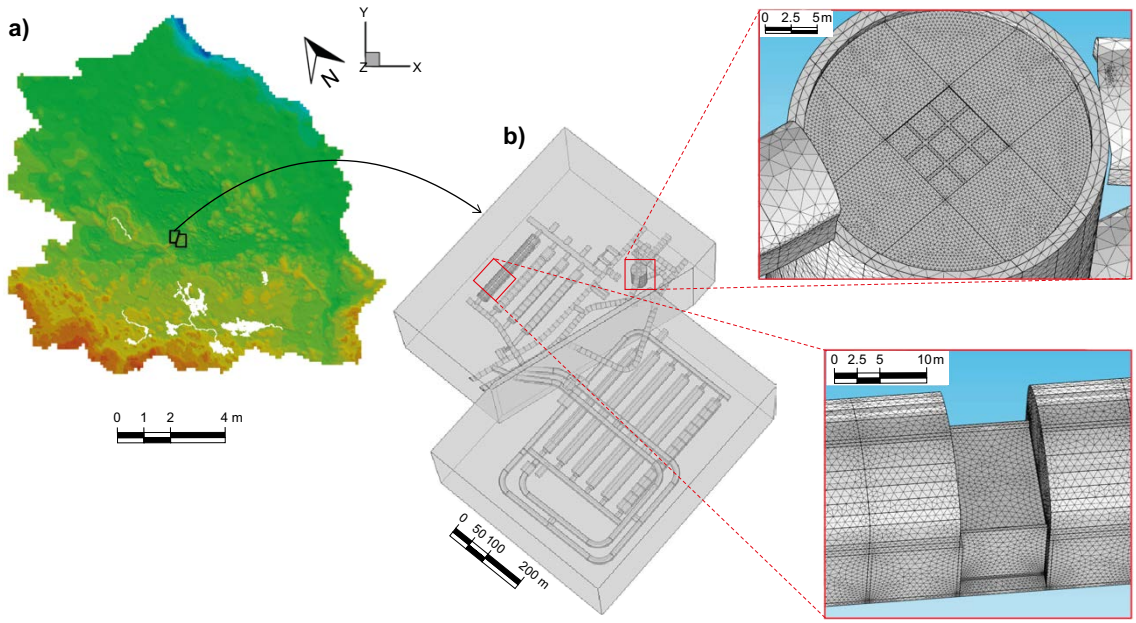

Figure 6-4. *Hydrological models; (a) the regional hydrogeological model providing boundary conditions to (b) the near-field hydrological models of SFR1 and SFR3. The near-field hydrological models include the structures in different vaults.*

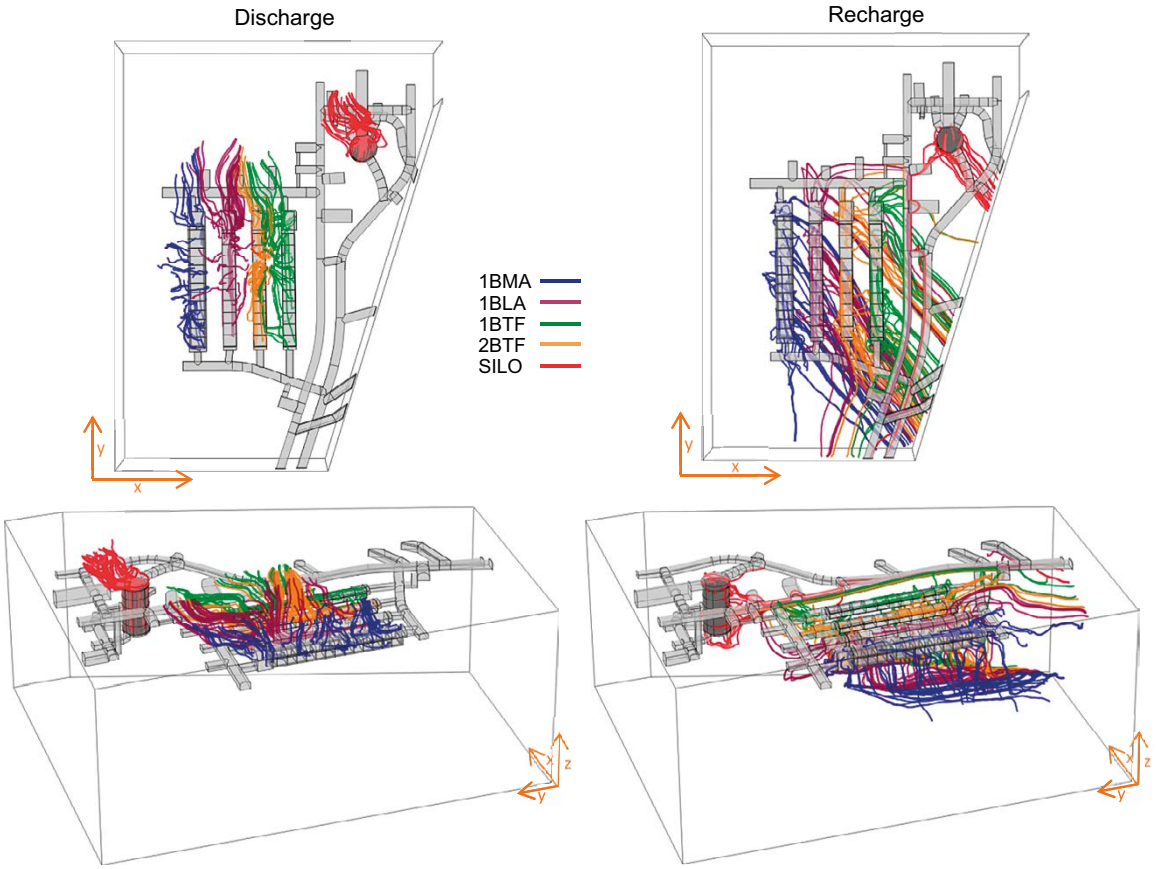

Figure 6-5. *Groundwater streamlines leaving (left) and reaching (right) individual vaults in SFR1 (colour tubes) at 2000 AD (Abarca et al. 2020).*

Bentonite barriers and sealed hydraulic sections of bentonite

To restrict groundwater flow through the waste vaults, the tunnel sections closest to the vaults will be sealed with sections of bentonite. These sections are supported by mechanical plugs. When the plugs are intact, the groundwater reaches the vaults in SFR mainly through deformation zones in the rock. These zones also connect vaults and distribute flow between them. Changes to the hydraulic properties of the bentonite barriers in the repository will be negligible during the initial period of submerged conditions (Section 6.2.9).

Transition towards terrestrial conditions

The flow pattern in the repository follows that described for the geosphere. When the shoreline regresses past the repository, the main flow direction gradually changes from vertically upwards to horizontal. The hydraulic gradient increases, which leads to increased flow rates in the repository, see further Section 6.3.7.

6.2.8 Evolution of the waste and of the repository chemical conditions

This section discusses the events and processes of importance for the evolution of the waste and of the repository chemical conditions. Waste is defined as all materials in the waste packages, including the waste matrix containing radionuclides, waste solidification or embedment material, and the waste packaging. This section describes the reference evolution of the waste, the water composition in the vaults, the speciation and sorption of radionuclides, corrosion of metals, organic complexing agents, microbiology, gas generation and gas transport during the initial period of submerged conditions.

A multitude of processes and reactions will occur between the waste, engineered barriers, and groundwater in the repository. The waste and barriers both contain large amounts of cement and steel. As such, processes related to these materials, e.g. sorption and corrosion, are important both in the waste and the engineered barriers. In consequence, parts of the evolution described in the present section apply to the entire repository including the reinforced concrete barriers, although most aspects of their evolution are described in Section 6.2.9.

The evolution described in this section is focussed on processes and chemical parameters that are important for radionuclide release from the waste and thus for repository function. Cement is ubiquitous in SFR, providing a high pH and calcium concentration, as well as a substantial ionic strength which is further influenced by the brackish groundwater that will saturate the repository after closure. These parameters directly affect the speciation and sorption of radionuclides which are further influenced by organic complexing agents present in the waste. The evolution of cementitious materials is mainly described in Section 6.2.9. Steel is another important waste material, setting reducing conditions which determines the speciation of some radionuclides. However, steel also produces hydrogen gas as it corrodes, and sufficiently low gas pressures are important for barrier integrity and radionuclide retention.

These and other important processes and parameters affecting the evolution of the waste and the repository chemical conditions are discussed in the following subsections. Most processes are fairly insensitive to temperature and to whether conditions above the repository are submerged or terrestrial; hence the description for the initial period of submerged conditions in the present section is mostly valid also for the subsequent terrestrial conditions in the variants of the reference evolution (Sections 6.3.8, 6.4.8 and 6.5.8). An exception is when the repository freezes, since freezing causes most relevant chemical processes to halt (Section 6.5.8).

Waste form and packaging

The waste in SFR is packed in packaging of steel or concrete and, in many cases, the waste inside the packaging is solidified in cement or bitumen, or embedded in concrete. A more detailed description of waste and packaging can be found in the **Initial state report**, Chapter 3.

Steel packaging

Steel packaging will start corroding during (and before) the operational period of SFR. Thus, its ability to function as a barrier to the transport of groundwater, gas and radionuclides after closure is uncertain. Nevertheless, thanks to anti-corrosion paint treatment, most packaging is expected to be in good shape at closure and thus expected to provide containment of radionuclides for some time after closure, ranging from years to many millennia depending on their sealing, material thickness, steel composition (e.g. stainless vs carbon steel), extent of corrosion at closure and resistance to hydrostatic pressure.

The corrosion products – iron oxides, oxyhydroxides and hydroxides – that are formed during the operational period and after closure can be good sorbents for radionuclides. Certain ions could also be co-precipitated with the corrosion products. Neither radionuclide sorption on, nor co-precipitation with, corrosion products have been considered within this safety assessment. Nevertheless, corrosion of iron and steel contribute to the reducing conditions in the repository, initially through consumption of oxidising agents like molecular oxygen and later by reduction of water which results in the formation of hydrogen gas (see further in the subsection *Metal corrosion* below).

Concrete packaging and cement matrices

Modelling of laboratory and natural analogue data shows that concrete packaging and cement matrices will not be subjected to any significant leaching of cement components during the initial period of submerged conditions (Höglund 2001, Gaucher et al. 2005, Cronstrand 2007, 2014). However, it cannot be excluded that local mineral alterations at the surface of the packages can take place.

Corrosion of rebar and the resultant volume increase could cause small cracks in the concrete adjacent to the rebar. This is not expected to be of importance for the properties of the concrete packages as a sorption barrier for radionuclides.

Another process that could eventually cause cracking of concrete packaging materials and cement matrices, is slow formation of expansive minerals in cement due to uptake of sulfate and/or (to a lesser extent) chloride and carbonate from evaporator concentrate, degraded ion-exchange resins and the incoming groundwater. Ion-exchange resins can release sulfate upon degradation, which hypothetically could lead to such extensive formation of expansive minerals that the integrity of the concrete packaging would be jeopardised. However, ion-exchange resins are not expected to degrade significantly under SFR chemical conditions (see subsection *Ion-exchange resin and filter aids* below for more details).

The integrity of both concrete and steel packages could also potentially be compromised if the gas pressure within them becomes too high (see subsections *Gas formation and transport*, *Microbiology* and *Metal corrosion* below).

Bitumen waste matrices

Bitumen is a colloidal material consisting mainly of high-molecular-mass aliphatic and aromatic hydrocarbons that can be used for solidifying low- and intermediate-level waste (Pettersson and Elert 2001). Ion-exchange resins are solidified in bitumen before being placed in waste packages, sometimes mixed with evaporator-concentrate salts (see subsection *Evaporator concentrate* below). In the bituminisation process, the waste is dried and then mixed with hot bitumen, resulting in a bitumen matrix with a dispersion of embedded waste particles. Although pure bitumen is a hydrophobic material, water can be transported into a bitumen matrix containing dried resins or salts. The properties of the bitumen–waste matrix can also change with time via radiolysis, chemical degradation, biodegradation and water uptake, all of which can result in swelling.

Depending on the properties of the waste, the driving force for water uptake can be described as a gradient in chemical potential (Sercombe et al. 2006), water activity or water concentration (Brodersen 1999). The evaporator-concentrate salts mixed in some bitumen waste matrices (Pettersson and Elert 2001, Table E-114 in SKB R-18-07) are often highly soluble (e.g. sodium salts such as $NaNO_3$ and Na_2SO_4), whereas other salts (e.g. $BaSO_4$) and sludges are relatively inert and not expected to dissolve.

As far as ion-exchange resins are concerned, the situation is more complex and depends on the type of resin used (cation- or anion-exchanger, powdered or bead, degree of cross-linking etc.) and the extent of drying and other pre-treatments of the resin such as heating (Pettersson and Elert 2001).

When dried ion-exchange resins and evaporated concentrates absorb water, they expand in volume. The degree of expansion of the waste depends on various factors including the mechanical properties of the bitumen, the waste loading and the homogeneity of the waste form. Many studies on bitumen-conditioned waste swelling have been conducted over the years.[22] One conclusion is that modelling results generally show greater swelling than corresponding experiments, tentatively attributed to simplifications in the models such as neglect of ion pairing in the ion-exchange resins.

In 1–2BMA, the placement of waste must be done in such a way that there is enough free volume available to accommodate the increased volume from swelling without jeopardising the integrity of the engineered barriers. Recent mechanical-strength calculations[23] on the effect of waste swelling in 1BMA indicate that the slab is the weakest point of the concrete structure surrounding the waste, whereas the walls between waste compartments could withstand pressures up to 12 kPa. Continued studies on the expected extent of swelling of bitumen-conditioned waste and the effect on the surrounding barriers are currently ongoing.

In the silo, engineered expansion cassettes are placed between the drums of bituminised waste from the Barsebäck nuclear power plant. Bituminised waste from the Forsmark nuclear power plant has between 5 and 10 % free void inside the moulds to accommodate swelling. More recent data indicate that this void may not be sufficient but, according to von Schenck and Bultmark (2014) and Olsson (2017), swelling bituminised waste forms may affect the internal structure of the silo but not the outer silo walls.

The main process affecting bitumen matrices that will promote release of radionuclides is expected to be water uptake and swelling. The time taken for water uptake and how this affects the matrix is highly uncertain. Some indication of how effective a bitumen matrix is as a barrier for radionuclide transport can be obtained from leaching experiments. Extrapolation of results from such leaching experiments conducted over periods that are short in a waste disposal context indicates that it could take several thousand years before all radionuclides have leached out of the bitumen matrix in a 200-litre steel drum (Pettersson and Elert 2001). A more reasonable timescale for the release of radionuclides is, according to Pettersson and Elert (2001), several hundred up to one thousand years, i.e. shorter than or equal to the length of the initial submerged period.

Ion-exchange resins and filter aids

The most abundant organic materials in the SFR repository are different forms of ion-exchange resins, used by the waste producers for decontamination of various process waters. Ion-exchange resins are found in all waste vaults, although most of the resins are found in 1BMA and the silo where they are solidified in cement or bitumen and packaged in steel moulds, concrete moulds or steel drums. In the BTF vaults, the situation differs from the other waste vaults in that the ion-exchange resins are stored without solidification but dewatered, in concrete tanks.

Ion-exchange resins consist of polystyrene chains where the active groups that bind radionuclides comprise tertiary amines in anion exchangers and sulfonic groups in cation exchangers (Allard and Persson 1985). Historically, some cation exchangers instead contained carboxylic active groups, more weakly binding than sulfonic groups, with a polyacrylate backbone (Allard et al. 2002).

Ion-exchange resins, as organic materials in general, can degrade by chemical, radiolytic, or microbial means. However, it has been shown that ion-exchange resins are chemically inert under the chemical conditions similar to those anticipated in SFR (Bradbury and Van Loon 1998, Van Loon and Hummel 1999a, b), so no chemical degradation of ion-exchange resins is expected in SFR.

[22] Rosdahl J, 2021. Utvärdering av redan utförda svällningsexperiment. SKBdoc 1928010 ver 1.0, Svensk Kärnbränslehantering AB. (In Swedish.) (Internal document.)

[23] Nytorp Jansson M, 2021. 1BMA – Svällande avfall. DMG1008837 1.0, Vattenfall AB. SKBdoc 1942931 ver 1.0, Svensk Kärnbränslehantering AB. (In Swedish.) (Internal document.)

As described in Van Loon and Hummel (1995), no chemical degradation is expected for sulfonate-type ion-exchange resins under high pH conditions. 1–2BMA, 1–2BTF and the silo are expected to retain a very high pH over the entire analysis period (see subsection *pH in waste leachate* below), so degradation of sulfonate-type ion-exchange resins is not expected. In 1–2BTF, the resins are not conditioned with cementitious materials but, because of the large amounts of cement present in these vaults, the mole fraction of $Ca(OH)_2$ exceeds the OH^--consuming reactions (SKB 2017b) and the chemical degradation will thus be negligible. Smaller amounts of ion-exchange resins are disposed in 1BLA, where degradation is more likely since it contains less cementitious materials, resulting in a more rapid pH decrease.

The carboxylate-type ion-exchange resins have been shown not to degrade (Allard et al. 2002) and are therefore expected to be stable throughout the assessment period.

The radiolytic decomposition of ion-exchange resins could cleave off functional groups during irradiation, in addition to producing hydrogen gas. During irradiation of sulfonate-type ion-exchange resins, sulfate ions are formed which may impact the integrity of concrete structures in the repository.

Anion-exchange resins are more susceptible to radiolytic degradation since the functional groups contain quaternary ammonium salts which could form amines. Irradiation of tertiary amine functional groups of anion-exchange resins will form a mixture of trimethyl amine, dimethyl amine, methyl amine, and ammonia. Water solutions of these amines could affect the solubility of radionuclides, especially for cations like Pd^{2+} and Ni^{2+} which form strong complexes with amines (more details in the subsection *Organic complexing agents* below).

In several studies (e.g. Van Loon and Hummel 1995, 1999b, Traboulsi et al. 2013, Rébufa et al. 2015), the radiolytic decomposition of ion exchange resins has been investigated. These studies can be divided into two categories:

1. Constant dose studies. Such studies aim to investigate and quantify the formed degradation products.
2. Studies with varying doses. Such studies aim to investigate how the dose influences the degradation.

The latter type is used to judge if the irradiation doses permitted in SFR, according to the waste acceptance criteria, can affect the degradation of ion exchange resins in SFR. Rébufa et al. (2015) performed a study of this nature. The results clearly indicate that, if ion-exchange resins of types relevant for SFR, are subjected to cumulative radiation doses lower than 4×10^6 Gy, only small amounts of amines are formed from the degradation of the quaternary amine moiety. At these doses, only low amounts of trimethyl amine were detected in the water phase when the ion-exchange resin was irradiated under anaerobic conditions. At tenfold higher doses, other amines started to form. According to Van Loon and Hummel (1995) the stability of the formed amine complexes decreases when larger, carbon-bearing ligands are bound to the nitrogen. From this reasoning, it is concluded that ammonia is the degradation product that influences the solubility of radionuclides the most. However, the monoamines formed from ion-exchange-resin degradation are too weak complexing agents to affect radionuclide sorption under SFR conditions; at least two coordinating groups are required for any noticeable effect (see subsection *Organic complexing agents* below and Keith-Roach and Shahkarami 2021).

Furthermore, these cumulative absorbed doses exceed the waste acceptance criteria for organic-containing wastes in the 1BMA and the silo[24] by more than an order of magnitude. Therefore, the radiation field in SFR is regarded as too low to result in appreciable release of amines and ammonia from ion-exchange resins.

The styrene backbone of the ion-exchange resins disposed in SFR is aerobically degradable by different types of bacteria (Omori et al. 1974, 1975, Sielicki et al. 1978, Shirai and Hisatsuka 1979, Grbić-Galić et al. 1990). It has also been shown to be degraded by an anaerobic consortium of microorganisms (Grbić-Galić et al. 1990). Whether microbial degradation will occur under the conditions expected in SFR remains uncertain. However, during the initial period of submerged conditions, the expected pH values are so high (see subsection *pH in waste leachate* below) that microbial activity is judged insignificant (see subsection *Microbiology* below), so the process is not regarded as a major degradation pathway.

[24] Södergren K, Snis K, Reitti M, 2021. Acceptanskriterier för avfall i SFR. SKBdoc 1336074 ver 5.0, Svensk Kärnbränslehantering AB. (In Swedish.) (Internal document.)

Filter aids are used by the waste producers together with the ion-exchange resins to prevent clogging. Dario et al. (2004) reported that a polyacrylonitrile filter aid was degraded by 15 % in less than two months. These results were used by Duro et al. (2012a) to derive a kinetic expression for the degradation. Applying this expression and the initial amounts of acrylonitrile polymer disposed in SFR reveals that the concentration of degradation products will not reach concentrations affecting the sorption of Eu(III) as reported Dario et al. (2004). Of the expected polyacrylonitrile degradation products under SFR conditions, those with possible complexing-agent properties are mainly ammonia, dicarboxylates, and small α-hydroxy carboxylates (Gaona et al. 2021), which are all too weak complexing agents to noticeably affect radionuclide sorption (see subsection *Organic complexing agents* below and Keith-Roach and Shahkarami 2021).

In conclusion, degradation of ion-exchange resins in SFR is considered unimportant both during the initial period of submerged conditions and throughout the assessment period.

After closure, radionuclides will be released from the ion-exchange resins at rates that vary between radionuclides and with the water flow through the waste. Radionuclides are generally expected to be released from the material and dissolved in the waste porewater during the initial submerged period.

Other organic materials

Like ion-exchange resins, other organic materials can also degrade chemically, radiolytically or microbially. In the **Waste process report**, Section 3.5.6, degradation of other organic materials, mainly plastics, is discussed in detail. Plastic materials can be divided into:

1. Addition polymers, e.g. polyethylene.
2. Condensation polymers, e.g. polyester, nylon and cellulose.

Polyethylene is not subject to alkaline degradation (Van Loon and Hummel 1995), an observation valid for addition polymers in general (Keith-Roach and Shahkarami 2021, Section 2.3). Condensation polymers, however, can be subjected to alkaline degradation, where degradation of cellulose is further described in the subsection *Cellulose* below. Degradation of polyamides such as nylon forms carboxylic acids and diamines and degradation of polyester forms dicarboxylic acids and diols.

Apart from the polymer molecule itself, plastic materials often contain smaller, non-polymeric additive molecules. One such commonly used additive in plastic materials is phthalates.

Radiolytic degradation of polyvinyl chloride (PVC) can generate hydrochloric acid which can lead to local pH changes. PVC is mainly found in BLA waste where the potential for radiolysis is low due to low activity levels compared to other vaults. The formed degradation products and plastic additives do not noticeably affect the sorption or solubility of radionuclides (Keith-Roach and Shahkarami 2021).

Evaporator concentrates

Some waste types, e.g. the bitumen-conditioned ion-exchange resins in BMA, may contain evaporator concentrates and these typically contain a significant amount of highly soluble salts. Chloride and sulfate salts can react with cement and form Friedel's salt and the expansive mineral ettringite, respectively (Höglund 2014). Such salts are expected to be dissolved from the evaporator-concentrate waste within the initial period of submerged conditions and can then potentially react slowly with adjacent cement waste matrices, concrete packaging materials and eventually surrounding concrete barriers.

To protect the surrounding barriers, cement-degrading salts in the waste can be immobilised within the waste form, either by additives that form insoluble salts (such as for example addition of $Ba(OH)_2$ which leads to formation of $BaSO_4$) or by inclusion of sufficient amounts of cement within the waste package so that all sulfate and chloride is consumed within the waste. As of 2021, such immobilisation is required according to the waste acceptance criteria for all vaults with concrete engineered barriers.[25]

[25] Södergren K, Snis K, Reitti M, 2021. Acceptanskriterier för avfall i SFR. SKBdoc 1336074 ver 5.0, Svensk Kärnbränslehantering AB. (In Swedish.) (Internal document.)

Cement-conditioned waste in concrete packaging, such as waste type R.29, contains sufficient cement to consume any plausible amounts of sulfate and chloride in the waste. But other waste types, such as F.17 that lack cement, disposed before 2021, may contain more salts than can be consumed within the waste package. Sulfate and chloride that is not consumed within the waste package will eventually be transported out to the compartment in 1BMA or caisson in 2BMA. Table 6-2 shows that there is sufficient cement in the waste domain for uptake of the estimated amounts of sulfate already deposited in the 1BMA compartments. In 2BMA and 1BMA compartments 12–15, the waste acceptance criteria will assure sufficiently high cement:sulfate ratios in the waste to protect the surrounding engineered barriers.

Table 6-2. Quantities of cement and soluble sulfate in the compartments of 1BMA where waste containing soluble sulfate is disposed (Initial state report).

Compartment	Cement[1] (kg)	Sulfate capacity[2] (mol)	Sulfate waste[3] (mol)	Capacity/Waste
2	163 600	264 900	2 700	9 850 %
3	159 200	257 700	33 800	760 %
4	536 400	868 300	300	259 550 %
5	158 900	257 300	19 400	1 330 %
6	166 900	270 100	50 200	540 %
10	254 000	411 200	32 600	1 260 %
11	124 900	202 200	1 800	11 170 %

[1] The concrete is assumed to have a density of 2 450 kg/m^3 (Table 4-1 in Höglund 2014), a cement content of 350 kg/m^3 (Table 2-4 in Höglund 2014) and of aluminium, iron and gypsum according to Table 2-3 in Höglund (2014).

[2] The capacity of sulfate uptake is calculated as $3 \times (Al_{mol} + Fe_{mol}) - Gypsum_{mol}$, where Al_{mol}, Fe_{mol} and $Gypsum_{mol}$ are the amounts of aluminium, iron and gypsum in the cement as mol/kg cement.

[3] The content of soluble sulfate in the waste is cautiously calculated based on the waste producers' analyses of sulfate contents in evaporator concentrate and amounts of concentrate per package, amounting to 1 kg $NaSO_4$ in each of B.05, B.05:2 and B.05:9 and 9.13 % of the weight of evaporator concentrates in each of F.17, F17:1 and F.17:2.

Trash and scrap metal

Large quantities of metals will be present in the SFR repository, predominantly carbon steel, followed by stainless steel, aluminium, zinc, lead and copper (SKB R-18-07). Carbon steel and stainless steel derive from various scrap metals in the waste, steel packaging and reinforcement in concrete packaging and concrete structures. Metals are subject to corrosion, as discussed in the subsection *Metal corrosion* below.

The trash fraction often contains organic materials, which may degrade chemically, microbially, and radiolytically (see subsections *Microbiology* and *Gas formation and transport* below).

Water composition

Groundwater

The repository water composition is mainly determined by materials in the vaults. However, the incoming groundwater also has a minor influence. During the initial submerged period, it is brackish with a distinct salinity, a pH of 6.6–8.0 and significant amounts of HCO_3^-, SO_4^{2-}, Ca^{2+} and Mg^{2+}, see Section 6.2.6.

Cement porewater

When the incoming groundwater interacts with the cementitious environment in the repository, a composition of cement porewater is adopted, as presented in Table 6-3.

Table 6-3. Cement porewater composition.

	Fresh cement porewater[1]	Leached cement porewater[2]
SO_4^{2-} (mg/L)	3.84	1.92
Cl^- (mg/L)	2.13	71
Na^+ (mg/L)	644	69
K^+ (mg/L)	3 237	3.9
Ca^{2+} (mg/L)	36	800
Si as SiO_2(aq) (mg/L)	22.4	0.084
Al_{tot} (mg/L)	1.08	0.054
OH^- (mg/L)	1 938	612
pH	> 13	12.5
Ionic strength (M)	0.12	0.061

[1] Lagerblad and Trägårdh 1994.
[2] Engkvist et al. 1996.

Cement and concrete are ubiquitous in both waste and surrounding barriers and the porewater composition described here is generally valid for both, but the evolution of the latter is further described in Section 6.2.9. The key impact of cement on aqueous speciation are high pH and an increase of ionic strength. As soon as the repository is saturated with water, these conditions arise from the leaching of alkali metal hydroxides and, later, from the leaching of calcium hydroxide (portlandite). The cement in the concrete barriers in SFR1 is of type Degerhamn Anläggningscement. Fresh SFR Degerhamn Anläggningscement porewater has a pH of around 13, with an ionic strength of ~0.1 M dominated by K^+, Na^+ and OH^- ions (Table 6-3). Such conditions are expected to remain valid for most cementitious materials in SFR during the initial period of submerged conditions (see subsection *pH in waste leachate* below).

During the subsequent portlandite phase, the pH is 12.5 and the ionic strength is ~0.06 M, dominated by Ca^{2+} and OH^- ions (Engkvist et al. 1996). When the portlandite has leached, incongruent dissolution of calcium silicate hydrate phases will occur, resulting in a gradual lowering of the pH to about 10 (Höglund 2014, Chapter 4).

The redox potential E_h of the cement porewater is expected to become reducing within months after closure, as expanded upon in the subsection *Redox potential* below.

pH in waste leachate

The cement porewater composition follows the mineralogical evolution of the cement, where the pH is one of the most important aqueous parameters for post-closure safety since it affects the speciation of some radionuclides (subsection *Radionuclide speciation*) as well as corrosion rates (subsection *Metal corrosion*). In the case of cement-conditioned waste, the leachate is expected to be dominated by the soluble species in the cement and the pH will be affected mainly by the amount of cement present and secondarily by certain waste materials, see Höglund (2014, 2018, 2019) and Cronstrand (2014).

Cement porewater pH can be lowered via carbonation, an important process in environments with CO_2 availability such as atmospheric conditions. Carbonation entails a replacement of $Ca(OH)_2$ with $CaCO_3$ via the hydroxide-consuming reaction (simplified):

$$CO_2 + 2OH^- \rightarrow CO_3^{2-} + H_2O$$

In SFR, CO_2 availability is expected to be low after closure. Some CO_2 could be produced by oxidative degradation of organic waste, but this process is expected to be unfavoured since the conditions are reducing (low redox potential) after closure (see subsection *Redox potential* below), instead favouring H_2 and CH_4 as the main gaseous degradation products of organic matter (**Waste process report**). Carbonation of cement is thus expected to be negligible in SFR after closure.

For the waste types with inhomogeneous waste (trash and scrap metal moulds) the cement availability and thus the pH could differ in different regions inside the package. Nevertheless, the water that saturates these packages will be equilibrated with the concrete in the surrounding structures and will therefore already have a high pH as it enters the package. Calculations show that the pH will remain above or near 12 in such waste even if all cellulose is pessimistically assumed to be oxidatively degraded to CO_2, protons and water (SKB 2017b). For a discussion about pH in waste types containing dewatered ion-exchange resins see subsection *Ion-exchange resins and filter aids* above.

Cronstrand (2014) modelled the pH evolution in SFR1 and the results are shown in Table 6-4. The modelling uses a simplistic stirred reactor tank approach for the examined model compartments, silo wall, silo waste domain, 1BMA wall, 1BMA waste compartment with bitumen-conditioned waste, 1BMA waste compartment concrete-conditioned waste, 2BTF, 1BTF and 1BLA. The model also accounts for reactions involving OH^- and H^+, i.e. the influence on pH by the waste materials including potential ions from ion-exchange resins and evaporator concentrates.

For SFR3, the pH evolution over time on the vault scale for 1BRT and 2BMA has been calculated by Höglund (2018, 2019), with results also shown in Table 6-4. Most calculations were performed at 25 °C, chosen as reference temperature since most thermodynamic data are defined at this temperature. Some comparative calculations were performed at 5 °C (Höglund 2018) and 10 °C (Höglund 2019), which is closer to the ~12 °C prevailing in SFR. These give a higher pH since portlandite has the unusual property of a retrograde solubility (more soluble at lower temperatures unlike most minerals), but do not significantly affect the mineralogical development over time.

In all vaults, the pH will be at least 12.5 during the initial period of submerged conditions. In 1BRT, the pH will remain at 12.5 for about 20 000 years and > 12 for at least 42 000 years and above 11 for about 70 000 years (Figure 2-5 in Höglund 2018). In 2BMA, the pH will remain above 12 (barriers) or 12.5 (waste) for the whole assessment period. On the outlet side, the pH will not drop below 12.5 for the whole assessment period and the same applies for the waste domain where pH slowly decreases from 13 to 12.5 during the assessment period (Höglund 2019, Figure 3-2).

In Cronstrand (2014), the pH in 1BMA was evaluated for the design described in SKB (TR-14-02) i.e. without an additional external concrete structure (**Initial state report**). The result is that the pH in the concrete walls surrounding the waste domain of 1BMA gradually decreases, reaching a value of 11.5 after 48 000 years in compartments with bituminised waste and 56 000 years in compartments with cement-conditioned waste. For the updated design of 1BMA, the pH decrease will be slower.

In 1BLA, the gradual pH decrease is faster due to smaller amounts of cementitious materials, finally reaching the pH of the intruding groundwater after about 19 000 years. No dedicated modelling of pH in 2–5BLA has been made but, the pH development in 2–5BLA is expected to be similar to that in 1BLA albeit somewhat slower due to greater amounts of concrete both in the constructions and in the waste (SKB 2017b, SKB R-18-07).

In 1BRT the pH is expected to be above 12 for about 20 000 years (Höglund 2018). The pH of 2BMA is estimated to be around 12.5 in the waste for the whole 100 000-year time period. On the inflow side of the concrete wall, the pH will start decreasing after about 10 000 years (Höglund 2019).

The 1BRT and 2BMA pH modelling illustrate that the results can vary depending on which thermodynamic database is used, on which minerals are taken into account and on the groundwater flow rates and cement quantities in the vaults (Höglund 2018, 2019). These variations give rise to data uncertainties regarding the pH evolution. However, the observed variation is mainly in terms of time for leaching of a certain mineral, translating to pH evolution curves that are highly similar in shape, but parallel-shifted in time. The entailing uncertainty in radionuclide speciation and retention is thus expected to be marginal, particularly since only a few radionuclides have speciation that is sensitive to the expected pH variations (**Data report**, Tables 7-4 to 7-7).

Table 6-4. Evolution of pH regimes in waste vaults as a function of time for the 100 000 years assessment period. Time is given in years (AD). Based on Cronstrand (2014) and Höglund (2018, 2019).

pH	Silo		1BMA-Cement [a)]		1BMA-Bitumen [a)]		1BLA
	Waste	Wall	Waste	Wall	Waste	Wall	
>12.5	2000–26 000	2000–34 000	2000–7000	2000–6000	2000–7000	2000–8000	
12.5	26 000–102 000	34 000–102 000	7000–102 000	6000–22 000	7000–102 000	8000–22 000	2000–8000
12.0–12.5				22 000–58 000		22 000–50 000	8000–9000
11.5–12				58 000–102 000		50 000–102 000	9000–9200
10.5–11.5							9200–11 000
9.0							11 000–21 000
7.5							21 000–102 000

pH	1BTF Ash section	2BTF	2BMA			1BRT
			Waste	Wall upstream	Wall downstream	
>12.5	2000–4000	2000–7000	2000–22 000	2000–3000	2000–22 000	2000–4000
12.5	4000–102 000	7000–102 000	22 000–102 000	3000–12 000	22 000–102 000	4000–21 000
12.0–12.5				12 000–22 000		21 000–42 000
11.5–12				22 000–102 000		42 000–87 000 [b)]
10.5–11.5						87 000–102 000 [b)]
9.0						
7.5						

[a)] Calculation based on the design given in SKB (TR-14-02).
[b)] Extrapolated depletion of CSH 1.2 in Figure 2-5 from Höglund (2018).

Dissolution and transport of dissolved species

Most radionuclides and many other materials in the waste are soluble to some extent, either directly or after degradation. This gives rise to various chemical species dissolved in the groundwater (in addition to dissolved radionuclides) that saturates the waste and the repository. These species can be transported by diffusion or advection with the groundwater flow, eventually leaving the waste package. Soluble species which may affect post-closure safety, apart from radionuclides, include cement-degrading salts (see subsection *Evaporator concentrate* above) and ligands that form soluble complexes with radionuclides (see subsection *Organic complexing agents* below).

Radionuclides and other soluble species contained within solid matrices will be released gradually, at a rate dependent on the water access inside the matrix and other factors. In particular, bitumen matrices are expected to delay the dissolution of radionuclides and other soluble compounds since the diffusivity of water, radionuclides and salt components is very low in intact bitumen. Water supply will therefore only be possible through cracks, bubbles and fissures in the waste matrix (see subsection *Bitumen waste matrices* above).

Colloids

Colloids, i.e. solid particles of diameter about 1–1 000 nm, could, in principle, enhance transport of radionuclides if the radionuclides sorb onto colloids, denoted *carrier colloids*, which are then transported with the groundwater. However, this is not expected to be a significant issue in SFR, based on the following considerations.

The amounts of colloids in the engineered concrete barriers in the silo, BMA, BTF and BRT vaults is expected to be negligible since the large amounts of concrete materials will supply a high ionic strength (chiefly from calcium ions) which suppresses colloid formation (Swanton et al. 2010). Furthermore, the intruding groundwater contains relatively large amounts of calcium and little natural organics, both of which help prevent extensive colloid formation in all vaults, including 1–5BLA even though they lack dedicated concrete barriers (SKB R-01-14).

SKB has studied the abundance of colloids in cement equilibrated water (Wold 2015). Two main types of samples have been studied:

1. Waste materials in contact with Äspö groundwater and crushed hardened cement paste.
2. Different types of hardened cement pastes in contact with water.

Results from the experiments that contained only hardened cement paste and water showed that the colloid concentration was below the detection limit (Wold 2015). Therefore, cement colloids are not likely to be formed in the repository.

Bitumen carrier colloids are likely to occur and would be stable and numerous in cementitious environments, based on evidence from experiments and natural systems and from the discussion in Bruno et al. (2013). However, the extent of radionuclide association to bituminous colloids is expected to be low (Bruno et al. 2013), and therefore their potential contribution to radionuclide transport through SFR is deemed to be negligible.

When the concentration of a given radionuclide increases to levels high enough for the radionuclide to precipitate and form a solid phase, the radionuclide will be distributed between dissolved and solid phases in ratios determined by the solubilities of the solid phases. A specific property, especially of tetravalent actinides such as Pu(IV), is that they have a high tendency to form *eigencolloids* or *intrinsic colloids*, i.e., waterborne particles composed of Pu(IV)-oxy-hydroxide polymers, having at least one dimension in the range 1–1 000 nm (Zänker and Hennig 2014).

The formation of intrinsic colloids requires sufficient concentrations of the radionuclide in question. Bruno et al. (2017) calculated the concentrations of Am and Pu in the waste, cautiously based on waste types containing the highest inventory of these radionuclides. The calculations were carried out cautiously assuming immediate release of the full radionuclide inventory from the waste matrix and accounting for the inorganic and organic complexation of the two radionuclides. The results showed that the concentrations of Am and Pu were higher than the solubility limit of $Am(OH)_3(s)$ and the solubility limit of PuO_2(am, hydr) and near the concentrations of Pu(IV) at which formation of colloids of Pu(IV) occurs. Nevertheless, when sorption equilibrium with the cement phases in the repository was considered, the concentrations decreased by more than four orders of magnitude for both radionuclides and their final concentrations are way below the solubility limit, thus decreasing the risk of formation of any solid phase, including intrinsic colloids. Literature data also indicate that intrinsic colloids of Cm(III), which is an analogue of Am(III), are destabilised in contact with cement phases (Stumpf et al. 2004), while Pu(IV) colloids are destabilised and dissolve within days in contact with montmorillonite (Begg et al. 2013). Intrinsic-colloid formation is consequently judged to be negligible in SFR.

Formation of bentonite carrier colloids is further discussed in Section 6.2.9.

Redox potential

The redox potential is a chemical parameter of aqueous solutions. It can influence the chemical speciation of many elements and its evolution in SFR is therefore of high relevance for post-closure safety. Redox-sensitive elements include selenium, technetium, neptunium and plutonium, and changes in oxidation state and speciation influence their sorption behaviour (see subsection *Radionuclide speciation* below).

An assessment of the evolution of the redox conditions in SFR1 has been performed (Duro et al. 2012b). It included evaluation of the evolution of redox conditions and reducing capacity in 14 waste types selected as being representative of most of the different wastes in SFR1. According to the results, the corrosion of steel (described further in the subsection *Metal corrosion* below) present in the repository can keep the system under reducing conditions for a long time. Upon repository closure and groundwater resaturation, the conditions are initially oxidising due to quantities of oxygen remaining from the operational period. However, the microbially mediated oxidation of organic matter causes the depletion of oxygen within days in such wastes. In waste without organic matter, steel oxidation will consume the oxygen, resulting in anoxia within about half a year. Corrosion of aluminium and zinc, present in some waste packages, can further hasten oxygen consumption. Consequently, anaerobic conditions will first develop locally and then gradually spread until they prevail in the whole repository, estimated to be completed within less than 5 years after resaturation (Duro et al. 2012b).

Anoxic corrosion of steel sets a redox potential of approximately $E_h = –0.75$ V at pH 12.5. The most stable corrosion product, magnetite, can be further oxidised to the Fe(III) minerals goethite, maghemite and/or hematite, setting a redox potential of about –0.65 V (Duro et al. 2012b). However, magnetite has a high kinetic stability, so its reliability for setting a low redox potential throughout the waste is uncertain. Therefore, calculations have been performed based on a simplified approach (Hedström 2019a), that cautiously disregards the Fe(II) in magnetite as an electron donor and uses the updated steel inventory from SKB (R-18-07), and updated corrosion rates (see subsection *Metal corrosion* below). Hedström (2019a) cautiously assumed that all steel begins to corrode immediately from all sides and keeps corroding, unimpeded by solubility limits or transport limitations, at a deterministic rate corresponding to the statistical mean for anoxic, near-neutral steel corrosion for 1–5BLA and anoxic, alkaline for all other vaults (**Data report**, Chapter 5). The results show that many tonnes of steel remain during the whole assessment period in the silo, 1–2BMA, 1BRT and 1–2BTF, see Figure 6-6. The presence of metallic iron within the steel thus ensures a reducing environment in these vaults during the entire initial period of submerged conditions and for the entire assessment period, as indicated in Figure 6-6 (see further Section 6.3.8).

Radionuclide speciation

The major factors affecting radionuclide speciation are pH, the redox potential E_h, and the concentration and type of other chemicals in the system, including complexing agents. A high pH increases the abundance of anionic species both through deprotonation by, and due to complexation with, hydroxide ions. E_h is of critical importance for redox-sensitive elements, and the low E_h in SFR (subsection *Redox potential* above) favours reduced oxidation states of radionuclides. A key example of a redox-sensitive element in wastes is iron, which corrodes from Fe(0) to Fe(II) and/or Fe(III), depending on the E_h and pH conditions. Technetium is another important example that can be reduced from Tc(VII), as the highly soluble TcO_4^-, to Tc(IV)O_2 which forms solid phases with low solubility. The oxidation state therefore affects the aqueous speciation and solubility of an element, as well as its reactions with other species.

Thermodynamic modelling is required to account for all the different interactions occurring within a complex system such as the SFR repository. Given the redox conditions within the SFR repository, thermodynamic modelling suggests that e.g. Se, Tc, Np and Pu will be present in their lower oxidation states as Se(–II), Tc(IV), Np(IV), Pu(III) and Pu(IV) (Duro et al. 2012b).

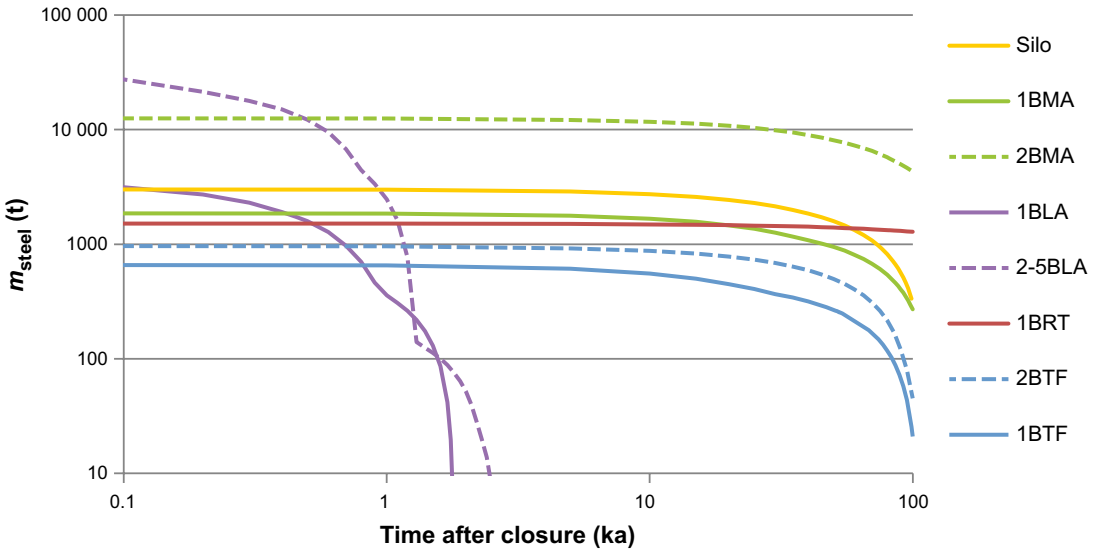

Figure 6-6. *The total mass of steel remaining uncorroded in each vault as a function of time, summed over all steel in all waste packages to be disposed within a vault, assuming a deterministic corrosion rate of 2.8 µm/a in 1–5BLA and 0.025 µm/a elsewhere. The 2–5BLA vaults are lumped into one series (adapted from Hedström 2019a).*

Later experiments have shown that the Pu aqueous species are likely Pu(IV) in a wide redox interval, encompassing SFR conditions (Tasi et al. 2018, 2021). Its dissolved concentration is limited by the poor solubility of PuO_2(s). Higher redox potentials could result in the formation of hydrated Pu(VI) oxide as the dominant solid phase and Pu(VI) oxy-hydroxide in solution. Pu(V) is not prone to solid-phase formation, but, as a dissolved oxycation, it has a narrow stability interval around $E_h = 0$ V vs the standard hydrogen electrode (SHE). Uranium can potentially be reduced to U(IV), but recent experiments indicate that it likely remains as U(VI) in the form of the uranyl oxycation UO_2^{2+} even at the low redox potentials of SFR (Bruno et al. 2018).

Aqueous speciation will affect the amount, composition, volume, pressure and degree of saturation of gases, because the saturation limit of a dissolved gas is affected by pH and aqueous speciation. An example of this is the solubility of CO_2 in water, which increases at higher pH because the OH^- ions shift the equilibrium towards CO_3^{2-}.

Radionuclide sorption on solid materials

Many elements in solution can become immobilised by physico-chemical attraction to solid materials via adsorption, absorption or ion-exchange, here collectively denoted by the term sorption. A certain fraction of sorbing radionuclides, quantified by radionuclide- and material-specific sorption coefficients K_d, will be immobilised by sorption on solid materials in the repository (**Waste process report**, Sections 3.5.3 and 4.4.3).

In SFR, sorption mainly occurs on hydrated cement surfaces in cementitious materials (**Data report**, Chapter 7). These materials are present in large amounts both in the waste and surrounding barriers and are good sorbents for many chemical species. Bentonite clay, present in the silo, can also sorb many radionuclides to a significant extent. The macadam backfill used in many vaults is also expected to sorb many radionuclides, but generally with substantially lower sorption coefficients than cement and bentonite. Other mineral materials, metals, and metal corrosion products in the repository may also act as sorbents but this has not been relied upon in the safety assessment.

The cement sorption coefficients of most radionuclides change as the cement degrades (subsection *pH in waste leachate* above), responding to both decreasing pH and altered mineralogical composition of the cement. Sorption coefficients as a function of cement degradation state are discussed further in the **Data report**, Chapter 7.

Organic complexing agents

Complexing agents are important because of their capacity to form molecular complexes with radionuclides (Hummel et al. 2005), primarily metal-ion radionuclides. Complexation increases the solubility of the radionuclides and hampers their sorption, promoting their mobility with faster transport out of the repository. Complexation and the resulting effect on radionuclide sorption in SFR are described in detail in Keith-Roach et al. (2021).

Most of the organic materials in SFR originate in the waste, including ion-exchange resins, bitumen, cellulose, filter aids, etc. Other organic materials are included in the structural components of the repository, i.e. concrete additives. Most organic materials are innocuous, but some have potential for complexation, either being able to complex radionuclides directly, or prone to degrade to form complexing agents *in situ* through chemical, physical, radiolytic and/or microbial processes. The impact of such organic materials on post-closure safety therefore depends on their stability and on the dominant degradation mechanism under repository conditions and the degradation products formed.

For an organic substance to significantly affect radionuclide speciation, they must be able to form a stable chelate. In a cementitious environment such as SFR with lots of competing OH^- and Ca^{2+}, sufficiently stable chelates can only be formed by a small set of ligands, requiring a chemical structure with 2+ functional groups capable of coordinating a cation (carboxylate, sub-quaternary amine, phosphate, sulfate, some alcohols) as well as a rather exact number of atoms (typically carbon) between the coordinating groups so the chelate becomes a 5- or 6-membered ring (Keith-Roach and Shahkarami 2021, Section 2.1). Further, the stability of a metal–chelate complex correlates strongly with the charge of the ligand (Means and Alexander 1981).

Detergents

Chemicals used for decontamination and cleaning at the Swedish nuclear installations sometimes contain complexing agents such as: oxalate, citrate, nitrilotriacetate (NTA) and gluconate. The amounts of different complexing agents present in SFR due to the use of detergents has been assessed (Keith-Roach et al. 2021). It is noted that the concentration and thus effect of several complexing agents is reduced because they precipitate as calcium salts in cementitious environments, primarily oxalate and citrate. NTA does not precipitate and has been identified as one of the most significant complexing agents from detergent use. NTA is a tetradentate ligand, coordinating the metal ion with the N atom as well as the three deprotonated carboxylic acid groups.

Due largely to updated requirements from SKB,[26] new methods for system decontamination have been implemented in recent decades at the Swedish nuclear power plants to use less and weaker complexing agents and avoid them reaching the SFR waste streams. Due to these efforts, the largest amounts of potent complexing agents are found in waste disposed during the earlier operation of SFR1. The current limits for complexing agents in waste to SFR are described and justified in Keith-Roach and Shahkarami (2021). 1–5BLA have less strict limits since sorption is not relied upon therein.

Chemical degradation of complexing agents from detergents is not expected to be significant within SFR during the initial period of submerged conditions. Chemical conditions more severe (e.g. higher pH or higher microbial activity) than those in the repository are considered necessary for degradation to occur (Keith-Roach 2008). However, the concentrations of this class of complexing agents are expected to decrease with time due to transport with the groundwater from the vaults (except the fraction precipitated as calcium salts or sorbed onto solid surfaces). This means that the effect of complexing agents is generally highest soon after closure and thereafter decreases with time.

[26] Södergren K, Snis K, Reitti M, 2021. Acceptanskriterier för avfall i SFR. SKBdoc 1336074 ver 5.0, Svensk Kärnbränslehantering AB. (In Swedish.) (Internal document.)

Cellulose

Under the conditions prevailing in SFR, i.e. a high pH and Ca^{2+}-rich environment, cellulose will degrade to shorter-chained organic compounds. Of the degradation products, the two isomers of isosaccharinate: 3-deoxy-2-C-hydroxymethyl-D-erythro-pentonate (α-ISA) and 3-deoxy-2-C-hydroxymethyl-D-threo-pentonate (β-ISA) are the most abundant. Calcium ions are more conducive than sodium ions towards ISA production (Machell and Richards 1960).

Analyses have confirmed the presence of both isomers of ISA in leachates from the degradation of cellulose in the presence of several types of cement, together with several other degradation products (Greenfield et al. 1993, 1994). Besides ISA, different carboxylates and hydroxycarboxylates have also been identified in other alkaline degradation studies (e.g. Bourbon and Toulhoat 1996, Glaus et al. 1999, Pavasars 1999).

Among the degradation products of cellulose, ISA has been identified conclusively as a key component and one of the organic compounds with the greatest impact on the speciation and mobility of radionuclides in SFR (Keith-Roach et al. 2021).

The rate of alkaline degradation is one of the factors determining the concentration of ISA in solution (Chambers et al. 2002, Askarieh et al. 2000). Relatively long-term experiments on cellulose degradation (Glaus and Van Loon 2008) were carried out under alkaline and anaerobic conditions and at room temperature over a time span of 12 years. In view of the data and the model presented in Glaus and Van Loon (2008), the range of uncertainty for complete degradation of cellulose under SFR conditions can be narrowed down to a best estimate of 1 000 to 5 000 years, hence encompassing the possible duration of the initial submerged period. Calculations for SFR estimate that ~99 % of all cellulose will be degraded within some 5 000 years after resaturation of the repository (Keith-Roach et al. 2014). The amounts of cellulose present in the SFR vaults are given in SKB (R-18-07).

The dissolved concentration of ISA is reduced due to its substantial sorption to cement minerals (Van Loon et al. 1997, Van Loon and Glaus 1998, Tasi et al. 2018). Therefore, the impact of ISA is highly dependent on the amount of cement, which varies between vaults and between compartments in 1BMA (Keith-Roach et al. 2021). However, the sorption means that ISA is expected to stay in the vault to a large extent and not be transported out like more soluble complexing agents such as NTA.

Superplasticiser cement additives

Certain cement additives, specifically superplasticisers, are potential complexing agents and are used in small amounts (up to a few percent) in many concrete materials. Superplasticisers are added to the concrete slurry to allow for good workability and low viscosity before curing and/or to reduce the amount of water required. They are long-chain organic polymers that sorb strongly to cement particles and reduce particle–particle interactions via electrostatic repulsion and/or steric hindrance. Dissolved superplasticisers can decrease radionuclide sorption, attributed to complexation (Dario et al. 2004, Section 2.3). However, superplasticisers present in SFR are not in the solution phase, but rather strongly bound to the hardened cement paste (HCP) in cured, solid concrete. Such bonds are generally so strong that studies have failed to show an effect on radionuclide sorption of superplasticisers in a solid concrete matrix (NDA 2017, Keith-Roach and Höglund 2018). On longer timescales than accessible by experiments, it is possible that the polymeric superplasticisers degrade to smaller molecules with weaker cement attraction, but some retained complexing capability, or that concrete degradation releases oligo- or polymeric superplasticisers. However, based on theoretical arguments, such degradation is expected to occur very slowly and result only in small concentrations of organic molecules with limited complexing strength (Hedström 2019a, Keith-Roach and Shahkarami 2021, Section 4.3), which would probably have a negligible effect on radionuclide sorption and certainly a smaller effect than other complexing agents present in SFR (see NDA 2017, Keith-Roach et al. 2021).

The additives used in the structural concrete in SFR1 are Sika plastiment BV-40 (concrete plasticiser) and Sika retarder (cement hydrating retarder); the amount of plasticiser varies between 0.05–0.5 % of the cement weight depending on the concrete recipe. Generally, 0.2 wt% retarder is added. The Sika plastiment BV-40 consists of a blend of lignosulfonates, an older class of superplasticisers. Lignosulfonates have been shown to not significantly reduce the sorption of Ni^{2+}, Eu^{3+} and Th^{4+} at the concentrations used in the structural concrete in SFR (Glaus and Van Loon 2004).

Polyamines in paint

Polyamines are present in many paint hardeners and, when the paint degrades over time, these amines may dissolve and act as complexing agents, particularly with Ni(II) to which they have a strong affinity (Hedström 2020, Keith-Roach and Shahkarami 2021, Section 4.6). Ni(II) is present in significant amounts throughout SFR in the form of Ni-59 and Ni-63, with modest sorption coefficients on bentonite and cement (**Data report,** Tables 7-4–7-7 and 7-9).

The Ni(II) affinity to polyamines has not been studied specifically for PSAR and the possible polyamine concentration in the vaults is uncertain. However, compared to complexing agents inside the waste packages, complexing agents on the outside have a smaller effect on radionuclide transport since they are initially separated by the packaging material from the radionuclides on the inside of the package. Only after transport through the packaging wall could they form complexes and subsequently experience reduced sorption.

Influence on sorption

Quantification of the effect of complexation is based on experiments which typically are performed under repository-like conditions. Consequently, the presence of stable Ca^{2+} is inherently accounted for, which is important since Ca^{2+} competes with the radionuclides for complexation to some extent, although the affinity of complexing agents to Ca^{2+} is often lower than to most relevant cationic radionuclides (oxalate and citrate are exceptions). Another effect important for complexation in SFR is the high concentration of hydroxide ions, which compete with the complexing agents for binding to the cationic radionuclides (Keith-Roach and Shahkarami 2021). In the PSAR, two complexing agents have been identified as dominating radionuclide complexation, NTA and ISA, and their effects on different radionuclides are quantified in the **Data report**, Chapter 7.

Transfer between vaults

Complexing agents are generally considered to mainly affect the sorption in the vault where they are present at closure. However, dissolved complexing agents may potentially travel with the groundwater from 1BLA to 1BMA, post closure. This issue is judged negligible for SFR3 since 2BMA is not situated downstream of 2–5BLA. The material judged to be most important in 1BLA with regards to complexation is cellulose (Table 4-27 in SKB R-18-07).

The transferred amount of ISA from 1BLA to 1BMA is expected to be small due to several factors: slow ISA formation, lower ISA yield due to lower pH and less Ca^{2+} in 1BLA than in other vaults, possible Ca-ISA precipitation due to solubility limits, protective concrete barriers in 1BMA and, most importantly, ISA sorption to cement in both vaults. It is thus judged likely to have a weaker effect on sorption in 1BMA than the complexing agents and cellulose already present in the 1BMA waste at closure.

Metal corrosion

SFR contains large amounts of metals prone to corrosion after closure, predominantly carbon steel and stainless steel, but also smaller amounts of aluminium, zinc, lead and some other base (non-noble) metals. Several parameters will affect the corrosion rate, in particular metallurgical and environmental factors including pH, redox potential, and to a lesser extent temperature (**Waste process report,** Section 3.5.9). Upon closure, the presence of molecular oxygen will result in a short period of oxic conditions and corresponding corrosion mechanisms (subsection *Redox potential* above). Once the oxygen is consumed, reducing conditions will prevail for the remainder of the initial submerged period and the entire assessment period. During this period, base metals will corrode anoxically, using water as oxidant and producing hydrogen gas (see subsection *Gas formation and transport* below). Many different oxides, hydroxides, and oxyhydroxides of iron can occur as products and intermediates of anoxic steel corrosion, but eventually, αFe_3O_4 (magnetite) is expected as the predominant product because of its thermodynamic stability.

The rate at which the metal corrodes is important for post-closure safety for a number of reasons. First, because it determines the radionuclide release rate from metal waste with irradiation-induced activity such as the reactor pressure vessels in 1BRT. Second, it determines how soon all steel in a vault becomes fully corroded, at which point the redox potential in the vault may increase noticeably and become more sensitive to possible intrusion of oxidants (subsection *Redox potential* above). Third, the rate at which the metal corrodes is directly proportional to the rate at which hydrogen gas is produced (subsection *Gas formation and transport* below). Fourth, corrosion will at some point breach the containment provided by certain steel packaging and possibly affect the integrity of reinforced concrete packaging as well, via expansion of corroding rebars.

Sulfate-reducing bacteria form sulfide, which can have a corrosive effect on metals. Under certain conditions, with local groundwater flow near metal surfaces and in the presence of organic compounds from the repository, some pitting corrosion can occur, but such sulfide-induced corrosion does not cause more material loss than general anoxic corrosion with water as the oxidant. Chlorides from the intruding brackish water typically hasten oxic corrosion, but the effect is generally insignificant for long-term anoxic, alkaline corrosion rates (**Data report**, Chapter 5).

For this safety assessment, a review has been performed of steel corrosion rates for various conditions relevant to the SFR repository. They are described in detail in the **Data report**, Chapter 5, and summarised here in Table 6-5.

Table 6-5. Corrosion rates for carbon and stainless steel in various chemical conditions (Data report, Chapter 5).

Conditions	Carbon steel (µm/a)	Stainless steel (µm/a)
Alkaline, oxic	< 1–100	
Alkaline, anoxic	0.001–0.1	0.001–0.01
Non-alkaline, near-neutral pH, oxic	10–400	0.1–0.5
Non-alkaline, near-neutral pH, anoxic	1–100	

Decreasing alkalinity may increase steel corrosion rates, particularly if the pH reaches 9 or lower, at which point steel surfaces are no longer passivated by protective layers of corrosion products that impede further corrosion (**Data report**, Section 5.1). Nevertheless, since the pH during the initially submerged period is not expected to go below 12 in 1–5BLA and 12.5 in all other vaults (Table 6-4), the corrosion rates for alkaline conditions are valid throughout this initial period.

Recent experiments on anoxic corrosion of aluminium and zinc embedded in concrete in artificial groundwater have been performed by Herting and Odnevall (2021) and compared to corrosion in artificial groundwater without concrete, i.e. near-neutral pH. The rates are initially relatively high but decrease over time and stabilize at lower values within two years (Table 6-6). Because of the relatively high corrosion rates of Al and Zn compared to e.g. steel, and the small material thickness expected, Al and Zn in SFR waste is generally expected to become oxidised well within the initial period of submerged conditions.

Table 6-6. Corrosion rates for aluminium and zinc embedded in concrete and/or in artificial groundwater (Herting and Odnevall 2021).

Conditions	Al (µm/a)	Zn (µm/a)
Anoxic, concrete-embedded for 2 weeks	977	50
Anoxic, concrete-embedded for 104 weeks	114	1
Anoxic, in near-neutral artificial groundwater for 2 weeks	3084	25
Anoxic, in near-neutral artificial groundwater for 104 weeks	54	3

Microbiology

Microbial activity plays an important role in organic degradation, corrosion and gas generation through the mediation of reduction–oxidation reactions. Under these conditions cellulose is chemically degraded to ISA, which in turn can be used by some microbes as substrate (e.g. Bassil and Lloyd 2017, 2019). Microbial growth will increase during the saturation phase due to the input of energy (e.g. H_2, which is an important energy source for sulfate-reducing bacteria, methanogens and acetogens) and other dissolved nutrients, but will slow down when saturation is reached and the recharge ceases. According to the modelling performed by Cronstrand (2014), hyperalkaline conditions will prevail when saturation is reached, and these conditions will last for a long time (Table 6-4). During that period, microbial activity is expected to slow down significantly. As the pH in SFR decreases with time, the influence of microbial processes will increase in magnitude concomitantly and could result in a further decrease in pH due to acidogenic activity such as fermentation. It has been shown by e.g. Small et al. (2008), in the large-scale gas generation experiment at the low- and intermediate-level waste repository in Olkiluoto, Finland, that microniches have a great potential to develop in such a heterogeneous environment. However, due to the extensive amount of cement, the development of low pH microniches is considered to be irrelevant and therefore ignored in SFR as hyperalkaline conditions are expected to dominate in all waste vaults. Formation of microbial biofilms on the waste surfaces and on the surfaces inside the packaging is likely to occur initially, but due to the harsh conditions in the vaults this is not considered to be relevant for post-closure safety.

The amount of organic carbon, nutrients and electron acceptors in the water interacting with the waste influences the microbial activity. Of great importance is the availability of electron acceptors, such as oxygen, nitrate, ferric iron, sulfate and carbon dioxide. SFR is rich in nutrients and energy, and these components will not be limiting for microbial activity *per se*. The magnitude, direction and distribution of water flow in the different waste vaults will influence the transport of microbes and, more importantly, the transport of electron acceptors to, and degradation products from, microbes present throughout SFR. The most favourable position for microbes, with respect to available energy, is inside the BLA packages with a large amount of organic waste. However, restricted availability of electron acceptors and build-up of toxic degradation products may reduce the diversity, but not necessarily the activity, of remaining organisms that can proliferate inside packages. Bitumen can be degraded by microbes and is therefore a possible substrate for microbial activity, but only to a minor extent in BLA, as the dominating substrate is cellulose. The growth of microbes will predominantly occur on bitumen surfaces inside waste packages, locally generating large numbers of microbes. The availability of electron acceptors will control microbial processes inside the waste packages.

Microbial growth is possible in a waste form that has been solidified with cement (Gorbunova and Barinov 2012) and on concrete structures. This diversity and activity may be significant if advective groundwater flow supplies the microbes with electron acceptors, removes degradation products and leaches the concrete. The effect may be less significant under stagnant hydraulic conditions. Microbial biofilms can develop on the surfaces of bitumen-solidified waste. Again, this growth may be significant if there is advective groundwater flow to supply the microbes with electron acceptors and remove degradation products. The bitumen will be degraded at a slow rate if conditions are anaerobic; access to oxygen is then an important limiting factor. Degradation is much higher under aerobic conditions.

Non-conditioned waste has the greatest potential for microbial degradation. The organic carbon content of this waste is often very high and its pH will be less alkaline than in cement-solidified waste. The large mobility of microbes and waste components inside a package suggests that gas production may become significant there. Microbial growth is possible on the outside of cement packages. The pH gradients will control microbial growth; the limit for microbial activity lies slightly below 12.7, but it varies somewhat between species and is highly dependent on the access to nutrients. In contrast to optimal conditions, survival at extreme conditions requires more nutrients to be able to maintain the cells. However, there are several studies showing that e.g. methanogens are not active at pH higher than slightly above 10 (e.g. Ferry 1993, Sorokin et al. 2015, Taborowski and Pedersen 2019). Development of CH_4 will not occur as long as pH remains above this limit.

The most important limiting factors are access to water and the high pH in the repository once it is saturated, because most of the waste is either encapsulated in concrete/cement or at least in close contact with it. The system is thus buffered with first NaOH and KOH and subsequently $Ca(OH)_2$, sustaining the high pH (Section 6.2.9). It has been demonstrated that microorganisms could grow

and be metabolically active under aerobic as well as anaerobic alkaline conditions, i.e. at pH 10–11 (Pedersen et al. 2004) and even higher pH (Yumoto 2007, Brazelton et al. 2013). However, since growth is slow, the numbers of bacteria will be low and metabolic activity will also be low.

Gas formation and transport

Gas can form in the repository by corrosion of metals in the waste, the waste packaging and the rebar in the concrete structures, as well as by microbial degradation of organic material in the waste. Radiation from the radioactive waste can also generate gas by radiolysis of water and of organic materials such as ion-exchange resins and bitumen (Maier 2021).

When the repository is closed and pumping ceases, the lower pressure in the repository will cause groundwater to flow in. Total saturation of the silo is estimated to take a few decades, whereas the other vaults are estimated to be saturated in just a few years (Börgesson et al. 2015, Holmén and Stigsson 2001). Remaining atmospheric oxygen and oxygen dissolved in water in the repository will be consumed within a few years thereafter (see subsection *Redox potential* above).

The quantities of gas formed can potentially be large. For the gas to escape into the surrounding rock, gas-conducting passages must be created in the repository. A possible consequence of the pressure build-up in absence of transport routes is the displacement of contaminated water, enhancing transport of radionuclides. In more severe cases, cracking of engineered barriers is imaginable, but this is not expected in SFR due to the appreciable permeability of the concrete barriers. These aspects of gas formation and transport are described in more detail under the following subheadings.

Gas formation due to corrosion

Anaerobic corrosion (oxidation) of base metals (subsection *Metal corrosion* above) is the process that is expected to contribute the largest quantities of gas in SFR. A prerequisite for hydrogen-generating corrosion is a supply of water. This is rarely a limiting factor in an underground repository after closure and even the initial content of water in the waste and the engineered barriers is often sufficient to generate gas. Theoretically, approximately 1 litre of water is needed to generate 1 Nm^3 (here, N stands for normal, i.e. 0 °C and 101.325 kPa) of hydrogen.

Another factor that affects corrosion is water chemistry – mainly pH, E_h and the concentration of dissolved salts (subsection *Metal corrosion* above). Temperature and radiation level can be of importance in repositories with high-level waste but are of lesser importance in repositories with low- and intermediate-level waste. It has also been found that high gas pressures that would inhibit the corrosion rate are not likely to occur in the repository since they exceed the pressures needed for the gas to escape through the surrounding barriers (Moreno et al. 2001).

Gas formation due to microbial activity

Microbial processes will utilise hydrogen from corrosion processes in SFR. Hydrogen gas will thereby have a profound influence on the extent and rate of microbial processes in SFR when the pH has fallen enough to allow uninhibited respiration by the microbes. Many microbial processes generate gases such as carbon dioxide, nitrogen, nitrous oxide and methane. Significant pressure build-up can consequently occur because of microbial processes. However, gases are also consumed by microbial processes, such as the reduction of CO_2 by 4 H_2 yielding 1 mole of CH_4 from 5 moles of gas (Equation 6-1).

Microbial degradation of organic materials under conditions expected to prevail in SFR1 after closure has been investigated by Pedersen (2001). Experiments cited there indicate that the rate of gas formation is initially rapid but decreases after the initial phase. According to Pedersen (2001), the environment in SFR1 is not optimal for microbial degradation, but even pH as high as 12 is not a complete hindrance to microbial activity. Gas formation due to microbial activity in SFR1 could be limited by the supply of oxidants and nutrients and the removal of reaction products. A possible positive aspect that could limit total gas formation in the repository is that many microorganisms can utilise hydrogen as an energy source and could thereby reduce the quantity of hydrogen formed by corrosion. This process, which is considered favourable, has not been included in the assessment.

Microbial decomposition of some organic materials under anaerobic conditions results in methane and carbon dioxide being generated in approximately equal amounts (Askarieh et al. 2000). Isosaccharinic acid (ISA) that is generated from chemical degradation of cellulose at hyperalkaline pH could be used in methanogenic microcosms. According to Rout et al. (2014) removal of ISA is associated with the production and removal of acetic acid and the generation of methane which comprised 54.7 % ± 3.3 of the gas generated in their study. Cellulose degradation rates corresponding to complete consumption in less than 200 years have been assumed in the calculations of gas formation. This is equivalent to a degradation rate of 0.2 mol kg^{-1} a^{-1} and a gas formation rate of about 2 L kg^{-1} a^{-1}, assuming that 50 % of the gases do not react with repository materials (Askarieh et al. 2000, Rout et al. 2014).

The few experiments that have been carried out on microbial degradation of bitumen, ion-exchange resins and plastics indicate that the processes are very slow. In the calculations here, it has been assumed that 0.002 mol kg^{-1} a^{-1} is degraded, corresponding to a degradation of all material in 15 000 years and a gas formation rate of 0.02 L kg^{-1} a^{-1}, assuming that 50 % of the gases do not react with repository materials (Moreno et al. 2001).

Methanogens are found in nearly every anaerobic environment. They can respire across a wide environmental pH range from 4 to 10, although their optimum pH generally ranges from 6 to 8 (e.g. Ferry 1993). The activity of microbes under anaerobic conditions may eventually lead to significant production of gases such as CH_4, CO_2 and H_2. However, autotrophic methanogenesis will also consume gas according to the reaction below:

$$CO_2 + 4H_2 \rightarrow CH_4 + 2H_2O \qquad \text{(Equation 6-1)}$$

One concern in SFR is the release of ^{14}C as $^{14}CH_4$ and $^{14}CO_2$, which will be generated largely by degradation of ^{14}C-labelled organic compounds within the waste. However, due to carbonation of the cement present in the near-field, radioactive $^{14}CO_2$, will be immobilised, subsequently preventing or at least limiting the formation of $^{14}CH_4$ by methanogenesis. The potential methanogenesis is not likely to start until the pH has dropped below hyperalkaline values (Ferry 1993). Thus, lowering of pH mitigated by acid production from fermentation by syntrophic bacteria present may activate methanogenesis. However, Brazelton et al. (2013) observed increased cell amounts at pH > 12, which is in contrast to the general view that microbial growth decreases with increased pH. This may open up the possibility of microbially produced metabolites that, could lower the pH to some extent under these conditions, but are not likely to have significance on the production of methane as pH needs to be lowered by several units in order to be favourable for methanogenesis. In a study by Taborowski and Pedersen (2019) it was shown that *in vitro* production of methane, using a pure culture of *Methanobacterium subterraneum* and indigenous methanogens (KFR in Figure 6-7) from SFR, was facilitated in presence of ion-exchange resins. Although these methanogens could be cultivated up to pH 10, their activity correlated negatively with increasing pH. There is a clear cut-off between pH 9.5 and 10 in both cases (Figure 6-7), further supporting that methane production slightly above pH 10 will be negligible.

Gas formation due to radiolysis

Radiation from the radioactive waste in SFR1 can act on materials and cause formation of gas and species that can affect the water chemistry. The materials in the waste and the immediate environs will be exposed to the greatest amount of radiation. The radiation chemical yields (*G* values), which express the number of molecules formed per amount of irradiation, are used in calculating gas formation due to radiolysis. *G* values have been determined experimentally for various materials and types of radiation. The effect of irradiation is proportional to the absorbed dose and dependent on the composition, including water content, of the material.

Hydrogen gas is formed at 0.1×10^6 Gy according to Rébufa et al. (2015) both for mixed bed and pure anion exchange resins. For cation resins with sulfonate as the functional group, hydrogen is formed at slightly higher doses (0.5×10^6 Gy). Due to this dose dependence, radiolytic gas production is expected to only be significant in waste with higher activity, i.e. silo and BMA waste. The main materials in the silo and BMA expected to produce gas via radiolysis are water, bitumen, and ion-exchange resins. For all of these, hydrogen H_2 is the main gaseous product under anaerobic conditions (Maier 2021).

Calculated gas quantities

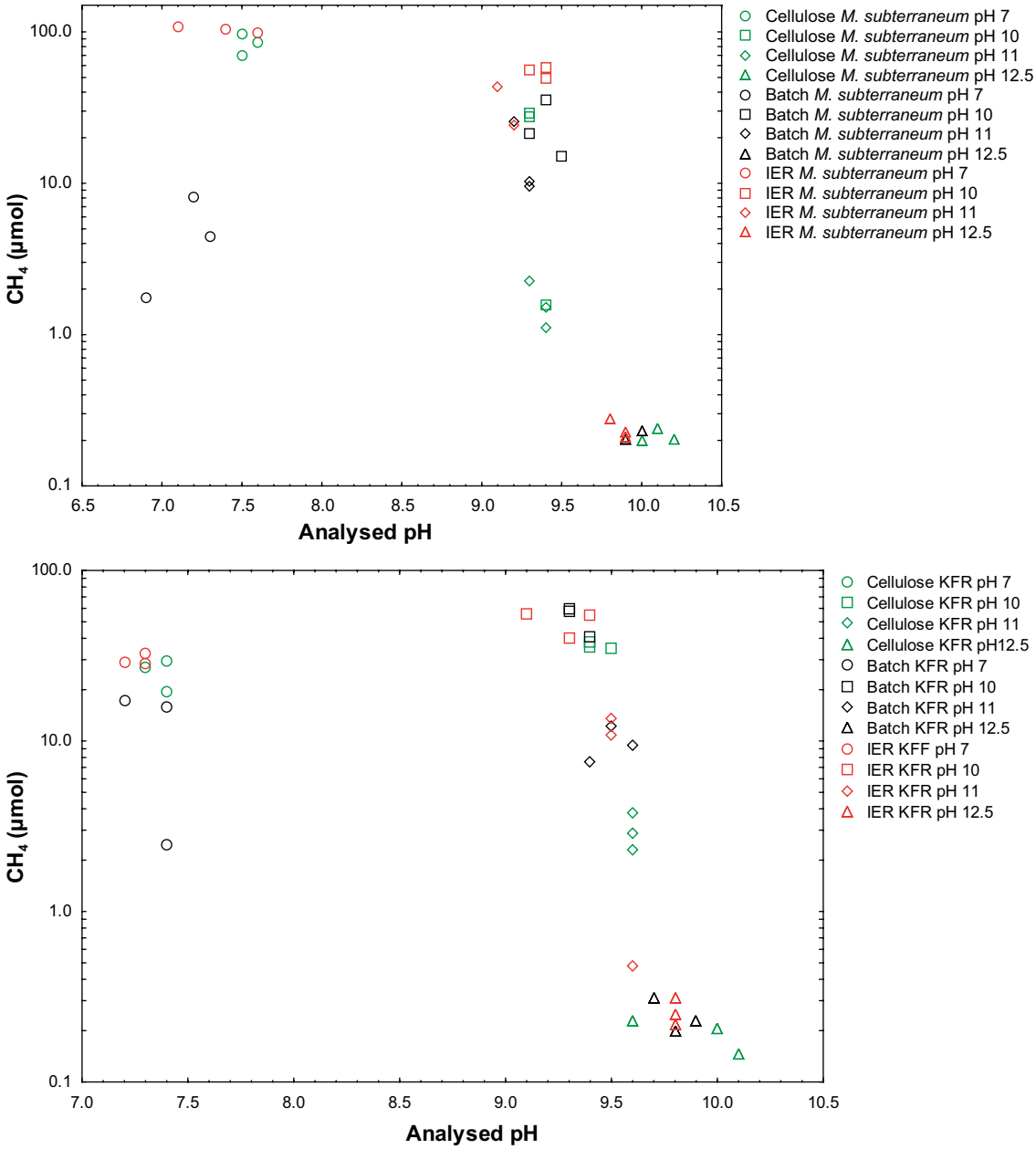

Figure 6-7. *Methane production plotted against measured pH from serum bottles after 8 weeks of incubation. The serum bottles contained 50 mL enrichment medium and were inoculated with M. subterraneum (top) and with KFR (bottom), respectively. Additionally, the serum bottles contained cellulose or IER. Bottles labelled "Batch" contained only medium. The pH in the name description indicates the expected pH. The detection limit for CH_4 was 0.04 µmol. Figure from Taborowski and Pedersen (2019).*

Gas is primarily produced in waste containing base metals. A secondary source is degradation of certain organic materials, in some cases exacerbated by radiation. Such wastes are present mainly in the silo, BMA and BLA vaults (scrap metal and organic wastes) as well as 1BRT (RPV steel). The waste in 1–2BTF generally does not contain metals (except steel in packaging materials), and too low radiation levels for appreciable radiolytic degradation of ion-exchange resins or water. The aluminium in the ash drums in 1BTF is expected to have become mostly oxidised during the incineration process, precluding future gas production.

The gas formation rates in the silo, 1BMA, and 1–2BTF have been estimated by Moreno and Neretnieks (2013), with separate contributions from microbes and from corrosion in structures, packaging, reinforcement in packaging and waste. They found that for the first few years after closure, corrosion of aluminium and zinc in the waste will completely dominate gas formation where

these metals are present, i.e. all vaults in SFR1 except 2BTF; they cautiously assumed the aluminium in 1BTF to be metallic rather than oxidised via incineration. Further, they assumed pessimistically high corrosion rates of aluminium and zinc of 1 mm/a; the rates have since been found to be significantly lower (Table 6-6). Considering the updated corrosion rates, aluminium corrosion is still expected to dominate early gas production, but with peak production rates about tenfold lower than estimated by Moreno and Neretnieks (2013) and extending over several decades after closure. Finally, Moreno and Neretnieks (2013) did not consider radiolysis of organic materials, which has since been found to possibly be of similar order of magnitude as radiolysis of water (Maier 2021).

Gas production rates have not been quantified for SFR3 but are generally expected to be similar to those in SFR1 since 2–5BLA and 2BMA contain less organics but more metals than 1BLA and 1BMA, respectively (Appendix E, Table E-3). The most impactful difference for SFR3 is that 2BMA contains significantly more aluminium than 1BMA, affecting early gas generation rates. The gas production in 2BMA will be quantified before determining the exact dimensions of its gas-evacuation system (Section 4.4).

Impact of gas formation

Gas formation can lead to pressure build-up if it is faster than the gas transport. This is most likely during the earliest part of the initially submerged period due to the fast corrosion of aluminium, as described above. Such pressures are expected to cause water from the waste domain to be expelled into the buffer or gravel/sand around the concrete structure and finally into fractures in the rock surrounding the vaults. The gas cannot escape until it reaches a sufficient pressure to overcome the capillary forces in the media surrounding the waste. Gas may flow through the buffer surrounding the silo or fine cracks in the concrete walls of the different concrete structures. The amount of water expelled depends on the volume of gas produced before the gas pressure becomes large enough to open a flow path through the barrier. Since most expulsion of water is expected to occur within decades after repository water saturation, the radiological consequences are expected to be limited because a large fraction of radionuclides are expected to still be bound to solid materials and not become dissolved until later.

In the silo and 2BMA, the barriers will have engineered gas-evacuation systems (Section 4.4) that will minimise the gas-pressure build-up and thus water expulsion. The gas evacuation systems are expected to mitigate pressure build-up and general cracking of engineered barriers (Section 6.2.9). The integrity of individual concrete waste packages containing high amounts of aluminium could potentially be affected by gas pressures.

Gas transport

Gases generated by the above processes will be dissolved in the groundwater according to the solubility equilibrium (Henry's law). Gases dissolved in water can be transported across the waste form to the outer part of the waste by diffusion or advection. If the solubility of the gas is exceeded, bubbles can form. The formation of a gas phase can produce two-phase flow. This process may expel water from the system, resulting in a certain degree of desaturation of parts of the repository. This process has not been quantitatively investigated for this safety assessment.

Gas transport through the porous materials of the matrices will follow the same laws as gas transport through the backfill and the engineered barriers in the repository. Gas can only affect the integrity of the concrete structures if the gas pressure exceeds the local hydrostatic pressure.

6.2.9 Evolution of engineered barriers

This section discusses the events and processes of importance for the evolution of the engineered barriers. However, during the initial period of submerged conditions, no significant effects of internal or external processes are expected.

Bentonite barriers

Bentonite consists mainly of montmorillonite, a clay mineral with plastic properties and a high capacity for ion exchange. As a barrier in a final repository, one of the most important properties of bentonite is its swelling capacity. It gives the material low hydraulic conductivity and also enables the clay to self-heal if cracks, channels or other forms of voids occur.

Montmorillonite transformation

Under normal groundwater conditions (Table 6-1), montmorillonite is considered to be stable during the time period covered in the assessment of the post-closure safety of the repository. However, for bentonite-cement installations the groundwater interacting with the bentonite will be significantly more alkaline and have higher contents of Ca^{2+}, Na^{+} and K^{+} than fresh groundwater. Under alkaline conditions the montmorillonite will start to dissolve and the hydraulic conductivity of the bentonite will change. The transformation will continue for as long as alkaline conditions prevail.

The composition of the altered groundwater as well as the processes that control the transformation of montmorillonite are thought to be known, but there are still uncertainties regarding reaction pathways and end products as well as the extent of the reactions and the kinetics of the transformation reaction. However, over the last twenty years, several relevant studies on montmorillonite dissolution rates under different conditions have been published (Rozalén et al. 2008, 2009, Sato et al. 2004, Satoh et al. 2013, Sato and Oda 2015, Ueta et al. 2016, Terada et al. 2019).

Cement–clay interactions have been studied both numerically (e.g. Marty et al. 2009, Idiart et al. 2020), experimentally (e.g. Jenni et al. 2014, Mäder et al. 2017, Yokoyama et al. 2021) and through natural analogues (Alexander and Milodowski 2014, Alexander et al. 2017).

Additional solutes are supplied by the alkaline solution itself. Depending on the degradation state of the concrete, solutions leaching out from cementitious silo components would mainly supply Na, K or Ca ions.

In comparison with the originally present montmorillonite, the secondary phases have a high molar volume but lack the swelling properties of the bentonite. This means that the transformation of montmorillonite can either lead to the available porosity being reduced or completely sealed or to a decrease in or complete loss of swelling pressure and changes in the hydraulic conductivity. The transformation is a slow process (Idiart et al. 2020) and during the initial period of submerged conditions changes to the bentonite barrier will be negligible.

Cementation

The term “cementation” has often been used in a broad sense to describe processes that lead to specific changes in rheology and swelling properties of the buffer material (**Barrier process report**, Section 7.4.14). A number of quite different chemical/mineralogical and mechanical underlying processes could conceivably cause such cementation effects. There are two main concerns about the effects of cementation on the bentonite buffer; one is an increase in hydraulic conductivity, and the other is an increase of shear strength.

Changes in hydraulic conductivity is generally related to mineral alteration, ion-exchange and changes in the composition of the external groundwater. In this assessment these processes are already covered by the studies of cement-bentonite interaction and groundwater composition.

Changes in shear strength may be caused by precipitation of accessory minerals, mineral alteration and heating. The shear strength of the bentonite in the silo is of low concern, since it only needs to be considered if there is a shear movement in the rock. The installed density of the bentonite in the silo is also low, which means that the strength will be low, even if the material is altered.

Bentonite colloid formation

In a confined space, such as outside the concrete wall of the silo, the water uptake by the bentonite leads to a swelling pressure developing in the bentonite. If openings occur in the confining walls (e.g. fractures), local swelling of the bentonite can progress until a thermodynamic equilibrium is reached. This free swelling may lead to separation of individual clay particles, which may result in a dispersion of the clay and the clay being eroded.

The dispersion behaviour of the montmorillonite is strongly dependent on the valence and concentration of ions in the pore space. Dispersion (formation of a clay sol) from aggregated clay (clay gel) is primarily relevant in the presence of dilute groundwater and especially at low concentrations of divalent cations in the groundwater (Ca^{2+}, Mg^{2+}).

During the initial period of submerged conditions, the salinity in the Forsmark groundwater (Table 6-1) and Ca^{2+} concentrations in the interface between bentonite and shotcrete are predicted to be high enough to avoid clay dispersion forming a clay sol (Gaucher et al. 2005, Birgersson et al. 2009, 2011).

Mobility of colloids

Colloid formed inside the silo could potentially carry radionuclides. In general, stable colloids can be transported with the groundwater through cracks and pores in the barriers. The extent of the transport and filtration of colloids depends on both the flow rate and the physical properties of the flow path and the colloids. The main mechanism of filtration is (pore) filtration, when colloids are too large to pass through the apertures, and sorption, when colloids attach to solid surfaces through for example electrostatic, van der Waals, physical or hydrophobic interactions. Another relevant process is ripening, an increase in pore surface roughness by colloid deposition which increases the probability for further colloid deposition. The sorption process is mainly dependent on solution and surface chemistry, while other transport mechanisms depend on the size and density of colloids as well as pore structure and flow rate. Colloid filtration can occur via either mechanical or electrostatic processes (e.g. Swanton et al. 2010).

For most colloids, the transport through compacted bentonite is negligible, due to the low hydraulic conductivity and the small pore sizes.

At present, it is difficult to decide what properties of relevance for release and filtration of colloids are possessed by the sand/bentonite mixture (90/10) which is placed under the concrete silo and which will also be placed on top of the silo at closure. The sand that will constitute the top layer of the backfill above the silo is, however, not expected to constitute an efficient filter, due to the large pore size and the relatively limited reactivity of the backfill material.

Montmorillonite–iron interaction

Several parts of the repository contain large amounts of Fe(0), which is not thermodynamically stable under repository conditions. The anaerobic corrosion that is expected to occur after closure of the repository will produce Fe(II), that can then react with the available barrier materials as well as with constituents dissolved in the pore water. Fe-bentonite interaction is a complex process which is not yet well understood.

An important consideration for the silo is that the iron and steel that occurs there is contained in concrete and/or cementitious grout. This means that corroding iron will primarily be in contact with cement and the effect on bentonite will depend on the transfer of dissolved Fe(II) through the cement mass. It can be expected that this transfer will be small enough to make the process non-significant in comparison with the interaction between bentonite and alkaline pore water from cement-based grout and concrete.

Piping and erosion in the bentonite surrounding the concrete silo needs to be considered. Piping is regarded as a hydraulic process with water transport through a channel or a pipe that is maintained for as long as the pore pressure is equal to, or exceeds, the swelling pressure in the surrounding bentonite. The flow rate is related to the hydraulic gradient and the radius of the channel.

When the drainage of the rock around the silo is terminated and the silo closed, the water pressure in the rock will increase until it either reaches the hydrostatic water pressure at the position equal to the

silo depth (64–133 m.b.s.l.) or until the water penetrates the bentonite barriers. Since the bentonite barrier in the silo has a swelling pressure that is not high enough to withstand the water pressure at silo depth (0.64–1.33 MPa), piping will most likely occur in the bentonite with subsequent bentonite erosion (Börgesson et al. 2015). An alternative is that piping does not occur due to valve formation in the bentonite, which means that the bentonite could be sealed locally and this can instead lead to the formation of closed water pockets.

Both processes lead to a local loss of bentonite and the formation of an open channel or void. The question is then how well this void is sealed by the swelling bentonite. It is possible that bentonite erosion will continue until the silo is filled with water or the pressure gradient has moved from the rock/bentonite interface into the bentonite barrier. The worst case is if the erosion creates an open hemisphere around the inflow point. A finite element calculation of self-sealing of a spherical void with a radius of 0.5 m, arbitrarily chosen by the bentonite thickness, has been made (Börgesson et al. 2015). Although the results cannot be used without reservation, they suggest that the bentonite is relatively unaffected close to the concrete silo, and that the sealing function still works for loss of half a metre of the bentonite filling.

Based on the study in Börgesson et al. (2015), it is judged unlikely that piping and erosion will have a significant impact on the performance of the bentonite barrier. Reasons for this are that the volume of water needed to resaturate the bentonite is limited and there will be many inflow points contributing to the resaturation. Thus, the loss of mass will be small in relation to the total amount of bentonite and be distributed across the bentonite in the silo. Voids created will be filled when the bentonite is resaturated due to the swelling pressure and associated self-healing of the bentonite.

Mechanical processes in the silo bentonite

The bentonite barrier around the silo was installed directly after the silo was constructed. Since the silo is kept open during the first ~50 years of operation, the rock wall surrounding the silo is provided with drainage which prevents water from entering the bentonite. After closure, the repository is filled with water and the clay absorbs water.

When the bentonite absorbs water, it will start swelling and after full water saturation, a swelling pressure of about 100 kPa is expected (Börgesson et al. 2015). With time, ion exchange in the clay between sodium and Ca^{2+} will transform the original Na-bentonite to a Ca-bentonite. This type of ion exchange may lead to a reduction in swelling pressure of up to a factor of five for the relevant dry density (about 1 000 kg/m^3) (Börgesson et al. 2015), a process that could cause subsidence in the bentonite.

The impact of gas on the silo bentonite barrier

There are a number of processes that generate gas in SFR i.e. corrosion of metal components, degradation of organic material and radiolysis (see Section 6.2.8).

As concluded from a relatively large set of tests of gas migration on bentonite and montmorillonite (Birgersson and Karnland 2015), the general picture is that diffusion is the only mass transfer mechanism for gas when the gas pressure is lower than the pressure in the bentonite. When the gas pressure exceeds the bentonite pressure, on the other hand, mechanical interaction between the two phases is inevitable. The mechanical interaction may manifest as gas breakthrough events, or possibly as a consolidation of the clay phase (with only diffusive transfer in the bentonite).

Gas–bentonite interaction is expected to happen mainly when the gas is expelled through the gas evacuation pipes in the top of the silo concrete structure. The silo is covered by a sealing layer of sand mixed with bentonite and an overpressure is needed to open flow pathways through the sealing layer. Pusch and Hökmark (1987) found that an overpressure of about 15 kPa is needed to open the sand-bentonite layer to the gas flow.

If the evacuation pipes are functional, there is no reason to assume that any significant gas pressure will form inside the silo.

Concrete barriers

Overview

The concrete barriers in SFR provide radiation shielding during the operational period and contribute to the prevention of release of radionuclides during the post-closure period. Great care must be taken during design and construction of the concrete barriers in order to ensure that the evolution of the chemical and hydraulic properties of the concrete barriers required can be assured.

The main constituents of concrete are hydrated cement clinker and aggregate materials such as sand and gravel. As a complement, concrete may also contain fly ash, blast furnace slag or inert fillers such as finely ground limestone, see Idiart et al. (2019). To adjust the workability and setting time of the fresh concrete, additives such as superplasticisers or retarders are also added to the mix in low amounts.

Further, most concrete structures also contain steel reinforcement bars whereas in some also form rods, used to keep the formwork together during casting, are embedded in the concrete.

Transport of radionuclides occurs either through advective flow through cracks in the concrete or by means of diffusion in the concrete pore system. Since concrete has a high specific surface area that provides sorption capacity, the mobility of many radionuclides is limited by sorption.

Over the period covered by the safety analysis, many different processes will affect the properties of the concrete barriers and their ability to prevent the release of radionuclides. These processes and their influence on properties of the barriers are described in the **Barrier process report**. Processes occurring in the waste, which also may influence the properties of the barriers, are described in the **Waste process report**, see also Section 6.2.8.

The reference evolution of the concrete barriers is determined by the combined action of processes occurring both inside the barriers but also in the waste. For that reason, the reference evolution described in this section will not follow the same system as in the process reports. Instead of describing the effect of each individual process, a number of events of critical importance for the post-closure safety of the repository will be defined.

The following events – described in more detail below – that can affect the function of the concrete barriers have been identified:

- General dissolution of the cement minerals and leaching.
- Chemical interactions with species in the groundwater and substances leached from the waste.
- Impact of gas formation in the waste.
- Impact of material expansion.
- Impact of local dissolution and leaching.
- Cracking due to freezing of the concrete pore water.
- Cracking due to loss of load bearing capacity.

This section begins with a general description of the concrete barriers followed by a description of the processes judged to be most important for the long-term function of those barriers. Furthermore, the section gives a description of the evolution of the concrete barriers based on the processes likely to affect the concrete barriers in the waste vaults (silo, 1BMA, 2BMA, 1BRT and 1BTF and 2BTF) during the initial period of submerged conditions.

General description of the concrete barriers in SFR

As mentioned in the overview section, the main constituents of the concrete barriers in SFR are hydrated cement paste in which calcium silicate hydrates (CSH) and portlandite ($Ca(OH)_2$) constitute the main binding phases and aggregates made of crushed rock, gravel and natural sand.

The composition of the hydrated cement paste is dependent on the initial composition of the cement clinker materials and the presence of other additives. The composition of the hydrated cement paste can be calculated. As an example, the composition of hydrated cement paste based on Degerhamn Anläggningscement from Cementa AB, used in the concrete structures in SFR1, is presented in

Table 6-7 (Höglund 2014). Degerhamn Anläggningscement is sulfate resistant which reduces the risk for formation of expanding minerals such as ettringite through interactions between the cement minerals and sulfate in the groundwater.

Table 6-7. Composition of hydrated cement used in SFR (Höglund 2014).

Hydrate	Amount in concrete (kmol/m^3)	Fictive[a)] concentration in pore water (kmol/m^3)
C_3FH_6 [b)]	0.1008	1.020
C_3AH_6 [c)]	0.02397	0.2424
Monosulfate	0.09613	0.9722
Ettringite	0	0
CSH-gel (Ca/Si=1.8)	1.225	12.39
Portlandite	1.036	10.48
Brucite	0.06079	0.6149
KOH	0.04607	0.4660
NaOH	0.007903	0.07993
$CaCO_3$	0.06295	0.6367
Porosity	0.099 m^3/m^3 concrete	

[a)] "Fictive concentration" refers to the calculated concentration, disregarding any solubility limitations and interactions with the solvent.
[b)] Hydrogarnet-Fe $(Ca0)_3Fe_2O_3 \cdot 3H_2O$.
[c)] Hydrogarnet $(Ca0)_3Al_2O_3 \cdot 3H_2O$.

The groundwater flow through the waste is determined by the hydraulic contrast, i.e. the ratio between the hydraulic conductivity of the concrete barrier and the backfill material. The implication of this is that a very low water flow through the waste compartment will be obtained for the combination of a dense concrete with a low porosity and no or only a few small cracks (below 0.1 mm) in combination with a backfill material with a high hydraulic conductivity.

The transport properties of the concrete are dependent on the effective porosity of the concrete as well as on the presence of penetrating cracks, whereas surface cracks have a negligible influence on the transport properties of the thick concrete structures in SFR. The aperture of the largest penetrating crack is a critical parameter, since the transmissivity of a crack increases with the cube of the crack aperture (Höglund 2014).

The initial total porosity of the hardened concrete depends on the water to cement ratio (w/c) of the fresh concrete and the pore system includes both connected and unconnected pores. In SFR1, different types of concrete have been used in the concrete structures of the different waste vaults. Of these, the porosity of the concrete used for construction of the silo with a w/c of 0.47 has been assigned an initial porosity of 15 % (Gaucher et al. 2005) whereas a more recent modelling study by Idiart et al. (2019) found the porosity of the silo concrete to be about 10 % and the concrete used in 1BMA with a w/c ratio of 0.63 to be 12–13 %. Finally, the findings by Höglund (2014) indicate a porosity of the silo concrete of just below 10 % even though the concrete in that report is denominated "1BMA construction concrete" due to previous lack of information regarding the mix-design of the 1BMA concrete.

The concrete structures in SFR may also contain surface cracks and/or cracks that penetrate the entire concrete structure. In principle, cracks are formed as a consequence of tensile stresses in the concrete structure exceeding the tensile strength of the material. The forces that cause these stresses can be either load dependent and thus caused by an external force such as weight from backfill material and water pressure or load independent and caused by processes within the concrete structure itself such as temperature gradients during cooling or uneven shrinkage caused by drying.

Cracking due to load-dependent forces can be prevented by correctly designing the concrete structure in combination with the use of reinforcement if permitted. However, reinforcement is only active after the formation of a crack and cannot prevent the crack entirely but only limit its width.

Cracking due to load-independent forces can be prevented by correct choice of material and methods of construction of the concrete structures. For examples of material and methods developed for use during construction of the concrete caissons for 2BMA, please refer to Lagerblad et al. (2017) and Mårtensson and Vogt (2019, 2020).

During the post-closure period, the hydraulic conductivity of the concrete barriers may increase due to increasing porosity and possibly also due to the formation of new cracks or widening of existing ones. Because of this, an increasing fraction of the total flow will be directed through the waste compartment with a possible increase in the release of radionuclides as a consequence.

In the following sections, the most important processes influencing the properties of the concrete barriers are discussed.

General dissolution of the cement minerals and leaching

General dissolution of the cement minerals and leaching affects the composition of the hydrated cement, its porosity as well as the composition and pH of the cement pore water. These changes mainly affect the chemical properties of the cement but for extensive leaching also the hydraulic properties may be affected.

Initially, interactions between concrete and the groundwater will lead to the leaching of the highly soluble alkali hydroxides. As these mainly occur as dissolved species in the cement pore water, the process is rather fast and is expected to occur early after resaturation of the repository. Leaching of the alkali hydroxides is followed by dissolution and leaching of $Ca(OH)_2$ (portlandite) and finally by incongruent dissolution of calcium silicate hydrates (CSH). The rate of dissolution and leaching is dependent on the pore structure of the concrete. For this reason, leaching of a dense concrete with small and poorly connected pores will be slower than leaching of a cracked concrete with larger and well-connected pores.

The leaching process leads to a gradual decrease of pH in the concrete pore water beginning at pH about 13 for the fresh concrete and finally ending up at a pH below 10 for the severely leached material. Leaching of concrete has been studied for the different waste vaults in SFR; see e.g. (Höglund 2001, 2014, Gaucher et al. 2005, Cronstrand 2007, 2014). These studies have shown that dissolution and leaching are both very slow processes, and that the interior of the concrete barriers are more or less unaffected by this process during several thousand years after closure.

Based on the findings discussed above it is concluded that general dissolution of the cement minerals and leaching will not affect the chemical and hydraulic properties of the concrete barriers in any of the waste vaults in SFR to a significant extent during the initial period of submerged conditions. This position is justified by the considerations that general dissolution and leaching are slow and the amounts of cement in the different waste vaults is very large.

Chemical interactions with species in the groundwater and substances leached from the waste

Chemical interactions with species in the groundwater and substances leached from the waste affect the composition of the hydrated cement, its porosity as well as the composition and pH of the cement pore water (Höglund 2001, 2014, Gaucher et al. 2005, Cronstrand 2007, 2014), thus affecting both the chemical and transport properties of the concrete.

After closure, the concrete barriers will become saturated by groundwater, containing a variety of dissolved species. However, some waste forms in 1BMA also contain significant quantities of soluble salts which can be dissolved once groundwater has reached the waste compartments. As an example, the main sulfate inventory in 1BMA is that in evaporator concentrates.

Dissolved substances, such as SO_4^{2-}, HCO_3^- and Cl^-, will react with the cement minerals, giving rise to precipitation of secondary phases. In addition, the exposure to increased concentrations of solutes released from the waste may give rise to dissolution–precipitation reactions. Especially for some waste compartments in 1BMA, this could lead to an increased rate of formation of new minerals in the

concrete and cement in the waste, compared with the parts of the concrete barriers exposed to pure groundwater. Examples of important dissolution and precipitation processes include:

- Formation of ettringite from monosulfate after increased sulfate exposure. Ettringite has the ability to bind large quantities of water as water of crystallisation, which means that this mineral has large potential for expansion when absorbing water. If insufficient pore volume is available for mineral expansion, this process could lead to the formation of cracks and mechanical degradation of the concrete (Höglund 2014).
- Precipitation of thaumasite as a result of increased exposure to CO_2/CO_3^{2-} and SO_4^{2-}.
- Carbonatisation. A recombination of the buffering mineral portlandite to calcite through this reaction in environments with a high content of carbon in either gaseous carbon dioxide or dissolved carbon as carbonate or carbon dioxide. Portlandite buffers pH to between 12 and 13, whereas calcite buffers pH to between 8 and 9.
- High magnesium water content may cause the buffering mineral portlandite to recombine to magnesium-rich minerals such as brucite or hydrotalcite (Höglund 2017). The magnesium content in the incoming groundwater used in the concrete degradation simulations (Höglund 2014) was chosen to not underestimate this effect (Höglund 2017, Auqué et al. 2013).
- Armouring of walls of cracks. If there are large cracks in the barriers, and the incoming groundwater contains a sufficiently high amount of carbon, a dense layer of calcite can be formed on the walls of the cracks. If the layer is dense and/or thick enough the interaction between the incoming groundwater and the barrier minerals could be reduced. With certain combinations of crack aperture, barrier thickness, hydraulic gradients and calcite layer porosity and thickness this may cause groundwater to reach the waste domain before it is fully equilibrated with the barrier minerals. However, with the slow water flow and thick barriers present in SFR, this effect is not expected to be important. The diffusive exchange between the barrier and waste is sufficient to keep the pH high in the waste even if armouring of cracks occurs (Höglund 2014). The formation of an armouring layer would decrease the crack aperture and/or porosity and thus reduce the advective transport through the barrier.
- Saline groundwater. Under submerged conditions the incoming groundwater is brackish (Auqué et al. 2013). This could lead to a formation of the mineral called Friedel's salt in or on the surface of the concrete barriers. Investigations of this indicate that the process leads to an increase in pH and could also alter the time for which the barrier will keep its buffering capacity (Höglund 2017, Honda et al. 2008). The formation of Friedel's salt is included in the concrete degradation studies (Höglund 2014, Idiart et al. 2019).

It must though be mentioned that the extent to which these reactions occur is dependent on the composition of the hydrated cement, the waste and the groundwater. The groundwater composition used in the concrete degradation modelling (Höglund 2014) is cautious in the sense that components that are expected to contribute to mineral alteration in the concrete are either realistic or more abundant than suggested by the statistical variation from the site studies (Auqué et al. 2013). Carbonatisation of the barriers during the operational period of the repository due to presence of atmospheric carbon dioxide has not been included in the concrete degradation calculations. The alteration depth may be in the order of centimetres over 100 years of atmospheric exposure (SS-EN 1992-1-1:2005) and the effect is therefore not important for the thick concrete structures in SFR. However, the effect may be of some importance for the structural integrity of waste containers that are stored in SFR during most of the operational period (Bultmark 2017).

Based on the studies summarised above it is concluded that chemical interactions between the cement minerals with groundwater and substances leached from the waste will have only a minor effect on the chemical and hydraulic properties of the concrete barriers during the initial period of submerged conditions.

This position is justified by the argument that during the initial period of submerged conditions ettringite will only form in a thin layer on the outer parts of the concrete barriers (Höglund 2014). It is also justified by the consideration that only small amounts of ettringite may form in the concrete barriers close to sulfate-containing waste. Further, the quantity of ettringite that can be formed inside waste

compartments is limited by the amount of SO_4^{2-} that can be released from the waste. Waste compartments in 1BMA containing evaporator concentrates also contain a sufficient quantity of cement for the largest fraction of SO_4^{2-} released from evaporator concentrates to form ettringite within the waste domain, see discussion around Table 6-2. Some local impact on the concrete barrier itself cannot, however, be fully excluded.

Impact of gas formation in the waste

Formation of cracks in the concrete barriers due to gas formation in the waste affects the hydraulic properties of the concrete barriers. Secondary effects such as increased leaching of the concrete in the vicinity of the crack are not considered in this section.

As the waste domain becomes saturated with water, decomposition of organic materials in the waste or anaerobic corrosion of metals will cause the formation of gas. If this gas cannot be dissipated from the waste domain, the pressure will increase inside the concrete structure which eventually may lead to the formation of one or several cracks in the concrete structure through which the gas can escape. For a description of processes occurring in the waste, see Section 6.2.8.

In materials with a fine pore structure, such as concrete, capillary forces determine the breakthrough pressure needed to expel gas. Gas will be expelled from the concrete first after a network of interconnected gas-filled pores has been formed in the barrier. Gas will escape while the pressure difference exceeds the capillary entry pressure. When the pressure drops below the breakthrough threshold, the pores will become resaturated until a sufficiently high pressure has built up once again form a transport path. In concrete waste packages and concrete structures, a few small cracks are sufficient to divert the gas. If the available transport paths are not enough to divert the formed gas sufficiently, additional cracking may occur.

To facilitate the release of the gas formed by these processes and avoid crack formation in the concrete barriers, the silo and 2BMA will be provided with engineered systems for gas release. For this reason, elevated gas pressures that may cause the formation of cracks in the concrete barriers in these waste vaults are not expected to occur during the initial period of submerged conditions.

Impact of material expansion

Formation of cracks in the concrete barriers due to material expansion affects the hydraulic properties of the concrete barriers. In this section, two important processes that may cause cracking are addressed; metal corrosion and swelling of organic waste through water uptake. Secondary effects such as increased leaching of the concrete in the vicinity of a crack are not considered in this section.

Initially, reinforcement bars and other steel components embedded in the concrete structures such as tie rods are passivated by the high pH of the concrete. With time, intrusion of Cl^- and CO_3^{2-}, in combination with groundwater leaching of the alkaline components and lowering of the concrete pore water pH, can depassivate the steel surfaces and initiate corrosion.

As a result of the corrosion processes, a layer of corrosion products will form on the metal surface. These corrosion products will mainly consist of iron oxides (Fe_xO_y) and iron hydroxides ($Fe(OH)_x$). As the molar volume of the corrosion products is larger than the volume of the iron, a gradual volume expansion will occur in the interface between concrete and metal with mechanical stress in the concrete surrounding the reinforcement bars as a result. If the stress exceeds the concrete tensile strength, cracks will form in the concrete (Höglund 2014). If the corrosion process is allowed to progress, the continued accumulation of corrosion products will lead to an increasing crack width and ultimately to spalling of the concrete covering layer. For penetrating steel components such as tie rods, corrosion can cause cracks that penetrate the barrier rather than spalling of the cover. If the corrosion products are instead dissolved in the water and transported away from the source, a void will form in the space that previously contained the corroding material.

The most important process involving the waste is swelling of the ion-exchange resins through water uptake after resaturation of the repository. Here, the degree of swelling and the maximum swelling pressure are dependent on the choice of conditioning method used. For example, for dewatered ion-exchange resins in concrete tanks the possible degree of swelling is much lower than for ion-exchange resins which have been dried and mixed with bitumen prior to disposal of the waste.

Contrary to crack formation caused by gas formation, cracking caused by material expansion is a local process which cannot be mitigated by a global engineered solution. Instead engineered solutions functioning on a local scale need to be sought.

To prevent the formation of cracks in the concrete barriers in 1BMA and 2BMA due to material expansion in the waste it has been decided that no grouting of the waste in 1BMA and 2BMA will be performed. In 1BRT, however, where grouting will be carried out, cracking due to the formation of voluminous corrosion products on the reinforcement bars, the tie rods as well on the segmented reactor pressure vessels can be anticipated.

In the silo, cracking of the outer concrete barrier caused by swelling of waste is prevented by the bitumen-solidified ion-exchange resins being disposed in some of the most central shafts. A study concerning these effects shows that even though the swelling pressure may cause damages in the interior of the silo, the outer walls will not be affected (von Schenck and Bultmark 2014).

Finally, the concrete tanks in 1–2BTF contain sufficiently large void volumes to prevent the pressure from potentially swelling waste causing damage to the walls of the tanks.

However, even though large-scale cracking caused by swelling of waste can be mitigated by engineered solutions, this is not the case for the local cracking caused by corrosion of reinforcement bars and form rods.

To avoid cracking caused by metal corrosion in the 2BMA concrete caissons, reinforcement bars and tie rods will not be used. To compensate for the exclusion of reinforcement bars, inner walls will be used instead, thus creating a structure similar to that of the silo.

For 1BMA, which contains steel reinforcement and tie rods, other solutions are being sought. SKB is currently developing a method for restoring the concrete barriers in 1BMA to their original initial state including strengthening of the walls as well as sealing of cracks. This also includes means to mitigate the effects of steel corrosion inside the barriers. The anticipated measures are described in the closure plan for SFR and references therein (Mårtensson et al. 2022).

Also, the silo contains large amounts of steel reinforcement bars. Here the bentonite surrounding the silo prevents any new measures to limit corrosion. However, the bentonite being the main hydraulic barrier of the silo limits the amount of water that can reach the concrete structure compared to a gravel backfill, thus dramatically reducing the rate of corrosion.

In summary, during the initial period of submerged conditions it is judged that the engineered solutions used in the different waste vaults will be sufficient to prevent the formation of cracks caused by material expansion processes in the waste that would seriously affect the hydraulic properties of the concrete barriers.

Crack formation caused by corrosion of metal components inside the concrete barriers is only expected to be an issue for the concrete tanks which might experience some cracking due to metal corrosion. Metal corrosion may also cause some cracks in the 1BMA barrier, but the effect of this is expected to be limited due to the planned restoration measures. For the silo, crack formation due to corrosion is not expected during this period and for 2BMA corrosion is not an issue. Finally, the reinforced concrete structure in 1BRT might experience some formation of cracks.

Impact of local dissolution and leaching

Widening of existing concrete cracks through local dissolution and leaching may influence the hydraulic properties of the concrete barriers but also the chemical properties in the direct vicinity of the existing crack.

After closure and resaturation of the waste vaults, the groundwater and solutes in the groundwater will react with the cement minerals in the concrete barriers. The processes that occur in connection with cracks and other local weaknesses are the same as generally apply for degradation of concrete in this type of environment – see above – and are not repeated here. In studies of local concrete degradation, water is assumed to flow mainly in the crack, while diffusion is the dominant transport mechanism in the concrete between cracks.

The effect of local leaching processes is the formation of a portlandite-depleted zone in connection with a crack, through which a certain amount of water could flow. This zone will be developed both along the length of the crack but also in a direction essentially perpendicular to the extent of the crack. For further details on widening of cracks through local dissolution and leaching, see Höglund (2014).

The portlandite-depleted zone may have a higher porosity and could be more permeable to water than intact concrete. However, this is dependent on the balance between the dissolution and precipitation processes as the water that enters the cracks will contain several solutes that can form secondary minerals. This may lead to closure of cracks or the formation of secondary minerals in the concrete close to the crack.

The hydraulic properties of a crack are not expected to change until the portlandite-depleted zone has penetrated the whole thickness of the concrete barrier. For cracks in the concrete barrier with apertures less than 0.1 mm, the water flow rate in the cracks is sufficiently low to ensure that this will not occur during the first 20 000 years after closure (Höglund 2014).

If, eventually, the portlandite-depleted zone has extended along the whole length of the crack, water which is unsaturated with respect to portlandite will start to flow in through the concrete wall. This will lower the pH of the water entering the waste domain. This may cause a loss of passivation of the steel components with an increased corrosion rate as a consequence.

For the concrete tanks in BTF, the local degradation due to portlandite leaching in cracks is not considered to cause any significant changes in the hydraulic properties of the tanks during the initial period of submerged conditions.

In summary, during the initial period of submerged conditions widening of existing cracks through local dissolution and leaching is not expected to alter the chemical and hydraulic properties of the concrete barriers in a way that affects the post-closure safety of any of the waste vaults in SFR.

Cracking due to freezing of the concrete pore water

Cracking of the concrete barriers due to freezing of the concrete pore water will not occur during the initial period of submerged conditions. This is because temperate climate conditions will prevail during this period.

Cracking due to loss of load bearing capacity

Cracks may form if the mechanical loads, e.g. from the backfill material, exceed the load bearing capacity of the concrete structure. The main process affecting the loadbearing capacity of the concrete structures is general dissolution of the cement minerals and leaching (Mårtensson 2017) in combination with loss of function of the reinforcement bars. These processes will not affect the mechanical properties of the concrete barriers in any of the waste vaults in SFR to a significant extent during the initial period of submerged conditions. Cracking of the concrete barriers due to loss of load-bearing capacity will not occur during the initial period of submerged conditions.

After closure of SFR, the vaults will gradually transition from unsaturated to saturated conditions as they are filled with groundwater. During this saturation period, the intruding water can exert an external mechanical load on the concrete structures. The concrete structures are designed to withstand such loads, so that their barrier properties remain unaffected. However, the ability of the concrete tanks in 1–2BTF to withstand the external water pressure is to some extent uncertain and is currently under investigation by SKB.

Backfill material

At closure, the voids outside the concrete barriers in 1BMA, 2BMA and 1BRT as well as the void on top of the concrete tanks in 1–2BTF will be backfilled with macadam, i.e. crushed rock with no or very small amounts of fine-grained material manufactured from rock material obtained from the excavation of the facility. The material planned for use is the same material that has been found to be suitable as aggregates in the concrete for the caissons in 2BMA (Lagerblad et al. 2016). Detrimental reactions between the backfill material and the alkaline pore water leached from the concrete barrier that could affect the hydraulic properties of the backfill material are unlikely.

During the initial period of submerged conditions, it is anticipated that groundwater flow in the backfill material may cause parts of the fine-grained material to settle towards the rock floor. Also, some fracture material from the surrounding bedrock may be transported into the vault. This is, however, not anticipated to affect the hydraulic properties of the backfill material during this period and thus not the post-closure safety of the repository.

Microbiology

Microbial growth is possible and may be significant in the backfill in the presence of an advective flow, which supplies the cells with nutrients and removes waste products. Because the rock walls are covered with shotcrete, the pH of the water in contact with the backfill materials will become slightly alkaline during a short initial period. However, the environment in the backfill will be less hostile toward microbial growth, than inside the cemented waste packages, as the pH is expected to be more affected by the surrounding crushed rock materials than by the cement and shotcrete. Microbial activity will be lower under stagnant hydraulic conditions.

Anderson et al. (2006a) showed that monolayer biofilms develop within a few months on polished rock surfaces exposed to anaerobic granitic groundwater. However, due to the high porosity of the backfill, clogging is unlikely to occur and is therefore not considered to affect the average hydraulic conductivity of the backfill to such an extent that water flow through the waste is affected.

Summary of the reference evolution of the barriers during the initial period of submerged conditions

In this section the reference evolution for the rock vaults in SFR has been described. The following summarising conclusions can be drawn from this work:

Silo: During the initial period of submerged conditions neither the hydraulic nor chemical properties of the barrier system of the silo are expected to be affected to such an extent that the post-closure safety of the silo is affected. This conclusion is justified by the consideration that the bentonite surrounding the concrete silo has a very low hydraulic conductivity and strongly limits any interactions with the groundwater.

1BMA: During the initial period of submerged conditions only the hydraulic properties of the concrete barriers in 1BMA may be affected due to minor formation of cracks caused by corrosion of tie rods or reinforcement bars. However, with the planned restoration measures, the effects of these cracks on the hydraulic properties are expected to be limited. The period is too short for anything other than a minor alteration of the chemical properties close to the surface of the concrete structure to occur. The hydraulic properties of the backfill are not expected to be affected during this period.

2BMA: During the initial period of submerged conditions only minor alterations of the chemical properties of the surface region of the concrete structure in 2BMA are expected to occur. Cracking is not expected during this period and thus the initial hydraulic properties are retained. The hydraulic properties of the backfill are not expected to be affected during this period.

1BRT: During the initial period of submerged conditions only the hydraulic properties of the concrete barriers in 1BRT may be affected due to minor cracking caused by corrosion of tie rods or reinforcement bars. The period is too short for anything else than a minor alteration of the chemical properties close to the surface of the concrete structure to occur. The hydraulic properties of the backfill are not expected to be affected during this period.

1–2BTF: During the initial period of submerged conditions, some cracking of the concrete tanks due to corrosion may occur, causing a slight change in the hydraulic conductivity of the walls of the tanks. Leaching of the concrete in the surface region may cause some changes of the chemical properties in this part. However, this is not expected to affect the properties of the water that penetrates the waste.

1–5BLA: There are no engineered barriers in 1–5BLA.

6.3 Present-day climate variant

This section describes the *present-day climate variant* of the reference evolution from the end of the initial submerged period, i.e. 1 000 years after closure, to the end of 100 000-year assessment period. The definition of the initial submerged period in the *present-day climate variant*, as well as the evolution of the repository system during this period, is described in Section 6.2.

6.3.1 External conditions

The *present-day climate variant* is chosen as a simplified development where initial state climate conditions (Section 4.5) and, consequently, temperate conditions prevail for the complete assessment period (Figure 6-1). Although the assumption of present-day climate conditions over the next 100 ka is not realistic, per se, the *present-day climate case* is considered to give a reasonable basis for evaluation of developments in the repository and its environs that occur under constant climate conditions. Also, the overall development is in agreement with the assessment that the Forsmark climate will likely remain temperate for the next 100 ka if current, or higher, levels of anthropogenic greenhouse-gas emissions continue over coming decades (**Climate report**, Section 4.3). Hence, despite its simplicity, the anticipated lack of transitions between climate domains within the assessment period is adequately captured by the *present-day climate variant*. The effects of a warmer climate than at present is described in the *warm climate variant* (Section 6.4).

6.3.2 Evolution of surface systems

This section summarises the natural processes and possible human impacts driving the development of the limnic and terrestrial systems at the Forsmark site under the *present-day climate variant* (from the **Biosphere synthesis report**, Chapter 4). The focus is on the development of the topography and regolith, near-surface hydrology, chemistry and ecology of limnic and terrestrial ecosystems. Historical land use is also described and used to sketch future human effects on the landscape development. Agricultural land is the most intensively managed part of the landscape. The development of marine systems is described in Section 6.2.2.

Development of regolith and topography

The distribution of regolith in the Forsmark area will change throughout the period considered in the safety assessment. In the present terrestrial area, the proportion of peat-covered areas will increase as the shallow lakes are infilled, and the low-lying wetlands are covered by a layer of peat. New lakes will form when the present seafloor becomes exposed due to isostatic rebound and these lakes will successively be filled with gyttja and peat that can be cultivated. A large proportion of the future land will become forested as bottoms with exposed bedrock and till emerge from the sea. The proportion of land suitable for agriculture is likely to increase significantly in the far future as the areas with water-deposited clay and sand in Öregrundsgrepen become exposed.

The RLDM (Section 6.2.2) was used to simulate and describe a potential future landscape. It is based on physical constraints and knowledge of the historical processes that have shaped the Forsmark landscape. The model is divided into one marine module (Section 6.2.2) and a lake module that simulates the lake infilling processes.

When enclosed sea bays become isolated as a result of the shoreline regression, the regolith development of each lake was modelled separately with the lake module (Brydsten and Strömgren 2013). The lake module initially estimates the vegetation ingrowth in the sea bay prior to isolation and then estimates sedimentation and ingrowth by vegetation in 100-year time steps until the lake is completely infilled. Raster maps of regolith layer depths, limnic sediments (i.e. clay gyttja) and peat, and an updated Digital Elevation Model (DEM) were outputs from the lake module for each time step.

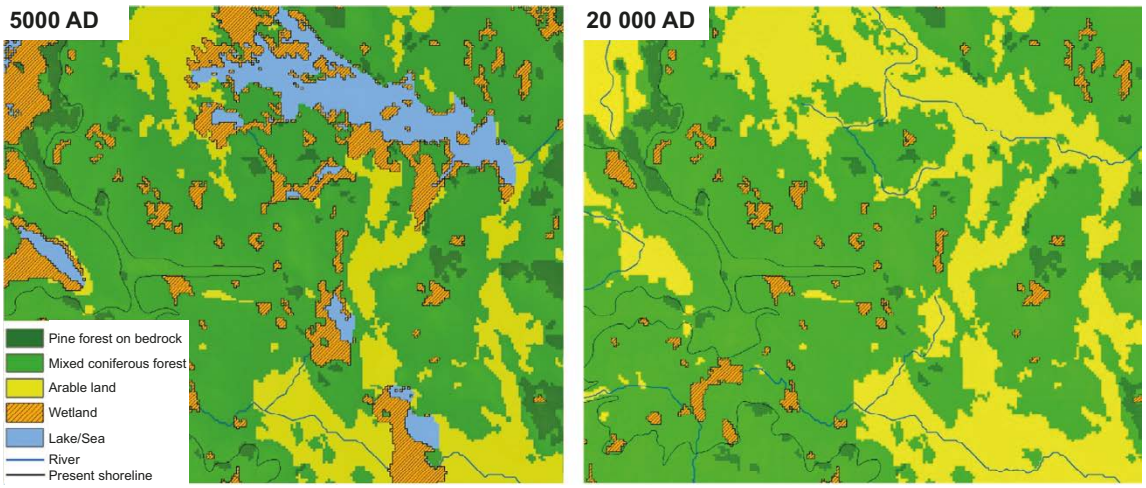

Figure 6-8. *Illustration of the landscape development in the present-day climate variant using the points 5000 AD and 20 000 AD (c.f. Figure 6-2 for 2000 AD and end of submerged period). The yellow colour represents land that could potentially be cultivated. Note that in this projection mires within lakes are not marked as potential arable land until the lake has been completely covered by mire vegetation (modified from Figure 4-6 in* ***Biosphere synthesis report****).*

The output from the RLDM was used to export three-dimensional regolith models as input to the hydrological modelling at different stages (2000 AD and 3000 AD in Figure 6-2, 5000 AD and 20 000 AD in Figure 6-8) for the landscape above the repository (Werner et al. 2013). The output from the RLDM is also used to identify and extract parameters describing geometries (e.g. water depths and regolith layer thicknesses) of potential future release areas of radionuclides from SFR that are used in the modelling of radionuclide transport and dose (Section 7.3). Uncertainties in the landscape development, related to e.g. properties of potential release areas and transport pathways of radionuclides, are considered in the radionuclide transport and dose modelling (Chapter 7 and **Biosphere synthesis report**, Chapters 10 and 11).

Development of near-surface hydrology

Hydrological processes play a role in the development of surface systems and are crucial for transport of dissolved substances and particles, including radionuclides. Conceptual and numerical models describing present and future hydrology were developed (Werner et al. 2013), based on SDM-Site (Bosson et al. 2008) and SR-Site (Bosson et al. 2010).

Modelling of future hydrology was conducted on a local spatial scale (Figure 6-9), supported by regional-scale boundary conditions, with the MIKE-SHE modelling tool. Hydrological models were developed for the times 2000 AD (present conditions), 3000, 5000 and 11 000 AD (Werner et al. 2013), using the meteorological data and assumed shoreline regression in the *present-day climate variant* (Sections 6.2.1 and 6.3.1).

Modelled average vertical head differences in the regolith in the local MIKE-SHE model area indicate whether the flow of groundwater has an upward or downward direction (illustrated for 5000 AD in Figure 6-9). In future land areas formed as a result of shoreline displacement, the modelled pattern of groundwater recharge and discharge areas in the regolith is similar to that observed in present land areas. This indicates that near-surface hydraulic gradients and flow directions are more dependent on topography than on the detailed distribution of regolith and the distance to the shoreline (at least for areas some metres above sea level). However, the stratigraphy and regolith depth may affect local recharge and discharge patterns in the regolith. Discharge areas for deep groundwater are concentrated into low-elevation areas. Regolith stratigraphy and depth in these areas are therefore important for near-surface transport of radionuclides.

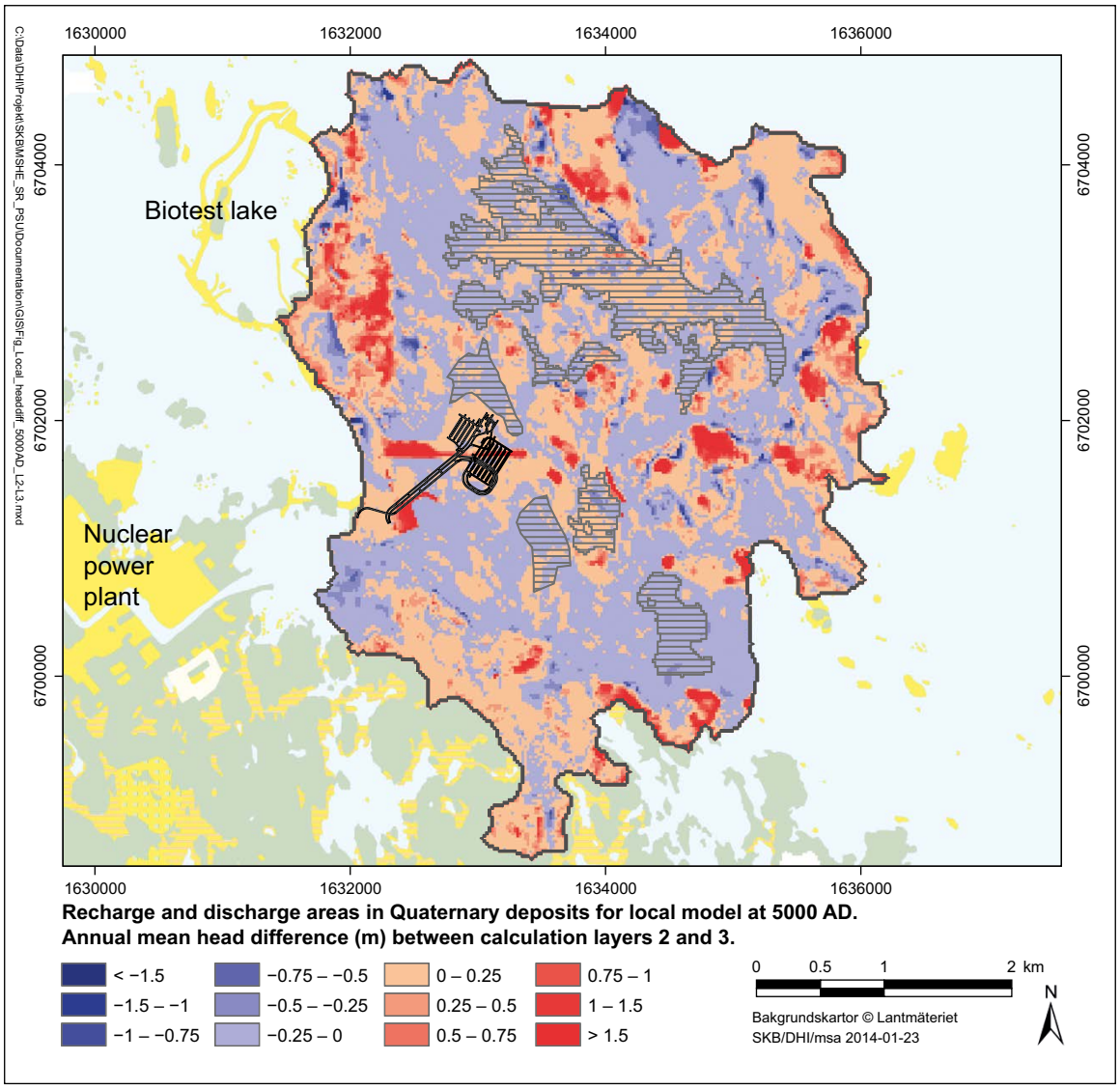

Figure 6-9. *MIKE-SHE calculated annual average vertical hydraulic head differences in the regolith at 5000 AD in the local model (modified from Figure 5-3 in Werner et al. 2013). Blue colours represent areas with upward flow (discharge) and red colours are areas with downward flow (recharge). Dashed areas indicate the potential radionuclide release areas (see Section 7.3.5).*

Groundwater discharge from the rock to the regolith increases (Sections 6.2.5 and 6.3.5) somewhat during the initial period after shoreline passage (3000 to 5000 AD) when the flow rates associated with the submerged period increase to those prevailing in the coastal terrestrial landscape. At 11 000 AD, all lakes within the local model area have been transformed to terrestrial areas, resulting in lower evapotranspiration and higher annual average stream discharges compared with 5000 AD.

Development of chemical conditions

The chemical conditions in the regolith and surface waters affect element transport and accumulation as well as the species present, communities, productivity and development of ecosystems. The Forsmark region is rich in calcite and calcite-bearing till deposits that has have a marked influence on the hydrochemistry in the area. When new areas of the present seafloor are raised above the sea level, weathering of the calcite ($CaCO_3$) is initiated, releasing Ca^{2+} and CO_3^{2-}/HCO_3^- ions. This process increases the alkalinity and pH in the shallow groundwater, streams, lakes and soils. This influences the sorption and transport of many elements, including radionuclides, and results in highly fertile soils. In limnic systems, on the other hand, secondary calcite precipitation and co-precipitation of e.g. phosphate results in nutrient-poor oligotrophic hard water lakes.

In the soil horizon farther away from Forsmark, calcite has been consumed down to considerable depths and there is a clear gradient with shallower depths towards the coast (Ingmar and Moreborg 1976). Estimates based on soil calcite inventories and present weathering rates suggest that the calcite in the regolith layers might be consumed within a time span of some 1 000 to more than 50 000 years (**Biosphere synthesis report**, Section 4.4).

In the long run, the decreasing calcium concentrations, pH and alkalinity will change element sorption and transport. This can potentially decrease the productivity in unmanaged soils and will increase the availability of phosphorus in limnic systems. When the surface water composition in the Forsmark area approaches inland brown-water systems, a relative shift from benthic to more pelagic primary production is expected in lakes (Andersson 2010). Possibly, weathering rates of less readily weathered minerals such as silicates will increase in the future when the calcite in the regolith is depleted (Lindborg 2010). The release of major constituents originating from these types of minerals, e.g. Al, Na and Mg, as well as release of trace elements incorporated in the bulk minerals, e.g. U and Th, and rare earth elements, are thus expected to increase in the future.

Typically, the mire formation in Forsmark initially results in a fen, i.e. a groundwater influenced mire, and succession could eventually lead to formation of a raised bog. The typical fen mire in the Forsmark area has a high pH and will undergo a natural long-term acidification when turning into a more bog-like mire (Löfgren 2010, Section 10.4).

Ecosystem development

In the following, the development of limnic and terrestrial ecosystems in the *present-day climate variant* are discussed (the development of marine ecosystems is described in Section 6.2.2). The ecosystem development is strongly affected by the shoreline displacement that turns the seabed into terrestrial areas. Relatively enclosed sea bays may become isolated and gradually turn into lakes. After isolation from the sea, sedimentation and ingrowth gradually transform the lake into a mire system (Figure 6-10 and Andersson 2010, Section 8.2). More open bays can turn directly into mires, without intermediate lake stages and more exposed bottoms often become forested.

Limnic

Most of the emerging lakes are expected to closely resemble the present-day shallow oligotrophic (i.e. nutrient-poor) hardwater lakes in Forsmark with high benthic primary production. However, if the calcite is depleted from regolith layers, it is possible that future lakes will be dystrophic (i.e. brown water lakes), dominated by respiration of the material produced in the surrounding terrestrial catchment.

A few future lakes, located further away from the repository, will have depths of more than 10 metres. These lakes will more closely resemble other deep lakes in surrounding areas that are deep enough to allow for thermal stratification during both summer and winter. Pelagic production may be more important in these lakes, but the losses through the outlet will probably be large due to large catchment areas.

In the future, small streams closely resembling the streams in the Forsmark area today (Section 4.6) will form in the area close to SFR. Further downstream in the model area, somewhat larger streams, more like the nearby Forsmarksån, will be formed.

Terrestrial

Forests are the most common terrestrial ecosystem type in Forsmark, but fen mires have been identified as the terrestrial ecosystem where deep groundwater (e.g. from a repository) most likely will discharge (SKB TR-10-09). Consequently, the focus here is on these mire ecosystems and their potential use as agricultural land after drainage.

Mire formation through filling-in of shallow lakes by sedimentation and establishment of vegetation (i.e. terrestrialisation) and the consecutive development of fen mires is probably the most important mire formation process in the areas that emerge from the sea. Primary mire formation, when peat is developed directly on fresh soils after emergence from water or ice, might also occur. The typical fen mire around Forsmark has a high pH and will undergo a natural long-term acidification when turning into a more bog-like mire (Figure 6-10 and Löfgren 2010, Section 4.1.1).

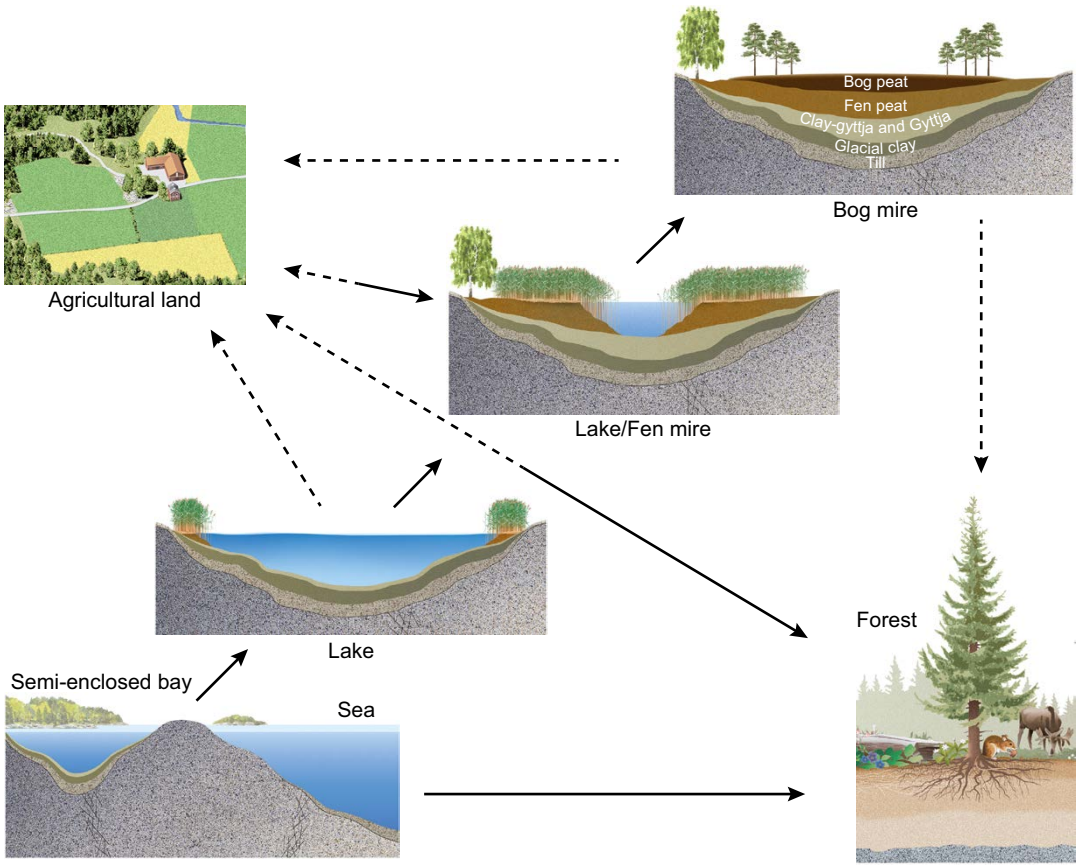

Figure 6-10. *A schematic illustration of the major ecosystems that may be found at certain points during a temporal sequence at the Forsmark site, where the original sea bottom slowly becomes land due to shoreline displacement. Black-line arrows indicate natural succession, while dashed arrows indicate human-induced changes to provide new agricultural land or improved forestry. Agricultural land may be abandoned and will then develop into forest or, if the hydrological conditions are suitable, into a fen. A forest may be "slashed and burned" and used as agricultural land. Through primary mire formation, some ecosystems transform straight from a sea bay directly to a mire without passing an intermediate lake stage (not illustrated in the figure).*

Land use and human influence on landscape development

Since large parts of the Forsmark area were submerged until recently, the earlier development of human land-use is largely based on information from other parts of Sweden. The early inhabitants constituted hunting, fishing and gathering societies (see further Section 7.3.6). In southern Sweden, the dense forests were cleared during the first phase of the Younger Stone Age (4000 BC–1 800 BC, Hyenstrand 1994) and then used as grazing land and, during the Bronze and Iron Ages (1 800 BC–1 100 AD), the areas with cultivated soils gradually increased.

Historically, only fairly dry soils in Sweden could be cultivated, but the modernisation of agriculture made it possible to drain peat and heavy-clay areas for cultivation. Extensive draining of mires started just over one hundred years ago and peaked in Sweden in the 1930s (Eliasson 1992). The thickness and properties of peat and the underlying regolith are of importance for the possibility to drain a mire and use it for agricultural purposes. Fen mires are more suitable for cultivation due to the higher nutritional value than bog peat and are also more relevant for the safety assessment since they, in contrast to raised bogs, are typically discharge areas of deep groundwater. Due to oxidation and compaction, peat subsides considerably when the groundwater is lowered after draining (discussed in Sohlenius et al. 2013a). Subsidence of peat is a fast process and sustainable cultivation for longer periods is possible only if the underlying deposits are suitable for cultivation.

To illustrate potential future landscapes at Forsmark, covering different climate conditions and land-use, maps of five different variants were presented in the SR-PSU (SKB TR-14-06, Section 5.5). These were constructed by coupling the RLDM output with different sets of assumptions with respect to the links between regolith, ecosystems and potential land use. In the *present-day climate variant* and assuming intensive cultivation, the area of terrestrial ecosystems, including mires (wetland in Figure 6-11) and potential arable land, gradually increases from 500 BC to 7000 AD. Potential arable land will continue to increase when the lakes have been completely filled with sediment and peat and can be drained and cultivated. At 15 000 AD, only 6 out of the 48 lakes remain. At 20 000 AD, no lakes remain in the area above the repository and, at the end of the simulation (40 000 AD), all lakes are filled with sediment and peat and most of them are classified as potential arable land.

In the SR-PSU, a comparison between the landscape projected by the RLDM for 2000 AD, including the resulting distribution of ecosystems and potential arable land, and the present-day conditions, showed that the RLDM captured many features of the present landscape (SKB TR-14-06, Section 5.6.2). The results from the RLDM give a comprehensive example of landscape development, based on well-known processes and physical constraints.

6.3.3 Thermal evolution

Due to the constant air temperature assumed in the *present-day climate variant* (Section 6.3.1), the thermal conditions in the repository and the bedrock are not expected to change during the assessment period in this variant.

6.3.4 Mechanical evolution

The description of the mechanical evolution in Section 6.2.4 are also considered to be valid for the *present-day climate variant*. Rock fall out will occur, but no damage to the concrete structures is foreseen due to the protective backfill material. As time progresses, the cumulative probability of an earthquake of a given magnitude increases.

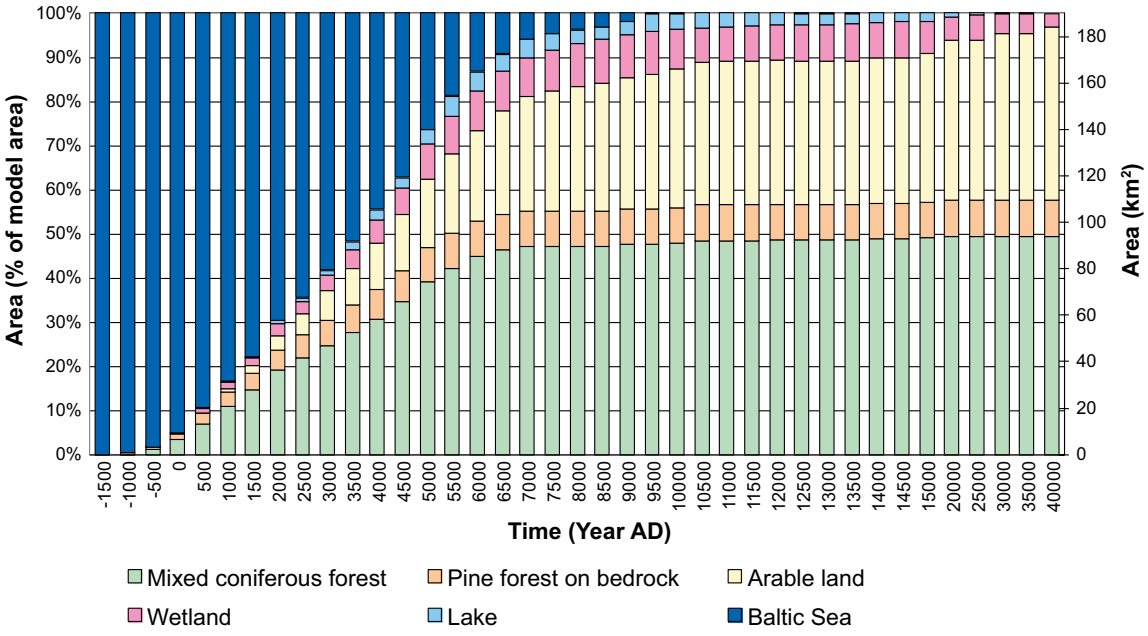

Figure 6-11. *Proportions of different ecosystems as a function of time, assuming intensive cultivation and present-day climate conditions. The time scale is in 500-year intervals from –1 500 AD (i.e. 1 500 BC) to 15 000 AD and 5000-year intervals from 15 000 AD to 40 000 AD.*

6.3.5 Hydrogeological evolution

As described in Section 6.2.5, the evolution of the hydrogeological system is driven by climate conditions and shoreline displacement. When the shoreline is located far away from the repository, its influence on the area for discharging groundwater flow becomes negligible. In the *present-day climate variant*, the climate conditions are assumed to remain constant for the entire assessment period, thus resulting in steady-state groundwater-flow conditions for the entire terrestrial period. In the regional hydrogeological modelling, fully steady-state flow conditions are reached about 9000 AD, when terrestrial conditions prevail in the entire model area. Steady-state conditions for the area relevant for flow paths from SFR1 and SFR3 are reached around 5000 AD (Figure 6-12). Groundwater flow through the waste vaults increases by two to three orders of magnitude from fully submerged to terrestrial conditions (Öhman and Odén 2018, Section 6.2). From 3500 AD to 5000 AD, only a minor increase in flow occurs. In the terrestrial period, particle tracking suggests that almost every particle released from SFR1 will emerge in a depression in the topography close to where deformation zones ZFMNNE0869 and ZFMNW0805A outcrop (Figure 6-12a, c, e; the locations of the deformation zones are indicated in Figure 6-3b). Particles from SFR3 mainly exit in the same depression. However, owing to the deeper location of SFR3, a number of particles from SFR3 discharge into lakes and streams further away from the repository (Figure 6-12b, d, f).

In addition, calculations with a large subhorizontal bedrock fracture located at shallow depth just north (downstream) of SFR have been performed. These calculations show more particles traveling longer distances than in the cases without a large subhorizontal fracture and a wider spread of the outflow locations. The likelihood of such a fracture however was estimated to be about 1 % based on stochastic generation of 1 000 realisations of the fracture network (Öhman and Odén 2017).

Future human actions may impact the groundwater flow system. Groundwater abstraction from a borehole may change the flow field in the vicinity of the borehole and lower the water table locally. The effects can extend for some distance from the borehole if it is drilled into a major permeable deformation zone, which is usually attempted to be able to abstract as much water as possible. If the repository is located within the zone of influence of a water-abstraction borehole (taking into account the effects of intersected fracture zones), then the flow through the repository may be affected by the abstraction. The construction of vaults, tunnels and shafts is likely to have a similar but greater effect on groundwater flow than water abstraction from boreholes. Activities that may affect groundwater flow are further discussed in the **FHA report**.

6.3.6 Geochemical evolution

During the period of terrestrial and temperate conditions, the groundwater changes from being brackish/saline to become slowly and increasingly influenced by meteoric water infiltrating. The timing of the transition to a complete dilute groundwater composition is however uncertain. When the area above the repository is terrestrial, meteoric water is expected to infiltrate, but this will likely occur relatively slowly.

A slower apparent dilution of the present brackish groundwater may also be the result of mixing with, or diffusion of, more or less saline groundwater-remnants in the rock (porewater and in fractures) occurring over time when meteoric water infiltrates. The most dilute brackish groundwater of the local Baltic Sea type is found at shallow depth down to 100 metres (Nilsson et al. 2011). When the ground surface above SFR is terrestrial, human activities such as drilling may influence the groundwater composition by mixing groundwaters with different hydrochemistries. Such induced changes in groundwater composition would then primarily affect the fracture-filling minerals and would not affect the rock matrix minerals to any significant extent within the assessment period.

The geochemical evolution of the groundwater at repository depth is the result of infiltration and geochemical processes from the surface of the domain to the repository. The infiltration occurs in an extended and complex network of deformation zones and fractures in which the infiltrating waters undergo geochemical reactions with the bedrock that may alter groundwater compositions over time. These rock–water interaction processes are relevant for determining the buffering capacity of the hydrogeological/geochemical system. Mass exchange between the transmissive zones and the low permeable matrix is simulated using a dual porosity approach (Román-Ross et al. 2014). The modelling assumes that the matrix is chemically inert as matrix diffusion processes are much slower than interactions with the fractured rock.

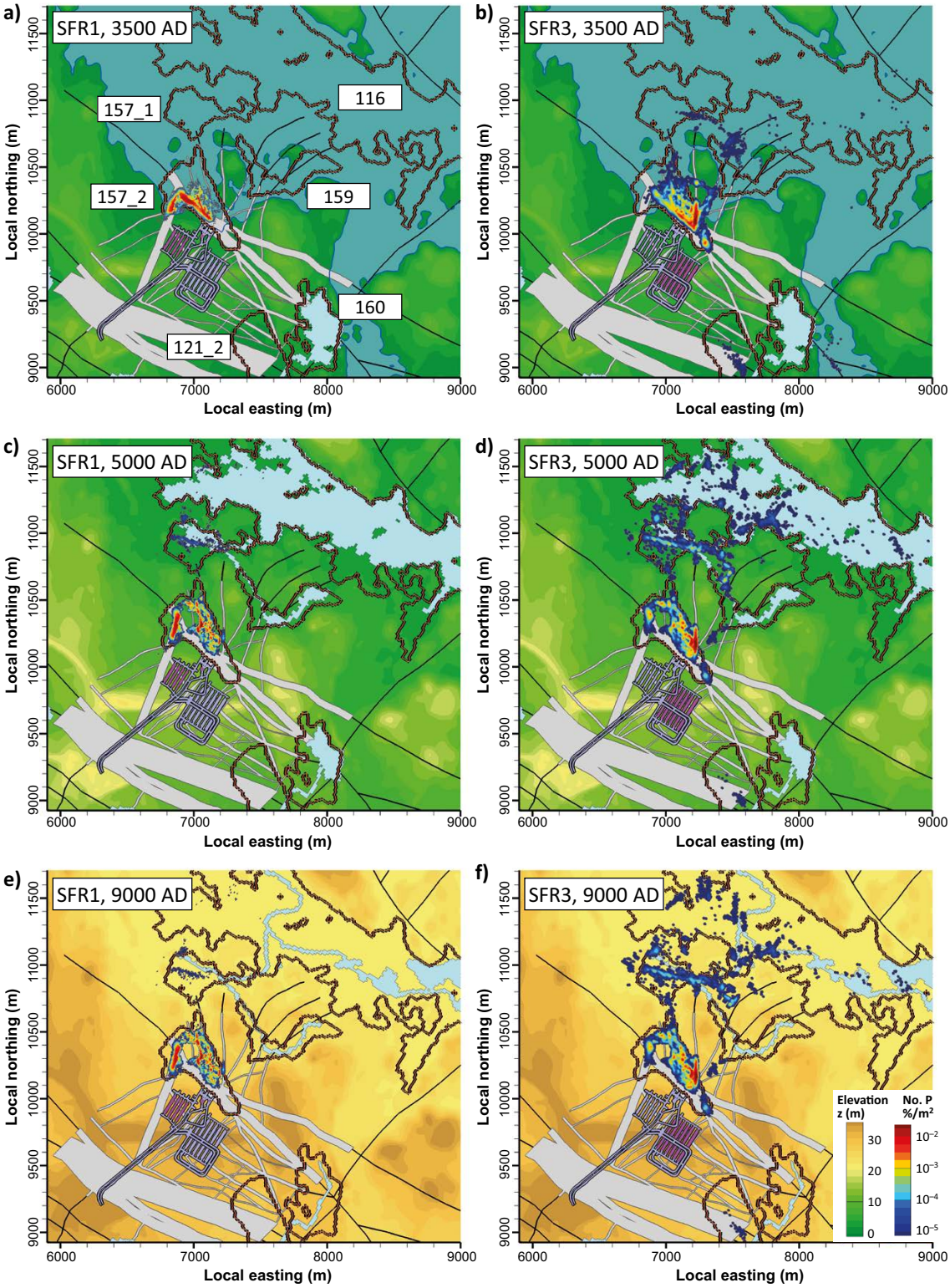

Figure 6-12. *Distribution of discharge to the surface systems from the SFR1 waste vaults (a, c and e) and the SFR3 waste vaults (b, d and f), based on density of particle exit locations (fraction of released particles/ surface unit) in the hydrogeological modelling (shading from blue to red). Results are shown for 3500 AD (a and b), 5000 AD (c and d) and 9000 AD (e and f). Waste vaults in SFR1 (panels a, c and e) and SFR3 (panels b, d and f) are indicated in magenta. Surface elevation above sea level is shown according to the elevation scale. The blue-grey colour indicates the sea and light blue areas specify lakes or streams. The grey areas indicate the thickness at ground surface of deformation zones that are represented in the SFR Regional domain of the hydrogeological model (Section 4.7.3). The black lines represent the location of deformation zones outside the SFR Regional domain. The orange contours and associated labels in (a) outline biosphere objects defined in Section 7.3.5. Figure is modified from Öhman and Odén (2018).*

Adjacent to and downstream the repository, high pH conditions may evolve in the surrounding groundwaters, originating from dissolution of the cement minerals in the repository (Section 6.3.9). The fracture geometry is considered to be unaffected by chemical processes such as dissolution and precipitation of fracture minerals and secondary formed mineral phases (**Geosphere process report**, Section 5.6). Changes in pH, ionic strength and possible changes in redox conditions of the groundwater may affect stability of colloids. However, since the natural colloidal concentrations in the geosphere are considered to be insignificant, the effect on colloidal-mediated radionuclide transport is of no concern for repository safety (**Geosphere process report**, Section 5.9.7).

The neutralisation of the high pH water in the geosphere has not been directly modelled. It is however expected that high pH cement leachate will be effectively neutralised by mixing with unaffected groundwater along flow paths in the geosphere within a relatively short distance from the repository (Crawford 2017). Thus, for the main part of the geosphere and the remainder of the assessment period in the *present-day climate variant*, pH < 10 is expected to prevail beyond the initial period of submerged conditions.

Dissolution/precipitation of fracture minerals may influence the groundwater composition and thus act as a buffer against acidification and changes in pH conditions. The expected groundwater composition under terrestrial temperate conditions in the *present-day climate variant* is given in Table 6-8.

Redox potential

Reducing conditions in groundwater are expected to prevail during the whole assessment period in the *present-day climate variant*. The reducing capacity as related to the content of iron-bearing minerals in terms of the valence state of the redox-pair Fe(II)/Fe(III) has been studied extensively both in groundwater and fracture minerals. For example, a study of divalent iron present in fracture minerals from Forsmark with an iron content with a minimum of 0.83 % and a maximum of 19 % (mean 9.9 %), indicates that 38 % to 66 % (25–75 percentile of maximum, by Mössbauer measurements) of all iron is in the divalent state Fe(II) (Yu et al. 2020). Even though the relative Fe(II) content in the fracture mineral is lower than in the rock, the Fe(II) concentration is higher, because the total content of Fe is higher in the fractures. The time required for exhaustion of all ferrous mineral in the matrix varies depends on the amount and surface area of the minerals, and the prevailing pore water composition in combination with the reactivity of the introduced groundwater given by pH, redox and ionic strength (in general). After the complete buffering from ferrous iron in fracture minerals, reducing capacity due to the presence of pyrite is modelled as maintaining reducing conditions in the geosphere with time (Román-Ross et al. 2014). Additionally, studies were performed to elucidate the content of divalent iron in fracture minerals of SFR to give an idea of its reducing capacity (Sandström and Tullborg 2011). The amount of reducing electrons, which is how the reducing capacity of the system is represented, gives an idea of the amount of oxidants that the system can buffer.

The overall microbial processes on-going in the bedrock contribute to the reducing conditions to a minor extent since the cell concentration and activity are projected to be very low. The microbial activity in the groundwater may be increased somewhat from otherwise low levels by a potential release of degraded organic components from the repository, but this is of minor importance for repository safety. Likewise, microbial activity is expected to be of minor importance after high-pH water from the repository has been somewhat neutralised by mixing with the near-neutral regional groundwater (**Geosphere process report**, Section 5.5).

The groundwater, initially similar to the present brackish marine groundwater, will successively become more and more dilute during prolonged temperate terrestrial conditions. The expected composition of the groundwater surrounding SFR can be simplified into ranges for an initial period and an extended period with more dilute groundwaters (Table 6-8).

Table 6-8. Expected composition of the groundwater surrounding SFR after the initial period of submerged conditions in the *present-day climate variant*. Table modified from Auqué et al. (2013).

	Reference composition	Range	Range
	For the initial period of temperate terrestrial conditions		For an extended period of temperate terrestrial conditions
pH	7.4	6.6–8.3	6.6–8.3
E_h (mV vs SHE)	–210	–135 to –300	–135 to –300
Cl^- (mg/L)	190	16–503	5–357
SO_4^{2-} (mg/L)	50	25–163	17–110
HCO_3^- (mg/L)	300	300–500	120–324
Na^+ (mg/L)	180	65–400	38–250
K^+ (mg/L)	5	5–15	2–5.3
Ca^{2+} (mg/L)	50	24–105	7–48
Mg^{2+} (mg/L)	12	7–24	2–13
SiO_2 (mg/L)	12	2–21	12–31

Organic complexing agents

See Section 6.2.6.

6.3.7 Near-field hydrological evolution

After terrestrial conditions have been established above the repository, the flow direction and the hydraulic gradient stabilise and can be assumed to be constant for as long as temperate conditions prevail. Once the shoreline has passed over the repository, the general groundwater flow direction in SFR1 and SFR3 gradually changes from vertically upward to horizontal and even locally downwards, see Figure 6-13 for SFR1.

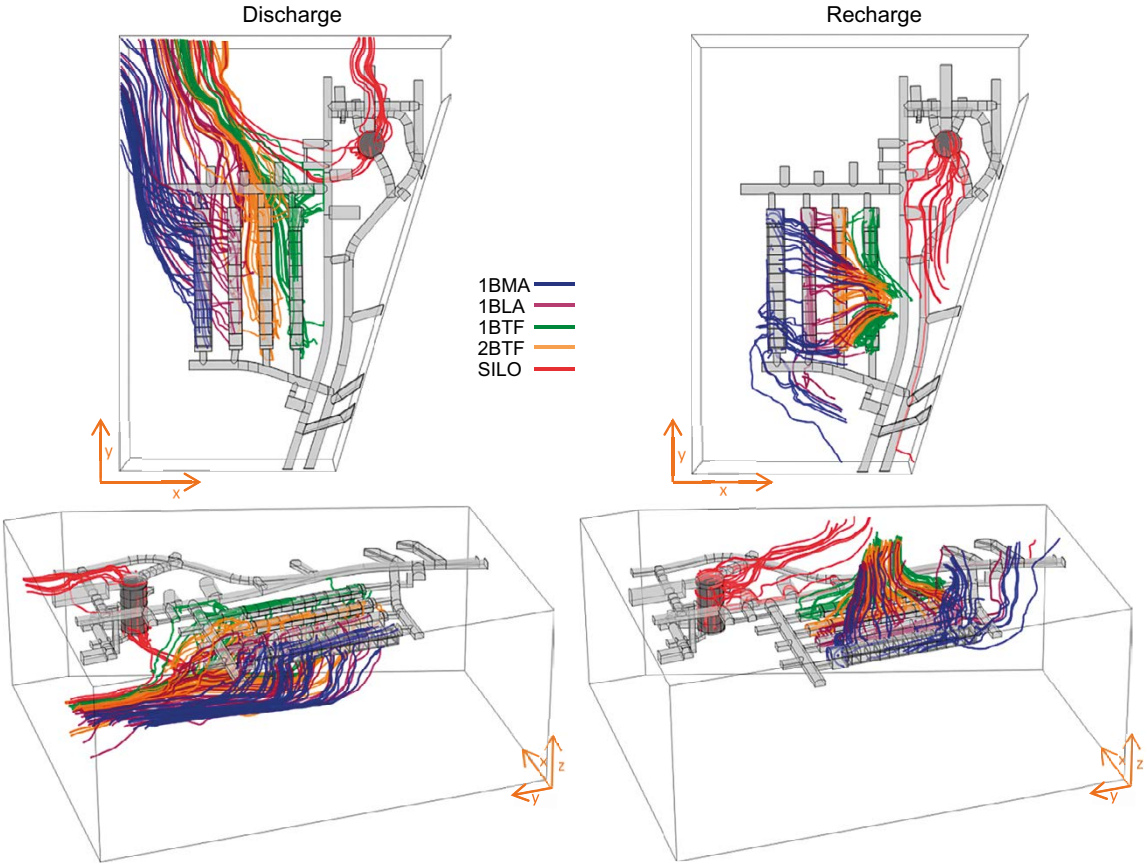

Figure 6-13. *Groundwater streamlines leaving (left) and reaching (right) individual vaults in SFR1 (colour tubes) at 5000 AD (Abarca et al. 2020).*

Concrete hydraulic barrier degradation

In the *present-day climate variant,* the evolution of the concrete barriers (described in Section 6.3.9) is expected to result in an increased hydraulic conductivity. The endpoints of the range of conductivities corresponds to the initial state of the concrete structures and a completely degraded state where concrete structures no longer constitute a hydraulic barrier (Abarca et al. 2013, 2020).

Degradation of sealed hydraulic sections of bentonite

In the reference evolution the hydraulic properties of the bentonite are considered constant throughout the analysis period (Section 6.3.9). However, the impact of the degradation of sealed hydraulic sections of bentonite on the groundwater flow through the repository has been studied by assuming that the sealed hydraulic sections no longer constitute a hydraulic barrier (Abarca et al. 2013, 2020).

As the sealed hydraulic sections degrade, groundwater flow is redistributed, and the preferential flow paths are along the access tunnels and the highly permeable backfill in the vaults. At the same time, flow decreases in the rock structures intersecting the vaults. The redistribution of flow is illustrated in Figure 6-14. The plot illustrates the increasing flows in the entire 1BLA vault and porous backfill of 1BMA. However, the BTF vaults, which exhibit the greatest increase in flow through the vaults as the sealed hydraulic sections degrade, display an increase in flow mainly in the loading areas, whereas flow through the waste domain decreases slightly.

6.3.8 Evolution of the waste and of the repository chemical conditions

At later times, following the initial period of submerged conditions, the chemical evolution is of importance for the release of radionuclides and other species, particularly with regards to sorption. The following description is a continuation of Section 6.2.8. The background and descriptions in Section 6.2.8 that are commonly valid for the entire assessment period are not repeated here.

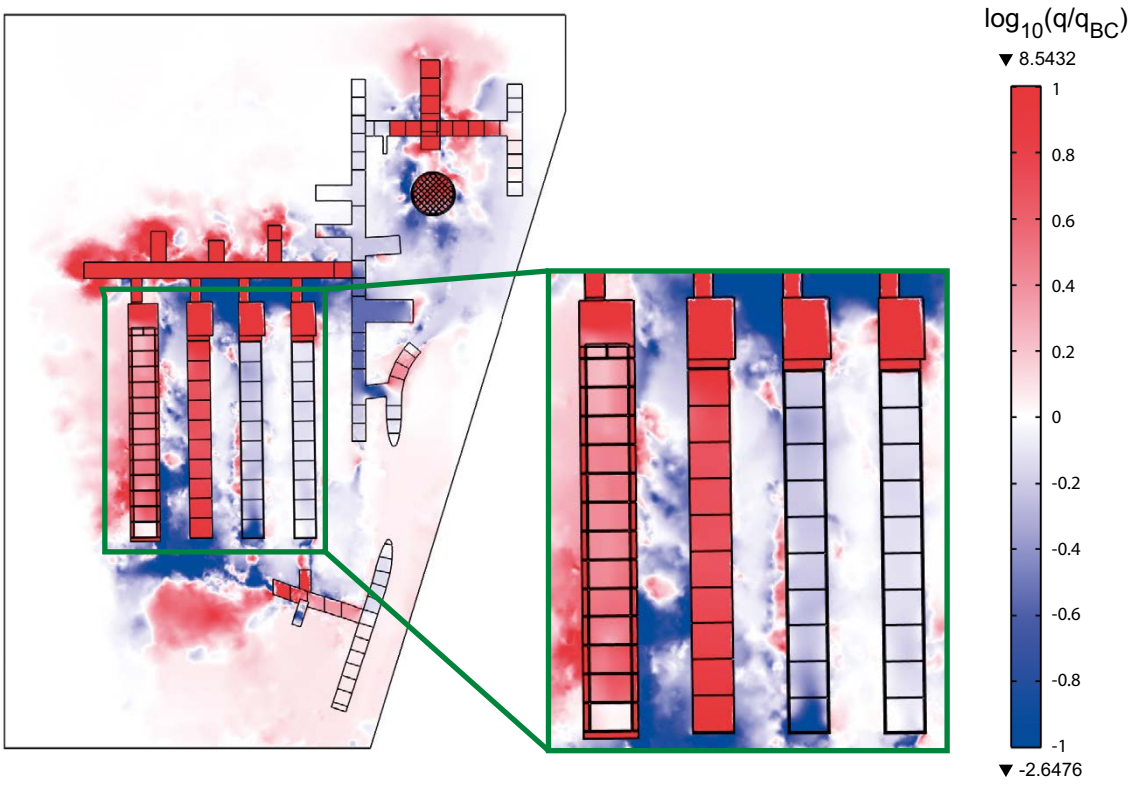

Figure 6-14. *Comparison of the logarithm of the ratio of the Darcy flux magnitude for completely degraded sections of bentonite and the initial state at the terrestrial position (5000 AD), in a horizontal cross section at 82.5 m depth. Values greater than zero indicate a higher flow in the case of completely degraded bentonite (adapted from Abarca et al. 2013).*

Among the few external changes that have a bearing on the chemical evolution is the fact that the groundwater after the initial submerged period is expected to be more dilute, see Section 6.3.6. The altered direction and magnitude of water flow due to shoreline migration is also of importance for some processes.

Waste form and packaging

Steel packaging

The steel packaging that has begun to corrode during the initial submerged period will continue to do so until the steel is fully corroded. Assuming uniform corrosion from two sides at a rate of 0.001–0.1 µm/a (Table 6-5), a steel mould of 5 mm thickness would be fully corroded within 25 000–2 500 000 years. In reality, the lower bound of this range is expected to be even shorter due mainly to the oxic corrosion that will have affected the steel packaging to some extent before anoxia has been reached in the repository.

Concrete packaging and cement matrices

Based on the calculations that have been carried out regarding leaching of concrete (Höglund 2001), the waste domain, concrete moulds and cement matrices are not expected to be subjected to significant leaching of cement components during the period up until 12 000 AD (end of the simulated study period) and for the silo vault up until 100 000 AD (Gaucher et al. 2005). However, it cannot be excluded that local mineral alteration at the surface of the concrete packaging can take place, see Cronstrand (2014, Section 6.2.8). See subsection *pH in waste leachate* below for more details including the period post 12 000 AD.

Bitumen waste matrices

All radionuclides and soluble salts are expected to have been released from the bitumen matrices during the submerged period (Section 6.2.8, subsection *Bitumen waste matrices*). However, if the integrity of bitumen matrices can mainly be maintained, for example if the surrounding steel packaging can contain the expanding bitumen waste matrix, salts and radionuclides may remain in bitumen matrices after 3000 AD and for thousands of years thereafter.

Ion-exchange resins and filter aids

Degradation of ion-exchange resins is initially not expected (Section 6.2.8). But, as the pH decreases with time, microbiological degradation may become increasingly viable. Sulfonate-type resins may produce sulfate which could affect concrete barriers or be transformed to sulfide by sulfate-reducing bacteria. Like most organic materials, microbial degradation into gases such as CO_2 and CH_4 is also possible (see further subsection *Microbiology* below).

Evaporator concentrates

The long-term effects of cement-degrading chloride and sulfate salts in 1BMA is described in detail in Höglund (2014) and accounted for in the evolution of cement porewater (subsection *Cement porewater* below) and of the concrete barriers (Section 6.3.9).

Trash and scrap metal

The metal corrosion and organic-material degradation described in Section 6.2.8 continues after the initially submerged period.

Water composition

Groundwater

When the shoreline has migrated past the repository, the groundwater flowing into the repository will be more dilute (non-saline) throughout the period. For details about the composition of the groundwater, see Section 6.3.6 and Table 6-8.

Cement porewater

The porewater composition follows the mineralogical evolution of the cement, where the pH is one of the most important aqueous parameters for post-closure safety. This is described in Section 6.2.8.

pH in waste leachate

The pH evolution is described in Section 6.2.8. After the submerged period, the pH will still be mainly determined by the leachate from cementitious materials in waste and barriers, with smaller influence from some waste materials. 1BRT and 1–5BLA are the only vaults where the pH falls below 12 within the assessment period, reaching ~10.5 in 1BRT and ~7.5 in 1–5BLA at the end of the assessment period (Table 6-4).

Dissolution and transport of dissolved species

Soluble species, including radionuclides, are expected to have leached out from bitumen waste packages during the submerged period (see subsection *Bitumen waste matrices* above). Due to higher conductivity and diffusivity, transport out of cement/concrete-conditioned waste is faster, but sorbing species are expected to be partly retained given their affinity to cement surfaces. In consequence, the most important fluxes during the subsequent period described in the present section are those occurring outside the waste packages, in the engineered barriers and macadam backfill, or vault void in 1–5BLA.

Colloids

See Section 6.2.8.

Redox potential

All aluminium and zinc are expected to be fully oxidised during the initial period, so steel is the dominant redox-determining material throughout the latter part of the *present-day climate variant* of the reference evolution, setting a low redox potential of about −0.75 V vs SHE (Duro et al. 2012b). The calculations by Hedström (2019a) based on cautious assumptions show that steel will remain throughout the entire assessment period in 1–2BMA, 1–2BTF, the silo, and 1BRT, assuming alkaline conditions and corrosion rates throughout (see Section 6.2.8, subsection *Redox potential*).

After all metallic steel in a vault is corroded, as is the case for the BLA vaults after a few thousand years after closure (Figure 6-6), the potential will increase but still be fairly reducing, as set by the incoming groundwater which holds an E_h of about −0.2 V (Section 6.2.6). Without reactive reductants such as steel, the vault redox potential becomes more sensitive to possible intrusion of oxidants. However, such intrusions are not expected under *present-day climate*, but could occur given other climate assumptions such as glaciations.

Radionuclide speciation

As the pH decreases, the speciation of some radionuclides may be affected, e.g. promoting $Ni(II)OH_2$ with lower solubility than $Ni(II)OH_3^-$ which is favoured at higher pH. This can influence the sorption coefficients for the affected elements (see subsequent subsection).

As per the previous subsection, the redox potential is expected to increase somewhat when steel is depleted. Tc(IV) and Se(−II) are then expected to increase their oxidation state to Tc(VII) and Se(IV). However, as noted above, this applies only to 1–5BLA within the assessment period wherein sorption is not credited.

Radionuclide sorption on solid materials

The evolution of the sorption coefficients during this period (**Data report**, Chapter 7) mainly responds to the evolution of cementitious materials (further described in Section 6.3.9), with decreasing porewater pH and altered mineralogical composition (Table 6-4). The sorption properties of bentonite and macadam are not expected to change noticeably during this period.

Organic complexing agents

During terrestrial conditions in the *present-day climate variant*, the concentrations of the highly soluble complexing agent NTA will decrease due to diffusive and advective transport out of the repository. The time when NTA has reached its no-effect concentration has been estimated to be between 4200 and 22 450 AD in different parts of the repository (Table 4-3 in Keith-Roach et al. 2021). ISA, however, is still being produced through at least the first part of the terrestrial period, while cellulose is still present and degrading. Since ISA sorbs to hydrated cement (Van Loon and Glaus 1998), it is also retained in the near-field over very long timescales.

These changes are reflected in the sorption reduction factors that quantify the impact of complexing agents over time (Keith-Roach et al. 2021).

Metal corrosion

Of the parameters affecting the corrosion rate (Section 6.2.8, subsection *Metal corrosion*), pH is the only one that significantly varies during the latter, terrestrial part of the reference evolution. The redox potential will be strongly reducing where steel is still present and moderately reducing elsewhere (subsection *Redox potential* above).

In most vaults, the pH remains highly alkaline (Table 6-4), so corrosion rates for alkaline, anoxic conditions are expected to be valid (Table 6-5). The main exception is in the BLA vaults where the pH decreases from 12.5 to ~9.0 during the period 3000–11 000 AD (Table 6-4). A pH above 9 is typically required for reliable passivation of steel surfaces (**Data report**, Section 5.1), so 1–5BLA will experience higher corrosion rates after 11 000 AD corresponding to non-passivating, near-neutral conditions, depleting the steel therein within a few millennia (Hedström 2019a). 1BRT also shows somewhat decreasing pH during the terrestrial period of the assessment, but never below pH 10.5 (Table 6-4). This is above the passivation limit, so corrosion is still expected to be slow in 1BRT, although associated with some uncertainty since the pH margin is smaller than for the other cementitious vaults.

Microbiology

As the pH of the system controls the microbial activity to great extent, extensive microbial activity will not occur until pH has dropped towards the optimum pH for microbial activity. Overall, the pH in the waste will be unfavourable for microbial activity during the assessment period for all vaults except the BLA and 1BRT vaults (Cronstrand 2014, Höglund 2018, 2019). Even in 1BRT the pH will not decrease below 11.5, see Table 6-4 and Figure 2-5 in Höglund (2018). The timescales on which microbial processes occur, is related to the amount of available nutrients and energy sources in the system. As regards the BLA waste vaults, the possibility cannot be excluded that microbial activity will be extensive. See further Section 6.2.8, subsection *Microbiology*.

Gas formation and transport

Gas formation due to corrosion

Following the initial period of submerged conditions in the *present-day climate variant*, it is foreseen that all aluminium and zinc will already be fully corroded and thus they will not produce additional gas. Anaerobic corrosion of iron in steel will be the dominating gas-producing process during this period, except in the BLA vaults after all steel is corroded (subsection *Metal corrosion* above) and microbial activity increases (see below).

Gas formation due to microbial activity

Microbial activity will increase as the pH decreases. Nevertheless, the pH in the waste will still be unfavourable for microbial activity during the assessment period. The exceptions are 1BRT and especially 1BLA where the pH will be about 10.5 after 7 200 years and the same as in the incoming groundwater after about 19 000 years. The BLA vaults also contain significant amounts of organic waste that can generate gases, unlike 1BRT.

Gas formation due to radiolysis

Gas formation due to radiolysis of water and organic materials will be lower during this period than the initial submerged period. It will decrease gradually, concomitantly with the decreasing activity in the waste due to decay and migration of radionuclides.

Calculated gas quantities

After all the aluminium has corroded, the gas generation rates are significantly lower. Following the initial period of submerged conditions in the *present-day climate variant*, gas generation is dominated by either degradation of organic material and/or steel corrosion. The gas production rates have been estimated to vary between 10 and 275 Nm^3/a between the different waste vaults in SFR1 (Moreno and Neretnieks 2013).

The rates in SFR3 are expected to be of similar magnitude as those in SFR1 (see further Section 6.2.8).

Gas transport

Gas transport through the porous material of the matrices will continue according to the description in Section 6.2.8.

6.3.9 Evolution of engineered barriers

Several internal and external processes are of importance for the post-closure safety of the engineered barriers in the repository. Shoreline displacement, as described in Section 6.2.1, has an impact on the groundwater flow which in turn has an impact on the barriers. The durability of the barriers is also affected by the interaction with the groundwater and naturally occurring solutes or agents formed by degradation of the waste in the groundwater (see also Section 6.2.8). Of these processes, leaching of portlandite and CSH gel caused by contact with groundwater is judged to have the greatest impact on the evolution of the barriers. Finally, the barriers may also be affected by pressure exerted by the waste and its packaging due to e.g. swelling waste.

Bentonite barriers in the silo

The montmorillonite component in the bentonite is gradually transformed to other minerals in contact with alkaline waters, see Section 6.2.9. Thermodynamic modelling of bentonite transformation in contact with high pH concrete leachate has been performed (e.g. Gaucher et al. 2005, Cronstrand 2007, 2016, Idiart et al. 2020). These four studies show different degrees of transformation. The two latest studies, that represent the current knowledge of the bentonite evolution, show that only a small part of the bentonite is affected during the first 30 000 years (Cronstrand 2016) and 100 000 years (Idiart et al. 2020). The transformation mainly happens at the contact between montmorillonite and concrete with philipsite being the main transformation product (Vidstrand 2015). Calcium silicate minerals, zeolites and new clays will form in the bentonite at the interfaces to the concrete silo and the shotcrete on the rock walls and roof.

The reactive transport modelling in Idiart et al. (2020) also indicates that the montmorillonite dissolution depths (extending from the bentonite-concrete interface into the bentonite) are limited compared to the thickness of the bentonite barrier. Taking this into consideration, it can be expected that local montmorillonite transformation does not affect the hydraulic properties of the bentonite barrier as a whole during the assessment period, i.e. the hydraulic properties of the bentonite can be considered constant during the entire assessment period.

The changes in porosity and mineral composition caused by the transformation processes are not expected to lead to higher diffusivities than for unaffected barriers. Regarding sorption, the values used are based on the occurrence of a sufficient fraction of montmorillonite for all time scales and the minerals likely to form, such as zeolites with generally high sorption of cations, are judged to have at least as good sorption properties as the original minerals (Rajec et al. 1999, Kyzioł-Komosińska et al. 2015). The values chosen for the unaffected bentonite barriers are, therefore, cautiously assumed to be representative for the entire assessment period.

Bentonite colloid formation

Even for the longest time frame considered in the post-closure safety assessment (up to 100 000 years after closure), sufficiently high Ca^{2+} concentrations are expected at the interface between bentonite and shotcrete to avoid the dispersion of clay and the formation of a clay sol (Gaucher et al. 2005). This process is therefore not deemed to have any significant impact on the design used in the silo. Based on these results, the safety assessment does not consider the possible impact on the bentonite from changes in groundwater composition.

Cement degradation in the concrete wall of the silo

No major changes in the volume/ porosity of the wall of the concrete silo are expected during the first 100 000 years or more after closure (Gaucher et al. 2005, Cronstrand 2007), see also subsection *Concrete barriers* below. Bentonite expansion/intrusion into the wall of the concrete silo can thus be neglected.

Concrete barriers

In this section, a description of the evolution of the concrete barriers based on the processes likely to affect the concrete barriers in the waste vaults (1BMA, 2BMA, 1BRT and 1BTF, 2BTF and the silo) in the *present-day climate variant* is presented.

General dissolution of the cement minerals and leaching

In the *present-day climate variant*, interaction with the groundwater leads to continued dissolution of the cement minerals and leaching of the dissolved species.

The evolution of mineral composition, pH and porosity in the concrete follows the general path as previously outlined in Section 6.2.9, subsection *Concrete barriers*. The main difference between the different waste vaults and between different parts of the concrete barriers within each vault is the time evolution of the composition, whereas the trend is expected to be basically the same regardless of waste vault. In Figure 6-15, the evolution of the mineral composition in the middle of the concrete barrier on the inflow side of a concrete caisson in 2BMA, is presented as a representative example for the concrete barriers in SFR (Höglund 2014).

As shown in Figure 6-15, the general trend includes first dissolution of the portlandite during a period with relatively constant pH (12.5) and porosity (about 11–13 %). This is followed by an incongruent dissolution of the CSH-phases from CSH_1.8 to CSH_0.8 and the final formation of large amounts of calcite. During this period, pH is reduced to about 10.5 and the porosity increases to about 25 % which taken together largely affect both transport and chemical properties of the concrete barriers.

Chemical interactions with species in the groundwater and substances leached from the waste

The evolution of the mineral composition of the concrete barriers in 2BMA shown in Figure 6-15 also illustrates effects of interactions between species in the groundwater and substances leached from the waste. Of interest here is the formation of rather large amounts of ettringite and thaumasite, two minerals which have greater molar volumes than the minerals they replace, hence potentially cause cracking of the concrete barriers.

However, as shown in Figure 6-15 changes in the amount of ettringite and thaumasite during the first 10 000 years is low and consequently also the risk of formation of cracks due to these processes. Significant changes in the amount of ettringite and thaumasite which could cause cracking first to occur during the period from 20 000 years up to about 70 000 years. However, as shown in Figure 6-15, the total porosity increases during this period which suggests that global cracking would be unexpected even though some minor local cracking could occur during this period.

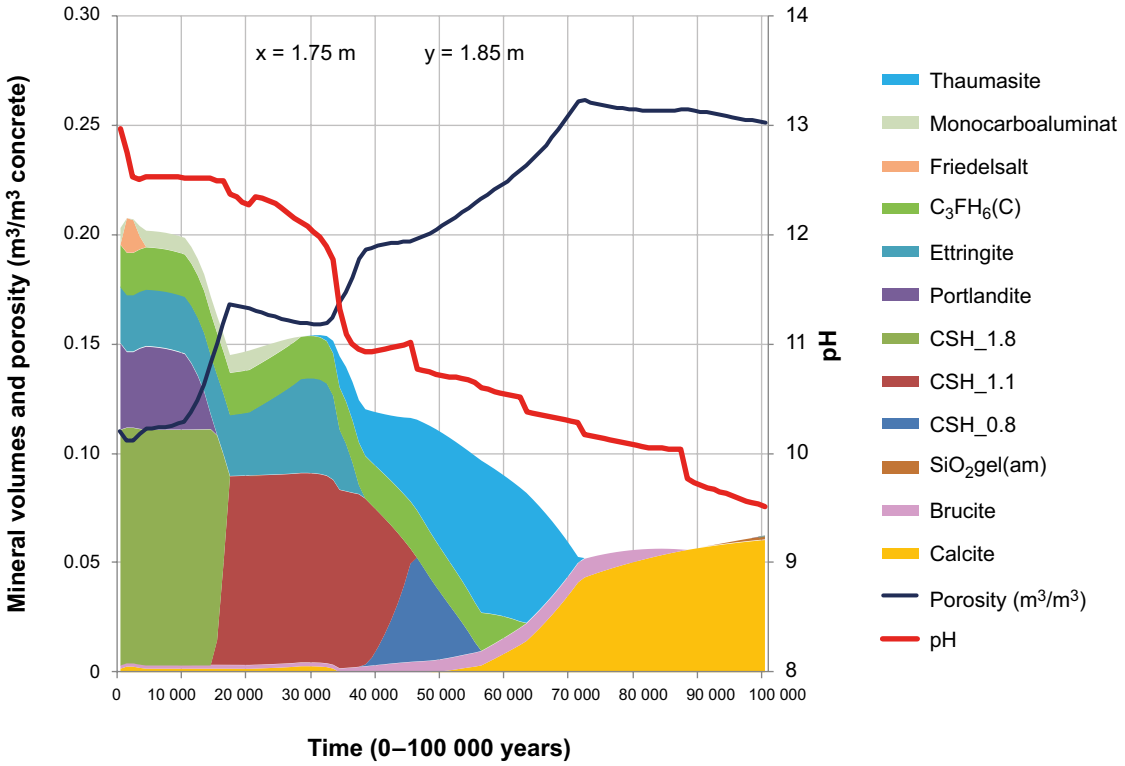

Figure 6-15. *Change in mineral volumes, pH and porosity over time in the middle of the most degraded concrete walls in 2BMA. Time is given in relation to the present, where 0 corresponds to 2000 AD (Höglund 2014).*

Impact of gas formation in the waste

From 1 000 years after closure and onward, gas-producing processes are expected to be slow in the *present-day climate variant*, dominated by steel corrosion since the easily degradable organic materials as well as Al and Zn are expected to already be consumed at this point (Section 6.2.8, subsection *Metal corrosion*). However, it is possible that minor amounts of metallic Al and Zn remain in more isolated parts of certain wastes with poor access to water, such as inside sealed steel containers that are not yet breached by corrosion.

During this period, gas transport can be facilitated through the engineered systems for gas release currently planned to be installed in the lids in the silo and 2BMA in combination with diffusion through the pore system of the concrete as well as transport in cracks and other permeable zones in the concrete structures. The risk for blocking of the sand-filled gas vents in the silo lid was investigated by Höglund and Bengtsson (1991) who concluded that the risk for blocking through the precipitation of calcite and brucite was unlikely and the function would therefore be ensured for an extensive period of time.

The risk for clogging of the gas vents in 2BMA (also including 1BMA and 1BRT in case it is decided to install gas vents also in these waste vaults) has not yet been evaluated because it has not yet been decided whether sand or a cementitious grout should be used to fill the gas vents. If sand is used, the findings of Höglund and Bengtsson (1991) indicate that clogging will be unlikely whereas the risk for clogging of vents filled with a cementitious grout as well as the impact thereof has not yet been explicitly studied. It should here be remembered that the impact of an internal gas pressure on the integrity of a concrete structure (risk of crack formation) is dependent on the original design of the concrete structure and extent of physical degradation and will therefore be unique for each individual concrete structure and degradation state.

In summary; in the *present-day climate variant*, gas production due to processes in the waste and barriers will be slow and the annual gas production low in all waste vaults in SFR. The need for a very efficient system for gas transport is therefore of less importance than during the first 1 000 years

after closure. In the vaults where systems for gas transport have been installed sufficient gas transport pathways through the barriers will most certainly prevail and ensure that high gas pressures that can cause the formation of cracks in the concrete barriers will not occur during this period. In vaults where no such systems have been installed – also including the concrete tanks in 1–2BTF – the gas transport capacity will be dependent on non-engineered solutions such as transport in the concrete pore system or through cracks and other permeable zones in the barriers. For that reason, the gas transport capacity in these vaults is associated with greater uncertainties.

Impact of material expansion

The formation of voluminous corrosion products due to corrosion of reinforcement bars and other metal components in the barriers is expected to cause the formation of zones conductive to water and gas through the barriers during this period.

According to current understanding crack formation due to corrosion of steel components in the barriers can only be avoided in 2BMA where the concrete barriers will not contain any metal components such as metal reinforcements.

For 1BMA, corrosion of steel within the existing barrier is likely to cause the formation of cracks and conducting channels in this part. However, the effects on the long-term properties have not yet been fully clarified. This is because the method for repairing the concrete barriers in 1BMA including strengthening of the walls as well as sealing of cracks, has not yet been decided upon. According to current requirements, restoration should utilise such methods that the negative effects of steel corrosion in the existing part of the barrier are avoided. The anticipated measures are described in the closure plan for SFR (Mårtensson et al. 2022) and in references therein.

In addition, the silo contains large amounts of steel reinforcement bars which eventually will corrode, even though the rate of corrosion will be restricted by the slow transport of water through the bentonite barriers surrounding the silo and the high pH in the concrete which is expected to prevail for the entire period. The formation of hydraulically conducting channels is less likely in the outer silo wall due to the lack of tie rods in the concrete structure.

In 1BRT, corrosion of the segmented reactor pressure vessels and the reinforcement bars in the concrete structure is expected to cause the formation of voluminous corrosion products and the formation of cracks in the concrete structure is therefore expected. However, this is not expected to affect the chemical evolution of the concrete barrier.

Finally, the concrete tanks in 1–2BTF contain various metal components embedded in the concrete walls which will corrode in the *present-day climate variant*. For that reason, it is anticipated that the concrete tanks in 1BTF and 2BTF will lose their integrity during this period. However, even cracked concrete will have remaining sorption capacity as long as there are cement minerals remaining.

In summary, in the *present-day climate variant*, local cracking due to metal corrosion is expected to occur in all concrete structures containing metal components or metallic waste. The effects of this on the hydraulic properties of the concrete structure are, however, dependent on the other components in the barrier system. The effects of swelling of organic waste on the properties of the concrete barriers in the different waste vaults are expected to be mitigated by the use of different engineered solutions, conditioning methods and waste deposition strategies used in the different waste vaults.

Impact of local dissolution and leaching

In the *present-day climate variant*, local dissolution of the cement minerals and leaching in the vicinity of cracks will affect the mineral composition, and porosity of the concrete as well as the pH of the cement pore water in these areas.

The effect of local leaching processes could be the formation of a portlandite-depleted zone in connection with existing cracks, but eventually this zone may be depleted from all its cement minerals which can be cautiously regarded as an effective widening of the crack.

As the mineral-depleted zone near the crack expands, the zone will eventually propagate throughout the entire concrete barrier. This may lead to an increased hydraulic conductivity in this zone, and thus result in a more localised flow through the concrete barrier. For a concrete structure where flow is localized to a few major cracks the breakthrough time for radionuclides becomes reduced. The impact of cracks on the transport of radionuclides through a concrete structure is further discussed in the **Radionuclide transport report**, Appendix B**.**

The rate and effect of local dissolution of the cement minerals and leaching is dependent on the width of the original crack. For cracks with apertures less than 0.1 mm, the water flow rate is sufficiently low to ensure that local dissolution will not occur during the first 20 000 years after closure (Höglund 2014). Eventually, though, the process will lead to the formation of wider cracks and the hydraulic conductivity of the concrete barriers will increase with a reduction of retaining capacity as a consequence. For the silo, this process will be much slower due to the flow-restricting properties of the bentonite surrounding the concrete structure.

For the concrete tanks in 1–2BTF, the local degradation due to leaching in cracks will eventually cause a significant change of the transport properties of the concrete tanks with a reduction in retaining capacity as a consequence.

In summary, in the *present-day climate variant*, widening of existing cracks through local dissolution and leaching will alter the chemical and hydraulic properties of the concrete barriers in SFR. The effect of this process will be more significant for the concrete tanks in 1BTF and 2BTF than for the other concrete barriers due to the comparatively thinner walls involved. For the silo, this effect is expected to be much slower and thus have a milder influence on the properties of the concrete structure whereas the effects are intermediate for 1–2BMA and 1BRT which are not protected by a bentonite barrier.

Cracking due to freezing of the concrete pore water

Cracking of the concrete barriers due to freezing of the concrete pore water will not occur in the *present-day climate variant*. This is because temperate climate conditions will prevail and freezing of the concrete pore water will thus not occur.

Cracking due to loss of load-bearing capacity

Cracks may form if the mechanical loads, i.e. from the backfill material, exceed the load-bearing capacity of the concrete structure. The leaching of cement minerals and loss of function of the reinforcement bars will, with time, reduce the load-bearing capacity of the concrete structures. The consequence of this process is dependent on the design of the structural part, the extent of degradation and the direction and magnitude of the loads to which it is exposed.

Backfill material

In the *present-day climate variant*, groundwater flow in the bedrock and in the backfill may cause an accumulation of fine-grained material in the backfill. This could lead to a slight reduction of the hydraulic conductivity of the backfill and a slight increase of groundwater flow through the waste. However, the effect of backfill clogging is expected to be minor compared to the processes affecting the hydraulic properties of the concrete structures themselves.

Studies (Anderson et al. 2006a, b) have shown that, even in low-nutrient environments such as granite, bacteria can form biofilms that may contribute to clogging and decreasing hydraulic conductivity and induce mineral precipitation. However, in the repository zones where pH remains above 12 for thousands of years, clogging due to microbial activity is not likely since microbial processes will be very limited as both activity and diversity decrease the more extreme the conditions. Pedersen et al. (2004) observed slow growth, low cell numbers and low metabolic activity in the alkaline springs of Maqarin, further supporting the assumption that microbial activity will be low during the alkaline phase of cementitious repositories.

Summary of the reference evolution of the engineered barriers in the present-day climate variant

In this section, the reference evolution for the different rock vaults in SFR in the *present-day climate variant* has been described. The following summarising conclusions can be drawn:

Silo: The concrete in the silo will undergo the same alteration as the concrete structure in 1BMA; see below. However, because of the presence of the bentonite layer surrounding the silo, the process will be much slower than in 1BMA and the hydraulic and chemical properties of the concrete barrier in the silo will therefore retain their initial status for a longer period than the concrete structure in 1BMA. Additionally, the combined effects of the concrete and bentonite barriers will restrict flow through the waste during a longer period than for the other waste vaults in SFR. Finally, as leaching will progress much slower, the mineralogical changes of the concrete will be slower than in the other concrete structures in SFR which are not protected by a bentonite barrier.

1BMA: In the *present-day climate variant*, the combined effects of several different processes will affect the chemical and hydraulic properties of the concrete barriers. Dissolution and leaching of the cement minerals will affect both the sorption capacity as well as the porosity of the concrete. Widening of existing cracks or the creation of new ones will increase the hydraulic conductivity of the concrete barriers with an increase in advective transport through the barriers as a consequence. During this period, cracks may also start to form due to corrosion of metals embedded in the concrete. The extent of this process is, however, difficult to determine as the method for restoration of the concrete barrier has not yet been finally determined. Of most importance for the hydraulic properties of the concrete barriers is the risk of extensive cracking due to loss of load-bearing capacity.

2BMA: See 1BMA but note that corrosion of metals embedded in the concrete will not be an issue.

1BRT: See 1BMA. Cracks may start to form due to corrosion of tie rods or reinforcement bars.

1–2BTF: The concrete tanks in 1–2BTF will undergo the same alterations as the concrete structure in 1BMA; see above. However, as the walls in the concrete tanks are much thinner than the concrete structure in 1BMA, the effects of these processes will be more significant. During the assessment period, the concrete tanks will become severely degraded. Sorption may, however, still occur as long as cement minerals are present.

1–5BLA: There are no engineered barriers in 1–5BLA.

6.4 Warm climate variant

This section describes the *warm climate variant* of the reference evolution from the termination of the initial submerged period, in this case occurring 4 500 years after closure, to the end of 100 000-year assessment period. The characteristics of the submerged period in the *warm climate variant*, as well as the reference evolution of the repository system during this period, is described in Section 6.2.

The anthropogenic greenhouse-gas emissions envisaged in this variant are expected to have a noticeable effect on the climate during the first half of the assessment period, whereas the effect is expected to be smaller during the latter half (**Climate report**, Section 3.4.5). Differences in external conditions between the *warm climate variant* and the *present-day climate variant* are therefore only relevant for the first half of the assessment period. These include:

- Higher air temperatures.
- Increased annual precipitation, whereas precipitation during the summer season may either increase or decrease.
- Longer initial duration of submerged conditions.

In this section, the reference evolution of the SFR repository system is only described for components that are considered to be significantly affected by these changes in external conditions. For remaining components, the descriptions of the reference evolution for the *present-day climate variant* are also considered valid for the *warm climate variant*.

6.4.1 External conditions

The *warm climate variant* assumes that anthropogenic greenhouse-gas emissions comparable to present levels will continue for the next few decades, after which they gradually decline towards net-zero emissions by the beginning of the 22nd century. To this end, this variant represents a likely development in line with the IPCC medium emissions scenarios RCP4.5 and RCP6.0 as well as recent projections of business-as-usual anthropogenic greenhouse-gas emissions (**Climate report**, Section 4.2). Most modelling studies of the long-term future climate evolution project that the current interglacial will be prolonged for at least 100 000 years under these levels of emissions (**Climate report**, Section 4.3). As a result, similarly to the *present-day climate variant* (Section 6.3.1), the *warm climate variant* is characterised by temperate climate conditions at Forsmark for the complete assessment period (Figure 6-1).

In the *warm climate variant*, the elevated concentrations of CO_2 and other greenhouse gases in the atmosphere result in a considerably warmer climate than in the *present-day climate variant*. Specifically, the mean annual air temperature at Forsmark is considered to increase by a maximum of 5 °C above the present level within the current millennium, after which it will slowly decline over the following tens of thousands of years (**Climate report**, Section 5.2.2). Annual precipitation is projected to increase with higher temperatures, with a maximum increase of 10–20 % relative to present-day for a 5 °C warming at Forsmark (**Climate report**, Section 3.4.4). The range represents an uncertainty in the precipitation response during the summer months (June to August) where the lower value of the range corresponds to a decrease in the summer precipitation compared to present, whereas the higher value corresponds to increased summer precipitation (**Climate report**, Section 5.2.2). Due to increased air temperatures, the annual potential evapotranspiration is also expected to increase. In the *warm climate variant*, the maximum increase in potential evapotranspiration, resulting from a 5 °C warming, is estimated to be ~34 % (**Climate report**, Section 5.2.2).

The *warm climate variant* is structurally similar to the extended global warming climate case which was included in the reference evolution in the SR-PSU (SKB TR-14-01, Section 6.2.1). Both developments describe warmer-than-present climate conditions with 100 000 years of temperate conditions at Forsmark, as well as a prolonged submerged period (Section 6.2).

6.4.2 Evolution of surface systems

A warmer climate mainly affects the development of the regolith and topography, the near-surface hydrology and the ecosystems. For the remaining components of the surface systems, the development under a warmer climate is broadly consistent with the description under the *present-day climate variant* (Section 6.3.2).

Development of regolith and topography

In a warmer climate, the landscape development and the resulting regolith stratigraphy and topography is expected to be substantially similar to the development in the *present-day climate variant* (Section 6.3.2), except for a temporal delay due to a later shoreline regression.

Development of near-surface hydrology

The influence of a warmer climate on surface hydrology was investigated using the 5000 AD hydrological model (Sassner et al. 2022). The hydrological simulations were based on the climate conditions described for the *warm climate variant* (Section 6.4.1). Thus, in one simulation, higher precipitation than at present was assumed for all seasons and a second simulation assumed higher precipitation for the winter, spring and fall seasons but lower precipitation for the summer season. In short, the *warm climate variant* is characterised by more annual precipitation and a higher potential evapotranspiration than that of the *present-day climate variant*. According to the hydrological model, the increased precipitation does not compensate for the higher evapotranspiration in a warmer climate. This results in a higher average water deficit (i.e. the potential evapotranspiration increases more than the precipitation) at the ground surface compared with model results using the *present-day climate variant* climate data. The influence of the warm climate is particularly large on the surface and near-surface water flow, but less so for deeper groundwater flow (Sassner et al. 2022).

Ecosystem development

Changes in limnic ecosystems under a warmer climate affect both abiotic (e.g. ice cover, mixing, carbon dioxide and oxygen concentrations) and biotic factors (e.g. biomass and production), but limited effects on radionuclide transport and exposure are expected (see further the **Biosphere synthesis report**, Section 4.5.2). For terrestrial ecosystems, a warmer climate is typically associated with increased biomass and net primary production, including higher production of crops (Chapin et al. 2002, BACC 2008). Potential plant functional types under warmer climate conditions were simulated with the dynamic global vegetation model LPJ-GUESS (Sitch et al. 2003). The modelling result suggests that Forsmark would be dominated by broad-leaved trees, with a larger biomass but with a net primary production similar to that of today. Other modelling approaches, e.g. BACC (2008), suggest that, in forests, both the productivity and the biomass increase in response to a warmer climate.

6.4.3 Thermal evolution

A warmer climate is also expected to result in higher temperatures in the bedrock and the repository. However, as argued in the *cold climate variant* (Section 6.5.3), the temperature change at repository depth is expected to be less than in the air or at the ground surface. No process relevant for the integrity of the repository has been identified that could be impacted by such a small temperature increase.

6.4.4 Mechanical evolution

See Sections 6.2.4 and 6.3.4.

6.4.5 Hydrogeological evolution

No regional hydrogeological modelling has been performed for the *warm climate variant*. The longer submerged period implies that hydraulic gradient across the repository is close to zero for a longer period of time and that the increased groundwater flow occurs later than in the *present-day climate variant*.

The assumed 10–20 % increase in precipitation and the ~30 % increase in potential evapotranspiration (Section 6.4.1) would result in a slight decrease in the potential infiltration rate, which could translate to slightly lower groundwater gradients. This would result in slightly lower groundwater flow rates through the waste vaults and in the bedrock surrounding the repository, but no significant changes to the groundwater flow direction.

6.4.6 Geochemical evolution

The geochemical evolution from the termination of the initial submerged period to the end of the 100 000-year assessment period is expected to be similar to that described for the *present-day climate variant* (Section 6.3.6).

A warmer climate is not expected to influence the geochemical properties of the rock matrix to any significant extent. An extended increase in temperature may affect the mineral reactions and influence the solubility of chemical components in the fracture groundwater by, for instance, increasing the ionic strength and thus leading to a decrease in solubility of dissolved elements in the fracture water. Increased infiltration of dilute meteoric water with lower ionic strength due to increased atmospheric precipitation may influence the fracture minerals to minor extent. Increased evapotranspiration may on the other hand increase the drawdown of infiltrating waters and decrease groundwater residence time. These effects are, however, expected to be minor and thus the groundwater composition in the *warm climate variant* is expected to follow that of the *present-day climate variant* described in Section 6.3.6 and as given by the range of the groundwater composition in Table 6-8.

6.4.7 Near-field hydrological evolution

The near-field hydrological system has a similar dependence on climate variations and shoreline displacement as the hydrogeological system, that is, in the *warm climate variant* the shoreline regression is assumed to be delayed by 3 500 years. Thus, a longer initial period of submerged conditions with lower groundwater flow is expected.

A warmer climate than at present is not expected to influence the hydraulic properties of the engineered barriers. Hence, concrete barrier degradation in the *warm climate variant* follows that of the *present-day climate variant* described in Section 6.3.7.

6.4.8 Evolution of the waste and of the repository chemical conditions

The thermodynamics of most chemical processes depend on the temperature and faster kinetics are generally favoured by increasing temperature; portlandite dissolution is an exception due to its retrograde solubility. However, the temperature sensitivity is small for the processes and temperature ranges relevant to SFR, so the minor possible repository-temperature increase due to a warmer climate (Section 6.4.3), is not sufficient to noticeably affect the evolution of the waste or the chemical conditions. Thus, the same evolution as described in Section 6.3.8 is applicable in the *warm climate variant* of the reference evolution.

6.4.9 Evolution of engineered barriers

The thermal (Section 6.4.3), mechanical (Section 6.4.4), hydrological (Section 6.4.7) and chemical (Section 6.4.8) conditions in the repository are not expected to differ significantly between the *warm climate variant* and the *present-day climate variant*. Therefore, the evolution of the engineered barriers in the *warm climate variant* of the reference evolution is considered to follow that of the *present-day climate variant* (Section 6.3.9).

6.5 Cold climate variant

This section describes the *cold climate variant* of the reference evolution from the termination of the initial submerged period, in this case 1 000 years after closure, to the end of 100 000-year assessment period. The description of the initial submerged period in the *cold climate variant*, as well as the reference evolution of the repository system during this period, is described in Section 6.2.

The *cold climate variant* assumes strong mitigation of current climate change within the next few decades (Sections 6.1 and 6.5.1), resulting in slightly warmer temperatures (< 2 °C) than in the *present-day variant* during the first thousand years after closure (**Climate report**, Section 3.4.4). However, as a warmer-than-present climate is already accounted for in the *warm climate variant*, the same climate conditions as in the *present-day climate variant* are for simplicity assumed during temperate conditions in the *cold climate variant*. Thus, the only difference in external conditions between the *cold climate variant* and the *present-day climate variant* relevant to post-closure safety is that the former includes periods of periglacial conditions in the latter half of the assessment period (Figure 6-1). The descriptions in this section therefore exclusively focus on the evolution of the repository system under periods of periglacial conditions at Forsmark.

These periods are characterised by the development of permafrost, defined as ground temperature that drops below 0 °C for at least two consecutive years (e.g. French 2007). As a result, permafrost does not always equate to frozen conditions in the bedrock, since, depending on the ambient pressure, chemical composition of the groundwater and on adsorptive and capillary properties of ground matter, water in the ground may freeze at temperatures below 0 °C (**Climate report,** Section 2.1). However, given the relatively shallow depths of the SFR repository and the low salinity of the groundwater at Forsmark, the difference between permafrost and frozen ground is small. In consequence, permafrost and frozen conditions are used interchangeably in this section, such that if "permafrost" is used, it is implicitly meant that the conditions are frozen.

6.5.1 External conditions

The *cold climate variant* represents a future development characterised by substantial reductions in anthropogenic greenhouse-gas emissions and/or removal of atmospheric CO_2 by technological measures. Under these developments, atmospheric CO_2 is projected to have returned to pre-industrial

levels within the first 50 000 years after closure (**Climate report**, Sections 3.4.1 and 4.3), resulting in the growth of Northern Hemisphere ice sheets in response to the next substantial minimum in summer insolation around 56 000 AD (**Climate report**, Section 3.4.5).

It is important to note that glacial inception in the Northern Hemisphere does *not* necessarily mean that the Forsmark site will be glaciated. Initial ice accumulation typically occurs in Arctic or sub-arctic high-altitude regions, such as the Scandinavian Mountain Range. Following this initial phase, it may take up to several tens of thousands of years for an ice sheet to grow sufficiently large to reach south-central Sweden (**Climate report**, Section 3.2) and the Forsmark area. Thus, although it cannot be excluded, it is considered unlikely that an ice sheet will reach the Forsmark site following the insolation minimum at 56 000 AD (**Climate report**, Section 4.4). Instead, build-up of ice sheets elsewhere in the Northern Hemisphere will likely induce further cooling of the climate at Forsmark too, resulting in periglacial conditions and permafrost development in the region (**Climate report**, Section 4.3). As a result, the *cold climate variant* includes the occurrence of periglacial conditions and permafrost development at Forsmark during the latter half of the assessment period (Figure 6-1).

The evolution of climate domains in the *cold climate variant* is structurally similar to the global warming climate case included in the reference evolution in the SR-PSU (SKB TR-14-01, Section 6.2.1). As in the *cold climate variant*, the SR-PSU global warming climate case also described temperate conditions for the first 50 000 years, followed by colder climate conditions with recurring periods of periglacial conditions during the last 50 000 years of assessment period. The timing and duration of each period with periglacial conditions in the SR-PSU global warming climate case were primarily inferred from reconstructed conditions of the Weichselian glacial cycle (SKB TR-13-05, Section 4.1). Whilst these data yield information on the climate development during the last glacial cycle (past 120 000 years), they are not representative for the next 100 000 years when external conditions related to e.g. insolation changes will be very different compared to the past 120 000 years (**Climate report**, Section 3.4.5). In consequence, the methodology for estimating the timing and duration of future periglacial periods has been updated since the SR-PSU. In the present safety assessment, these periods are derived from modelling of the long-term future climate at Forsmark by Lord et al. (2019) (**Climate report**, Section 5.2.3). Based on air temperature data from that study, periglacial conditions at Forsmark are estimated to occur from 61 000 AD to 69 000 AD and from 81 000 AD until the end of the assessment period (Figure 6-1).

6.5.2 Evolution of surface systems

As with a warmer climate (Section 6.4.2), a periglacial climate is considered to mainly affect the near-surface hydrology and ecosystems. For the remaining components of the surface systems, the development under warmer climate conditions is considered to be broadly consistent with the description under the *present-day climate variant* (Section 6.3.2). This also includes the landscape development as all lake-mire systems in the area above the repository are considered to have reached a mature state before periglacial conditions occur at 61 000 AD (Section 6.3.2).

Development of near-surface hydrology

Periglacial conditions influence the hydrology and were described and analysed by Werner et al. (2013). Periglacial environments are typically characterised by permanently frozen ground that controls the general distribution and routing of surface water across the landscape. There is a relatively short hydrologically active period in the spring and summer months. At the top of the permafrost there is a relatively thin, hydrologically active layer which undergoes a seasonal freeze-thaw cycle. A large part of the snowmelt occurs when the active layer is still frozen thus preventing infiltration of surface water into the regolith and bedrock. Once the active layer thaws, it is quickly water-saturated, which promotes ground-surface storage, pond formation and surface-water runoff. In discontinuous permafrost, most groundwater recharge is assumed to occur via through taliks that connect the unfrozen groundwater flow system under the permafrost to the active layer at the ground surface (Figure 6-16). In a periglacial environment without frozen conditions near the surface, groundwater flow in the uppermost regolith is the largest part of the total runoff, whereas with frozen conditions the surface runoff makes the largest contribution to total runoff.

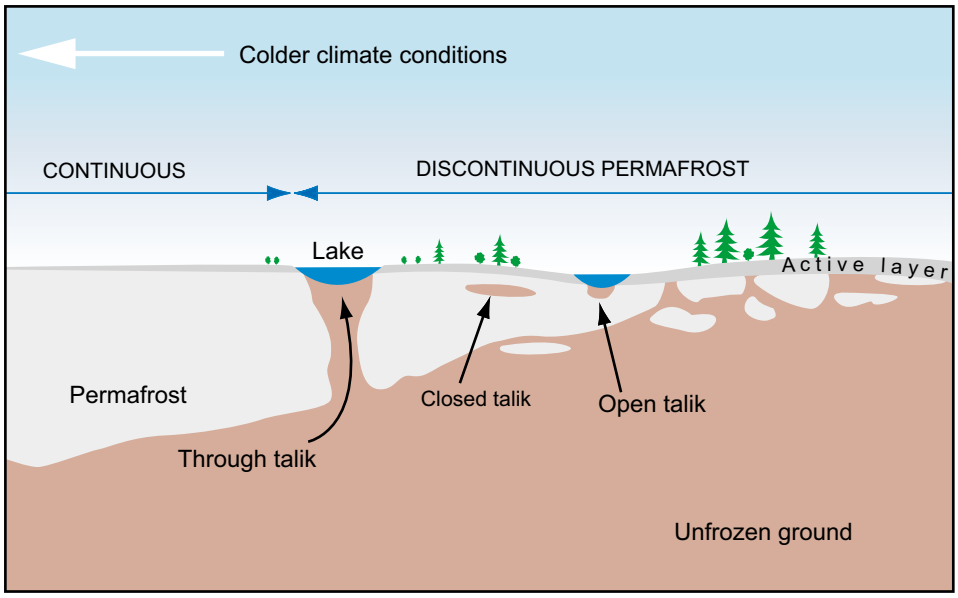

Figure 6-16. *A schematic profile through a permafrost area with an active layer and different types of taliks (Bosson et al. 2010).*

The spatial distribution of taliks in periglacial landscapes is influenced by several factors, including air temperature, topography, snow cover, availability of water bodies and vegetation (Johansson et al. 2006, Hartikainen et al. 2010). Discharge taliks (or through taliks) are typically formed below lakes. Results from regional hydrogeological modelling suggest that groundwater from the extended repository could be discharged to large future lakes in Öregrundsgrepen (Section 6.5.5). Furthermore, mire vegetation might inhibit permafrost development and discharge taliks below mires cannot be excluded (Cohen-Corticchiato and Zwinger 2021).

Ecosystem development

Expected changes in limnic ecosystems under periglacial conditions include decreased production and biomass of primary producers and fish (**Biosphere synthesis report**, Section 4.5.3). With sufficiently reduced air temperatures, terrestrial systems will eventually change from temperate or boreal to more tundra-like ecosystems. This will lead to a lower primary production and biomass in both forested taiga and tundra peatlands. The areas that have been classified as mires during periods of temperate conditions will likely be mires also in a periglacial landscape. A lower mean annual temperature will reduce the yield of crop production and dramatically change the potential for cultivation. For a detailed discussion on terrestrial ecosystems and how they are expected to change under different climate conditions, see Löfgren (2010); a summary is provided in Lindborg (2010).

6.5.3 Thermal evolution

The thermal evolution within the repository is primarily determined by the temperature in the surrounding bedrock and groundwater, which is in turn controlled by the climate. For permafrost and frozen conditions to develop in the bedrock, modelling studies suggest that the annual average air temperature, at a minimum, needs to drop below freezing (Hartikainen et al. 2010, Brandefelt et al. 2013). The colder climate during periglacial conditions emerges from the combination of a relatively low atmospheric CO_2 concentration and a reduced insolation during the boreal summer season, resulting in the growth of ice sheets elsewhere in the Northern Hemisphere (Section 6.5.1). These global-scale changes naturally are associated with considerable uncertainties, resulting in a wide range of possible air temperatures that could influence the development of permafrost and frozen conditions at Forsmark. For example, it has been estimated that permafrost development in response to the insolation minimum at 56 000 AD could be accompanied by air temperatures at Forsmark ranging from approximately −11 °C to −1 °C, depending on e.g. atmospheric greenhouse-gas concentrations and Northern Hemisphere ice cover (Brandefelt et al. 2013).

Owing to the late onset of periglacial conditions at 61 000 AD, potential freezing of concrete pore water in the repository is expected to be less important for the hydraulic properties in the concrete compared to other degradation mechanisms (Section 6.5.9). The thermal evolution in the bedrock in response to the uncertainty in air temperature was investigated in simulations by Brandefelt et al. (2013). For the 0 °C isotherm to reach SFR1 and SFR3, they estimated that the annual mean air temperature would need to be at least −1 °C and −3 °C, respectively, over a period of approximately 2 000 years. Such development thus opens the possibility of a relatively shallow permafrost development, where bedrock conditions are frozen in areas above the repository while they, at least partially, remain unfrozen at repository depth. A further lowering of the air temperature would naturally result in a faster vertical permafrost propagation and colder conditions at repository depth. For example, for air temperatures of −7 °C, the 0 °C isotherm is estimated to reach SFR1 in less than 500 years and SFR3 in approximately 800 years (Brandefelt et al. 2013). For such low air temperatures, the simulations suggest that the bedrock temperature at SFR1 and SFR3 depths would reach approximately −5 °C and −3 °C, respectively. Under such conditions, most of the water in the bedrock is expected to be frozen also at repository depth.

6.5.4 Mechanical evolution

In the periods of periglacial climate domain, lower ground temperatures and permafrost conditions are expected. This temperature change and the freezing process of the groundwater can lead to mechanical processes, including deformation of intact rock, fracture opening and the formation of new fractures (**Geosphere process report**, Section 2.2 and Chapter 4). The near-surface air temperature evolution and associated geosphere temperatures during periglacial periods are described in the **Climate report**.

Rock fall will occur but no damage to the concrete structures is foreseen due to the protective backfill material. As with the other variants (Sections 6.3.4 and 6.4.4), the probability of an earthquake increases as time progresses.

6.5.5 Hydrogeological evolution

Under periglacial conditions, advective transport is restricted due to the low permeability of frozen ground. However, unfrozen taliks in the otherwise frozen landscape may occur under lakes, streams and mires. All lakes in the Forsmark area are expected to be infilled and transformed into mires by the time of occurrence of periglacial conditions in the *cold climate variant*. So-called through taliks may form in these mires in periods of shallow permafrost (Section 6.5.2).

During periglacial conditions, the main factor of importance for groundwater flow is the extent of perennially frozen ground. If the permafrost is relatively shallow, so that virtually unfrozen conditions prevail at repository depth, the groundwater flow through the repository is determined by the regional hydrogeology. If the permafrost reaches the waste vaults and their structures, the flow of groundwater through the waste will effectively stop. The presence of frozen ground will also change the locations of recharge and discharge and drive groundwater flow to greater depth. Near unfrozen areas, potential gradients may be high.

Regional hydrogeological modelling of potential future situations, ranging from a few to many through taliks were reported by Odén et al. (2014). The latter situation is not relevant for the periods of periglacial conditions in the *cold climate variant* because all lakes are projected to be filled with sediment and peat prior to the onset of the first periglacial period (Section 6.3.2). For situations with a few through taliks, lower total flow through the waste vaults and higher flow-related transport resistance values are expected compared with those under temperate conditions (Odén et al. 2014). In addition, longer path lengths and travel times are expected.

Particle tracking shows that the particle exit locations are predominantly found within the physical boundaries of the regional model domain (Figure 6-17). More than 99 % of the particles discharge in the through taliks to the northeast (in Öregrundsgrepen), whereas some particles discharge through the permafrost layer. The latter is due to a low but non-zero permeability of the rock, reduced by up to five orders of magnitude as compared to temperate conditions. In other words, the permafrost still has a residual permeability in the assessment modelling. It should also be noted that the deformation zones govern the exit locations in the permafrost.

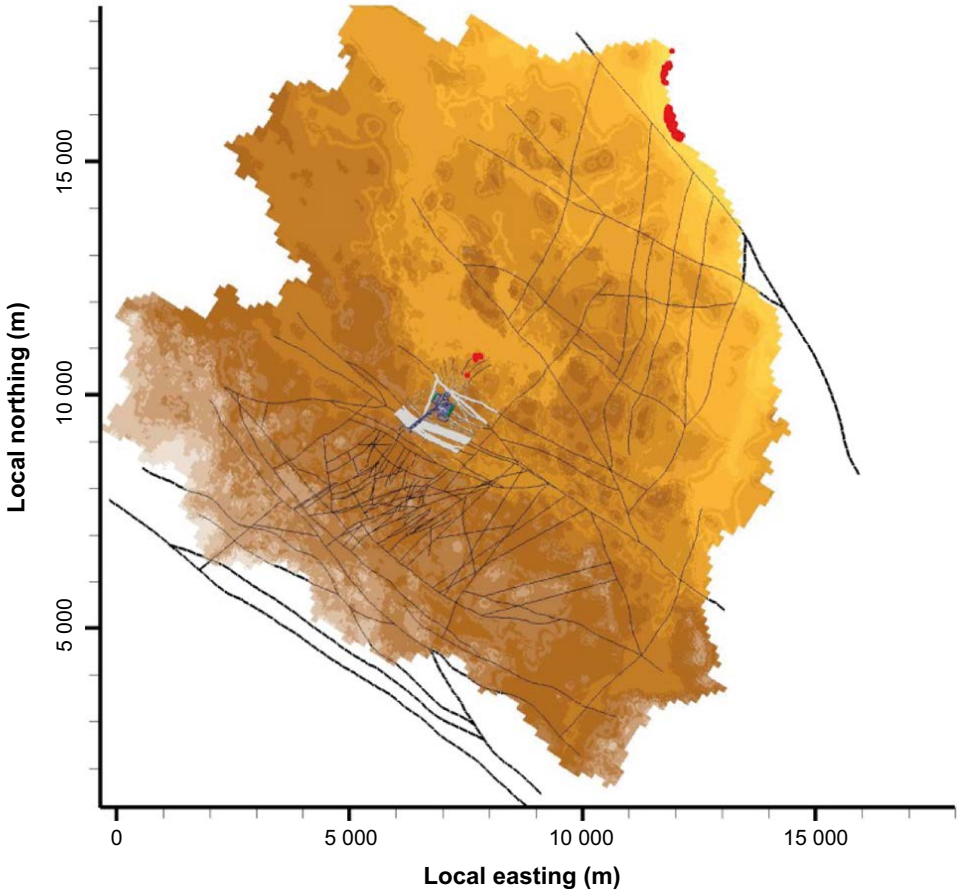

Figure 6-17. *Distribution of discharge to the surface systems from SFR (red dots) for a situation with shallow permafrost that does not reach SFR and a few through taliks at the model boundary far to the north-east of SFR. The light grey areas indicate the thickness at ground surface of deformation zones that are represented in the SFR Regional domain of the hydrogeological model. The black lines represent the location of deformation zones outside the SFR Regional domain. Figure is modified from Odén et al. (2014).*

In frozen parts of the geosphere, the hydraulic conductivity will decrease substantially, and no significant groundwater flow will occur. Since the groundwater flow that transports released radionuclides through the geosphere ceases during periods of continuous permafrost, no significant release to the biosphere from frozen parts of the geosphere occurs during these periods.

6.5.6 Geochemical evolution

The prevailing periglacial climate domain affects the groundwater composition around the repository, especially during permafrost. However, since the groundwater is expected to be diluted after an extended period of terrestrial conditions, the effects are expected to be minor.

Generally, water flow and solute transport to and from SFR ceases or is substantially decreased during times of periglacial conditions, except in the presence of taliks (Section 6.5.2). Advective solute transport is limited by the restricted flow during this period and no exchange between fracture water and the rock matrix by diffusion is expected.

Based on currently available hydrogeochemical information, the groundwater around the repository during periods of a periglacial climate domain is expected to be similar in composition to that present during the temperate domain under terrestrial conditions, when the repository is not submerged. Freeze-out of constituents dissolved in the groundwater can increase the salinity of the liquid phase. Although somewhat dependent of the timing of this period, the effect of such a process is not expected to have any major impact on the salinity distribution in a groundwater that will be substantially diluted by meteoric water by that time. Redox conditions will not change during permafrost. All relevant

processes affecting the redox conditions will cease under such conditions. No microbial activity is deemed possible during frozen bedrock conditions. Gas formation processes are dependent on liquid water, so gas formation and gas transport are not expected to take place during periods of permafrost at repository depth. In addition, speciation of radionuclides is not expected to change during periods of permafrost. Thus, the groundwater composition during periglacial periods of the *cold climate variant* is expected to follow that of the *present-day climate variant* described in Section 6.3.6 and as given by the range of the groundwater composition for an extended period of temperate terrestrial conditions in Table 6-8.

Other processes, e.g. mixing with older groundwater types in unfrozen regions of the geosphere, may still be important for the spatial distribution of the groundwater composition.

During periods of permafrost at repository depth, water will be in the solid state, hence chemical reactions will cease. The radionuclides already complexed will remain as metal–organic complexes. No new complexation between radionuclides and organic complexing agents is expected when frozen. The radionuclides already sorbed or precipitated will also remain so. After thawing, the chemical processes are expected to resume as before the permafrost.

6.5.7 Near-field hydrological evolution

If the permafrost is relatively shallow, so that virtually unfrozen conditions prevail at repository depth, the groundwater flow in the repository is determined by the regional hydrogeology, see Section 6.5.5. If the permafrost reaches the waste vaults and their structures, the flow of groundwater through the waste will effectively stop since most of the water in the surrounding rock and inside the repository will be frozen.

Concrete hydraulic barrier degradation

Owing to the relatively late onset of periglacial conditions at 61 000 AD, potential freezing of concrete pore water in the repository is expected to be less important for the hydraulic properties in the concrete compared to other degradation mechanisms (Section 6.5.9).

6.5.8 Evolution of the waste and of the repository chemical conditions

As explained for the w*arm climate variant* (Section 6.4.8) the temperature dependence is very weak for the relevant processes in the waste. However, when the water in the repository is frozen, all relevant chemical processes and radionuclide transport will proceed at negligible rates. When the water becomes liquid again, the processes continue as described in Sections 6.2.8 and 6.3.8. As described in Section 6.5.9, the concrete may freeze if the ground temperature at repository depth drops below the freezing point of leached concrete, affecting the structural integrity of the repository. However, the sorption partitioning coefficients between water and concrete are considered to be unaffected by the concrete structural changes occurring after permafrost. Hence sorption of radionuclides is expected to fully resume after the permafrost.

Water composition

Groundwater

Under periglacial conditions, salt exclusion due to freezing could increase the salinity of the groundwater (Vidstrand et al. 2007), but the groundwater is not particularly saline before the onset of permafrost and the salts that are formed are moved to the bottom of the permafrost. Thus, the deeper the permafrost, the greater salt exclusion can be. Since SFR is located at such a shallow depth and the salinity of the groundwater is low before the onset of permafrost, the effect of salt exclusion is negligible.

Cement pore water

During periods of permafrost at repository depth, all water will be in the solid state. The pH is controlled by fast chemical reactions and permafrost is not expected to have any appreciable impact on the overall pH evolution.

Dissolution and transport of dissolved species

There will be no advective fluxes of water when it is in the solid state and diffusion of species through solid ice is also negligible.

Permafrost and glaciation effects on colloids

Colloids are not mobile when water is present in the solid state.

Redox potential

Redox conditions are not expected to change due to temperature or permafrost. All relevant processes affecting the redox conditions of the waste domain will halt under frozen conditions but are expected to resume unaffected after melting.

Radionuclide speciation

Speciation of radionuclides is not expected to change due to temperature or permafrost.

Metal corrosion

Like chemical processes in general, corrosion slows down with decreasing temperature, but the deceleration is negligible for the small temperature decrease expected due to cold climate. However, for noticeable corrosion of steel to occur, liquid water must be present. During periods of permafrost at repository depth, water will be in the solid state, so corrosion will be absent or negligibly slow.

Organic complexing agents and sorption

During periods of permafrost at repository depth, water will be in the solid state, hence chemical reactions are practically halted. The radionuclides already complexed with organic complexing agents are expected to remain as metal–organic complexes. No new complexation between radionuclides and organic complexing agents is expected. The radionuclides already sorbed to cementitious materials will remain sorbed. For periods after the permafrost, sorption will resume as before permafrost. At this time, soluble complexing agents are expected to have become washed out of the repository to an extent.

Microbiology

During periods of permafrost at repository depth, no microbial activity is deemed possible, but microorganisms can survive.

Gas formation and transport

The gas formation processes are dependent on liquid water, so gas formation and gas transport are expected to be negligibly slow during periods of permafrost at repository depth.

6.5.9 Evolution of engineered barriers

Bentonite barriers

Low ground temperatures may lead to the development of permafrost, which if it reaches deep enough can cause freezing of the water contained in the engineered barriers.

Ice lens formation

In partially frozen bentonite, non-frozen water may contribute to the formation and growth of an ice lens. The process, which ends when there is no longer access to non-frozen water, may lead to increased pressure and displacement of material in connection with the lens. Any possible ice lens

formation in the bentonite surrounding the silo will likely be distributed on several lenses. With the current knowledge (Birgersson and Andersson 2014), it cannot be excluded that frost heave will occur in the bentonite. This could occur exclusively during periods of permafrost at repository depth.

Consequences of possible ice lens formation

If the bentonite in the silo is compressed by 1 m, corresponding to approximately 2 % of its total height, without water loss, it may lead to a relatively high-pressure build-up. However, it has been demonstrated that no detrimental pressure on the rock wall and the waste packages will be caused by ice-lens formation in the silo (Birgersson and Andersson 2014).

Ice lens formation in the silo wall is a slow process, since the hydraulic conductivity of the bentonite is low. Extensive ice lens formation requires that the freezing temperature/front stays at exactly the same level of the silo height for long time. If the front moves downwards, the water supply will cease and if the front move upwards the lens will melt. This makes ice lens formation a highly unlikely event.

The ability of the bentonite surrounding the silo to self-heal after thawing is dependent on how the ice lenses are distributed in the material.

Freezing of entrapped water

If permafrost reaches repository depth, a situation could arise where all drainage passages to bentonite components in various parts of the repository (silo, tunnel plugs and backfill) are blocked due to ice-filled fractures in the rock. If the temperature in this case continues to decrease, more water will in turn be converted to ice in the bentonite, which contains substantial amounts of unfrozen water even at temperatures of –10 °C or lower and so-called frost weathering pressure peaks may then occur. An estimate of the maximum value for such peaks, based on simple elastic mechanical reasoning, has been made. The analysis clearly showed that pressure peaks in a range of a few hundred kPa cannot be excluded (Birgersson and Andersson 2014). In the *cold climate variant*, permafrost occurs at times when the concrete of the silo is considered to be completely degraded and thus any potential damage to the concrete will not have any effect on calculated radionuclide releases. The pressures are judged not to be high enough to cause any permanent damage to the bedrock surrounding the silo. The bentonite is completely recovered at thawing and thus any deterioration of the bentonite properties due to the pressure peak is of no concern for the bentonite itself.

Concrete barriers

As explained in Section 6.5.1, the onset of periglacial conditions is expected to occur at about 61 000 AD and up until then the evolution of the properties of the concrete barriers will follow that of the *present-day climate variant* (Section 6.3.9).

During periglacial climate domain beyond 61 000 AD all processes will continue to progress as long as there is liquid water available at repository depth and the evolution of the properties of the concrete barriers will continue to follow that of the present-day climate variant (Section 6.3.9). During periods with frozen conditions at repository depth, the only process of concern is freezing of the concrete pore water. This process is described below.

Freezing of the concrete pore water

The resistance of concrete against cracking due to freezing of the concrete pore water is dependent on the degree of water saturation, the diameter of the pores in which the water is confined and, finally, on the tensile strength of the concrete. For concrete which has a pore structure comprising pores with varying diameter, water will freeze at different temperatures depending on the dimensions of the individual pores. Water which is not frozen will be relocated to other unfrozen parts of the pore system during this period. For concrete, the critical parameter determining the degree of damage is the amount of the concrete pore water that freezes at a certain temperature.

At the point in time of the first possible onset of periglacial conditions (61 000 AD) it is expected that the physical structure of the concrete has been considerably altered compared to the original material with abundant cracks and a high porosity. Even though it is not possible to predict the detailed structure of 60 000 years old concrete it is considered reasonable to assume that the additional degradation caused by freezing of the concrete pore water will have a limited influence on the structure and properties of the concrete barriers in SFR. Instead, at this stage freezing of the concrete pore water as well as the water in the surrounding bedrock will prevent the release of any radionuclides as long as the water remains frozen.

Backfill material

During periglacial climate domain all processes will continue to progress as long as there is liquid water available at repository depth; see Section 6.3.9, subsection *Backfill material*.

During periods with frozen conditions at repository depth, the only process of concern is freezing of the water in the backfill material. If this occurs, transport of fine-grained material will cease as well as transport of water and gas to/from the waste domain.

7 Main scenario

7.1 Introduction

The assessment of the capability to protect human health and the environment is based on a set of scenarios that together illustrate the most important courses of development of the repository and its environs (Section 2.6.8). In general, each scenario describes a sequence of events and conditions of the repository and its environs and how they affect the protective capability of the repository. According to the regulations, the set of scenarios shall include a main scenario, which takes into account the most probable changes within the repository and its environs. This chapter describes the main scenario including the evolution in the repository, bedrock and surface systems accounting for identified uncertainties. The evolution described is based on the initial state (Chapter 4), the reference external conditions (Section 2.6.3 and Chapter 6) and the reference evolution (Chapter 6). The scope of the main scenario, including the management of uncertainties in the scenario, is further described in Section 7.2.

To estimate radiological consequences, the scenarios are evaluated with the aid of calculation cases that are analysed with mathematical models (Section 2.6.9). The models built to calculate the radionuclide transport from the repository (near-field) through the bedrock (geosphere) to the surface system (biosphere) are briefly described in Section 7.3, including the radionuclides considered in the calculations. For each calculation case, radionuclide transport is quantified, and the resulting doses that humans can incur from exposure to repository-derived radionuclides are evaluated (Sections 7.4 to 7.7). The effects on non-human biota are also assessed (Section 7.8). The results from the calculations constitute the basis for the assessment of annual risk and protection of the environment (Chapter 10). A detailed presentation of the modelling and analysis of the results is given in the **Radionuclide transport report**.

The main scenario also constitutes the starting point for the evaluation of uncertainties. These are in turn related to the status of the safety functions that are the basis for the selection of the less probable scenarios. The status of the safety functions in the main scenario is described in Section 8.2.

7.2 Description of the main scenario

The main scenario includes a set of calculation cases that are defined based on the reference external conditions, complemented by a set of supporting calculation cases (Table 7-1). The initial state implemented in the main scenario is defined by the characteristics of the waste and its packaging such as radionuclide inventory and the chemical composition, as well as the conditions of the engineered barriers, the geosphere and the surface systems at closure of the repository (Chapter 4). These are also manifested in the definitions of the conceptual and mathematical models used in the radionuclide transport calculation (Section 7.3) together with the chosen parameterisations at the time of repository closure (Sections 7.4 to 7.6).

Table 7-1. Calculation cases described in this chapter.

Scenario	Calculation case	
Main scenario	Present-day climate (base case)	
	Warm climate	
	Cold climate	
	Supporting calculation cases	Timing of shoreline regression
		Delayed release from repository
		Subhorizontal fracture
		Alternative landscape configurations

Included in the risk assessment.

The external conditions implemented in the main scenario are described in the three calculation cases that relate to the reference external conditions:

- The *base case* is defined based on the *present-day climate variant* of the reference evolution. It represents present-day conditions in the repository environs, including the effect of shoreline displacement following the last glaciation (Section 7.4).
- Two calculation cases representing the range of probable evolution of external conditions: the *warm* and *cold climate calculation cases* (Sections 7.5 and 7.6) defined based on the *warm* and *cold climate variants* of the reference evolution, respectively.

The evolution of conditions in the near-field, geosphere and biosphere during the assessment period are included in the description of the calculation cases. The descriptions are comprehensive for the *base case*, while the descriptions of the other calculation cases focus on the differences from the *base case*. The handling of the following aspects of the near-field, geosphere and biosphere is included in the descriptions of the calculation cases:

- Hydrological conditions in the near-field.
- Physical properties of cementitious materials in concrete barriers and waste.
- Chemical conditions of concrete barriers and waste.
- Properties of bentonite in the engineered barriers.
- Properties of the backfill.
- Flow and non-flow related migration properties in the geosphere.
- Landscape properties.
- Surface hydrology.
- Ecosystem parameters.
- Potentially exposed groups.

The management of uncertainties within the safety assessment in general is described in Section 2.5. Within the main scenario, data uncertainties and, to some extent, scenario and modelling uncertainties are handled. Uncertainties in most input data for the calculation cases are handled by using a probabilistic approach, whereby stochastic values of the parameters are drawn from the corresponding probability density functions (PDFs). The impact of these uncertainties on the resulting dose in the *base case* is analysed in Section 7.4.6. For some input parameters, the probabilistic approach is not considered feasible. This is the case, for example, for parameters that are already handled cautiously or pessimistically in the radionuclide transport and dose modelling. Other parameters that are typically not handled probabilistically are those that are subject to a considerable modelling or scenario uncertainty. Such modelling uncertainties include, for example, uncertainties in parameters that are derived from underlying modelling activities, for which a probabilistic approach was not considered feasible. This concerns e.g. the modelling of the landscape development and the surface hydrology (Sections 6.2.2 and 6.3.2). Scenario uncertainties are, for example, related to significant changes in external conditions and/or the timing of an event. To maintain internal consistency in parameters depending directly on the external conditions and to avoid temporal risk dilution (Section 10.6), such uncertainties are most appropriately handled by considering alternative sets of input data that bracket the potential variability. These uncertainties include e.g. the timing of concrete degradation in the engineered barriers.

Modelling and scenario uncertainties are covered by the number of calculation cases in the main scenario and less probable scenarios. To this end, the main scenario includes a set of supporting calculation cases (Table 7-1), described in Section 7.7. These supporting calculations are defined to provide a sensitivity analysis of specific uncertainties in external conditions and internal processes potentially important to radionuclide transport through the repository system. The reason for evaluating these uncertainties in the main scenario, in contrast to the less probable scenarios, is that assigning a low probability of occurrence (≤ 10 %; see further Section 8.2) may not be appropriate (*timing of shoreline regression calculation case*) or that they do not relate to uncertainties in the safety functions of the repository system (*delayed release from repository*, *subhorizontal fracture* and *alternative*

landscape configurations calculation cases). The selection of the supporting calculation cases is based on experiences from previous safety assessment iterations including the regulatory reviews. The calculations are used as input for the selection of assumptions in the *base case* and, thereby, ensures that the evaluated uncertainties do not contribute to underestimate the dose in the main scenario. Therefore, the resulting doses in the supporting calculations are similar, or lower, than the dose of the *base case* and, thus, it is not necessary to propagate the calculations to the risk assessment in Chapter 10. It can be noted that in order to support the selection of assumptions the supporting cases are evaluated before the assumptions in the *base case* are set.

Developments from the SR-PSU

The set of scenarios and calculation cases included in the PSAR has been developed from the SR-PSU, but still covers the same range of future developments that could influence repository safety as the corresponding set in the SR-PSU. For the calculation cases included in the main scenarios of both safety assessments, the following holds:

- The PSAR *base case* is almost identical to the SR-PSU global warming calculation case for the first 50 000 years after closure. However, radionuclides from the waste start to be released at closure in the PSAR, rather than after 1 000 years in the SR-PSU. For the latter 50 000 years of the assessment period, the PSAR *base case* is similar to the SR-PSU extended global warming calculation case.
- The PSAR *delayed release from repository calculation case* assumes that the radionuclide release from the waste is delayed for 1 000 years after closure, in agreement with the assumptions made in the SR-PSU global warming calculation case.
- The PSAR *warm climate calculation case* is comparable to the SR-PSU extended global warming calculation case.
- The PSAR *cold climate calculation case* is comparable to the SR-PSU global warming calculation case.
- Radiological consequences of permafrost development within the first 50 000 years of the assessment period, evaluated in the SR-PSU early periglacial variant of the main scenario and in an associated complementary study (Näslund et al. 2017a), are illustrated in a residual scenario in the PSAR (see Section 9.3 for details).

7.3 Radionuclide transport and dose modelling

7.3.1 Modelling chain and general methodology

The radionuclide transport modelling methodology is based on experiences from SKB's previous safety assessments, in particular the SR-PSU (SKB TR-14-09) and the safety evaluation SE-SFL (SKB TR-19-06). Radionuclide transport and dose modelling is performed with a set of models representing different parts of the repository and its environs: the near-field, the geosphere and the biosphere (**Radionuclide transport report**).

The model chain starts with the near-field model that describes the transport, retention and release of radionuclides in and from the waste domain and the surrounding engineered barriers in a vault (Figure 7-1). The radionuclide release to the geosphere at the waste vault–bedrock interface is also calculated. The geosphere model describes the subsequent transport and retention of radionuclides through and in the fractured bedrock towards the surface. Finally, the biosphere model describes transport and accumulation of radionuclides in aquatic and terrestrial ecosystems. To calculate exposure from cultivation, the model includes stylised representations of agricultural systems.

The calculation endpoint is the *annual dose* to humans and *adsorbed dose rates* to non-human biota (Section 2.6.9). Annual doses to humans are effective doses and are calculated for representative individuals of four exposed groups, each associated with a unique variant of land-use (Section 7.3.6). The highest dose from any exposed group is carried on to the risk assessment (Chapter 10).

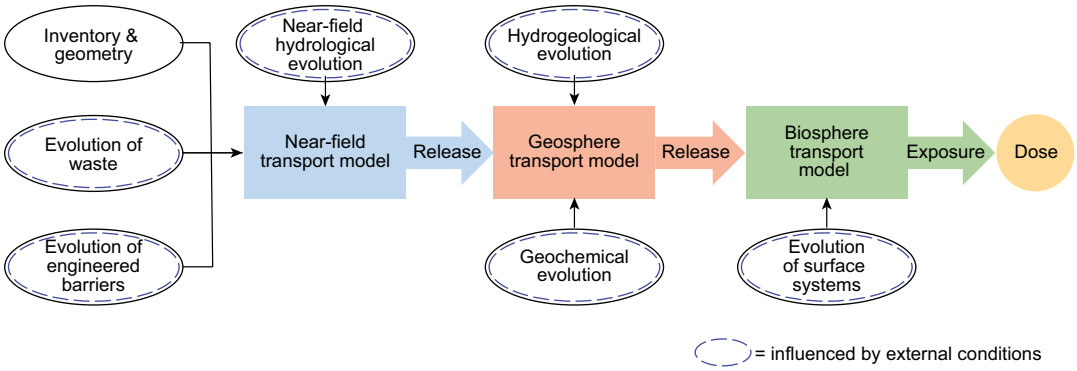

Figure 7-1. *Models and data used for the radionuclide transport and dose calculations. Boxes represent modelling activities and ovals represent data. Dashed ovals indicate that the data are influenced, directly or indirectly, by external conditions.*

All models are implemented as compartment models. This approach assumes that the system can be adequately represented by discretisation into a limited number of model compartments, each of which is internally homogeneous and connected to other compartments (**Radionuclide transport report**, Section 4.1.1). The near-field and biosphere models are implemented in the Ecolego compartment modelling software (**Model tools report**), and the geosphere model is implemented in Matlab (SKB TR-19-06, Appendix B). A brief overview of the models is given in Sections 7.3.4 to 7.3.6.

The radionuclide transport calculations are carried out as dynamic simulations, where the output from one model, in terms of the annual activity release for each radionuclide, is used as input for the next. The modelling tools are coupled indirectly, i.e. the model chain has been executed for one entity at a time followed by a semi-automatic transfer of results to the calculation tool for the subsequent model. To ensure functional coupling between the three models, the models have been designed to use compatible definitions of the parameters, so that the inputs and outputs are not only numerically compatible but also that the same FEPs are represented consistently along the whole modelling chain.

The calculations cover the entire assessment period of 100 000 years, starting from the closure of the repository.[27] Calculations are performed both deterministically and probabilistically for most calculation cases. In this report, results from probabilistic calculations are presented unless otherwise noted. The probabilistic calculation cases are analysed using 1 000 simulations selected using Monte Carlo methods. For each simulation, random parameter values are sampled from pre-defined PDFs that aim to capture the uncertainties in the input data. Parameters that are used in several transport models are only sampled once to ensure consistency in the handling between the models. The presentation and discussion of the calculation cases are based on the *mean* across the 1 000 probabilistic simulations, which is used to calculate risk (Section 2.6.9). In Section 7.4.6, it is shown that 1 000 simulations are sufficient to obtain an acceptable level of convergence of the mean value.

7.3.2 Overview of input data

The radionuclide transport and dose modelling use input data from several sources (Figure 7-1). The radionuclide activity at closure (i.e. the radionuclide inventory at closure) constitutes the starting point for the calculations. To calculate transport and retention of radionuclides from the near-field to the surface, data describing the post-closure evolution of the three sub-systems are used. The near-field data describe changes in the repository physical and chemical conditions, which affect e.g. groundwater flow and sorption in the waste and the engineered barriers. Characteristics of the groundwater flow, water-bearing fractures and sorption properties in the bedrock matrix are important for the description of geosphere transport. Transport and accumulation of radionuclides in the biosphere

[27] Note that most figures in this report present releases and doses from 2000 AD to 100 000 AD. This is a simplification as the planned closure of the repository is at 2075 AD and the assessment period in the calculations is 100 000 years. Thus, the figures present the first 98 000 years after closure and 2000 AD represents the time of closure.

are calculated using representative data for the surface systems, including landscape development, ecosystem properties and characteristics of the discharge areas.

The input data in all transport models are also influenced by the evolution of external (climate) conditions (Figure 7-1). Important aspects of external conditions include the timing of shoreline regression in the area above the repository and the temporal succession of climate domains (temperate, periglacial and glacial; see Section 2.6.3). A description of the input data flows for the radionuclide transport and dose modelling is presented in Appendix H. The input data used in the radionuclide transport calculations for the near-field are described in Section 7.4.2, the **Data report**, the **Initial state report** and the **Radionuclide transport report**, Appendix A. Input data used in the geosphere modelling are found in the **Data report** and the **Radionuclide transport report**, Appendix A, whereas data for the biosphere modelling are described in the **Biosphere synthesis report**, Chapter 8.

7.3.3 Radionuclides included in the analysis

The initial radionuclide inventory is described in Section 4.3.7. Not all radionuclides in the waste are relevant for post-closure safety and so do not need to be included in the radionuclide transport and dose calculations (Section 2.4.2). The screening of radionuclides with respect to their relevance in the post-closure safety assessment follows the methodology used in previous SKB safety assessments, e.g. the SR-PSU (SKB TR-14-09). The methodology is summarised in the following and described in detail in the **Radionuclide transport report**, Section 3.3.

A first screening of relevant radionuclides from the given initial inventory at closure to be considered in the radionuclide transport calculations is based on the following two criteria:

- the half-life of a radionuclide is 10 years or longer, and
- the radiotoxicity by ingestion at the time of repository closure exceeds 10 mSv.

Using these criteria, the set of radionuclides considered in the inventory in the PSAR is the same as in the SR-PSU. Thus, six radionuclides with a non-zero initial inventory (Cs-134, Eu-154, Fe-55, Sb-125, Pm-147 and Eu-155)[28] are screened out due to their short half-lives, and two radionuclides (Be-10 and In-115) have a radiotoxicity below 10 mSv and are therefore screened out due to the second criterion.

Regardless of the given initial inventory, decay products must be considered for their safety-relevance. The criterion used for explicitly taking decay products into account in the radionuclide transport calculations is that their half-life is longer than 100 days (in contrast to the half-life criterion for the initial inventory above). Decay products with half-lives less than 100 days are not explicitly modelled in the transport calculations, but are implicitly accounted for in the dose calculation, assuming that they are in secular equilibrium with their parent radionuclides when calculating the dose conversion coefficient of that parent (see **Radionuclide transport report**, Appendix A for details). In addition, two radionuclides that were explicitly modelled in the SR-PSU (Th-228 and Cm-242) are pessimistically added to the parent radionuclide assuming secular equilibrium, even though their half-lives are slightly longer than 100 days.

Another reason for excluding decay products is if their half-life indicates that no dose-relevant activity could possibly build up during the assessment period. Thus, decay products not present in the disposed inventory with a half-life greater than 10^{10} years are excluded in the radionuclide transport and dose calculations. Due to this criterion, two radionuclides that were included in the SR-PSU (Th-232 and its decay product Ra-228) are now screened out.

Radionuclide decay chains included in the radionuclide transport modelling are presented in the **Radionuclide transport report**, Section 3.3.3.

[28] Due to its relatively high radiotoxicity, Co-60 with a half-life of about five years is also included even though it does not fulfil the first criterion.

Handling of uncertainties in the radionuclide inventory

Uncertainties in the radionuclide inventory are described in Section 4.3.7. The uncertainties are handled differently in the PSAR as compared to the SR-PSU where uncertainties were accounted for by the high inventory scenario (SKB TR-14-01, Section 7.6.1), which contributed to the risk assessment as a less probable scenario. In the present assessment, an improved methodology is applied where uncertainties are instead handled in a probabilistic manner. In summary, PDFs of the inventory of individual radionuclides are constructed based on information about the uncertainty in e.g. measurements and models (**Data report**, Chapter 4). The probabilistic representation of the uncertainty in the radionuclide inventory is achieved through sampling these PDFs. This results in 1 000 samples (or realisations) of the inventory that are propagated to the radionuclide transport calculations. In addition to the probabilistic handling of uncertainties, three alternative inventories representing a selection of operational changes are evaluated in a residual scenario (Section 9.6).

7.3.4 Near-field transport models

The near-field models describe the transport and retention of radionuclides in the waste domain and the surrounding engineered barriers as well as releases of radionuclides from the waste vaults to the geosphere. To account for different barrier designs and waste types, separate models have been developed for each waste vault. The models are described in detail in the **Radionuclide transport report**, Section 4.2 and in Åstrand et al. (2022). A brief overview is given in the following.

The most important input data for the near-field models include the initial activity in the waste vaults (Section 7.3.3), properties of the waste and engineered barriers and their changes with time (Sections 4.3, 4.4, 6.2.8, 6.2.9, 6.3.8, 6.3.9, 6.4.8, 6.4.9, 6.5.8 and 6.5.9) and the modelled groundwater flow through the barriers and waste (Sections 6.2.7, 6.3.7, 6.4.7 and 6.5.7).

The engineered concrete barriers and bentonite barriers (only for the silo) limit the release of radionuclides from the near-field by reducing the groundwater flow through the waste and by providing sorption capacity for many radionuclides. These barriers are explicitly represented by several model compartments in the near-field models. The access tunnels and plugs are also important for post-closure safety. However, they are not explicitly represented in the radionuclide transport models. Instead, their impact on radionuclide transport is accounted for through their effect on groundwater flow because plug flow resistance limits groundwater flow in the vaults.

The near-field models include several simplifying assumptions. The level of detail used in the models varies between the waste vaults depending on the character of their barriers and their expected relative importance for overall system performance. The vault models have been developed to consider the main retaining properties of the barriers in the vaults but, depending on the vault, some retaining abilities are neglected. Most importantly, sorption is pessimistically not considered in the 1–5BLA vault models, despite the presence of significant amounts of cement and other sorbents. Other simplifications in the near-field modelling are:

- The repository is assumed to become instantly saturated with groundwater upon closure (Section 4.4.9) and to remain so for the full assessment period.
- Radionuclides are assumed to be instantaneously and fully dissolved in the waste porewater, with the exception of the fractions sorbed on barrier materials or induced in reactor pressure vessels (RPVs) disposed in 1BRT.
- The sorbent properties of metals and their corrosion products are pessimistically disregarded.
- The potential transport-limiting effect of waste matrices and steel packaging is neglected. This assumption has the greatest effect on bitumen-solidified wastes.

Taken together, these simplifications result in earlier releases from the near-field compared to when more realistic parameterisations of these processes were included in the modelling. Radiological consequences of these simplifications are evaluated in the *delayed release from the repository calculation case* (Section 7.7).

Processes handled in the near-field models

A large number of physical and chemical processes have been identified as potentially important and they have been thoroughly analysed in the near-field of SFR (see the **Waste process report** and the **Barrier process report**). The analyses show that only a few of these processes have a significant impact on radionuclide transport; these are summarised in Table 7-2. The mathematical description of these processes is given in the **Radionuclide transport report**, Section 4.2.4.

Table 7-2. Near-field processes considered in the radionuclide transport modelling. The implementation of these processes is further described in Section 7.4.2.

Process	Comment
Radionuclide decay and ingrowth	Explicitly included.
Speciation	Implicitly included in pre-calculated, time-dependent sorption coefficients and diffusivities.
Advection	Explicitly included.
Diffusion	Explicitly included.
Dispersion	Implicitly included as numerical dispersion resulting from the compartmental modelling approach.
Sorption	Explicitly included.
Complexation	Complexing agents are implicitly included.
Corrosion-controlled release	Included for the RPVs in 1BRT.

Coupling to the geosphere

The transport in the macadam backfill is dominated by advection. Thus, the release of radionuclides from the near-field, for all vaults except the silo, is calculated as the sum of the advective transfers from the backfill compartments to the geosphere.

As bentonite constitutes the main hydraulic barrier in the silo, the transport of radionuclides to the geosphere from this vault is predominately diffusive rather than advective. Therefore, transport from the silo to the geosphere is represented by an equivalent water flow, Q_{eq}, which depends both on the diffusivity of radionuclides in water and the flow-related migration properties of the geosphere (see further the **Radionuclide transport report**, Section 4.2.4).

7.3.5 Geosphere transport model

The geosphere transport model describes the transport and retention of radionuclides through and in the fractured bedrock towards the surface. Radionuclides from the near-field are released at the waste vault–bedrock interface. Transport in the geosphere is modelled with FARFCOMP, described in detail in the **Radionuclide transport report**, Section 4.3 and in SKB (TR-19-06, Appendix B); only a brief overview is given in the following.

The geosphere model incorporates a compartmental representation of the fracture–matrix system as a dual porosity model. In the dual porosity approach, the rock is divided into two distinct domains with different types of porosity: 1) fractures with advecting groundwater and 2) rock matrix with porosity accessible only by diffusion in the porewater.

Processes handled in the geosphere

All the physical and chemical processes identified as potentially important in the geosphere are discussed in the **Geosphere process report**. However, only a few of them are relevant for radionuclide transport modelling in the geosphere and these are summarised in Table 7-3. The mathematical descriptions of these processes are given in the **Radionuclide transport report**, Section 4.3.2.

Table 7-3. Geosphere processes considered in the radionuclide transport modelling. The implementation of these processes is further described in Section 7.4.3.

Process	Comment
Radionuclide decay and ingrowth	Explicitly included.
Advection	Explicitly included.
Rock-matrix diffusion	Exchange of solutes between groundwater flowing in the fractures and the adjacent rock matrix is explicitly included in the geosphere model.
Dispersion	Longitudinal hydrodynamic dispersion along the individual trajectories is explicitly included by means of the constant Péclet number that quantifies the ratio between advective and dispersive transport.
Sorption	Retardation of radionuclides is accomplished by sorption onto the internal surfaces of the rock matrix porosity (accessible by diffusion), while sorption on the fracture surface, or possible fracture fill, is pessimistically omitted in the model.

Coupling to the biosphere: biosphere objects and the well interaction area

Radionuclide releases from the geosphere are discharged to the deepest regolith layer in the biosphere transport and exposure model (described in Section 7.3.6). The discharge locations in the landscape are defined by *biosphere objects* where each object is an area in the modelled landscape that is predicted to receive a substantial portion of the radionuclides following release from the geosphere (**Biosphere synthesis report**, Chapter 5). The biosphere objects identified in the SR-PSU are also used in the PSAR; these are shown in Figure 7-2 and Figure G-1. They were identified by mapping simulated flow paths from the repository in hydrogeological simulations to present marine basins and the postulated locations of future lake basins (Odén et al. 2014).

Following the completion of the SR-PSU, new hydrogeological simulations were carried out under temperate conditions to address uncertainties in the bedrock modelling (Section 6.3.5 and Öhman and Odén 2018). The simulations consisted of 30 sets of parameterisation variants (referred to as bedrock cases) and the results confirmed the pattern of discharge locations reported in the SR-PSU (Odén et al. 2014); for 22 of the 30 bedrock cases, almost all particles released from SFR1 and most particles from SFR3 were discharged into biosphere object 157_2 (**Biosphere synthesis report**, Section 5.1.3). In the remaining eight bedrock cases, an anomalous low probability realisation of the bedrock was used, representative of a large subhorizontal fracture under object 157_2 (Section 6.3.5). The presence of such a fracture caused a third of the released particles to be directed to the two downstream objects 157_1 and 116 in the simulations (**Biosphere synthesis report**, Section 5.1.3). Radiological consequences of the presence of such a subhorizontal fracture are evaluated in the *subhorizontal fracture calculation case* (Section 7.7).

The results from Odén et al. (2014) and Öhman and Odén (2018) indicate that, for most calculation cases, it is sufficient to use biosphere object 157_2 as the primary discharge area for examining the effects of a geosphere release, i.e. the entire geosphere release is discharged to this object. During the marine period, the surface water in all seven basins will receive radionuclides via advective fluxes of the surface water across the basin boundaries. During the terrestrial period, the two objects downstream of 157_2, i.e. 157_1 and 116, are considered to receive radionuclides via surface and/or groundwater flow from object 157_2.

Under periglacial conditions, it is postulated that the only pathways available for groundwater to reach the surface ecosystem will be via through taliks (Section 6.5.2). Results of the hydrological modelling studies (Bosson et al. 2010, Odén et al. 2014, Vidstrand et al. 2014b) conducted for the SR-PSU indicate that the mire in object 157_1 and the lake in object 114 could potentially evolve to become through taliks. These objects are therefore considered under periglacial conditions.

Different types of water wells and well locations are represented in the biosphere model. Dug wells are included as an exposure pathway for agricultural, self-sustained communities existing within the biosphere objects. Drilled wells, placed outside of the repository footprint, are also included in the analyses as water pumped from these wells could be contaminated by radionuclides. The fraction of the geosphere release reaching wells drilled within the path of the contaminant plume was examined and quantified in the SR-PSU (Werner et al. 2013, Section 6.4). The area within which radionuclides

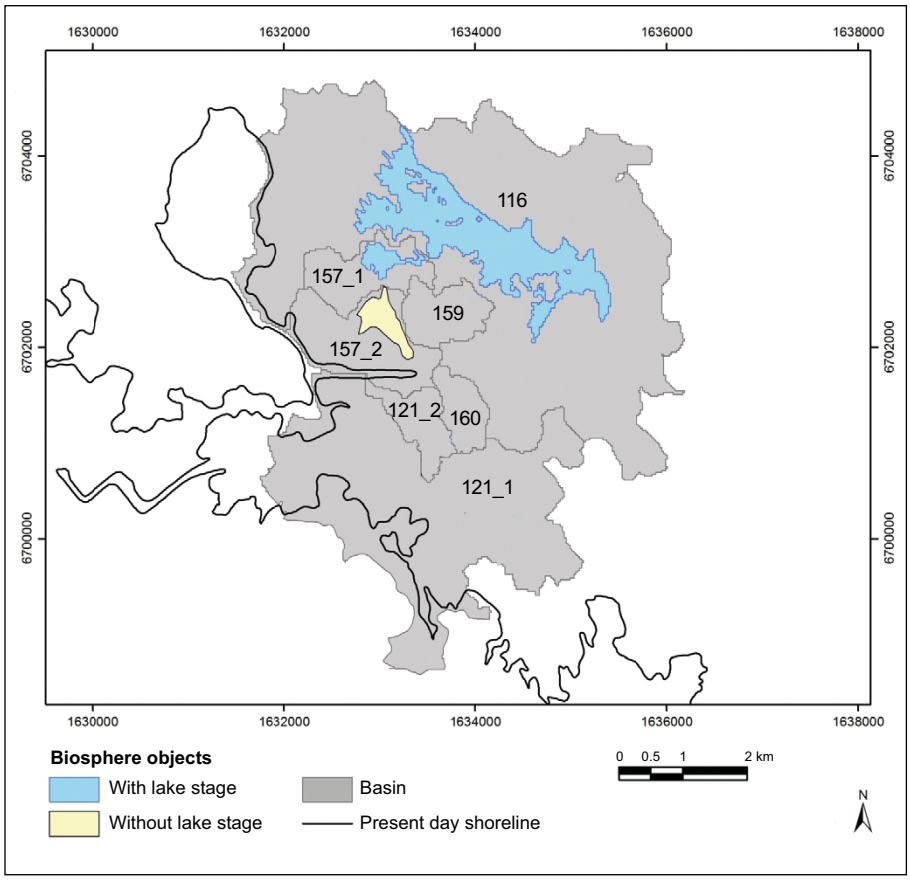

Figure 7-2. *Map of biosphere objects. When the area is submerged, the biosphere objects are in their marine stage and all the delineated objects are used simultaneously to assess the potential exposure from the marine object. However, significant fractions of the geosphere release are only expected to be discharged to basin 157_2 in most cases, and to 157_1, 157_2 and 116 given the presence of an atypical subhorizontal fracture (Section 6.3.5). Thus, these three objects are considered sufficient for assessing dose in the terrestrial stage. In the terrestrial stage, the biosphere object is defined as the original lake basin (blue) or the mire (yellow). Biosphere object 114 is shown in Figure G-1, which includes a map covering a greater area than the present figure.*

released from SFR would intersect the area of influence of a theoretical future bedrock well is called the *well interaction area* (Werner et al. 2013, Öhman and Vidstrand 2014). The spatial coverage of the well interaction area is the same as in the SR-PSU.

The probability of drilling a well into the well interaction area is not taken into account. Instead, the drilled well is treated as an exposure pathway (with a probability of one) and the dose from this pathway is evaluated considering a small exposed group that uses the water for household needs (the garden-plot household, see Section 7.3.6). The spatial variability of the radionuclide concentration in the well interaction area is accounted for as data uncertainty (**Biosphere synthesis report**, Section 8.2.4). In accordance with the general advice to SSMFS 2008:21, detriment to humans intruding into the repository is handled in residual scenarios. This includes drilled wells which directly penetrate the repository (Section 9.11.2).

7.3.6 Biosphere transport and exposure model (BioTEx)

Radionuclide transport in the biosphere is described using the BioTEx model which describes radionuclide transport and accumulation in the near-surface environment and ecosystems as well as calculating potential doses to humans and dose rates to non-human biota (NHB). The BioTEx model is based on the model developed for the SR-PSU (Saetre et al. 2013a). However, in response to SSM's reviews of the SR-Site and the SR-PSU (e.g. SSM 2017, 2018, Walke et al. 2017), and

from SKB's own research and development program, the BioTEx model was somewhat modified in SE-SFL (SKB TR-19-05). Most of these updates, in addition to several other improvements, are included in the BioTEx model for the PSAR. All updates since the SR-PSU are documented and evaluated in the **Biosphere synthesis report**, Section 7.5.

Discharge of radionuclides into the biosphere is evaluated over thousands of years. The discharge area is considered at the scale of a coastal basin or a lake–mire complex (Section 7.3.5) and the annual dose to future inhabitants is considered for an adult lifetime. At these temporal and spatial scales, it is assumed that most biogeochemical interactions can be approximated by equilibrium or steady-state conditions. Thus, ecosystem states are represented by average conditions and fluxes of water, solid matter and gas are typically described as functions of empirical parameters that capture the combined outcome of the underlying processes.

Radionuclides released from the repository enter the surface system through deep groundwater discharge and then reach the soil, sediments, water and air. Two main types of ecosystems are simulated, namely aquatic ecosystems (including sea basins, lakes and streams) and terrestrial ecosystems (including mires and agricultural land). The distribution of radionuclides in aquatic ecosystems is represented by six compartments associated with several regolith layers, two compartments associated with the water, and one compartment associated with aquatic primary producers. Correspondingly, the distribution of radionuclides in mire ecosystems is represented by eight compartments associated with several regolith layers and one compartment associated with the mire vegetation. In addition, a garden plot is used to evaluate consequences of irrigation with water from a drilled well in the bedrock (Section 7.3.5). The processes that are represented by flow of radionuclides between the compartments are summarised in the subsection *Processes handled in the biosphere* below.

The final step in the biosphere modelling consists of calculating annual doses to humans and dose rates to NHB that are exposed to repository derived radionuclides in the environment, see subsections *Assessment endpoints for humans* and *Assessment endpoints for non-human biota* below.

Processes handled in the biosphere

The dynamic change in the radionuclide content of each compartment is the result of radionuclide fluxes and ingrowth/decay; these are summarised in Table 7-4. The processes have been checked against the processes in the SKB FEP list (**Biosphere synthesis report**, Chapter 6) and are described in detail in the **Biosphere synthesis report**, Chapter 7.

Assessment endpoints for humans

The primary assessment endpoint for humans in the biosphere assessment is the annual dose to a representative individual in the group exposed to the greatest risk (Section 2.6.9). To select an appropriate group, or groups, to address in the analysis, all exposure pathways relevant for post-closure safety must be identified. These include doses from external exposure (radiation from the ground, air and seawater), inhalation of radionuclides and, most importantly, by ingestion of radionuclides through food and water, depending on the type of ecosystem (Figure 7-3).

A comprehensive pathway analysis for exposure of humans was conducted for the SR-PSU (SKB R-14-02) and this is also valid for the present assessment. The outcome of that analysis was that 22 exposure route cases were identified as important for post-closure safety, and that they could be covered in the dose calculations by establishing four potentially exposed groups (PEGs).

The degree to which future humans will inhabit and/or utilise natural resources in the biosphere object have been handled according to Swedish regulations (SSMFS 2008:37) and in line with U.S. and international standards and guidance (e.g. ATSDR 2005, ICRP 2006). The assigned characteristics and habits of the potentially exposed group are reasonable and sustainable with respect to physical constraints of the landscape, to human needs for nutrients and energy, and to present and/or historical land use. Land-use variants, which resulted in relatively high exposure have primarily been identified from historically self-sustainable communities (Saetre et al. 2013b). The PEGs are briefly described below and are considered credible to use as bounding cases for a representative individual in the group exposed to the greatest risk, with respect to exposure through all relevant exposure pathways (**Biosphere synthesis report**, Section 6.2).

Table 7-4. Overview of radionuclide fluxes (processes) included in the BioTEx model. The processes have been categorised with respect to the underlying mechanism, namely mass-fluxes of solids (MS), water (MW) or gas (MG), diffusion in water (DW) or in gas (DG), or incorporation into or release from organic matter due to photo-synthesis (PP) or mineralisation (Min). "Y" indicates that the process is included as a dynamic flux between compartments in the aquatic (Aqua), mire (Mire) or agricultural (Agri) sub-model. * indicates that only the steady-state outcome of the process is taken into account. Superscripts indicate that fluxes can occur between ecosystems (BTW), that the initial inventory in agricultural soil is conditioned on environmental concentrations in natural ecosystems (INIT). Superscripts also specify the system(s) of cultivation; drained mire (DM), infield-outland agriculture (IO) or a garden plot (GP). ** Indicates that the process is restricted to a warm climate for DM and IO.

Process	Type	Radionuclide flux		
		Aqua	Mire	Agri
Biological				
Bioturbation	MS	Y		Y^{DM}
Plant (root) uptake	PP	Y	Y	*
Leaf retention/translocation	PP			Y^{**}
Litter respiration/release	Min	Y	Y	Y^{IO}
Litter production	PP	Y	Y	
Regolith Mineralisation	Min	Y	Y	Y
Vegetation ingrowth^{BTW}	MS	Y	Y	
Water bound				
Advective horizontal^{BTW}	MW	Y	Y	
Advective vertical	MW	Y	Y	Y
Diffusion (vertical)	DW	Y	Y	
Water uptake	MW			Y^{DM}
Solid liquid phase dissociation		*	*	*
Sediment dynamics				
Sedimentation	MS	Y		
Resuspension	MS	Y		
Burial	MS	Y	Y	
Gas transport/transition				
Degassing	MG/DG	Y	Y	Y
Gas uptake	MG	Y	Y	
Human behaviour				
Drainage/cultivation$^{BTW, INIT}$	MS			Y^{DM}
Fertilisation^{BTW}	MS			$Y^{GP,IO}$
Irrigation	MW			Y^{**}
Radiological				
Radionuclide decay/ingrowth		Y	Y	Y

Hunter-gatherers (HG) – A hunter and gatherer society uses the undisturbed biosphere for living space and food. The major exposure pathways to a hunter-gatherer are related to foraging discharge areas in the landscape (fishing, hunting, and collecting berries and mushrooms), and from drinking water from surface water (streams or lakes). Land use and habits of a typical HG community have been extracted from historical records (Saetre et al. 2013b and the associated electronic supplementary material), and the group is assumed to be made up of 30 individuals that forage an area of approximately 20 km^2.

Infield–outland farmers (IO) – Self-sustained agriculture in which infield farming of crops is dependent on nutrients from mires (outland). Radionuclides in wetland hay reach the cultivated soil through fertilisation with manure. The major exposure pathways are from growing food and raising livestock, and from drinking water either from a dug well or surface water. A self-sufficient community of IOs is assumed to be made up of 10 persons. A wetland area of 0.1 km^2 (10 ha) is needed to supply winter fodder to the herd of livestock corresponding to the amount of manure needed to support infield crop production for this group.

Drained mire farmer (DM) – Self-sustained agriculture on a former lake or wetland, where both crops and fodder are cultivated on organic soils. Radionuclides that have accumulated for an extended time prior to drainage is the main source of activity, but radionuclides reaching the cultivated soil through groundwater uptake is also taken into account. The major exposure pathways are from growing food and raising livestock, and from drinking water from a dug well (or from surface water). A self-sufficient community of DM farmers is assumed to be made up of 10 persons. A wetland area of 6 ha is needed to support food production for this group, assuming a level of technology similar to that from the turn of the nineteenth century.

Garden-plot households (GP) – A household that is self-sustained with respect to vegetables and root crops produced through small-scale horticulture. Radionuclides reach the cultivated soil through fertilisation (with algae or biomass ash) and irrigation. The major exposure pathways are from growing food and from drinking water from a dug or drilled well (or from surface water). A GP household is assumed to be made up of five persons and a 270 m^2 area garden plot is assumed to be sufficient to support the family with vegetables and root crops. The garden-plot is also associated with support areas providing fertilizers. These depend on the productivity of seaweed, the productivity of wood, or the depth of the peat layer in the biosphere object. In the two latter cases, ash from biofuel combustion is used as fertilizer. The productivity of the garden-plot and the diet for this group have been determined from present-day habits.

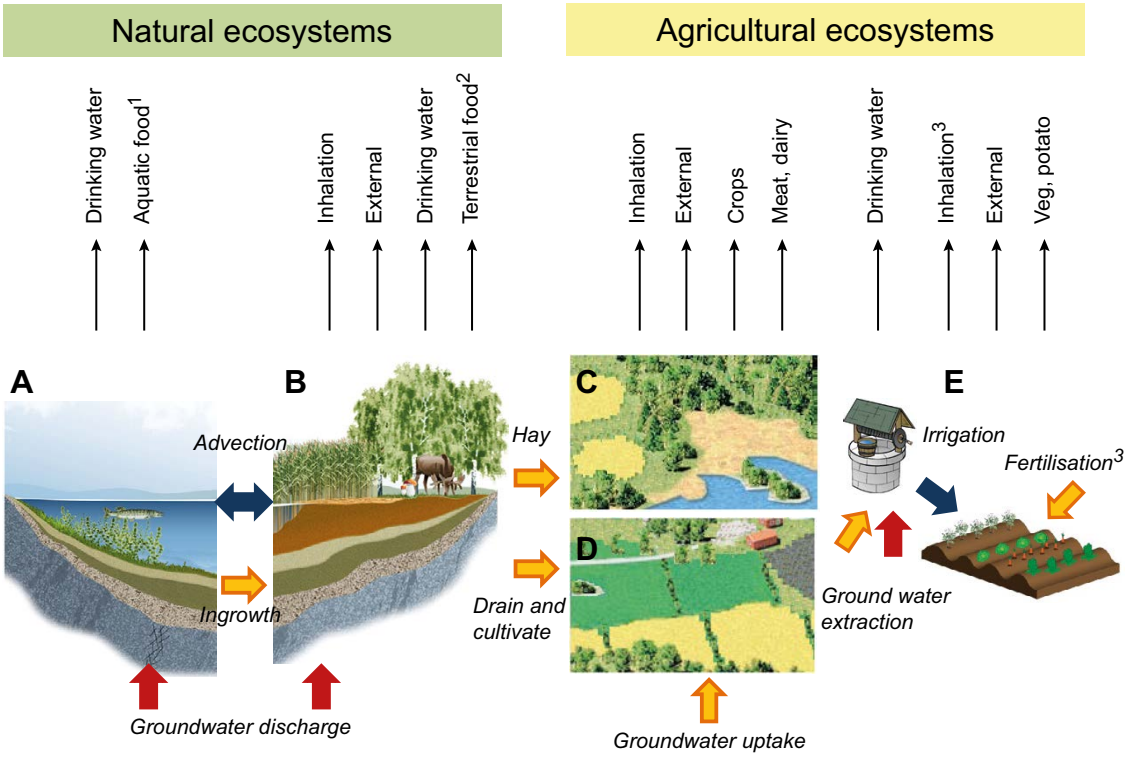

Figure 7-3. *Exposure pathways included in the dose calculations for exposed populations using natural resources and/or living in biosphere objects. HGs use natural aquatic (A) and mire (B) ecosystems. The other three exposed populations represent different uses of arable land, namely infield-outland agriculture (C), draining and cultivating the mire (D) and small-scale horticulture on a garden-plot (E). Thick arrows represent input of radionuclides from the bedrock (red), from natural ecosystems or deep regolith deposits (orange), or water-bound transfer of radionuclides within the biosphere (blue). The thin arrows (top) represent exposure routes: 1 = fish and crayfish, 2 = game, berries and mushroom, 3 = inhalation and fertilisation that include radionuclides from combustion of biofuel. Figure from* ***Biosphere synthesis report****.*

Assessment endpoints for non-human biota

The assessment endpoint for NHB is absorbed dose rate to a set of reference organisms (**Biosphere synthesis report**, Section 6.3). As for humans, an exposure pathway analysis for NHB was conducted in the SR-PSU (SKB R-14-02), which is valid also for the present assessment. The outcome of the exposure pathway analysis was that eight exposure route cases were screened in: internal exposure due to seawater, lake/stream water or peat, and external exposure from seawater, lake/stream water, sea sediment, lake/stream sediment or peat (SKB R-14-02, Table 3-9).

It is practically impossible to consider and ensure protection of every single population of organisms at the site, so generalisations are necessary to allow assessments to focus on a few representative targets, i.e. reference organisms, characterising the range of species and their habitats present. Species at the site are represented by several *reference organisms* included in ERICA in terrestrial, freshwater and marine ecosystems. Reference organisms are a set of organism types selected as assessment targets to represent organisms that are likely to get the highest exposure in the ecosystems of relevance. Thus, they mirror the reference man concept employed in human dose calculations.

Since the SR-PSU, the reference organisms have been updated (Brown et al. 2016), along with updates to the ERICA tool (Brown et al. 2008, the present assessment is based on v2.0, public release: November 2021). Key changes include removal of the "Bird-egg" organism type, as it was deemed inconsistent with the general protection strategy, while adding the freshwater "Reptile", as some protected reptile species in Europe were identified. In total, 38 organism types have been included in the PSAR: 13, 14 and 11 for terrestrial, freshwater and marine ecosystems, respectively (Table 7-5).

Table 7-5. Organism types included in the analysis of NHB.

Terrestrial ecosystem	Freshwater ecosystem	Marine ecosystem
Amphibian	Amphibian	Benthic fish
Annelid	Benthic fish	Bird
Arthropod – detritivorous	Bird	Crustacean
Bird	Crustacean	Macroalgae
Flying insects	Insect larvae	Mammal
Grasses & herbs	Mammal	Mollusc – bivalve
Lichen & bryophytes	Microphytobenthos	Pelagic fish
Mammal – large	Mollusc – bivalve	Phytoplankton
Mammal – small-burrowing	Mollusc – gastropod	Polychaete worm
Mollusc – gastropod	Pelagic fish	Vascular plant
Reptile	Phytoplankton	Zooplankton
Shrub	Reptile	
Tree	Vascular plant	
	Zooplankton	

7.4 Base case

7.4.1 General description

The *base case* constitutes the basis for the analysis of the main scenario, and thus the radionuclide transport and dose calculations. The conditions in the repository and its environs at closure and post closure are chosen based on the initial state (Chapter 4) and the *present-day climate variant* of the reference evolution (Sections 6.2 and 6.3). Thus, the *base case* considers present-day climate conditions for the entire assessment period (Section 6.2.1). This calculation case also fulfils the regulatory requirement that an assessment of a repository's protective capability should include a case where the biosphere conditions prevailing at the time of the application will not change (SSMFS 2008:37).

The shoreline displacement in the *base case* is dominated by the isostatic rebound following the last glaciation. This results in 1 000 years of submerged conditions in the area above the repository (Section 6.2.1). Radiological consequences of using longer periods with submerged conditions are evaluated in the *timing of shoreline regression calculation case* (Section 7.7). A submerged period shorter than 1 000 years is not considered realistic due to the current and future sea level rise (Section 6.2 and the **Climate report**, Section 3.5).

The *base case* serves as a starting point for the analysis of uncertainties in other calculation cases. Models configured, and assumptions made, for the other calculation cases are therefore only described if they deviate from the *base case*, and results from these cases are compared with those for the *base case*. Thus, the description of the *base case* is far more detailed than the descriptions of the other calculation cases. A comparison of the radionuclide transport between the *base case* and the SR-PSU base case, the global warming calculation case, is given in the **Radionuclide transport report**, Appendix C.

The description of the *base case* follows the structure established by the radionuclide transport modelling chain (Figure 7-1), starting with the near field (Section 7.4.2), followed by the geosphere (Section 7.4.3) and the biosphere (Section 7.4.4). A summary of the *base case* transport calculations, including the resulting annual dose to humans, is given in Section 7.4.5. The results are presented as the mean of 1 000 probabilistic simulations, each of which has a unique set of parameter values which are sampled from pre-defined uncertainty ranges. A statistical analysis of the annual dose across the 1 000 simulations is presented in Section 7.4.6. Finally, the conclusions from the analysis of the *base case* are documented in Section 7.4.7. A detailed description of the radionuclide transport and dose modelling for the *base case*, as well as a detailed analysis of the results from each model used in the calculations, is given in **Radionuclide transport report**, Chapter 5.

7.4.2 Handling in the near-field

The transport of radionuclides in the near-field is primarily controlled by the hydrological conditions, which in turn depend on the shoreline regression and the conditions of the engineered bentonite and concrete barriers (Section 6.2.7). The latter degrades over time due to leaching and cracking, causing deteriorating hydraulic barrier properties. The degradation of cementitious materials also affects their mineralogical–chemical properties, in turn causing changes to the sorption of many radionuclides over time. The sorbent properties of the silo bentonite and the macadam backfill are also considered, whereas those of metals and their corrosion products are pessimistically disregarded (Section 7.3.4). Sorption may also be reduced due to the presence of organic complexing agents in most vaults, considered in the modelling in terms of sorption reduction factors (SRFs).

The radionuclide transport calculations in the near-field require information on flow-related and non-flow-related migration properties and their development in time. The data used are described in the **Data report** and the **Radionuclide transport report,** Appendix A. For more details on the implementation, see the **Radionuclide transport report,** Section 5.3.

Hydrological conditions

The near-field hydrological evolution is mainly controlled by the shoreline displacement and the conditions of the engineered barriers, but also to some extent by changes in the natural (rock) barriers (Section 6.2.7). No significant changes to the mechanical properties of the bedrock are expected over the next 100 000 years (Section 6.3.4) and such changes are thus omitted in the *base case*. However, the effects of shoreline displacement and degradation of the engineered barriers on the hydrological conditions are considered.

The evolution of the near-field groundwater flow in the *base case* is based on the modelling by Abarca et al. (2020)[29], using regional hydrogeological conditions (Section 7.4.3) and rock hydraulic properties as boundary conditions (see the **Radionuclide transport report**, Section 5.3.1 for further details on the implementation). The near-field groundwater flow was calculated for four shoreline positions (at

[29] Note that the ”base case” mentioned in Abarca et al. (2020) represents the flow obtained when the barriers are intact, whereas the flow selected for the *base case* in the main scenario also accounts for degradation of the barriers.

2000, 2500, 3500 and 5000 AD) covering the transition from submerged to fully-terrestrial conditions above the repository. The transition results in an increase of the groundwater flow by two orders of magnitude or more in all waste vaults. The groundwater flow through the vaults in the base case (intact barriers) from Abarca et al. (2020) is shown in Figure 7-4.

Concrete physical properties

The degradation of cementitious materials in the waste packages and engineered barriers can be divided into two main categories; physical degradation and chemical degradation. In the following, the physical concrete degradation considered in the *base case* is described. The chemical degradation of the concrete is described in the subsection *Chemical conditions of concrete barriers and waste* below.

Physical degradation of cementitious materials includes cracking and other changes of the pore structure, caused by, for example, degradation of reinforcement, leaching and formation of new mineral phases (Section 6.2.9). The physical changes influence radionuclide transport mainly due to changes in hydraulic conductivity, porosity and diffusivity. The evolution of the concrete physical degradation is evaluated in Höglund (2014) and is simplified to be used in the radionuclide transport calculations.

Following Abarca et al. (2020), the evolution of the hydraulic properties of concrete is described by four stages; (i) intact concrete, followed by (ii) moderately, (iii) severely and (iv) completely degraded concrete. Intact concrete is considered to have a hydraulic conductivity of 1×10^{-9} m/s or lower. For each degradation state, the hydraulic conductivity of the concrete structures increases by two orders of magnitude until a limiting value of 1×10^{-3} m/s is reached for complete degradation.

The effect of these degradation states on groundwater flow through the waste domains in each vault is shown in Figure 7-5. As expected, groundwater flow generally increases the more degraded is the concrete. The increase is largest in 1BMA and 2BMA, where the flow increases by approximately two and four orders of magnitude, respectively, for completely degraded concrete compared with intact concrete. In these vaults, the concrete barriers are thus more important for limiting groundwater flow through the waste domains than for the other vaults. For the silo, the influence of concrete degradation on groundwater flow is very small. For this vault, bentonite constitutes the main hydraulic barrier rather than concrete (Sections 4.4.1 and 6.2.9). In comparison, flow through the waste in 1–2BTF and 1BRT increases by less than one order of magnitude as the concrete degrades.

The total groundwater flow through the vaults (grey bars in Figure 7-5) is generally unaffected by the degradation of concrete, because flow is primarily limited by the bentonite in the silo and diverted through the backfill in the other vaults. The properties of bentonite and backfill do not change with time (see below). The BLA vaults are not credited with any hydraulic barriers in the modelling and thus are unaffected by physical concrete degradation.

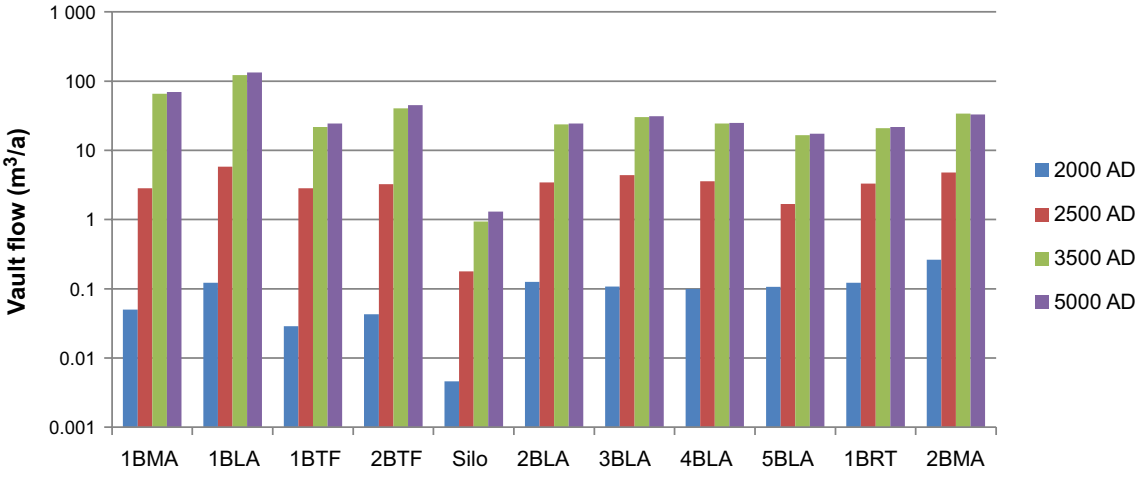

Figure 7-4. *Modelled flow (m^3/a) in the waste vaults for different shoreline positions corresponding to the years given by the legend. Modified from Abarca et al. (2020).*

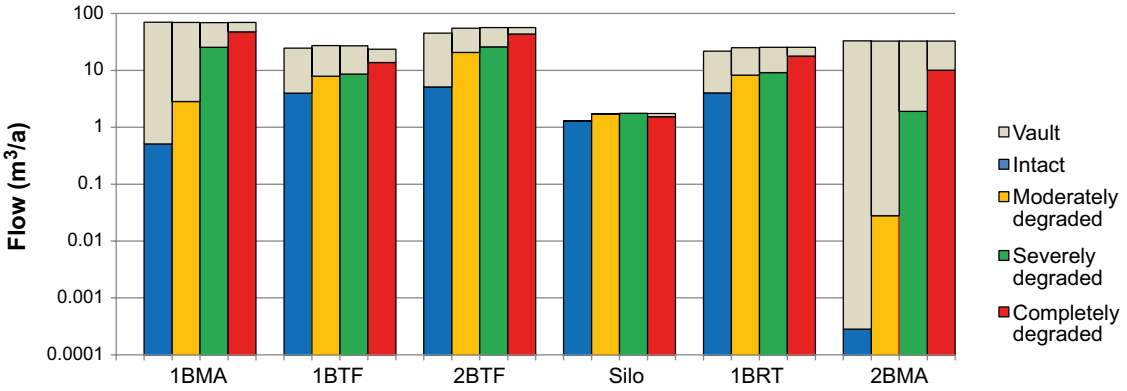

***Figure 7-5**. Modelled flow rates (m^3/a) in the waste vault (grey bars) and waste domains (coloured bars) for different concrete degradation states for terrestrial conditions above the repository (shoreline position corresponding to 5000 AD). Modified from Abarca et al. (2020).*

In the modelling, two vaults are considered to have intact concrete at initial state, namely all structures in 2BMA and the new outer walls in 1BMA and (Figure 7-6). The initial hydraulic conductivity of the structural concrete in 2BMA is set to 1×10^{-9} m/s. This value is more than a factor of 100 higher than the values obtained in measurements of fresh concrete planned to be used for 2BMA, and can therefore be considered to cover uncertainties associated with the construction of the concrete structures and the development of their properties during the operational period (e.g. Mårtensson and Vogt 2019).

The properties of the new outer walls in 1BMA corresponds to the repair and strengthening measures that are planned to be taken before repository closure (Section 4.4.2). These measures will limit groundwater flow through the waste in 1BMA and compensate for the cracking that has been observed in some places on the existing structure. The external walls are considered to replace the existing structures as the main hydraulic barrier, as the hydraulic conductivity (K) is more than four orders of magnitude lower than in the existing structure (8.3×10^{-10} m/s vs. 1×10^{-5} m/s, see the **Data report**, Chapter 9).

All other waste vaults are considered to have a hydraulic conductivity corresponding to degraded concrete at the initial state (Figure 7-6); this is motivated in the following.

- For the silo, the hydraulic conductivity of the structural concrete at initial state and during the entire submerged period is set to 1×10^{-7} m/s. This value will likely be much lower, especially in the beginning of this period, but it is cautiously assumed to successively increase due to expansive corrosion of reinforcement bars (Section 6.2.9 *Impact of material expansion*).
- The concrete barriers in 1BRT are not required to constitute a hydraulic barrier (Table 5-1). During the initial period of submerged conditions, the hydraulic properties of the concrete barriers in 1BRT may be affected due to minor cracking caused by corrosion of tie rods or reinforcement bars (Section 6.2.9). Thus, the concrete barriers in 1BRT are considered to already have a hydraulic conductivity corresponding to severely degraded concrete at closure.
- For 1–2BTF, small cracks (< 1 mm wide) in the concrete tanks cannot be ruled out during the operational period (Section 4.4.5). Thus, the concrete is considered to have a hydraulic conductivity corresponding to moderately degraded concrete at initial state.

The leaching of cement minerals and loss of function of the reinforcement bars will over time reduce the load-bearing capacity of the concrete structures. The consequence of this process is dependent on the design of the structural part, the extent of degradation as well as the direction and magnitude of the loads to which it is exposed. Following the approach in the SR-PSU, the concrete structures in all waste vaults are considered to be completely degraded ($K = 10^{-3}$ m/s) at the latest by 52 000 AD due to leaching and cracking (SKB TR-14-01, Section 7.4.3). The concrete of the existing structure in 1BMA and the tanks in 1–2BTF are envisaged to become completely degraded prior to the other vaults, namely at 22 000 AD and 12 000 AD, respectively (Figure 7-6). The main reason for the earlier degradation in these vaults is that existing cracks are expected to widen, and new cracks may form due to corrosion of tie rods or reinforcement bars in the concrete (Section 6.3.9 *Summary*). The relatively thin concrete of the tanks in 1–2BTF is the reason why the complete physical degradation in that vault occurs earlier than in the existing 1BMA structures.

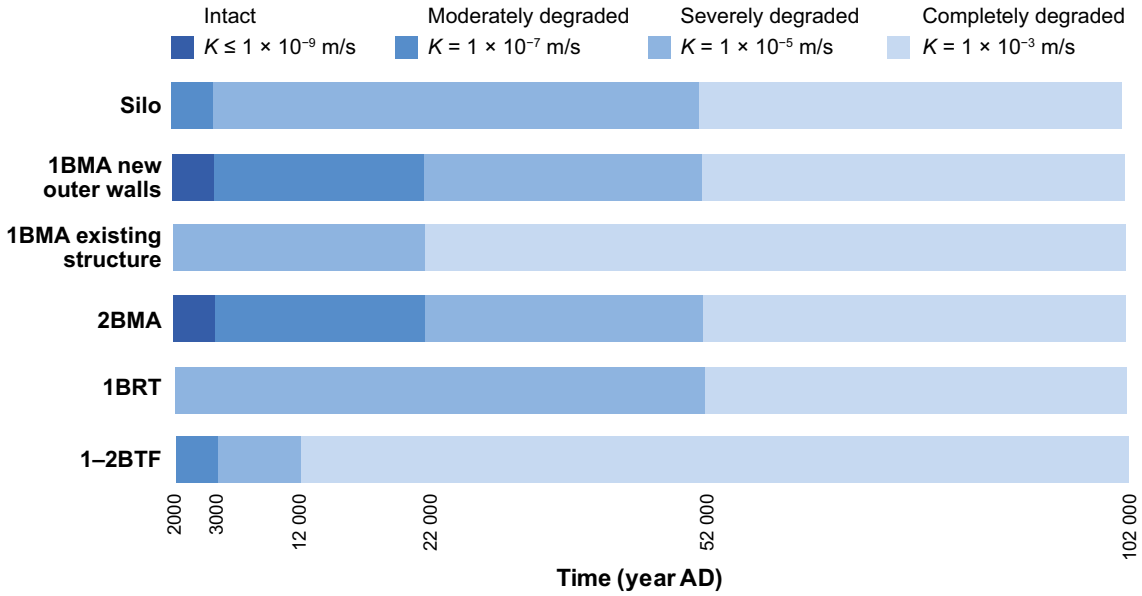

Figure 7-6. *Succession of the hydraulic conductivity of concrete in the base case.*

The transitions to moderately and severely physical concrete degradation states in Figure 7-6 are motivated by the following considerations:

- Silo:
  - 3000 AD; corrosion of reinforcement bars due to intrusion of chloride (Section 6.3.9 *Impact of material expansion*).
- 1BMA new outer walls and 2BMA:
  - 3000 AD, chemical interaction with species in the groundwater and substances leached from the waste (Section 6.2.9 *Chemical interaction with species in the groundwater and substances leached from the waste*).
  - 22 000 AD, widening of existing cracks due to dissolution of cement minerals (Section 6.3.9 *Impact of local dissolution and leaching*).
- 1–2 BTF:
  - 3000 AD, corrosion of reinforcement bars due to intrusion of chloride causing some cracking of the concrete tanks (Section 6.2.9).

As the concrete degrades over time, the diffusion-available porosity and the effective diffusivity of radionuclides in the concrete structures increase (Höglund 2014). The evolution of these parameters varies between the different barriers of the waste vaults, see the **Data report** for further details.

Cracks in concrete

Advective transport through concrete barriers is modelled either through a homogenous porous medium or a cracked medium. Cracks affect the sorption of radionuclides by forming a channel for advective transport in which the radionuclides can travel without having access to the sorption sites. In general, for intact or moderately degraded concrete, the groundwater flow is considered to be relatively slow and to be distributed over several small cracks. However, for a severely or completely degraded concrete, the magnitude of the groundwater flow is larger and considered to be localised to a few major cracks to such an extent that it reduces the mean transit time of radionuclides. For 1–2BMA and 1BRT, advective transport through the concrete structures has been modelled using a crack (a transfer directly from the waste domain to the crushed-rock backfill) during periods with severely and completely degraded concrete (Figure 7-6). Thus, the existing structure of 1BMA, including the slab, is assumed to be cracked at initial state. For the new outer walls in 1BMA and the walls in 2BMA, advective transport through the concrete structures has been modelled as transport through a homogenous porous medium up to 22 000 AD. A more detailed discussion on the applicability of the model with cracked media, based on how cracks affect the mean transit time for radionuclides through the concrete barriers, is presented in the **Radionuclide transport report**, Appendix B.

Chemical conditions of concrete barriers and waste

The chemical–mineralogical properties change over time as the cement minerals in the concrete degrade. The chemical degradation of the cementitious materials mainly influences radionuclide transport by changing their ability to sorb radionuclides (Sections 6.2.8 and 6.3.8). The chemical degradation is much slower than the physical degradation. This implies that even when concrete has lost its hydraulic barrier function it will still provide a chemical barrier function, and substantial amounts of many radionuclides will be sorbed to the barriers throughout the assessment period.

The chemical degradation of cementitious materials can be divided into four steps (**Data report**, Section 7.4): degradation state I (dissolution of sodium and potassium hydroxides from the concrete pore water, pH > 12.5), degradation state II (leaching of portlandite, pH ≈ 12.5), degradation state IIIa (incongruent dissolution of calcium silicate hydrates (CSH) phases, presence of Ca-aluminates, pH ≈ 12) and degradation state IIIb (incongruent dissolution of CSH phases, absence of Ca-aluminates, pH ≈ 10.5). The rate of degradation will vary somewhat between different parts of a waste vault (Section 6.2.9). The differences are however judged to have a limited effect on the average sorption in a vault. Hence, for simplicity, it is assumed that degradation occurs at the same rate in all cementitious materials within a single vault. The duration of the degradation states for each waste vault in the *base case* is shown in Figure 7-7. It is based on the pH calculations performed by Cronstrand (2014) for SFR1 and Höglund (2018, 2019) for 1BRT and 2BMA, respectively. The resulting pH development is presented in Table 6-4. However, unlike Höglund (2018, 2019), Cronstrand (2014) assumed a constant water flow post 7000 AD. Thus, the 1–2BTF transport model cautiously assumes a faster chemical degradation rate (Figure 7-7) than given in Cronstrand (2014) and Table 6-4.

Modelling of sorption is implemented using a linear approach, based on sorption coefficients (K_d values) specific to the chemical species. The sorption coefficients for cement paste of different chemical degradation states are presented in the **Data report**, Tables 7-4–7-7. The percentage of cement paste in different cementitious materials is given in the **Data report**, Table 7-8. To represent the uncertainty of the sorption capacity of the cementitious materials, the coefficients are implemented in the form of probability density functions. For some radionuclides, the K_d values are independent of the chemical degradation e.g. the sorption coefficients of organic carbon (10^{-5} m^3/kg) and iodine (10^{-3} m^3/kg).

Several of the radionuclides are redox-sensitive, with varying retention behaviour depending on their oxidation state. However, reducing conditions will prevail in the repository throughout the assessment period in the *base case*, due to the strongly reducing metallic steel present in large amounts in waste and barrier materials, as well as the slightly reducing intruding groundwater (Sections 6.2.8 and 6.3.8).

The high pH provided by the cementitious materials suppresses microbial activity (Section 6.2.8 *Gas formation due to microbial activity*). Since pH is considered to never go below 10.5, it is assumed that microorganisms do not affect conditions in the repository.

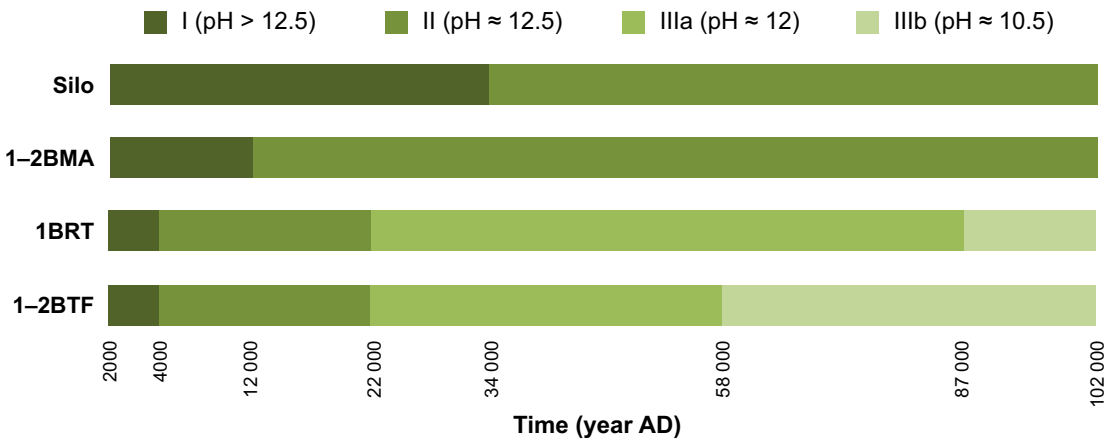

Figure 7-7. *Succession of the four chemical concrete degradation states (I–IIIb) in the base case.*

A slow corrosion-controlled release of irradiation-induced radionuclides in steel from reactor pressure vessels in 1BRT is accounted for in the modelling. The corrosion is assumed to progress at a constant anoxic-corrosion rate based on statistical analyses of literature data (**Data report**, Table 5-13), and the activity is assumed to be evenly distributed within the metal. A further simplifying assumption is that all steel retains the same surface area throughout the corrosion process. Hence, the rate of release of radionuclides from the 1BRT steel waste is constant until it is fully corroded. In the *base case*, it is pessimistically assumed that release of the entire induced activity from the reactor pressure vessels occurs within the first 30 000 years (Section 9.7 in Åstrand et al. 2022). Based on the amount of concrete in 1BRT, a decreasing pH evolution is applied according to Figure 7-7. Although the corrosion rates are expected to remain low even as the pH approaches ~10, the distribution of rates for near-neutral, anoxic conditions are pessimistically applied already from 22 000 AD (**Data report**, Table 5-14).

Complexing agents

Complexing agents tend to associate with cationic radionuclides, forming coordination complexes (Sections 6.2.8 and 6.3.8). This primarily affects metal-ion radionuclides, and the formation of complexes increases their solubility. This directly lowers the fraction sorbed on solid surfaces, predominantly cement minerals, which leads to a decrease in sorption of these radionuclides. Hence, due to the presence of complexing agents in the repository, the sorption coefficients (K_d values) of many radionuclides are divided by a unitless SRF before application in the transport calculations. The SRF depend on the complexing-agent concentrations, which vary spatially in SFR between vaults and 1BMA compartments. (Keith-Roach et al. 2021).

The concentrations of complexing agents and amounts of materials that degrade to complexing agents, e.g. cellulose, allowed in each waste package is restricted and regulated by the waste acceptance criteria (WAC). The amounts allowed according to the most recent WAC[30] are restricted so that the sorption of radionuclides will not be influenced by the amounts of complexing agents and cellulose present in future wastes.

The SRFs are radionuclide-specific because the interaction strength with a complexing agent can vary significantly for different central ions. SRF values are defined for five groups of species (SRF Groups) with assumed analogous complexation properties within each group (Table 7-6). The SRFs are generally greatest for tetravalent radionuclides (SRF Groups 3 and 4), whereas anions and monovalent cations show such small complexing-agent affinities that no sorption reduction is assumed for such species, i.e. SRF = 1 (Keith-Roach et al. 2021). The SRF values are described in detail in Keith-Roach et al. (2021), and their full statistical distributions are used in the probabilistic radionuclide transport modelling (**Radionuclide transport report**, Section 5.3).

Table 7-6. Radionuclides grouped by assumed analogous complexation properties and thus SRF values. Denoted by their oxidation states and relevant isotopes, respectively.

SRF Group	Elements by oxidation state	Relevant isotopes in the transport modelling
Group 1	Ac(III), Eu(III), Am(III), Cm(III), Ho(III), Sm(III), Po(IV),	Ac-227, Am-241, Am-242m, Am-243, Cm-243, Cm-244, Cm-245, Cm-246, Eu-152, Ho-166m, Po-210, Sm-151
Group 2	Pb(II), Pd(II)	Pb-210, Pd-107
Group 3	Th(IV), Np(IV), Pa(IV), Tc(IV), Zr(IV), Sn(IV), Pa(V)	Np-237, Pa-231, Sn-126, Tc-99, Th-229, Th-230, Zr-93
Group 4	Pu(IV)	Pu-238, Pu-239, Pu-240, Pu-241, Pu-242
Group 5	U(VI)	U-232, U-233, U-234, U-235, U-236, U-238
Other	Elements assumed unaffected by complexing agents	Ag-108m, Ba-133, C-14-ind, C-14-inorg, C-14-org, Ca-41, Cd-113m, Cl-36, Co-60, Cs-135, Cs-137, H-3, I-129, Mo-93, Nb-93m, Nb-94, Ni-59, Ni-63, Ra-226, Se-79, Sr-90

[30] Hedström S, Ahlford K, Rosdahl J, Rasmusson M, Maier A, 2021. Krav på avfall från säkerhetsanalysen av SFR1. SKBdoc 1533189 ver 4.0, Svensk Kärnbränslehantering AB. (In Swedish.) (Internal document.)

Properties of bentonite

The bentonite in the silo and plugs is considered to retain its initial-state hydraulic properties for the entire assessment period (Section 6.3.9). The lower part of the silo bentonite wall has a hydraulic conductivity of 9×10^{-12} m/s and the upper part about 9×10^{-11} m/s (**Initial state report**). The hydraulic conductivity of the bentonite in the plugs is 1×10^{-12} m/s. The porosity and the diffusivity of radionuclides in the bentonite in the silo is given in the **Data report**.

Sorption coefficients, K_d values, for the bentonite were selected to be representative for both saline and non-saline groundwaters and are applicable to the full assessment period. The values are given in the **Data report**, Table 7-9. K_d values for the mixture of sand and bentonite are obtained by using a weighted average from the K_d values selected for macadam and bentonite and the weight proportions of the two materials. This approach is used because of the limited amount of experimental data available on sorption on mixtures of sand and bentonite.

Properties of backfill

Changes in the hydraulic properties of the backfill (macadam) due to clogging are expected to be minor (Section 6.3.9 *Backfill material*). Thus, the hydraulic conductivity in the backfill (10^{-3} m/s) is considered to be maintained throughout the entire assessment period (**Data report**, Section 9.12). This choice includes some margin for uncertainties related to clogging of the backfill that potentially could reduce its hydraulic conductivity. The diffusivity and solid density of the macadam are given in SKB (R-01-14, Table 6-10) and the porosity is given in the **Initial state report**, Chapter 12.

Sorption coefficients for the macadam backfill are taken from the geosphere bedrock sorption data (**Data report**, Table 8-8), selecting values for high pH where applicable. Thus, due to different chemical conditions between near-field and geosphere, particularly pH, the K_d values applied in the modelling differ between the two domains for some radionuclides.

7.4.3 Handling in the geosphere

As with the near-field, the geosphere radionuclide transport calculations require both flow and non-flow related radionuclide migration properties as input. Flow-related migration properties are calculated using a site-specific hydrogeological model (Odén et al. 2014, Öhman and Odén 2018). The non-flow related migration properties are primarily based on data used in the SR-PSU. In the following, an overview of the assumptions made in the geosphere modelling for the *base case* is provided. The data used are described in the **Data report** and the **Radionuclide transport report**, Appendix A. For more details on the implementation, see the **Radionuclide transport report**, Section 5.5.

Flow-related migration properties

In the most recent hydrogeological study, three bedrock cases (model-parameterisation variants), namely 1, 11, and 15, were considered to be representative of future flow conditions: a reference case and two bounding cases with low and high flow, respectively (Öhman and Odén 2018). These cases are therefore selected to represent the regional hydrogeological conditions in the *base case*. The variation in vault flow between these three cases is similar to, or greater than, the variation across all bedrock cases used in the SR-PSU (Öhman et al. 2014). For each of the three bedrock cases, steady-state groundwater flow solutions at nine stages of shoreline retreat were evaluated (2000 AD, 2100 AD, 2250 AD, 2500 AD, 2750 AD, 3000 AD, 3500 AD, 5000 AD and 9000 AD). These are representative for resolving the transition from submerged conditions into fully matured terrestrial conditions in the *base case*. The simulations showed that the groundwater flow through the geosphere increases from very low levels, less than 1 % of the maximum flow, during fully submerged conditions, until about 3000 AD when a transition towards a maximum stationary flow occurs. At around 3500 AD, the flow regime around SFR approaches stationary conditions, i.e. the flow regime is largely unaffected by the continued shoreline regression (Figure 7-8).

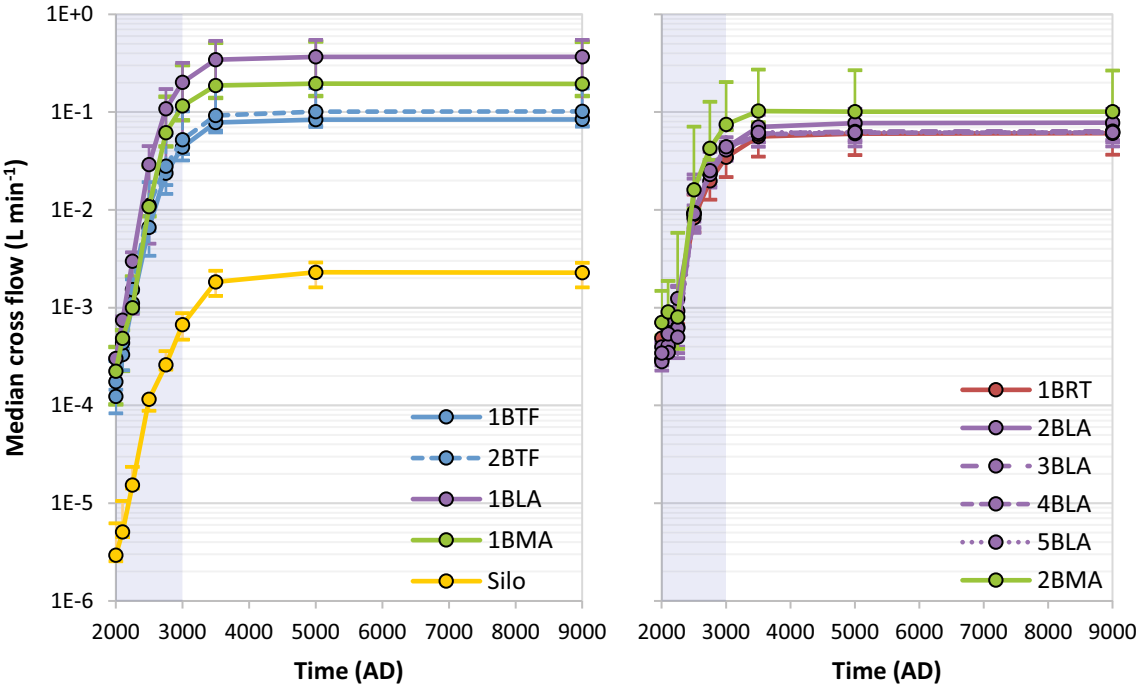

Figure 7-8. *Vault flow (Q) from 2000 AD to 9000 AD in the base case for SFR1 (left) and SFR3 (right). Circles indicate median of the three representative bedrock cases (1, 15, and 11), and bars indicate the variability between these cases. Reproduced from Figure 6-34 in Öhman and Odén (2018).*

For each time-slice, particle tracking was performed with 10 000 particles starting at the bedrock entry (i.e. the vault-rock interface) of each waste vault and terminating at its exit (i.e. rock-regolith interface). Particle tracking was initiated with particles uniformly distributed over the waste vaults under stationary flow conditions for all model permutations (Öhman and Odén 2018). The trajectories collectively describe the potential macro dispersion[31] in the transport through the geosphere.

Advective travel times through the shallow geosphere for groundwater flow are relatively short, typically a couple of years for fully terrestrial conditions above the repository (**Radionuclide transport report**, Table 5-14).[32] Thus, radionuclide residence times in the geosphere are generally considerably shorter than those in the engineered barriers of the waste vaults. Therefore, a simplified approach describing the transport of radionuclides through the geosphere is adopted, using so-called "effective trajectories". For each bedrock case, waste vault and time slice, these trajectories are computed as the median values of the advective travel time (t_w, in units of a m^{-1}) and the flow-related transport resistance (F, in units of a m^{-1}) for the 10 000 trajectories (for details, see the **Radionuclide transport report**, Section 5.5.1). A comparison with a more comprehensive approach, where all individual trajectories are used, shows that the use of effective trajectories is a reasonable simplification of the radionuclide transport calculations (**Radionuclide transport report**, Appendix A).

To describe the patterns of variation and co-variation of the flow-related parameters, t_w, F and the vault flow Q, the three representative bedrock cases are analysed in a mixed linear model (for further details, see the **Radionuclide transport report,** Section 5.5.1). In this analysis, the variation in the flow properties in the silo, SFR1 (apart from the silo), SFR3 are treated as independent. This assumption is reasonable based on the physical distance between the repository units and is supported by previously reported patterns of vault cross flows (Öhman et al. 2014). The linear model calculates the co-variance of the flow-related parameters and describes how these are expected to vary with bedrock realisation across repository units and time. Based on this information, random sets of correlated flow properties are calculated that are propagated as input to the probabilistic simulations.

[31] Macro dispersion is here defined as the dispersion due to splitting of the release in different pathways with varying lengths, transport times and flow-related transport resistances.

[32] Note that the travel times for elements that sorb onto the rock matrix is considerably longer than for the groundwater.

During submerged conditions, topography has a minor effect on the groundwater flow. Thus, during this period, groundwater flow components are mainly vertical and particles follow fracture paths directed upwards (Section 6.2.5). As the shoreline regresses over the repository, conductive fractures and hydraulic pressure gradients due to the surface terrain also influence the path of the particles. As the horizontal flow components successively grow, the trajectory paths are expected to be directed mainly towards the mire in biosphere object 157_2 situated north of the repository (Sections 6.2.5, 6.3.5 and 7.3.5). Therefore, in the *base case,* it is cautiously assumed that all paths are directed towards biosphere object 157_2.

Non-flow related migration properties

The mechanical conditions in the bedrock around SFR are not expected to change significantly during the assessment period (Section 6.3.4). Therefore, changes in the mechanical conditions in the bedrock are not considered in the *base case*.

The density and porosity of the rock matrix and the Peclet number are the same values as in the SR-PSU. Hence, the density is 2 700 kg m^{-3} (Thomson et al. 2008), the porosity is set to 0.18 % (SKB TR-10-52, Table 6-90) and the Peclet number is selected to be 10 (SKB R-01-14, Table 7-3). The penetration depth of the radionuclides, i.e. how far they are allowed to diffuse into the rock matrix, is updated to 0.9 m in the PSAR from 1.4 m in the SR-PSU. This updated distance corresponds to half the average spacing between conductive fractures in the area around the SFR site (**Radionuclide transport report**, Appendix A). The lower effective diffusivity for anions is cautiously used for all radionuclides (Löfgren 2014).

As in the handling in the near-field, modelling of sorption is implemented using a linear approach, based on K_d values specific to the chemical species. The K_d values are obtained from the **Data report**, Table 8-8. Some radionuclides exhibit different sorption characteristics depending on the prevailing pH, redox conditions and groundwater salinity (Sections 6.2.6 and 6.3.6). For these radionuclides, K_d values corresponding to pH < 10 and reducing conditions are selected for the *base case*, and the lowest K_d are cautiously selected with respect to the salinity conditions (temperate saline groundwater conditions).

Due to the lack of detailed investigations and minor impact on dose (**Radionuclide transport report**, Section 5.5.1), the effects of a plume of high pH and complexing agents from the near-field are neglected in the geosphere modelling.

7.4.4 Handling in the biosphere

The biosphere transport and exposure model accounts for landscape development and surface hydrology for the relevant ecosystems (Section 7.3.6). The model relies on several ecosystem parameters and definitions of the exposed human groups as described in the following. Parameters used in the modelling are described in the **Biosphere synthesis report,** Chapter 8, and details regarding their implementation in the *base case* are described in the **Radionuclide transport report,** Section 5.7 and the **Biosphere synthesis report,** Chapter 9.

Landscape properties

The evolution of biosphere object 157_2 and the *well interaction area* resulting from the shoreline regression in the *base case* is summarised in Table 7-7. The deepest parts of object 157_2 are presently approximately 6 m below sea level and, when the object emerges from the sea, the shallowest (southern) parts of the object will emerge first. During the submerged period, radionuclides are expected to reach all basins in direct or indirect contact with basin 157_2, through lateral exchange of water between basins (Figure 7-9). However, during periods of fully terrestrial conditions (after ~4500 AD for object 157_2), radionuclides will only reach objects that are connected with the primary discharge area via surface runoff (Figure 7-10).

In the *base case*, the biosphere description is focused on the primary discharge area (object 157_2). Transport and accumulation of radionuclides in regolith layers and water bodies are described for both the marine and terrestrial periods of object 157_2. Exposure from downstream objects is also evaluated but, for these recipients, water is the only environmental transport medium considered.

The transport and accumulation of radionuclides is simulated in a landscape that is undisturbed by humans. Only after the biosphere object has emerged sufficiently above sea level to prevent intrusion of saline water are the consequences of draining and cultivating the mire complex and extraction of water from a dug well evaluated in parallel. Similarly, the effects of water extraction from a well drilled into the geosphere are evaluated when the *well interaction area* is sufficiently elevated above sea level. The threshold for cultivation and extraction of well water has been set to one metre above sea level, approximately corresponding to the highest storm-surge levels in the area (**Climate report**, Section 3.5 and Grolander 2013, Werner et al. 2013). In the *base case*, the upland parts of object 157_2 and of the *well interaction area* will have emerged one metre above sea level at around 3200 AD and 3000 AD, respectively (Table 7-7).

Table 7-7. Overview of the evolution of biosphere object 157_2 and the well interaction area, resulting from the initial shoreline displacement assumed in the *base case* (Section 6.2.1).

Year AD	Surface above SFR	Biosphere object 157_2	Well interaction area
2000	Submerged	Submerged	Submerged
2500	Shoreline located directly above SFR	Submerged	Submerged
3000	> 75 % terrestrial	Highest point (southern part) above sea level*	Highest area > 1 m above sea level
3500	Terrestrial	20 % of object above sea level, and highest point > 1 m, above sea level	25 % of area > 1 m above sea level
4000	Terrestrial	90 % of object above sea level	67 % of area > 1 m above sea level
4500	Terrestrial	Whole object > 1 m above sea level, mire fully developed.	Whole area > 1 m above sea level

* Dug well and draining possible.

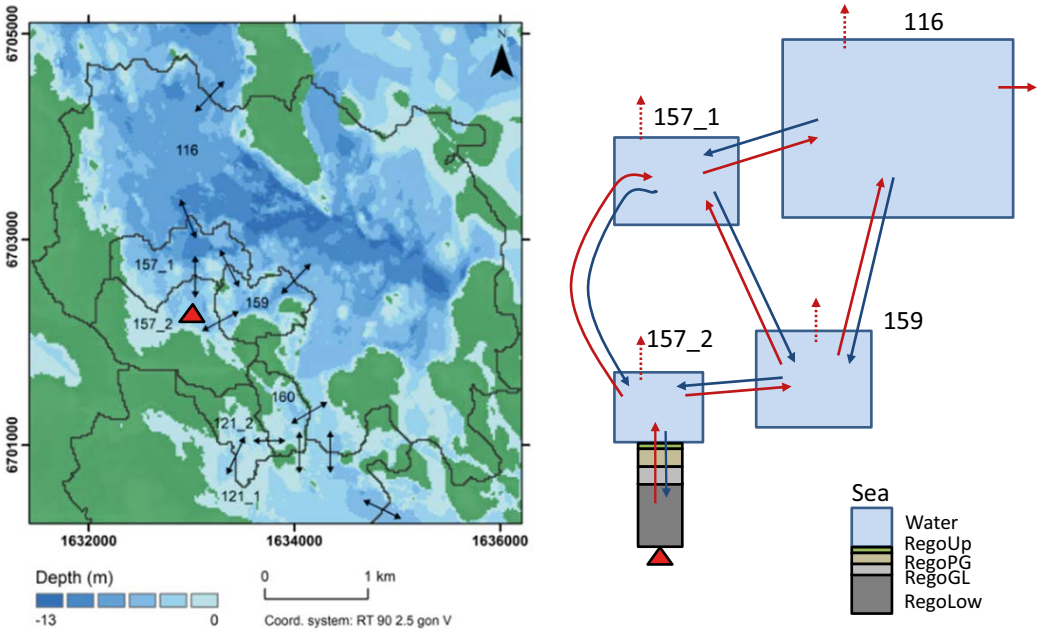

Figure 7-9. *Conceptual model of discharge and dispersion of radionuclides that reach the biosphere via groundwater from the geosphere during the marine stage. The red triangle represents the location of the geosphere release (object 157_2). Left) Water depth and dispersion routes of radionuclides between basins at 3000 AD. Biosphere object 157_2 receives radionuclide-containing groundwater from below. All biosphere objects receive radionuclides via lateral seawater flow during the marine stage. Right) Schematic sketch of the dispersion of radionuclides between regolith layers and surface seawater volumes within and between biosphere objects. The light blue boxes represent seawater. Red arrows show transport of radionuclides along a declining solute concentration gradient. Blue arrows show the transport of radionuclides in the opposite direction. The regolith layers included are (from below); till (RegoLow), glacial clay (RegoGL), post-glacial clay-gyttja (RegoPG), biologically active surface sediments (RegoUp). Dashed arrows represent loss of C-14-org to the atmosphere. Note that the figure represents a snapshot in time and that exchange with basins south of 116 has been excluded for clarity.*

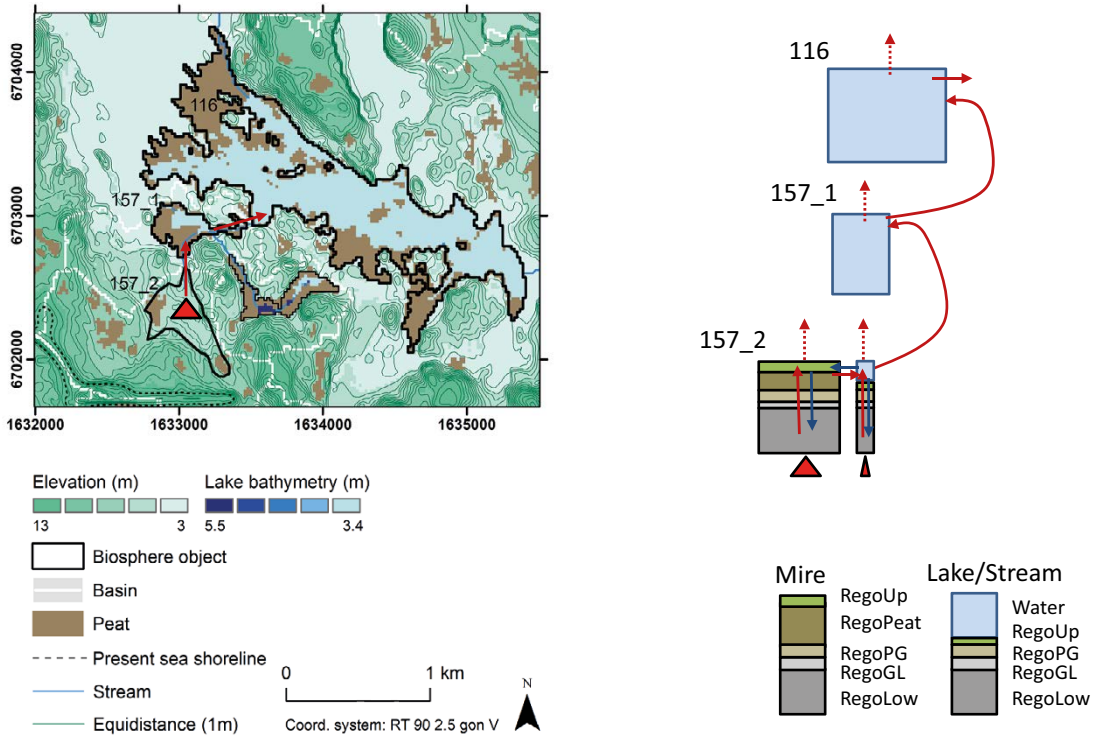

Figure 7-10. *Conceptual model of discharge and dispersion of radionuclides that reach the biosphere via groundwater from the geosphere during the terrestrial stage. The red triangle represents the location of the geosphere release (object 157_2). Left) Ground surface elevation and water depths in lakes at 5000 AD. Downstream objects 157_1 and 116 receive radionuclides via surface water during the terrestrial stage. Right) Schematic sketch of the transport of radionuclides between regolith layers and surface waters within and between biosphere objects. In both the panels, red arrows show transport of radionuclides along a declining solute concentration gradient. Blue arrows show transport in the opposite direction. The regolith layers for aquatic ecosystems are labelled as in Figure 7-9. In terrestrial parts deep peat (RegoPeat) and surface peat (RegoUp) are stratified on top of clay-gyttja. The light blue boxes represent lake and stream water. Dashed arrow represents loss of C-14-org to the atmosphere. Note that the figure represents a snapshot in time and that the lake basins in 157_1 and 116 will ultimately be infilled with peat so that the lakes disappear and only a stream remains.*

Surface hydrology

Surface and groundwater flow rates in the regolith were modelled for future biosphere objects (areas potentially affected by releases) at three points in time: 3000 AD (end of submerged period), 5000 AD (terrestrial period, when objects are either lake-mire complexes or mires) and 11 000 AD (terrestrial period, all objects are mires) (Section 6.3.2). Temperature, precipitation and potential evapotranspiration from present-day conditions, corresponding to the initial-state climate (Section 4.5.1), were used as input data to the simulations.

It is assumed that the runoff from object 157_2 reaches the downstream object 157_1 via a stream (Section 7.5.2 in Werner et al. 2013). The effects of assuming diffuse overland-water transport, rather than stream transport, are examined in the *alternative landscape configuration calculation case* (Section 7.7).

Ecosystem parameters

Ecosystem parameters are based on site data from lakes, wetlands and marine basins in the area and applied to future ecosystems by assuming present-day conditions concerning nutrients and temperatures. The parameters updated since the SR-PSU include those used to describe the accumulation of organic carbon and those describing the crop and water regime of the GP exposed group (Section 7.3.6). In addition, new parameters for chlorine are derived from recent field measurements at Forsmark (**Biosphere synthesis report**, Section 8.2).

Potentially exposed groups and populations

The annual dose to a representative human is calculated for the four different exposed populations described in Section 7.3.6. Exposure pathways included are the ingestion of food and drinking water, inhalation from breathing air, and direct external radiation (**Biosphere synthesis report**, Section 6.2). The exposure from a well drilled in the *well interaction area* is only considered to be relevant for a small group (Section 7.3.6). The pathways considered for this group are the ingestion of water and small-scale irrigation (GP). As the group is small, a risk criterion of 10^{-5} is considered appropriate.[33]

7.4.5 Radionuclide transport and dose

Retention in the waste vaults

Retention of radionuclides in the near-field is primarily achieved by the engineered barriers, as these promote low groundwater flow through the waste and retain many radionuclides by sorption. As a result, most of the initial activity has decayed or is still present within the waste vaults by the end of the assessment period, with only a small fraction having been released. This is illustrated in Figure 7-11, which shows how much of the initial radiotoxicity in the *base case* (including radiotoxicity produced due to ingrowth in the waste vaults) is eventually released to the geosphere at some point during the assessment period. Such a comparison should arguably be interpreted with some caution as the simplifying assumptions adopted in the modelling (e.g. those listed in Section 7.3.4) may affect individual radionuclides differently. However, as the strategy in the modelling is to opt for the cautious or pessimistic choice for uncertain parameters (Section 2.5), the releases shown in Figure 7-11 are more likely overestimated than underestimated. The figure shows that for most of the radionuclides considered in the analysis, especially those with the highest radiotoxicity, more than 90 % of the initial or produced radiotoxicity remains or decays within the waste vaults during the assessment period. Importantly, most radionuclides that have a large fraction of their inventory released from the near-field also have a relatively low initial or produced radiotoxicity, typically less than 0.1 % of the total initial radiotoxicity in SFR (Figure 7-11).

The efficacy of containment also varies depending on the properties of the waste vaults, generally correlating positively with the effectiveness of the engineered barriers in the waste vaults. However, the engineered barriers were designed based on the total radiotoxicity in the waste vaults, such that the waste with the highest initial radiotoxicity typically is disposed in the vaults with the most effective barriers and vice versa (Section 1.3). For example, the silo contains about 80 % of the total initial radiotoxicity (stacked vertical bar in Figure 7-12), but a much smaller fraction of the total near-field release comes from this vault due to the high retention capacity of its barriers (**Radionuclide transport report**, Section 5.3.8). This stands in contrast to the BLA vaults, whose release to the geosphere constitutes a disproportionally large portion of the initial activity, such that most of the disposed radionuclides with half-lives longer than ~1 000 years are released at some point. As a result, despite large differences in the initial inventory between the waste vaults, each of the vaults has a relatively similar contribution to the total dose, with only one-order-of-magnitude difference between the vault with the highest maximum contribution (silo) and the vault with the lowest contribution (1BTF) (Figure 7-12). This result indicates that the initial radiotoxicity of the waste is properly distributed between the individual waste vaults.

Annual dose to the potentially exposed group

The resulting annual doses to the four land-use variants in the *base case* are shown in Figure 7-13. During the initial submerged period, when the groundwater flow is low (Figures 7-4 and 7-8) and agriculture in biosphere object 157_2 is not possible, the HG group is the most exposed group and the resulting doses are low. At 3000 AD, when drilling of wells is possible (Table 7-7), the doses to the GP group utilising the drilled well results in the highest dose for the 200 following years. At 3200 AD, it is considered feasible to drain the peat land in object 157_2, resulting in the DM farmers becoming the most exposed group for the rest of the assessment period (Figure 7-13). This is primarily because radionuclides can accumulate in peat over a long period of time prior to exposure and

[33] To make the dose comparable to that of other exposed populations, it is divided by a factor of ten to allow for the different criteria applied to large and small exposed groups (**Biosphere synthesis report**, Section 7.5.4).

because cultivated ecosystems are highly productive. The maximum annual dose, 5.6 µSv, occurs around 7000 AD. Thus, it remains below the dose corresponding to the regulatory risk criterion (14 µSv) throughout the entire assessment period.

The most important exposure pathways from the drained mire are through ingestion of cultivated crops and of animal products. Both these pathways are linked to uptake of radionuclides by plants, either directly in the edible crops or indirectly via the fodder consumed by livestock. Ingestion of cereals is the most important exposure pathway during the entire assessment period, and accounts for 30–70 % of the total dose (**Biosphere synthesis report**, Section 9.3).

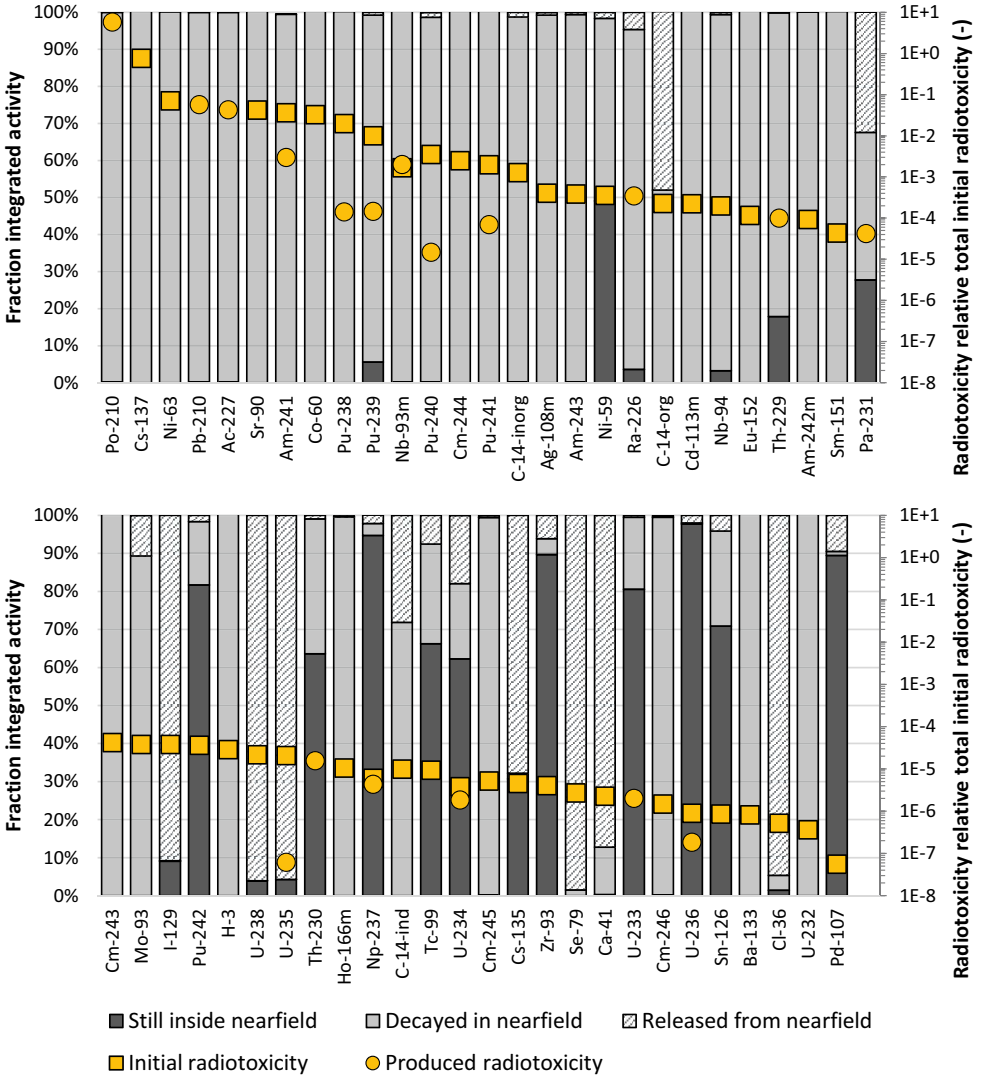

Figure 7-11. *Fates of radionuclides in the near-field in the base case. The radionuclides are sorted from the top-left to the bottom-right in descending order of initial (yellow squares) or ingrown radiotoxicity within the repository summed over the whole assessment period (yellow circles). Both the yellow squares and circles are shown as fractions of the total initial radiotoxicity in SFR (right vertical axis). The bars illustrate the retention capacity of the repository for different radionuclides (left vertical axis); dark grey shows the fraction of the integrated activity (i.e. the initial disposed activity plus the activity produced by ingrowth) still contained in the repository at the end of the assessment period, light grey shows the fraction that has decayed inside the repository and the hatched part shows the fraction that has been released.*

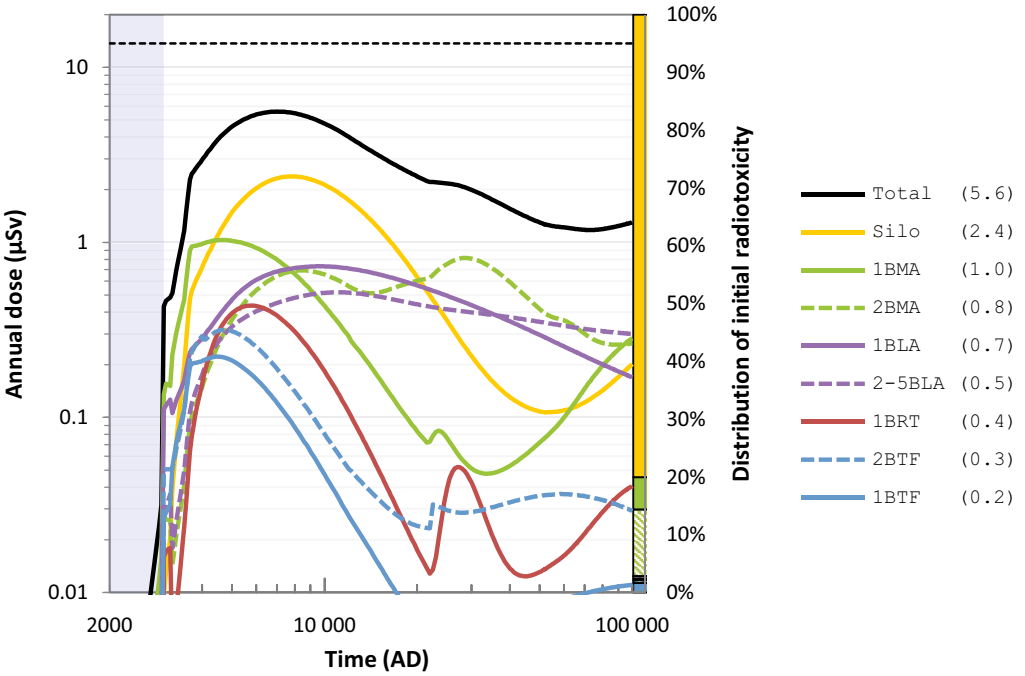

Figure 7-12. *Annual dose in the base case and contributions from individual waste vaults. The stacked vertical bar shows the relative distribution of the initial radiotoxicity in the waste vaults (colours are the same as those given by legend, and the hatched areas in the bar correspond to the dashed lines in the legend). The submerged period is indicated by the blue shading. The total and vault-specific dose maxima are shown in parentheses and the annual dose (14 µSv) corresponding to the regulatory risk criterion is indicated by the black dashed line. Note that the annual dose is the mean across the 1 000 probabilistic realisations (Section 7.3.1). Unless otherwise noted, the mean across the probabilistic simulations are shown in all dose figures presented in this report.*

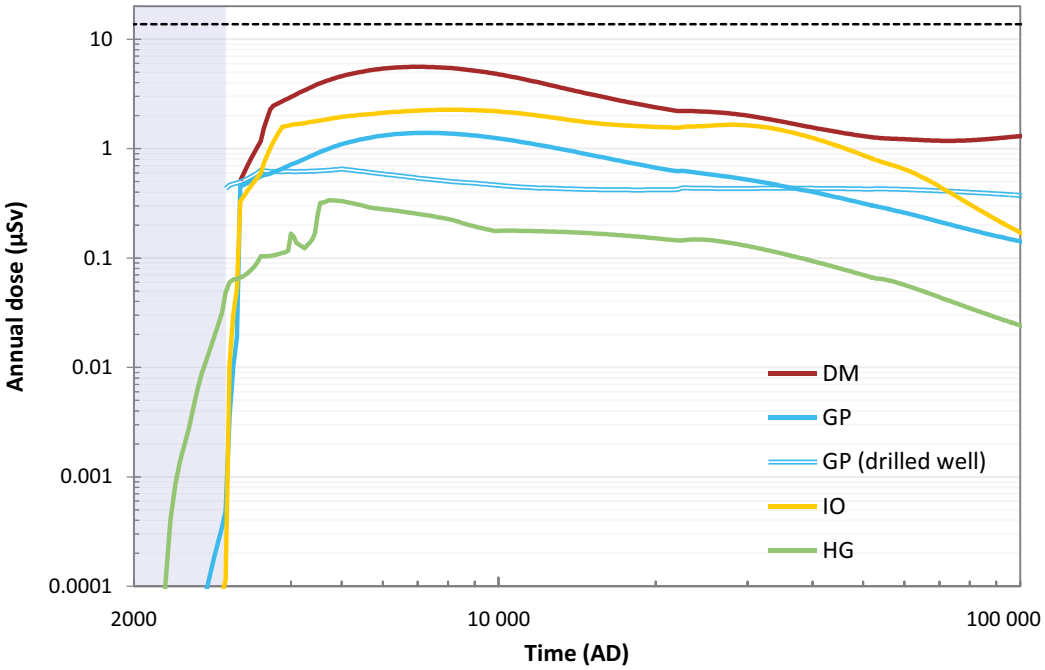

Figure 7-13. *Annual dose to the exposed groups in the base case, that is to hunter-gatherers (HG), infield-outland farmers (IO), drained-mire farmers (DM) and garden-plot households (GP). The dose to the GP group from a dug and drilled well are shown separately (blue lines). The submerged period is indicated by the blue shading and the black dashed line indicates the annual dose (14 µSv) corresponding to the regulatory risk criterion.*

Radionuclide-specific transport and dose

Most radionuclides have only modest dose contributions to the total dose in the *base case*. This is illustrated by the fact that only 11 of the 53 radionuclides explicitly considered in the analysis contribute at any point with more than 0.1 μSv[34] to the total dose. One important reason for the minor dose contributions from most radionuclides is the high retention in the waste vaults (see above). However, other radionuclide-specific properties are also important for dose, namely (i) initial radiotoxicity of the inventory, (ii) radioactive decay and ingrowth, (iii) retention in the geosphere and the biosphere and (iv) uptake in plants and transfer to animal products.

Radionuclides that contribute with more than 0.1 μSv to the annual dose at some point during the assessment period are shown in Figure 7-14. Each of the radionuclides featured in the figure has different transport properties that explain their respective dose contributions. For example, I-129 has a relatively low initial inventory (Figure 4-2) but it is also very long-lived and has a low retention during transport through the repository system. U-235 and U-238 originate mostly from the BLA-vaults, which are not credited with any transport retention properties. However, unlike the other radionuclides in Figure 7-14, uranium sorbs strongly in the rock matrix and so the contributions to dose from U-235 and U-238 are mitigated due to retention in the geosphere.

The most important radionuclides for the total annual dose are Mo-93 and C-14-org that contribute most during the period of maximum dose, Ca-41 that contributes most in the middle of the assessment period, and Ni-59 that contributes most at the end of the assessment period[35] (Figure 7-14). To illustrate the properties of these dose-dominating radionuclides, as well as their transport through the repository system, Figure 7-15 shows their relative activity remaining in each repository-system component (including that which has left the modelled system, denoted “Export” in Figure 7-15) at the time point of their respective dose maxima (circles). In addition, the figure shows the corresponding distribution between repository-system components of the activity that has decayed until the same point in time (triangles). The transport and retention of the four dose-dominating radionuclides, based on the results shown in Figure 7-15, are discussed in the radionuclide-specific subsections below.

[34] 0.1 μSv is approximately 0.7 % of the dose corresponding to the regulatory risk criterion.

[35] In addition to Ni-59, Cs-135 contributes somewhat to the dose at the end of the assessment period. Both radionuclides also show an increasing dose trend at the end of the assessment period. A supporting calculation (not shown) covering the next 1 million years shows that, while the doses from both radionuclides continue to increase for some time after 102 000 AD, their contributions remain well below the dose corresponding to the risk criterion for the entire period of one million years (**Radionculide transport report**, Section 5.7.2).

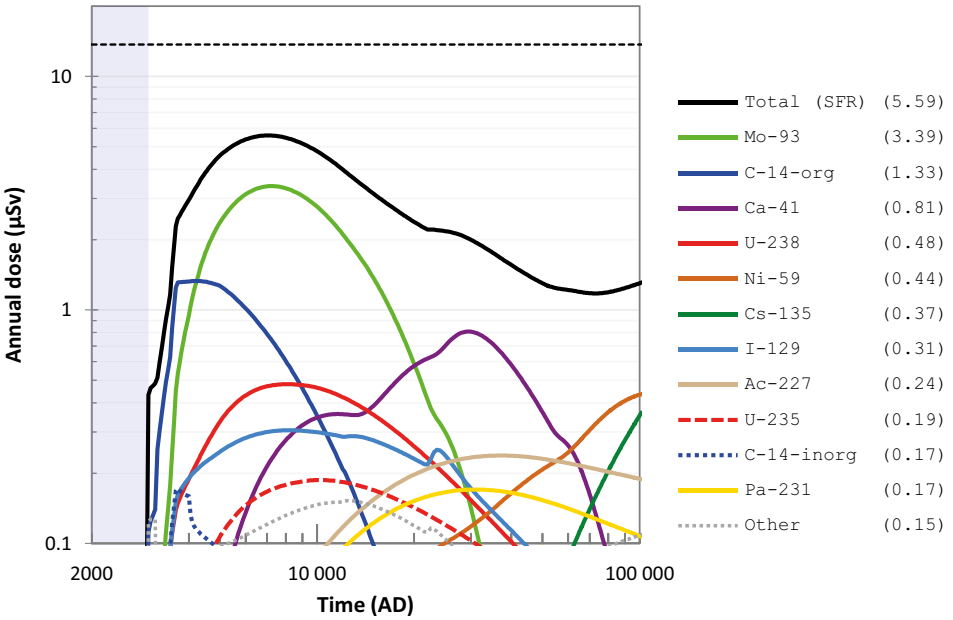

Figure 7-14. *Annual dose to the most exposed group, including radionuclides contributing most to the total dose, for releases from all waste vaults in the base case. Only radionuclides that contribute with more than 0.1 µSv to the total dose at some point during the assessment period are shown. The blue shading indicates the submerged period. The radionuclide-specific dose maxima are shown in parentheses and the annual dose (14 µSv) corresponding to the regulatory risk criterion is indicated by the black dashed line.*

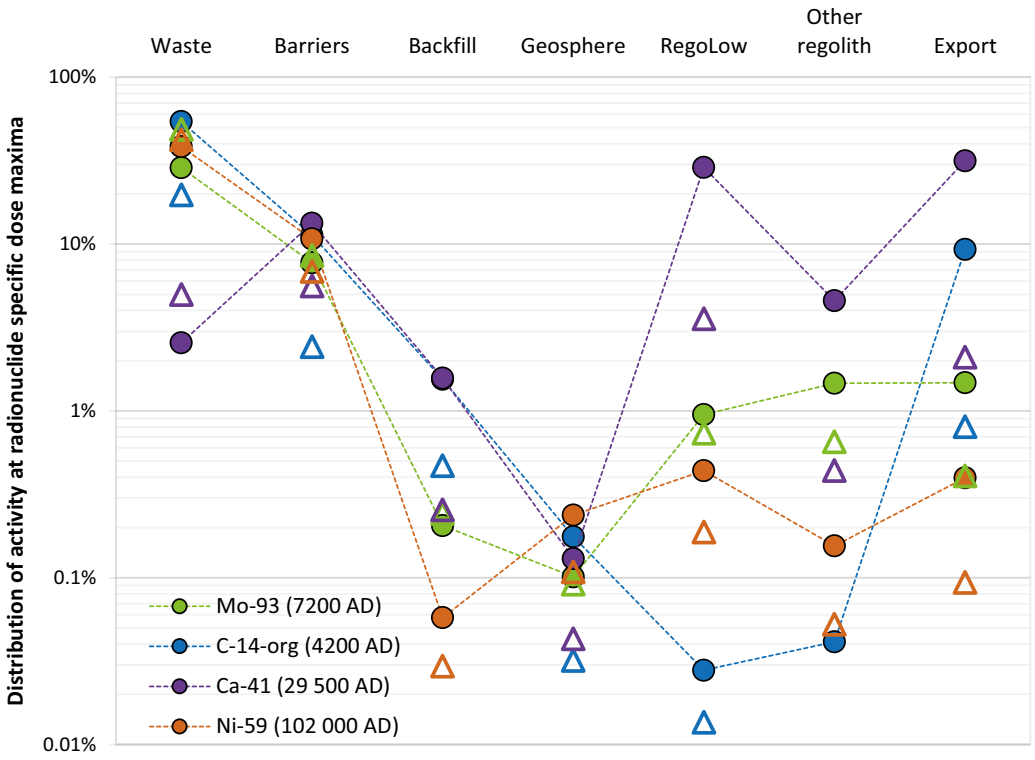

Figure 7-15*. Distribution of activity between repository-system components, including outside the model (Export, far right), of the remaining activity (circles) and accumulated decay (triangles) of the four dose-dominating radionuclides at the time of their respective dose maxima to the DM group in the base case. The timing of the maximum dose from each radionuclide is noted in the legend.*

C-14-org

C-14-org has a high initial inventory in the silo and 1BMA (Figure 7-16) and displays negligible sorption in all repository-system components as modelled here. As a result, it is relatively quickly transported through the repository, the geosphere and the regolith layers. It is ultimately exported out of the system by degassing or is transported downstream via surface water. Owing to its mobile nature and relatively short half-life, the dose maximum occurs relatively early for this radionuclide, at about 2000 years after repository closure. The total dose contribution from each waste vault correlates positively to the initial activity within the vaults, but 1–2BTF have disproportionally large releases considering their inventory. Residence times of C-14-org are slightly shorter in 1BMA than in the silo, implying that releases from 1BMA contribute more to dose for the first few thousands of years, whereas the silo contributes more for the reminder of the assessment period (Figure 7-16). Thus, the fact that most of the C-14-org is still present within the waste and barriers at the time of its dose maximum, as seen in Figure 7-15, is primarily due to the strong retention properties of the silo. In addition, owing to its mobile nature, accumulation is of minor importance for exposure. Instead, groundwater uptake is the primary source for C-14-org in the drained and cultivated mire (**Biosphere synthesis report**, Section 9.3).

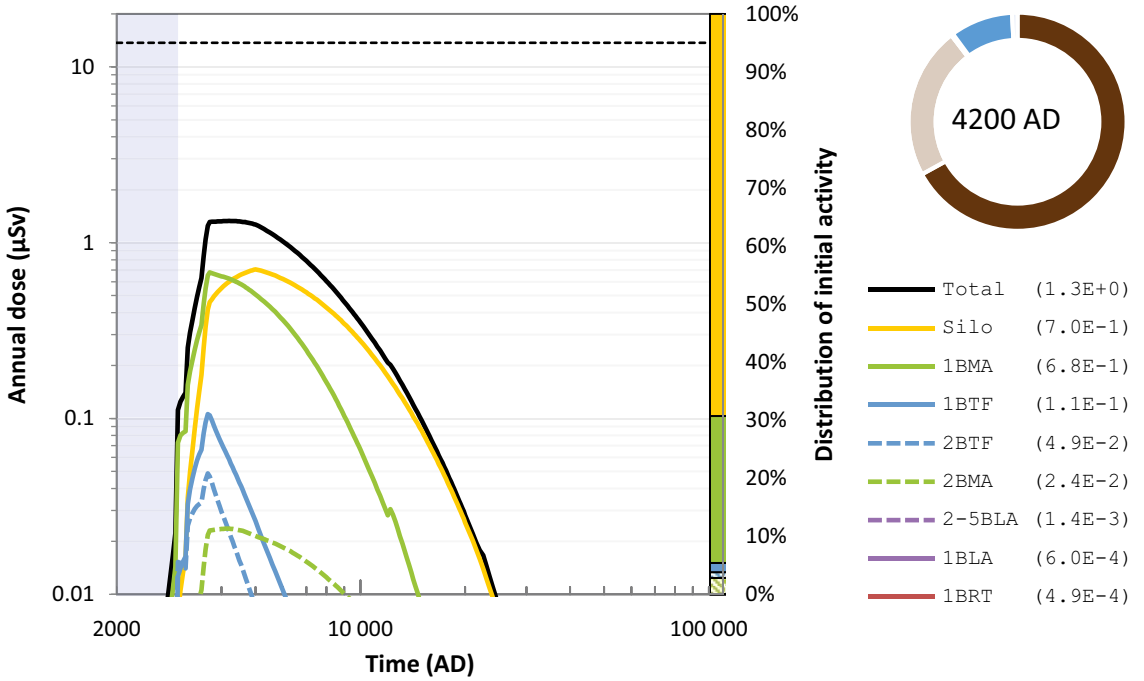

Figure 7-16. *Annual dose from C-14-org to the most exposed group in the base case, including contributions from individual waste vaults. The stacked vertical bar shows the relative distribution of the initial C-14-org activity in the waste vaults (colours are the same as those given by legend, and the hatched areas in the bar correspond to the dashed lines in the legend). The submerged period is indicated by the blue shading. The total and waste-vault specific dose maxima of C-14-org are shown in parentheses and the annual dose (14 µSv) corresponding to the regulatory risk criterion is indicated by the black dashed line. The circle diagram shows the distribution of the activity in the near-field (brown) and the export from the system (blue) and the cumulative decay in the near-field (pale brown) at the time for maximum dose (data from Figure 7-15). Note that the activity in the geosphere and the biosphere are too small to be visible in the circle diagram.*

Mo-93

Most of the initial activity of Mo-93 is found in the silo, with significant, albeit lower, activities also in 2BMA and 1BRT. These waste vaults also contribute most to the dose from this radionuclide (Figure 7-17). Doses from Mo-93 are significant in the *base case*, contributing more than 50 % to the total dose maximum (Figure 7-14). Nevertheless, the engineered barriers inhibit Mo-93 transport; the analysis demonstrates that, despite relatively weak sorption onto cement, only a couple of percent of the total Mo-93 inventory has been released to the geosphere by the time of its dose maximum (7200 AD, Figure 7-15).[36] Further, Mo-93 has a half-life of 4000 years, implying that more than half of its initial activity has decayed in the vaults at the time of dose maximum.

Mo-93 sorbs weakly to the rock matrix, so it is virtually unaffected by transport through the geosphere. It sorbs more strongly in the biosphere, particularly in the organic-rich upper regolith layers (cf. "Other regolith" vs "RegoLow" in Figure 7-15). Most of the accumulated activity of Mo-93 in the biosphere will be exposed when those layers are cultivated by the DM group. The doses from Mo-93 are dominated, almost entirely, by ingestion of cultivated crops (**Biosphere synthesis report**, Section 9.3).

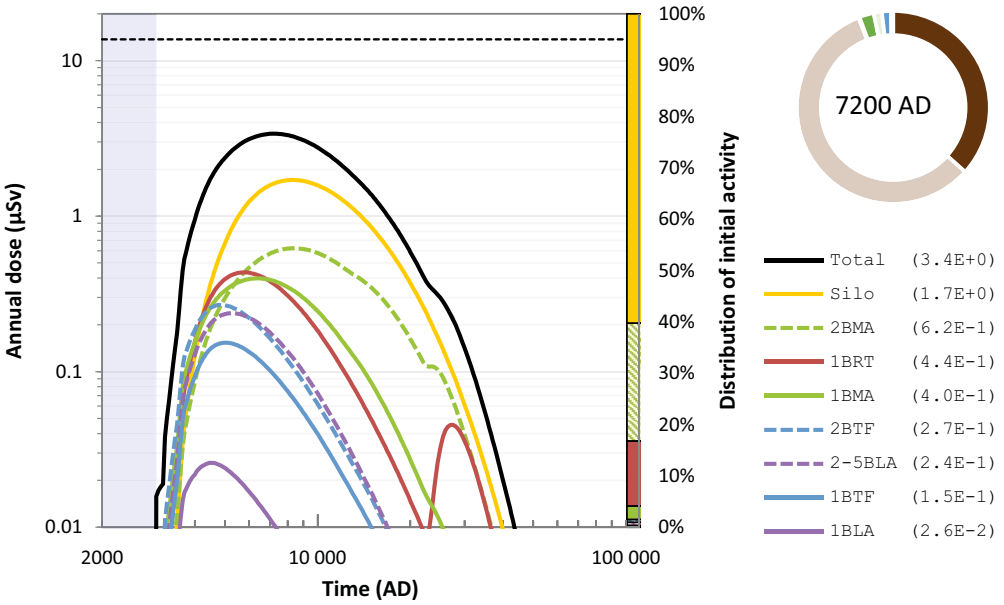

Figure 7-17. *Annual dose from Mo-93 to the most exposed group in the base case, including contributions from individual waste vaults. The stacked vertical bar shows the relative distribution of the initial Mo-93 activity in the waste vaults (colours are the same as those given by legend, and the hatched areas in the bar correspond to the dashed lines in the legend). The submerged period is indicated by the blue shading. The total and waste-vault specific dose maxima of Mo-93 are shown in parentheses and the annual dose (14 µSv) corresponding to the regulatory risk criterion is indicated by the black dashed line. The circle diagram shows the distribution of the activity (solid colours) in the near-field (brown) and biosphere (green), the export from the system (blue) and the cumulative decay (pale colours) at the time for maximum dose (data from Figure 7-15). Note that the activity in the geosphere is too small to be visible in the circle diagram.*

[36] Over the entire assessment period, ~10 % of the total Mo-93 inventory is released to the geosphere, while the remaining ~90 % decays in the waste vaults (**Radionuclide transport report**, Figure 5-36).

Ca-41

The initial Ca-41 activity is present only in 2BMA and in 2–5BLA, which have very different transport properties. The waste containers in the BLA vaults are not credited with any transport retention capability, so significant releases of Ca-41 from those vaults start immediately after the shoreline recedes past the repository and groundwater flow becomes appreciable. This results in a relatively early dose contribution of Ca-41 from 2–5BLA (Figure 7-18). In 2BMA, the residence time of Ca-41 in the concrete caissons is relatively long until 12 000 AD and 22 000 AD, when the concrete undergoes physical and chemical degradation, respectively (Figures 7-6 and 7-7). Given its long half-life (102 000 years), Ca-41 releases from 2BMA increase significantly in response to these two degradation events. Thus, 2BMA contributes considerably later to the dose of Ca-41 than the BLA vaults (Figure 7-18). A further consequence of sorption onto cementitious materials in 2BMA is that the Ca-41 activity inside the barriers is higher than in the waste at the time of maximum dose (Figure 7-15).

Sorption of Ca-41 is not considered in the geosphere (**Data report**, Section 8.6), so the geosphere release of this radionuclide is similar to its near-field release. In the biosphere, Ca-41 is strongly sorbing in inorganic regolith layers and is primarily retained within the lowest regolith layer (Figure 7-15). At the time of maximum dose, ca. 30 000 AD, similar amounts of activity have decayed as remain in the near-field (~15 %). However, twice as much activity has accumulated in the biosphere or has left the surface system (ca 30 % each) (Figure 7-15). Ingestion of food, especially animal products, is the dominant exposure pathways for this radionuclide (**Biosphere synthesis report**, Section 9.3).

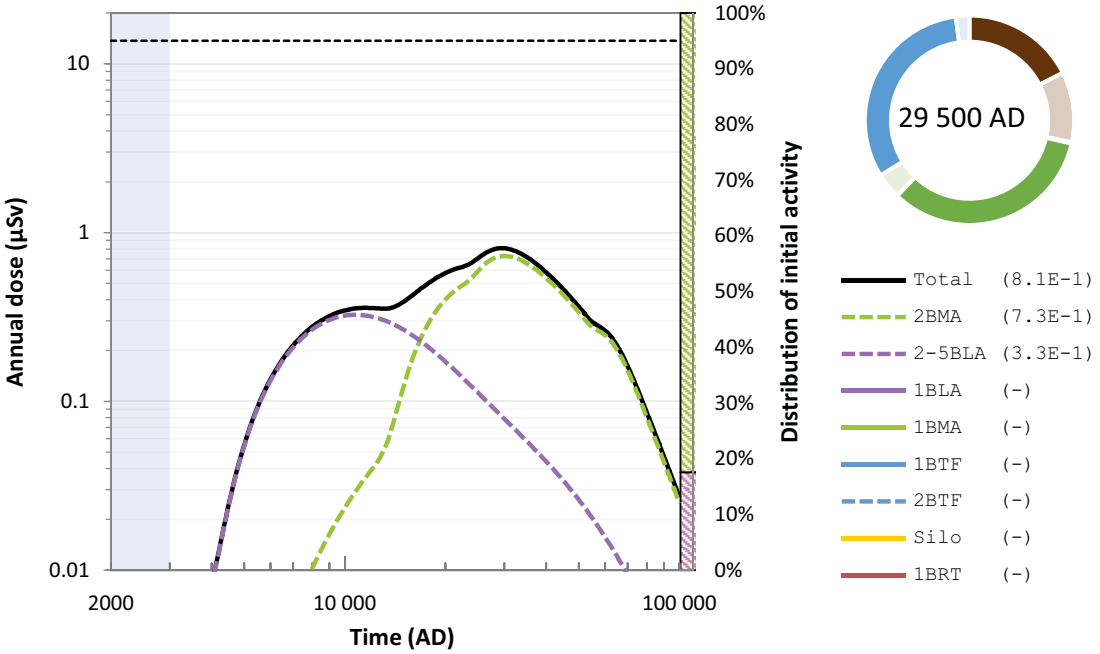

Figure 7-18. *Annual dose from Ca-41 to the most exposed group in the base case, including contributions from individual waste vaults. The stacked vertical bar shows the relative distribution of the initial Ca-41 activity in the waste vaults (colours are the same as those given by legend, and the hatched areas in the bar correspond to the dashed lines in the legend). The submerged period is indicated by the blue shading. The total and waste-vault specific dose maxima of Ca-41 are shown in parentheses and the annual dose (14 µSv) corresponding to the regulatory risk criterion is indicated by the black dashed line. The circle diagram shows the distribution of the activity (solid colours) in the near-field (brown) and biosphere (green), the export from the system (blue) and the cumulative decay (pale colours) at the time for maximum dose (data from Figure 7-15). Note that the activity in the geosphere is too small to be visible in the circle diagram.*

Ni-59

Although most of the Ni-59 inventory is present in the silo, 1BMA and 2BMA, other waste vaults with relatively small inventories contribute notably to the annual Ni-59 dose (Figure 7-19). The reason is that the activity disposed in the silo and the BMA vaults is effectively retained by sorption onto cement and bentonite. Therefore, 98 % of the total Ni-59 activity either decays or remains in the repository by the end of the assessment period (which coincides with its dose maximum, see Figure 7-15). Ni-59 is a long-lived radionuclide (half-life is 101 000 years), so releases from the near-field to the geosphere are largely controlled by concrete degradation in 1BMA and 2BMA at later stages of the assessment period. Overall, however, annual releases of Ni-59 from SFR are relatively constant throughout the assessment period (**Radionuclide transport report**, Figure 5-42).

In contrast to the other dose-dominating radionuclides, Ni-59 sorbs, albeit relatively weakly, to the rock matrix (**Data report**, Table 8-8). Consequently, the release of Ni-59 from the geosphere is slightly lower than that from the near-field and the fraction of its total activity in the geosphere is higher than for the other dose-dominating radionuclides (Figure 7-15).

As with Ca-41, Ni-59 sorbs more strongly onto the inorganic lower regolith layers than to the organic upper layers (Figure 7-15). However, Ni-59 sorption in these layers is substantially stronger than for Ca-41 (**Biosphere synthesis report**, Table 9-2), resulting in longer biosphere residence times. This together with the relatively constant release of Ni-59 results in higher doses towards the end of the assessment period.

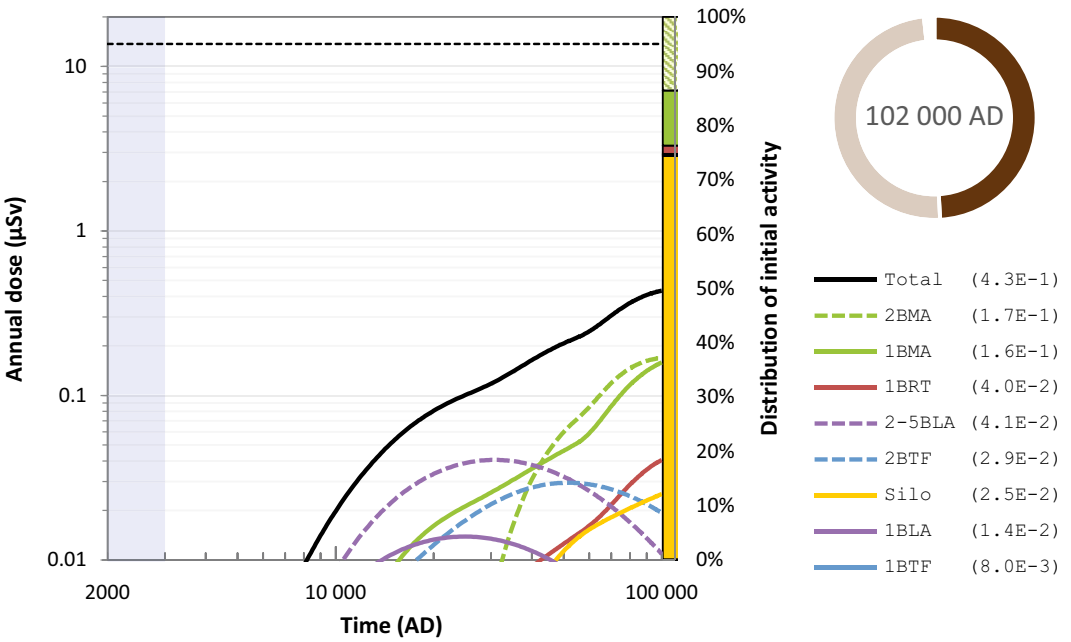

Figure 7-19. *Annual dose from Ni-59 to the most exposed group in the base case, including contributions from individual waste vaults. The stacked vertical bar shows the relative distribution of the initial Ni-59 activity in the waste vaults (colours are the same as those given by legend, and the hatched areas in the bar correspond to the dashed lines in the legend). The submerged period is indicated by the blue shading. The total and waste-vault specific dose maxima of Ni-59 are shown in parentheses and the annual dose (14 µSv) corresponding to the regulatory risk criterion is indicated by the black dashed line. The circle diagram shows the distribution of the activity (solid colours) in the near-field (brown) and the cumulative decay in the near-field (pale brown) at the time for maximum dose (data from Figure 7-15). Note that the activity in the geosphere and the biosphere as well as the activity exported from the system are too small to be visible in the circle diagram.*

7.4.6 Impact of data uncertainty

In the preceding subsections, only the mean doses across all 1 000 probabilistic simulations in the *base case* were presented and discussed. However, each of the simulations uses a different combination of input parameter values originating from the uncertainty in individual parameters. Thus, the releases and doses are unique for each simulation and deviate from the mean values across all simulations. In the following, the effect on the resulting dose of these parameter uncertainties is further examined.

The uncertainty in input parameters causes a significant variation in the calculated dose between the 1 000 realisations that underlies the mean, i.e. the expected value, of the annual dose. The difference between the 5th and the 95th percentiles of the dose typically span an order of magnitude, and this span tends to widen with time (Figure 7-20). Although uncertainties will inevitably increase far into the future, the pattern in the simulations primarily reflects the differences in uncertainties associated with the individual radionuclides that contribute to the dose in sequence. That is, the uncertainties in the dose from C-14-org and Mo-93 that contribute early, are relatively small compared to the uncertainties of dose from Ca-41 and Ni-59 that contribute later (for further details on uncertainties for individual radionuclides, see the **Radionuclide transport report**, Appendix D and the **Biosphere synthesis report**, Section 11.2).

In Figure 7-20, the mean dose is consistently above the median dose. This is to be expected, because the total dose (at each point in time) is approximately log-normally distributed. This reflects that most of the important input parameters in the *base case* affect the dose multiplicatively and have positively skewed distributions (**Radionuclide transport report**, Appendix D and the **Biosphere synthesis report**, Section 11.2). Based on the central limit theorem (see Ekström 2017 for details), the confidence intervals of the mean value (thin blue lines in Figure 7-20) can be estimated with good precision assuming that it is normally distributed. It can be noted that the confidence interval of the mean exhibits small variability (less than 10 % of the mean dose), clearly indicating that the number of realisations (1 000) is sufficient for an acceptable level of convergence.

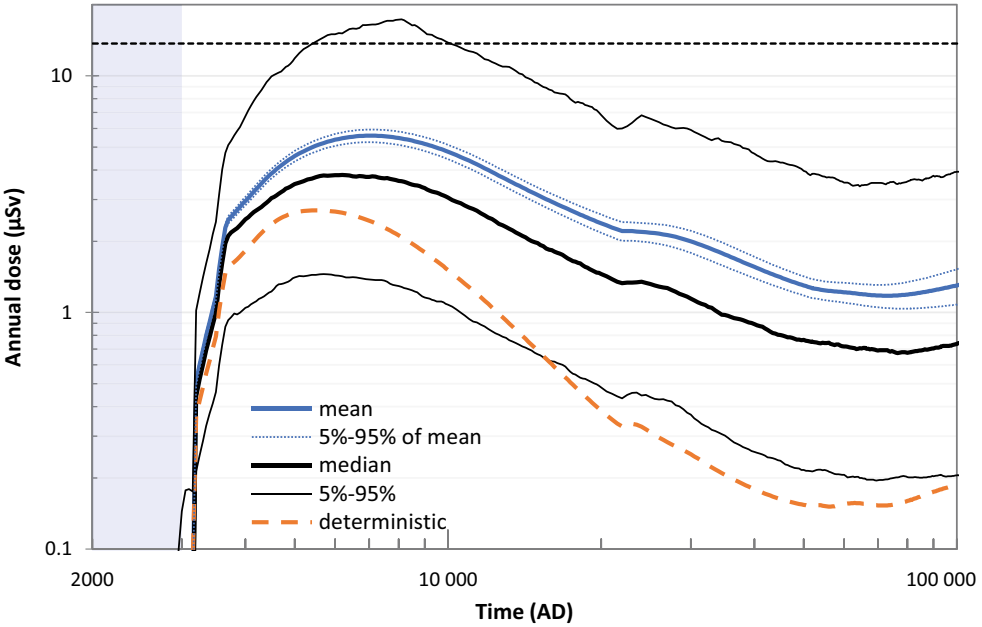

Figure 7-20*. Distribution and characteristics of the total annual dose in the base case. Blue colour represents the mean (expectation) value of the dose from probabilistic simulations, with the 90-percent confidence interval of the mean (thin blue dotted lines). The span of the 1 000 realisations is shown as the 5th and the 95th percentile of the simulations (thin black lines) and the 'typical dose' (i.e. the median) from the realisations is shown in black. The dose calculated from one deterministic simulation using best estimates for all input parameters is shown for comparison (dashed orange line). The submerged period is indicated by the blue shading and the annual dose (14 µSv) corresponding to the regulatory risk criterion is indicated by the black dashed line.*

It can also be noted that a deterministic simulation, with best estimates for each input parameter, yields a systematically lower dose than the mean dose from probabilistic calculations. This indicates that data uncertainty does not lead to an underestimation of the dose. After about 20 000 AD, only 5 % of the probabilistic simulations result in doses that are lower than the deterministic calculations (i.e. the 5th percentile curve is then above that for the deterministic results in Figure 7-20). This somewhat counter-intuitive result is primarily caused by parallel pathways for accumulation and exposure in the biosphere. That is, for some radionuclides several regolith layers contribute similarly to the accumulation in the drained and cultivated soil and several separate ingestion pathways contribute similarly to dose. When parallel pathways have similar importance and the underlying parameters are positively skewed in a direction that increases exposure, the dose from probabilistic simulations has a strong tendency to be higher than that of the deterministic simulation, which uses the best-estimate values.[37] In addition, for a few biosphere parameters, the PDFs have been biased towards increased exposure by selecting the PDFs with a central value above the best estimate. The effects of parallel pathways and biased PDFs on dose can be seen most clearly in the period between 20 000 AD and 60 000 AD when Ca-41 contributes most to the dose, see **Biosphere synthesis report**, Section 9.4 for further details.

The potential for risk dilution due to the probabilistic simulations is evaluated in Section 10.6.

7.4.7 Concluding remarks

In the *base case*, the total annual dose throughout the entire 100 000-year assessment period is below the dose corresponding to the regulatory risk criterion, 14 μSv, with a maximum of 5.6 μSv occurring at around 7000 AD. Draining and cultivation of a mire (DM farmers) in biosphere object 157_2 is the land use variant resulting in the highest doses and four radionuclides were found to be of specific interest for the total dose. Mo-93 and C-14-org contribute most to the total dose from the time of repository closure up until the time of dose maximum, Ca-41 contributes the most in the middle of the assessment period and Ni-59 contributes the most at the end of the assessment period.

The outcome of the analysis of the *base case* is consistent with SKB's general understanding, acquired from previous safety assessments, of radionuclide transport through the SFR repository system. Differences in transport patterns of individual radionuclides are explained by radionuclide-specific properties and by properties of individual waste vaults. Deterministic simulations with best estimates for each input parameter were found to systematically yield a lower dose than the average dose from probabilistic calculations, indicating that data uncertainty does not lead to an underestimation of the dose. Sensitivity analyses of specific assumptions in the *base case* are illustrated in dedicated supporting calculations in Section 7.7. Taken together, the analysis of the *base case* helps to build confidence that the model results are reliable, robust and that they serve as a credible starting point for the analysis of uncertainties in other calculation cases evaluating the main scenario, less probable scenarios and residual scenarios.

7.5 Warm climate calculation case

7.5.1 General description

The *warm climate calculation case* is selected to evaluate the effects on post-closure safety of a future development characterised by business-as-usual anthropogenic greenhouse-gas emissions. The conditions in the repository and its environs at closure and post closure are chosen based on the initial state (Chapter 4) and the *warm climate variant* of the reference evolution (Sections 6.2 and 6.4). External conditions at Forsmark are characterised by temperate climate conditions for the entire assessment period, albeit with a warmer climate than in the *base case* (Section 6.4.1). The warmer climate results in 4 500 years of submerged conditions above the repository (Section 6.2.1).

Precipitation is projected to increase because of a warmer climate during the winter, spring and autumn seasons, but may either increase or decrease during the summer season (Section 6.4.1).

[37] When parameters are log-normally distributed, the geometric mean is typically used as the best estimate and the central value of the PDF for biosphere parameters.

Because of this uncertainty, the effects of a warmer climate are examined in two variants: the *high summer precipitation* variant and the *low summer precipitation* variant.

In the *base case*, it is assumed that DM farmers cultivate crops that obtain the water required via groundwater uptake. However, as the climate becomes warmer, the potential evapotranspiration is projected to increase at a faster rate than the precipitation (Section 6.4.1), resulting in increased water demand for crops and potential use of irrigation water to satisfy this demand. In the *warm climate calculation case*, it is therefore assumed that the increased water demand is satisfied either by groundwater uptake or by sprinkler irrigation. To this end, an additional exposed group is considered in the calculations: DM farmers practicing large-scale irrigation.

A detailed description of the radionuclide transport and dose modelling for the *warm climate calculation case*, as well as a more detailed analysis of the results, is given in the **Radionuclide transport report**, Section 6.2.

7.5.2 Handling in the near-field and geosphere

The near-field and geosphere conditions are not expected to be affected by a warmer climate in a way that significantly affects repository performance (Section 6.4). The longer submerged period compared to the *base case* influences the groundwater flow and is handled by imposing a delay of the shoreline regression (**Data report**, Chapter 12). Thus, the progression of the groundwater flow in the near-field and geosphere is shifted 3 500 years forward in time compared to the *base case*. Except for this change, the handling in the near-field and geosphere is identical to the *base case*. Thus, the entire geosphere release is still assumed to be discharged to biosphere object 157_2.

7.5.3 Handling in the biosphere

The modelling of the *warm climate calculation case* in the biosphere considers changes in surface hydrology and ecosystem parameters and includes an additional potentially exposed group: DM farmers practicing large-scale irrigation.

Surface hydrology

Ground- and surface-water flow for the mire state of biosphere object 157_2 in a warmer climate has been simulated with the MIKE SHE tool (**Biosphere synthesis report**, Appendix F). The simulations are based on climates consistent with the two variants described above (*high/low summer precipitation*), and hydrological parameter values are derived from simulated water balances (**Biosphere synthesis report**, Section 8.3.1). In addition to object-specific flows, the net precipitation from the new hydrological simulations was used to characterise percolation in the unsaturated agricultural soils (left panel in Figure 7-21).

In a warmer climate, the projected increase in evapotranspiration is greater than the projected increase in precipitation leading to an increase of the plant water deficit during the vegetation period. This is true for both variants of the calculation case. An increased demand for water could either fully or partly be supplied by an increased groundwater uptake through capillary rise and/or it could be satisfied by irrigation. A multi-model approach is used to forecast the response of crop water demand in agricultural systems (right panel in Figure 7-21).[38] Moreover, it is cautiously assumed that the crop water demand is fully compensated by water containing radionuclides originating from the repository, either from groundwater or from irrigation with surface water.

[38] For this purpose, output data for sixteen combinations of global climate and hydrological models were utilised (**Biosphere synthesis report**, Section 10.2.1).

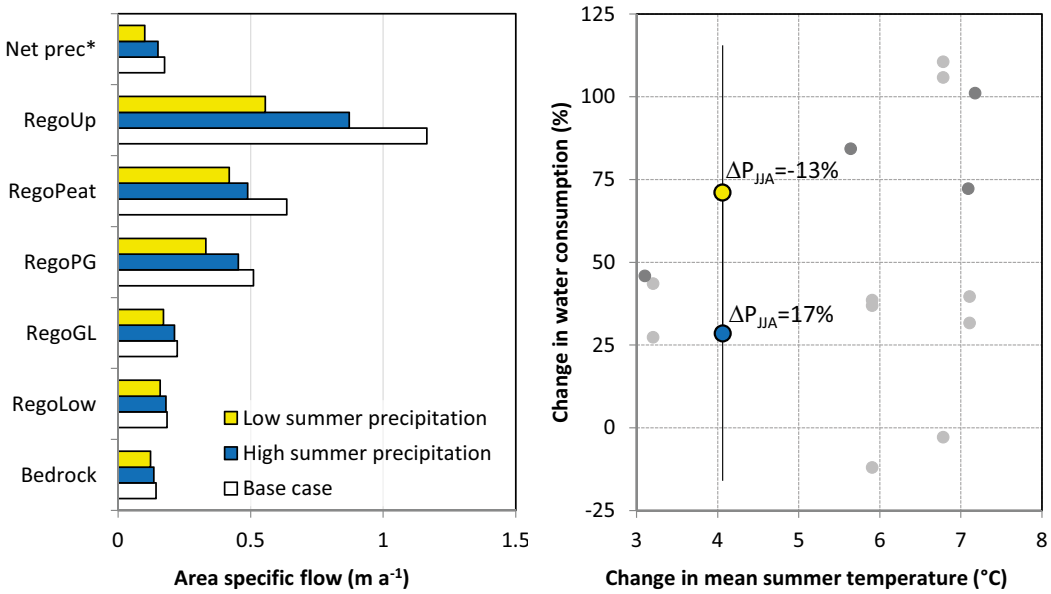

Figure 7-21. *Response in the surface hydrology and the water demand for arable land for the two variants of the warm climate calculation case. Left) Area-specific upward groundwater flow in the regolith layers for the wetland in object 157_2 and net precipitation (*), as predicted with hydrological modelling (**Biosphere synthesis report**, Appendix F). Yellow represents flows in the variant with low summer precipitation, blue flows in the variant with high summer precipitation, and white the flows given present day climate used in the base case. Right) Changes in crop water demand due to changes in summer temperature and precipitation as estimated from a global multi-model approach (Gosling et al. 2019). Coloured symbols represent the mean changes as compared to the demand in the base case. Error bars represents the standard deviation corresponding to the uncertainty in projections between hydrological models (**Biosphere synthesis report**, Appendix G). Dark grey circles correspond to results for the grid point closest to Forsmark, whereas light grey circles represent the average response for entire Scandinavia.*

Ecosystem parameters

Values for ecosystem parameters, such as biomass, net primary production and crop yield are adjusted to increased air temperature based on literature data from warmer locations (Grolander 2013). The concentration of stable CO_2 in the atmosphere is adjusted to elevated levels in accordance with the RCP4.5 emissions scenario (540 ppm; **Climate report**, Section 3.4.1).

Large-scale irrigation of cereal and fodder production is not practiced in Forsmark under present conditions. Adding large-scale irrigation as an exposure pathway to DM farming thus requires the definition of new parameters describing this practice (**Biosphere synthesis report,** Section 8.3.1). Moreover, the processes for accumulation on edible parts of crop (cereals), element translocation to edible parts (potatoes) and weathering of intercepted radionuclides (fodder) are added to the models describing agriculture in warmer conditions. The amount and frequency of irrigation of a garden plot are also adjusted to reflect warmer conditions.

Owing to their different representations of the summer climate, the crop water deficit during the vegetation season, and thus the irrigation and plant groundwater uptake, is higher in the *low summer precipitation* variant than in the *high summer precipitation* variant.

Potentially exposed groups

In addition to the PEGs of humans defined in the *base case*, a variant of DM farmers practicing large-scale irrigation at a relatively low intensity is added (two irrigation events per season at a scale of several hectares, evaluated over 50 years of cultivation). Long-term large-scale irrigation (500 consecutive years) is assessed for the IO farming group (two irrigation events per season). The effects of short-term irrigation at higher intensities (ten irrigation events per season) with well water, either from a dug or a drilled well, are assessed for the GP household group.

7.5.4 Radionuclide transport and dose

As in the *base case*, long-term accumulation in natural ecosystems is also the most important exposure pathway in a warmer climate. Thus, DM farmers are the group exposed to the highest doses in the *warm climate calculation case* (**Biosphere synthesis report**, Figure 10-4). A warmer climate leads to a slight reduction of the maximum dose to this group with respect to the *base case* (Figure 7-22). This is primarily a result of a delayed and reduced release from the near-field of the radionuclides that contribute most to the maximum dose in the *base case*, i.e. C-14-org and Mo-93 (**Radionuclide transport report**, Section 6.2.5). The prolonged submerged period, and the consequently lower groundwater flow, ensures that a larger amount of these radionuclides decay in the waste vaults than in the *base case*.

Despite a lower release from the near-field and the geosphere, the maximum dose from C-14-org is higher in the *low summer precipitation* variant than in the *base case* (Figure 7-23). The dose from C-14-org is near proportional to the rate of groundwater uptake and its activity concentration, as this is the primary source for C-14-org in the drained mire (Section 7.4.5). In the *low summer precipitation* variant, the groundwater uptake increases by 70 % (right panel in Figure 7-21) and the dilution of groundwater decreases by ~15 % (RegoLow in Figure 7-21). Thus, almost twice the amount of radionuclide released from the geosphere reaches the cultivated soil, which affects both root and atmospheric uptake of C-14-org proportionally.

Maximum releases from the near-field of radionuclides with half-lives orders of magnitude longer than the submerged period (e.g. Ca-41 and Ni-59) are generally only marginally affected by the longer submerged period in this calculation case (**Radionuclide transport report**, Section 6.2.5).

In the biosphere, accumulation of radionuclides in the regolith layers generally increases in the *warm climate calculation case* as compared to the *base case*. The accumulation is the greatest in the *low summer precipitation* variant, where the upward groundwater flow is reduced by between ~20 % (glacial clay RegoGL) and 35 % (deep peat RegoPeat) in layers that are exposed by draining (left panel of Figure 7-21). The increased accumulation leads to a noticeable increase in the dose from e.g. Ca-41, Ni-59 and Ac-227, and the dose is consistently higher than in the *base case* for the period after 20 000 AD (Figure 7-23).

The effect of irrigation is evaluated using stream water to compensate for the crop water deficit. This is reasonable because stream water is generated locally and is readily available in the discharge area. As stream water is diluted with the runoff generated in the catchment, the dilution is more than a factor four larger than in groundwater used to meet the crop water demand assuming capillary rise from the saturated lower regolith layer. The effect of surface water dilution is only noticeable in the early stage when C-14-org contributes to the dose and, in this stage, the annual dose is consistently lower in variants with irrigation (Figure 7-22). However, after ~20 000 AD there is no difference in doses with respect to the source of water covering the crop water deficit. This is because accumulation in mire regolith layers is the dominating source for activity for the other dose-contributing radionuclides (e.g. Mo-93, Ca-41, Ni-59 and Ac-227).

7.5.5 Concluding remarks

A future development characterised by business-as-usual anthropogenic greenhouse-gas emissions will result in a warmer climate at Forsmark than at present and lead to a longer period of submerged conditions than in the *base case*. The analysis of the *warm climate calculation case* shows that these changes are unlikely to result in a higher maximum dose than in the *base case*. The main reason is that the near-field and geosphere releases of the radionuclides that contribute most to the maximum dose in the *base case* (C-14-org and Mo-93) are reduced due to the extended submerged period. The postulated changes associated with a warmer climate serve to increase doses from longer-lived radionuclides during the period subsequent to the dose maximum (i.e. after 20 000 AD). However, this increase is modest (approximately a factor of two) and the dose during this period does not exceed the maximum dose in the *base case*.

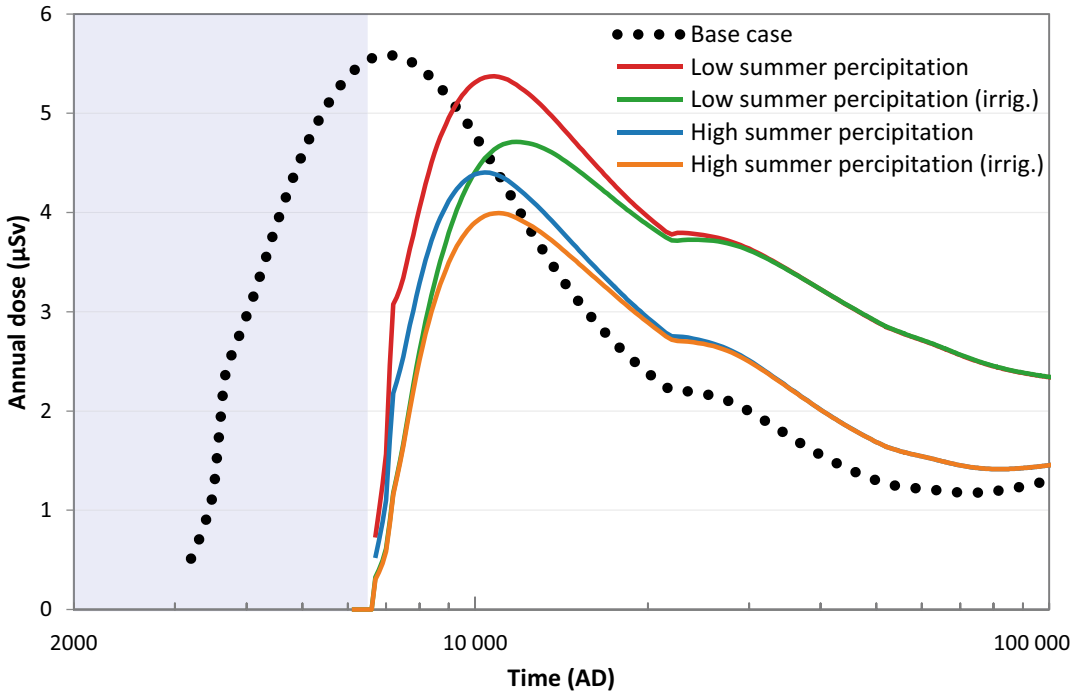

Figure 7-22. *Annual dose to the DM group, with and without large-scale irrigation, in the two variants of the warm climate calculation case. The annual dose in the base case is shown for comparison (black dotted line). The blue shading indicates the submerged period.*

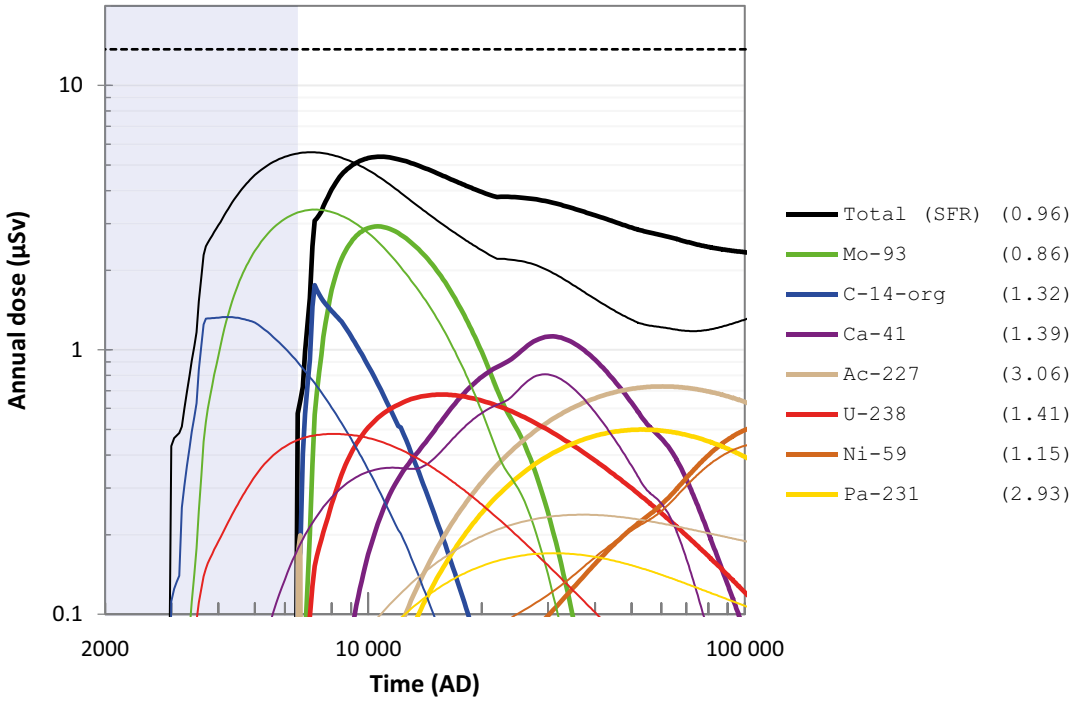

Figure 7-23. *Annual dose to the most exposed group, including radionuclides contributing most to the total dose, for releases from all waste vaults in the low summer precipitation variant of the warm climate calculation case. The annual dose in the base case is shown for comparison (thin lines). Values in parentheses show the ratio between the maximum dose in the present calculation case and the base case. The submerged period is indicated by the blue shading and the annual dose (14 µSv) corresponding to the regulatory risk criterion is indicated by the black dashed line.*

7.6 Cold climate calculation case

7.6.1 General description

The *cold climate calculation case* is selected to evaluate the effects on post-closure safety of a future development characterised by substantial reductions in anthropogenic greenhouse-gas emissions and/or removal of atmospheric CO_2 by technological measures. The conditions in the repository and its environs at closure and post closure are chosen based on the initial state (Chapter 4) and the *cold climate variant* of the reference evolution (Sections 6.2 and 6.5). External conditions are characterised by the termination of the current interglacial in response to the next substantial minimum in summer insolation at 56 000 AD. To this end, the evolution of climate domains at Forsmark is considered to be identical to the *base case* except for two periglacial periods between 61 000 AD and 69 000 AD and between 81 000 AD and 102 000 AD (Section 6.5.1).

Periods of periglacial conditions are characterised by considerably lower air temperatures than at present, resulting in the development of permafrost and frozen bedrock conditions at Forsmark. There is a wide range of potential air temperatures that could influence the post-closure development of frozen conditions in the bedrock (Section 6.5.3). Motivated by this uncertainty, two simplified bounding variants are selected to evaluate radiological consequences of periglacial conditions in this calculation case.

The *continuous permafrost* variant describes a situation where the climate becomes sufficiently cold such that frozen bedrock conditions extend from the surface to depths below the repository. In this variant, frozen conditions are considered to hinder the release of radionuclides to the surface during periglacial conditions, and doses are evaluated in the active layer of the biosphere object that receives geosphere release during temperate conditions (object 157_2).

In the *permafrost with talik* variant, the climate is assumed to be sufficiently cold to enable a shallow freezing of the bedrock, yet warm enough to maintain unfrozen conditions at all depths occupied by the repository. In this variant, the geosphere release is assumed to reach the surface ecosystem by discharge via a through talik (Section 6.5.2). Doses to humans are evaluated in two different ecosystems: a mire and a lake.

Although these variants represent simplifications of the temporal and spatial development of a periglacial landscape (**Climate report**, Section 2.1), they are considered to bracket the uncertainty in radionuclide transport due to development of permafrost and frozen conditions in the geosphere and the biosphere. Freezing of pore water that could cause potential damage to the concrete barriers is not considered in this calculation case. In the *base case*, the concrete barriers are assumed to degrade to such an extent within the first 50 000 years (Section 7.4.2) that a potential subsequent period of freezing would no longer significantly influence the hydraulic properties of the concrete. Radiological consequences of an earlier hypothetical freezing of the concrete pore water are evaluated in a residual scenario (Section 9.3).

A detailed description of radionuclide transport and dose modelling for the *cold climate calculation case*, as well as a more detailed analysis of the results, is given in the **Radionuclide transport report**, Section 6.3.

7.6.2 Handling in the near-field and the geosphere

During temperate conditions, including the initial period of submerged conditions, the handling in the near-field and the geosphere models are identical to the *base case*. In the *continuous permafrost* variant, the frozen conditions are considered to result in a complete cessation of the groundwater flow in the near-field and geosphere. As the geosphere release only occurs in temperate periods in the *continuous permafrost* variant, all release is directed to the one single discharge area, object 157_2, as in the *base case*.

In the *permafrost with talik* variant, the conditions in the near-field are considered to be the same as during temperate conditions, i.e. identical to the *base case*. In this variant, the geosphere release during periglacial periods reaches the biosphere by discharge via a through talik, typically formed below lakes (Section 6.5.2). Results from regional hydrogeological modelling shows that groundwater from the extended repository could be discharged to large future lakes in the area of

Öregrundsgrepen (Section 6.5.5). Furthermore, discharge taliks below mires cannot be excluded (Section 6.5.2). Thus, in the *permafrost with talik* variant, the entire geosphere release during periglacial conditions is either directed to a future lake in object 114 (in Öregrundsgrepen) or to a mire in object 157_1 (see Figure 7-2 and Figure G-1 for the locations of the biosphere objects).

In the *permafrost with talik* variant, the geosphere release is assumed to be equally large as in the *base case*. This simplification is overall considered to be cautious, since periglacial conditions are associated with a higher rock matrix K_d for a few radionuclides, a lower groundwater flow and, consequently, longer travel times than during temperate conditions (see the **Radionuclide transport report**, Section 6.3.3 for further details).

7.6.3 Handling in the biosphere

The biosphere model is adjusted to account for a lake and a mire through talik in the biosphere objects. Furthermore, hydrological and ecosystem parameters are adjusted to reflect periglacial conditions (**Biosphere synthesis report**, Section 10.3.1).

Landscape description

The evolution of the landscape in the *cold climate calculation case* is identical to the *base case* up until the onset of the first periglacial period at 61 000 AD.

All lake-mire systems in the area above the repository are considered to have reached a mature state before 50 000 AD (Section 6.5.2). Thus, effects of ecosystem succession are not accounted for in the periglacial periods. Instead, a stationary representation of the mire in object 157_1 at its mature state is adopted. Lake infilling is considered to be slow in periglacial conditions (Brydsten and Strömgren 2010) and thus a stationary representation of a hypothetical deep lake (i.e. a permanent lake without ecosystem succession) in object 114 farther out in Öregrundsgrepen is also used to evaluate dose.

Surface hydrology

In the SR-PSU, near-surface water-flow components were derived for the same potential future taliks as considered in this calculation case (**Biosphere synthesis report**, Sections 4.3 and 5.5 and Odén et al. 2014). These are also used in this calculation case. The hydrological modelling of taliks is described in Werner et al. (2013) and the hydrological parameters for the two taliks in Grolander (2013).

Biosphere object 157_2 is assumed to have continuous permafrost during periglacial periods. Thus, in the biosphere modelling all solute transport (advection and diffusion) in object 157_2 is halted in the till layer (RegoLow). However, as the active layer thaws in summer, transport processes are assumed to be maintained to some extent in the regolith layers on top of the till. The net precipitation and runoff are assumed to increase by about 25 % in a future permafrost landscape (**Biosphere synthesis report**, Section 7.5.5).

Ecosystem parameters

The parameter values for the concentration of stable CO_2 in the atmosphere, primary production, production of edible fish and crayfish are altered to reflect permafrost conditions based on literature data from colder environments (**Biosphere synthesis report**, Section 8.3). Parameter changes as compared to temperate conditions are further described in Grolander (2013).

Potentially exposed groups

During periglacial conditions, cultivation is not possible due to permafrost and wells will not yield any water from the frozen ground. Thus, during periglacial periods, the only PEG is HGs foraging in the Forsmark landscape. HGs are assumed to collect food from a large area and can thereby utilise food from several biosphere objects at the same time (i.e. objects 157_2, object 157_1 and object 116). In the *permafrost with talik* variant with a lake through talik (object 114), no additional downstream objects are considered. During temperate conditions, the potentially exposed groups are identical to those assessed in the *base case* (Section 7.4.4).

7.6.4 Radionuclide transport and dose

Before the first onset of periglacial conditions at 61 000 AD, the resulting dose in the *cold climate calculation case* is identical to the *base case*. The main result in the *cold climate calculation case*, in both variants, is that the maximum dose during periglacial periods is at least one order of magnitude lower than in the *base case* at the corresponding time (Figure 7-24). The main reason is that hunting and gathering during periglacial conditions results in lower doses than cultivation and well water usage during temperate conditions. While doses to DM farmers after 61 000 AD are dominated by radionuclides like Ca-41 and Ni-59 that sorb and accumulate in regolith layers that become cultivated (Section 7.4.5), I-129 dominates the dose to HGs. This radionuclide is transported relatively quickly through the regolith and exposure arises mainly through ingestion (wildlife and berries), but also through drinking surface water.

Doses to HGs are similar in the *continuous permafrost* and the *permafrost with talik* variants both during temperate and periglacial periods. The reason is that the doses are generally dominated by exposure from radionuclides (e.g. I-129) that have accumulated in object 157_2 during the preceding temperate period. The effect of taliks on the dose is thus small and only seen during the second periglacial period. As this period is considerably longer than the first periglacial period, the geosphere release has enough time to reach the upper regolith in object 157_1 and start contributing to the dose (Figure 7-24). Doses due to exposure from the lake talik in object 114 are even lower than from object 157_1 and are therefore not shown in Figure 7-24.

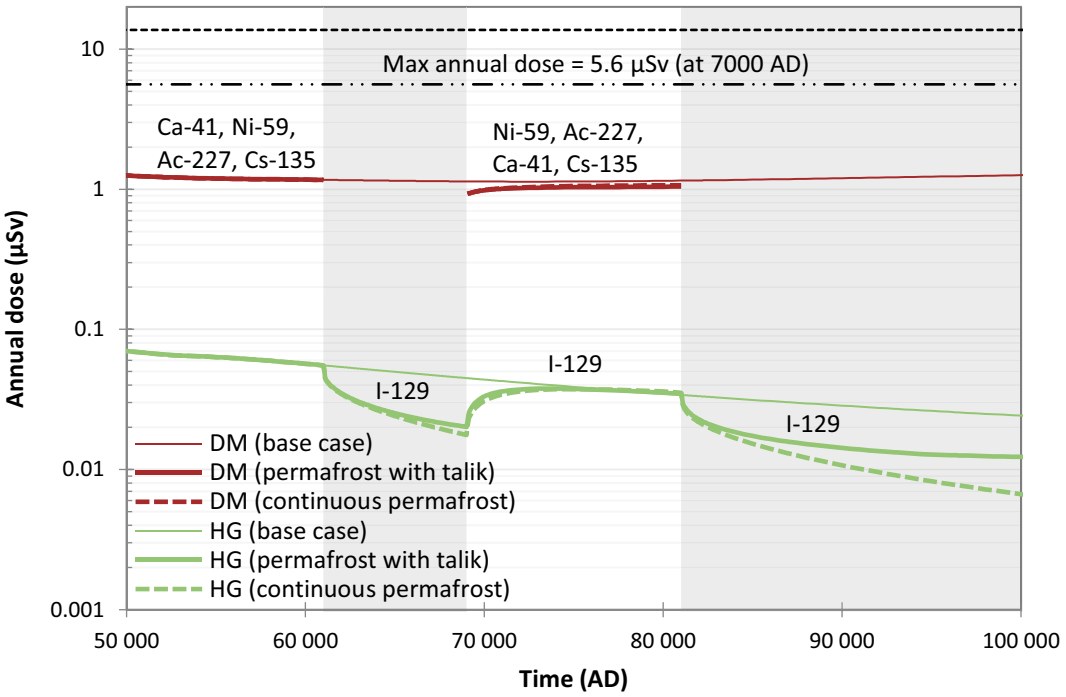

Figure 7-24. *Annual dose to the DM (red) and HG (green) groups during the latter 50 000 years of the assessment period in the continuous permafrost variant (dashed coloured lines) and permafrost with talik variant (solid lines) of the cold climate calculation case. The annual dose in the base case is shown for comparison (thin lines). The radionuclides contributing most to the dose to the DM and HG groups are also indicated. The annual dose resulting from a release through a talik into a lake in biosphere object 114 is below 0.001 µSv and is therefore not shown. Periods of periglacial conditions are indicated by grey shading. During the first 50 000 years of the assessment period, the annual dose is identical to the base case; the maximum annual dose from this period is indicated by the black dashed-dotted line. The annual dose (14 µSv) corresponding to the regulatory risk criterion is indicated by the black dashed line.*

In the *continuous permafrost* variant, radionuclides and their decay products are trapped in the near-field and geosphere by the permafrost. Once groundwater flow again increases during the subsequent temperate period, releases of radionuclides with long half-lives are similar to those immediately prior the onset of the preceding periglacial period. This means that releases of these radionuclides during the subsequent temperate period are marginally higher than the releases during the corresponding time in the *base case* (**Radionuclide transport report**, Figure 6-7). This slight increase in the release does not affect doses significantly. Instead, the doses are initially somewhat lower during the post-periglacial temperate period than during the corresponding time in the *base case* for both variants. The main reason is the lack of releases to object 157_2 and the depletion of accumulated inventory in the regolith due to leaching during the preceding periglacial period.

7.6.5 Concluding remarks

A future development characterised by a large reduction of anthropogenic greenhouse-gas emissions within this century is likely to result in the development of periglacial climate condition within the latter half of the assessment period. The analysis of the *cold climate calculation case* shows that this change will not result in a higher dose than in the *base case*. The main reason is that hunting and gathering is the only possible exposure pathway during periglacial conditions and this results in lower doses than cultivation and well-water usage. Furthermore, potential accumulation of decay products in the near-field and the geosphere does not result in doses that exceed the dose in the *base case* during the post-periglacial temperate period in this calculation case.

7.7 Supporting calculation cases

7.7.1 General description

The main scenario also includes a set of supporting calculation cases, selected to provide a sensitivity analysis of specific uncertainties in external conditions and internal processes that are potentially important for radionuclide transport through the repository system (Section 7.2). As the *base case* constitutes the basis for all radionuclide transport and dose calculations in the present safety assessment, evaluating the sensitivity to specific uncertainties in this case also contributes to increasing confidence in the other scenarios and calculation cases in the assessment. Therefore, the supporting calculation cases are configured with respect to the conditions in the *base case*.

Four supporting calculation cases are presented in this report (Table 7-1), covering uncertainties in future sea level rise (*timing of shoreline regression calculation case*), the timing of initial releases from the repository (*delayed release from repository calculation case*), the spatial dispersion of the release (*subhorizontal fracture calculation case*) and transport pathways within the landscape (*alternative landscape configuration calculation case*).

In this section, a short description of the supporting calculations is given together with the most important results from the calculations. More detailed descriptions and analyses of the *timing of shoreline regression calculation case* and *delayed release from repository calculation case* are given in the **Radionuclide transport report**, Section 5.8. The *subhorizontal fracture calculation case* and *alternative landscape configuration calculation case* are presented in detail in the **Biosphere synthesis report**, Chapter 10. These two calculation cases build on complementary studies carried out within the SR-PSU to address uncertainties with respect to the future landscape (Saetre and Ekström 2016, 2017).

In addition to the supporting calculations presented in this report, an additional four cases have also been developed specifically for the biosphere analysis (**Biosphere synthesis report**, Chapter 11). These calculations evaluate, among other things, uncertainties with respect to biosphere properties (*mire object properties calculation case*) and delineation (*alternative delineation calculation case*) of biosphere object 157_2, as well as uncertainties in how ecosystems are handled in the modelling (*ecosystem properties calculation case*) and the effect of calcite depletion on sorption in the regolith (*calcite depletion calculation case*).

In the *mire object properties*, *ecosystem properties*, and *calcite depletion* calculation cases, the resulting maximum annual dose is slightly lower than the maximum dose in the *base case*. In the *alternative delineation calculation case*, the entire radionuclide release is assumed to occur pessimistically to the part of biosphere object 157_2 that is most suitable for cultivation, which corresponds to one fifth of its total area. The assumption is considered hypothetical, since it is not in line with the modelling of discharge areas in the landscape (Figure 6-12). Despite this, the doses in the calculation case are only about a factor of two higher than in the *base case*, showing that the resulting dose is not very sensitive to the object delineation. In summary, the results from the calculations indicate that the parameterisations made for the biosphere properties in the *base case* of the evaluated uncertainties are adequate.

7.7.2 Description of the calculation cases

Timing of shoreline regression

This calculation case addresses the uncertainty in the initial duration of the submerged conditions in the area above SFR. In the *base case*, the initial period of submerged conditions is 1 000 years based on the assumption that the global sea level rise up until repository closure and post closure is negligible (Section 7.4.1). This assumption is arguably not fully realistic when taking the ongoing and anticipated future sea level rise into account (Section 6.2.1). Therefore, in the *timing of shoreline regression calculation case*, radiological consequences are evaluated for delayed shoreline regressions of 5 000, 10 000, 15 000 and 20 000 years relative to the *base case*. The delayed shoreline regression is handled by letting the shoreline position corresponding to 2000 AD in the *base case* prevail for the duration of the delay, after which the shoreline regression of the *base case* is assumed to follow (**Data report**, Chapter 12).

Delayed release from repository

This calculation case is developed to evaluate radiological consequences of simplifying assumptions whereby several processes are omitted in the near-field modelling (Section 7.3.4). The overall consequence of these simplifications is an earlier release from the near-field than if more realistic parameterisations were to be used. Thus, the simplifications could possibly result in an increased release during the submerged period in the *base case*, when doses to humans are significantly lower than during the subsequent terrestrial period. In this calculation case, radionuclide releases from the near-field are therefore set to zero for the first 1 000 years and thus do not begin until the conditions in the area above SFR are terrestrial. Prior to this, the only process affecting the magnitude of the inventory is the radioactive decay and in-growth of decay products.

Subhorizontal fracture

This calculation case is developed to evaluate the influence of distribution of the geosphere release over a greater area than in the *base case*, caused by a large subhorizontal fracture in the bedrock (Section 7.3.5). In this calculation case, the geosphere release from the *base case* is not restricted to object 157_2, but some fraction of the total release is also discharged to the regolith of the two downstream objects 157_1 and 116 (Figure 7-2). Specifically, the geosphere release from each waste vault is partitioned to the three biosphere objects 157_2, 157_1 and 116 according to results from particle tracking simulations with the presence of a large subhorizontal fracture (Öhman and Odén 2018; see also Section 6.3.5). In the terrestrial period, ~40 % of the particles released from SFR1 and SFR3 were calculated to reach the basins of either of the two downstream objects (157_1 and 116). In addition to this change, groundwater flow to the objects is modified according to the regional hydrogeological simulations (Öhman and Odén 2017).[39] These hydrogeological simulations show that the bedrock discharge to object 157_1 may increase considerably as a result of the presence of the subhorizontal fracture.

[39] An alternative calculation with unmodified bedrock discharge to the three biosphere objects is presented in the **Biosphere synthesis report**, Section 10.5. This calculation is considered less realistic given a subhorizontal fracture than the case with a modified bedrock discharge.

Alternative landscape configurations

This calculation case addresses uncertainties with respect to the transport pathways and development of the future Forsmark landscape. This calculation case is evaluated in two variants: *no stream* and *release to surface water*. In the *base case*, radionuclides from the primary biosphere object (157_2) are discharged to a stream and reach the surface water of the downstream object (157_1) (Section 7.4.4). The *no stream* variant assumes that there is no stream connecting object 157_2 and 157_1. Instead, flow of shallow groundwater, from the wetland in 157_2 to the downstream lake-mire complex in 157_1, is conceptualised as a diffuse outflow of near-surface water (see e.g. Section 6.2.3 in Werner et al. 2013). In order not to underestimate accumulation of radionuclides in the peat of the downstream object, it is further assumed that all radionuclides will reach the mire part of the recipient. This variant largely corresponds to the biosphere base case in the SR-PSU. Thus, besides illustrating potential effects of extensive accumulation in the downstream object, it facilitates a comparison with the previous assessment.

The *release to surface water* variant addresses the uncertainty related to transport pathways to the downstream lake. In this variant, the entire geosphere release has been directed directly to the stream water in object 157_2, resulting in only negligible amounts of C-14-org being lost to the atmosphere before the stream water enters the lake in object 157_1.

7.7.3 Radionuclide transport and dose

The calculated maximum dose in the supporting calculations and the *base case*, including the radionuclide contributions to this dose, is shown in Figure 7-25. In the following, the results are discussed separately for each calculation case.

Timing of shoreline regression

The extended submerged period in the *timing of shoreline regression calculation case* implies that the radionuclides that dominate the maximum dose in the *base case*, i.e. Mo-93 and C-14-org, have decayed more before they are available for exposure in the surface system. Consequently, the total maximum dose in this calculation case is noticeably lower than the maximum dose in the *base case*, and the maximum dose decreases with increasing duration of the submerged period (Figure 7-25). Owing primarily to its long half-life (102 000 years), Ca-41 contributes most to the maximum dose for the longest submerged periods (Figure 7-25).

Delayed release from the repository

This calculation case gives a higher dose than in the *base case* during the first few centuries after 3000 AD. This is primarily due to elevated releases of C-14-inorg from the bituminised waste in 1BMA. However, these elevated releases have only a marginal influence on the maximum dose. Thus, the maximum dose in this calculation case, including the individual radionuclide contributions to this dose, are very similar to the *base case* (Figure 7-25).

Subhorizontal fracture

The distributed release in the *subhorizontal fracture calculation case* results in a maximum dose that is approximately halved in object 157_2 as compared to the *base case* (Figure 7-25). Directing part of the geosphere release directly to biosphere object 157_1 gives a maximum dose from this object early in the assessment period (~4000 AD). This is primarily caused by increased exposure to C-14-org from draining the mire in the object. However, the maximum dose from object 157_1 is still about 30 % lower than that from object 157_2 (Figure 7-25).

Alternative landscape configurations

In the *no stream* variant, export of radionuclides with diffuse overland-water flow from object 157_2 results in a considerable accumulation in the downstream mire in object 157_1. As a result, exposure from object 157_1 gives higher doses than object 157_2 after approximately 10 000 years. However, the accumulation of radionuclides in object 157_1 by the time of maximum dose from object 157_2 (~7000 AD) is limited. Thus, the maximum dose in this variant, including the individual radionuclide contributions to this dose, is very similar to the *base case* (Figure 7-25).

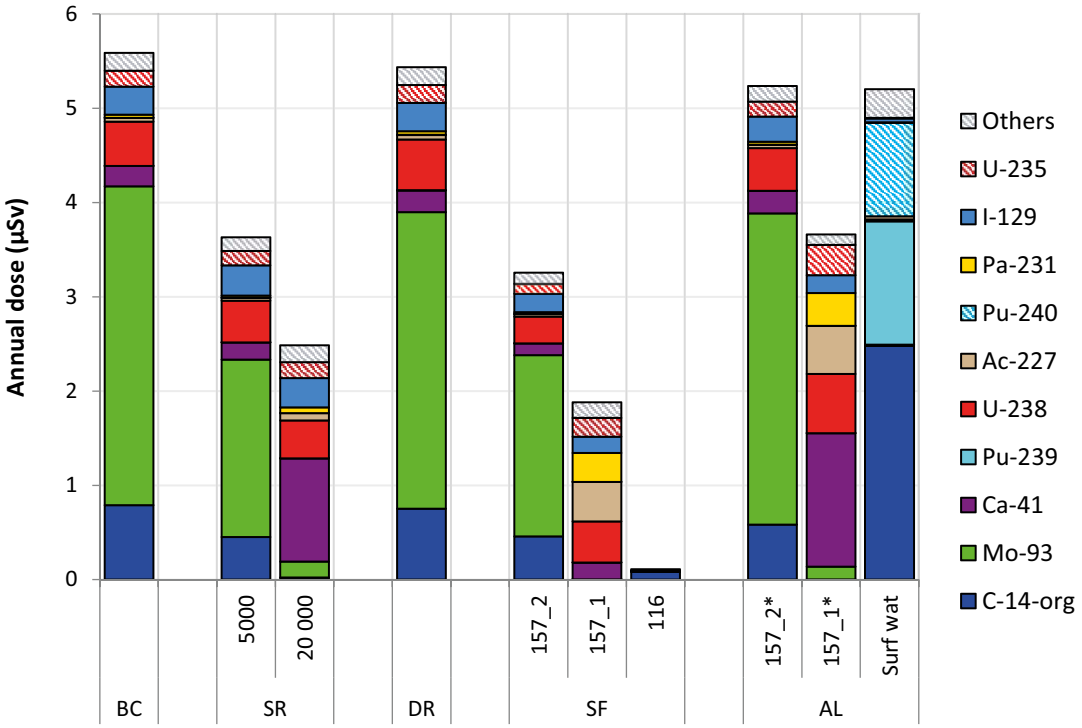

Figure 7-25. *Maximum annual dose to the most exposed group, including the contribution to the maximum dose from individual radionuclides, in the main scenario (i.e. the base case) and the supporting calculation cases. The calculation cases are written in an abbreviated form, where BC = base case, SR = timing of shoreline regression, DR = delayed release from repository, SF = subhorizontal fraction and AL = alternative landscape configurations. * indicates that the results are from the no stream variant of the alternative landscape configurations calculation case. The results for SR are shown for a 5 000 and 20 000-year delay of the shoreline regression with respect to the base case. For the SF and the no stream variant of AL, the maximum dose from different biosphere objects is shown.*

The resulting dose in the *release to surface water* variant is comparable to the *base case* until ~5000 AD due to exposure to HGs to mainly C-14-org (Figure 7-25). However, for the remainder of the assessment period, the dose is considerably lower than in the *no stream* variant as well as the *base case* (**Biosphere synthesis report**, Section 10.6.2).

7.7.4 Concluding remarks

In conclusion, the uncertainties evaluated in the supporting calculation cases are unlikely to result in a significantly higher maximum dose than in the *base case*. Thus, the assumption of a relatively short submerged period in the *base case* and *cold climate calculation case* is pessimistic, as using longer, more realistic, submerged periods result in lower annual doses. Further, the calculated maximum dose from the *delayed release from repository*, *subhorizontal fracture* and *alternative landscape configurations calculation cases* are not higher than the maximum dose in the *base case*. Thus, the relatively simplistic representations in the main scenario, where (i) several near-field processes are omitted, (ii) the entire geosphere release is discharged into object 157_2 and (iii) radionuclides are transported to the downstream biosphere object 157_1 through a small stream, are considered to be adequate.

7.8 Dose rate to non-human biota

7.8.1 Introduction

Radiation exposures of plants and animals are the result of external exposure (i.e. radiation from radionuclides in water, sediment or soil) and internal exposure (i.e. from radionuclide uptake or intake). Both external and internal exposure depend directly on the activity concentrations in the

environmental media, and thus temporal and spatial variations in dose rates for any organism group are expected to follow those of the environmental media. The geosphere releases contain different radionuclides and their impacts on biota differ, depending on their half-lives, decay modes (reflected in the *dose conversion coefficients*), and their availability for uptake, physiological/metabolic processes and trophic transfer in biota and their food webs (described by *concentration ratios*).

Exposures of NHB to radionuclides originating from SFR are estimated by calculating absorbed dose rates with the BioTEx model (Section 7.3.6). The method underpinning the calculations is described in more detail in the **Biosphere synthesis report**, Section 12.3. The results are interpreted with respect to the ERICA screening dose rate of 10 μGy h^{-1} across all organism types, as recommended in the ERICA Integrated Approach (Larsson 2008).

The ecosystem types are separated into aquatic and terrestrial. During the initial submerged period, the aquatic portion of the biosphere object is considered to be fully marine, whereas the site is, in fact, brackish. Thus, the ecosystem is assumed to be equivalent to marine conditions. However, as isostatic rebound occurs and lake basins and wetlands are isolated, the aquatic ecosystem is considered to transition to terrestrial and so becomes freshwater. Some organism types (e.g. Annelid) were included in the terrestrial ecosystem, where un-drained wetland ecosystems are clearly an inappropriate choice as a habitat. However, the use of such organism types in a wetland has been maintained in this assessment to give a cautious assessment for such organism types that may exist in surrounding non-wetland terrestrial ecosystems, including marginal areas in transition from wetland to terrestrial.

Dose rates to NHB are evaluated for the *base case*, *warm climate calculation case* and *cold climate calculation case*. In addition, dose rates are evaluated for the *alternative delineation calculation case*, which is a supporting calculation case for the biosphere included to illustrate potential effects of a release restricted to a habitat relevant for a protected species and/or to areas smaller than the original outline of object 157_2. This case is presented in the **Biosphere synthesis report**, Section 12.7. This section summarises the evaluations of dose rates under the *base case* (Section 7.8.2). Key points from the *warm climate calculation case* and the *cold climate calculation case* are presented in Sections 7.8.3 and 7.8.4, respectively. Finally, concluding remarks are made in Section 7.8.5.

7.8.2 Base case

The general description and the handling in the near-field and geosphere, described in Sections 7.4.1 to 7.4.3, also applies for calculating dose rates to NHB in the *base case*. The handling in the biosphere is identical with the description in Section 7.4.4, with the exception that the assessment endpoint is absorbed dose rate to the set of organism types presented in Table 7-5.

Dose rates to organisms in the aquatic ecosystem

The aquatic ecosystem that receives geosphere release can be divided into two stages, the marine stage prior to the full emergence of biosphere object 157_2 (2000 AD to ~4300 AD; see Table 7-7), and the freshwater stage, which occurs once the biosphere object is fully terrestrial (~4300 AD to 102 000 AD). Release of radionuclides and subsequent exposures of organisms are considered to begin shortly after repository closure (Figure 7-26). Dose rates to marine organisms increase steadily until object 157_2 has fully emerged due to the combined effect of increasing activities of C-14-org reaching the biosphere and decreasing water exchange in the basin of the biosphere object. After emergence of object 157_2, the dose rates to organisms increase sharply when the radionuclides are released to a relatively small stream. This is due to a marked decrease in the amount of flowing water that dilutes the radionuclide release. About half of the organisms experience their dose rate maximum at the transition (4300 AD), followed by a steady decline, reflecting the ambient concentrations of C-14-org. The remaining half of the organism types maintain a higher dose rate, with a maximum occurring later (~16 000 AD), attributable to dose rates from Ac-227.

The highest dose rates are found in (freshwater) Bird, followed by Microphytobenthos, with dose rates of around 1×10^{-2} μGy h^{-1}, thus approximately three orders of magnitude lower than the screening dose rate. These two organism types correspond to the earlier maximum of exposures (4300 AD), with dose rates dominated by C-14-org (freshwater Bird: 99 %). Details of the dose rates from specific radionuclides over time in the freshwater Bird are depicted in Figure 7-27.

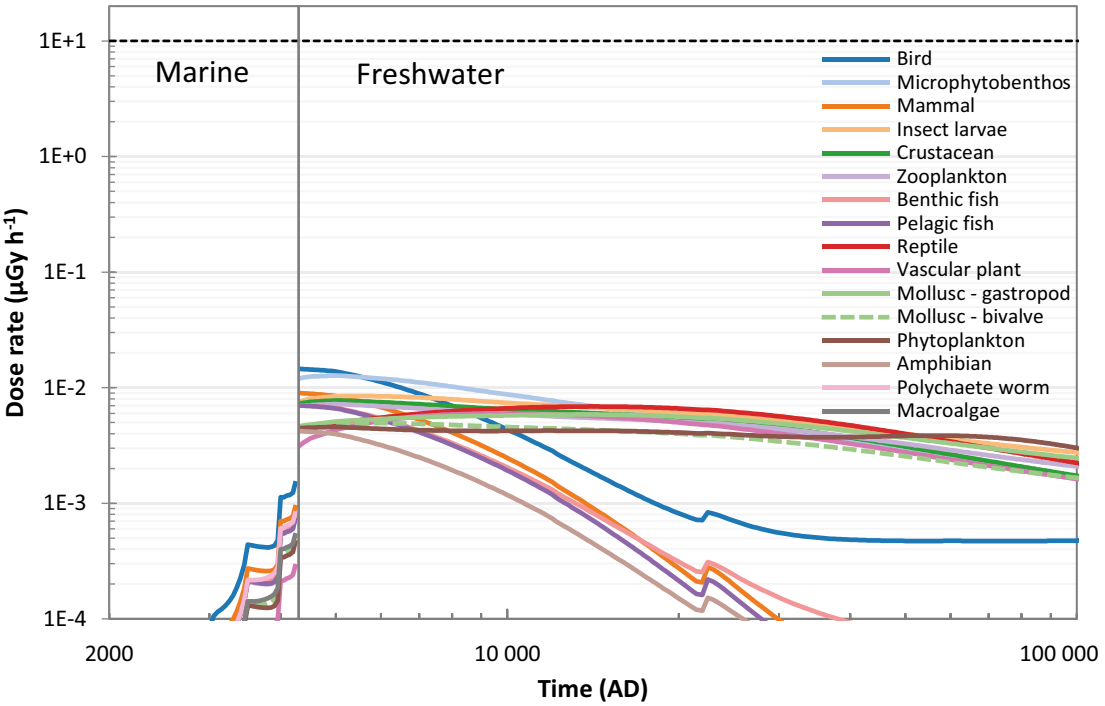

Figure 7-26. *Dose rates to aquatic organisms before emergence in the marine era (to the left of the vertical line) and after emergence (to the right of the vertical line) of the biosphere object, under the base case. The horizontal dashed line indicates the screening dose rate (10 µGy h^{-1}).*

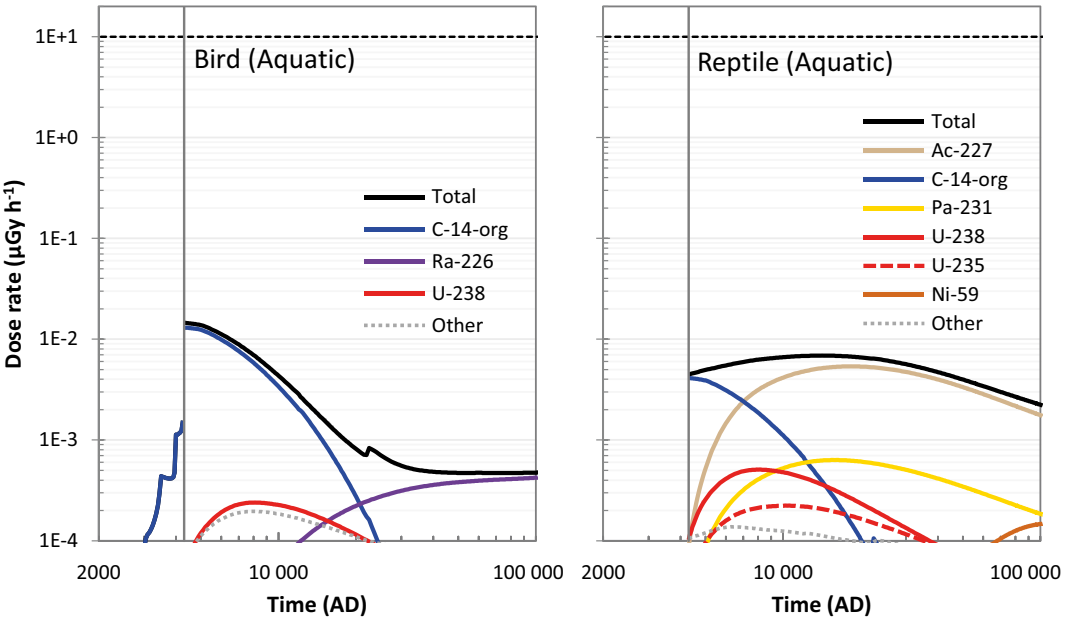

Figure 7-27. *Radionuclide-specific dose rates to freshwater Bird (left) and freshwater Reptile (right), the aquatic organisms with highest dose rate maxima in the first and second peak, under the base case. The horizontal dashed line indicates the screening dose rate (10 µGy h^{-1}). The vertical line indicates the emergence of freshwater and terrestrial systems replacing the marine system.*

The most exposed organism types of the second dose rate maximum (~16 000 AD) are Reptile, Insect Larvae and Zooplankton, with maximum dose rates lower than 10^{-2} µGy h^{-1}, dominated by Ac-227 (freshwater Reptile: ~80 %). Details of the dose rates from specific radionuclides over time in the freshwater Reptile are depicted in Figure 7-27. Radionuclides such as Ac-227 become dominant as U-235 and its decay products accumulate in peat. An important factor for variation in exposures in the later period is the concentration ratios of radionuclides (particularly, Ac-227) in freshwater organisms. The concentration ratios of Ac-227 in organisms exhibiting lower total dose rates in the later stage (i.e. Bird, Benthic and Pelagic fish, Mammal and Amphibian) are approximately three orders of magnitude lower than those in the organism types that exhibit higher dose rates throughout this period.

Dose rates to organisms in the terrestrial ecosystem

Exposures in the terrestrial ecosystem begin at 3000 AD (Figure 7-28), when the first parts of object 157_2 start to emerge from the sea. The exposure increases as isostatic rebound continues, levelling-off (in most organism types) at the point of complete emergence of the land from the sea (~4300 AD).

Organisms show two patterns of exposure (Figure 7-28, left panel). Most of the species experience their maximum dose rates around 10 000 AD, but a few organisms receive maximum dose rates earlier, at the point of complete emergence (4300 AD). The organisms at 10 000 AD experience greater exposure and the dose rates are dominated by uranium isotopes. The maximum dose rates experienced are around 1×10^{-2} µGy h^{-1} (Lichen & Bryophytes), with the next most exposed organisms in the range of 4–7 $\times 10^{-3}$ µGy h^{-1} (Annelid, Mollusc-gastropod, Arthropod-detritivorous and Reptile). These values are at least three orders of magnitude lower than the screening dose rate. In Lichen & Bryophytes, U-238 and U-235 together contribute to approximately 95 % of the total dose rate. Bird, Tree, and Grasses & Herbs are most exposed at emergence, with dose rates of just below 1×10^{-3} µGy h^{-1}. Dose rates to the Bird are dominated by C-14-org (70 %). Cl-36 contributed significantly to the dose rate to terrestrial plants (Tree, Grasses & Herbs and Shrub), due to the high concentration ratio of chlorine. In all three plant types, the dose rates from Cl-36 exceed those from C-14-org.

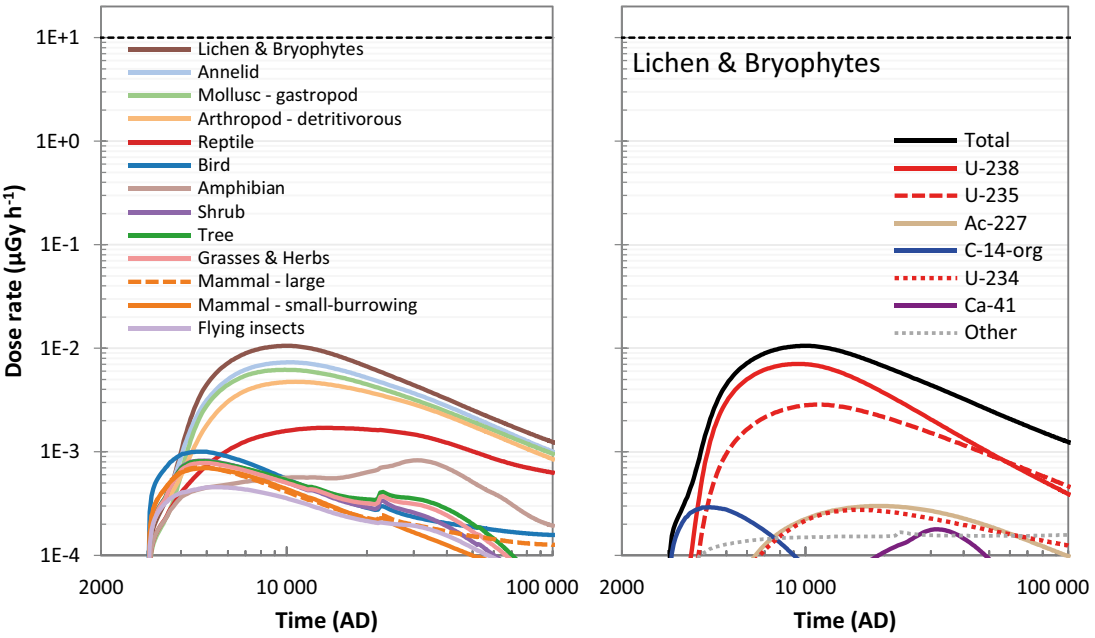

Figure 7-28. *Total dose rates to terrestrial organisms, under the base case (left). Radionuclide-specific dose rates to Lichen & Bryophytes, the terrestrial organism with highest dose rate maximum, under the base case (right). The horizontal dashed line indicates the screening dose rate (10 µGy h^{-1}). The vertical line indicates the emergence of freshwater and terrestrial systems replacing the marine system.*

7.8.3 Warm climate calculation case

The *warm climate calculation case* is characterised by an increased sea level that delays the shoreline regression; object 157_2 starts to emerge at 6500 AD and is fully isolated at 7800 AD. The calculation case is evaluated by the *high summer precipitation* variant and *low summer precipitation* variant (see Section 7.5.1 for a general description). The delayed evolution of the terrestrial and freshwater ecosystems means that the radionuclides have decayed for longer (about 3500 years) before reaching these ecosystems and this reduces dose rates from radionuclides with shorter half-lives (such as C-14-org). Delayed shoreline regression will also delay the transition from marine to freshwater ecosystems, as compared with the *base case*.

The effect of warming of the environment alone has little impact on the magnitude of dose rates. However, the later emergence of the biosphere object from the sea leads to a delayed release of radionuclides to freshwater and terrestrial ecosystems. As the highest dose rates to freshwater organisms in the *base case* occurred immediately after emergence, the delay in emergence under the *high summer precipitation* variant leads to a lower maximum dose rate to freshwater organisms. Lichen & Bryophytes is the most exposed organism in the terrestrial ecosystem, with a maximum dose rate approximately the same as in the *base case*.

The *low summer precipitation* variant also exhibits a delayed exposure of the freshwater and terrestrial organisms relative to the *base case*. However, the maximum dose rates are greater than in the *high summer precipitation* variant, in particular from radionuclides that are important in the later stages of the assessment period (i.e. isotopes of uranium and decay products from U-235). This is the result of decreased ground and surface water flow associated with the drier summer climate (Figure 7-21), which reduces the dilution of radionuclides. For aquatic organisms, freshwater Reptile experiences the highest dose rate (Figure 7-29). In terrestrial organisms, the highest dose rate, almost 2×10^{-2} µGy h^{-1}, is experienced by Lichen & Bryophytes due to mainly exposure of U-238. While this dose rate is the highest across all organisms, ecosystems and variants of the *warm climate calculation case*, it is still about three orders of magnitude below the screening dose rate.

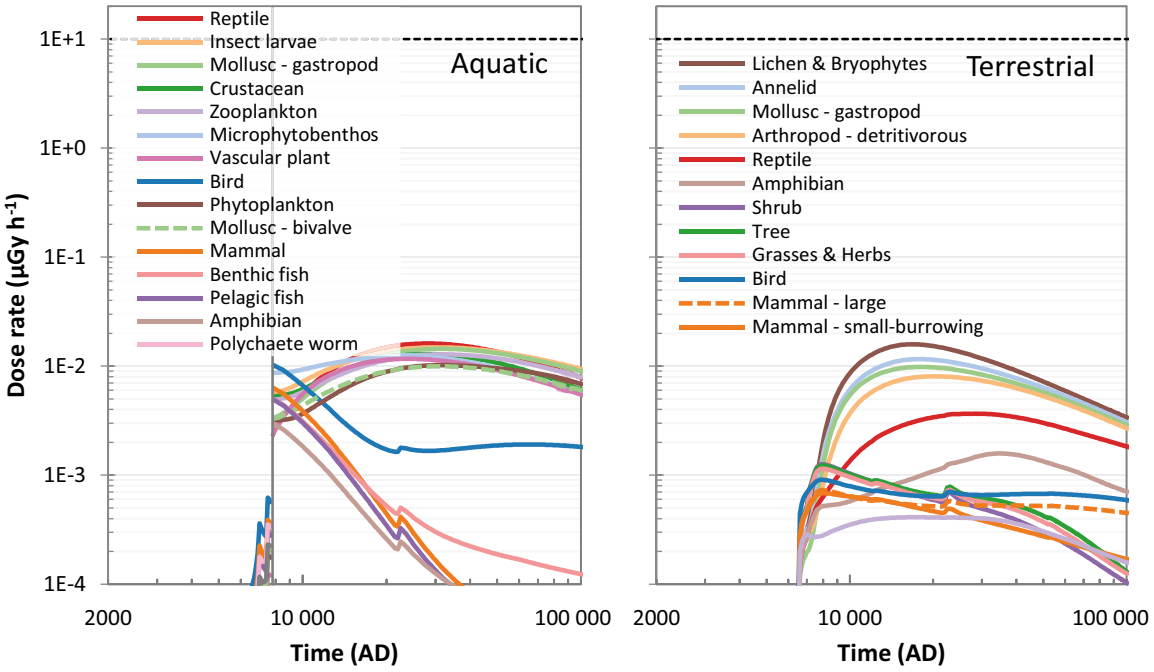

Figure 7-29. *Dose rates to aquatic organisms (left) and terrestrial organisms (right), under the low summer precipitation variant of the warm climate calculation case. The horizontal dashed line indicates the screening dose rate (10 µGy h^{-1}). Organisms are colour-labelled as in Figure 7-26 (aquatic) and Figure 7-28 (terrestrial). The vertical line indicates the emergence of freshwater and terrestrial systems replacing the marine system.*

7.8.4 Cold climate calculation case

Under the *cold climate calculation case*, the evolution of climate domains at Forsmark is considered to be identical to the *base case* except for two periglacial periods between 61 000 AD and 69 000 AD and between 81 000 AD and 102 000 AD (Section 7.6.1). Two variants are selected to evaluate radiological consequences of periglacial conditions, namely the *continuous permafrost* variant without talik and the *permafrost with talik* variant. The same organisms as in the *base case* are assessed in the cold climate. However, limnic amphibians and mammals along with terrestrial trees, gastropods, amphibians, reptiles and annelids may not be viable and might no longer be present at the site in a cold climate (Jaeschke et al. 2013).

In both variants, dose rates are identical to those in the *base case* during the first temperate period (before 61 000 AD), and the maximum dose rates (in object 157_2) are also similar during the second temperate period. However, during the periglacial periods, the dose rates decrease by up to a factor of five (Figure 7-30). The reason is that biosphere object 157_2 is isolated from geosphere releases during periglacial periods, and thus environmental concentrations decrease as accumulated radionuclides leach out from the object.

As with exposure to humans (Section 7.6.4), taliks have only a marginal effect on the dose rates. For aquatic organisms, the dose rates from the stream in object 157_2 are always higher than the dose rates from the aquatic ecosystems above a discharge talik. Thus, for these organisms, the highest dose rates in the *permafrost with talik* variant are near identical with that from the *continuous permafrost variant* (Figure 7-30). For terrestrial organisms in the *permafrost with talik variant*, the dose rates from the mire in object 157_2 are higher than the dose rates from the mire talik in object 157_1 for most of the periglacial periods. However, radionuclides released from the repository during the first periglacial period are transported up through the regolith layers in the mires of object 157_1 during the temperate period. Consequently, activity concentrations build up in surface peat during the second periglacial period and, at about 95 000 AD, dose rates in the mire talik start exceeding those in up-stream object.

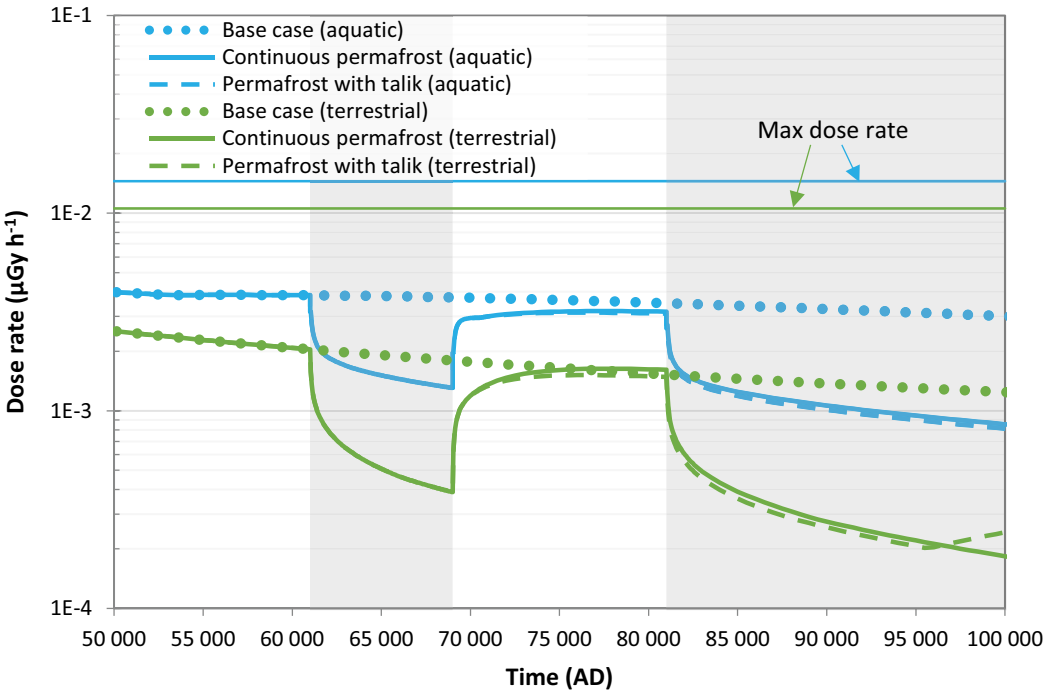

Figure 7-30. *Highest dose rates to aquatic organisms (top) and terrestrial organisms (bottom) in the cold climate calculation case. Periglacial periods are indicated by the light grey shaded areas. The maximum dose rate from the temperate period (solid thin lines) and the dose rate from the base case (dotted lines) are shown for comparison. Note that the time on the x-axis is presented on a linear scale.*

7.8.5 Concluding remarks

In all calculation cases presented above, the maximum dose rates over all organism types are three orders of magnitude below the ERICA screening dose rate (10 μGy h^{-1}) and occur relatively early in the assessment period. All dose rates are thus also considerably below 4 μGy h^{-1}, which is the lower boundary of the most restrictive ICRP Derived Consideration Reference Levels (DCRL, ICRP 2008), which only applies to certain vertebrate animals and coniferous trees.

In the aquatic system, C-14-org dominates the maximum dose rate and it arises at the time when the biosphere object first fully emerges from the sea. In the terrestrial system, uranium isotopes (or their decay products) contribute most to the dose rates and the maximum rates typically occur several thousands of years after emergence. Freshwater Bird and Lichen & Bryophytes are the most exposed organisms in aquatic and terrestrial ecosystems, respectively, except for the aquatic environment under the *low summer precipitation* variant of the *warm climate calculation case* where freshwater Reptile was slightly more exposed than freshwater Bird.

8 Less probable scenarios

8.1 Introduction

Three different categories of scenarios are included in the present safety assessment: the main scenario, less probable scenarios, and residual scenarios (Section 2.6.8). The main scenario is addressed in Chapter 7 and takes into account the most probable changes in the repository and its environs. The aim of less probable scenarios, as discussed in this chapter, is to evaluate scenario uncertainties and other uncertainties that are not evaluated within the framework of the main scenario, as recommended in SSM general advice to SSMFS 2008:21. Residual scenarios primarily aim to illustrate the significance of individual barriers and barrier functions and these are presented in Chapter 9.

This chapter first presents the selection of less probable scenarios based on a systematic assessment of scenario uncertainties related to each safety function (Section 8.2). The less probable scenarios are then described and analysed in Sections 8.3 to 8.6. For each less probable scenario, a general description is given together with an assessment of the probability of occurrence of the scenario. The description of the calculation cases for the scenarios focusses on differences from the main scenario. Each scenario is analysed in terms of activity releases and doses to humans, and dose-rates to non-human biota are not evaluated. Relevant scenarios are also evaluated with respect to collective dose. Section 8.7 addresses the handling of the different climate cases in relation to the less probable scenarios and combinations of scenarios.

8.2 Selection of less probable scenarios

The approach for selecting less probable scenarios is described in Section 2.6.8. The selection is based on the safety functions and the FEPs identified as potentially affecting the safety function indicators as presented in Chapter 5. For each safety function, uncertainties in how the initial state, internal processes and external conditions are specified in the main scenario, especially in the *base case*, are evaluated to determine if there is a possibility that the status of the safety function deviates from that in the main scenario in such a way that post-closure safety may be impaired. It can be noted that the status of the safety functions evolves in the main scenario and that some safety functions are not upheld for the entire assessment period in the main scenario due to e.g. expected degradation processes of the engineered barriers. Safety is not necessarily compromised if a safety function is poorly upheld, it is rather an indication that more in-depth analyses are needed to further evaluate safety (Chapter 5). The safety functions generally become less important over time as the activity of the inventory decreases due to radioactive decay. Adequate limitations on the inventory of long-lived radionuclides in each waste vault ensures acceptable dose and risk consequences in the very long term.

The probabilities of each less probable scenario are assessed in the context of the scenario descriptions in Sections 8.3 to 8.6. The actual probability for deviations in the safety function in question is judged to be equal to or less than the probability selected for the scenarios. In most cases, the actual probability of occurrence is judged to be considerably less than the selected probability. The probabilities are also an indication of the magnitude of uncertainty handled within the main scenario – less probable scenarios handle evolutions that are judged to have a probability of 10 % or less to occur.

In the following (Sections 8.2.1–8.2.11), the safety functions are evaluated primarily with respect to the key scenario uncertainties affecting the safety function indicators, but also considering relevant system and modelling uncertainties. The safety functions are categorised as

- waste form and waste packaging,
- engineered barriers,
- repository environs,

and thus follow the structure in Table 5-1. The evaluation systematically addresses uncertainties in the state of the safety function indicators relating to the initial state, internal processes and external

conditions, i.e. relating to scenario uncertainty as defined in Section 2.5. These uncertainties are discussed based on information given in the reference evolution (Chapter 6), the **Initial state report**, the **Waste process report**, the **Barrier process report**, the **Geosphere process report** and the **Climate report**. It should be noted that uncertainties on a technical/scientific level, as expressed in the process reports, do not necessarily impact the results of the safety assessment. The scenario selection process can, in this respect, be seen as an identification of uncertainties that are not already handled in the main scenario and that potentially have an important effect on the results of the safety assessment. The process reports describe the FEPs in general and thus include, but are not limited to, the FEPs that relate to the safety functions as described in Chapter 5 (Tables 5-2 to 5-4). By systematically addressing uncertainties affecting the safety function indicators, the relevant FEPs are considered in the selection of scenarios. The status of the safety functions in the main scenario is discussed for each safety function indicator in Sections 8.2.1–8.2.11.

8.2.1 Waste form and waste packaging – Safety function limit quantity of activity

The safety function *limit quantity of activity* is assessed with the aid of the safety function indicator *activity of each radionuclide in each waste vault* (Table 5-1).

Status of the safety function in the main scenario

The radionuclide inventory in the waste is limited by the WAC which allows only certain kinds of waste in SFR, and by regulating the amount of activity of different radionuclides in each waste vault (Section 4.3). The amounts of different radionuclides are included in the variable *radionuclide inventory* (**Initial state report**, Section 12.1). The radionuclide inventory applied in the main scenario (Section 4.3.7) is based on forecast operational and decommissioning wastes. In the main scenario, the safety function is established initially by taking radioactive decay during the operational period into account. The initial activity used in the main scenario is illustrated in Figure 4-2. The disposal strategy and procedures ensure, together with waste type descriptions, that the waste acceptance criteria (WAC) are met. Considering the WAC, the waste will be emplaced in the correct waste vault.

Uncertainties in the initial state

Uncertainties in the radionuclide inventory are discussed and the 95th percentile is presented in Appendix E, Table E-2. In Section 7.3.3, the selection of radionuclides that are included in the radionuclide transport calculations is described. Deviations in radionuclide inventory are considered to be caused by uncertainties that relate to characteristics of both waste already deposited and to forecast wastes (**Initial state report**, Section 3.8). These uncertainties are, in the main scenario, handled by creating probability density functions (PDFs) for the inventory selected (Section 7.3.3).

Uncertainties in internal processes and external conditions

Radioactive decay and ingrowth are the only internal processes identified that affect the radionuclide inventory. The processes are well-known, and uncertainties are small. Thus, the safety function indicator *activity of each radionuclide in each waste vault* will not deviate from the evolution in the main scenario in a way that impairs safety.

Scenario selection

Since the uncertainties related to the safety function *limit quantity of activity* are, in principle, only driven by uncertainties in the waste deposited, and these are accounted for by probabilistic handling in the main scenario, no less probable scenario is selected for further analysis. Uncertainty in waste volume and uncertainties related to unforeseen changes in operational conditions at the waste producers are not considered within the main scenario. Such changes are considered within the residual scenario *alternative radionuclide inventory* (Section 9.6). In any case, increased waste volumes could be accounted for in future safety assessments and would need to be compatible with WAC.

8.2.2 Waste form and waste packaging – Safety function low gas formation

Gas can be formed in the repository by corrosion of metals in the waste, metals in the waste packaging, and the steel reinforcement in the concrete structures. Microbial degradation of organic material in the waste can also generate gas. Moreover, radiation from the radioactive waste can generate gas by radiolysis of water and of organic materials such as ion-exchange resins and bitumen (Section 6.2.8 and the **Waste process report**, Sections 3.5.10 and 4.4.8). The so-produced gas may potentially lead to faster transport of radionuclides via either gas-driven advection or cracking of the barriers. The safety function *low gas formation* is relevant for the waste in vaults with credited engineered barriers, i.e. the silo, 1–2BMA, 1BRT and 1–2BTF and is assessed with the aid of the safety function indicator *amount of gas-forming materials* (Table 5-1).

Status of the safety function in the main scenario

The selected safety function indicator relates to the initial-state amounts of materials, as given in Appendix E. Materials that rapidly produce gases are most relevant, of which the main ones that the waste may contain are metallic aluminium and zinc. In particular, materials with large surface areas may contribute to rapid gas formation, e.g. metal swarf. Furthermore, easily degradable organic waste such as paper contributes to gas generation. There are WAC (Section 4.3.4) that relate to the amount of gas-forming materials in the waste that aim at limiting gas formation to levels that do not affect barrier safety. Moreover, gas venting systems are installed in the silo and 2BMA. Finally, there is work ongoing in relation to the operation of SFR1 regarding WAC and gas-forming materials and the design of the repair measures for 1BMA (Section 8.2.7). The results of that work are not yet available and have therefore not been considered in this assessment. However, future wastes arising will be subject to the revised WAC.

Uncertainties in the initial state

Most of the waste that will be disposed in SFR has not yet been produced and hence the final inventory, as well as the amounts of gas-forming materials, used in the main scenario are based on forecast operational and decommissioning wastes. Uncertainties in the estimated amounts of gas-forming materials in the operational waste is here handled probabilistically (SKB R-18-07, Section 3.3). The ongoing work relating to gas formation and repairs to 1BMA, including the study of the need for a gas venting system, aims at ensuring that the initial state with respect to gas formation is well characterised and that barrier safety is not impaired by gas formation. The disposal strategy and procedures, together with the waste type descriptions, ensure that the WAC are met.

Uncertainties in internal processes and external conditions

As noted above, the two expected main sources of gas generation are anaerobic corrosion of metals and microbial degradation of organic materials, but radiolysis may also contribute. There are uncertainties in both the mechanistic understanding of these processes and in the simplifications made in the gas generation models used (**Waste process report**, Section 3.5.10). The uncertainties relating to the understanding of the processes are judged to be of minor importance given the uncertainties in the forecast amounts of wastes.

Uncertainties in external conditions

Uncertainties in external conditions are judged to be of no importance for this safety function.

Scenario selection

Uncertainties related to gas formation are dominated by uncertainties in the estimation of the initial amount of gas-forming materials in the inventory, which is judged to be mainly due to data uncertainties in forecast operational and decommissioning wastes. Corrosion rates contribute less uncertainty since they have recently been statistically compiled for steel (**Data report**, Chapter 5), and measured for Al and Zn (Herting and Odnevall 2021), under repository-like conditions. These uncertainties are accounted for in the main scenario. Revised WAC are currently being derived to ensure adequate

limitation on the amounts of gas-forming materials and hence gas formation. The design of the repair measures for 1BMA also accounts for the possibility of gas generation, as do the gas-evacuation systems for 2BMA and the silo. Gas formation will thus be low enough not to impair barrier safety by adequate design measures and limitations on the amount of gas-forming materials. No less probable scenario has been selected to assess uncertainties related to this safety function.

8.2.3 Waste form and waste packaging – Safety function limit advective transport

The safety function *limit advective transport* is defined for the waste packaging in the form of concrete tanks in 1–2BTF and is assessed with the aid of the safety function indicator *hydraulic conductivity* in the concrete tanks (Table 5-1).

Status of the safety function in the main scenario

The status of the safety function indicator *hydraulic conductivity* in the concrete tanks evolves in the main scenario following concrete degradation. The temporal succession of the hydraulic conductivity of the concrete considered in the main scenario is described in Section 7.4.2 and illustrated in Figure 7-6. During the first 1 000 years after closure, the concrete tanks are considered to be moderately hydraulically degraded ($K = 10^{-7}$ m/s) and then severely degraded ($K = 10^{-5}$ m/s) from 3000 AD to 12000 AD. After that they are considered to be completely degraded ($K = 10^{-3}$ m/s).

Uncertainties in the initial state

The conditions in the 1–2BTF waste vaults are controlled and inspected during the operational period and at closure of the repository (**Initial state report**, Section 8.3), and uncertainties are therefore judged to be small. The initial state of the concrete tanks in 1–2BTF at closure is not expected to deviate from the status in the main scenario, since cautiously chosen hydraulic conductivity values are applied. Undetected, more extensive cracking of the tanks at closure of the repository is judged to be unlikely but imaginable due to e.g. tanks being impacted during transport with the forklift in 1–2BTF, and so cannot be excluded. However, directly after closure, one-sided hydraulic pressure during resaturation of the repository might affect the tanks adversely, which is currently being investigated. The effects could be related to those described in the scenarios *initial concrete cracks* (Section 9.8) and *alternative concrete evolution* (Section 8.5) which both affect the tanks since they constitute the main hydraulic barrier in 1–2BTF. The results of the investigation relating to one-sided hydraulic pressure during resaturation were not available during the work with present assessment and are therefore not taken into account. The initial state and evolution that were assigned before the issue was raised are therefore kept in present assessment. The effect of the issue on post-closure safety is being assessed as part of the ongoing work in relation to the operation of SFR1.

Uncertainties in internal processes

The safety function indicator *hydraulic conductivity* in the concrete tanks is influenced by the degradation of concrete, which is caused by several interacting processes as described in Sections 6.2.8–6.2.9 and 6.3.8–6.3.9 with references to the **Barrier process report**. More extensive and more rapid physical degradation leads to increased cracking and thereby increased hydraulic conductivities in the concrete structures. The uncertainty in the degradation of concrete for the engineered barriers in 1–2BTF and 1–2BMA is discussed in Section 8.2.6 and the general descriptions are also valid for the concrete tanks in 1–2BTF. However, there are also specific considerations for the engineered barriers and the concrete tanks of 1–2BTF, for instance, faster degradation of the concrete tanks than the outer concrete structures of 1–2BMA. The hydraulic conductivity values in the main scenario are chosen cautiously for the intact concrete tanks and related uncertainties are thus accounted for in the main scenario. As in uncertainties in the initial state, faster degradation than considered in the main scenario, for instance as a consequence of undetected more extensive cracking of the tanks at closure of the repository, is judged to be unlikely (but the issue of one-sided pressure build up is also not accounted for, see previous subsection) but could potentially occur due to mishaps.

Uncertainties in external conditions

Glacial conditions may affect the structural integrity of the concrete tanks, and periglacial conditions could possibly affect the hydraulic conductivity by freezing. In the climate cases considered in this assessment (Section 2.6.3), glacial and periglacial conditions occur at a time when the concrete tanks are considered to be already completely degraded due to other reasons and uncertainties relating to freezing or glaciation are therefore not of concern.

Potential consequences of an earthquake are not assessed within the main scenario. Earthquakes can affect the stability of the rock as well as the stability of the engineered barriers and may potentially lead to increased hydraulic conductivity in the concrete tanks. It is not possible to predict when future earthquakes will occur and what magnitude they will have, and large intraplate earthquakes cannot be excluded to take place within the assessment period (Section 6.2.4).

Scenario selection

Due to uncertainties, mainly in the rate of concrete degradation processes, but also uncertainties in the initial state, the scenario *alternative concrete evolution* has been selected to assess uncertainties related to this safety function indicator. In principle, uncertainties related to earthquakes could also be analysed in the *earthquake scenario*. However, the limited inventory in 1–2BTF, containing mostly radionuclides with shorter half-lives, combined with a low yearly probability of earthquakes of relevant magnitudes, implies that an analysis of effects of earthquakes in the scenario is not required.

8.2.4 Waste form and waste packaging – Safety function limit corrosion

The safety function *limit corrosion* is defined for the metal waste with induced activity in 1BRT and is assessed with the aid of the safety function indicators *pH in porewater* and *redox potential* (Table 5-1).

Status of the safety function in the main scenario

In the main scenario, the evolution of the safety function indicators for *limit corrosion*, i.e. pH in porewater and redox potential in 1BRT is as follows.

pH in porewater – The pH is controlled by the degradation of cementitious materials (Section 6.2.8). During the initial 2 000 years, sodium and potassium hydroxides set the pH to above 12.5. Thereafter, pH is controlled by the dissolution of portlandite until 22 000 AD. During the period 22 000 AD to 87 000 AD pH is about 12. At the end of the assessment period, the pH in 1BRT decreases to about 10. The evolution of the pH in 1BRT in the main scenario is shown in Figure 7-7.

Redox potential – Highly reducing conditions are quickly established after closure and resaturation of the 1BRT vault (Section 6.2.8) provided by the corrosion of iron. When all the steel is corroded, after about 30 000 years in the *base case*, the redox potential will increase but still be fairly reducing, as set by the incoming groundwater (Sections 6.2.8 and 7.4.2).

Uncertainties in the initial state

The large amount of concrete in 1BRT ensures that the pH is initially high, and uncertainties are judged to be small. The large amount of steel ensures initially reducing conditions with high certainty.

Uncertainties in internal processes

The uncertainties in the general dissolution and leaching of the cement minerals are of minor importance for the safety function *limit corrosion* since the amount of concrete in 1BRT is large and the effects of uncertainties in the pH evolution on corrosion rates are handled cautiously in the main scenario (Section 7.4.2). Rates for near-neutral, anoxic conditions are cautiously applied earlier than predicted based on the pH evolution (Figure 7-7) and the pH sensitivity of steel corrosion (**Data report**, Section 5.1). This leads to a depletion of steel after about 30 000 years within the vault. Nevertheless,

since the incoming groundwater is still reducing (Section 6.3.6, Table 6-8), a correspondingly low redox potential, albeit higher than when steel corrosion still prevails, is expected to be upheld throughout the assessment period in the main scenario. Thus, uncertainties in internal processes related to the evolution of the safety function *limit corrosion* are judged to be handled within the main scenario.

Uncertainties in external conditions

Potential consequences of a glaciation are not assessed within the main scenario. During glaciation, the possible intrusion of oxygenated water might affect corrosion rates. However, the cautious handling of the corrosion rates in the main scenario leads to a depletion of steel in 1BRT before the time a glaciation could possibly occur (Section 6.3.8 and the **Climate report**, Section 4.4) and the effect of glaciation is thus of no concern.

Scenario selection

The corrosion of the segmented steel reactor pressure vessels comprising induced activity is handled cautiously in the main scenario in relation to the evolution of the safety function indicators. No credible way for the safety function indicators to deviate from the main scenario adversely and impairing repository safety is identified. Hence, no less probable scenario related to metal corrosion is defined. The effect of oxidising conditions in the repository on the corrosion of the waste in 1BRT is illustrated in the residual scenario *oxidising conditions* (Section 9.7).

8.2.5 Waste form and waste packaging – Safety function sorb radionuclides

The safety function *sorb radionuclides* is defined for the waste form and packaging in the silo, 1–2BMA, 1BRT and 1–2BTF, and is assessed with the aid of the safety function indicators: *amount of cementitious material, pH in porewater, redox potential*, and *concentration of complexing agents* (Table 5-1). Corresponding indicators are also defined for the engineered barriers, described in Section 8.2.8.

Status of the safety function in the main scenario

Amount of cementitious material – Sorption of radionuclides onto cementitious materials is a key aspect for this safety function, as cement retards many radionuclides efficiently in degradation states I through IIIb (**Data report**, Chapter 7). The amounts of cement in the vaults are sufficient to maintain these states over the whole assessment period (Section 7.4.2 and Cronstrand 2014, Höglund 2018, 2019).

pH in porewater – The development of the average pH in the waste vaults following the four defined degradation states is shown in Figure 7-7.

Redox potential – Highly reducing conditions are quickly established in all waste vaults after closure and resaturation of the vaults (Section 6.2.8). Corrosion of iron will provide a reducing environment for all wastes. After all the steel is corroded the redox potential will increase but still be fairly reducing, as set by the incoming groundwater (Section 6.2.8).

Concentration of complexing agents – The concentrations of complexing agents in SFR are evaluated in Keith-Roach et al. (2021) and the handling in the main scenario is summarised in Section 7.4.2. For most of the compartments in 1BMA, and in the silo and 1–2BTF, the levels of nitrilotriacetate (NTA) imply that sorption of some radionuclides is reduced. After the NTA has been flushed out, the cellulose-degradation product isosaccharinate (ISA) has an enduring effect on some radionuclides in 1BMA. The amounts allowed according to the most recent WAC[40] are restricted so that the sorption of radionuclides will not be influenced by the amounts of complexing agents and cellulose present in future wastes. Degradation of cellulose to ISA and mobilisation of radionuclides due to complex formation will not take place during periods of frozen conditions at repository depth, which is addressed in the *continuous permafrost variant* of the *cold climate calculation case* in the main scenario (Section 7.6).

[40] Hedström S, Ahlford K, Rosdahl J, Rasmusson M, Maier A, 2021. Krav på avfall från säkerhetsanalysen av SFR1. SKBdoc 1533189 ver 4.0, Svensk Kärnbränslehantering AB. (In Swedish.) (Internal document.)

Uncertainties in the initial state

The uncertainties in the initial state regarding amount of cementitious material, pH and redox potential are judged to be of minor importance, and no deviation of these safety function indicators from the initial state used in the main scenario is judged likely. The concentrations of complexing agents are regulated in the WAC (**Initial state report**, Section 3.1) and uncertainties in the concentration of complexing agents are handled probabilistically in the main scenario (Section 7.4.2). For instance, the uncertainties associated with the mass of cellulose, that degrades to ISA, were assessed using a Monte Carlo approach. Generally, the uncertainties in the initial state are therefore handled within the main scenario.

Ni(II) is in the main scenario considered unaffected by complexing agents, since it does not have a strong affinity for the dominant complexing agents ISA and NTA (Section 6.2.8). However, Ni(II) has a strong affinity for polyamines, which are not accounted for in the main scenario and whose concentrations are uncertain. The likelihood of polyamines affecting Ni(II) transport out from the waste is judged to be small (see further Section 6.2.8) and such effects are therefore not considered in the main scenario.

Uncertainties relating to the safety function indicator *concentration of complexing agents* are generally handled within the main scenario. However, the potential degradation of superplasticisers that are strongly bound to the hardened cement paste has not been considered in the main scenario. On longer timescales than accessible by experiments, it cannot be ruled out that superplasticiser degradation products will be released from the solid concrete matrix (Section 6.2.8). However, based on theoretical arguments, such degradation is expected to occur very slowly and result only in small concentrations of organic molecules with limited complexing strength (Section 6.2.8, Hedström 2019b, Keith-Roach and Shahkarami 2021). Thus, the evolution of the safety function indicator might deviate from the evolution in the main scenario, but this is judged unlikely.

Possible future discoveries of previously unknown amounts of complexing materials that reach the waste producers' waste streams cannot be ruled out. Such discoveries have occurred since SFR was commissioned and were then included in the assessments. However, as the waste producers' understanding and avoidance of complexing agents have improved in recent years, future discoveries of sufficient magnitude to affect sorption are deemed unlikely.

The uncertainties related to the initial state, Ni(II) complexation and future discoveries of previously unknown complexing materials might lead to a deviation of the safety function indicator *concentration of complexing agents* compared to the main scenario. Such deviations are judged to be less probable and are therefore not considered in the main scenario.

Uncertainties in internal processes

Large amounts of cementitious materials are present in 1–2BMA, 1BRT and 1–2BTF (**Initial state report**) and uncertainties in upholding effective sorption for relevant radionuclides throughout the assessment period are small.

The evolution of the pH in the porewater is treated cautiously in the main scenario (Section 7.4.2), based on the studies of Cronstrand (2014) for SFR1 and Höglund (2018, 2019) for 1BRT and 2BMA. The effect of potential uncertainties in the pH evolution on radionuclide speciation and retention is, in any case, expected to be marginal, particularly since only a few radionuclides' speciation is sensitive to the expected pH variations (Section 6.3.8). It is judged that there is no credible way for the safety function indicator *pH in porewater* to deviate from the evolution in the main scenario in a way that impairs post-closure safety.

The calculations by Hedström (2019a) show that steel will remain and set reducing conditions throughout the assessment period in 1–2BMA, 1–2BTF and the silo (Sections 6.2.8 and 6.3.8). For 1BRT, the metallic waste ensures reducing conditions for as long as the waste is not completely corroded. After all steel is corroded, after about 30 000 years in the main scenario (using assumptions to ensure a cautious handling of the release of activity induced in the steel, see Section 7.4.2), the redox potential will increase but still be fairly reducing, as set by the incoming groundwater (Sections 6.2.8 and 7.4.2). Given the cautious assumptions underlying the analysis of redox conditions and that reducing groundwater conditions will prevail, the uncertainties are judged to be handled adequately within the main scenario.

An uncertainty relating to the concentration of complexing agents in 1BMA that is not accounted for in the main scenario is the potential groundwater transport of complexing agents from 1BLA to 1BMA. Sorption is not accounted for in 1BLA and the amount of complexing agents is therefore not of concern for 1BLA. The amount of complexing agents in 1BLA is largely undocumented, but there is an inventory estimate for cellulose, which can degrade to form ISA that acts as a complexing agent, and the amount of ISA transferred between 1BLA and 1BMA is expected to be small, because:

- ISA is only slowly formed with a low yield in 1BLA due to the prevailing chemical conditions,
- the potential for Ca-ISA precipitation due to solubility limits,
- the protective concrete barriers in 1BMA, and
- ISA sorption occurs in both vaults.

Treating all these factors cautiously, the safety function indicator *concentration of complexing* agents in 1BMA could potentially deviate from the evolution in the main scenario.

Uncertainties in external conditions

Varying groundwater composition, as a result of varying external conditions, has been considered in the reference evolution and in the main scenario; by this the effects of varying external conditions have been included indirectly in the selection of parameter values for the internal conditions.

Uncertainties in the climate evolution that are not covered by the main scenario are primarily related to the possibility of a glaciation at Forsmark within the assessment period (**Climate report**, Section 4.4). The intrusion of oxygenated water occurring under glacial conditions might affect the redox-state of redox sensitive radionuclides if the redox-buffering capacity is depleted by the intruding oxygen. Oxidising conditions may affect the speciation of the radionuclides and consequently their sorption on bentonite and cement.

Scenario selection

Based on the discussion above, uncertainties of interest for the scenario selection are related to several aspects coupled to the concentration of complexing agents due to uncertainties in the initial state and internal processes that may lead to a deviation of the safety function indicator status in comparison to the main scenario. The *high concentration of complexing agents scenario* is selected to assess these uncertainties that are judged to be less probable and thus not part of the main scenario.

Uncertainties in the future climate evolution that are not addressed in the main scenario may lead to glacial conditions which affect the safety function indicator *redox potential*. This may lead to a deviation of this indicator in comparison to the main scenario. The *glaciation scenario* has been selected to assess the impact of glacial conditions considering its effect on the redox potential at repository depth.

8.2.6 Engineered barriers – Safety function limit advective transport

The safety function *limit advective transport* is assessed with the aid of two safety function indicators. The indicator *hydraulic conductivity in concrete and bentonite* applies to the outer concrete structures in 1–2BMA and to the bentonite in silo and plugs. The indicator *hydraulic conductivity in backfill* applies to 1–2BMA and 1–2BTF (Table 5-1).

Status of the safety function in the main scenario

The initial state hydraulic conductivity of the engineered barriers in the 1–2BMA and 1–2BTF waste vaults is described in Section 7.4.2. The indicator *hydraulic conductivity in concrete* is influenced by degradation processes in the concrete. The outer concrete structures of 1–2BMA evolve from being intact during the initial submerged period to being moderately degraded during the following period up until 22 000 AD (Figure 7-6 and the **Data report**, Section 9.12). Over the following 30 000 years, the concrete becomes severely degraded, being completely degraded at 52 000 AD. Fully penetrating

cracks are present in the concrete slab of 1BMA at closure. In the outer concrete structures of 1–2BMA, cracks might occur when the concrete is severely degraded. The evolution of the hydraulic conductivity in the outer concrete structures in the main scenario follows these degradation states with hydraulic conductivity values less-or-equal to 10^{-9} m/s, 10^{-7} m/s, 10^{-5} m/s and 10^{-3} m/s, respectively (see Section 7.4.2 and the **Data report**, Chapter 9 for details).

The low hydraulic conductivity of the bentonite in the silo and tunnel plugs is assumed to be maintained throughout the analysis period in the main scenario. The lower part of the silo wall has a hydraulic conductivity of 9×10^{-12} m/s and the upper part about 9×10^{-11} m/s. The hydraulic conductivity of the bentonite in the plugs is 1×10^{-12} m/s (Section 7.4.2).

The hydraulic conductivity in the backfill, that consists of highly permeable macadam (10^{-3} m/s), is in the main scenario maintained throughout the entire analysis period (Section 7.4.2).

Uncertainties in the initial state

The state of the outer concrete structures of 1–2BMA will be inspected during construction, operation and before backfilling (**Initial state report,** Sections 5.3 and 6.3) and thus uncertainties with respect to the initial state are limited. Design deviations due to undetected mishaps during construction should therefore also be unlikely. Formation of fully penetrating cracks caused by shrinkage processes during the early period after casting (Section 6.2.7) are avoided by adequate choice of material and methods of construction (Section 6.2.9). If, despite the precautions, fully penetrating cracks should occur they should be detected during checks and can then be repaired. The analysis in Höglund (2014, Section 9.3) shows that the width of cracks is more critical than the frequency, and it is easier to detect and repair wide cracks. Narrow cracks (< 0.1 mm) also tend not to be penetrating, which was concluded from the investigations in SFR1 (Mårtensson 2014). A deviation in the initial state of the indicator hydraulic conductivity of the outer concrete structure of 1–2BMA in comparison to the main scenario thus requires an unlikely mishap leading to the event that cracks form, and that they would either be undetected or the repairs would be less effective than expected. It should be noted that the hydraulic conductivity for undegraded concrete in the main scenario is already at least a factor of 100 higher than the values obtained in measurements of fresh concrete corresponding to the 2BMA concrete. The initial state in the main scenario can therefore be considered to already cover uncertainties associated with construction of the concrete structures and the structural development during the operational period.

The hydraulic conductivity of the bentonite in the silo has been assessed (**Initial state report**, Section 12.3.3, Pusch 1985, Johannesson et al. 2015, Tables 2-3 and 2-4) and the values used in the main scenario are thus judged to be valid.

The initial state of the backfill in 1–2BMA and 1–2BTF is handled cautiously in the main scenario. Measurements of the hydraulic conductivity resulted in values that were about two orders of magnitude higher than the values used in the calculations (**Data report**, Chapter 9). Since the flow is diverted from the waste domain due to the high conductivity in the backfill, assuming a lower conductivity in the calculations is cautious. It is judged that there is no credible way for the initial status of the hydraulic conductivity of the backfill in 1–2BMA and 1–2BTF to deviate from the value applied in the main scenario in such a way that post-closure safety may be impaired.

Uncertainties in internal processes

The durability of the concrete barriers is evaluated by long-term reactive transport modelling, accounting for the coupling between dissolution/precipitation of minerals and porosity/diffusivity/hydraulic conductivity changes (Section 6.2.9 and the **Barrier process report**, Section 5.4.6). There are uncertainties, at the conceptual level, in the model applications, and in the interpretation of the model results over long timescales (Höglund 2014). The uncertainties in the hydraulic conductivity of the concrete are mainly related to the existence of cracks in the concrete, the degradation rate of the concrete and the hydraulic properties of the degraded concrete (**Barrier process report**, Section 5.2.2). Due to the absence of reinforcement bars and other steel components in the concrete barriers of 2BMA, the impact of steel corrosion on the barrier function does not need to be considered for the 2BMA vault.

In principle, thermal shrinkage of the concrete structures as a result of groundwater filling the vaults after closure could cause formation of cracks within a few years (**Data report**, Section 9.3), however, cracking due to such load independent forces can be prevented by correct choice of material and methods of construction of the concrete structures (Section 6.2.9). The uncertainties described in this paragraph are accounted for by the selection of a cautious parameter set in the main scenario (**Data report**, Section 9.12 and Höglund 2014).

In the unlikely event that the initial status of the indicator hydraulic conductivity of the outer concrete structure of 1–2BMA should deviate from the main scenario, as described in the previous subsection, due to undetected or ineffectively repaired fully penetrating cracks before closure, the degradation rate of the concrete during the post-closure period could also be affected. The penetrating cracks could potentially lead to a more pronounced effect of coupling between physical degradation and chemical leaching at a local scale. The effect of the thin cracks that are considered in the initial state of the main scenario on the chemical degradation is judged to be small (Höglund 2014, Section 9.3) and is handled with the cautious parameterisation of the degradation processes. As a consequence of a more pronounced effect of coupling between physical degradation and chemical leaching due to undetected or ineffectively repaired fully penetrating cracks, the indicator hydraulic conductivity of the outer concrete structures of 1–2BMA could deviate from the evolution in the main scenario. Given the low probability of such an event relating to the initial state, deviations from the subsequent post-closure evolution are also judged to be unlikely.

The chemical composition of the groundwater and surrounding materials used in the modelling of concrete degradation cover the likely range that can occur in the post-closure period (SKB 2017a). Substantially higher amounts of chloride or sulfate ions could potentially lead to increased concrete degradation. This could lead to a deviation (from the evolution in the main scenario) of the safety function indicator *hydraulic conductivity in the outer concrete structure* of 1–2BMA. Furthermore, some local impact of salts on the concrete barriers in waste compartments in 1BMA that contain evaporator concentrates cannot be fully excluded (Section 6.2.9). However, such geochemical conditions in general or local impacts of evaporator concentrates in 1BMA are judged to be unlikely.

In the **Barrier process report**, Section 5.1, the conclusion is drawn that the probability of cracking of the outer concrete barriers in 1–2BMA due to low temperature and freezing of the concrete pore water is negligible. It can also be noted that permafrost occurs only after the concrete has been degraded due to other processes in the main scenario. Therefore, uncertainties regarding internal processes related to freezing are not of importance in relation to the main scenario. The handling of uncertainties in external processes that affect the safety function indicator *hydraulic conductivity in the outer concrete structures* of 1–2BMA is given in the following subsection.

The hydraulic conductivity in bentonite might potentially be affected by uncertainties relating to processes during the initial resaturation phase (Section 6.2.9 and the **Barrier process report**, Section 7.2). The initial water pressure gradient at the rock-bentonite interface could cause piping/erosion that could potentially lead to bentonite loss from the barrier and reduced swelling pressure and thus increased hydraulic conductivity. Based on the study in Börgesson et al. (2015) it is, however, judged that piping and erosion will not have a significant impact on the performance of the bentonite barrier (Section 6.2.9) and thus on the safety function indicator *hydraulic conductivity in bentonite*.

The evolution of the safety function indicator *hydraulic conductivity in the bentonite* might be influenced by uncertainties related to montmorillonite transformation due to interactions with cementitious materials or cementation (Sections 6.2.9, 6.3.9, and the **Barrier process report**, Sections 7.4.10 and 7.4.14). Results from modelling show that only a small part of the bentonite is affected within the 30 000-year period that was studied in Cronstrand (2016) (see Section 6.3.9) and indicate that the montmorillonite dissolution depths are small compared with the thickness of the bentonite barrier, even after 100 000 years (Idiart et al. 2020). With limited dissolution depths, transport through the bentonite barrier surrounding the silo will remain diffusion controlled. It is judged to be unlikely that uncertainties in montmorillonite transformation and cementation cause transport to be dominated by advection in the bentonite, and this situation is therefore not considered within the main scenario.

The interaction of bentonite with iron is a complex process and there are uncertainties related to process understanding (Section 6.2.9 and the **Barrier process report**, Section 7.4.11). However, as the iron is enclosed in the concrete, direct interaction with the bentonite is unlikely. It can therefore be expected that this transfer will be small enough to make the process non-significant in comparison with the interaction between bentonite and alkaline pore water from cement-based grout and concrete (Section 6.2.9 and the **Barrier process report**, Section 7.4.11).

If permafrost occurs at repository depth and leads to freezing of the bentonite, non-frozen water might be transported towards the already-frozen parts and potentially lead to the formation of an ice lens. This can be considered a highly unlikely event (Section 6.5.9). In the even more unlikely event that all drainage passages to the bentonite are blocked due to the presence of ice-filled fractures in the host rock (Section 6.5.9), so called frost weathering pressure peaks may occur. In such a situation, pressure peaks of a few tens of MPa cannot be excluded (Birgersson and Andersson 2014). In the main scenario, permafrost occurs at times when the concrete of the silo is considered to be completely degraded and thus any potential damage to the concrete will not have any effect on calculated radionuclide releases. The pressures are judged not to be high enough to cause any permanent damage to the bedrock surrounding the silo. The bentonite is completely restored after thawing, and thus any deterioration of the bentonite properties due to the pressure peak is of no concern. For both cases of ice-lenses and frost weathering, it is judged unlikely that the hydraulic conductivity of the bentonite surrounding the silo would be affected to a magnitude that results in advective transport becoming dominant over diffusion.

The bentonite earth dam plugs are subject to similar process uncertainties as the bentonite in the silo. However, the large amount of bentonite in the earth dam plugs and their distance to concrete structures make them less sensitive to degradation processes.

The effect of backfill clogging due to accumulation of fine-grained material in the backfill, chemical reactions or microbial activity, could lead to a slight reduction of the hydraulic conductivity (Section 6.2.9). However, given the cautious parameter values used, this uncertainty is handled within the main scenario. Moreover, the processes affecting the hydraulic properties of the concrete structures themselves are judged to be of greater importance. Hence, no credible deviation in the safety function indicator *hydraulic conductivity of the backfill* that could impair post-closure safety has been identified.

Uncertainties in external conditions

Uncertainties in the climate evolution that are not covered by the main scenario are primarily related to the possibility of a glaciation at Forsmark within the assessment period (**Climate report**, Section 4.4). The structural integrity of the waste vaults cannot be expected to remain intact after a glaciation and bentonite might be affected by potentially high groundwater flow and low ionic strength of the glacial meltwater. However, a glaciation may realistically only occur within the last 50 000 years of the assessment period (**Climate report**, Section 4.4), i.e. when the structural concrete is already considered to be physically degraded due to other processes in the main scenario (Section 7.4.2). Therefore, a glaciation only affects the properties of the bentonite, i.e. the status of the safety function indicator *hydraulic conductivity of the bentonite*. If permafrost were to lead to freezing at repository depth at earlier times, uncertainties related to the safety function indicator *hydraulic conductivity of outer concrete structures* of 1–2BMA and bentonite, as described above, could potentially lead to deviations in comparison to the evolution in the main scenario. Permafrost occurring at early times is, however, highly unlikely and regarded as a hypothetical event (**Climate report**, Section 4.3).

Potential consequences of an earthquake are not assessed within the main scenario. Earthquakes can affect the stability of the rock as well as the stability of the repository and may potentially lead to increased hydraulic conductivity in concrete and bentonite. It is not possible to predict when future earthquakes will occur nor what magnitude they will have; large intraplate earthquakes cannot be excluded to occur within the assessment period (Section 6.2.4). Thus, an earthquake can potentially cause a deviation of the safety function indicator *hydraulic conductivity of the outer concrete structures* of 1–2BMA and of the silo bentonite.

Other uncertainties related to the external conditions are judged to not influence the indicators hydraulic conductivity in the concrete and bentonite or backfill to a degree that is not already handled within the main scenario. For instance, the shoreline regression's influence on the degradation processes in the concrete (Höglund 2014) is judged to be considerably smaller than the other uncertainties discussed in relation to the internal processes. In addition, a significantly delayed shoreline regression is expected to result in a delay of the concrete degradation due to a lower water flow. This process is handled cautiously in the main scenario since the concrete degradation is based on the fastest foreseeable shoreline regression (**Climate report**, Section 3.5.3 and **Data report**, Chapter 12).

Scenario selection

Due to the uncertainties in the initial state of the degradation processes in the outer concrete structures of 1–2BMA described above, the *alternative concrete evolution scenario* has been selected to assess uncertainties related to the safety function indicator *hydraulic conductivity* for these structures. It is also noted that, for 1BMA, a calculation case without repair measures of the current concrete barrier is presented within a residual scenario (Section 9.9). In principle, the *earthquake scenario* could be used to study the impact of earthquakes on the hydraulic conductivity of the concrete structures of 1–2BMA. However, the effect of the silo being damaged is judged to be the main contributor to dose increase after an earthquake. In SAR-08 (SKB R-08-130, Section 10.3.1), the risk contribution from 1BMA is more than an order of magnitude lower than that from the silo. The 2BMA vault is located further from the surface, which results in both lower groundwater flow and less risk of being affected by earthquakes (SKB R-08-130, Bäckblom and Munier 2002). Given the pessimistic assumptions made in the calculation case including the silo (Section 8.6) contributions from 1–2BMA are omitted. The effect of uncertainties in the climate evolution on the hydraulic conductivity of the bentonite is accounted for in the *glaciation scenario*. The scenario also illustrates the effect of loss of the bentonite barrier due to other reasons such as uncertainties in the montmorillonite transformation. Such transformations are very slow and effects on the flow-limiting properties of the bentonite barrier are unlikely to occur, particularly before the latter half of the assessment period, when the onset of the glaciation occurs. The effects of hypothetical early permafrost leading to freezing at repository depth is illustrated in the residual scenario *hypothetical early permafrost* (Section 9.3). In that case, the effect of an ice lens on the bentonite in the silo is accounted for as well as degradation of the concrete during the permafrost event. The residual scenario *loss of engineered barrier functions* (Section 9.4) includes a calculation case that illustrates the effect of neglecting the hydraulic barriers in the repository and the *initial concrete cracks scenario* (Section 9.8) evaluates the effect of initially damaged hydraulic concrete barriers in the repository.

8.2.7 Engineered barriers – Safety function allow gas passage

The safety function *allow gas passage* is defined for the silo, 1–2BMA and 1–2BTF, and is assessed with the aid of the safety function indicator *permeability* (Table 5-1).

Status of the safety function in the main scenario

In concrete structures, a few small cracks are generally sufficient to allow all the generated gas to escape, however, the bentonite in the silo is not as permeable. In order to facilitate the release of the gas generated in the waste, the silo and 2BMA will be provided with engineered systems for gas release, and therefore adverse effects of gas formation on the concrete barriers are not taken into account in the main scenario. For 1BMA, no engineered system for gas release is included in the current version of the closure plan underlying the PSAR.[41] Gas formation within 1BMA is however mostly slow. The steel drums in 1BTF and the grouting allow for gas transport and the WAC for 1–2BTF and, in particular for the concrete tanks, aims at limiting the amount of gas-forming materials (Section 8.2.2).

[41] The closure plan for SFR is gradually being developed by SKB. Ongoing developments for 1BMA include detailed investigations of the requirements on the repair measures planned for the concrete structure, including requirements on withstanding detrimental effects of gas formation, water and soil pressure.

Uncertainties in the initial state

The initial state for the safety function *allow gas passage* is not subject to any significant uncertainties, because the status of the barriers and engineering systems for gas release are well known at closure.

Uncertainties in internal processes

Gas formation inside the silo and 2BMA has been studied and judged to be acceptably slow to allow the gas to escape through the engineered systems for gas release without any harmful pressure build-up (Section 6.2.8). For 1BMA, pressure inside the waste domain is unlikely to build up given limited gas formation and the existing cracks in the concrete slab. Furthermore, there is ongoing work related to the repair measures for 1BMA that relate to gas-formation and transport (Section 8.2.2).

During the very early period after closure when most gas generation is predicted to occur, the function of the systems for gas release through the concrete barriers in silo and 2BMA will be intact. After this early period, gas production due to processes in the waste and barriers will be slow and low. Thus, uncertainties related to engineered systems for gas release and hence the status of the safety function indicator *permeability* in the main scenario are judged to be small.

Uncertainties in external conditions

Uncertainties in external conditions are judged to be of no importance for this safety function.

Scenario selection

Uncertainties related to gas formation (Section 8.2.2) and to the capabilities of the waste vaults to allow passage of the generated gas are small. No less probable scenario has been identified that would imply a need to evaluate uncertainties related to this safety function.

8.2.8 Engineered barriers – Safety function sorb radionuclides

The safety function *sorb radionuclides* is defined for the concrete barriers in silo, 1–2BMA, 1BRT and 1–2BTF. The safety function is assessed with the aid of the four safety function indicators: *amount of cementitious material*, *pH in porewater*, *redox potential* and *concentration of radionuclide complexes* (Table 5-1).

Status of the safety function in the main scenario

The discussion in Section 8.2.5 for the safety function indicators *amount of cementitious material, pH in porewater, redox potential* and *concentration of complexing agents* relating to the waste form and packaging is valid also for the engineered barriers. One difference is, however, that complexing agents are not expected to be formed within the concrete barriers (for a discussion on superplasticisers, see Section 8.2.5), but the complexing agents initially present or formed within the waste form may also affect the sorption in the barriers. Another difference is that the *amount of cementitious material* that is accessible for radionuclide sorption can be affected by cracks in the concrete barriers that may lead to transport dominated by advection.

Uncertainties in the initial state

The uncertainties in the initial state regarding the amount of cementitious material, pH in porewater and redox potential are judged to be of minor importance (Section 8.2.5). The only complexing agents initially present in the structural concrete are superplasticisers, and since they are strongly bound to solid cement particles rather than dissolved in the porewater they contribute little to the uncertainty in the initial state regarding radionuclide sorption.

Uncertainties in internal processes

The uncertainties discussed in Section 8.2.5 are also relevant for the respective processes and safety function indicators in the concrete barriers in 1–2BMA, 1BRT and 1–2BTF. Uncertainties related to

the formation of cracks in the concrete barriers are discussed in Section 8.2.6. The formation of more cracks than accounted for in the main scenario could lead to smaller accessible amounts of cement for sorption for advection dominated transport paths through the cracks.

Uncertainties in external conditions

The uncertainties discussed in Section 8.2.5 are also relevant for respective processes and safety function indicators in the concrete barriers in 1–2BMA, 1BRT and 1–2BTF. Potential consequences of an earthquake are not assessed within the main scenario. Earthquakes may potentially lead to cracks in the concrete structures and could lead to smaller accessible amounts of cement for sorption for advection dominated transport paths through the cracks.

Scenario selection

Given the similarities with the uncertainties in the indicators related to the safety function *sorb radionuclides* in waste form and waste packaging (Section 8.2.5), the same scenarios are selected, i.e. the *high concentration of complexing agents scenario* and the *glaciation scenario*. In addition, uncertainties in the formation of cracks in the outer concrete structures of 1–2BMA, as described in Section 8.2.6, can lead to smaller accessible amounts of cement for sorption for advection dominated transport paths through the cracks. The *alternative concrete evolution scenario* is selected to assess this effect. The same effect of more cracks can also be the result of an earthquake that damages the concrete barriers. This effect is analysed in the *earthquake scenario*. The residual scenario *initial concrete cracks scenario* (Section 9.8) evaluates the effect of large cracks in all concrete structures directly after closure and the effects of such cracks on sorption.

8.2.9 Geosphere – Safety function provide favourable hydraulic conditions

The safety function *provide favourable hydraulic conditions* is assessed with the aid of the safety function indicators *hydraulic conductivity* and *hydraulic gradient* (Table 5-1).

Status of the safety function in the main scenario

In the main scenario, the hydraulic conductivity of the fractures in the bedrock at initial state (Section 4.7) is assumed to prevail throughout the assessment period (Section 7.4.3).

Since the repository is located beneath the sea at initial state (Section 4.5), the hydraulic gradient at SFR is very low. After the land over the repository has risen above sea level, the hydraulic gradient and flow direction stabilise and are in the *base case* constant from around 5000 AD to the end of the assessment period (Section 7.4.3). The land relief is low and thus the hydraulic gradients are small. In the *warm climate calculation case*, the regression of the shoreline in the Forsmark area is delayed 3500 years compared to the *base case* (Section 7.5.2). In the *cold climate calculation case*, the hydraulic gradients evolve in the same way as in the *base case*, although flow will cease during frozen periods (Section 7.6).

Uncertainties in the initial state

The hydraulic conductivity applied in the initial state is based on the site investigations, as described in Section 4.7. In the site investigations, treatment of uncertainties was given thorough attention. In the main scenario, data uncertainties are handled by probabilistic treatment of relevant parameters in the hydrogeological and radionuclide transport calculations (Section 7.4.3). Initially, when the area above SFR is submerged, the uncertainties in the gradient are negligible.

Uncertainties in internal processes

The hydraulic conductivity is not expected to change significantly within the assessment period (Section 6.2.5). Internal processes potentially affecting the evolution of the hydraulic conductivity are discussed together with related uncertainties in the **Geosphere process report**, Sections 3.2, 4.4, 4.5, 5.6. No uncertainties in internal processes that are not already handled in the main scenario

and that would impair repository safety have been identified to be important for the safety function. The hydraulic gradient is affected by uncertainties in the external conditions (see next subsection), however, no uncertainties in internal processes affecting the hydraulic gradient have been identified in the **Geosphere process report**.

Uncertainties in external conditions

The occurrence of a glaciation during the assessment period is judged to be unlikely and is not assessed within the main scenario. Under glacial conditions, the hydraulic gradients may change significantly (Section 8.3.2) and the mechanical load from an inland ice sheet affects the hydraulic conductivity of the geosphere. To quantify such effects of the mechanical load on the hydraulic conductivity, a coupled hydro-mechanical model would be needed. However, ignoring hydro-mechanical couplings has the effect of exaggerating the Darcy fluxes at depth (Neuzil 2012) and uncertainties are thus handled cautiously in the main scenario. Uncertainties in the shoreline displacement and its timing affect the time periods with hydraulic gradients controlled by the Baltic Sea. This is evaluated in the *warm climate calculation case* and in a supporting calculation case in the main scenario (Sections 7.5 and 7.7).

Potential consequences of an earthquake are not assessed within the main scenario. The seismic activity in the Fennoscandian shield is currently very low. However, large intraplate earthquakes cannot be excluded to take place within the assessment period (Section 6.2.4). Earthquakes may cause displacement along fractures in the geosphere, which alter the hydraulic conditions of the geosphere. The extent to which the geosphere is affected is associated with large uncertainties, dependent on the location and magnitude of the earthquake, but can be handled by pessimistic assumptions (**Geosphere process report**, Section 3.2.7).

Scenario selection

Uncertainties in the future development of the climate may lead to glacial conditions which affect the safety function indicators *hydraulic conductivity* and *hydraulic gradient*. This may lead to a deviation of the safety function indicator status in comparison to the main scenario which may affect repository safety. Glacial conditions are unlikely to occur within the assessment period and are therefore not included in the main scenario. The less probable *glaciation scenario* has been selected to assess the impact of glacial conditions. In addition, due to uncertainties as to whether an earthquake will occur and its effects on the safety function indicator *hydraulic conductivity*, the *earthquake scenario* is selected.

8.2.10 Geosphere – Safety function provide chemically favourable conditions

The safety function *provide chemically favourable conditions* is applied since the inflowing groundwater acts as a hydrochemical boundary condition for the waste vaults. The safety function is assessed with the aid of the safety function indicator *redox potential* (Table 5-1).

Status of the safety function in the main scenario

In the main scenario, reducing conditions prevail in the geosphere around the repository for the entire assessment period (Section 7.4.3).

Uncertainties in the initial state

The water composition at initial state and related uncertainties are described in Section 4.7.8. The supply of hydrochemical data and predictability with regard to the expected composition of the groundwater are good. It is not likely that any extreme water compositions other than those already encountered will be discovered during the construction phase. Uncertainties in the initial groundwater composition and in mineralogical conditions in the geosphere are judged to be insignificant in relation to the safety function indicator *redox potential*.

Uncertainties in internal processes

The groundwaters reaching the repository are not expected to contain appreciable concentrations of oxidising species, due to the redox buffer capacity in the biosphere and geosphere. There are various chemical processes in the geosphere that will affect the composition of the groundwater; for example, diffusional exchange between ground- and porewaters, mineral dissolution and precipitation in fractures and the rock matrix (Sections 6.2.6 and 6.3.6 and the **Geosphere process report**, Chapter 5). Freezing of the geosphere also affects the groundwater composition in terms of salt exclusion (Section 6.5.6). Considering the uncertainties in all these processes, the groundwater redox state is unlikely to change significantly during temperate or periglacial conditions (Sections 6.3.6 and 6.5.6). In addition, the redox potential in the near-field is controlled by the corrosion of steel, which leads to even stronger reducing conditions in the repository near-field (Duro et al. 2012a, Hedström 2019a).

Uncertainties in external conditions

The occurrence of a glaciation during the assessment period is judged to be unlikely and is not assessed within the main scenario (Section 7.2 and the **Climate report**, Section 4.4). If a glaciation should occur, it cannot be excluded that oxygen-rich waters will infiltrate the repository (Auqué et al. 2013).

Scenario selection

Uncertainties in the future development of the climate may lead to glacial conditions which affect the safety function indicator *redox potential*. This may lead to a deviation of the safety function indicator status in comparison to the main scenario that might affect repository safety. Glacial conditions are unlikely to occur within the assessment period and are therefore not included in the main scenario. The *glaciation scenario* has been selected to assess the impact of glacial conditions. In the residual *oxidising conditions scenario* (Section 9.7), the redox potential of the geosphere is assumed to be oxidising throughout the assessment period.

8.2.11 Surface system/sub-sea location – Safety function avoid boreholes in direct vicinity of the repository

The safety function *avoid boreholes in the direct vicinity of the repository* is assessed with the aid of the safety function indicators *boreholes downstream of the repository* and *intrusion boreholes* (Table 5-1).

Status of the safety function in the main scenario

As long as the area above SFR remains submerged, the potential for boreholes being drilled in the vicinity of the repository is very low, and no boreholes are assumed in the main scenario during this time. When the shoreline has regressed and when terrestrial conditions prevail above the repository, wells drilled downstream of the repository for the purpose of extracting water are considered in the main scenario (Section 7.3.5). The probability of such a well is cautiously assumed to be one in the main scenario. Intrusion into the repository is handled as part of the analysis of future human actions (FHAs) and the safety function indicator *intrusion boreholes* is therefore not handled in the main or less probable scenarios. FHAs and related scenarios are discussed in Chapter 9.

Uncertainties in the initial state

Initially, the area above SFR is submerged and there are thus no boreholes suitable for water extraction in the vicinity of the repository.

Uncertainties in internal processes

The exposure from a well in the area where groundwater is expected to have the highest concentrations of radionuclides, i.e. the *well interaction area*, is included in the main scenario (Section 7.3.5). Thus, the handling is cautious in the main scenario. Moreover, the uncertainty with respect to the position of the well is handled probabilistically (**Biosphere synthesis report**, Section 8.2.4).

Uncertainties in external conditions

There are uncertainties in the evolution of the climate at Forsmark, especially related to future sea level changes over the next few thousand years (Section 6.2.1). These uncertainties are handled within the main scenario, by including three variants of reference external conditions in the reference evolution (Section 6.2.1) and supporting calculation cases with different lengths of submerged conditions (Section 7.7). Hence, uncertainties in the length of the initial period of submerged conditions are handled within the main scenario.

Scenario selection

No less probable scenario is selected for further analysis of the safety function related to the *avoiding boreholes in direct vicinity of the repository*. It cannot be entirely ruled out that intrusive boreholes may be drilled in the future. Intrusion boreholes are handled within FHA scenarios (Section 9.11).

8.2.12 Selected less probable scenarios

Table 8-1 summarises the selected less probable scenarios and the safety functions underpinning their selection. Based on the evaluation of each of these safety functions in Sections 8.2.1–8.2.11, four less probable scenarios are selected for further analysis. Radionuclide transport and dose are evaluated in one calculation case for each scenario (Table 8-2). The scenarios and the associated calculation cases are further described in Sections 8.3–8.6.

Table 8-1. Less probable scenarios and associated safety functions that deviate from the status in the main scenario.

Less probable scenario	Safety function										
	Waste form and waste packaging					Engineered barriers			Repository environs		
	Limit quantity of activity	Limit gas formation	Limit advective transport	Limit corrosion	Sorb radionuclides	Limit advective transport	Allow gas passage	Sorb radionuclides	Provide favourable hydraulic conditions	Provide chemically favourable conditions	Avoid boreholes in the direct vicinity of the repository
Glaciation scenario					X	X		X	X	X	
High concentrations of complexing agents scenario					X			X[3)]			
Alternative concrete evolution scenario			X			X		X			
Earthquake scenario			X[1)]			X[2)]		X	X		

[1)] In principle the concrete tanks in 1–2BTF can be affected by an earthquake, however the contributions to risk are judged to be small and 1–2 BTF are thus not explicitly considered in this scenario.

[2)] In principle 1–2BMA can be affected by and earthquake, however the contributions to risk are judged small in comparison to the silo, because pessimistic assumptions are made (Sections 8.2.6 and 8.6). 1–2BMA is thus not explicitly considered in this scenario.

[3)] The scenario is not directly related to this safety function, but its safety function indicator *concentration of radionuclide complexes* is strongly correlated to the safety function indicator *concentration of complexing agents* in the waste, for which this scenario is selected for analysis.

Table 8-2. Less probable scenarios and associated calculation cases.

Scenario		Calculation case
Less probable scenarios	Glaciation	Glaciation
	High concentrations of complexing agents	High concentrations of complexing agents
	Alternative concrete evolution	Alternative concrete evolution
	Earthquake	Earthquake

Included in the risk assessment.

8.3 Glaciation scenario

8.3.1 General description and probability assessment

This scenario is selected to assess uncertainties in the climate evolution, related to the occurrence of glacial conditions above SFR within the assessment period. The underlying assumption is that the glacial conditions will influence the safety function indicators *hydraulic conductivity in bentonite* (silo and plugs), *redox potential* (waste, engineered barriers and geosphere) and *hydraulic conductivity/gradient* (geosphere) to such extent that the safety functions *limit advective transport* in the engineered barriers, *sorb radionuclides* in the waste and engineered barriers as well as *provide favourable hydraulic conditions* and *provide chemically favourable conditions* in the geosphere will deviate from the main scenario (Sections 8.2.5, 8.2.6, 8.2.8, 8.2.9 and 8.2.10).

The approach in the main scenario is to make assumptions based on the range of probable climate evolution, as defined by the reference external conditions (Chapter 6). Radiological consequences of a colder-than-present climate in the main scenario are evaluated by the *cold climate calculation case* (Section 7.6). That calculation case assumes that the atmospheric CO_2 concentration has decreased sufficiently within the first 50 000 years after closure, such that ice sheets begin to grow in the Northern Hemisphere in response to the next substantial insolation minimum at 56 000 AD, but without an ice sheet reaching Forsmark. This results in the development of periglacial climate conditions at Forsmark within the latter half of the assessment period for that calculation case.

The *glaciation scenario* assumes that the development towards colder climate conditions after 50 000 years will result in ice-sheet development to such an extent that glacial conditions occur at Forsmark. In this context, a potential glaciation at Forsmark resulting from the 56 000 AD insolation minimum is of particular interest for post-closure safety as this enables radiological consequences to be evaluated during temperate climate conditions subsequent to glacial conditions at the site. Periods of temperate conditions subsequent to Forsmark glaciations that result from later insolation minima (around 79 000 and 98 000 AD, see **Climate report**, Figure 3-29) would emerge after the 100 000-year analysis period. Therefore, the probability of the *glaciation scenario* is inferred from the estimated probability of a glaciation at Forsmark resulting specifically from the 56 000 AD insolation minimum.

As discussed in the **Climate report**, Section 4.4, glaciation at Forsmark in response to the 56 000 AD insolation minimum would require an unprecedented growth rate of the Eurasian ice sheet, considerably faster than past growth rates from ice-free conditions inferred from geological records. As a result, the likelihood of a glaciation at Forsmark during this time is assessed to be low, even under the assumption of zero future anthropogenic carbon emissions (**Climate report**, Section 4.4). Furthermore, unless future technological advances will result in the removal of all anthropogenically-produced CO_2 from the atmosphere, a certain fraction of the CO_2 emissions is projected to persist in the atmosphere for the entire assessment period regardless of emissions size (**Climate report**, Section 3.4.1). Hence, even under the assumption of a strong reduction of anthropogenic emissions within the coming decades, a perturbation of anthropogenic CO_2, albeit small, is expected to remain in the atmosphere also after 50 000 years. It is likely that these elevated CO_2 concentrations would serve to reduce the extent of the Northern Hemisphere glaciation, and thus also the likelihood of a glaciation at Forsmark within the coming 100 000 years.

In summary, quantifying the probability of the *glaciation scenario* requires a probability assessment of (i) the growth rate of the Eurasian ice sheet, and (ii) future pathways of anthropogenic carbon emissions. Whilst the probability of the former theoretically could be quantified by extensive ice-sheet modelling, a probability quantification of the latter is more challenging as it depends on the global socio-economic development, including future policy decisions. The probability of the *glaciation scenario* is therefore based on expert judgement taking the argumentation outlined above into account. According to this assessment, the probability of the *glaciation scenario* is judged to be low, likely into single percent digits. However, in the assessment of radiological risk, the probability is for simplicity selected to be 10 %.

8.3.2 Description of the calculation case

The *glaciation calculation case* is selected to evaluate radionuclide transport and dose from the *glaciation scenario*. A detailed description and analysis of the calculation case is given in the **Radionuclide transport report**, Section 7.2. A summary of the calculation case, including the description of external conditions, is presented in the following and the key results are presented in Section 8.3.3.

External conditions

The development of external conditions in the *glaciation calculation case* is described by the glaciation climate case (**Climate report**, Section 5.3.1). The succession of climate domains is shown in Figure 8-1 and Table 8-3. The initial shoreline regression is the same as in the *base case*. As discussed in Section 6.2.1, this is a reasonable assumption for a future development towards a colder climate. As a result, external conditions in the *glaciation calculation case* are the same as in the *base case* up until the onset of the first period of periglacial conditions at 56 600 AD. The development of external conditions for the remainder of the assessment period is summarised in the following subsections. A more detailed description of the glaciation climate case, representing the external conditions in this calculation case, is given in the **Climate report**, Section 5.3.1.

Development of permafrost and frozen ground

Permafrost and frozen ground develop during periglacial climate conditions, but may, or may not, also prevail beneath an ice sheet during glacial conditions. For an ice sheet to advance over a region, below-freezing annual air temperatures are required for some time prior to the ice-sheet migration (**Climate report**, Section 3.2.3). Thus, the landscape at Forsmark is considered to be dominated by periglacial conditions prior to the ice-sheet advance over the region (Table 8-3). The duration of these periods is estimated based on modelling of the future climate at Forsmark (Lord et al. 2019), as further described in the **Climate report**, Section 5.3.1. In order not to underestimate the duration of the temperate period following the first glaciation at the site, pessimistic assumptions were employed to ensure that the second period of periglacial conditions was kept as short as possible (**Climate report**, Section 5.3.1).

In this calculation case, it is also assumed that the frozen depth always exceeds the depth of the repository. The case of a shallower permafrost development, including the presence of taliks in the landscape, is analysed in the *cold climate calculation case* (Section 7.6).

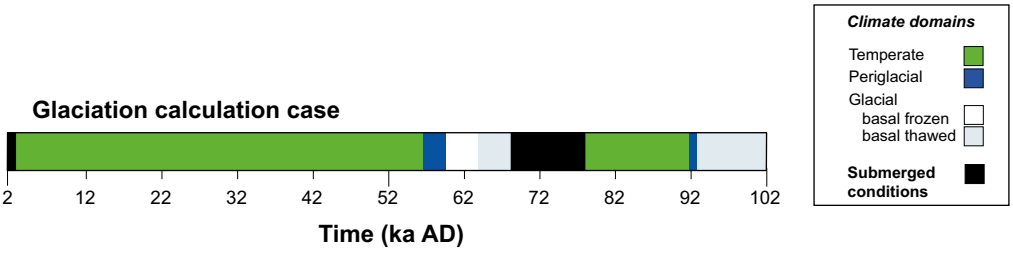

Figure 8-1. *Succession of climate domains in the glaciation calculation case.*

Table 8-3. Summary of the glaciation calculation case, including conditions in the repository and its environs during periods of different climate domains.

Time period	Duration (years)	Climate domain above repository	Thermal conditions at all repository depths	Repository barrier integrity	Repository and geosphere redox conditions	Geosphere groundwater flow [a]	Biosphere discharge area
2000–56 600 AD	54 600	Temperate	base case	*base case*	Reducing	*base case*	*base case*
Periglacial conditions 56 600–59 600 AD	3 000	Periglacial	Frozen bedrock	*base case*	Reducing	No flow	Cold climate (*continuous permafrost*)
Ice-sheet advance 59 600–63 900 AD	4 300	Glacial	Frozen bedrock	No barriers	Reducing	No flow	No recipient/no exposure
Peak glaciation 63 900–66 200 AD	2 300	Glacial	Thawed bedrock	No barriers	Oxidising	*base case* 9000 AD [b]	Deep sea basin
Ice-sheet retreat 66 200–68 150 AD	1 950	Glacial	Thawed bedrock	No barriers	Oxidising	Linear interpolation to 3 × *base case* 9000 AD [b]	Deep sea basin
Transition from glacial to submerged conditions 68 150–68 200 AD	50	Glacial	Thawed bedrock	No barriers	Oxidising	Linear interpolation to *base case* 2000 AD [c]	Deep sea basin
Submerged conditions 68 200–76 900 AD	8 700	Temperate, submerged conditions	Thawed bedrock	No barriers	Reducing	*base case* 2000 AD [c]	*base case* 2000 AD
Transition from submerged to terrestrial conditions 76 900–77 900 AD	1 000	Temperate, submerged conditions	Thawed bedrock	No barriers	Reducing	*base case* 2000–3000 AD	*base case* 2000–3000 AD
Terrestrial conditions 77 900–91 800 AD	13 900	Temperate	Thawed bedrock	No barriers	Reducing	*base case* 3000–16 900 AD	*base case* 3000–16 900 AD
Periglacial conditions 91 800–92 800 AD	1 000	Periglacial	Frozen bedrock	No barriers	Reducing	No flow	Cold climate (*continuous permafrost*)
Ice-sheet advance 92 800–102 000 AD	9 200	Glacial	Thawed bedrock	No barriers	Oxidising	*base case* 9000 AD [b]	Shallow sea basin

[a] The geosphere groundwater flow is based on the *base-case* flow, scaled by a time-dependent factor. The repository groundwater flow is based on the *base case* and a "no barriers" flow case (Abarca et al. 2020). The same scaling factor as for the geosphere groundwater flow is also applied for the near-field flow.
[b] "*base case* 9000 AD" is taken as a representative for the flow under fully terrestrial temperate conditions.
[c] "*base case* 2000 AD" corresponds to the flow under fully submerged temperate conditions

Periods of glacial conditions

The timing and duration of the glacial periods, including the thermal conditions (frozen/unfrozen) beneath the ice sheet, are adopted from the Weichselian glacial cycle climate case in the SR-PSU (SKB TR-13-05, Section 4.4). The same glacial conditions were also used in the reference glacial cycle climate case in the SR-Site (SKB TR-10-49, Section 4.5). These climate cases represent a projection into the future of conditions reconstructed for the last 120 000 years. Although changes in insolation over the next 100 000 years will be considerably different from those during the past 120 000 years, periods of glacial conditions in the climate cases coincide reasonably well with the timing of anticipated future periods of colder climate conditions and ice-sheet growth in the Northern Hemisphere (**Climate report**, Sections 3.4.5 and 4.4).

In accordance with the SR-PSU Weichselian glacial cycle climate case, the 100 000-year long assessment period encompasses two glacial periods at Forsmark. The first glacial period begins at 59 600 AD, a few thousand years after the summer insolation minimum at 56 000 AD, and the second glacial

period begins at 92 800 AD (Figure 8-1 and Table 8-3). Further, frozen conditions beneath the ice sheet are considered to persist during the initial 4 300 years of the first glacial period. During the remaining time of the first glacial period (also 4 300 years), as well as the entire second glacial period, thawed conditions are considered at repository depth as well as at the surface (Table 8-3).

The corresponding calculation case in the SR-PSU (the "glaciation and post-glacial conditions calculation case", see SKB TR-14-01, Section 8.5.8) evaluated dose consequences of a glaciation in a residual scenario. In that calculation case, the second periglacial and glacial periods were omitted from the calculations and, consequently, temperate conditions prevailed from the post-glacial submerged period until the end of the assessment period. An important distinction to the SR-PSU is that the radiological consequences of a glaciation in this safety assessment are evaluated in a less probable scenario rather than a residual scenario. Thus, as the resulting doses contribute to the radiological risk in this safety assessment, the description of the glacial climate evolution is designed to be more consistent with the prevailing scientific knowledge than was the case in the SR-PSU. Specifically, the inclusion of a second glaciation in this safety assessment conforms to the general understanding of climate and ice-sheet dynamics of the past ~800 000 years and is supported by contemporary projections of the future climate (**Climate report**, Sections 3.4.5 and 5.3.1).

Post-glacial submerged and temperate-terrestrial conditions

After the first glaciation, the Forsmark site is considered to be submerged beneath the sea for almost 10 000 years (Figure 8-1 and Table 8-3). The duration of this period is adopted from the SR-PSU Weichselian glacial cycle climate case (SKB TR-13-05, Section 4.4). The shoreline regression during the last 1 000 years of this post-glacial submerged period and the subsequent terrestrial period of temperate conditions is assumed to follow the initial regression of the *base case* (Table 8-3).

In order not to underestimate the radiological consequences of a glaciation, the period of temperate-terrestrial conditions after the first glacial period is assigned a relatively long duration of 13 900 years. Together with the preceding submerged period, this results in almost 24 000 years of uninterrupted temperate conditions after the first glaciation in this calculation case. Such a long sequence of temperate conditions embedded within a glacial cycle is considered to be pessimistic as it is neither supported by geological data from the last glacial (the Weichselian) nor by modelling (see further the **Climate report**, Section 5.3.1).

Handling in the near-field

The handling in the near-field models is identical to the *base case* up until the onset of the first period of periglacial conditions at 56 600 AD. For the remainder of the assessment period, sorption due to changes in redox and hydrological conditions are adjusted in the near-field with respect to the *base case*. The changes are summarised in Table 8-3 and described below.

Hydrology

The structural integrity of the engineered barriers cannot be expected to remain intact after a glaciation. However, at the time of the first ice-sheet advance over the site (59 600 AD), the concrete barriers are already completely degraded in the main scenario (Section 7.4.2). This calculation case also assumes that the bentonite will be affected by high groundwater flow rates and low ionic strength of the glacial meltwater. Thus, the hydraulic conductivity of the bentonite in the silo is pessimistically assumed to be 10^{-3} m s^{-1} from the first ice-sheet advance over the site until the end of the assessment period (as opposed to the main scenario for which the conductivities are applied for the entire assessment period, see Section 7.4.2). Furthermore, the hydraulic resistance of the plugs is pessimistically omitted after the ice-sheet advance.

The influence of the changes described above on the hydrology was examined in the "no barriers" flow case by Abarca et al. (2020). It was concluded that groundwater flow through the waste increased for all waste vaults in comparison to a case with intact concrete and bentonite barriers. The most affected vault by far is the silo, for which the groundwater flow is increased by almost three orders of magnitude in the "no barriers" case with respect to the case with intact barriers (Abarca et al. 2020).

During periods of frozen conditions at repository depth (Table 8-3), near-field groundwater flow and diffusion are considered insignificant and therefore set to zero. From the onset of thawed conditions beneath the ice sheet at 63 900 AD until the end of the first glacial period at 68 200 AD, the near-field groundwater flow will increase with the gradient of the ice-sheet surface, as described in the simulations of Vidstrand et al. (2013, 2014a). When the slope of the ice-sheet surface is flat over the repository site, i.e. when the ice-sheet margin is located far from Forsmark, groundwater flow is comparable to that during temperate terrestrial conditions (Figure 9 in Vidstrand et al. 2014a). When the ice sheet retreats, its southward margin gradually propagates closer to the repository site, at which point the slope of the ice sheet becomes steeper. In the ice sheet used for this calculation case, which is assumed to be the same as reconstructed for the last glacial cycle, the slope of the ice-sheet surface begins to gradually steepen during approximately the last 2 000 years of the first glacial period (**Climate report**, Appendix E). In the radionuclide transport calculations, groundwater flow rates are therefore set to increase linearly from 66 200 AD to a maximum value at 68 150 AD and the maximum is achieved when the ice-sheet margin is located above the repository. This maximum change is derived from the simulations of Vidstrand et al. (2013), where the maximum increase of groundwater flow during ice-sheet retreat varies in the range 3 to 20 times the magnitude simulated for present-day conditions. In order not to overestimate the radionuclide activity that is transported out of the repository during the glacial period (when dose consequences are expected to be marginal), the lower value (3 times the "no barriers" flow) is selected as the maximum flow during ice-sheet retreat (Table 8-3).

After the ice sheet has retreated from the site, the ice-free bedrock is isostatically depressed, and thus the site is submerged beneath the sea. Based on typical propagation rates of ice-sheet retreat from the last glacial cycle, the transition between glacial and submerged conditions at the Forsmark site is estimated to take approximately 50 years (**Climate report**, Appendix F). Thus, the transition from high to low groundwater flow is selected to occur during the last 50 years of the glacial period, i.e. between 68 150 AD and 68 200 AD (Table 8-3). During this short period, groundwater flow is reduced to "no barriers" flow under fully submerged conditions (i.e. conditions are assumed to be the same as at 2000 AD). This flow rate is then kept constant for 8 700 years of the post-glacial submerged period. For the remaining 1 000 years of the submerged period, as well as for the subsequent 13 900-year long period with temperate terrestrial conditions, the "no barriers" flow between 2000 AD and 16 900 AD is applied.

The second glacial period prevails beyond the assessment period of 100 000 years (see subsection *External conditions* above). Potential changes in the groundwater flow are not considered in the modelling due to the retreat and advance of this ice sheet, see further **Radionuclide transport report**, Section 7.2.3.

Sorption

The vault-specific concrete chemical degradation development in the *glaciation calculation case* is the same as in the *base case* (Figure 7-7). This is a cautious choice since the degradation rate is expected to slow down or halt during periods of frozen repository conditions. Hence, this calculation case does not affect the sorbents. Sorption is instead affected in terms of the properties of the sorbates, particularly in terms of altered speciation of some radionuclides in response to altered redox conditions.

Glacial meltwater is oxygen rich; Auqué et al. (2013, Tables 5-1–5-3) propose a redox potential of +400 mV for glacial groundwater and around −225 mV for non-glacial groundwater. The combination of abundant meltwater supply and high water pressures caused by the ice sheet may cause injection of glacial meltwater to greater depths than oxygen-rich waters would penetrate under non-glacial conditions. In addition, the consumption of oxygen close to the surface may be limited due to the lack of organic matter and microbiological activity (**Climate report**, Section 2.3). During the periods with sub-glacial meltwater production (63 900–68 200 AD and 92 800–102 000 AD), it is therefore cautiously assumed that oxygen-rich water penetrates from the surface to the repository, resulting in oxidising conditions in the repository and its environs. After the first glacial period, the surface groundwater becomes reducing again which in itself is sufficient to provide reducing conditions in the repository, even without any remaining reducing materials such as metallic steel.

Several redox-sensitive radionuclides are expected to change oxidation state during oxidising conditions in the near-field. This affects the speciation and consequently the sorption coefficients on bentonite and cement of Np, Pa, Pu, Se and Tc as discussed in the **Data report**, Chapter 7 and summarised in the **Radionuclide transport report**, Section 7.2.3. Of the five affected elements, four show weaker sorption during oxidising conditions. Only selenium, which is non-sorbing during reducing conditions, has a higher (albeit still quite low) sorption coefficient during oxidising conditions.

As a result of the altered speciation of these radionuclides under oxidising conditions, their interactions with complexing agents are expected to change in terms of moving to a different sorption reduction factor (SRF) group, where each SRF group has a certain sensitivity to complexing agents (Keith-Roach et al. 2021). Thus, the vault-specific SRF are altered upon changed redox conditions for Np, Pu and Tc, whereas Pa and Se remain in the same SRF group (**Radionuclide transport report**, Table 7-3).

Handling in the geosphere

Groundwater flow is modified according to Table 8-3. The temporal evolution of the groundwater flow is described and justified in the subsection *Handling in the near-field* above.

The handling of sorption coefficients during glacial conditions in the geosphere follows that of the near-field. To this end, K_d-values from the *base case* are used for the entire assessment period, apart for the periods of sub-glacial meltwater production from 63 900 AD to 68 200 AD and from 92 800 AD to 102 000 AD. During these periods, the groundwater is considered to be oxygen-rich, resulting in modified K_d values for Ba, Cs, Np, Ra, Sr, Tc and U (**Data report**, Chapter 8). For some of these elements, the altered redox conditions cause a change in oxidation state, whereas others change their K_d in response to the altered water composition and mineralogy without changing redox state, as noted in the **Data report**, Chapter 8.

During the latter part of the first glacial period (63 900–68 200 AD), when the bedrock is unfrozen, radionuclides are transported from the geosphere to a single sea basin. Due to the isostatic depression of the bedrock at SFR, a substantial water depth is considered in this part of the Baltic Sea during the first glaciation. A similar approach is used during the second glaciation (92 800–102 000 AD). In contrast to the first glaciation, the second glaciation is characterised by thawed bedrock conditions when the ice-sheet margin advances to the site (Figure 8-1). At this time, however, the isostatic depression of the bedrock is moderate, resulting in a significantly lower water depth compared to the time of thawed bedrock conditions during the first glacial period. Thus, during the second glaciation, radionuclides from the geosphere are assumed to be released to a shallow sea basin instead of a deep sea basin (see further subsection *Handling in the biosphere* below).

During the post-glacial submerged period and the following temperate period (68 200–92 800 AD), radionuclides are transported through the geosphere to biosphere object 157_2, as in the *base case*.

Handling in the biosphere

The handling in the biosphere model is identical to the *base case* during temperate conditions (Section 7.4.4) and to the *continuous permafrost* variant of the *cold climate calculation case* during periglacial conditions (Section 7.6.3).

The evolution of the discharge area is summarised in Table 8-3. When the bedrock is unfrozen during glacial conditions (59 600–63 900 AD and 92 800–102 000 AD), the historical sea basin of object 116 (dating to 8500 BC) is used as an open sea recipient. As the second glacial period is characterised by thawed bedrock conditions when the ice sheet advances over the site (Table 8-3), it is associated with a lower water depth compared to the time of thawed bedrock conditions during the first glacial period (subsection *Handling in the geosphere* above). Therefore, during the second glaciation, the same basin is used, but with a shallower water depth (corresponding to year 3000 AD). Further details on the parameterisations of the open sea basins are given in the **Radionuclide transport report**, Section 7.2.5.

During ice-covered periods, most unconsolidated regolith layers on top of the till are expected to be removed by glacial erosion and the remaining regolith is assumed to be flushed by large quantities of surface water. Thus, the radionuclide inventory in all regolith layers of object 157_2 is assumed to

be negligible at the start of the post-glacial submerged period. The dose consequence of such an out flush of radionuclides is evaluated separately by postulating that the entire radionuclide inventory that has accumulated in object 157_2 during the temperate period (i.e. until 56 600 AD) is released, at a constant rate, into an open sea basin over a period of 50 years, see further the **Radionuclide transport report**, Section 7.2.5.

As for periglacial conditions, hunters and gatherers (HG) is the only potentially exposed group during periods with glacial conditions. This is motivated by the consideration that the discharge area is covered by the sea and catches from the postulated open sea basin provide the only source of food considered to contain repository-derived radionuclides for the potentially exposed group (Saetre et al. 2013a, Section 9.3).

8.3.3 Radionuclide transport and dose

The annual dose during periods of periglacial conditions was analysed in the *cold climate calculation case*. In summary, the dose during the periglacial periods is more than one order of magnitude lower than the corresponding dose in the *base case* (Section 7.6.4). The doses during the post-glacial submerged and glacial periods, including the out flush of radionuclides to the open sea in conjunction with the ice-sheet retreat (Section 8.3.2 *Handling in the biosphere*), are several orders of magnitude lower than the doses at the corresponding time in the *base case*. Since the effect of an increased oxygen content in the groundwater is only considered during the glacial periods, when the doses are considerably lower than during temperate periods, it is of limited importance for the results in this calculation case. Radionuclide transport and dose during the post-glacial submerged and glacial periods are discussed in detail in the **Radionuclide transport report**, Sections 7.2.6–7.2.8. In the following, only the results related to the radionuclide transport and dose during the post-glacial temperate-terrestrial period, i.e. when draining and cultivation of the mire in object 157_2 is possible, are discussed.

The activity of many radionuclides, including e.g. Mo-93 and C-14-org, have decreased considerably due to decay at the onset of the first glacial period. For some radionuclides with longer half-lives, e.g. Ca-41 and U-238, most of the activity has already been released during the initial temperate period. Thus, for these radionuclides, post-glacial releases are low and their contributions to the dose are not affected by the glaciation.

The radionuclide most affected by glaciation is Ni-59. This long-lived radionuclide dominates the activity release towards the end of the assessment period in the *base case* and contributes most to dose during that period (Figure 7-14). In the present calculation case, the annual near-field and geosphere release of Ni-59 during the post-glacial temperate period increases by almost two orders of magnitude compared with the same time period in the *base case* (**Radionuclide transport report**, Figure 7-3). This increase is primarily caused by the reduced hydraulic barrier function of the bentonite in the silo where most of the Ni-59 inventory is disposed. As a result, more than 30 % of the Ni-59 inventory is released from the near-field in this calculation case compared with only 2 % in the *base case*.

The higher release of Ni-59 from the geosphere has a significant impact on dose during the post-glacial temperate period. Ni-59 sorbs strongly in the lower regolith, and thus transport to the glacial clay (and to regolith layers above it) is slow (see also subsection about Ni-59 in Section 7.4.5). Therefore, during the first ~5000 years of the post-glacial temperate-terrestrial period, draining and cultivating of the mire in object 157_2 gives a lower exposure than in the *base case*, and the dose during this period is primarily caused by exposure to water extracted from a drilled well (Figure 8-2). This effect is somewhat elevated compared with the same group in the *base case* (~factor 2 at similar times) and is primarily attributed to the increased geosphere release of Ni-59. After the initial 5000 years of the post-glacial temperate period, draining and cultivating of the mire in object 157_2 gives the highest exposure due to the transport of Ni-59 from the lower regolith. From this time, the annual doses increase continuously and towards the end of the period the dose is ~4 μSv. This is about 3 times higher than in the *base case* at this time (or later times) but is still lower than the maximum dose that occurs during the first temperate period (Figure 8-2). Hence, even assuming a pessimistically long period of temperate conditions after the glaciation (considering it is embedded in a glacial cycle, see Section 8.3.2 *External conditions*), the maximum dose resulting from a glaciation does not exceed the maximum dose of the *base case*.

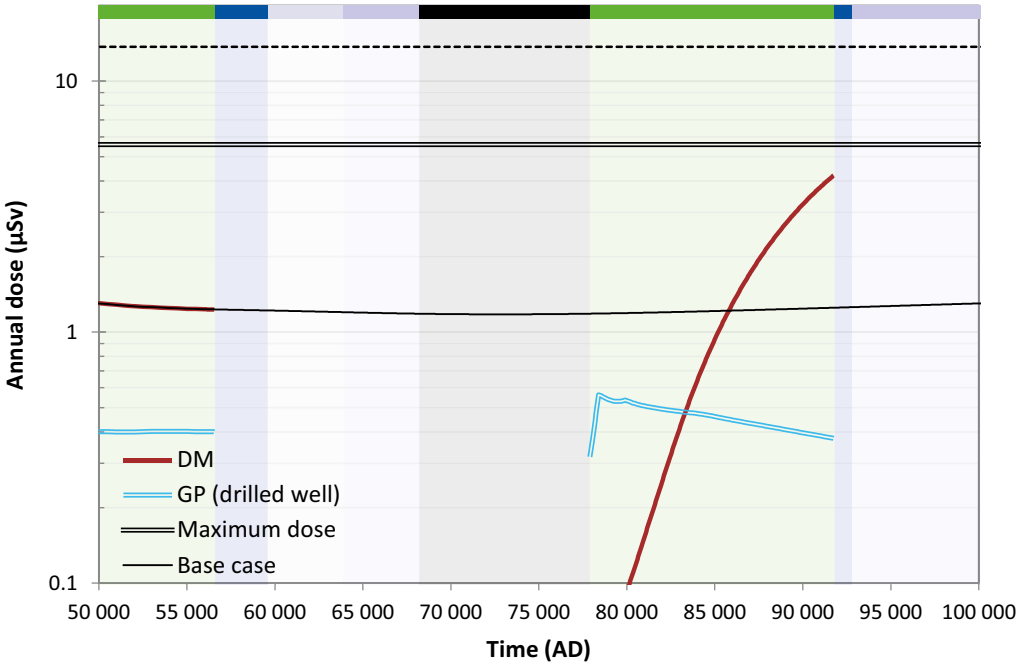

Figure 8-2. *Annual doses (µSv) to the two most exposed groups in the glaciation calculation case: drained-mire farmers (DM, red line) and garden-plot households (GP, blue line) utilising a drilled well. The maximum annual dose (at ~7000 AD; same as in the base case) and the annual dose in the base case are indicated by a double black line and a thin black line, respectively. The annual dose corresponding to the regulatory risk criterion (14 µSv) is indicated by the black dashed line. Coloured bars at the top with matching background shading represent the succession of climate domains in the glaciation calculation case (cf. Figure 8-1). Note that the timescale is shown only for the second half of the assessment period and is presented on a linear scale.*

8.3.4 Concluding remarks

This scenario is selected to evaluate radiological consequences of glacial conditions above SFR, resulting in the deviation from the main scenario of the safety functions *limit advective transport* in the engineered barriers, *sorb radionuclides* in the waste and engineered barriers as well as *provide favourable hydraulic conditions* and *provide chemically favourable conditions* in the geosphere. Due to these changes, this scenario yields significantly higher doses than in the main scenario during the temperate period following the first glaciation. The duration of the post-glacial temperate period is pessimistically assigned to be relatively long considering it is embedded in a glacial cycle. Even under this pessimistic assumption, the highest dose during this period remains below the maximum dose in the main scenario and, consequently, below the annual dose corresponding to the regulatory risk criterion (14 µSv).

8.4 High concentrations of complexing agents scenario

8.4.1 General description and probability assessment

The underlying assumption in this scenario is that, due to uncertainties in the safety function indicator *concentrations of complexing agents*, there is large enough reduction in sorption that the safety function *sorb radionuclides* in the waste form and packaging deviates from the main scenario (Section 8.2.5).

Complexing agents used at the nuclear facilities are present in the waste and can also be produced in the repository by degradation of waste components such as superplasticisers and cellulose. These may reduce sorption and enhance radionuclide transport. As described in Section 8.2.5, and in greater detail in Section 6.2.8, there are four sources of uncertainty that could affect the concentrations of complexing agents in the waste: (i) degradation of superplasticisers, (ii) dissolved complexing agents that may potentially travel with the groundwater from 1BLA to 1BMA, (iii) possible yet unidentified amounts of complexing materials that reach the waste producers' waste streams, and (iv) polyamines and their interaction with Ni(II).

Uncertainties in the concentrations of complexing agents are, to a certain degree, considered in the main scenario as statistical distributions of SRFs which are used in the probabilistic calculations (Section 7.4.2 *Complexing agents*). The amounts allowed according to the most recent WAC[42] are restricted so that the sorption of radionuclides will not be influenced by the amounts of complexing agents and cellulose present in future wastes. This, and the careful control over the amounts deposited, mean that the probability of the *high concentrations of complexing agents scenario* occurring is low, less than 10 %. However, in the assessment of radiological risk, the probability is cautiously selected to be 10 %.

8.4.2 Description of the calculation case

The *high concentrations of complexing agents calculation case* is selected to evaluate the dose from the *high concentrations of complexing agents scenario.* A detailed description and analysis of the calculation case is given in the **Radionuclide transport report**, Section 7.3. A summary of the calculation case is presented below and the key results are presented in Section 8.4.3.

In the near-field transport calculations, the SRF values for cement, bentonite and crushed rock in SRF Groups 1–5 are increased by a factor of 10 compared with the *base case*, including radionuclides whose *base case* SRF = 1 (Table 7-6). This tenfold increase is applied throughout the assessment period, regardless of whether ISA or NTA determines the *base case* SRF. The affinity of Ni(II) to the dominant complexing agents ISA and NTA is modest and so it is placed in the SRF Group "Other" which comprises radionuclides that in the *base case* are considered unaffected by complexing agents (Section 7.4.2). However, due to its affinity to polyamines, whose concentration in the vaults is uncertain (Section 8.2.5), the present calculation case applies the same tenfold SRF increase for Ni(II) as well; it is the only radionuclide from the SRF Group "Other" for which this increase is applied. The increased SRFs are applied to all waste vaults credited with the safety function *sorb radionuclides* and where complexing agents and/or cellulose are, or could be, disposed. As such, the waste vaults 1BRT and 1–5BLA are not affected in this calculation case.

The tenfold SRF increase is considered to be cautious, even taking all considered uncertainties into account. As argued in the **Radionuclide transport report**, Section 7.3.1, the SRFs considered in this calculation case are judged to significantly exceed the potential effects of superplasticisers in SFR and complexing agents transported from 1BLA to 1BMA. Although it is difficult to assess the probability and severity of still undiscovered amounts of complexing materials, the sorption reductions resulting from earlier discoveries are generally smaller than those applied in this calculation case. Furthermore, the waste producers' understanding and avoidance of complexing agents have in recent years improved, so the SRFs considered in this calculation case are judged to be cautious with respect to yet unidentified complexing agents (**Radionuclide transport report**, Section 7.3.1).

Values for hydraulic conductivity and porosity of the cementitious materials (and bentonite in the silo), as well as the diffusivity of radionuclides, evolution of the pH and K_d values are identical to those applied in the *base case* (Section 7.4.2).

When radionuclide–organic complexes enter the geosphere where the complexing-agent concentration is smaller than in the repository, a large fraction of complexes is expected to dissociate, reaching new equilibrium concentrations as determined by their stability constants. As noted in Section 6.2.6, complexing agents from the repository may still reduce the sorption of radionuclides in the geosphere. This effect has not been quantified, but the effect of sorption reduction is smaller than in the near-field since sorption is much stronger to cement than to bedrock for all radionuclides significantly affected in this calculation case: Ni(II), Pu(IV), Pd(II), Tc(IV), Zr(IV) (**Data report**, Chapters 7 and 8). Thus, the SRFs in the geosphere are, for simplicity, not altered in this calculation case.

The handling in the biosphere is the same as in the *base case*.

[42] Hedström S, Ahlford K, Rosdahl J, Rasmusson M, Maier A, 2021. Krav på avfall från säkerhetsanalysen av SFR1. SKBdoc 1533189 ver 4.0, Svensk Kärnbränslehantering AB. (In Swedish.) (Internal document.)

8.4.3 Radionuclide transport and dose

The presence of additional complexing agents has a minor effect of the maximum dose, because the radionuclides contributing most to the maximum dose in the *base case* (Mo-93 and C-14-org) are unaffected by complexing agents. However, the contribution of Ni-59 to the total dose increases significantly, especially towards the end of the assessment period when the dose from Ni-59 is almost one order of magnitude higher than in the *base case* (Figure 8-3). The higher contribution of Ni-59 results in a second dose peak around 80 000 AD. This peak is however lower than the maximum dose around 7000 AD (which is the same as in the *base case*).

The higher dose from Ni-59 is explained by increased activity releases of this radionuclide from the waste vaults. The total release of Ni-59 over the entire assessment period increases by about one order of magnitude compared with the *base case* (**Radionuclide transport report**, Section 7.3.7).

Several other radionuclides are also affected by the presence of additional complexing agents (**Radionuclide transport report**, Section 7.3.7). These are however not important for the dose, either in this calculation case or in the *base case*.

8.4.4 Concluding remarks

This scenario is selected to evaluate radiological consequences of reduced sorption due to higher concentrations of complexing agents than in the main scenario, resulting in the deviation from the main scenario of the safety function *sorb radionuclides*. This change results in a several-fold increase of the dose towards the end of the assessment period when compared to the main scenario. However, the maximum dose in this scenario does not exceed the maximum dose in the main scenario and, consequently, it remains below the dose corresponding to the regulatory risk criterion (14 µSv).

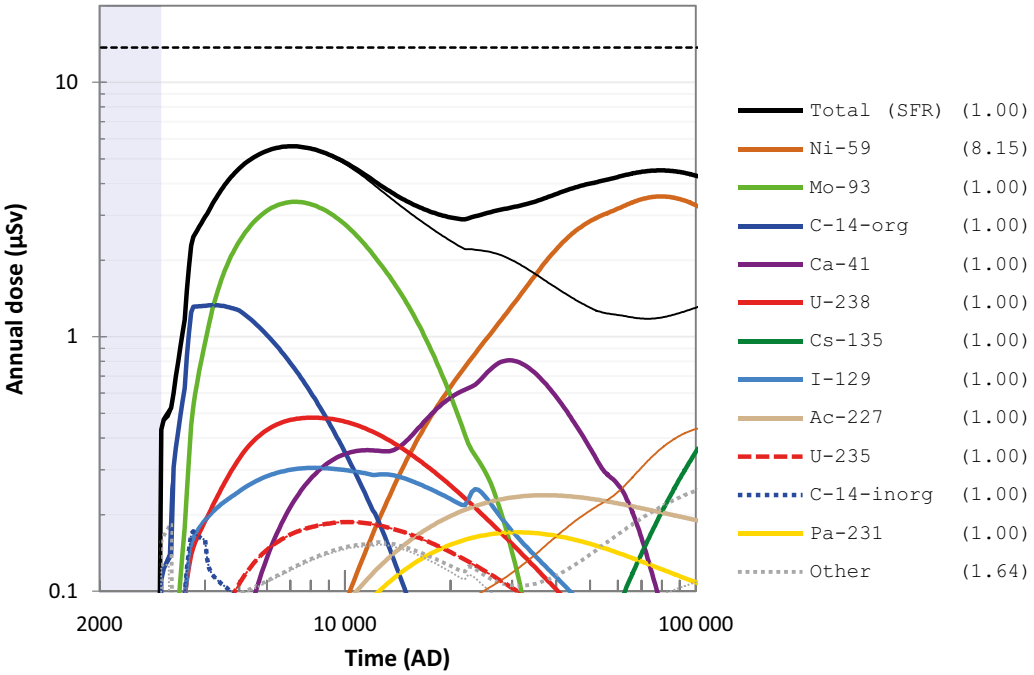

Figure 8-3. *Annual dose (µSv) to the most exposed group (black line), including radionuclide specific contributions (coloured lines), in the high concentrations of complexing agents calculation case (thick lines) and the base case (thin lines). The combined contribution from radionuclides not shown is indicated by the grey dotted line. The ratio between the maximum doses in the present calculation case and the base case are shown in parentheses in the key. The annual dose corresponding to the regulatory risk criterion (14 µSv) is indicated by the black dashed line and the submerged period is illustrated by the blue shading.*

8.5 Alternative concrete evolution scenario

8.5.1 General description and probability assessment

This scenario is selected to assess uncertainties related to the initial state and the physical degradation of cementitious materials in the waste vaults. To this end, effects of an earlier physical degradation than in the main scenario are evaluated. One underlying assumption is that due to uncertainties in the safety function indicators *hydraulic conductivity* in the concrete tanks (1–2BTF) and the outer concrete structures of 1–2BMA there is great enough groundwater flow such that the safety function *limit advective transport* in the engineered barriers, waste form and packaging deviates from the main scenario (Sections 8.2.3 and 8.2.6). For consistency, however, the hydraulic conductivity of the concrete in the silo and 1BRT are also adjusted in this scenario. Another underlying assumption is that the safety function *sorb radionuclides* deviates from the main scenario due to an earlier formation of cracks which leads to smaller accessible amounts of cement for sorption along advection-dominated transport paths through the concrete (Section 8.2.8).

Apart from the advective flow paths through cracks, sorption is not altered in this scenario. The same chemical evolution of the concrete barriers and waste is used as in the main scenario. The repository sensitivity to chemical-degradation uncertainties is instead illustrated by the sorption-related scenario *high concentrations of complexing agents* (Section 8.3) as well as the residual scenarios *loss of engineered barrier function* (Section 9.4) and *oxidising conditions* (Section 9.7).

As discussed in Sections 8.2.3 and 8.2.6, the uncertainties in the hydraulic conductivity of the concrete are mainly related to the existence of cracks in the concrete, the degradation rate of the concrete and the hydraulic properties of the degraded concrete. In general, however, physical degradation of concrete and associated values of the hydraulic conductivity are chosen cautiously in the main scenario (Section 7.4.2). Therefore, the probability of the *alternative concrete evolution scenario* occurring is low, considerably less than 10 %. In the assessment of radiological risk, the probability is cautiously selected to be 10 %.

8.5.2 Description of the calculation case

The *alternative concrete evolution calculation case* is selected to evaluate the dose from the *alternative concrete evolution scenario.* A detailed description and analysis of the calculation case is given in the **Radionuclide transport report**, Section 7.4. A summary of the calculation case is presented in the following and the key results are presented in Section 8.5.3.

The handling of the geosphere and the biosphere is identical to the *base case*. The near-field modelling includes an earlier physical degradation of the structural concrete than in the *base case*. Specifically, the following differences with respect to the *base case* are considered:

- The hydraulic conductivity of the structural concrete (and thus groundwater flow through the waste) is higher initially and increases earlier than in the *base case*.
- The diffusivities of radionuclides in the structural concrete increase earlier than in the *base case* and the uncertainties in diffusivities are considered greater.
- The porosity of the structural concrete increases earlier than in the *base case*.
- Earlier occurrence of cracks due to the earlier concrete degradation.

The increase in diffusivity and porosity considered in this calculation case are described in the **Radionuclide transport report**, Section 7.4. The hydraulic conductivities considered in this calculation case are shown in Figure 8-4. This can be compared with the corresponding conductivities considered in the *base case*, shown in Figure 7-6. In general, concrete degradation occurs earlier in this calculation case, such that periods in the *base case* with intact concrete ($K \leq 10^{-9}$ m/s) as well as moderately ($K = 10^{-7}$ m/s) or severely ($K = 10^{-5}$ m/s) degraded concrete in the waste vaults are assigned a higher hydraulic conductivity in this calculation case, whereas periods with completely degraded concrete in the *base case* have the same hydraulic conductivity ($K = 10^{-3}$ m/s) in this calculation case. Since the concrete is considered to be completely degraded during the last 50 000 years in the *base case*, the conditions in the near-field are thus identical to the *base case* for this period, whereas they deviate from the *base case* during the first 50 000 years of the assessment period.

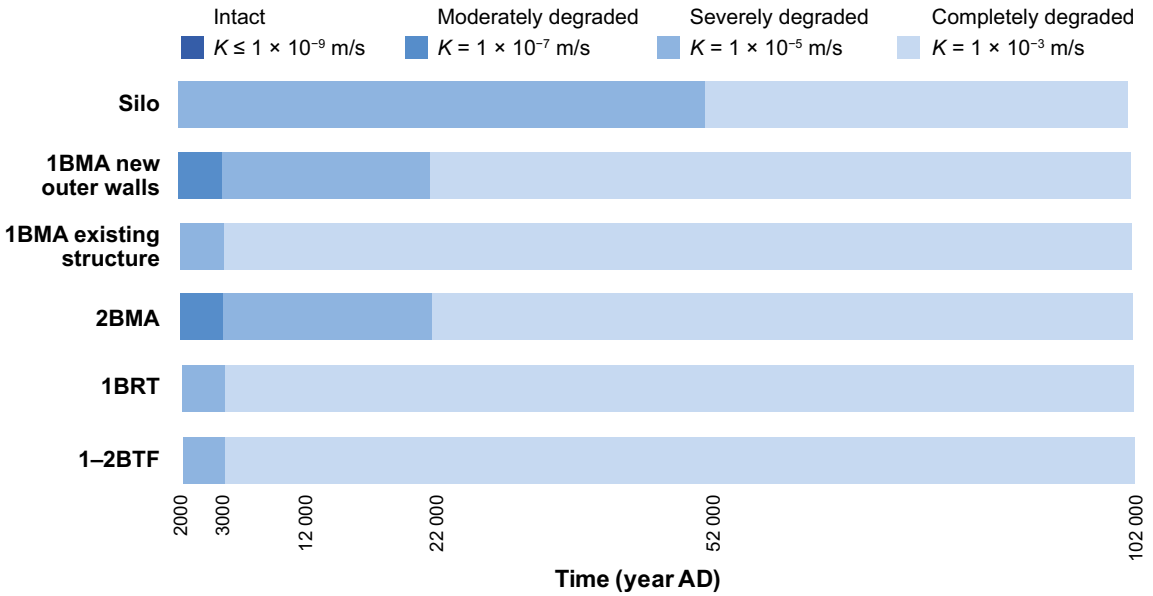

Figure 8-4. *Succession of hydraulic conductivity of concrete in the alternative concrete evolution calculation case. The corresponding succession for the base case is shown in Figure 7-6.*

The relationship in the *base case* between the hydraulic conductivity and the modelling of the advective flow is also considered to be valid in this calculation case, i.e. a moderately degraded concrete structure is modelled as a homogeneous medium whereas a severely or completely degraded concrete structure is modelled as a cracked medium (Section 7.4.2). Thus, as a consequence, the transition from a homogeneous to a cracked flow regime will occur earlier for 1–2BMA in this calculation case than in the *base case*. Moreover, as in the *base case*, the slab in 1BMA is considered to be cracked upon closure.

Apart from the changes described above, the handling in the near-field is the same as in the *base case*. Thus, properties of bentonite, macadam and complexing agents as well as the chemical evolution of cementitious materials are the same as in the *base case*. The handling is also identical to the *base case* for 1–5BLA that do not have any credited engineered barriers in the modelling.

8.5.3 Radionuclide transport and dose

For radionuclides that are primarily disposed in the BLA-vaults (e.g. U-235 and U-238), including decay products (e.g. Ac-227), the maximum annual dose in this calculation case, as expected, is the same as in the *base case*. However, all other radionuclides contribute to a higher dose in this calculation case than in the *base case* (Figure 8-5). As a consequence, the total dose is higher than in the *base case* throughout the entire assessment period, and the maximum dose is increased by almost 50 %. However, the maximum dose is still below the dose corresponding to the regulatory risk criterion.

Another result is that the maximum dose occurs earlier in this calculation case than in the *base case* (Figure 8-5). This is explained by higher groundwater flow through the waste early in the assessment period in this calculation case, resulting in earlier transport of the radionuclides to the geosphere and the biosphere than in the *base case*.

As in the *base case*, the radionuclides contributing most to the maximum dose are Mo-93 and C-14-org. The contribution of these radionuclides to the total dose is approximately doubled in this calculation case compared with the *base case*. The reason is primarily due to higher releases of these radionuclides from the BMA vaults (**Radionuclide transport report**, Section 7.4). In those vaults, especially the transition to severely degraded concrete at 3000 AD results in releases that are up to one order of magnitude higher than in the *base case*. The comparatively modest increase of the total dose from these radionuclides (Figure 8-5) is explained by dilution from the other vaults, where the increase is smaller than from the BMA vaults. Most importantly, for the silo, where most of the Mo-93 is disposed (Figure 4-2), the earlier concrete degradation has only a small effect on the groundwater flow as the hydraulic properties are mainly controlled by the bentonite in that vault.

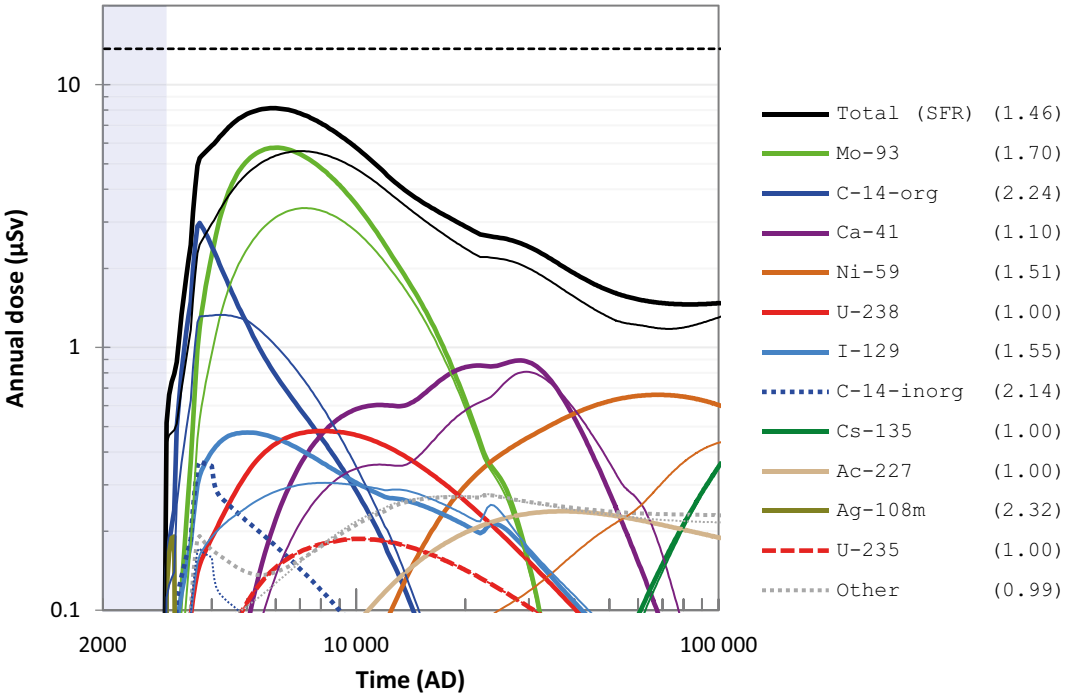

Figure 8-5. *Annual dose (µSv) to the most exposed group (black line), including radionuclide specific contributions (coloured lines), in the alternative concrete evolution calculation case (thick lines) and the base case (thin lines). The combined contribution from radionuclides not shown is indicated by the grey dotted line. The ratio between the maximum doses in the present calculation case and the base case are shown in parentheses in the key. The annual dose corresponding to the regulatory risk criterion (14 µSv) is indicated by the black dashed line and the submerged period is illustrated by the blue shading.*

8.5.4 Concluding remarks

This scenario is selected to evaluate radiological consequences of an earlier physical degradation of cementitious materials, including earlier formation of cracks, than in the main scenario. This results in deviation from the main scenario of the safety function *limit advective transport* in the engineered barriers (1–2 BMA) and waste form and packaging (1–2 BTF) as well as the safety function *sorb radionuclides* in the engineered barriers. These changes result in a maximum dose that is almost 50 % higher than that of the main scenario. However, the maximum dose in this scenario remains below the dose corresponding to the regulatory risk criterion (14 µSv).

8.6 Earthquake scenario

8.6.1 General description and probability assessment

This scenario is selected to assess the uncertainty related to damaged engineered barriers and adverse effects on the natural barriers resulting from an earthquake during the assessment period. One underlying assumption is that due to uncertainties in the safety function indicator *hydraulic conductivity/gradient* the hydraulic resistance in the geosphere will be sufficiently compromised such that the safety function *provide favourable hydraulic conditions* deviates from the main scenario (Section 8.2.9). Another underlying assumption is that the safety function *sorb radionuclides* deviates from the main scenario due to a reduced amount of cementitious material being accessible for sorption along the transport paths out from the repository (Section 8.2.8).

In principle, an earthquake can also affect the hydraulic conductivity of the concrete tanks in 1–2BTF and the outer concrete structures of 1–2BMA. However, the BTF tanks are excluded from the analysis due to a limited initial inventory containing mostly radionuclides with relatively short half-lives (Section 8.2.3). The BMA vaults are omitted, either because the consequences of an earthquake have been reported to be small in previous assessments (1BMA) or because it is located at a depth less affected by earthquakes (2BMA) (Section 8.2.6). Further, a pessimistic handling of the silo is adopted which more than compensates for the omittance of the BMA and BTF vaults from the analysis.

An analysis of the mechanical consequences of an earthquake for the integrity of the silo has been conducted (Georgiev 2013). Three different load spectra with annual probabilities of 10^{-5}, 10^{-6} and 10^{-7} were used (SKI 1992, Appendix 1). The conclusion from the analysis in Georgiev (2013) is that damage to the silo concrete structure cannot be ruled out for a load spectrum with a probability of 10^{-6} a^{-1}. Thus, the assigned yearly probability of damaged barriers due to earthquakes is 10^{-6} in this scenario, corresponding to a 10 % probability for such an earthquake during the assessment period.

8.6.2 Description of the calculation case

The *earthquake calculation case* is selected to evaluate the dose from the *earthquake scenario.* A detailed description and analysis of the calculation case is given in the **Radionuclide transport report**, Section 7.5. A summary of the calculation case is presented below and the key results are presented in Section 8.6.3.

This calculation case assumes that an earthquake damages the silo concrete structure and also adversely affects the structural and mechanical properties of the rock. As a detailed quantification of the effects of an earthquake on radionuclide transport is associated with large uncertainties, a highly simplified modelling methodology is used that intentionally overestimates the radiological consequences of an earthquake. The same methodology was used in the SR-PSU (SKB TR-14-01, Section 8.4.5) and in SAR-08 (SKB R-08-130, Section 8.4.3).

Up until the time of an earthquake, radionuclide transport occurs in the same way as in the *base case.* After the event, the concrete structure is assumed to be damaged to such extent that the concrete barriers in the silo are no longer fully functional. The effects on radionuclide transport of the damaged concrete structure are highly uncertain; with current knowledge, it is not possible to rule out that radionuclide transport pathways out from the silo would change compared with the main scenario. It is reasonable to believe that most of the transport would not be radically altered due to the integrity of the silo bentonite. However, as alternative transport pathways may be created (e.g. larger cracks), it is not possible to rule out a reduced transport-interaction with the engineered barriers.

Groundwater flow through the silo following concrete structural damage was analysed in the safety assessment SAFE (SKB 2001). Since the bentonite constitutes the main hydraulic barrier of the silo, the change of groundwater flow used in this calculation case is relatively small compared to the *base case*. However, because of eventual new transport pathways after concrete structure failure, both sorption and the diffusive resistance in the engineered barriers in the silo are pessimistically disregarded. Consequently, the remaining radionuclide activity is assumed to be distributed in the full network of pores in the silo, with releases linked to the turnover time of the flow of groundwater through the silo. This is a pessimistic assumption because radionuclides can be expected to sorb (both onto the cement in the damaged concrete as well as to the bentonite) and the repository's pore network cannot be expected to be fully interconnected, even after an earthquake.

The conditions in the geosphere are assumed to be adversely affected by an earthquake of sufficient magnitude to damage the silo concrete structure, but such effects on the geosphere have not been quantified here. Therefore, it is pessimistically assumed that there is no transport retention in the geosphere in this calculation case. Because of this simplification, and since the activity release into the till in the discharge area (from which groundwater from a dug well is extracted) is highly overestimated, exposure from a drilled well downstream the repository is not considered in this calculation case.

Calculations over the entire assessment period are made for single earthquakes, and the calculations are repeated for earthquakes occurring every 100th year from repository closure up until the end of the assessment period. Due to the large number of simulations, fully probabilistic calculations are not deemed feasible considering the available computational capacity. Instead, a combination of a deterministic approach using best-estimate values and a probabilistic approach using random samples based on PDFs is applied in this calculation case. Specifically, deterministic simulations using best-estimates are used for all radionuclides, except Ni-59, for which fully probabilistic simulations are performed. The reason for excluding other radionuclides from the probabilistic calculations is either that (i) the dose from the deterministic simulations is similar to the mean of the probabilistic simulations; (ii) dose consequences occur only in the beginning of the assessment period (e.g. shorter-lived Mo-93 and C-14-org), when the cumulative probability of an earthquake event is very low (Figure 8-6, lower panel); (iii) no, or very little, activity is disposed in the silo (Ca-41 and uranium isotopes) or; (iv) the initial activity in the silo is not retained in the *base case* (I-129, see e.g. Figure 7-11) implying that the potential increase in dose consequence from an earthquake is expected to be limited, see the **Radionuclide transport report**, Section 7.5.2 for further details.

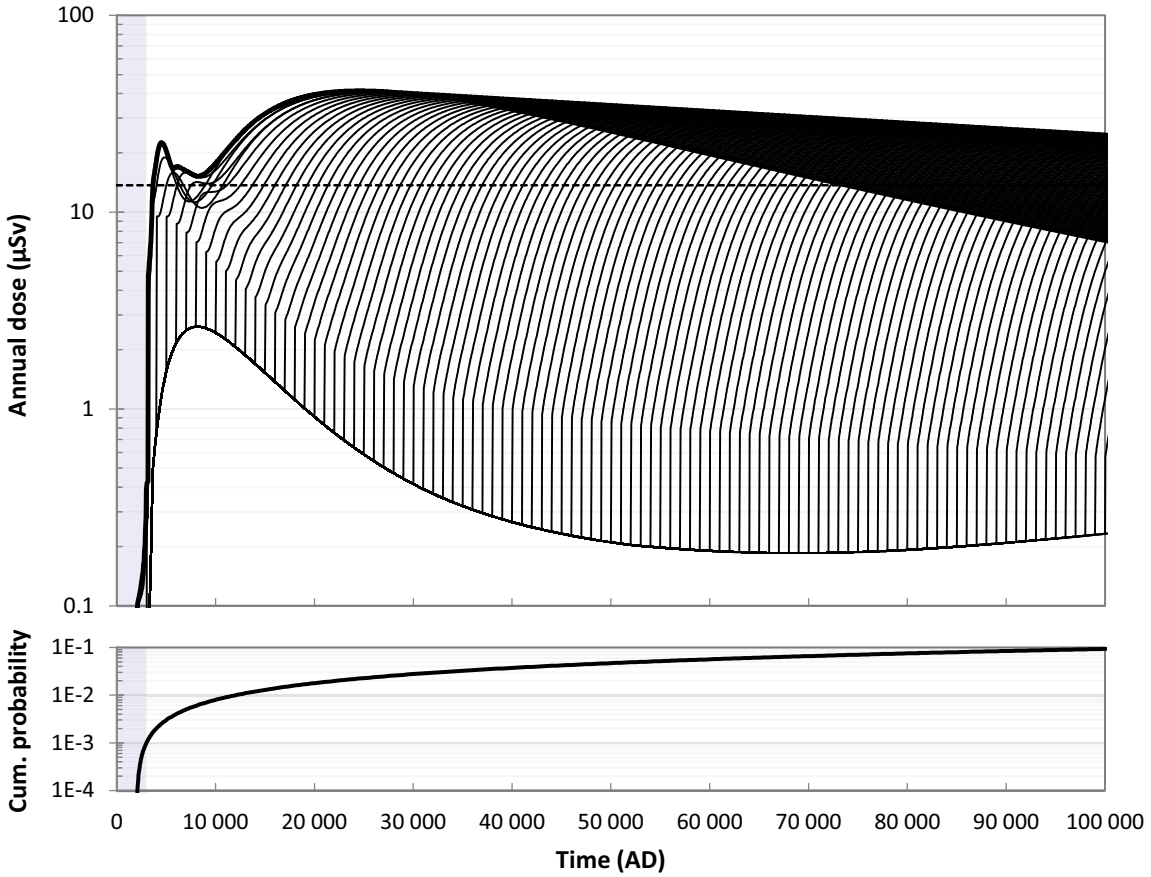

Figure 8-6. *Upper panel: annual dose (µSv) to the most exposed group from releases from the silo calculated for earthquakes occurring at times separated by intervals of one thousand years (thin lines) and the highest annual dose from all calculations (upper thick line) in the earthquake calculation case. The lower line shows the dose from the silo in the absence of earthquakes during the assessment period. The annual dose corresponding to the regulatory risk criterion (14 µSv) is indicated by the black dashed line. Lower panel: cumulative probability of an earthquake event. The submerged period is illustrated by the blue shading in both panels.*

8.6.3 Radionuclide transport and dose

The annual dose to the most exposed group from releases from the silo is presented in Figure 8-6 for several calculations. The difference between the calculations is the timing of the earthquake. For all evaluated earthquakes, the highest annual dose is shown in the figure for each point in time, irrespective of when the earthquake occurs. The calculation with the highest maximum dose (41 μSv), at 24 500 AD, is caused by an earthquake occurring at repository closure. After reaching its maximum, the dose gradually decreases and is approximately halved by the end of the assessment period. The delayed dose maximum with respect to the earthquake is primarily caused by the time it takes for Ni-59 to break through the bottom till layer in the surface system and thus become available for exposure after draining the mire (**Radionuclide transport report**, Section 7.5.3). The elevated doses from Ni-59 in this calculation case are explained by the rapid release of the remaining inventory[43] due to the assumed lack of sorption in the silo after an earthquake.

8.6.4 Concluding remarks

This scenario evaluates radiological consequences of an earthquake which is pessimistically assumed to (i) damage the concrete structure in the silo which also loses its capability to sorb radionuclides and to (ii) eliminate retention in the geosphere. These effects result in deviations from the main scenario of the safety functions *sorb radionuclides* in the engineered barriers and *provide favourable hydraulic conditions* in the geosphere. The maximum dose from the silo in this scenario is almost 20 times higher than the corresponding maximum dose in the main scenario. However, due to the pessimistic assumptions in this scenario, radiological consequences of an earthquake are overestimated. This scenario is therefore considered to provide an upper-bound estimate of the dose resulting from an earthquake rather than a realistic assessment. Furthermore, for most of the assessment period, the cumulative probability of an earthquake is lower than the probability assigned for the other less probable scenarios (see Figure 8-6, lower panel). This reduces the impact on the risk from this scenario, see further details in Chapter 10.

8.7 Less probable scenarios – handling of climate cases and scenario combinations

In the method for selecting less probable scenarios, the effects of uncertainties that have not been addressed within the main scenario are analysed with respect to the status of each safety function regarding the initial state, internal processes, and external conditions. In principle, the uncertainties that lead to the definition of the less probable scenarios could occur in different combinations in a single scenario. Moreover, three different climate cases are analysed in the main scenario whereas only the calculation case based on present-day climate (*base case*) is applied in the less probable scenarios. In this section the handling of the other two climate cases in relation to the less probable scenarios and possible combinations of less probable scenarios are discussed.

8.7.1 Handling of climate cases in relation to less probable scenarios

In the general advice to SSMFS 2008:37 it is recommended that the risk is evaluated for each climate case. The main scenario shows that the *base case* results in the highest maximum dose (Sections 7.4.7, 7.5.5, and 7.6.5) and it is therefore also likely that the present-day climate case gives the highest maximum doses for the less probable scenarios. However, it is not obvious that this is the case and therefore supporting calculations have been performed. In Table 8-4, the effect of the cold and warm climate cases on the maximum doses for each less probable scenario are discussed. The cold climate case yields lower doses for all scenarios compared to the present-day climate case. The warm climate case results in lower doses for the main scenario and the *alternative concrete evolution scenario*. For the *earthquake* and *high concentration of complexing agents scenarios*, the warm climate case leads to a marginal increase in maximum doses. It is thus expected that the *base case* (present-day) climate is limiting with respect to the risk criterion. This is further discussed in the assessment of risk (Section 10.4).

[43] > 99 % of the Ni-59 activity is retained or has decayed in the silo in the *base case*.

Table 8-4. Combinations of climate cases and less probable scenarios and their effect on maximum doses.

Scenario	Cold climate case	Warm climate case
Glaciation scenario	Mutually exclusive	Mutually exclusive
High concentrations of complexing agents scenario	There are only marginal differences affecting the dose dominating radionuclide (Ni-59) at late times in the *cold climate calculation case* in the main scenario and these occur long after the maximum dose. Therefore, combining the *high concentrations of complexing agents scenario* with cold climate yields lower doses than the *base case* climate.	Both the *warm climate calculation case* in the main scenario and the less probable scenario assuming high concentrations of complexing agents lead to higher doses at late times than the *base case* in the main scenario. A second peak occurs at late time that is dominated by Ni-59. The second peak is marginally higher than the first.
Alternative concrete evolution scenario	The *cold climate calculation case* in the main scenario only marginally differs from the *base case* at late times in the assessment period and results in lower doses. The doses resulting from the *cold climate calculation case* in the main scenario are identical with the *base case* before the first onset of periglacial conditions at 61 000 AD, i.e. long after the maximum dose has occurred.	The *warm climate calculation case* gives a lower maximum dose than the *base case* if combined with the *alternative concrete evolution scenario*. The maximum dose in the *alternative concrete evolution scenario* is dominated by the same radionuclides as the *base case* and therefore also the effect on the peak is similar.
Earthquake scenario	There are only marginal differences affecting the dose-dominating radionuclide (Ni-59) at late times in the *cold climate calculation case* in the main scenario and these occur long after the maximum dose. Therefore, combining the *earthquake scenario* with cold climate yields lower doses than with the *base case* climate.	The difference between the *warm climate calculation case* and the *base case* in the main scenario for the dose-dominating radionuclide (Ni-59 in the *earthquake scenario*) is marginal. Given the pessimistic handling of Ni-59 in the *earthquake scenario*, in which retardation in the repository and in the geosphere is omitted, the difference between the base-case climate and the warm climate is marginal.

8.7.2 Combinations of less probable scenarios

In the following, all possible combinations of less probable scenarios are discussed to show that none of them yield significantly higher doses than the less probable scenarios by themselves. The probability of the scenario combinations is the product of the probabilities of the less probable scenarios assuming their independence, i.e. 1 % or lower (*earthquake scenario*). Thus, the contribution to the total risk becomes very small unless the combinations yield significantly higher doses than the individual less probable scenarios.

Glaciation scenario and alternative concrete evolution scenario

A combination of the *glaciation* and *alternative concrete evolution scenarios* is identical to the latter until the onset of glaciation. Looking at the dose resulting in the *alternative concrete evolution scenario* after the point in time when the glaciation occurs in the *glaciation scenario* it can be noted that the dose is similar to the *base case*. It can also be noted that the concrete structures are already completely degraded at onset of the glaciation at around 60 000 AD. Due to the increased early time releases of Ni-59 in comparison to the *base case*, which is a consequence of the alternative concrete evolution, the second dose peak that arises after the glaciation and that is dominated by Ni-59 becomes smaller than in the *glaciation scenario* due to depletion. Thus, the maximum dose resulting from the combination of these scenarios will be equal to the maximum dose for the alternative concrete evolution scenario.

Glaciation scenario and earthquake scenario

The *earthquake scenario* is very pessimistic, assuming no sorption in the silo after an earthquake. Combining this handling with additional degradation resulting from the glaciation is judged to be overly pessimistic. A combination of the assumptions of the earthquake and glaciation scenario would, however, most likely not lead to higher doses than the earthquake scenario, since the amount of Ni-59 that dominates the late dose peak in the glaciation scenario has diminished in the silo at the onset of glaciation due to the releases at earlier times, as a consequence of the neglected sorption. After a glaciation, post-glacial earthquakes may occur. However, in the analysis the glaciation already has led to the degradation of the barriers and the increased probability of an earthquake due to the glaciation would not have any impact on the analysis.

Glaciation scenario and high concentrations of complexing agents scenario

The *high concentrations of complexing agents scenario* implies increased releases of Ni-59 in comparison to the *base case*. This leads to a partial depletion of Ni-59 in the repository before glaciation occurs and therefore a less pronounced, Ni-59 dominated, dose peak after glaciation. The maximum dose is equal to the dose for the complexing agents scenario, which in turn is equal to the *base case*.

Alternative concrete evolution scenario and earthquake scenario

The *earthquake scenario* is very pessimistic, assuming no sorption in the silo after an earthquake. Combining this handling with additional increased concrete degradation is judged to be pessimistic. In any case, the maximum dose should be controlled by the earthquake's effect on the silo, which yields the maximum dose in the latter part of the assessment period, when the doses due to releases from the other waste vaults are relatively small in the alternative concrete evolution scenario. The maximum dose of a combined scenario is therefore unlikely to give a significantly higher maximum dose than the *earthquake scenario*.

Alternative concrete evolution scenario and high concentrations of complexing agents scenario

The combination of the *alternative concrete evolution scenario* and the *high concentrations of complexing agents scenario* results in a maximum dose that equals that of the *alternative concrete evolution scenario*. The combination leads to a higher second dose peak dominated by Ni-59 in comparison to the *alternative concrete evolution scenario*, in a similar way to the *high concentrations of complexing agents scenario*. However, this dose peak is lower than the maximum dose dominated by Mo-93, which is equal to the maximum dose in the *alternative concrete evolution scenario*.

Earthquake scenario and high concentrations of complexing agents scenario

The earthquake scenario pessimistically assumes that the sorption within the silo is neglected from the time when the earthquake occurs. Therefore, a combination with high concentrations of complexing agents will have no effect on the maximum doses.

Conclusion regarding combination of less probable scenarios

The discussion in this section shows that none of the possible combinations of less probable scenarios is likely to yield significantly higher doses than the less probable scenarios themselves. Given that the probability of the combinations assuming independence is 1 % or lower, it can be concluded that combinations of the less probable scenarios do not yield any significant contributions to the risk calculations. Scenario combinations are therefore not further considered.

9 Residual scenarios

9.1 Introduction

Three different categories of scenarios are included in the present safety assessment: the main scenario, less probable scenarios and residual scenarios (Section 2.6.8). The main scenario is addressed in Chapter 7 and takes into account the most probable changes in the repository and its environs. Less probable scenarios are presented in Chapter 8, which evaluate scenario uncertainties related to alternative evolutions of the repository, or uncertainties in the specified initial state or external conditions, that are not evaluated within the framework of the main scenario.

This chapter addresses the residual scenarios. Primarily, residual scenarios aim to illustrate the significance of individual barriers and barrier functions and how they contribute to the protective capability of the repository. They are also selected to contribute to the discussion of the robustness of the repository regarding the protection of human health. To this end, residual scenarios may include hypothetical assumptions that are associated with a low degree of realism or events with exceptionally low likelihood of occurrence. The descriptions of the calculation cases for the scenarios focus on the differences from the main scenario. Each scenario is analysed in terms of activity releases and doses to humans; dose-rates to non-human biota are not evaluated. Residual scenarios comprise sequences of events and conditions that are selected and studied independently of probabilities and doses to humans are thus not propagated to the assessment of risk.

The general advice to the regulations gives recommendations on how to select the residual scenarios; this is further described in Section 9.2 together with the approach for selecting the scenarios. In Sections 9.3–9.11, the residual scenarios are described and analysed.

9.2 Selection of residual scenarios

The general advice to SSMFS 2008:21 recommends that residual scenarios should be selected to illustrate the significance of individual barriers and barrier functions, detriment to humans intruding into the repository and the consequences of an unsealed repository that is not monitored.

The approach for selecting residual scenarios that illustrate the significance of individual barriers and barrier functions is based on the safety functions that are defined in Chapter 5. In Table 5-1, the safety functions are grouped into the categories waste form and waste packaging, engineered barriers and repository environs. These are used as a basis for selecting residual scenarios.

For the safety function *limit quantity of activity* that is related to the waste form and packaging, a scenario is selected to illustrate the effect of changes in the radionuclide inventory. To obtain calculation cases that are credible, alternative radionuclide inventories are estimated from a selection of operational changes at the Swedish nuclear power plants that do not necessarily comply with the current licensing conditions given for SFR. The selected conditions are related to extended operation of reactors, increased fuel-damage frequency and extended use of molybdenum-alloy fuel spacers (Table 9-1).

For the engineered barriers, residual scenarios are selected that relate to physical and chemical state of the repository and relevant safety functions. A complete loss of the engineered barrier functions is postulated, including a calculation case with loss of sorption in the repository and a calculation case with loss of hydraulic barriers in the repository. Oxidising conditions in the repository are analysed and, furthermore, hypothetical less favourable initial states of the engineered barriers are postulated in the calculation cases *initial concrete cracks* and *unrepaired 1BMA* (Table 9-1).

For the geosphere, the loss of the safety function *provide favourable chemical conditions* is analysed by postulating oxidising conditions, which is included in the *oxidising conditions scenario*. Moreover, the role of retardation in the geosphere is evaluated with the *no sorption in the geosphere calculation case* and the *no transport retention in the geosphere calculation case* (Table 9-1).

The effect of permafrost occurring at a relatively early time in the assessment period is analysed in the *hypothetical permafrost scenario*. This includes a calculation case that evaluates effects of permafrost on the engineered barriers (Table 9-1).

A scenario stipulating an unsealed repository is selected and analysed. Furthermore, a set of scenarios is selected to evaluate the impact of a broad range of potential future human actions (FHAs). This set includes two scenarios related to human actions directly intruding into the repository (the *drilling into the repository scenario* and the *intrusion well scenario*) and two scenarios related to human actions not leading to direct intrusion (the *water management scenario* and the *underground constructions scenario*) (Table 9-1).

Table 9-1. Residual scenarios and associated calculation cases.

Scenario		Calculation case
Residual scenarios	**Hypothetical early permafrost**	No effect on engineered barriers [a] Effect on engineered barriers
	Loss of engineered barrier function	No sorption in the repository No hydraulic barriers in the repository
	Loss of geosphere barrier function	No sorption in the geosphere No transport retention in the geosphere
	Alternative radionuclide inventory	Extended operation of reactors Increased fuel damage frequency Extended use of molybdenum-alloy fuel spacers
	Oxidising conditions	Oxidising conditions
	Initial concrete cracks	Initial concrete cracks
	Unrepaired 1BMA	Unrepaired 1BMA
	Unsealed repository	Unsealed repository
	Drilling into the repository [b]	Drilling event Construction on drilling detritus landfill Cultivation on drilling detritus landfill
	Intrusion well [b]	Intrusion well
	Water management [b]	Construction of a water impoundment
	Underground constructions [b]	Rock cavern in the close vicinity of the repository Mine in the vicinity of the repository

[a] Described in the **Radionuclide transport report**.

[b] FHA scenarios.

9.3 Hypothetical early permafrost scenario

9.3.1 General description

The aim of the *hypothetical early permafrost scenario* is to illustrate the significance of individual barriers and barrier functions under the hypothetical assumption of permafrost development and freezing of engineered barrier structures within the first 50 000 years after closure. To this end, the scenario illustrates the significance of the safety function *limit advective transport* by considering the effect of freezing of the engineered barriers.

This scenario is reminiscent of the early periglacial variant of the main scenario in the SR-PSU. However, owing to its very low likelihood of occurrence (**Climate report**, Section 4.3) and its demonstrated low impact on annual dose in the SR-PSU (SKB TR-14-01, Brandefelt et al. 2016, Näslund et al. 2017a, b), an early period of permafrost development is analysed in a residual scenario rather than in the main scenario in the present safety assessment.

The development of external conditions is described by the hypothetical early permafrost climate case (**Climate report**, Section 5.4.1). The timing and duration of the early periglacial period in this climate case are inferred from the SR-PSU supplementary study of Näslund et al. (2017a). Thus, the evolution of climate domains is identical to the *base case* with the exception of a hypothetical periglacial period between 12 000 AD and 17 000 AD (Figure 9-1).[44]

The potential effects of a hypothetical early permafrost period on the engineered barriers include:

- Freezing of the concrete pore water resulting in a complete physical degradation of the structural concrete in the repository.
- Formation of an ice-lens in the silo bentonite, causing damage that lasts throughout the subsequent temperate period.

Both of these effects are evaluated in *effect on engineered barriers calculation case*, described in detail in the **Radionuclide transport report**, Section 8.2. A summary of the calculation case is presented in the following subsections together with the key results.

This scenario also includes an additional calculation, the *no effect on engineered barriers calculation case*, which is described only in the **Radionuclide transport report**, Section 8.2. This calculation case is identical to the *cold climate calculation case* of the main scenario (Section 7.6), apart from an earlier occurrence of periglacial conditions. Thus, the *no effect on engineered barriers calculation case* is not designed to illustrate how individual barriers and barrier functions contribute to the protective capability of the repository, but rather to support the analysis of periglacial conditions in the safety assessment, and it is therefore not further presented in this report.

9.3.2 Effect on engineered barriers calculation case

Description of the calculation case

This calculation case is evaluated in two variants, *frozen concrete* and *bentonite degradation*. In both variants, the handling in the geosphere and biosphere are the same as in the *continuous permafrost* variant of the *cold climate calculation case*. The handling in the near-field models is summarised below.

Frozen concrete – Following Näslund et al. (2017a), the concrete barriers are assumed to transition to a completely degraded state (i.e. hydraulic conductivity is $K = 10^{-3}$ m/s; see Figure 7-6) due to freezing at the beginning of the periglacial period (12 000 AD). As the concrete degrades, the diffusion-available porosity of the concrete barrier and radionuclide diffusivities change. The hydraulic conductivity, porosity and diffusivity values are from this point in time until the end of the assessment period assumed to be identical to those of the *base case* for the period 52 000–102 000 AD. Chemical degradation of cementitious materials, and thus changes in sorption coefficients, are also adopted from Näslund et al. (2017a), see the **Radionuclide transport report**, Table 8-1.

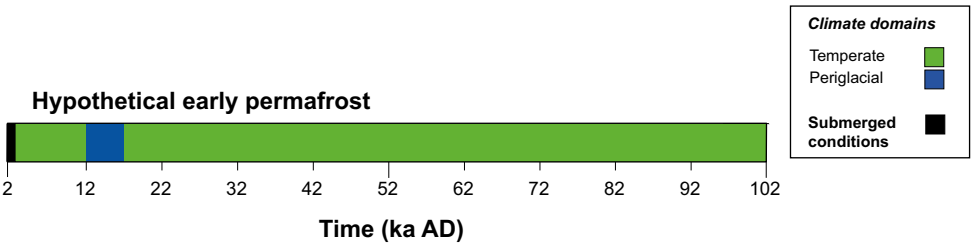

Figure 9-1. *Succession of climate domains in the hypothetical early permafrost scenario*

[44] The periglacial periods of the last 50 000 years of the assessment period in Näslund et al. (2017a), originally developed for the SR-PSU global warming climate case are, for simplicity, omitted in this scenario. Radiological consequences of periglacial periods within the last 50 000 years of the assessment period are analysed in the *cold climate calculation case* of the main scenario (Section 7.6).

Bentonite degradation – The hydraulic properties of the bentonite around the silo are assumed to deteriorate due to the formation of an ice-lens in the bentonite during the periglacial period, with the consequence of higher groundwater flow in the silo during a subsequent period of temperate climate conditions. A set of water flux parameters has been calculated specifically for the ice-lens case in the detailed modelling of the near-field hydrology (Abarca et al. 2020). In this variant, radionuclide release calculations are performed using these specific water fluxes for the silo. The other vaults are modelled as in the *continuous permafrost* variant of the *cold climate calculation case*.

Radionuclide transport and dose

The resulting maximum annual dose after the periglacial period is slightly lower in the *bentonite degradation* variant than in the *frozen concrete* variant (**Radionuclide transport report**, Section 8.2.3). Therefore, only the results from the *frozen concrete* variant are summarised in the following.

Similar to the *cold climate calculation case*, doses during periods of periglacial conditions are more than one order of magnitude below the doses in the *base case* at the corresponding time (Figure 9-2). The reason is mainly that hunting and gathering is the only possible land use during periglacial conditions and this generally results in lower doses than cultivation and well water usage (Section 7.6.4).

The enhanced degradation of the concrete barriers results in elevated doses for the entire post-periglacial temperate period compared with the *base case* (Figure 9-2). The highest dose during the post-periglacial temperate period is obtained a few thousand years after the periglacial period, when it is approximately 30 % higher than in the *base case* at the corresponding time. The highest dose during this period is, however, well below the maximum dose at about 7000 AD (same as in the *base case*; Figure 9-2). The radionuclides that contribute most to increased dose after the periglacial period in this calculation case are primarily Ca-41 and Ni-59 (Figure 9-2). These radionuclides dominate the dose in the *base case* after 20 000 AD (Figure 7-14) and this is partly a result of concrete degradation in that calculation case (Section 7.4.2). The enhanced concrete degradation in this calculation case leads to a higher accumulation of these radionuclides in the biosphere and, thus, to higher doses than in the *base case*.

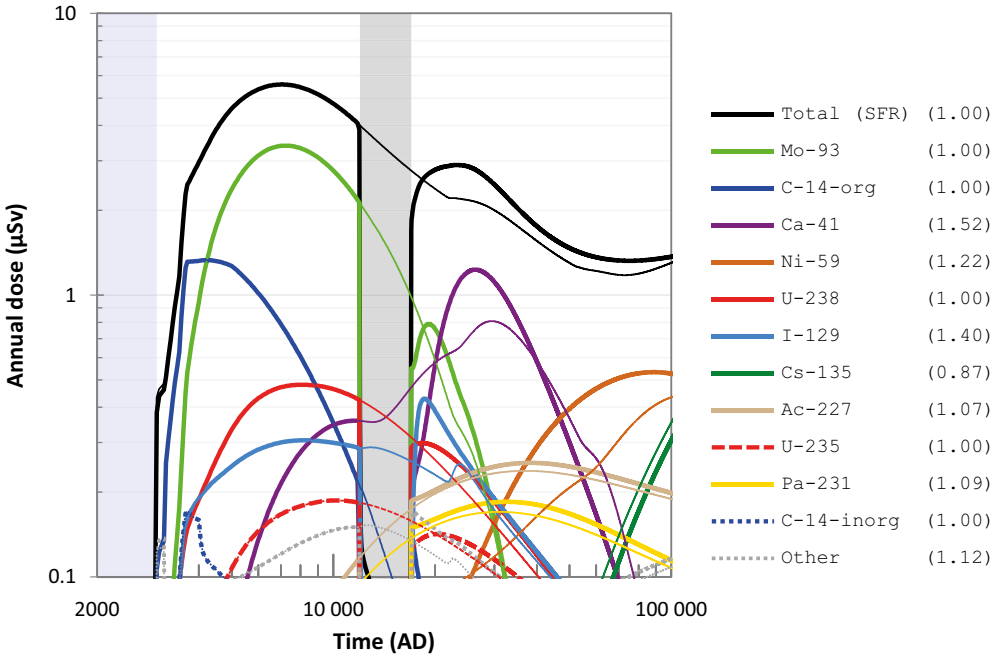

***Figure 9-2**. Annual dose (µSv) to the most exposed group (black lines), including radionuclide-specific contributions (coloured lines), in the frozen concrete variant of the effect on engineered barriers calculation case (thick lines) and the base case (thin lines). The combined contribution from radionuclides not shown is indicated by the grey dotted lines. The ratio between the maximum doses in the present calculation case and the base case are shown in parentheses in the key. The submerged and periglacial periods are illustrated by the blue and grey shading, respectively.*

9.3.3 Concluding remarks

This scenario illustrates the significance of a hypothetical freezing of the engineered barriers for the protective capability of the repository. The results show that freezing of engineered barriers early in the assessment does not result in higher maximum annual dose than in the main scenario. After the periglacial period, the doses do increase but only marginally. This confirms the results in the complementary study of Näslund et al. (2017a). In conclusion, freezing of engineered barriers early in the assessment period does not result in a deviation of the safety function *limit advective transport* to such extent that the protective capability of the repository is compromised.

9.4 Loss of engineered barrier function scenario

9.4.1 General description

The aim of the *loss of engineered barrier function scenario* is to illustrate how the engineered barriers contribute to the protective capability of the repository, i.e. to illustrate the significance of the safety functions *sorb radionuclides* and *limit advected transport* in the engineered barriers. To this end, two calculation cases are selected to analyse the importance of sorption and hydraulic barriers in the repository:

- No sorption in the repository calculation case.
- No hydraulic barriers in the repository calculation case.

A detailed description and analysis of the calculation cases is given in the **Radionuclide transport report**, Section 8.3. In the following, a summary of the calculation cases is presented together with the key results.

9.4.2 No sorption in the repository calculation case

Description of the calculation case

The *no sorption in the repository calculation case* is selected to illustrate the importance of sorption in the repository. This is done by setting sorption coefficients for all radionuclides in the near-field materials to zero. This change affects releases from all vaults except for the BLA vaults, for which sorption is not credited (Section 7.3.4). Other than setting the sorption coefficients to zero, all other input data used in radionuclide transport models are identical to the *base case*.

Radionuclide transport and dose

Assuming no sorption in the near-field results in a total annual dose that is significantly higher than in the *base case*, with the maximum dose being almost one order of magnitude higher than the maximum dose in the *base case* (Figure 9-3). Mo-93 contributes most to the dose during the first ~10 000 years in the *base case* and it has a significant contribution during this time in this calculation case too (**Radionuclide transport report**, Figure 8-6). However, Ni-59 contributes most to the total dose in this calculation case. This radionuclide displays strong sorption in the *base case*. Thus, neglecting sorption serves to increase annual releases from all waste vaults (except the BLA vaults) by several orders of magnitude compared with the *base case*, with the largest increase found in the silo (Figure 9-4). In summary, more than 90 % of the entire initial Ni-59 activity in the waste vaults is released in this calculation case, whereas the corresponding value is less than 5 % in the *base case*. Owing to its long half-life (101 000 years) and long residence times in the biosphere (Section 7.4.5), the dose from Ni-59 increases towards to the end of the assessment period. As a result, the total dose maximum occurs significantly later in this calculation case (~30 000 AD) than in the *base case* (~7000 AD).

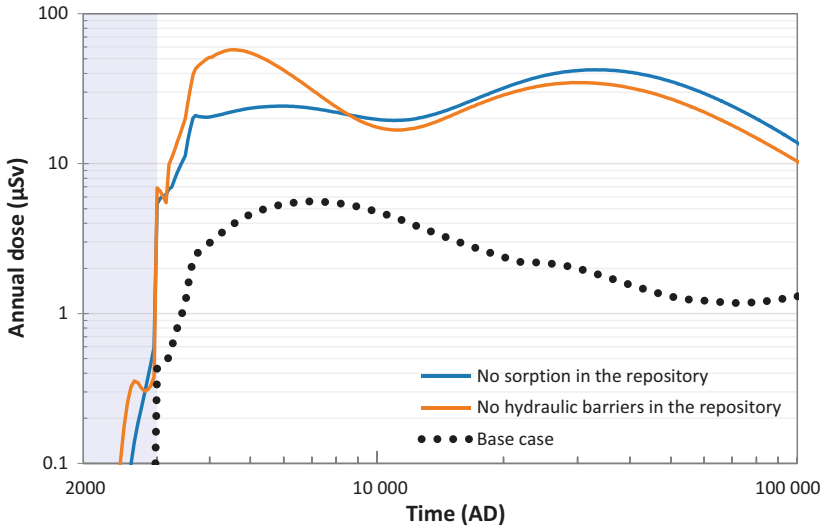

Figure 9-3. *Annual dose (µSv) to the most exposed group in the calculation cases in the loss of engineered barrier function scenario (coloured lines) and the base case (black dotted line). The submerged period is illustrated by the blue shading.*

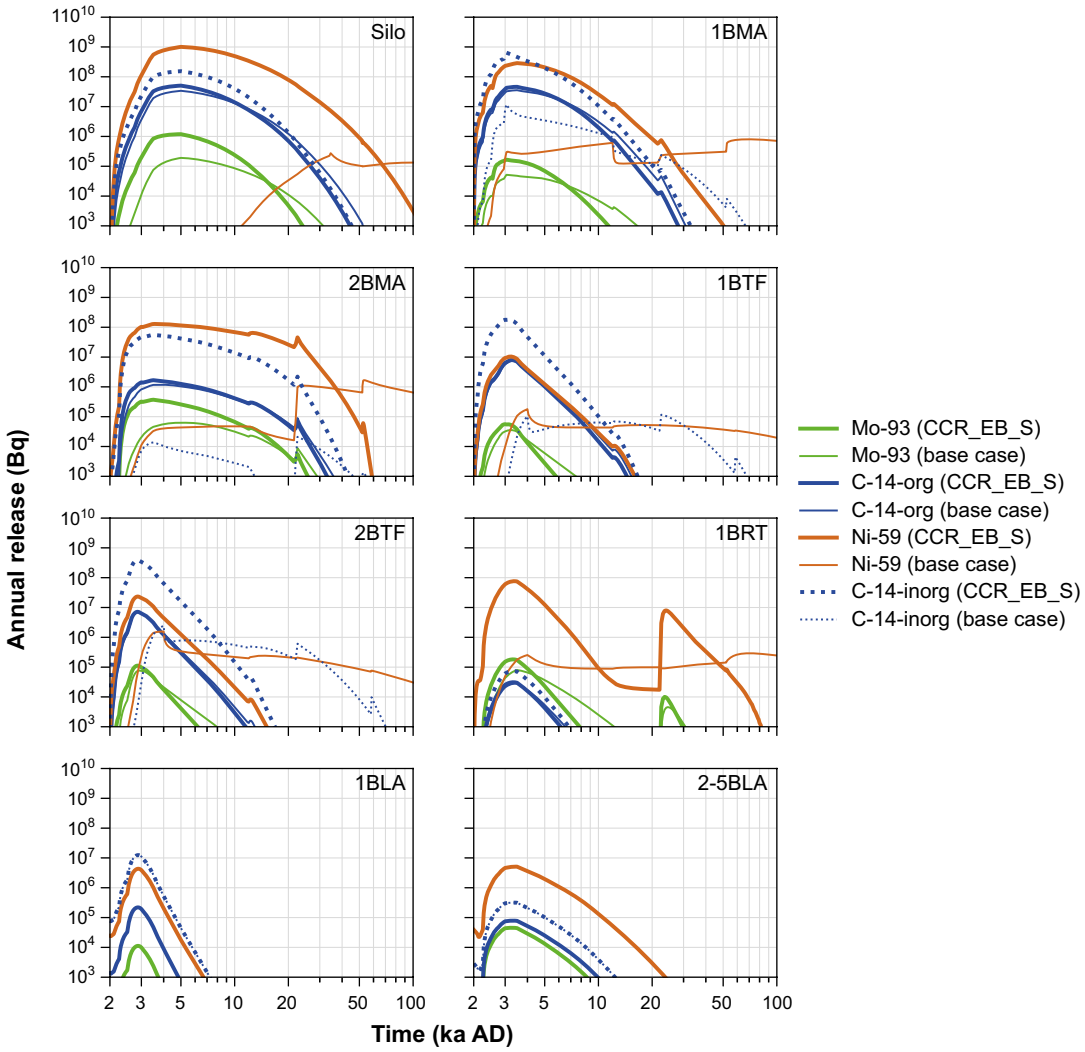

Figure 9-4. *Annual activity releases (Bq) from different waste vaults (panels) in the no sorption in the repository calculation case (thick lines) and the base case (thin lines). Note that for 2–5BLA the sum of the releases from all four vaults is shown.*

9.4.3 No hydraulic barriers in the repository calculation case

Description of the calculation case

The *no hydraulic barriers in the repository calculation case* is selected to illustrate the importance of the engineered barriers capability to limit the groundwater flow through the waste. In this calculation case, the near-field water-flow from the "no barriers" case in the hydrological calculations (Abarca et al. 2020) were used during the whole assessment period (see also Section 8.3.2). The groundwater flow is calculated assuming no resistance to flow due to concrete and bentonite barriers in the vault structures. Furthermore, the effect of tunnel closure plugs is neglected. Other conditions, including sorption, are the same as in the *base case*.

Radionuclide transport and dose

Assuming no hydraulic barriers in the near-field results in a total annual dose that is more than one order of magnitude higher than the maximum dose in the *base case* (Figure 9-3). As with the *no sorption in the repository calculation case*, there is a significant increase of the dose from Ni-59 in this calculation case too, particularly towards the end of the assessment period (**Radionuclide transport report**, Figure 8-9). In contrast to the *no sorption in the repository calculation case*, however, the contribution from Ni-59 to the total dose maximum is considerably reduced. The reason is that the release of Mo-93 from the waste vaults, especially the silo and 2BMA, is significantly increased in this calculation case (Figure 9-5). As a result, Mo-93 contributes most to the maximum dose and this occurs earlier than in the *no sorption in the repository calculation case* (Figure 9-3).

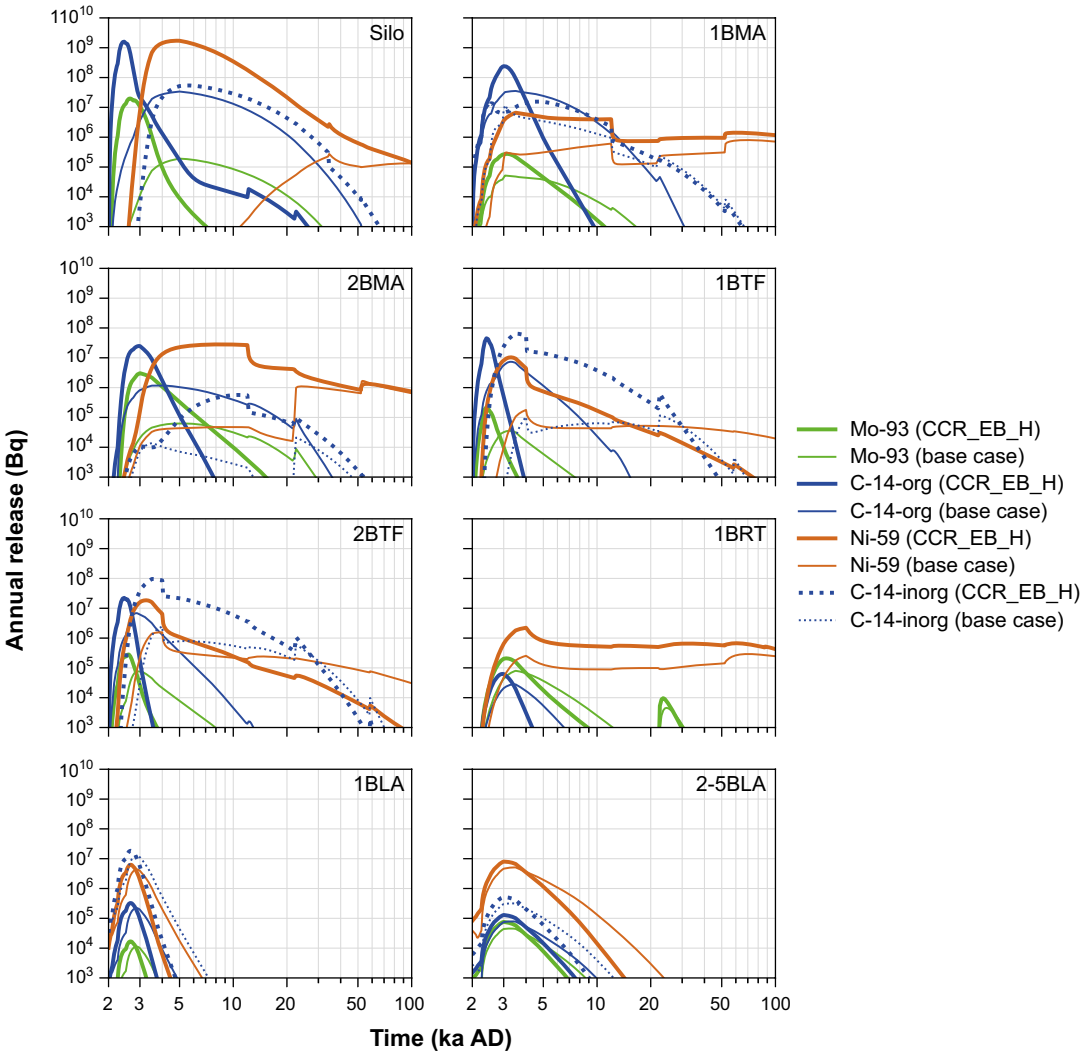

Figure 9-5. Annual activity releases (Bq) from different waste vaults (panels) in the no hydraulic barriers in the repository calculation case (thick lines) and the base case (thin lines). Note that for 2–5BLA the sum of the releases from all four vaults is shown in the figure.

It can also be noted that the calculations performed for the *construction of a water impoundment calculation case* (Section 9.11.2) relate to the capability of the repository and the bedrock to limit advective transport. Increasing the groundwater flow rates ten times with respect to the *base case*, in both the near-field and geosphere, leads to doses of about 20 μSv in that calculation case.

9.4.4 Concluding remarks

This scenario illustrates the significance of the engineered barriers for the protective capability of the repository. The calculations show that neglecting sorption and hydraulic barriers in the near-field, respectively, result in doses within the range 20–50 μSv for almost the entire assessment period. This illustrates the importance of the safety functions *sorb radionuclides* and *limit advective transport* for keeping the dose in the main scenario below the dose corresponding to the regulatory risk criterion (14 μSv).

9.5 Loss of geosphere barrier function scenario

9.5.1 General description

The aim of the *loss of geosphere barrier function scenario* is to illustrate how the geosphere contributes to the protective capability of the repository, i.e. to illustrate the significance of the safety functions *provide favourable hydraulic conditions* and *provide favourable chemical conditions* in the geosphere. To this end, two calculation cases are selected to analyse the importance of sorption and hydraulic conditions in the geosphere:

- No sorption in the bedrock calculation case.
- No transport retention in the geosphere calculation case.

A detailed description and analysis of the calculation cases is given in the **Radionuclide transport report**, Section 8.4. In the following, a summary of the calculation cases is presented together with the key results.

9.5.2 No sorption in the bedrock calculation case

Description of the calculation case

The assumption in this calculation case is that there is no sorption in the bedrock matrix, which is implemented by setting all sorption coefficients in the geosphere to zero. Aside from this change, the representation of the geosphere as well as the near-field and biosphere are identical to the *base case*.

Radionuclide transport and dose

The highest doses are, as in the *base case*, received by the drained-mire farmers (DM) throughout the terrestrial period, apart from the first few hundred years when garden-plot households (GP) with a drilled well receive higher doses (Figure 9-6). In general, total doses to the DM are somewhat higher without sorption in the geosphere than in the *base case* and the maximum total dose is about 75 % greater than in the *base case*. One reason for the relatively limited increase in total dose is that the radionuclides that dominate in the *base case* are almost unaffected by disregarding sorption in the bedrock matrix, as sorption was cautiously set to zero (C-14-org and Ca-41), close to zero (Mo-93) or relatively low (Ni-59) already in the *base case* (Section 7.4.3). Thus, the limited increase in dose relative to the *base case* could, to some extent, be attributed to cautious choices of sorption coefficients in that calculation case.

The uranium isotopes U-235 and U-238 contribute most to the increased maximum doses in this calculation case compared with the *base case*. Uranium sorbs strongly in the rock matrix in the *base case* (Section 7.4.5), resulting in geosphere releases of U-235 and U-238 increasing by more than one order of magnitude when sorption is omitted (**Radionuclide transport report**, Figure 8-14). This results in five to ten times higher doses from those uranium isotopes as well as the decay products of U-235: Pa-231 and Ac-227 (Figure 9-6). Furthermore, U-235 and U-238, together with Pu-238, Pu-239 and Am-241, also contribute to the exposure from the drilled well to GP during the initial terrestrial period. The dose due to exposure from a drilled well is higher than in the *base case*, but still lower than the maximum dose to DM.

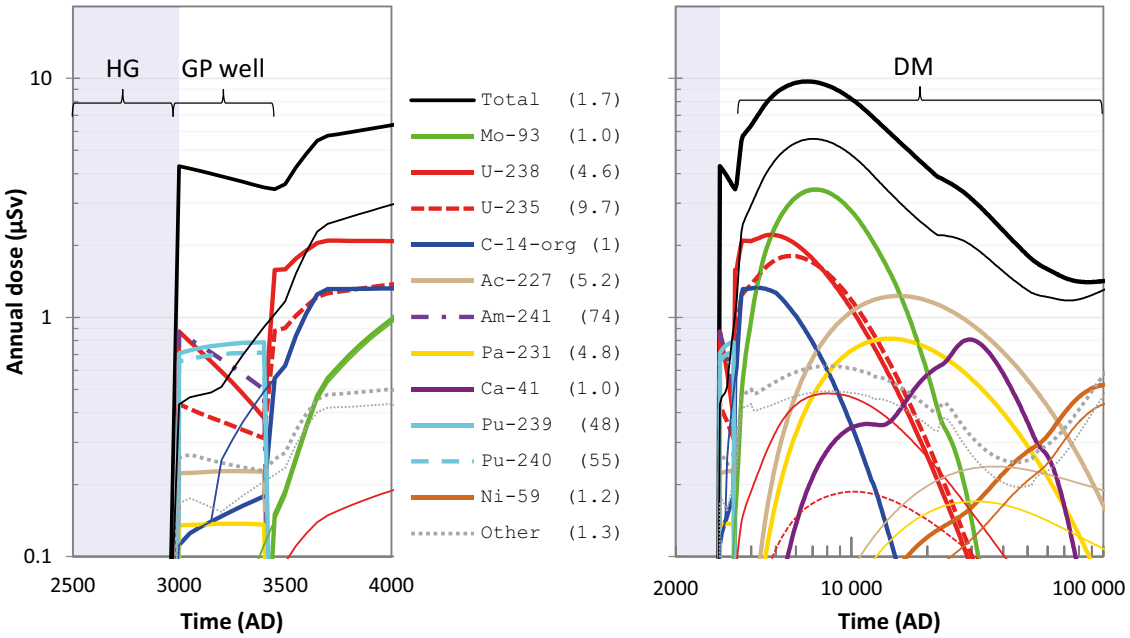

***Figure 9-6**. Annual dose (µSv) to the most exposed group (black lines), including radionuclide-specific contributions (coloured lines), in the no sorption in the geosphere calculation case (thick lines) and the base case (thin lines). The combined contribution from radionuclides not shown is indicated by the grey dotted lines. The ratio between the maximum doses in the present calculation case and the base case are shown in parentheses in the key. The submerged period is illustrated by the blue shading. The left panel shows annual doses between 2000 AD and 4000 AD (linear scale on the x-axis), whereas the right panel shows doses during the entire assessment period (log-scale on the x-axis). The most exposed groups during different periods of the simulation are indicated in the upper part of the panels; hunter-gatherers (HG), garden plot household with a drilled well (GP well) and drained-mire farmers (DM), see Section 7.3.6.*

9.5.3 No transport retention in the bedrock calculation case

Description of the calculation case

In this calculation case, the retention in the bedrock is disregarded by setting the transport time through the geosphere to zero, i.e. the geosphere release is identical to the near-field release. All other input data in the near-field and the biosphere models are identical with the *base case*, including the geosphere properties that affect the near-field, such as hydrological conditions and redox state.

Radionuclide transport and dose

The total dose and the radionuclides contributing significantly to the total dose in the *no transport retention in the geosphere calculation case* are almost identical to the *no sorption in the geosphere calculation case*. The reason is that the groundwater travel time through the geosphere is already limited in the *base case*. Median advective groundwater travel times through the geosphere are only a few years during fully terrestrial conditions after 3000 AD (**Radionuclide transport report**, Table 5-14). This time is too short to noticeably influence the release of any radionuclide that contributes to dose. Therefore, excluding the effects of sorption is functionally equivalent to eliminating transport retention.

9.5.4 Concluding remarks

This scenario illustrates the significance of the geosphere for the protective capability of the repository. The results show that neglecting sorption and retention in the geosphere, respectively, result in a maximum annual dose of ~10 µSv during the assessment period. Thus, the results indicate that geosphere barrier functions are less critical for the maximum dose than the engineered barriers evaluated in Section 9.4. In conclusion, the geosphere safety functions *provide favourable hydraulic conditions* and *provide favourable chemical conditions* contribute to the protective capability of the repository. However, even if the safety functions are not fulfilled, post-closure safety is unlikely to be compromised.

9.6 Alternative radionuclide inventory scenario

9.6.1 General description

The *alternative radionuclide inventory scenario* is selected to illustrate how the safety function *limit quantity of activity* contribute to the protective capability of the repository. To this end, three hypothetical radionuclide inventories that deviate from that used in the main scenario are considered. These are based on the assumptions that the operating time of the reactors at the nuclear power plants is prolonged, the frequency of fuel damage during the remaining period of operation increases and that the use of molybdenum alloy fuel spacers is extended, respectively. Thus, this scenario is analysed by the following three calculation cases:

- Extended operation of reactors calculation case.
- Increased fuel damage frequency calculation case.
- Extended use of molybdenum alloy fuel spacers calculation case.

It should be noted that the inventories used in these three cases are estimated from a selection of operational changes at the Swedish nuclear power plants, and do not necessarily comply with the licensing conditions given for SFR. A detailed description and analysis of the calculation cases is given in the **Radionuclide transport report**, Section 8.5. In the following, a summary of the calculation cases is presented together with the key results.

9.6.2 Extended operation of reactors calculation case

Description of the calculation case

The calculation case analysing the effects of prolonged operation of the remaining reactors from 60 to 80 years only affects future waste and sites (including Clab) that are still in operation (**Data report**, Section 4.5.1). The increase in waste volume that prolonged operation could give rise to is not considered. This is a cautious assumption as the amount of sorbing material in the waste is underestimated. Hence, only the change in radioactivity is evaluated in this alternative inventory. All other properties of the modelling are handled in the same way as in the *base case,* i.e. the extension of the operating time of the reactors is here not assumed to affect the time of repository closure.

Figure 9-7 shows the ratio of the inventory between this calculation case and the *base case* for affected radionuclides.

Radionuclide transport and dose

The radionuclide-specific doses, as well as the total dose, are higher than in the *base case* with an extended operation of the reactors (Figure 9-8). However, the increase of the maximum dose is relatively small, amounting to less than 20 % higher than in the *base case* for most radionuclides.

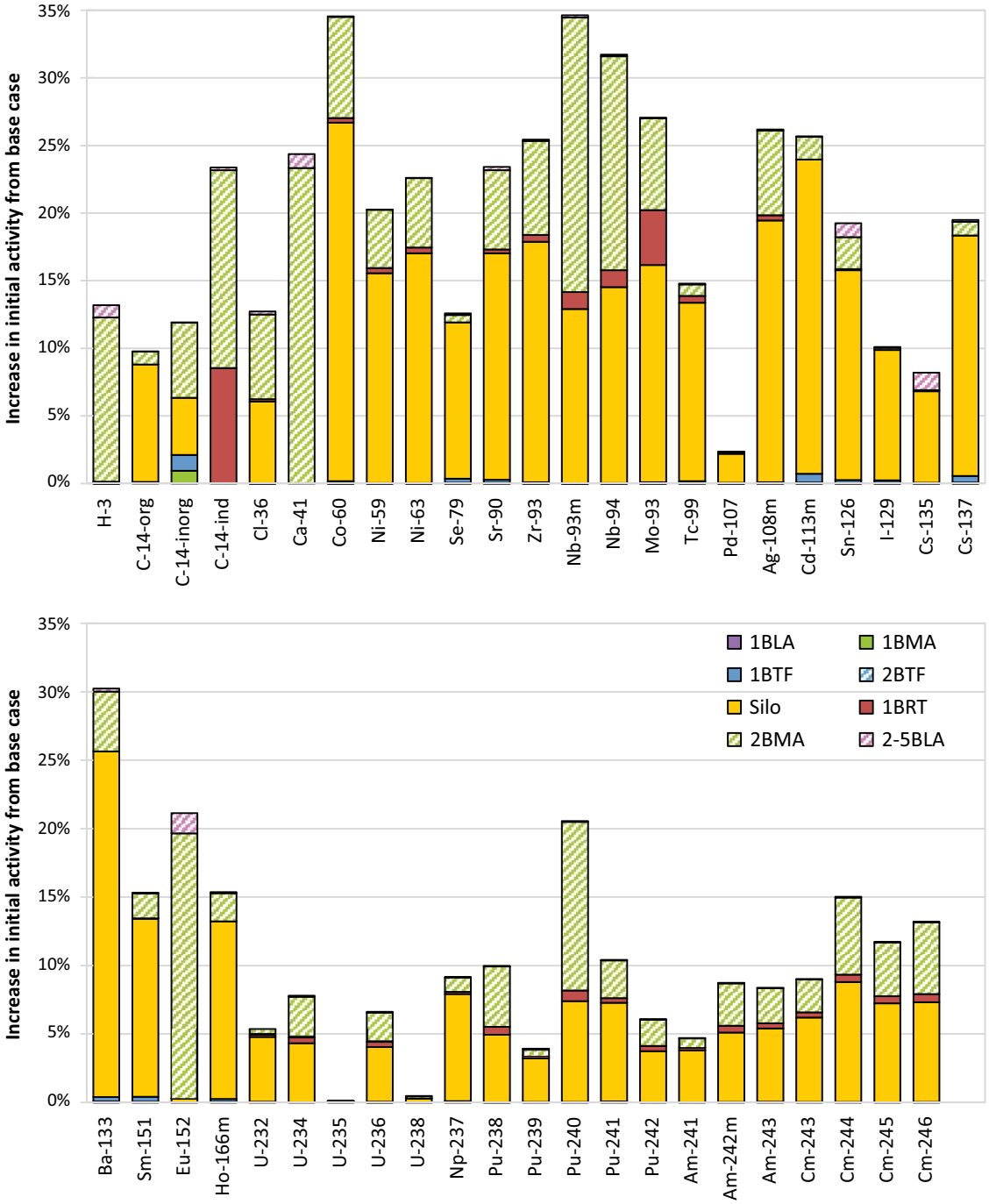

Figure 9-7. *Increase of the total initial radionuclide inventory in SFR in the extended operation of reactors calculation case compared with the base case.*

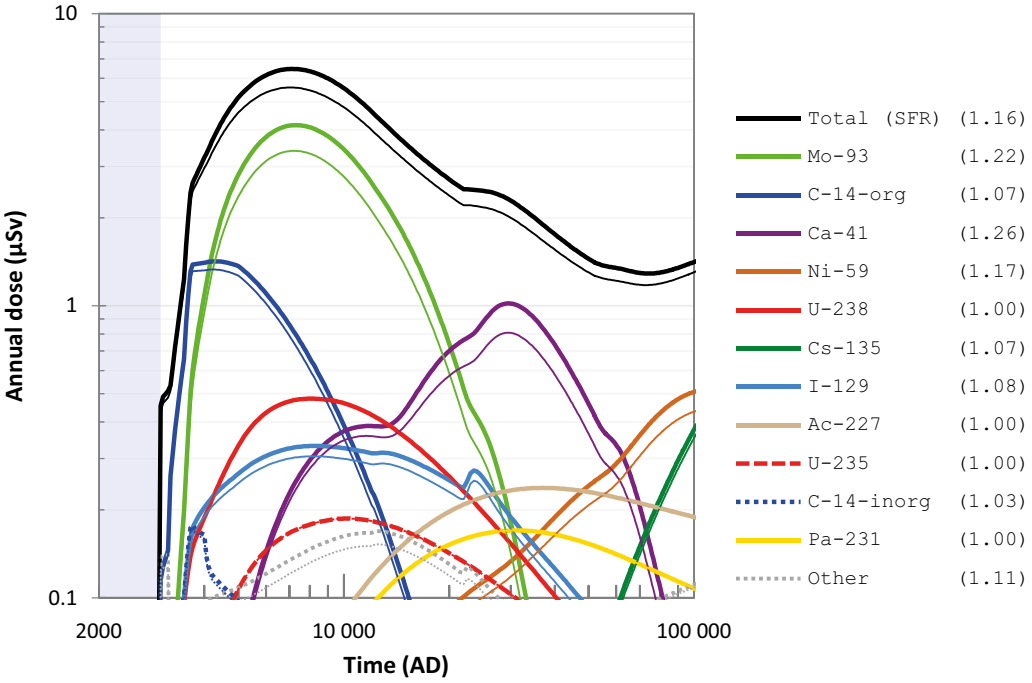

Figure 9-8. *Annual dose (µSv) to the most exposed group (black lines), including radionuclide-specific contributions (coloured lines), in the extended operation of reactors calculation case (thick lines) and the base case (thin lines). The combined contribution from radionuclides not shown is indicated by the grey dotted lines. The ratio between the maximum doses in the present calculation case and the base case are shown in parentheses in the key. The submerged period is illustrated by the blue shading.*

9.6.3 Increased fuel damage frequency calculation case

Description of the calculation case

The calculation case evaluates potential effects of increased fuel damage frequency during the remaining operation of the reactors, which affects only future waste and sites (including Clab) that are still in operation. Radionuclides related to fuel and fission in both forecast operational waste and decommissioning waste, most importantly I-129 and Cs-135, are assumed to be affected (**Data report**, Section 4.5.2). The assumption in this calculation case is that the activity of these radionuclides is increased by a factor of 10. The increase in activity is not applied to waste that has already been disposed in SFR.

Radionuclide transport and dose

The increased inventory of I-129 contribute most to the increased doses in this calculation case. The total maximum dose is however only about 15 % higher than in the *base case*, even with increased fuel damage frequency (Figure 9-9).

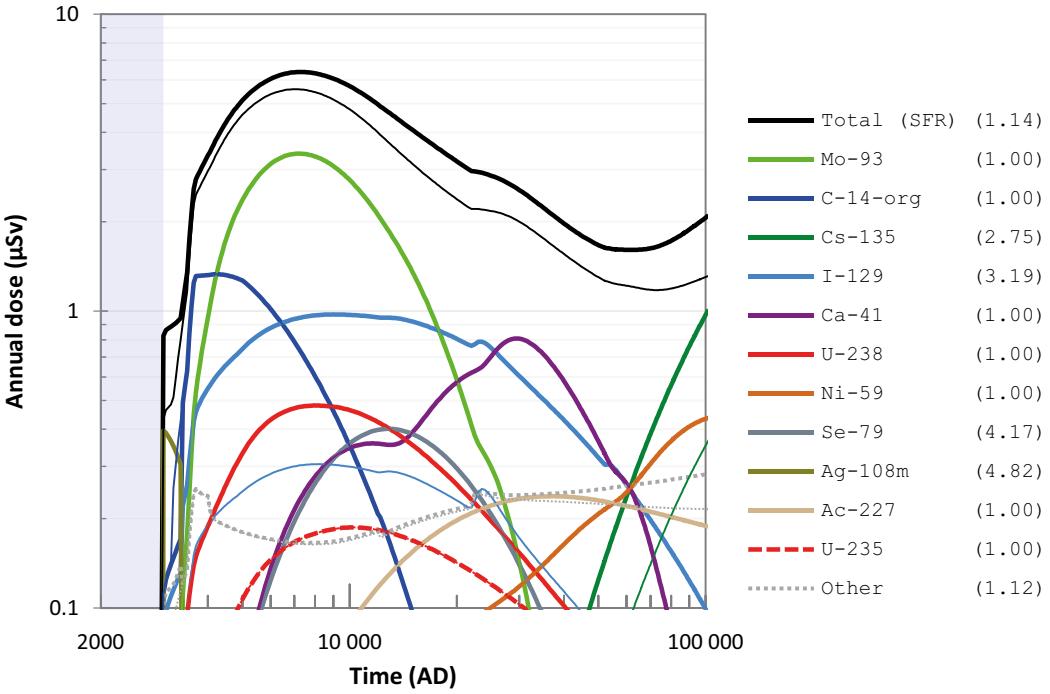

Figure 9-9. *Annual dose (µSv) to the most exposed group (black lines), including radionuclide-specific contributions (coloured lines), in the increased fuel damage frequency calculation case (thick lines) and the base case (thin lines). The combined contribution from radionuclides not shown is indicated by the grey dotted lines. The ratio between the maximum doses in the present calculation case and the base case are shown in parentheses in the key. The submerged period is illustrated by the blue shading.*

9.6.4 Extended use of molybdenum alloy fuel spacers calculation case

Description of the calculation case

This calculation case evaluates potential effects of extended use of molybdenum alloy fuel spacers. This only affects future waste from sites with BWRs still in operation, as well as Clab. The molybdenum activity of this waste is multiplied by a factor 10 (**Data report**, Section 4.5.3), resulting in a total inventory of Mo-93 in SFR that is approximately four times higher than in the *base case*.

Radionuclide transport and dose

The hypothetical increase of the Mo-93 inventory leads to a maximum dose from SFR that is almost three times higher than the corresponding dose in the *base case* (Figure 9-10). Apart from the effect of Mo-93, a small effect can also be seen for its decay product Nb-93m (included among "Other" in Figure 9-10), although the effect of this is insignificant for the total dose.

9.6.5 Concluding remarks

This scenario illustrates the potential effects of radionuclide inventories estimated for three unlikely changes in the operational conditions at the Swedish nuclear power plants. These conditions are that the operating times of the nuclear power plant reactors are extended by 20 years, that the fuel damage frequency during the remaining operation increases and that the period of use of molybdenum alloy fuel spacers is extended. All in all, the results from these calculations show that a fractional increase in the radionuclide inventory yields a similar fractional increase in the maximum dose. This illustrates the importance of fulfilling the safety function *limit quantity of activity* by accepting only certain kinds of waste in SFR and by regulating the quantity of the activity of different radionuclides in each waste vault.

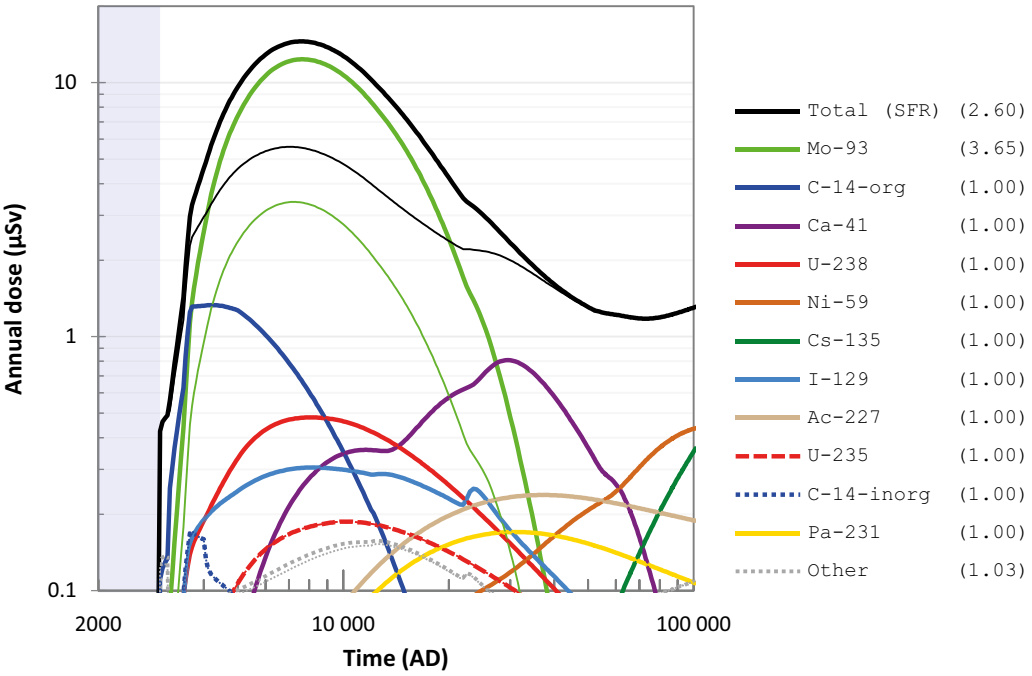

Figure 9-10. *Annual dose (µSv) to the most exposed group (black lines), including radionuclide-specific contributions (coloured lines), in the extended use of molybdenum alloy fuel spacers calculation case (thick lines) and the base case (thin lines). The combined contribution from radionuclides not shown is indicated by the grey dotted lines. The ratio between the maximum doses in the present calculation case and the base case are shown in parentheses in the key. The submerged period is illustrated by the blue shading.*

9.7 Oxidising conditions scenario

9.7.1 General description

The aim of the *oxidising conditions scenario* is to illustrate how redox conditions in the repository and the bedrock contribute to the protective capability of the repository. This scenario illustrates the significance of the safety functions *limit corrosion* in 1BRT, *sorb radionuclides* in the waste and engineered barriers, and *provide favourable chemical conditions* in the geosphere with the aid of the safety function indicator *redox potential*. In contrast to the main scenario, which considers reducing redox conditions for the entire assessment period (Sections 7.4.2 and 7.4.3), this scenario is based on the hypothetical assumption of oxidising conditions throughout the assessment period.

This scenario is evaluated with the *oxidising conditions calculation case*. A detailed description and analysis of the calculation case is given in the **Radionuclide transport report**, Section 8.6. In the following, a summary of the calculation case is presented together with the key results.

9.7.2 Oxidising conditions calculation case

Description of the calculation case

The modelling of sorption in the near-field and geosphere is analogous to the periods with oxidising conditions in the *glaciation calculation case* (Section 8.3.2). In addition, higher corrosion rates are applied in 1BRT in this calculation case. The long-term corrosion rate of carbon steel for oxidising, alkaline conditions is assumed to range between 1 and 100 µm/a (**Data report**, Table 5-12), which is three orders of magnitude greater than range for reducing, alkaline conditions that is applied at the start of the *base case* (Section 7.4.2). The evolution of both the physical and the chemical concrete degradation is assumed to be identical to those in the *base case* (Figures 7-6 and 7-7). Thus, at 22 000 AD, the pH in 1BRT decreases to 12.0 and, after this point, corrosion rates for near-neutral, oxidising conditions are pessimistically assumed (**Data report**, Table 5-11). This is a very high corrosion rate, but it has little impact since most of the 1BRT steel is already corroded before it is applied.

Except for these changes, the conditions in the near-field, the geosphere and the biosphere are handled as in the *base case*.

Radionuclide transport and dose

The results show that the maximum total annual dose roughly doubles compared with the *base case*, exceeding 10 µSv (Figure 9-11), if oxidising conditions are assumed in the near-field and geosphere. This is mainly due to the dose-dominant Mo-93. This radionuclide is not redox-sensitive but still exhibits increased releases in this calculation case, particularly its maximum release, due to the increased corrosion rate in 1BRT. Significant increases are also observed for U-235 and U-238, including decay products Pa-231 and Ac-227. These increases are explained mainly by their lower sorption due to oxidising conditions in the geosphere.

9.7.3 Concluding remarks

This scenario illustrates the significance of reducing redox conditions in the repository and the bedrock for the protective capability of the repository. The results show that changing the redox potential in the near-field and the geosphere throughout the assessment period results in a maximum dose exceeding 10 µSv. In conclusion, the safety functions *limit corrosion* in 1BRT, *sorb radionuclides* in the waste and engineered barriers, and *provide favourable chemical conditions* in the geosphere due to changes in the indicator *redox potential* contribute to the protective capability of the repository. However, even with the hypothetical assumption of prevailing oxidising conditions during the entire assessment period, post-closure safety is unlikely to be compromised.

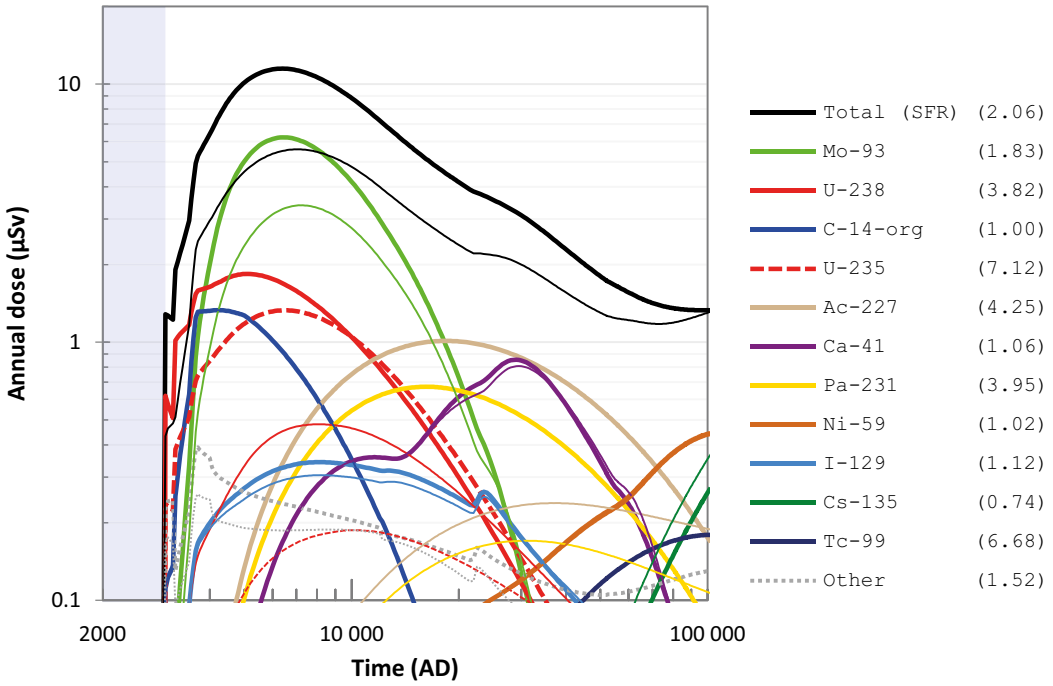

Figure 9-11. *Annual dose (µSv) to the most exposed group (black lines), including radionuclide-specific contributions (coloured lines), in the oxidising conditions calculation case (thick lines) and the base case (thin lines). The combined contribution from radionuclides not shown is indicated by the grey dotted lines. The ratio between the maximum doses in the present calculation case and the base case are shown in parentheses in the key. The submerged period is illustrated by the blue shading.*

9.8 Initial concrete cracks scenario

9.8.1 General description

The aim of the *initial concrete cracks scenario* is to illustrate how an absence of cracks in the concrete barriers contributes to the protective capability of the repository, i.e. to illustrate the significance of the safety functions *limit advective transport* and *sorb radionuclide* in the engineered concrete barriers of the silo, 1–2BMA and the concrete tanks in the 1–2BTF. This scenario is included as a complement to the *alternative concrete evolution scenario* (Section 8.5). However, in contrast to that scenario, this scenario is based on the hypothetical assumption that cracks exist in the concrete already at the initial state, corresponding to the conditions in the severely degraded physical degradation state (Section 7.4.2).

This scenario is evaluated with the *initial concrete cracks calculation case*. A detailed description and analysis of the calculation case is given in the **Radionuclide transport report**, Section 8.7. In the following, a summary of the calculation case is presented together with the key results.

9.8.2 Initial concrete cracks calculation case

Description of the calculation case

The concrete structures are assumed to be in the severely degraded physical degradation state (hydraulic conductivity of $K = 10^{-5}$ m/s, see Section 7.4.2) at initial state. As in the *base case,* the hydraulic conductivity of the main concrete barrier increases to 10^{-3} m/s at 52 000 AD for the silo and 1–2BMA and at 12 000 AD for 1–2BTF. Moreover, as in the *base case*, sorption is omitted during advective transport through the cracked concrete barriers. The calculation case does not affect 1BRT and 1–5BLA as 1BRT also has initial cracks in the *base case* and 1–5BLA have no credited concrete barriers.

This is implemented in the model by adding advective transfer directly from the waste domain to the gravel backfill without taking any sorption in the concrete structure into account.

Radionuclide transport and dose

The results from this calculation case largely confirm the results from the *alternative concrete degradation calculation case* (Section 8.5.3). Thus, in this calculation case, the maximum annual dose throughout the assessment period is also about 50 % higher than in the *base case*, mainly due to elevated releases of Mo-93 from 2BMA (**Radionuclide transport report**, Section 8.7.3).

9.8.3 Concluding remarks

This scenario illustrates the significance of cracks in the concrete structures for the protective capability of the repository. The similarity in the results between this scenario and the *alternative concrete evolution scenario* suggests that the timing of formation of cracks in the concrete structures in the silo, 1–2BMA and 1–2BTF has only a marginal impact on the resulting doses. Taken together, the results from both scenarios suggest that the safety function *limit advective transport* due to enhanced concrete degradation contributes to the protective capability of the repository. However, even if the safety function is not fulfilled, post-closure safety is unlikely to be compromised.

9.9 Unrepaired 1BMA scenario

9.9.1 General description

The closure plan for SFR (Mårtensson et al. 2022) outlines extensive repair and strengthening measures that need to be adopted to achieve the desired hydraulic and mechanical properties of 1BMA at closure. The measures include the erection of new reinforced outer concrete walls on the outside of the existing ones (Section 4.4.2). In accordance with the closure plan, the external concrete walls in 1BMA are included in the calculations of the main scenario (Section 7.4.2).

The aim of this scenario is to illustrate the importance of these repair and strengthening measures for post-closure safety. To this end, an alternative initial state of 1BMA where no additional concrete structure has been erected around the existing concrete structure is evaluated with the *unrepaired 1BMA calculation case*. This calculation case is set up to resemble as close as possible the *No repair* case in the updated analysis of the post-closure safety for 1BMA (Elfwing et al. 2018). A detailed description and analysis of the *unrepaired 1BMA calculation case* is given in the **Radionuclide transport report**, Section 8.8. In the following, a summary of the calculation case is presented together with the key results.

9.9.2 Unrepaired 1BMA calculation case

Description of the calculation case

The difference in this calculation case with respect to the *base case* is the omission of the new outer concrete barrier in 1BMA. Thus, the groundwater flow in 1BMA is limited by the already existing concrete structure and not the planned reinforced outer concrete walls in this calculation case. The hydraulic conductivity of the existing concrete is the same as in the *base case*, thus corresponding to severely degraded concrete ($K = 10^{-5}$ m/s) for the first 20 000 years and completely degraded concrete ($K = 10^{-3}$ m/s) for the remainder of the assessment period.

Apart from this change, the handling in the radionuclide transport and dose modelling is identical to the *base case*.

Radionuclide transport and dose

The maximum annual dose from 1BMA increases by approximately a factor of two from the *base case* (Figure 9-12). The elevated dose from C-14-org, Mo-93 and I-129 is a direct result of the increased groundwater flow through the waste due to the increased hydraulic conductivity in 1BMA. After ~20 000 AD, Ni-59 dominates the dose from 1BMA (Figure 9-12) due to elevated releases resulting from increased groundwater flow and earlier formation of cracks.

The elevated doses from 1BMA also have an impact on the total dose from the entire repository (Figure 9-13), although these changes are considerably smaller than from 1BMA since the release and doses from the other vaults are the same as in the *base case.* Specifically, the maximum total dose from SFR is about 5 % higher than in the *base case.* Furthermore, the dose curve exhibits a steeper and earlier rise in this calculation case due to the elevated releases from 1BMA. In the period approximately between 20 000 AD and 90 000 AD, the total dose is slightly elevated due to the fast breakthrough of Ni-59 (Figure 9-13).

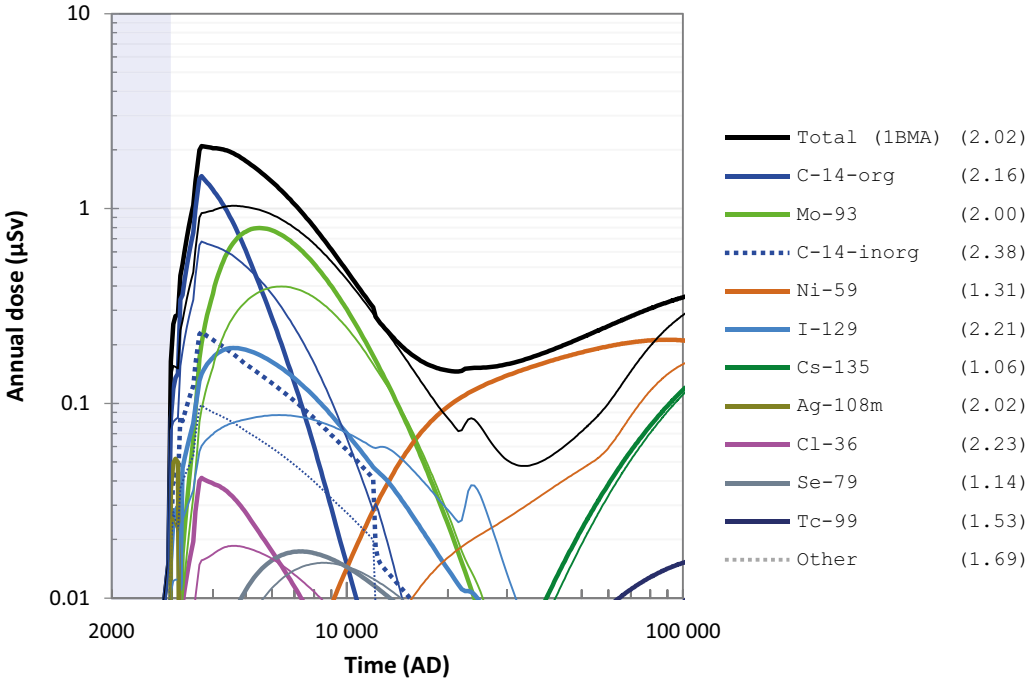

Figure 9-12. *Annual dose (µSv) to the most exposed group (black lines), including radionuclide-specific contributions (coloured lines), due to releases from 1BMA in the unrepaired 1BMA calculation case (thick lines) and the base case (thin lines). The combined contribution from radionuclides not shown is indicated by the grey dotted lines. The ratio between the maximum doses in the present calculation case and the base case are shown in parentheses in the key. The submerged period is illustrated by the blue shading.*

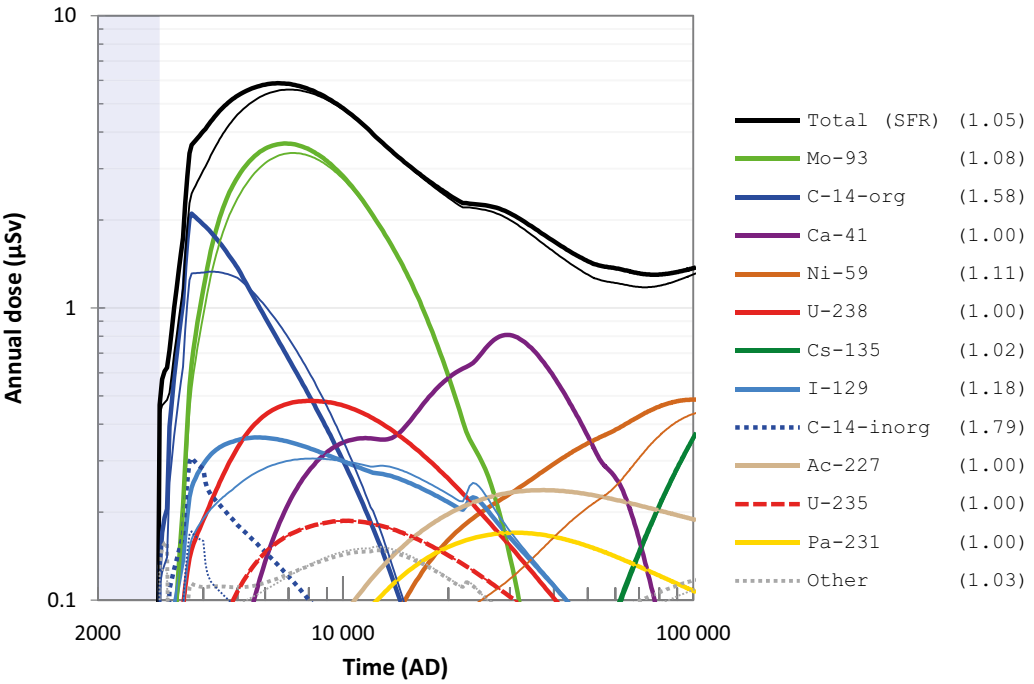

Figure 9-13. *Annual dose (µSv) to the most exposed group (black lines), including radionuclide-specific contributions (coloured lines), due to releases from all waste vaults in the unrepaired 1BMA calculation case (thick lines) and the base case (thin lines). The combined contribution from radionuclides not shown is indicated by the grey dotted lines. The ratio between the maximum doses in the present calculation case and the base case are shown in parentheses in the key. The submerged period is illustrated by the blue shading.*

9.9.3 Concluding remarks

This scenario illustrates the significance of the planned repair and strengthening measures of 1BMA to the protective capability of the repository. Neglecting the hydraulic properties of the new outer concrete structure in 1BMA results in a 5 % increase in the maximum dose from SFR compared with the main scenario. This minor difference in dose suggests that the planned repair and strengthening measures of 1BMA are not of critical importance for post-closure safety.

9.10 Unsealed repository scenario

9.10.1 General description

According to regulations, the residual scenarios should address the consequences of an unsealed repository that is not monitored (Section 2.6.8). In the *unsealed repository scenario*, it is assumed that the repository, following completion of waste disposal, is abandoned without being closed as planned (Mårtensson et al. 2022) and left without oversight. No assumptions are made for the reason for this to occur.

Today, groundwater is pumped out continuously from the repository. Abandoning the repository would halt pumping and the unsealed repository would be expected to become water filled within a few years. This scenario assumes that the abandoning of the repository occurs during the period when the area above the repository is submerged beneath the sea. During this period, hydrogeological flow is small and, consequently, it will take a fairly long time to replace the water in the repository. In this scenario, it is therefore pessimistically assumed that the water in the repository will not be replaced and the radionuclides that dissolve remain in the repository.

The repository will become filled with water within a few years. Since the groundwater that is pumped out of the repository today is relatively saline, it is not likely that the water that fills the repository will be used as a water supply for as long as the repository is situated in the vicinity of the shoreline. However, it is not unreasonable to assume that the influx of meteoric water and limited mixing due to the difference in salinity and temperature could lead to the formation of a freshwater pool near the access tunnel entrance. Over an extended period, freshwater could seep down into the repository and replace the saline water present there today with potable water. Hence, exposure to humans in this calculation case is assumed to occur due to utilising water from the tunnel entrance as drinking water; this is the only considered exposure pathway in this calculation case.[45]

As in the considerations of FHA (Section 9.11 and the **FHA report**), this calculation case addresses only inadvertent actions, meaning that the people pumping the water out of the repository have no knowledge of the potential radiological hazard. It is assumed that inadvertent FHAs are only possible after memory of the repository is lost, i.e. the existence and location of, and/or the nature of, the repository is forgotten. Memory is assumed to be preserved for at least 300 years after closure in the FHA scenarios. However, that is under the presumptions that present-day social conditions and technical capabilities will prevail and that the repository is closed as planned. The premise for the *unsealed repository scenario* is that the repository is neither closed nor monitored. For this to occur, it may be reasonable to assume that social conditions have drastically changed. This implies that memory might not be preserved for a minimum of 300 years. In this scenario, it is assumed that memory may be lost earlier, already after 100 years. Thus, doses are calculated from 100 years and onward after the repository has been abandoned.[46]

This scenario is evaluated with the *unsealed repository calculation case*. A detailed description and analysis of the calculation case is given in the **Radionuclide transport report**, Section 8.9. In the following, a summary of the calculation case is presented together with the key results.

[45] It is thus cautiously assumed that radionuclides uniformly mix between the saline water and the freshwater pool, but that the salinity does not mix.

[46] The repository is assumed to be abandoned at the planned time of closure.

9.10.2 Unsealed repository calculation case

Description of the calculation case

The only exposure pathway considered in this calculation case is ingestion of drinking water, taken directly from the tunnel entrance of the unsealed repository. As presented in Section 9.10.1, the usage of the drinking water is assumed to begin 100 years after the repository has been abandoned. Releases of radionuclides from the waste to other parts of the repository system are neglected in this calculation case. As this calculation case is highly simplified and pessimistic, it is considered appropriate to apply only deterministic calculations.

Radionuclide transport and dose

The maximum annual dose occurs at the start of the calculation. At this time, radionuclides with a high initial radiotoxicity and rather short half-life contribute most to the maximum dose, e.g. Cs-137 and Ni-63 (Table 9-2).

As discussed in Section 9.10.1, it is considered pessimistic to assume only 100 years for the period during which the memory of the repository is preserved. Therefore, for comparison, Table 9-2 also presents the resulting dose maximum with the assumption that the memory of the repository will be kept for at least 300 years, as is assumed in the FHA scenarios (Section 9.11). As can be seen, the dose decreases by more than one order of magnitude from 100 years to 300 years after closure, mainly due to decay of Cs-137.

Table 9-2. Annual doses from ingestion of water from the tunnel entrance 100 and 300 years after abandoning the repository.

Time of exposure (years after the repository was abandoned)	Annual dose (mSv)	Most contributing radionuclides
100	14.3	Cs-137 (90 %), Ni-63 (6.0 %), Sr-90 (1.8 %)
300	0.59	Ni-63 (36 %), Cs-137 (22 %), Ag-108 (22 %)

9.10.3 Concluding remarks

In conclusion, the maximum dose due to exposure of radionuclides in the drinking water from an unsealed repository is several orders of magnitude higher than in the main scenario. These results clearly demonstrate the importance of adequate closure and sealing of the repository.

9.11 Future human actions scenarios

9.11.1 General description

Considering the time perspective of the post-closure safety assessment of SFR, it cannot be ruled out that humans in the future, in some way, will conduct activities at, or near, the Forsmark area that potentially may affect the conditions of the repository. Therefore, FHAs are considered. Those are the actions potentially resulting in 1) changes to the barrier system affecting, directly or indirectly, the rate of the release of radionuclides from SFR, and 2) radioactive waste being brought to the surface giving rise to exposure of people at the surface. Only inadvertent FHAs are addressed, which are defined as actions carried out without knowledge of the repository and/or its nature (the location of the repository, its purpose and the consequences of the actions).

Four stylised FHA scenarios have been identified, based on present-day social conditions and technical capabilities prevailing throughout the assessment time frame. This set of selected FHA scenarios is intended to comprise an illustrative set of credible FHAs but should not be considered to be fully comprehensive or complete. Two of them are related to direct intrusion into the repository by drilling. These two are the *drilling into the repository scenario*, which focuses on radioactive material being brought to the surface during the drilling event, giving rise to exposure of people, and the *intrusion well scenario*, in which drilling for a household water supply is addressed. The two other FHA scenarios

are related to human actions not directly intruding into the repository, but which may have impacts on the repository due to potentially altered groundwater flow in the bedrock and through the waste vaults: the *water management scenario* and the *underground construction scenario*.

Details on the FHA scenarios, and the analysis of them, are presented in the **FHA report**, Chapter 4. Below is a summary of the scenarios and the key results are presented.

9.11.2 Calculation cases and results

Calculation cases for the drilling into the repository scenario

Three calculation cases are analysed in the *drilling into the repository scenario*, exposure to the drill crew during a drilling event, and exposure to people either cultivating or performing construction on land containing contaminated drilling detritus. For these cases, the effective dose maximum is 0.014 mSv, related to bringing a 1 m drill core from 2BMA to the surface resulting in exposure of the drill crew (Figure 9-14). At the time of the maximum, Am-241 is the main contributor to the dose, followed by Pu-239. With time, as Am-241 decays, Pu-239 dominates the dose to a member of the drill crew, followed by the contributions from Nb-94 and Pu-240.

The doses for the cases related to utilising the land containing contaminated drilling detritus from the drilling event are lower. The effective dose maximum to a construction worker, conducting work for one year on a landfill containing contaminated drilling detritus, is 0.0022 mSv, and the annual dose maximum to a person cultivating vegetables and tubers on a similar landfill is about 0.0036 mSv.

Intrusion well calculation case

The *intrusion well into the repository calculation case* is defined to analyse the *intrusion well scenario*. It is assumed that a water well is drilled into a waste vault of the repository and, consequently, radionuclides released from this vault are mixed into the well water. The exposure pathway considered is utilising the well water as a source of drinking water. The dose maximum for this case is 1.3 mSv, for a well drilled into one of the 2–5BLA waste vaults at 3000 AD (Figure 9-15). 3000 AD is assumed to be the earliest time a well can be drilled into the repository as this corresponds to the point when the shoreline has regressed sufficiently that about 75 % of the surface above the repository is terrestrial. At the dose maximum for 2–5BLA, the radionuclides most contributing to the total dose are Am-241, Pu-239 and Pu-240.

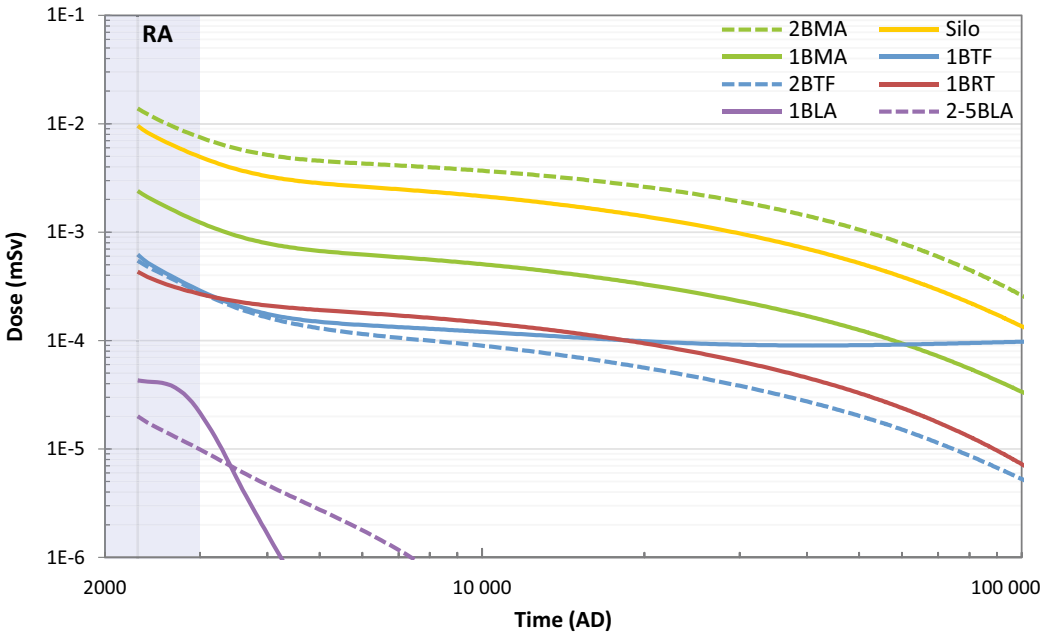

Figure 9-14. *Effective dose to a member of the drill crew during drilling into the different waste vaults, using rotary drilling with air (RA). The submerged period is indicated by the blue shaded area and the earliest time when it is assumed that memory of SFR may be lost is marked with a grey vertical line.*

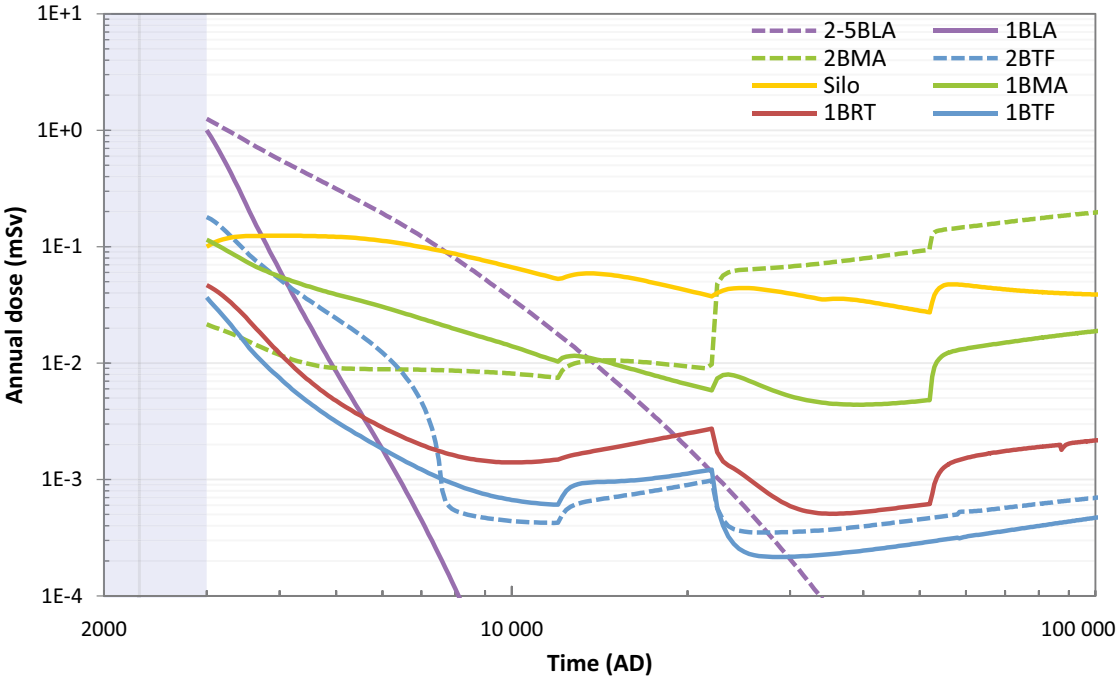

Figure 9-15. *Annual dose for a well drilled into the different waste vaults in the intrusion well into the repository calculation case. The submerged period is indicated by the blue shaded area and the earliest time when it is assumed that memory of SFR may be lost is marked with a grey vertical line.*

Construction of a water impoundment calculation case

The *construction of a water impoundment calculation case* is defined to analyse the *water management scenario*. It is assumed that the SFR pier and/or other artificial causeways in the area are utilized and modified as part of a dam for a future water impoundment in the close vicinity of SFR. Annual doses are calculated by postulating that the impoundment results in a four- or tenfold increase of the groundwater flow rates in the bedrock and through the waste vaults compared with the *base case* (Section 7.4.3). Apart from the increased groundwater flow rate, the radionuclide transport and dose calculations in this case are based on the *base case*. The annual doses to the most exposed groups in the *base case* and for the postulated higher flow rates in the bedrock and through the waste vaults are shown in Figure 9-16. To be consistent with the assumption of a present-day level of technology in all FHA scenarios, the potentially exposed groups included here are GP households and DM farmers (Section 7.3.6). For the four-fold increase in flow rate, the dose maximum is 0.012 mSv. This is about twice the dose maximum in the *base case*. For the ten-fold higher flow rate, the dose maximum is 0.019 mSv, which is about 3.5 times higher than in the *base case*.

As expected, it is radionuclides that are non-sorbing in the repository and in the geosphere, such as C-14-org, Mo-93 and I-129, for which doses increase most when the flow rates increase. The doses from these radionuclides increase about 2.5–3 times for the four-fold increase in flow rate and by about 5 times for the ten-fold increase in flow rate. Mo-93 is the radionuclide contributing most to the dose maximum in the *base case* and also in this calculation case.

Calculation cases for the underground construction scenario

Two calculation cases are identified and analysed in the *underground construction scenario*: the *mine in the vicinity of the Forsmark site calculation case* and the *rock cavern in the close vicinity of SFR calculation case*. In the case involving a mine, it is judged that the potential hydraulic impact on SFR from a hypothetical mine in the vicinity of the Forsmark site would be insignificant. In the case with the rock cavern, the same increase of the flow rates in the bedrock and through the waste vaults as in the *construction of a water impoundment* calculation case are assumed. Hence, the resulting annual doses in this calculation case are comparable to the doses in the *construction of a water impoundment calculation case*.

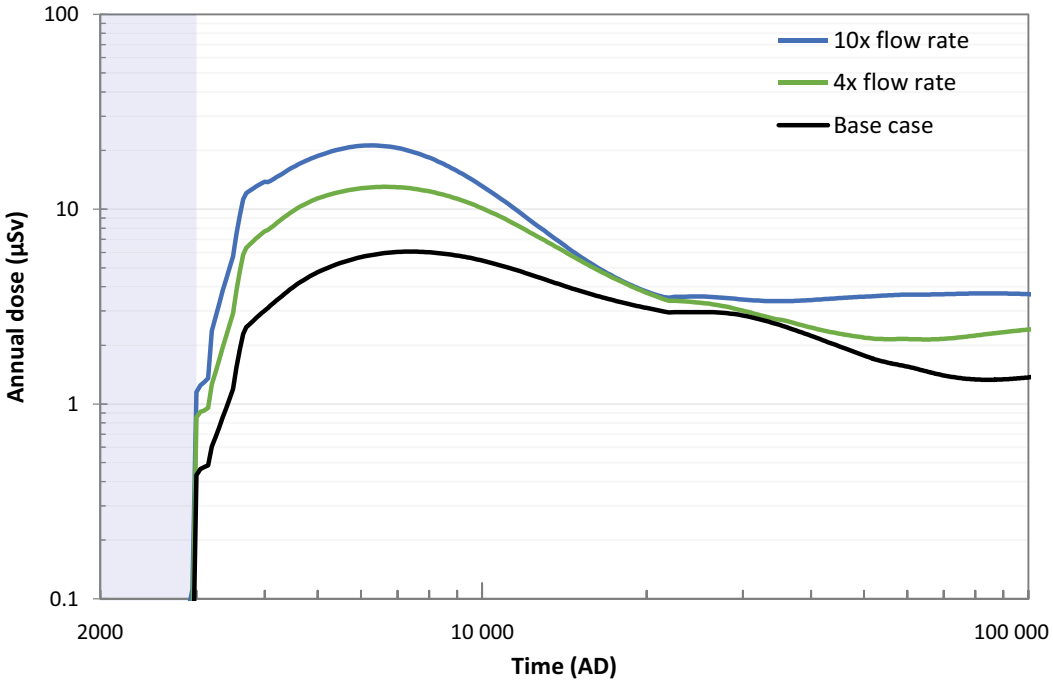

Figure 9-16. *Annual dose to the most exposed group in the construction of a water impoundment calculation case, applying four- and ten-fold higher flow rates in the bedrock and through the waste vaults (coloured lines). The black line shows the annual dose in the base case. The submerged period is indicated by the blue shaded area.*

9.11.3 Concluding remarks

The FHA scenarios identified and analysed are considered to cover a wide range of credible human activities. A key outcome from the dose calculations is that most of the doses are below 1 mSv, which is the criterion set out by the IAEA (2011) below which efforts to reduce the probability of intrusion or to limit its consequences are not warranted. Only in the calculation with an intrusion well in the BLA vaults does the dose exceed 1 mSv for a well drilled at the earliest time possible (3000 AD) or within a few hundreds of years after that. After about 3300 AD, all doses are below 1 mSv. If, according to IAEA (2011), annual doses in the range 1–20 mSv are indicated, then reasonable efforts are warranted at the stage of development of the facility to reduce the probability of intrusion or to limit its consequences by means of optimisation of the facility's design. This has already been done for SFR, since the selection of geological disposal is widely deemed as the most effective measure to reduce the potential for human intrusion.

The results from analysing the scenarios without a direct intrusion into SFR, water management and underground constructions in the vicinity of the repository, show that safety functions of the geosphere and engineered barriers to provide favourable hydrological conditions and limit advective transport are influenced in these scenarios. However, the resulting annual doses are significantly lower than 1 mSv, and within a factor of five higher than those in the *base case* (Section 7.4.5). This clearly indicates that SFR is robust against these types of FHAs.

The scenarios involving direct intrusion into SFR, drilling into the repository and intrusion wells, have a larger influence on the safety functions of the geosphere and engineered barriers to provide favourable hydrological conditions and limit advective transport. Considering a single bore hole, the impairment is local, and it is considered that the performance of the repository as a whole is not significantly weakened.

10 Annual risk and protection of the environment

10.1 Introduction

In this chapter, the results from the analysis of the scenarios in Chapters 7–8 are assessed with respect to the protection of human health and the environment.

Protection of human health is assessed against SSM's regulatory criterion (SSMFS 2008:37, Section 5) for annual radiological risk of harmful effects after closure for a representative individual in the group exposed to the greatest risk. The risk assessment is part of the ninth step in SKB's ten step safety assessment methodology for SFR (Section 2.6.9). The procedure used for calculating the annual risk is described in Section 10.2. This procedure is implemented to evaluate the annual risk as a function of time for the main scenario and each of the less probable scenarios and results are presented in Section 10.3. The annual risk for all scenarios is then used to evaluate the total annual risk according to the procedure in Section 10.4. Additional considerations regarding the total annual risk are discussed in Section 10.5, including the contribution to the annual risk from different waste vaults and radionuclides. A comparison to the annual risk results from SR-PSU is also made in this section. In Section 10.6 the consequence of risk dilution is described. In the general guidance to SSMFS 2008:37, it is recommended that additional safety indicators should be evaluated. As an additional safety indicator, the estimated activity concentrations in the environment from repository release of two naturally occurring radionuclides are compared to measured background concentrations (Section 10.7).

The protection of the environment in connection to final management of nuclear waste implies that biodiversity and the sustainable use of biological resources shall be protected against the harmful effects of ionising radiation (SSMFS 2008:37, Section 6). Furthermore, biological effects of ionising radiation in the habitats and ecosystems concerned shall be described (SSMFS 2008:37, Section 7). In Section 10.8, protection of the environment is assessed based on the results presented in the **Biosphere synthesis report**.

10.2 Risk calculation procedure

The total annual radiological risk ($Risk_M^{tot}$) is calculated accounting for contributions from the main scenario and the less probable scenarios (Equation 10-1). Total annual risk is calculated separately for each of the different climate cases in the main scenario (index M) and is separately compared with the risk criterion. The annual conditional risk for a calculation case in the main scenario is evaluated by multiplying the arithmetic mean value of the annual dose to an individual in the most exposed group, obtained at each point in time (T) from probabilistic calculations ($Dose_M(T)$), with the nominal risk coefficient (α) of 7.3 percent per Sievert (ICRP 2006, 2007). For the less probable scenarios (index i), apart from the *earthquake scenario*, the annual conditional risk (conditioned on the climate case M) is calculated in the same way as the conditional risk for the main scenario ($\alpha \cdot Dose_{i|M}(T)$, Equation 10-2). The risk for the main scenario $Risk_M(T)$ and the individual less probable scenarios ($Risk_{i|M}(T)$) are then obtained by multiplication by the probability of the scenario (p_M and p_i, respectively). A probability of one is assigned ($p_M = 1$) to a climate case of the main scenario, however, in the risk summation, the probability of the main scenario is reduced by the probabilities of the less probable scenarios associated with it, details of the risk summation are further described below. Less probable scenarios and their probabilities are described in Chapter 8 and listed in Table 10-1.

In the *earthquake scenario*, the annual risk is linked to the timing of an earthquake that may damage the structural integrity of the silo and the probability of occurrence at that time (Equation 10-3). The probability of the first such earthquake occurring at a given point in time is the yearly probability multiplied by the probability that it has not yet occurred (since the modelled consequence of such an earthquake is assumed to only happen once). This conditional probability follows an exponential distribution, which is expressed in the first term within the integral in Equation 10-3. The corresponding cumulative probability for an earthquake that can damage the silo structure during the analysis period is given in Equation 10-4 and shown in Figure 10-1. In practice, the annual risk in the *earthquake scenario* is calculated using a series of separate dose calculations with earthquake events occurring at discrete time intervals T_{per} (100 years) throughout the full assessment period (Section 8.6.3). Thus,

the integral is approximated by a sum of the annual dose at each point in time from each earthquake calculation, weighting the doses with the probability of each earthquake, and multiplying with the nominal risk coefficient (Equation 10-3). This approach of approximating the risk-integral in Equation 10-3 was also used in SAR-08 and SR-PSU, where it is further described (SKB R-08-130, Section 7.6.1).

The risk from a less probable scenario is included in the risk summation when the dose of the scenario exceeds that of the main scenario (Equation 10-5 is applied to all less probable scenarios apart from the earthquake scenario for which Equation 10-6 is applied). When this happens, the probability of the less probable scenario is subtracted from the probability of the main scenario, accounting for the fact that the main and less probable scenarios are mutually exclusive. This approach ensures a cautious total risk estimate, and is consistent with the purpose of the less probable scenarios (i.e. they are designed to illustrate an elevated risk associated with identified uncertainties and are not included when they yield lower doses than the main scenario).

$$Risk_M^{tot}(T^{47}) = \alpha \cdot Dose_M(T) \cdot \left(p_M - \sum_{i=LP} \omega_i(T) \cdot p_i\right) + \sum_{i=LP} \omega_i(T) \cdot Risk_{i|M}(T) + v(T) \cdot \left(Risk_{EQ|M}(T) - Risk_M(T) \cdot p_{Cuml,EQ}(T)\right) \quad \text{(Equation 10-1)}$$

$$Risk_M(T) = \alpha \cdot Dose_M(T) \cdot p_M, \qquad Risk_{i|M}(T) = \alpha \cdot Dose_{i|M}(T) \cdot p_i \quad \text{(Equation 10-2)}$$

$$Risk_{EQ|M}(T) = \alpha \cdot \int_0^T p_{EQ} \cdot e^{-t \cdot p_{EQ}} \cdot Dose_{EQ|M}(T,t)\, dt \approx \alpha \cdot \sum_{j=0}^{\lfloor T/T_{per} \rfloor} Dose_{EQ|M}(T, j \cdot T_{per}) \cdot p_{EQ} \cdot T_{per} \cdot e^{-j \cdot T_{per} \cdot p_{EQ}} \quad \text{(Equation 10-3)}$$

$$p_{Cuml,EQ}(T) = \int_0^T p_{EQ} \cdot e^{-t \cdot p_{EQ}}\, dt = 1 - e^{-T \cdot p_{EQ}} \quad \text{(Equation 10-4)}$$

$$\omega_i(T) = \begin{cases} 1, & Dose_{i|M}(T) > Dose_M(T) \\ 0, & otherwise \end{cases} \quad \text{(Equation 10-5)}$$

$$v(T) = \begin{cases} 1, & Risk_{EQ|M}(T) > Risk_M(T) \cdot p_{Cuml,EQ}(T) \\ 0, & otherwise \end{cases} \quad \text{(Equation 10-6)}$$

where

M	main scenario climate case M used as basis to calculate total annual risk; *base case* (*present-day climate)*, *warm climate* or *cold climate*,
LP	less probable scenarios; *glaciation*, *high concentration of complexing agents* and *alternative concrete evolution*,
EQ	less probable scenario; *earthquake*,
α	nominal risk coefficient (7.3 percent per Sievert, ICRP 2006 and 2007),
$Dose_M(T)$	annual dose (Sv) at time T after closure for main scenario climate case M,
$Dose_{i\|M}(T)$	annual dose (Sv) at time T after closure for less probable scenario i, conditioned on main scenario climate case M,
$Dose_{EQ\|M}(T, t)$	annual dose (Sv) at time T after closure, for an *earthquake* at time t after closure, conditioned on main scenario climate case M
p_M	probability of the main scenario climate case M,
p_i	probability of less probable scenario i (except earthquake scenario),
$p_{EQ}{}^{e^{-t \cdot p_{EQ}}}$	exponential distribution for the probability of first occurrence of an earthquake at time t,
$p_{Cuml,\,EQ}(T)$	cumulative probability of the first earthquake event at time T (see Figure 10-1) and
T_{per}	length of time interval for modelling earthquake consequences (100 years).

[47] The unit of the time variables in Equations 10-1 to 10-6 are defined as "years after closure" instead of "years AD" as shown in result presentations, the reason for this is to simplify the equations.

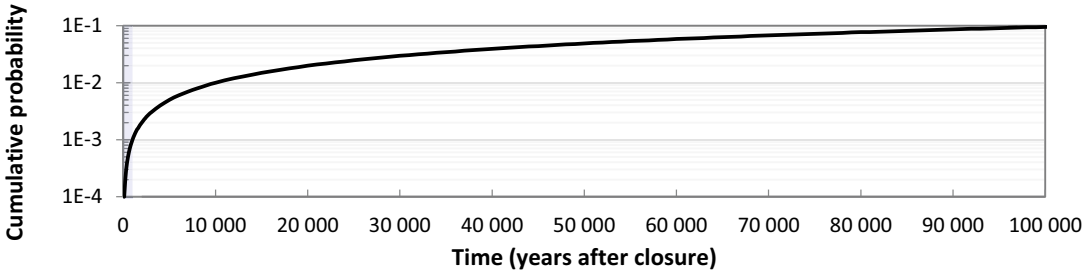

Figure 10-1. *Cumulative probability of the first earthquake event that may damage the silo structure as a function of time (Equation 10-4). Based on a yearly probability of an earthquake event of 10^{-6} (Table 10-1). Blue shaded area shows the period of submerged conditions in the base case (present-day climate).*

10.3 Annual risk for the main and each of the less probable scenarios

The calculated annual radiological risks for the main scenario and the less probable scenarios are presented in Figure 10-2. The annual risks are calculated using Equations 10-2 and 10-3 and the scenario probabilities are given in Table 10-1. The annual doses for each scenario are presented in Chapters 7–8. The highest dose from any of the four exposed groups considered in the dose calculations (DM, HG, IO and GP) is carried on to the risk assessment (Section 7.3.1).

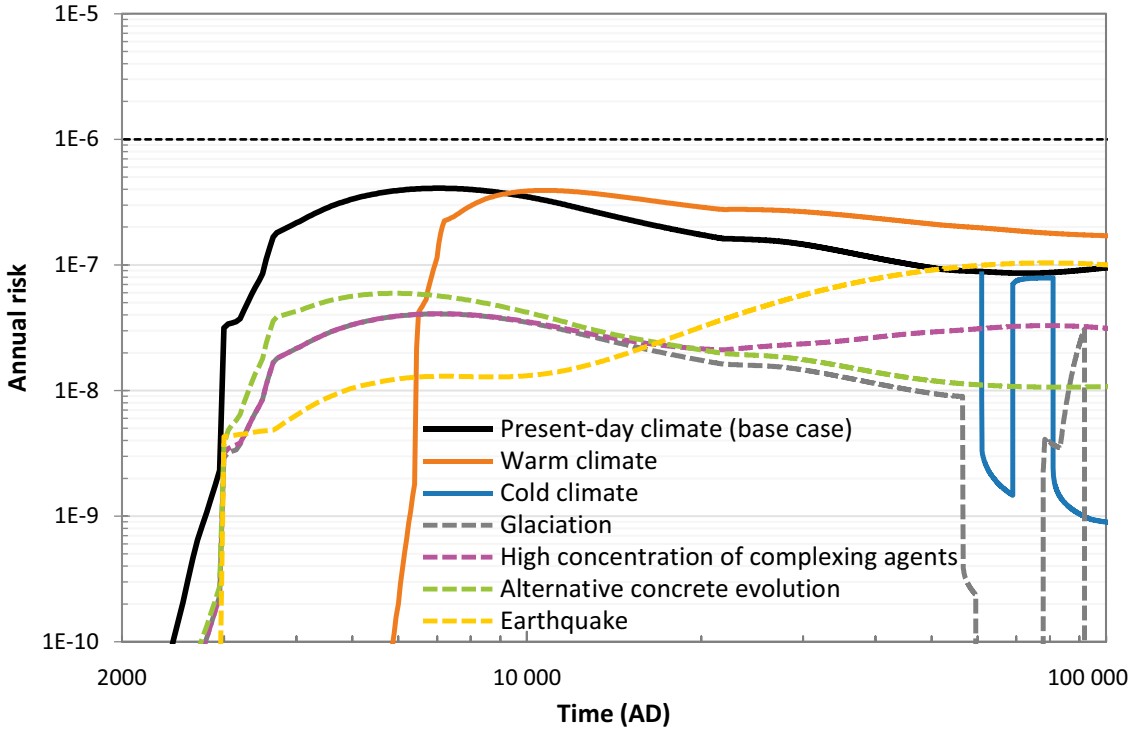

Figure 10-2. *Annual risk as a function of time, for the calculation cases in the main scenario (solid lines) and in the less probable scenarios (dashed lines). The annual risk for the calculation cases is calculated according to Equations 10-2 and 10-3. The annual risk of the less probable scenarios is calculated with respect to the base case (present-day) climate. The dashed black line represents the regulatory risk criterion.*

Table 10-1. Probabilities of the scenarios included in the risk calculations. The probabilities of the less probable scenarios are discussed and assigned in Sections 8.3–8.6. For the earthquake scenario, the yearly probability of an earthquake event that would damage the silo structure is presented.

Scenario	Probability
Main	1
Glaciation*	< 0.1
High concentration of complexing agents*	< 0.1
Alternative concrete evolution*	< 0.1
Earthquake	10^{-6} a^{-1}

* 0.1 is used in the risk calculations.

The main scenario includes three calculation cases, namely the *base case* (present-day climate), the *cold climate calculation case* and the *warm climate calculation case*. The *base case* yields the highest maximum annual risk, which occurs at 7000 AD (Table 10-2, Figure 10-3). The annual risk of the *cold climate calculation case* is identical to the *base case* (including the maximum annual risk) up until the onset of the first periglacial period at 61 000 AD, from which the annual risk becomes smaller than in the *base case*. The annual risk of the *warm climate calculation case* is initially lower than in the *base case*. From approximately 10 000 AD it provides a slightly higher annual risk (Figure 10-2). However, as noted above, the maximum annual risk of the *warm climate calculation case* never exceeds that of the *base case* (Table 10-2).

The less probable scenarios generally result in lower annual risks than in the *base case*. An exception is the *earthquake* scenario that yields an annual risk that is similar to the *base case* during the latter half of the assessment period. The increasing trend with time for the *earthquake scenario* is explained by the increasing cumulative probability that an earthquake event will occur before a given point in time (Figure 10-1) and that releases of Ni-59 contributes significantly to the annual dose at the end of the assessment period irrespective of when the silo structure is damaged (Figure 8-6 and the **Radionuclide transport report**, Figure 7-31).

It can be noted that each of the examined scenarios results in a risk that is clearly below the regulatory risk criterion (Table 10-2, Figure 10-3). Combinations of less probable scenarios are not included in the risk summation as their contribution to the total annual risk is considered to be insignificant (Section 8.7).

Table 10-2. Maximum annual risk for each of the calculation cases in the main scenario and the less probable scenarios based on the base case (present-day climate). The year at which the maximum annual risk is obtained is also indicated.

Scenario	Maximum annual risk	Year of maximum annual risk (AD)
Main – Present-day climate (base case)	4.1×10^{-7}	7000
Main – Warm climate	3.9×10^{-7}	10 800
Main – Cold climate	4.1×10^{-7}	7000
Glaciation	4.1×10^{-8}	7000
High concentration of complexing agents	4.1×10^{-8}	7100
Alternative concrete evolution	5.9×10^{-8}	5900
Earthquake	1.0×10^{-7}	79 000

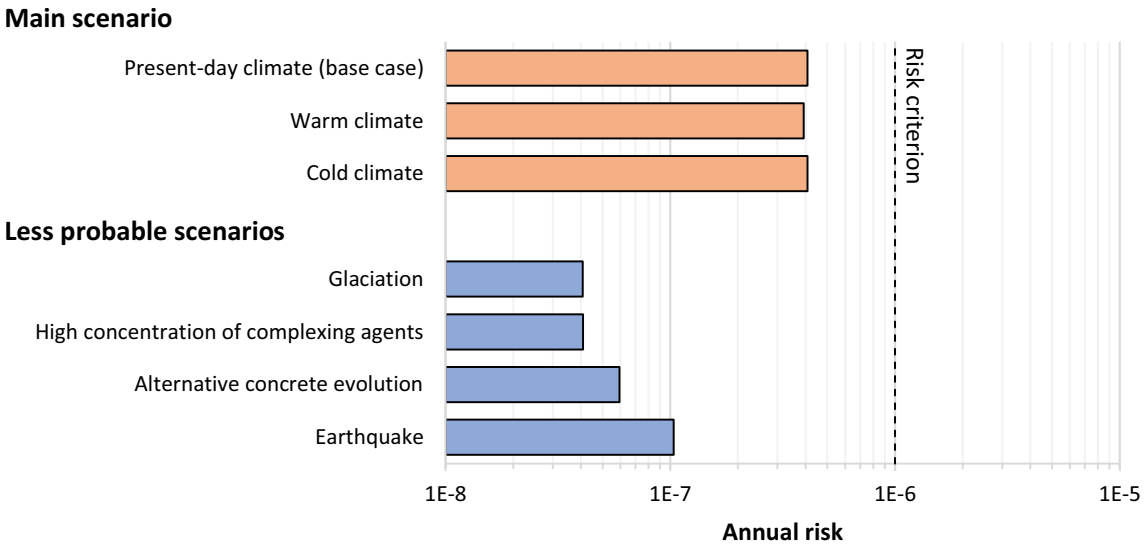

Figure 10-3. *Maximum annual risk for each of the calculation cases in the main scenario and the less probable scenarios.*

10.4 Total annual risk

Figure 10-4 shows the total annual radiological risk from SFR as a function of time. The risk is calculated using the procedure described in Section 10.2. The maximum total annual risk that occurs at 6900 AD is 4.4×10^{-7}. This is below SSM's risk criterion, which states that a repository for nuclear waste shall be designed so that the annual risk of harmful effects after closure does not exceed 10^{-6} for a representative individual in the group exposed to the greatest risk (SSMFS 2008:37, Section 5).

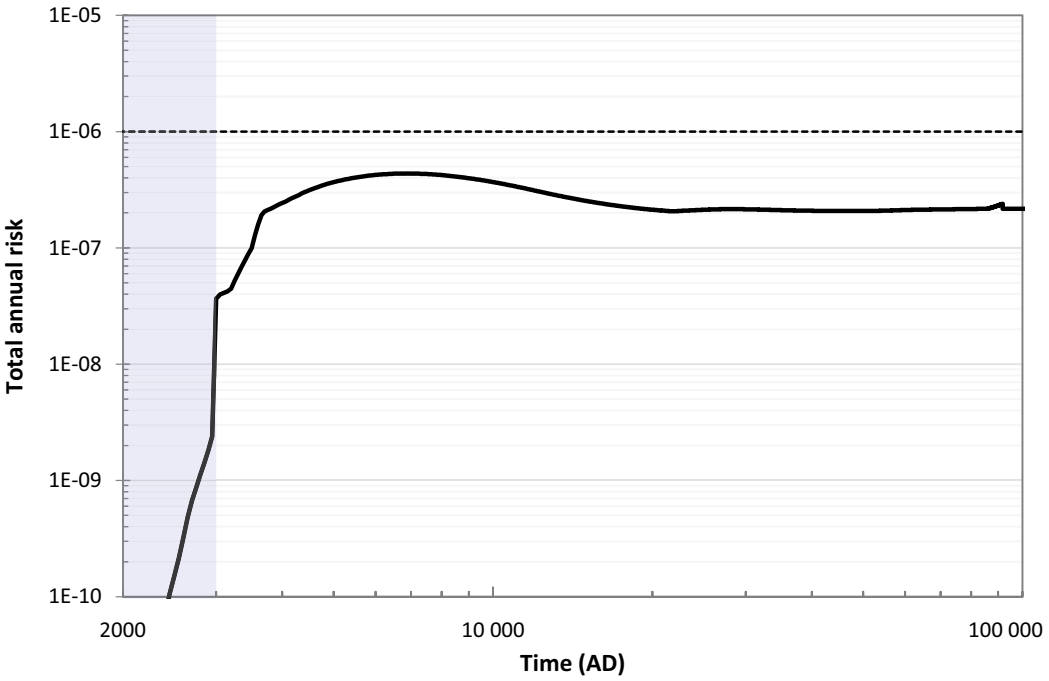

Figure 10-4. *Total annual risk as a function of time, obtained from the summation of the main scenario and all less probable scenarios using the base case (present-day) climate parameterisation. The blue shaded area shows the period of submerged conditions in the base case (present-day climate). The dashed black line represents the regulatory risk criterion.*

The contribution from the main scenario dominates the total annual risk until about 40 000 AD, after which the *earthquake scenario* gives the largest contribution to the total annual risk (Figure 10-5). The less probable scenarios only contribute to the total annual risk if their annual dose is higher at a given time than the main scenario, as explained in Section 10.2. This is the reason why the *complexing agent scenario* does not contribute before around 10 000 AD and the *glaciation scenario* only contributes during the limited terrestrial post-glacial period around 90 000 AD (little "shark fin", far right end of the curve in Figure 10-5).

The calculated total annual risk displayed in Figure 10-4 and Figure 10-5 is based on the *base case*, i.e. the *present-day climate calculation case* of the main scenario and the corresponding parameterisation of the less probable scenarios. Figure 10-2 suggests that the present-day climate considered in the *base case* yields the highest maximum total annual risk compared to the other climate cases. However, a parameterisation of the less probable scenarios based on the *warm climate calculation case* could possibly yield a higher total risk than for the *base case*, in particular at later times in the assessment period. The discussion in Section 8.7 regarding the effect of the different climate cases on the results of the less probable scenarios suggests that the present-day climate parameterisation is limiting with respect to the risk criterion., i.e. using the *base case* as basis gives the highest maximum risk.

To confirm that this really is correct, a supporting calculation of total annual risk has been performed using the *warm climate calculation case* of the main scenario and applying parameter values from this case for all of the relevant less probable scenarios (note that it is not considered relevant to combine the warm climate with the *glaciation scenario* in this supporting calculation). The maximum total annual risk for the warm climate is 4.1×10^{-7}, which is lower than the maximum total annual risk of 4.4×10^{-7} using the *base case* as the basis. This confirms that applying the *base case* is limiting with respect to SSM's risk criterion. Figure 10-6 shows a comparison of the total annual risk of the two calculations. The total annual risk, when based on the warm climate parameterisation, yields a later maximum due to the longer submerged conditions and, as expected from the individual annual risk curves, a somewhat higher annual risk in the later parts of the assessment period. The maximum annual dose for the *high concentration of complexing agents scenario* for the warm climate is 4.5×10^{-8} (81 250 AD) and for the *earthquake scenario* 1.2×10^{-7} (91 000 AD). They are thus marginally higher than corresponding values for the *base case* (Table 10-2). Nevertheless, the maximum total annual dose is lower when based on the *warm climate calculation case* as compared to the *base case*.

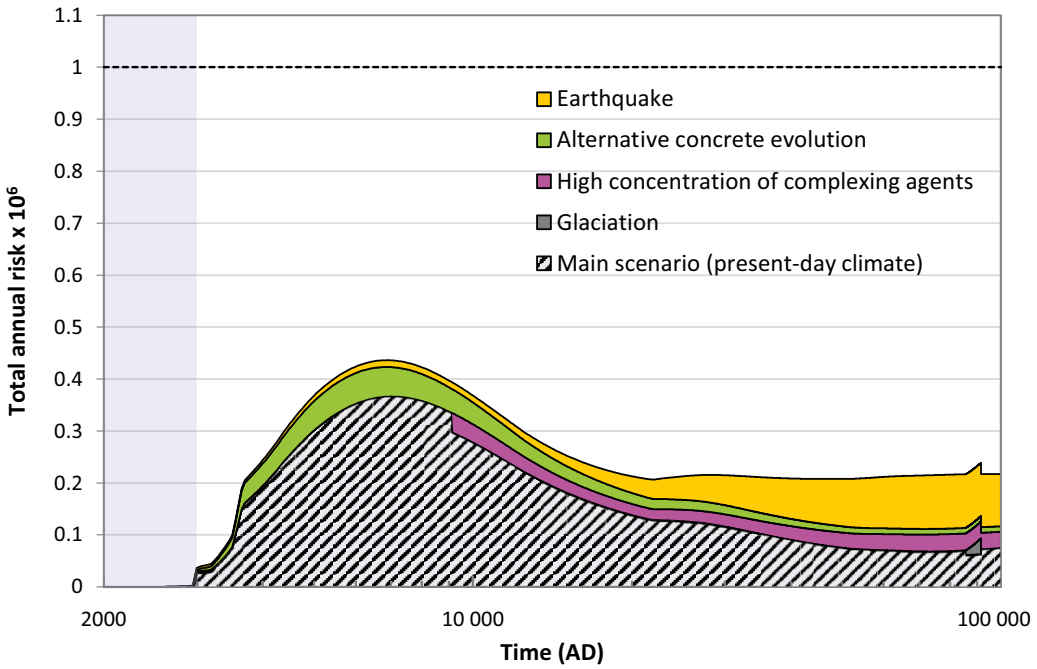

Figure 10-5. *Contributions of the main and less probable scenarios to the total annual risk as a function of time, using the base case (present-day) climate parameterisation. The blue shaded area shows the period of submerged conditions in the base case (present-day climate). The dashed black line represents the regulatory risk criterion. Note that the y-axis is linear.*

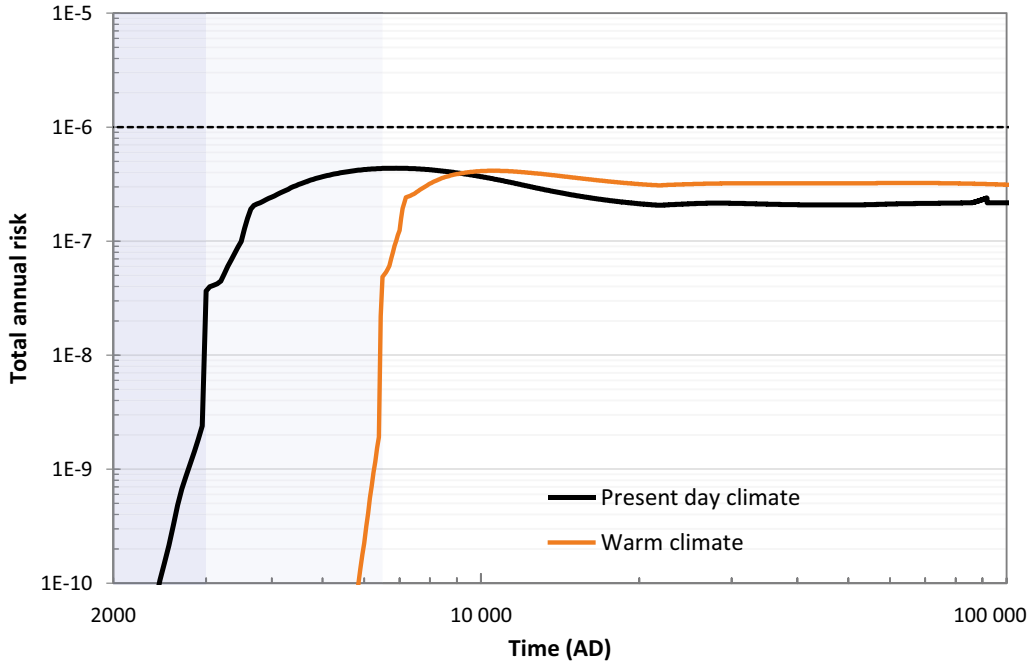

Figure 10-6. *Total annual risk as a function of time, obtained from the summation of the main scenario and all less probable scenarios according to Equations 10-1 to 10-6 using the base case (present-day) climate parameterisation (black line) and the warm climate calculation case as basis (orange line). The initial blue shaded area shows the period of submerged conditions in the base case (present-day climate) and the extended period (paler colour) for the warm climate calculation case. The dashed black line represents the regulatory risk criterion.*

In Figure 10-7, the contribution of each scenario to the total annual risk in the supporting calculation is displayed. It can be noted that the less probable scenarios have less influence on the total annual risk when using the parameterisation for the *warm climate calculation case* as basis compared to using the *base case* (compare Figure 10-7 and Figure 10-5). As the less probable scenarios only contribute to the total annual risk if their annual dose is higher at a given time than the main scenario, the contribution of the *alternative concrete evolution scenario* ends at around 30 000 AD.

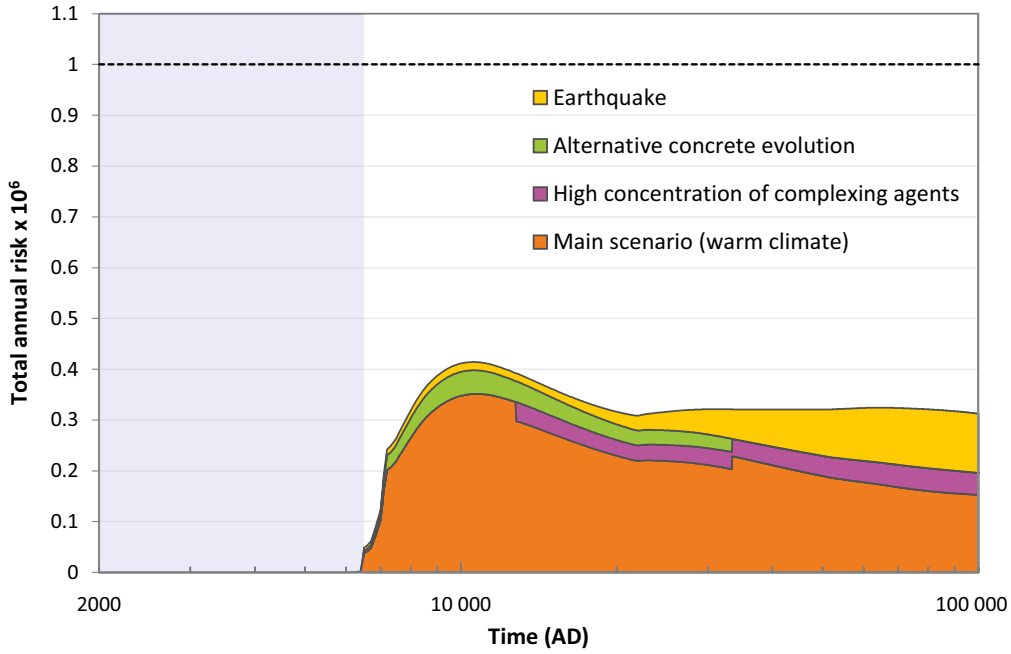

Figure 10-7. *Contributions of the main and less probable scenarios to the total annual risk as a function of time, using the warm climate parameterisation. The blue shaded area shows the period of submerged conditions in the warm climate calculation case. The dashed black line represents the regulatory risk criterion. Note that the y-axis is linear.*

10.5 Additional considerations regarding total annual risk

It is of interest to consider the contribution to total annual risk from the different waste vaults and radionuclides. This can increase the understanding of the results and thus support future improvements of the safety assessment. In Section 10.5.1, the total annual risk is presented with respect to contributions from the different waste vaults, i.e. the silo, 1BMA, 1BLA, 1–2BTF of SFR1 and 2BMA, 1BRT and 2–5BLA of SFR3. In Section 10.5.2, the total annual risk is illustrated with respect to contributions of different radionuclides.

10.5.1 Contribution to total annual risk from different waste vaults

The contribution to total annual risk from different waste vaults depends to a large degree on the radionuclide inventory and the associated ingestion radiotoxicity of the waste disposed in the vaults. The comparison of the radiotoxicity in the inventory of the vaults with the annual risk over time can give insight into the functioning and effectiveness of the barrier system of the different vaults.

Radiotoxicity serves to quantify the radiological hazard from individual radionuclides in a simple way, here defined as the product of the activity of a radionuclide and its corresponding ingestion dose coefficient (see Section 1.2.2). In Figure 10-8, the relative radiotoxicity of the disposed waste at closure (assumed at 2075) and its development during the full assessment period is shown for each waste vault. The radiotoxicity only shows changes owing to radioactive decay and ingrowth of radioactive decay products and does not account for transport from the repository. The largest part (about 80 percent) of the initial radiotoxicity is from waste disposed in the silo, which is also the waste vault having engineered barriers with highest retention capabilities, followed by 2BMA and 1BMA (Figure 10-8). Less than 2 % of the radiotoxicity at closure is located in the other waste vaults. After 200 years, when the activity of relatively short-lived radionuclides has declined, the waste disposed in 2BMA constitutes the largest part of radiotoxicity until the end of the assessment period. The radiotoxicity disposed in 1–5BLA increases due to ingrowth of decay products after a couple of thousand years, but the levels are still relatively low. It can also be noted that almost 98 % of the radiotoxicity has been lost due to decay before the submerged period has ended. Initially, 88 % of the radiotoxicity is located in SFR1 and thus 12 % in SFR3.

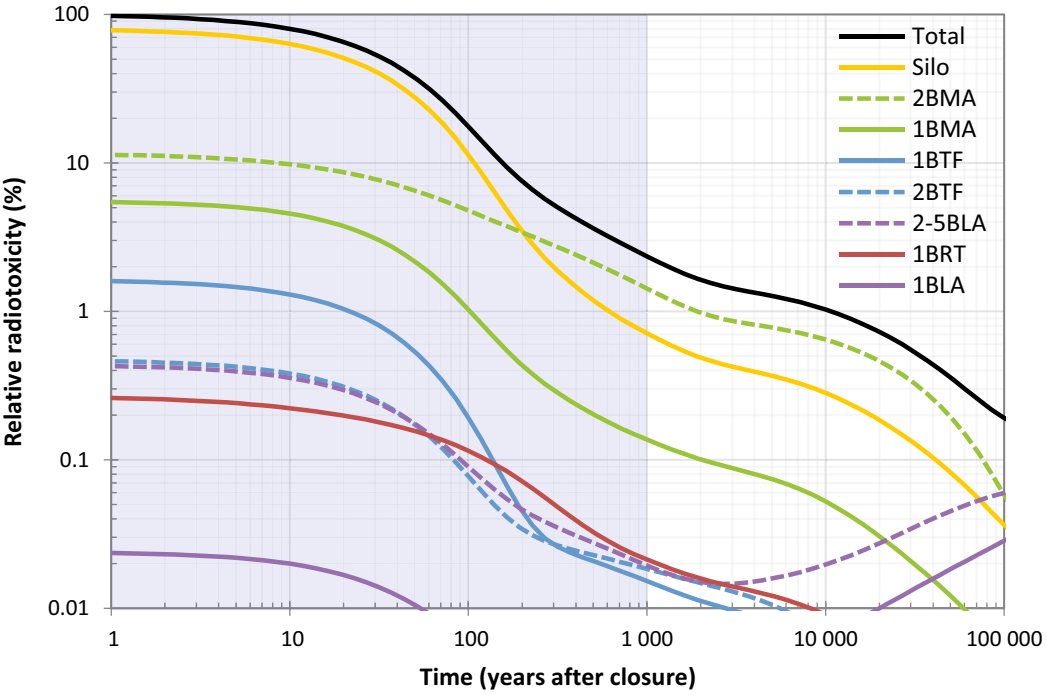

Figure 10-8. *Contribution to total radiotoxicity from each waste vault as a function of time after closure (assumed at 2075), ignoring transport out from the waste vaults. Note that the horizontal axis is displayed in units "years after closure" enabling clear visualisation of the initial development. The blue shaded area shows the period of submerged conditions in the base case (present-day climate).*

The relative contribution to the annual risk from different waste vaults is plotted in Figure 10-9. The contributions to total annual risk from different waste vaults depends on several factors. These are the radiotoxicity of the radionuclides in the disposed waste, retention capacity of the barrier system, radionuclide-specific transport and accumulation in the surface system, and the relative importance of different exposure pathways. The resulting annual risk also depends on the degree of pessimism in the assumptions and assigned parameter values, which may vary between the models for the different waste vaults and radionuclides. Finally, the annual risk also depends on the probabilities of the scenarios that contribute to the total annual risk.

The influence of the radiotoxicity of the radionuclide inventory, and the retention capacity of the barrier system from different waste vaults on resulting dose, are explained in detail for the main scenario *base case* in Section 7.4.5 (Figure 7-12). Since the main scenario dominates the contribution to the total annual risk, apart from late times (Figure 10-5), the explanations for the total dose can also be generalized to the total annual risk. However, at later times, the *earthquake scenario* becomes dominant (Figure 10-5). As the earthquake calculation is simplified to only affect the properties of, and releases from, the silo, the contribution of the silo to the total annual risk increases. Thus, release from the silo is the dominant contributor to risk for most of the assessment period (Figure 10-9).

As discussed in Section 7.4.5, the largest part of the radiotoxicity is placed in vaults (silo and 2BMA) having engineered barriers with the highest retention capabilities, and the contribution to the annual dose or risk is therefore not as high as indicated by the fraction of radiotoxicity placed in these vaults. This result shows that the initial distribution of radiotoxicity of the waste between the individual waste vaults is appropriate. It can be noted that at the time of the maximum risk, SFR1 contributes with 72 % to the total annual dose and SFR3 with 28 %. When interpreting Figure 10-9, it should be kept in mind that only a very small fraction of the total radiotoxicity contributes to dose or risk and that radionuclide-specific contributions need to be considered and this is discussed in Section 10.5.2. It should also be kept in mind that the annual risk results for 1–5BLA are judged to be overestimated more than other vaults due to simplifying assumptions. In the modelling of the BLA vaults, sorption is neglected despite the presence of significant amounts of cement and other sorbents (Section 7.3.4). By including sorption processes in the transport calculations, a significant delay of the release of risk-contributing radionuclides from the BLA vaults is expected.

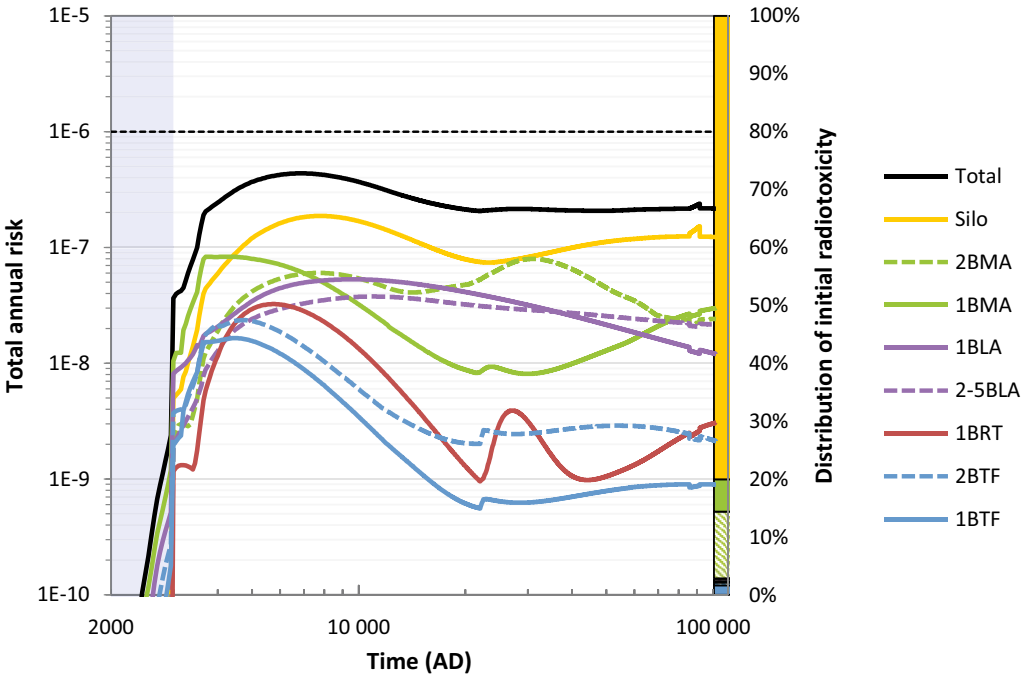

Figure 10-9. *Contribution to total annual risk from each waste vault as a function of time, for base case (present-day) climate parameterisation. The stacked vertical bar on the right shows the relative distribution of the initial radiotoxicity in the waste vaults. The blue shaded area on the left shows the period of submerged conditions in the base case (present-day climate). The dashed black line represents the regulatory risk criterion.*

10.5.2 Contribution to total annual risk from different radionuclides

In Figure 10-10, the level of radiotoxicity as a function of time, assuming no radionuclide transport from the waste vaults, is shown for the radionuclides with the highest relative radiotoxicity. This figure can be compared with Figure 10-11 that shows the contribution of radionuclides to the total annual risk. It is evident that none of the radionuclides that contribute most to the radiotoxicity of the disposed inventory is contributing significantly to the total annual risk. Radionuclides that contribute most to the radiotoxicity are all relatively immobile (e.g. isotopes of Am and Pu) or decay significantly within the period of submerged conditions (e.g. Cs-137, Ni-63, Sr-90, and Co-60). Instead, other more mobile and long-lived radionuclides contribute most to the total annual risk. The most important radionuclides contributing to the total annual risk as well as the total annual dose in the *base case* are C-14-org, Mo-93, Ca-41, and Ni-59 (Figure 10-11 and Figure 7-14, respectively). However, these four radionuclides together account for only ~0.06 % of the radiotoxicity of the initial inventory (Section 7.4.5), which shows that the safety principle *limitation of the activity of long-lived radionuclides* is of importance and has been implemented adequately.

The less probable scenarios have limited impact on the contributions of individual radionuclides to the maximum total annual risk. The reason is that the less probable scenarios contribute a relatively small fraction (16 %) to the maximum total annual risk (Figure 10-5) and the relative importance of the contributing radionuclides is similar to the *base case*. However, the *earthquake scenario* and the *high concentrations of complexing agents scenario* have a significant impact on the contributions of Ni-59 to the total annual risk from about 10 000 AD. This relates to reduced sorption of Ni-59 in the *high concentration of complexing agents scenario* and that Ni-59 sorption is neglected in the silo after an earthquake in the *earthquake scenario*. In the following, the contributions of key radionuclides to the total annual risk are briefly discussed.

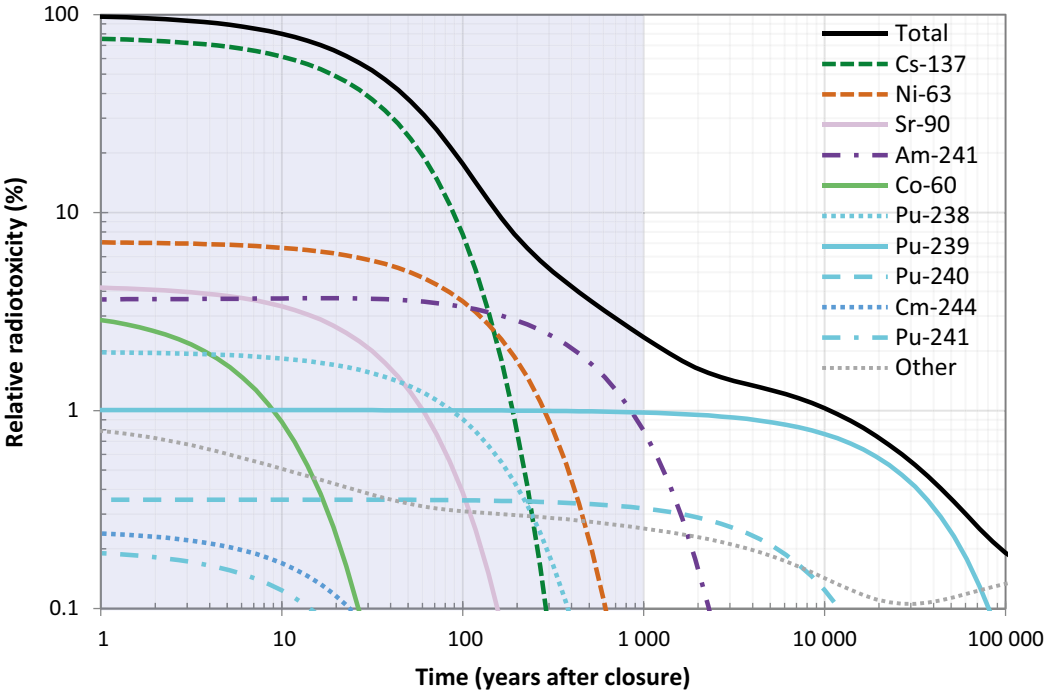

Figure 10-10. *Contributions to total radiotoxicity from individual radionuclides as a function of time, assuming no transport from the waste vaults. Other (grey dotted line) comprises contributions from all radionuclides not visible in the figure. Note that the horizontal axis is displayed in units "years after closure" enabling clear visualisation of the initial development. The blue shaded area shows the period of submerged conditions in the base case (present-day climate).*

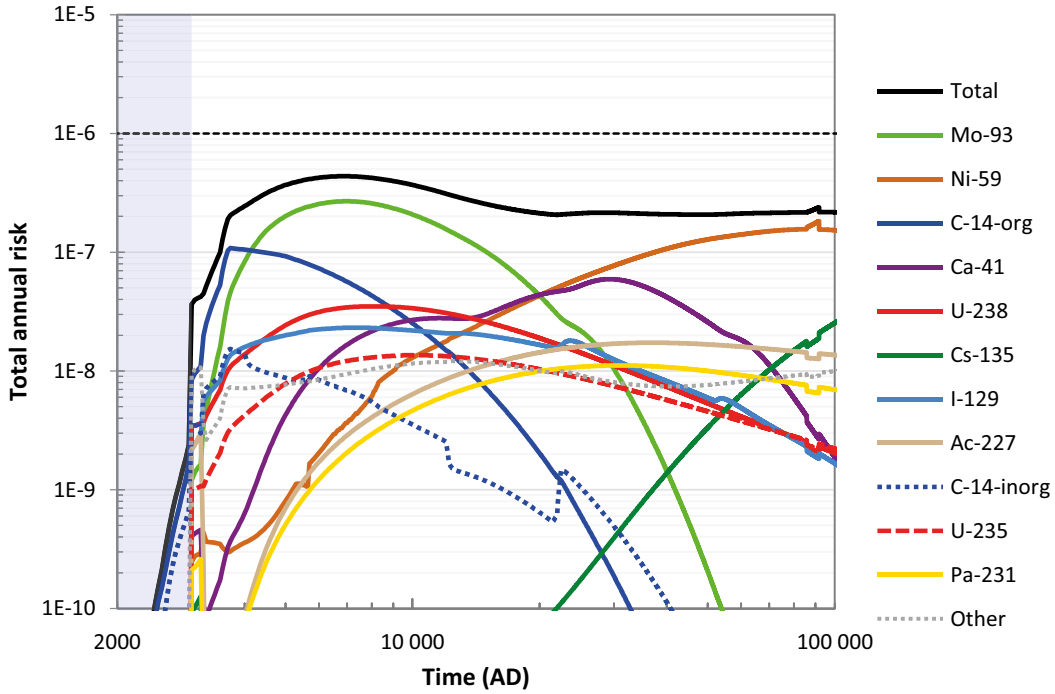

Figure 10-11. *Contribution to total annual risk from individual radionuclides as a function of time, for base case (present-day) climate. The blue shaded area shows the period of submerged conditions in the base case (present-day climate). The dashed black line represents the regulatory risk criterion.*

Contribution of carbon-14

C-14 dominates the total annual risk during the initial marine period (Figure 10-11) due to releases from SFR1 and contributes significantly to the dose during the early terrestrial period. The major part of the inventory of C-14 (Figure 10-12) is in inorganic form (84 %), the remaining part of disposed C-14 is either in organic form (15 %) or is irradiation-induced (1 %). The organic C-14, mainly present in the silo and 1BMA, is more mobile in the near-field than the more abundant inorganic C-14 (Figure 10-12 and Section 7.4.5). Consequently, organic C-14 from these two waste vaults contributes most to the annual dose from this radionuclide in the main scenario *base case* (Figure 7-16). With a half-life of 5 700 years, the contribution to annual risk becomes less important after about 10 000 AD.

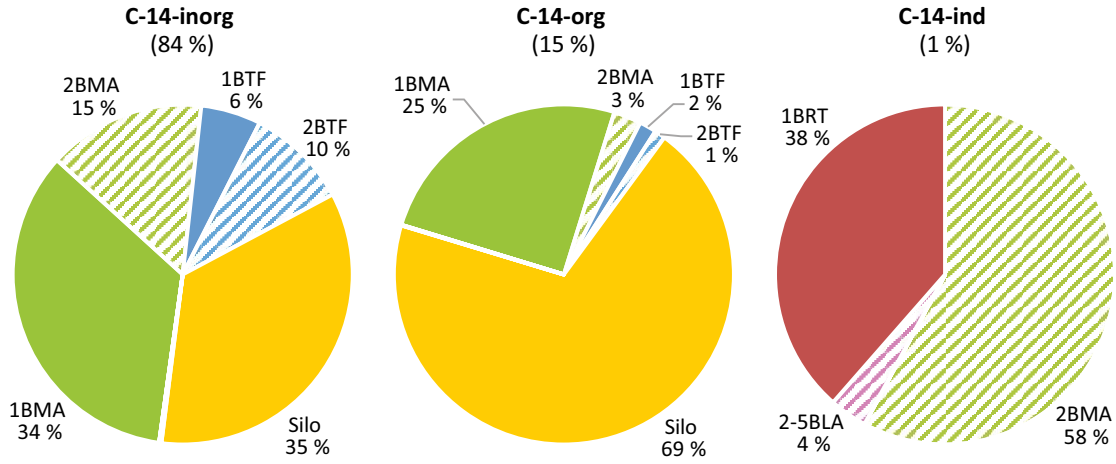

Figure 10-12. *Distribution of disposed inventory of C-14 per form and waste vault (inorg = inorganic, org = organic and ind = irradiation-induced). Labels only shown for vaults with at least 1 % of total disposed inventory.*

As can be seen from Figure 10-5, C-14 contributes mainly to the total annual risk from the main scenario (for annual dose results, see Figure 7-14). However, increased releases of organic C-14 from 1BMA in the *alternative concrete evolution scenario* also influences the annual risk (for annual dose results see Figure 8-5). Releases of C-14 in the *earthquake scenario* do not significantly increase the annual risk (for annual doses, see **Radionuclide transport report**, Figure 7-31). As the three forms of C-14 are not affected by complexing agents (**Data report**, Chapter 7) and most C-14 has decayed before a possible glaciation, there is no or very small effect due to C-14 from the *high concentrations of complexing agents* and the *glaciation scenario* on the total annual risk. As clearly reflected by the distribution of the organic C-14 in the initial inventory (Figure 10-12), the silo and 1BMA contribute most to total annual risk from C-14.

Contribution of molybdenium-93

Mo-93 dominates the total annual risk between 3000 AD and 20 000 AD and contributes 62 % of the maximum total annual risk at 7000 AD (Figure 10-11). Mo-93 is an activation product with a half-life of 4000 years and most of the initial inventory of Mo-93 is found in the silo, with significant, albeit lower, inventories in 2BMA and 1BRT (Figure 10-13). It can be derived from Figure 10-5 that Mo-93 contributes mainly to the maximum annual risk through the main scenario (for annual dose results, see Figure 7-14), but also through the *alternative concrete evolution scenario* (for annual dose results, see Figure 8-5), and to a lesser extent through the *earthquake scenario* (**Radionuclide transport report**, Figure 7-31). As for C-14, there is no, or very small, effect from Mo-93 from the *high concentrations of complexing agents* and the *glaciation scenario* on the total annual risk. For Mo-93, the silo contributes most to the total annual risk followed by 2BMA and 1BRT (noting that about 90 % of Mo-93 is in induced form in 1BRT, leading to slow release), reflecting the distribution of the initial inventory.

Contribution of calcium-41

Ca-41 is one of the largest contributors to the total annual risk from around 10 000 AD to about 60 000 AD (Figure 10-11). Ca-41 has a half-life of 102 000 years and will only be disposed in SFR3. The main part of the inventory (83 %) is located in 2BMA and the rest is evenly distributed between the 2–5BLA vaults (Figure 10-13). As can be seen from Figure 10-5, Ca-41 contributes mainly to the total annual risk through the main scenario (for dose results, see Figure 7-14). However, the earlier and higher release of Ca-41 from 2BMA in the *alternative concrete evolution scenario* means that Ca-41 also influences the total risk from this scenario (for dose results, see Figure 8-5). The annual risk from Ca-41 from other less probable scenarios does not have any significance compared to the *base case*. 2BMA contributes most to total annual risk and 2–5BLA to a smaller extent, which is as expected from the distribution of the initial inventory.

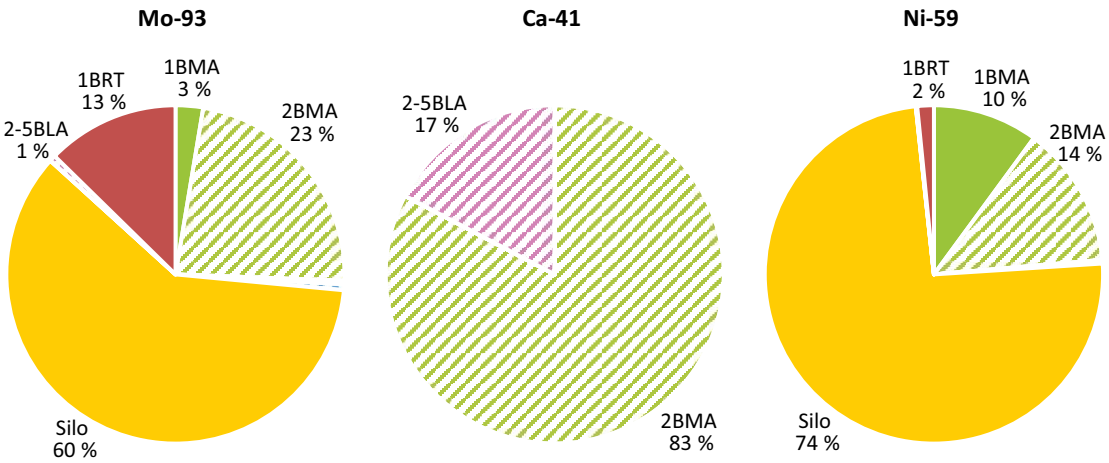

Figure 10-13. *Distribution of disposed inventory of Mo-93, Ca-41 and Ni-59 per waste vault. Labels only shown for vaults with at least 1 % of total disposed inventory in SFR.*

Contribution of nickel-59

Ni-59 is the radionuclide that contributes most to the total annual risk from 20 000 AD and dominates the total annual risk in the later part of the assessment period (Figure 10-11). It has a half-life of 101 000 years and most of the Ni-59 inventory (about 75 %) is found in the silo. The remaining part is placed in 1–2BMA and, to a lesser extent, also in 1BRT (Figure 10-13). In the main scenario, annual dose from Ni-59 increases steadily throughout the full assessment period (Figure 7-14), with 1–2BMA contributing most to the annual dose, followed by 1BRT and the silo (Figure 7-19). The contribution from Ni-59 to the total annual risk occurs earlier compared to the results for the total annual dose in the *base case* (cf. Figure 10-11 and Figure 7-14). In addition, the silo is of increased importance and is the primary source for the total annual risk from 20 000 AD (Figure 10-9).

The reason for the earlier breakthrough and increased contribution from Ni-59 and the silo, as compared to the main scenario, is the relatively significance of less probable scenarios in the risk summation (Figure 10-5). The increase of the annual doses in the less probable scenarios is ~10 times in the *glaciation scenario*, ~8 times in the *high concentrations of complexing agents scenario*, ~50 % in the *alternative concrete evolution scenario* and almost 100 times higher in the *earthquake scenario*. After about 20 000 AD, Ni-59 dominates the annual dose in the *earthquake scenario* (**Radionuclide transport report**, Figure 7-31) and, given the contribution of this scenario to the total annual risk, Ni-59 dominates the contribution to the total annual risk at late times in the assessment period. As the *earthquake scenario* only includes effects on the silo, the silo becomes a more important contributor to the total annual risk than to the annual dose in the main scenario (Figure 7-19). Additionally, mainly due to large contributions from the main scenario and the *high concentrations of complexing agents scenario*, Ni-59 releases from 1–2BMA have a significant influence on the total annual risk at later times. Thus, the resulting contribution of Ni-59 to annual risk reflects mainly the combination of annual risk contributions of the main, the *earthquake* and the *high concentrations of complexing agents* scenarios. As the assumptions in the analysis of the *earthquake scenario* are judged to be pessimistic, the role of Ni-59 in the total annual risk results when the influence of this scenario is large, is likely to be overestimated.

10.5.3 Total annual risk – comparison to SR-PSU results

The present safety assessment is a development from the previous assessment SR-PSU and it might therefore be of interest to compare the results of the two assessments. In Figure 10-14, the total annual risk is shown for the present assessment and for the previous SR-PSU assessment and there are several notable differences. For example, the shape of risk curves in the initial period after submerged conditions and the last 50 000 years of the assessment period are clearly different and the magnitude of total risk is somewhat lower in the PSAR than in SR-PSU. These differences are explained and discussed below.

The differences in the initial period with terrestrial conditions are primarily due to changes in assumptions underlying the biosphere calculations and the handling of intrusion wells. That is, cultivation was not considered until approximately 4500 AD in SR-PSU (**Biosphere synthesis report**, Section 7.5.2) and, thus, the total annual risk in the period between 3000–4500 AD primarily reflected exposure from wells drilled directly into 1BLA and 1BMA[48] and a drilled well down-stream of the repository (see below). In PSAR, the risk from this period mainly reflects early cultivation of a drained mire, as intrusion wells are no longer part of the main scenario (instead they are treated as FHAs, Section 2.6.8) and cultivation of emerged areas of the discharge object is considered.

The sharp and repeated depressions in the annual risk curve in the latter half of the assessment period in SR-PSU are related to periglacial climate conditions that were previously included in the *base case*. In the PSAR, present-day climate conditions are assumed in the *base case* during the full assessment period. The effect of a colder climate can be seen as a small shark's fin at about 90 000 AD in the total annual risk curve, reflecting the contributions from increased post-glacial releases (of Ni-59 from the silo) in the less probable *glaciation scenario* (Figure 10-2). A cold climate with repeated periods of periglacial conditions is also evaluated in the main scenario in the present assessment (Section 7.6). As in SR-PSU, periods with permafrost yielded significantly lower risk than periods with temperate conditions (Figure 10-2). However, as the *base case* always yields a higher annual risk in these periods, the cold climate parameterisation is not limiting with respect to the risk criterion and has therefore not been evaluated with respect to total annual risk (Section 10.4).

[48] Treated as less probable scenarios, with the risk contributions added to the total risk without decreasing the probability of the main scenario by the probability of the less probable scenarios, thus overestimating the dose.

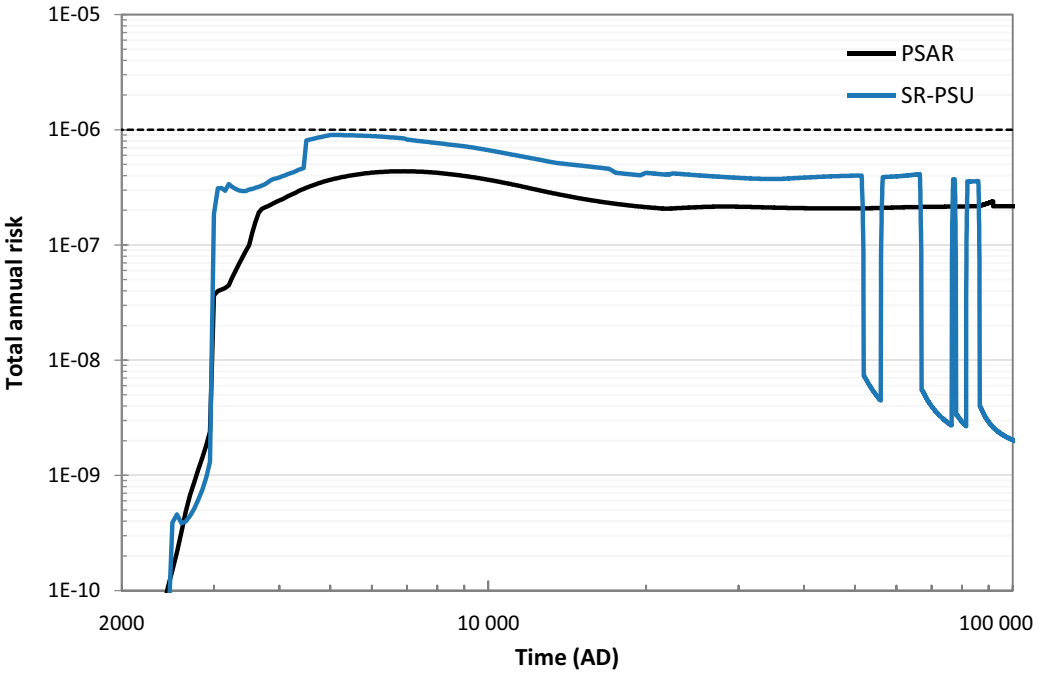

Figure 10-14. *Total annual risk in the present assessment (black line; Figure 10-4) and in the SR-PSU assessment (blue line; SKB TR-14-01, Figure 10-6). The dashed black line represents the regulatory risk criterion.*

The generally lower annual risk in the PSAR than in SR-PSU is due to the combined effect of parameter and modelling updates (**Radionuclide transport report**, Appendix C) and handling of uncertainties within the main scenario that has led to a reduction of the number and influence of less probable scenarios. Moreover, intrusion wells are in PSAR handled as FHA and thus outside the risk assessment. In particular, deterministic approaches were used in SR-PSU to describe geosphere groundwater flow in radionuclide transport calculations and the release of radionuclides to a drilled well downstream of the repository. The fraction of the release that reached the drilled well was set to 10 % for all waste vaults, which was a cautious handling. In the PSAR, the corresponding parameter values are represented by PDFs that are based on multiple underlying realisations. Thus, the characteristics of groundwater flow are centred on typical flow across representative bedrock cases and the characteristics of the release to drilled wells are based on particle tracking to multiple wells from individual waste vaults (**Radionuclide transport report**, Section 5.5). This has resulted in lower average groundwater flow through (and slower transport from) the silo and a lower release to well water for most waste vaults (including 1BLA that contributed most to the annual risk in SR-PSU). It can be noted that the bedrock realisation that was implemented in the main scenario in SR-PSU was judged to result in an uncharacteristically high flow through the silo in comparison to the other representative bedrock realisations. The methodology for including less probable scenarios in the total risk is inherently cautious as the assigned probability represents an upper bound and because the scenarios are only included in the summation when they increase the total risk. In SR-PSU, uncertainties associated with the initial activity of the inventory, with groundwater flow and with the presence of downstream wells, were all handled in separate, less probable, scenarios. In PSAR, these uncertainties are incorporated in the main scenario as data uncertainties and therefore there is no need for the cautious handling connected to less probable scenarios and their probabilities. This contributes to reduce the total risk as compared to SR-PSU. Furthermore, it is also of note that the updated inventories of C-14-org and Mo-93 are approximately 15 % lower in the PSAR than in SR-PSU, resulting in a lower risk.

10.6 Risk dilution

In the context of radionuclide transport, dose and risk calculations, risk dilution in a broad sense refers to a situation in which an increase in the uncertainty of the values of important input parameters, or in the assumptions with respect to the timing of an event, leads to a decrease in the calculated

annual dose and associated annual radiological risk. This can occur even if the inclusion of parameter uncertainty in dose calculations often leads to the opposite effect with broader confidence intervals and higher expected values of the calculated dose, due to positively skewed distributions of key parameters (SKB TR-14-06, Section 10.9 and the **Radionuclide transport report**, Section 10.3). The general cause of risk dilution is an overestimation of the spatial and/or temporal spread of annual dose or risk. In the case of calculations of annual dose from SFR in the PSAR, where all geosphere release is discharged into one biosphere object, the potential causes for dilution are primarily factors influencing the spread of annual dose in time. These include, for instance, probabilistically handled parameters that influence the retardation of radionuclide transport or events occurring at a distinct point in time, such as earthquakes. SSMFS 2008:37 provides guidance on how to deal with the issue of risk dilution that can arise in probabilistic calculations of annual risks for certain types of scenarios.

In the PSAR, the expected value for the annual dose is calculated by running 1 000 simulations with different randomly drawn parameter sets, and then summing the annual dose over all simulations for each point in time, giving each realisation the probability of 0.001. This probability weighted average is referred to as the *expectation value* of the annual dose (or mean annual dose). While this is clearly the expected value of the annual dose for each fixed point in time, it may not give a fair description of the expectation value of the maximum annual dose for all points in time. Thus, if the timing of the maximum (or peak) annual dose differs between simulations, e.g. due to uncertainties in parameters affecting the retardation of radionuclides, then the annual dose to the generation of humans associated with the maximum annual dose in each of the realisations will be underestimated when the average is calculated for a fixed point in time. This is because, even for the time point that yields the highest average annual dose, there will be simulations where the maximum annual dose occurred earlier or later in time. The dilution that occurs from such averaging is expected to be larger for narrow annual dose peaks than for broad annual dose peaks.

A simple method for examining the potential effects of risk dilution is to compare the mean annual dose from the probabilistic calculations with the annual dose calculated from one deterministic realisation based on the best estimate for each input parameter. If the maximum of the mean annual dose from probabilistic calculations is not below the corresponding maximum annual dose from the deterministic calculation, the effects of temporal spread are not likely to have diluted the calculated annual dose significantly. By comparing annual doses using the *base case* it can be noted that a deterministic simulation with best estimate for each input parameter yields a systematically lower annual dose than the average annual dose from probabilistic calculations (Figure 7-20). This indicates that parameter uncertainty does not lead to an underestimation of the annual dose (for further details and discussion about management of uncertainties see the **Radionuclide transport report**, Section 10.3 and the **Biosphere synthesis report**, Section 9.4).

Another method that can be used to assess risk dilution is to utilise the maximum annual dose from each of the probabilistic simulations, irrespective of the time of the maximum. The mean of such maximum annual doses is referred to as the *mean-of-peaks* and it can be contrasted against the maximum expectation value over the assessment period, referred to as the *peak-of-means*. The *mean-of-peaks* is, by definition, greater than (or equal to) the *peak-of-means*. The ratio between the two is hereby referred to as the risk dilution ratio (Wilmot and Robinson 2004). Note that in a deterministic calculation, the maximum annual dose from different radionuclides may also be separated by thousands of years, due to the specific properties of the individual radionuclides, of the repository and of its environment. Thus, some caution must be applied when interpreting annual *mean-of-peak* doses, so that appropriate temporal spread of the annual dose and risk is not unduly disregarded. A comparison between the *mean-of-peaks* and *peak-of-means* for the main scenario *base case* (vertical axis position of grey and orange cross-hairs, respectively, in Figure 10-15) shows that the risk dilution ratio is 1.26, indicating that temporal dilution is not likely to have any significant effect on the results.

Approximately 80 % of the simulations yield maximum annual dose values that occur before 10 000 AD, mainly reflecting the dose from C-14 and Mo-93 (upper histogram in Figure 10-15). However, in a portion of the calculations the maximum annual dose occurs after 10 000 AD. This results in a bimodal distribution of the maximum annual dose with time after 10 000 AD, reflecting the separate contributions of Ca-41 and Ni-59 to the annual dose (second and third peak respectively). Thus, the *mean-of-peaks* calculation combines annual doses from peaks that are separated in time partly due to systematic differences in parameter values between radionuclides in combination with the reference evolution of the repository. Including the second and third peak in the *mean-of-peak* calculations will

over-estimate the potential for risk dilution by not fully accounting for expected effects of retention and dispersion. The picture can be balanced by studying the risk dilution ratio of individual radionuclides, which amounts to 1.05, 1.08, 1.19 and 1.04 for C-14, Mo-93, Ca-41 and Ni-59, respectively. Consequently, the potential for a temporal dilution appears to be 8 % or less for the first 10 000 years when the maximum annual dose (and risk) occurs. This strengthens the conclusion that temporal dilution introduced by probabilistic simulations are unlikely to have any significant effect on the results.

For certain situations where a short-term release may occur at a highly uncertain point in time, it is appropriate to apply alternative methods to calculate the annual risk. The reason for this is that calculating the annual risk as an average per generation may provide an insufficient picture of how risk is allocated between the future generations most affected by the release (Appendix 1 in the general advice to SSMFS 2008:37). Such an approach is applied for an alternative estimate of the annual risk resulting from barrier failure of the silo following an earthquake. In these calculations, the probability of an earthquake that damages the structural integrity of the silo within a specific interval of time is combined with the maximum consequences of an earthquake occurring in that interval (see Appendix F for details). The annual risk calculated with this method represents a type of *mean-of-peak* estimate, that accounts for the increase in the probability of an earthquake having occurred with time since closure. The calculated annual risk based on the results in Section 8.6.3 and using the approach to calculate annual dose described in Appendix F is shown in Figure 10-16. The results are broadly similar. A risk dilution ratio is calculated by dividing the estimate by the *peak-of-means* from the earthquake calculation case. The resulting risk dilution ratio of 1.9 implies that the risk from the alternative way to calculate risk is less than a factor two larger than the standard calculation. It thus indicates that the potential for temporal dilution is limited and that effects of risk dilution on the results are thus also limited.

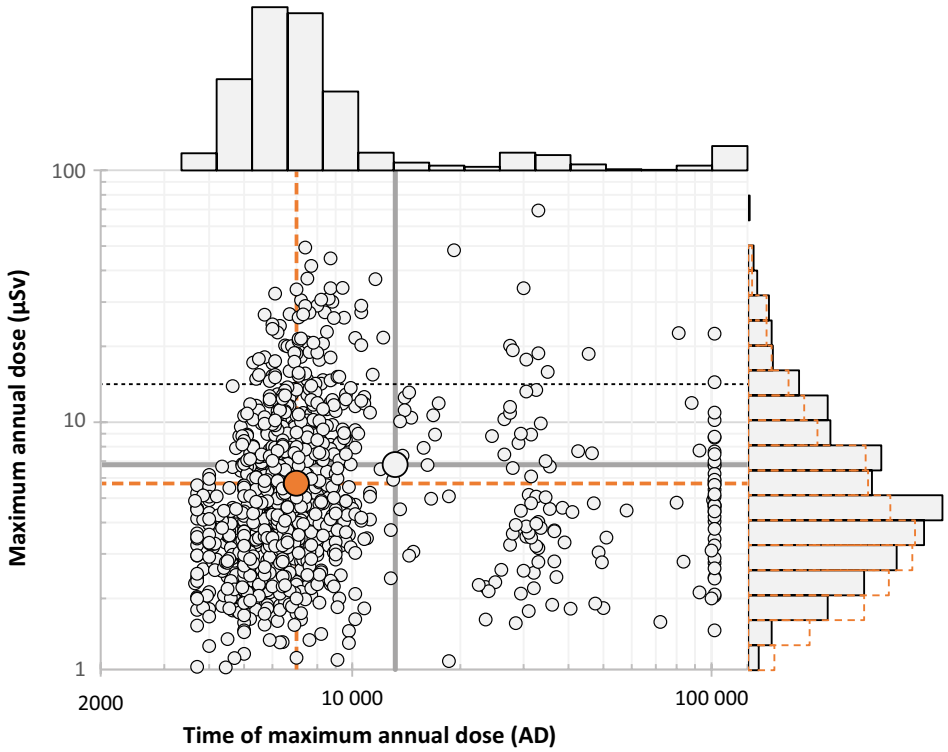

Figure 10-15. *Distribution of peak characteristics for the total annual dose from the 1 000 realisations used in the probabilistic calculations in the base case. The histogram on the right shows the distribution of the peak annual doses and the histogram at the top shows the distribution of the corresponding peak times. The scatter plot in the centre shows these two characteristics for each of the 1 000 realisations. The distribution of the annual dose from each of the simulations at the time of maximum for the average annual dose (~ 7000 AD) is indicated by the orange dashed line in the right-hand histogram for reference. The mean-of-peaks is 26 % higher than the peak-of-means, as indicated by the horizontal grey line being above the horizontal orange dashed line. The mean-of-peaks occurs later than the peak-of-means. The annual dose (14 µSv) corresponding to the regulatory risk criterion is indicated by the thin black dashed line. Figure reproduced from Section 9.4 in the* ***Biosphere synthesis report****.*

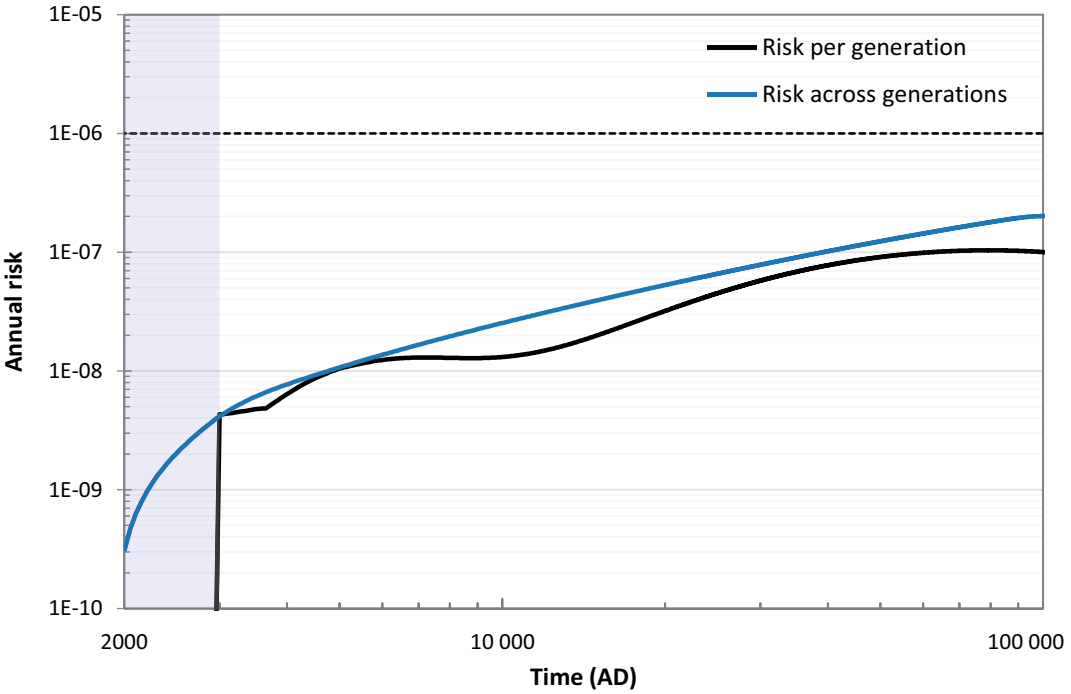

Figure 10-16. *Annual risk resulting from alternative calculations of annual risk in the earthquake scenario representing a mean-of-peak estimate and thus annual risk across generations (blue line) and the annual risk resulting from the earthquake scenario as presented in Section 8.6.3, representing a peak-of-means and thus risk per generation (black line). The blue shaded area shows the period of submerged conditions in the base case (present-day climate). The dashed black line represents the regulatory risk criterion.*

10.7 Additional safety indicators

The general advice in SSMFS 2008:37 and SSMFS 2008:21 suggests that alternative safety indicators should be used for time periods beyond 1 000 years. Below, the estimated activity concentrations in the environment for the main scenario *base case* are compared with activity concentrations of naturally occurring radionuclides.

U-238 and Ra-226 are both naturally occurring radionuclides. In order to illustrate the radiological consequence of the repository, a comparison of calculated activity concentrations in environmental media for the main scenario *base case* and natural activity concentrations in Forsmark is presented in Table 10-3. It can be seen that the calculated concentrations obtained for the *base case* for these two radionuclides are below the naturally occurring levels. Thus, potential releases from the repository will not lead to a significant increase of environmental activity concentrations of U-238 and its decay products.

A study of 818 Swedish wells made by SGU and SSI (Ek et al. 2007) also shows that the calculated activity concentrations in well water obtained in the *base case* (Table 10-3) are far below those occurring in natural groundwaters, Table 10-4.

Table 10-3. Comparison of activity concentration maxima obtained for the main scenario base case (present-day climate) against typically occurring concentrations in Forsmark (SKB TR-10-09).

Radionuclide	Concentration in soil* (Bq kgDW^{-1})		Concentration in surface waters (Bq L^{-1})		Concentration in well water (Bq L^{-1})		
	Base case	Top soil, Forsmark	Base case	Lake water, Forsmark	Base case, dug well	Base case, drilled well	Near surface groundwater, Forsmark
U-238	1.7×10^{0}	4.6×10^{1}	1.3×10^{-4}	1.5×10^{-2}	3.0×10^{-3}	1.5×10^{-2}	7.4×10^{-2}
Ra-226	9.7×10^{-4}	3.9×10^{1}	3.2×10^{-7}	6×10^{-3}	2.7×10^{-5}	9.8×10^{-4}	7.2×10^{-2}

* Dry weight, RegoUp, see the **Biosphere synthesis report**.

Table 10-4. Activity concentration in 818 wells in Sweden (Ek et al. 2007).

Radionuclide	Min (Bq L^{-1})	Average (Bq L^{-1})	Max (Bq L^{-1})
U-238*	3.7×10^{-4}	2.2×10^{-1}	1.3×10^{1}
Ra-226	2×10^{-2}	9.4×10^{-2}	6.0×10^{0}

* In the report given as 0.03 µg L^{-1}, 18 µg L^{-1} and 1.014 µg L^{-1}.

10.8 Protection of the environment

According to SSM's regulations (SSMFS 2008:37, Section 6) it is required that *the final management of spent nuclear fuel and nuclear waste shall be implemented so that biodiversity and the sustainable use of biological resources are protected against the harmful effects of ionising radiation*.

To assess the biological effects of ionising radiation in the habitats and ecosystems concerned, the ERICA Integrated Approach (Larsson 2008) is applied. Within this framework, absorbed dose rates to reference organisms are calculated using the ERICA code (**Biosphere synthesis report,** Section 12.3 and Appendix D). The ERICA reference organisms are judged to be suitably representative of species in Sweden, including sensitive species presently living in the Forsmark area (Jaeschke et al. 2013). The methodology meets the regulatory requirement to account for the existence of genetically distinctive populations such as isolated populations, endemic species and species threatened with extinction and in general any organisms worth protecting. The results of the calculations are interpreted with respect to the ERICA screening dose rate, as recommended in the ERICA Integrated Approach (**Biosphere synthesis report**, Section 12.2). The ERICA approach utilises a single screening dose rate of 10 µGy h^{-1} across all organism types. Consideration is also given to relevant screening benchmarks recommended by ICRP (4–4 000 µGy h^{-1}; ICRP 2008), where these are more restrictive than the generic ERICA screening value. Given that there are no quantitative regulatory criteria for protection of the environment with regard to ionising radiation, these values are considered to be relevant for the assessment of regulatory compliance, noting that the methodology is in line with the general guidance in ICRP (2003) that SSM recommends in the general guidance to SSMFS 2008:37.

In all calculation cases, the maximum dose rates are three orders of magnitude below the ERICA screening dose rate (10 µGy h^{-1}) and occur relatively early in the assessment period (**Biosphere synthesis report**, Section 12.8). Furthermore, all dose rates are considerably below the lower boundary of the most restrictive ICRP derived consideration reference level (4 µGy h^{-1}; which only applies to certain vertebrate animals and coniferous trees). The calculations are based on all climate cases considered in the main scenario as well as the supporting calculation case addressing alternative delineations of biosphere object 157_2 (**Biosphere synthesis report** Section 12.8). The results show that, compared with the margin between the calculated dose rates and the screening dose rates of concern, the dose rates are relatively insensitive to the considered span in climate conditions and object properties.

The results indicate that no adverse impacts on populations of NHB are expected from radionuclides released from the repository. Hence, it can be concluded that the repository ensures that biodiversity and sustainable use of biological resources in the Forsmark area are protected against the harmful effects of ionising radiation and that this conclusion is robust with respect to uncertainties in the future climate and the development of the landscape.

11 Conclusions

The main objective of the post-closure safety assessment documented in the present report is to demonstrate that SFR is, after closure, radiologically safe for humans and the environment. For this purpose, the safety assessment has been performed using a methodology that follows the requirements and general advice given in the Swedish Radiation Safety Authority's (SSM's) regulations (SSMFS 2008:21 and 2008:37). The results of the safety assessment thus allow for the evaluation of the authority's requirements concerning post-closure safety and the protection of human health and the environment.

In Section 11.1, both compliance with regulations regarding the protection of human health and the environment, as well as the robustness of the barrier system, are demonstrated. The compliance with these requirements as stated in Section 11.1 is based on an extensive underlying understanding of the repository and its environs supported by a broad analysis of these systems as presented in the previous chapters of this report. The results and discussions in these chapters are, in turn, supported by the main references. Where appropriate, additional scientific literature is cited throughout the different parts of the analysis. In Section 11.2, important aspects that support the confidence in the compliance stated in Section 11.1 are discussed. In the framework of the process of successive safety assessments coupled to stepwise licensing, each assessment is developed in the context of earlier assessments and feedback is given to facilitate the subsequent steps in the repository programme. These developments and feedback are discussed in Section 11.3.

11.1 Demonstration of compliance

In the following, compliance is demonstrated with regard to both requirements on the protection of human health and the environment, as well as the robustness of the barrier system. These aspects are considered to be the central parts of SSM's post-closure regulations SSMFS 2008:37 and 2008:21. A discussion of compliance with each requirement of these regulations, together with how the recommendations in the related general advice have been considered, is presented in Appendices B and C.

11.1.1 Protection of human health and the environment

The protection of human health after closure is regulated in Section 5 of SSMFS 2008:37, which states that *a repository for spent nuclear fuel or nuclear waste shall be designed so that the annual risk of harmful effects after closure does not exceed 10^{-6} for a representative individual in the group exposed to the greatest risk. […]*.

During the entire assessment period of 100 000 years, the total annual risk is shown to be below the risk criterion. This statement is based on the results presented in Figure 10-4 that illustrate the total annual risk obtained from the summation of the risk contributions from the main scenario and all less probable scenarios over the assessment period. The results are explained and interpreted in depth with respect to the contribution of the different scenarios, individual waste vaults and specific radionuclides in Sections 10.4–10.5. It can be concluded that SFR is designed such that the annual risk of harmful effects after repository closure does not exceed 10^{-6} for a representative individual in the group exposed to the greatest risk.

The protection of the environment after closure is regulated in Section 6 of SSMFS 2008:37, which states that *the final management of spent nuclear fuel and nuclear waste shall be implemented so that biodiversity and the sustainable use of biological resources are protected against the harmful effects of ionising radiation.*

The results of the assessment of the biological effects of ionising radiation on the habitats and ecosystems concerned show that biodiversity and sustainable use of biological resources in the Forsmark area are protected against the harmful effects of ionising radiation (Section 10.8). The calculations performed are based on the framework of the ERICA Integrated Approach (**Biosphere synthesis report**, Section 12.2) and consider all climate evolutions of the main scenario and a range of biosphere object properties. In all calculation cases, the maximum dose rates are three orders of magnitude below

the ERICA screening dose rate (10 μGy h^{-1}) and occur relatively early in the assessment period (**Biosphere synthesis report**, Section 12.8). Furthermore, all dose rates are considerably below the lower boundary of the most restrictive ICRPs derived consideration reference levels (4 μGy h^{-1}; which only applies to certain vertebrate animals and coniferous trees, ICRP 2008). If dose rates are below these screening values, any potential release from the repository is highly unlikely to cause detrimental effects on the survival and reproduction of individual organisms. As no effects are expected at the level of individual organisms, effects at the levels of populations, communities and ecosystems are also highly unlikely. It can thus be concluded that the extended SFR complies with SSM's regulations regarding the protection of the environment.

11.1.2 Robustness of the barrier system

The regulations concerning safety in connection with the disposal of nuclear material and nuclear waste require that *safety after closure shall be maintained through a system of passive barriers* (SSMFS 2008:21, Section 2) and that *the function of each barrier shall be to, in one or several ways, contribute to the containment and prevention or retention of dispersion of radioactive substances, either directly or indirectly by protecting other barriers in the barrier system* (SSMFS 2008:21, Section 3).

The system of passive barriers is described as part of the initial state, including the waste form and waste packaging (Section 4.3), engineered barriers (Section 4.4) and natural barriers (Section 4.7). Each barrier is assigned one or several safety functions based on the safety principles for SFR that are formulated as *limitation of the activity of long-lived radionuclides* and *retention of radionuclides* (Section 2.2). The safety functions all contribute to the containment and prevention or retention of dispersion of radionuclides, either directly or indirectly by protecting other barriers in the barrier system (Chapter 5). The barrier system effectively retains, or prevents the dispersion of, radionuclides initially present in the waste. This can be illustrated by the results of the risk calculations that show that none of the radionuclides that contribute most to the total radiotoxicity at closure give any significant contribution to the total annual risk after closure (Section 10.5.2, Figures 10-10 and 10-11).

SSM's regulations include requirements on the design and construction of the barrier system. *The barrier system shall be able to withstand such features, events and processes that can affect the post-closure performance of the barriers* (SSMFS 2008:21, Section 5).

The safety assessment includes a thorough discussion on all features, events and processes (FEPs) potentially relevant for the post-closure performance of the barriers (Chapter 3). The reference evolution is based on these FEPs and describes the evolution of the waste form and waste packaging, engineered barriers and natural barriers for the duration of the assessment period. The reference evolution is the basis for the selection of the scenarios, which are assessed in Chapters 7–8 and address FEPs coupled to the performance of the barriers, including their initial state, as well as internal and external processes affecting the barriers during the assessment period. The subsequent risk assessment demonstrates that the total annual risk is below the regulatory risk criterion (Chapter 10). The conclusion is that the barrier system will withstand the FEPs that have been identified as being able to affect the post-closure performance of the barriers.

This conclusion is strengthened by the results of the analysis of a set of residual scenarios that primarily aim to illustrate the significance of individual barriers and barrier functions and how they contribute to the protective capability of the repository (Chapter 9). These show that, even in cases of hypothetical defects that strongly affect the safety functions of the repository in an unrealistic way, as in the *loss of engineered barrier function* and *loss of geosphere barrier function scenarios,* the calculated maximum annual dose to the most exposed group is of the same order of magnitude as the annual dose corresponding to the risk criterion. It can be noted that the risk criterion corresponds to a dose that is two orders of magnitude lower than the annual natural background radiation in Sweden of about 1–2 mSv.

According to the regulations, *the barrier system shall be designed and constructed taking into account the best available technique* (BAT; SSMFS 2008:21, Section 6). The license that the government granted for the extended SFR implies that the facility, as described in SKB's application filed 2014 and associated amendments, was considered to comply with requirements on BAT. Thus, the discussion related to BAT in the present step in the stepwise licensing regards only changes to the barrier system

made since F-PSAR. The barrier system of the extension of SFR (SFR3) has not been modified in relation to F-PSAR. The representation of the barrier system of the existing SFR (SFR1) has, however, been developed since F-PSAR. The initial state of the present post-closure safety assessment differs from F-PSAR with regard to the repair measures adopted for 1BMA. Moreover, further refinements of the repair measures, as presented in this assessment, are ongoing. The objective of the repair measures is to prevent, limit and delay releases from the engineered barriers and thereby to comply with the BAT requirement. It can be noted that the effect on radionuclide releases of assuming that repair measures are not carried out are relatively small, as shown in the residual scenario *unrepaired 1BMA* (Section 9.9). In conclusion, the barrier system of SFR is designed and constructed taking BAT into account.

BAT is related to preventing, limiting and delaying releases of radionuclides from both engineered and geological barriers of the repository. In addition to BAT, also *optimisation must be performed* (SSMFS 2008:37, Section 4). In general, the consideration of BAT also leads to optimisation of the protective capability of the repository with respect to risk (unless, for instance, an early release and dilution in the Baltic Sea should lead to lower annual doses than retention in the repository and later, less diluted, releases to a terrestrial area). The update of the waste acceptance criteria (WAC) since SR-PSU improves the control of future waste disposed and thus leads to smaller uncertainties regarding the actual initial state. Consequently, the protective capability of the repository has been optimised. The revision of the WAC also leads to further optimisation of this capability via the distribution of the wastes between the waste vaults.

A further requirement by SSM is that *the barrier system shall comprise several barriers so that, as far as possible, the necessary safety is maintained despite a single deficiency in a barrier*. (SSMFS 2008:21, Section 7). The different waste vaults have multi-barrier systems that have been adapted to match the waste characteristics and associated risk of harmful effects. The inventory with the highest radiotoxicity is placed in vaults having engineered barriers with the highest retention capabilities, i.e. the silo followed by 1–2BMA. The implications of single deficiencies in individual barriers are analysed in the less probable and residual scenarios (Chapters 8–9) and the results show that the post-closure safety is not unduly dependent on a single barrier or barrier function.

The conclusions in this section demonstrate that the extended SFR complies with SSM's regulations regarding the robustness of the barrier system.

11.2 Confidence in compliance

There are several aspects of the present post-closure safety assessment that strengthen confidence in the compliance as stated in Section 11.1. These are discussed below.

11.2.1 Safety assessment methodology

The applied assessment methodology is well developed and tried and tested. SKB has, over the last few decades, performed a series of post-closure safety assessments for SFR and the spent nuclear fuel repository, along with a safety evaluation of SFL, with successive enhancements of different parts of the methodology. This work has been subject to several regulatory reviews, the latest being SSM's reviews of SE-SFL, SR-SPU, SR-Site, SAR-08 and SR-Can (SSM 2021, 2019, 2018, 2009, SKI/SSI 2008). SSM concluded that the regulatory requirements regarding methodological aspects were addressed in an acceptable way in the SR-PSU. SSM commented on some methodological aspects in their review of the SR-PSU and these comments have been addressed in the present post-closure safety assessment. For instance, the description of the management of uncertainties and the selection of scenarios has been developed. The programme for the extension of SFR (PSU) follows the steering documents and process instructions that are part of SKB's ISO certified (ISO 9001:2015) integrated management system. Furthermore, programme-specific steering documents have been established (Section 2.8). This includes e.g. the *Quality plan for the SFR extension programme* (see Table 2-2). For the reporting of the post-closure safety assessment, process instructions on formal review have been implemented. In summary, the methodology is considered adequate to be able to draw firm conclusions from the results of the post-closure safety assessment regarding regulatory compliance.

11.2.2 Foundations of barrier design and repository system understanding

The post-closure safety assessment of SFR is based on a well-defined and understood initial state (Chapter 4). The repository has been designed and its location has been chosen so as to ensure safe disposal of the low- and intermediate-level radioactive waste included in the inventory. The barrier design is coupled to the overall post-closure safety principles *limitation of the activity of long-lived radionuclides* and *retention of radionuclides* (Section 2.2). The barrier design is adapted to the waste form and packaging and the characteristics and radiotoxicity of the radionuclides in the inventory. The main part of the radiotoxicity is disposed in the silo and 1–2BMA that have the engineered barrier systems with the highest retention capabilities. For low radiotoxicity wastes, a simpler barrier design is accordingly adapted. During construction, operation and before closure, the barriers are inspected to ensure they are in an adequate state for their required purpose (Section 4.4). The radionuclide inventory at closure is estimated accounting for uncertainties (Section 4.3.7) and SKB's requirements, particularly the WAC and the waste type descriptions, ensure that the waste's properties are appropriate in relation to post-closure safety.

The assessment of post-closure safety is based on an adequate understanding of the evolution of the repository and its environs. The site of SFR has been thoroughly investigated and characterised in the site descriptive model (SKB TR-11-04), and the evolution of the repository system has been analysed over the assessment period. Supplementary investigations at the site have been performed in five core-drilled boreholes as a part of the preparations for construction of SFR3 (Earon et al. 2022). The investigations confirm the understanding of the site presented in the site descriptive model.

The reference evolution is based on a scientifically founded process understanding regarding the evolution of the repository with its barriers and the environs, as described in the FEP analysis (Chapter 3) and associated reports, including the process reports. The main scenario is based on probable evolutions of external conditions and credible assumptions with respect to internal conditions. Additional scenario uncertainty is addressed in supporting calculation cases (Section 7.7) and in the less probable scenarios (Chapter 8). In some instances, pessimistic or cautious assumptions are applied when a thorough substantiation is not possible or justified. It can be noted that the main contribution of the post-closure safety assessment to the preliminary safety analysis report is to demonstrate that SFR is radiologically safe for humans and the environment after closure. Thus, cautious or pessimistic assumptions imply that the risk is expected to be overestimated. Analyses conducted to optimise the protective capability of the repository need to account for such assumptions.

The well-defined initial state and the well-founded understanding of the evolution of the repository system underpins SKB's confidence in the compliance stated in Section 11.1.

11.2.3 Post-closure performance of the repository system

As long as the area above the repository is submerged beneath the Baltic Sea, groundwater flow through the repository is low due to low hydraulic gradients. This, together with the initial state of the engineered barriers ensures that release of radionuclides is minimised. Human intrusion, in particular due to drilling into the repository for potable water, is restricted by the subsea location. The uncertainties regarding the protective capability of the repository during this period are low. During this period, a large part of the initial radiotoxicity is lost owing to decay in the repository of radionuclides with relatively short half-lives, such as Cs-137 and Ni-63 (Figure 10-10).

When the area above the repository becomes terrestrial, groundwater flow will increase and the groundwater flowing through the repository is expected to discharge along the shoreline, in lakes, and in terrestrial areas north of SFR. Due to the flat topography in the area around SFR, the hydraulic gradients and so groundwater flow will still be limited. The flow-limiting concrete barriers degrade slowly and, in the main scenario, it is not until 20 000 years post-closure that the flow-limiting capabilities of the engineered barriers in 1–2BMA are expected to be lost. The less probable scenario with alternative concrete evolution shows that deviations of the safety function *limit advective transport* is relevant, but uncertainties in flow-limiting properties due to degradation of the cementitious materials are unlikely to compromise the protective capability of the repository. The bentonite hydraulic barrier in the silo is expected to be maintained throughout the assessment period. Even for the radionuclides that dominate the total risk in the first 20 000 years post-closure, retention and

decay in the repository is effective. For instance, for Mo-93 and C-14 which provide the largest contributions to the total annual risk, about 90 % and 50 % of their initial inventory, respectively, are retained and decay in the repository in the *base case* (Section 7.4.5).

For the time after 20 000 years post-closure, only very long-lived radionuclides or their decay products have any significant effect on the total annual risk. Ni-59 provides a relatively large contribution to the total annual risk at late times. In the *base case*, about 97 % of the initial inventory is expected to be retained in the repository (mainly the silo) due to sorption and scenarios where there is a substantial release of Ni-59 are less probable (Section 10.5.2).

Concrete remains a good sorbent of many radionuclides for a very long time. The cementitious materials in the silo and 1–2BMA degrade mineralogically, in the main scenario they reach a state characterised by portlandite dissolution (pH ~ 12.5) after 32 000 and 10 000 years, respectively. This state is then maintained throughout the entire assessment period. Thus, the sorption properties of the most important very long-lived radionuclides, such as Ni-59, are upheld until the end of the assessment period. Uncertainties in sorption in the repository are evaluated by probabilistic handling in the main scenario and furthermore in a less probable scenario assuming high concentrations of complexing agents in the waste. The results from this scenario show that a reduction in sorption may lead to an eightfold increase in the contribution from Ni-59, but the maximum annual dose to the most exposed humans still does not exceed the dose in the main scenario. Radionuclides that are weakly or non-sorbing under repository conditions and have very long half-lives, such as I-129 or Ca-41 (noting that Ca-41 sorbs significantly during chemical concrete degradation state I, but not thereafter), are difficult to retain over very long time periods. Therefore, the limitation of the inventory of such radionuclides is important to be able to meet the risk criterion.

Uncertainty in the climate evolution is addressed in the main scenario and in the less probable *glaciation scenario*. The effect of an earthquake occurring that is strong enough to affect the barriers of the silo is analysed in the *earthquake scenario*. Both scenarios contribute to the total annual risk and thus these uncertainties are included in the evaluation of the post-closure safety.

The results of the radionuclide transport and dose calculations are analysed in depth in the **Radionuclide transport report**. Uncertainties in the biosphere and dose calculations are discussed in depth in the **Biosphere synthesis report**, Chapter 13. The discussions include the sensitivity of the results to different uncertainties and assumptions. For example, through a combination of alternative models and sensitivity analyses in the **Biosphere synthesis report**, it is shown that the results from the *base case* are robust with respect to uncertainties in the landscape development, in object properties and in the local hydrology. Thus, the interpretations of the results are well-founded, strengthening them as a basis for the compliance discussion.

As required by SSM's regulations the collective dose has been calculated. The *base case* of the main scenario as well as several additional calculation cases have been the basis for the calculations of collective dose to the global population from C-14 (1.6–2.0 man Sv) and collective dose to the regional population around the Baltic Sea from all radionuclides (0.12–0.14 man Sv; **Radionuclide transport report**, Chapter 9).

In addition to the analysis of post-closure safety based on the reference evolution, the effects of future human actions (FHA) are analysed as required in SSM's regulations (SSMFS 2008:37, Section 9). The results of the FHA calculation cases do not directly relate to compliance with the risk criterion or the robustness of the barrier system (Sections 11.1.1–11.1.2). However, they can be compared with the criterion set out by the IAEA (2011) for when efforts to reduce the probability of intrusion or to limit its consequences are warranted. The conclusion from such a comparison is that no further efforts are warranted (Section 9.11.3).

In summary, the understanding of the evolution of the repository system, together with credible or pessimistic assumptions in the radionuclide transport and dose calculations, and thoroughly interpreted results, lend confidence in the compliance stated in Section 11.1.

11.2.4 Management of uncertainties

SKB's safety assessment methodology has been developed accounting for regulatory requirements on management of uncertainties. In Section 2.5, it has been made more transparent than in previous assessments that uncertainty management is an integral part of the methodology. In Section 2.6, the management of uncertainties in each safety assessment step is described. The uncertainties are classified into scenario uncertainty, system uncertainty, modelling uncertainty and data uncertainty and all these types of uncertainties have been addressed in the risk assessment. Moreover, the residual scenarios can be used to discuss uncertainties as their parameterisation lies outside the realistic range and they can be viewed as bounding cases.

The *base case* within the main scenario has been defined as the basis for the radionuclide transport, dose and risk calculations. Scenario and modelling uncertainties are addressed by a set of additional simulations (e.g. alternative climate evolutions within the main scenario). Potential risk from several less probable scenarios is also taken into account. The selection of less probable scenarios is based on an analysis of uncertainties to determine if there is a possibility that the status of the safety functions deviates from that in the main scenario in such a way that post-closure safety may be impaired (Section 8.2).

System uncertainty is accounted for in the FEP-analysis described in Chapter 3. That is, the FEP analysis ensures that all aspects important for post-closure safety have been identified and properly addressed in the safety assessment. This includes, for instance, handling of FEPs that relate to uncertainties in the repository evolution and to uncertainties due to defects in engineered barriers and the initial state of the repository.

Modelling uncertainty is addressed in several steps in the safety assessment methodology. Many internal processes considered are handled with modelling and in relation to the description of the internal processes in the process reports, modelling uncertainty is addressed (Section 2.6.4). Modelling uncertainty and data uncertainty may be coupled to each other and, in the methodology for qualification of input data, (Section 2.6.6 and the **Data report,** Section 2.3), discussion of the role of modelling uncertainty is included. Moreover, modelling uncertainty is addressed in some less probable scenarios and in supporting calculation cases in the main scenario (Sections 2.6.8 and 2.6.9).

To account for data uncertainty, the radionuclide transport and dose calculations have been performed with a probabilistic approach and, where justified, cautious or pessimistic assumptions have been made. To evaluate specific uncertainties in external conditions and internal processes that are potentially important for radionuclide transport, supporting calculation cases have been performed as part of the main scenario (**Radionuclide transport report**, Section 5.8 and the **Biosphere synthesis report,** Chapters 10 and 11).

An in-depth discussion of system, scenario, modelling and data uncertainties relating to the biosphere analysis, including their effect on the results of the dose calculations, is presented in the **Biosphere synthesis report**, Chapter 13.

Residual scenarios can be viewed as bounding cases and it can be noted that the results of some of the residual scenarios are rather similar to less probable scenarios that relate to the same barrier functions. For instance, the results of the residual scenario *initial concrete cracks*, that evaluates the effects of the concrete structures of the silo, 1–2BMA, and 1–2BTF initially being severely degraded (Section 9.8), gives approximately the same maximum annual dose as the less probable scenario *alternative concrete evolution* (Section 8.5). This illustrates that the uncertainties in concrete evolution are handled cautiously in the less probable scenario. It also indicates that the dose results are not very sensitive to any additional uncertainties in the underlying processes that may impact the hydraulic properties of the concrete barriers. Another aspect is that uncertainties in underlying processes, which are thoroughly documented in relation to the selection of less probable scenarios (Section 8.2), do not necessarily have a significant impact on the results. For instance, the effect of a more rigorous coupling of physical and chemical concrete degradation is not likely to have large effects on the annual risk.

The residual scenarios that neglect either sorption in the repository or the hydraulic barrier function of the bentonite in the silo (Sections 9.4.2 and 9.4.3), both show significant effects on the annual dose compared with related less probable scenarios (*high concentrations of complexing agents*

scenario, Section 8.4; and *glaciation scenario*, Section 8.3). But, as noted in Section 11.1.2, these hypothetical cases still only yield annual doses on the same order of magnitude as the annual dose corresponding to the risk criterion. Neglecting geosphere retention in the residual scenario *loss of geosphere barrier function* (Section 9.5) shows that geosphere retention affects the resulting dose but the results indicate that geosphere barrier functions are less critical for the maximum dose than the engineered barriers evaluated in Section 9.4.

Results from the residual scenario *alternative radionuclide inventory* (Section 9.5) confirm that a fractional increase in the radionuclide inventory yields a similar fractional increase in the maximum dose. This illustrates the importance of controlling uncertainties in the inventory and upholding the safety function *limit quantity of activity*. This is achieved by accepting only certain kinds of waste in SFR (Section 4.3.4) and by regulating the radionuclide activity in each waste vault (Section 4.3.7).

Significant effort has been made in the safety assessment to manage uncertainties, in particular in the radionuclide transport and dose calculations. The annual doses resulting from residual scenarios that are related to the barrier functions are, due to their hypothetical nature, considered to be higher than from any realistic scenario. Still, the annual doses from these residual scenarios, that can be viewed as bounding cases, are close to the annual dose corresponding to the risk criterion. Taken together, confidence is high that uncertainties are adequately managed and that the calculated total annual risk is not underestimated. This strengthens confidence in the compliance stated regarding both the protection of human health and the environment as well as the robustness of the barrier system.

11.3 Development of the safety assessment and feedback to subsequent steps in the repository programme

11.3.1 Developments since SR-PSU

At a general level, a description of significant changes since SR-PSU is given in Section 1.5.2. Since the SR-PSU assessment, SKB's RD&D program has continued with efforts that are related to the safety assessment (SKB TR-19-24, SKB TR-22-11).

In relation to the repository, several projects have had the objective of improving the basis for the post-closure safety assessment, summarised below.

- The concrete caissons of 2BMA have been examined in detail to demonstrate that an adequate initial state without detrimental cracking can be achieved (SKB TR-19-24, Section 10.2.1; Mårtensson and Vogt 2020). Thus, the confidence in the initial state of 2BMA has been strengthened since SR-PSU.
- The confidence in the initial state of 1BMA has been strengthened by efforts in relation to the repair measures to be adopted (SKB TR-22-11, Chapter 9). Since SR-PSU, SKB has carried out further work on mechanical stability of the concrete barriers in 1BMA and anticipated measures including the construction of concrete walls outside the existing structure and casting a concrete lid on top of the concrete structure.
- The closure plan for SFR (Mårtensson et al. 2022) has been updated with the updated layout.
- Work is ongoing regarding the analysis of gas generation and transport in 1BMA.
- Further investigations have been carried out regarding sorption of very long-lived radionuclides of importance for the post-closure safety. This includes new information concerning sorption on cementitious materials (**Data report**, Chapter 7) that is based on Nagra's database (Wieland 2014) and specific experimental studies (Tits et al. 2014, Bruno et al. 2018, Tasi 2018).
- Additional information on sorption reduction factors is also given based on Keith-Roach et al. (2021). Thus, confidence in the quantification of sorption for some of the assessed radionuclides, including Ni(II), Pu(IV), and Th(IV), has increased since SR-PSU.
- A literature review of data on metal corrosion has been carried out and data used in the present post-closure safety assessment have been updated accordingly (Section 6.2.8 and the **Data report**, Chapter 5). This increases confidence in the quantification of metal corrosion processes that are important for release of irradiation-induced activity in 1BRT and gas generation.

- The inventory has been updated (Chapter 4) and smoke detectors that were part of the SR-PSU inventory have now been reallocated to SFL, significantly lowering the radiotoxicity of the inventory.
- The WAC have been updated since SR-PSU to ensure adequate limitation of organic complexing agents in the newly produced waste (Keith-Roach and Shahkarami 2021).
- Finally, the layout of the tunnels and vaults of SFR3 has been updated and refined (Chapter 4).

In relation to the safety analysis calculations, the following improvements have been made.

- Probabilistic methods have been introduced in the present post-closure safety assessment for some aspects that were handled deterministically in the SR-PSU. For instance, the estimation of the inventory, calculation of corrosion in 1BRT and groundwater flow in the radionuclide transport calculations.
- Radionuclide transport calculations for 2BMA using a model that better reflects the actual design has been implemented to create a more transparent approach.
- Further analysis of risk dilution has been carried out (Section 10.6).
- The handling of drilled wells in the dose calculations has been updated (**Biosphere synthesis report**, Section 7.5.4).
- Since SR-PSU, the representation of climate and climate-related processes used for the post-closure safety assessment have been reviewed and updated based on the latest scientific developments (**Climate report**). In particular, the potential duration of the periods during which the area above the repository is submerged have been updated based on recent studies on future sea level rise (**Climate report**, Section 3.5). Consequently, radiological consequences related to the duration of the submerged period are more thoroughly investigated in this safety assessment than in the SR-PSU (Section 7.7).
- The biosphere assessment has been further developed, for instance the discretisation of the BioTEx model has been improved, the data used in the assessment have been updated and a set of calculation cases has been selected to improve the evaluation of key uncertainties (**Biosphere synthesis report**, Section 1.3.2).

11.3.2 Feedback to subsequent steps in the repository programme

The main objective of the safety assessment is to demonstrate that SFR is radiologically safe for humans and the environment after closure. The assessment is a basis for SSM to evaluate regulatory compliance and to approve the start of facility construction. In addition, the safety assessment is also used by SKB to guide the detailed design of the facility, including the barrier systems, to identify future needs for RD&D and site investigations and to enhance the safety assessment for future steps.

The requirements that arise from the post-closure safety assessment are considered in the detailed design process (Section 2.8). This relates mainly to the extension of the facility, but also to the repair measures of 1BMA. It also relates to the closure measures for both the existing and extension parts, such as grouting of waste domains. In the general advice to SSM's regulation on post-closure safety it is recommended that *a number of design basis cases should be identified based on scenarios that can be shown to be especially important from the standpoint of risk. Together with other information, such as regarding manufacturing method and controllability, these cases should be used to substantiate the design basis, such as requirements on barrier properties*.

The scenarios that are important from the standpoint of risk are the scenarios that contribute to the total annual risk. The main scenario dominates the maximum risk (Figure 10-5) and illustrates which barriers and safety functions are central to the repository performance given the FEPs represented in the scenario. The importance of the barriers and safety functions is further highlighted by the less probable scenarios. To achieve the demonstrated safety after closure, the initial state of the barrier system underpins the detailed design of the barrier system and informs the planning of repository construction. As noted above (Section 11.3.1), several efforts have been made to strengthen the confidence that the initial state will be achieved as planned.

The most important barrier properties relate to limitation of advective flow and to sorption of radionuclides. Requirements are, for instance, established regarding the hydraulic conductivity of the concrete barriers in 1–2BMA based on the initial state (Chapter 4, **Initial state report**). The selection of the hydraulic conductivity in the assessment is based on results from different underlying analyses that relate to different FEPs that influence the evolution of the hydraulic conductivity of the concrete barriers and their design (**Data report**, Chapter 9). This includes the mechanical influence on the concrete barriers as well as chemical degradation. Information and efforts relating to the manufacturing methods are described in the RD&D programme (SKB TR-22-11, Section 9.2). A requirement that is related to the safety function sorb radionuclides is the amount of cement in 1–2BMA and 1BRT. For 1BRT the requirement on amount of cement is also connected to achieving a high pH that ensures limited corrosion of the metallic waste that contains induced activity. A further example of a requirement is the chemical inventory of the waste, which is regulated in the WAC with respect to complexing agents and other reactive materials.

The scenario analysis shows that the required barrier properties, as expressed in the initial state and that form the design basis from a post-closure safety perspective, are adequate for fulfilling regulatory requirements on risk and robustness of the barrier system (Section 11.1). In the process of detailed design, it may show that changes in the design are beneficial. Change control management is implemented to ensure that requirements related to post-closure safety are maintained (Section 2.8). The needs and plans for research and development are described in the RD&D programme that SKB publishes every third year (SKB TR-22-11). The post-closure safety assessment is an important input to SKB's work with the RD&D programme. This can relate to technical developments, such as the experimental work linked to demonstrating that the concrete barriers in 2BMA can be constructed with adequate quality or the further development of closure measures. Beneficial efforts can also relate to developments of the safety assessment, such as refinements of the radionuclide transport and dose calculations. The assessment can point to aspects of the site investigations that could be further considered. Moreover, part of the development work is carried out in relation to the operation of the SFR1, for instance, the investigations of the 1BMA repair measures or updates of the inventory or WAC. In general, the safety assessment is based on the layout, design, and data that is available at the point in time when the assessment is carried out, i.e. a data freeze is applied. The present post-closure safety assessment that is part of PSAR thus constitutes a baseline for subsequent developments carried out in relation to the operation of the SFR1. In the results and reporting of such work, the differences with respect to the present post-closure safety assessment will be discussed. For instance, this can apply to potential future changes of the details of the inventory which is subject to licensing conditions. When the developments are finalised, the results will be incorporated in the work on the subsequent post-closure safety assessment that is to be reported as part of the renewed SAR (FSAR).

References

SKB's (Svensk Kärnbränslehantering AB) publications can be found at www.skb.com/publications. SKBdoc documents will be submitted upon request to document@skb.se.

References with abbreviated names

Barrier process report, 2023. Post-closure safety for SFR, the final repository for short-lived radioactive waste at Forsmark. Engineered barrier process report, PSAR version. SKB TR-23-04, Svensk Kärnbränslehantering AB.

Biosphere synthesis report, 2023. Post-closure safety for SFR, the final repository for short-lived radioactive waste at Forsmark. Biosphere synthesis report, PSAR version. SKB TR-23-06, Svensk Kärnbränslehantering AB.

Climate report, 2023. Post-closure safety for SFR, the final repository for short-lived radioactive waste at Forsmark. Climate and climate-related issues, PSAR version. SKB TR-23-05, Svensk Kärnbränslehantering AB.

Data report, 2023. Post-closure safety for SFR, the final repository for short-lived radioactive waste at Forsmark. Data report, PSAR version. SKB TR-23-10, Svensk Kärnbränslehantering AB.

FEP report, 2014. FEP report for the safety assessment SR-PSU. SKB TR-14-07, Svensk Kärnbränslehantering AB.

FHA report, 2023. Post-closure safety for SFR, the final repository for short-lived radioactive waste at Forsmark. Handling of future human actions, PSAR version. SKB TR-23-08, Svensk Kärnbränslehantering AB.

Geosphere process report, 2014. Geosphere process report for the safety assessment SR-PSU. SKB TR-14-05, Svensk Kärnbränslehantering AB.

Initial state report, 2023. Post-closure safety for SFR, the final repository for short-lived radioactive waste at Forsmark. Initial state of the repository, PSAR version. SKB TR-23-02, Svensk Kärnbränslehantering AB.

Model tools report, 2023. Post-closure safety for SFR, the final repository for short-lived radioactive waste at Forsmark. Model tools summary report, PSAR version. SKB TR-23-11, Svensk Kärnbränslehantering AB.

Radionuclide transport report, 2023. Post-closure safety for SFR, the final repository for short-lived radioactive waste at Forsmark. Radionuclide transport and dose calculations, PSAR version. SKB TR-23-09, Svensk Kärnbränslehantering AB.

Waste process report, 2023. Post-closure safety for SFR, the final repository for short-lived radioactive waste at Forsmark. Waste form and packaging process report, PSAR version. SKB TR-23-03, Svensk Kärnbränslehantering AB.

Other references

Abarca E, Idiart A, de Vries L M, Silva O, Molinero J, von Schenck H, 2013. Flow modelling on the repository scale for the safety assessment SR-PSU. SKB TR-13-08, Svensk Kärnbränslehantering AB.

Abarca E, Silva O, Idiart A, Nardi A, Font J, Molinero J, 2014. Flow and transport modelling on the vault scale. Supporting calculations for the safety assessment SR-PSU. SKB R-14-14, Svensk Kärnbränslehantering AB.

Abarca E, Sampietro D, Sanglas J, Molinero J, 2020. Modelling of the near-field hydrogeology. Report for the safety assessment SR-PSU (PSAR). SKB R-19-20, Svensk Kärnbränslehantering AB.

Alexander W R, Milodowski A E, 2014. Cyprus Natural Analogue Project (CNAP) Phase IV Final report. Posiva Working Report 2014-02, Posiva Oy, Finland.

Alexander W R, Reijonen H M, MacKinnon G, Milodowski A E, Pitty A F, Siathas A, 2017. Assessing the long-term behaviour of the industrial bentonites employed in a repository for radioactive wastes by studying natural bentonites in the field. Geosciences 7, 5. doi:10.3390/geosciences7010005

Allard B, Persson G, 1985. Organic complexing agents in low and medium level radioactive waste. Nagra Technical Report NTB 85-19, Nagra, Switzerland.

Allard B, Dario M, Borén H, Torstenfelt B, Puigdomenech I, Johansson C, 2002. Karboxylatjon-bytarmassans egenskaper. SKB R-02-40, Svensk Kärnbränslehantering AB. (In Swedish.)

Anderson C R, Pedersen K, Jakobsson A-M, 2006a. Autoradiographic comparisons of radionuclide adsorption between subsurface anaerobic biofilms and granitic host rocks. Geomicrobiology Journal 23, 15–29.

Anderson C R, James R E, Fru E C, Kennedy C B, Pedersen K, 2006b. In situ ecological development of a bacteriogenic iron oxide-producing microbial community from a subsurface granitic rock environment. Geobiology 4, 29–42.

Andersson E, 2010. The limnic ecosystems at Forsmark and Laxemar-Simpevarp. SKB TR-10-02, Svensk Kärnbränslehantering AB.

Andersson E, Aquilonius K, Sivars Becker L, Borgiel M, 2011. Site investigation SFR. Vegetation in streams in the Forsmark area. SKB P-11-18, Svensk Kärnbränslehantering AB.

Andersson J, Riggare P, Skagius K, 1998. Project SAFE. Update of the SFR-1 safety assessment. Phase 1. SKB R-98-43, Svensk Kärnbränslehantering AB.

Andersson P, Garnier-Laplace J, Beresford N A, Copplestone D, Howard B J, Howe P, Oughton D, Whitehouse P, 2009. Protection of the environment from ionising radiation in a regulatory context (PROTECT): proposed numerical benchmark values. Journal of Environmental Radioactivity 100, 1100–1108.

Aquilonius K (ed), 2010. The marine ecosystems at Forsmark and Laxemar-Simpevarp. SR-Site Biosphere. SKB TR-10-03, Svensk Kärnbränslehantering AB.

Askarieh M M, Chambers A V, Daniel F B D, FitzGerald P L, Holton G J, Pilkington N J, Rees J H, 2000. The chemical and microbial degradation of cellulose in the near field of a repository for radioactive wastes. Waste Management 20, 93–106.

ATSDR, 2005. Public health assessment guidance manual (Update). U.S. Department of Health and Human Services, Public Health Service Agency for Toxic Substances and Disease Registry, Atlanta, Georgia.

Auqué L, Gimeno M, 2017. On the PCA methodology of mixing calculation and correlated variables for SKB's hydrogeochemical evaluations and interpretations of groundwater conditions. SKBdoc 1594812 ver 1.0, Svensk Kärnbränslehantering AB.

Auqué L F, Gimeno M J, Acero P, Gómez J B, 2013. Compositions of groundwater for SFR and its extension, during different climate cases, SR-PSU. SKB R-13-16, Svensk Kärnbränslehantering AB.

Auqué L, Gimeno M, Nilsson A-C, Tullborg E-L, 2017. Further clarification and guidance to the discussion about redox conditions and related processes in the geosphere, SR-PSU. SKBdoc 1594783 ver 1.0, Svensk Kärnbränslehantering AB.

BACC, 2008. Assessment of climate change for the Baltic Sea basin. The BACC (BALTEX Assessment of Climate Change for the Baltic Sea basins) author team. Berlin: Springer.

Bassil N M, Lloyd J R, 2017. Draft genome sequences of four alkaliphilic bacteria belonging to the Anaerobacillus genus. Genome Announcements 5, e01493-16. doi:10.1128/genomeA.01493-16

Bassil N M, Lloyd J R, 2019. *Anaerobacillus isosaccharinicus* sp. nov., an alkaliphilic bacterium which degrades isosaccharinic acid. International Journal of Systematic and Evolutionary Microbiology 69, 3666–3671.

Begg J D, Zavarin M, Zhao P, Tumey S J, Powell B, Kersting A, 2013. Pu(V) and Pu(IV) sorption to montmorillonite. Environmental Science & Technology 47, 5146–5153.

Berglund S, Lindborg T (eds), 2017. Monitoring Forsmark – evaluation and recommendations for programme update. SKB TR-15-01, Svensk Kärnbränslehantering AB.

Berglund Ö, Berglund K, Sohlenius G, 2009. Organogen jordbruksmark i Sverige 1999–2008. Uppsala: Swedish University of Agricultural Sciences, Department of Soil Sciences. (Rapport 12) (In Swedish.)

Bergström U, Barkefors C, 2004. Irrigation in dose assessments models. SKB R-04-26, Svensk Kärnbränslehantering AB.

Birgersson M, Andersson L, 2014. Freezing of bentonite components in SFR. Modelling and laboratory testing. SKB R-14-29, Svensk Kärnbränslehantering AB.

Birgersson M, Karnland O, 2015. Flow and pressure response in compacted bentonite due to external fluid pressure. SKB TR-14-28, Svensk Kärnbränslehantering AB.

Birgersson M, Börgesson L, Hedström M, Karnland O, Nilsson U, 2009. Bentonite erosion, Final report. SKB TR-09-34, Svensk Kärnbränslehantering AB.

Birgersson M, Hedström M, Karnland O, 2011. Sol formation ability of Ca/Na-montmorillonite at low ionic strength. Physics and Chemistry of the Earth, Parts A/B/C 36, 1572–1579.

Bosson E, Gustafsson L-G, Sassner M, 2008. Numerical modelling of surface hydrology and near-surface hydrogeology at Forsmark. Site descriptive modelling, SDM-Site Forsmark. SKB R-08-09, Svensk Kärnbränslehantering AB.

Bosson E, Sassner M, Sabel U, Gustafsson L-G, 2010. Modelling of present and future hydrology and solute transport at Forsmark. SR-Site Biosphere. SKB R-10-02, Svensk Kärnbränslehantering AB.

Boulton G S, Kautsky U, Morén L, Wallroth T, 2001. Impact of long-term climate change on a deep geological repository for spent nuclear fuel. SKB TR-99-05, Svensk Kärnbränslehantering AB.

Bourbon X, Toulhoat P, 1996. Influence of organic degradation products on the solubilisation of radionuclides in intermediate and low level radioactive wastes. Radiochimica Acta 74, 315–320.

Bradbury M H, Van Loon L R, 1998. Cementitious near-field sorption data bases for performance assessment of a L/ILW disposal facility in a Palfris Marl Host Rock. CEM-94: Update I, June 1997. PSI Bericht 98-01, Paul Scherrer Institute, Switzerland.

Brandefelt J, Näslund J-O, Zhang Q, Hartikainen J, 2013. The potential for cold climate conditions and permafrost in Forsmark in the next 60 000 years. SKB TR-13-04, Svensk Kärnbränslehantering AB.

Brandefelt J, Näslund J-O, Andersson E, 2016. Kompletterande information om hantering av klimatscenarierna i ansökan om utbyggnad av SFR. SKBdoc 1541317 ver 1.0, Svensk Kärnbränslehantering AB. (In Swedish.)

Brandefelt J, Åstrand P-G, Liakka J, 2023. Post-closure safety assessment flowchart (PSAR SFR). SKBdoc 1998708, ver 1.0. Svensk Kärnbränslehantering AB.

Brazelton W J, Morrill P L, Szponar N, Schrenk M O, 2013. Bacterial communities associated with subsurface geochemical processes in continental serpentinite springs. Applied Environmental Microbiology 79, 3906–3916.

Brodersen K, 1999. Hygroscopic materials in bituminised waste: experiments and modelling. In Vanbrabant R, Selucky P (eds). Radwaste bituminization ’99: proceeding of the International Workshop on the Safety and Performance Evaluation of Bitumenization Processes for Radioactive Waste, Řež near Prague, 29 June – 2 July 1999.

Brown E T (ed), 1981. Rock characterization testing & monitoring: ISRM suggested methods. Oxford: Pergamon.

Brown J E, Alfonso B, Avila R, Beresford N A, Copplestone D, Pröhl G, Ulanovsky A, 2008. The ERICA tool. Journal of Environmental Radioactivity 99, 1371–1383.

Brown J E, Alfonso B, Avila R, Beresford N A, Copplestone D, Hosseini A, 2016. A new version of the ERICA tool to facilitate impact assessments of radioactivity on wild plants and animals. Journal of Environmental Radioactivity 153, 141–148.

Brunberg A-K, Nilsson E, Blomqvist P, 2002. Characteristics of oligotrophic hardwater lakes in a postglacial land-rise area in mid-Sweden. Freshwater Biology 47, 1451–1462.

Brunberg A-K, Carlsson T, Blomqvist P, Brydsten L, Strömgren M, 2004. Forsmark site investigation. Identification of catchments, lake-related drainage parameters and lake habitats. SKB P-04-25, Svensk Kärnbränslehantering AB.

Brundell P, Kanlén F, Westö A-K, 2008. Water use for irrigation. Report on Grant Agreement No 71301.2006.002–2006.470, Statistiska centralbyrån (Statistics Sweden).

Bruno J, Alexander W R, Van Loon L R, Thorne M, 2013. The potential radionuclide migration role of bitumen colloids at SFR. SKB P-13-41, Svensk Kärnbränslehantering AB.

Bruno J, Duro L, Riba O, 2017. Supplementary information on colloid interactions in SFR. SKBdoc 1569690 ver 1.0, Svensk Kärnbränslehantering AB.

Bruno J, González-Siso M R, Duro L, Gaona X, Altmaier M, 2018. Key master variables affecting the mobility of Ni, Pu, Tc and U in the near field of the SFR repository. Main experimental findings and PA implications of the PhD thesis. SKB TR-18-01, Svensk Kärnbränslehantering AB.

Brydsten L, 2009. Sediment dynamics in the coastal areas of Forsmark and Laxemar during an interglacial. SKB TR-09-07, Svensk Kärnbränslehantering AB.

Brydsten L, Strömgren M, 2010. A coupled regolith-lake development model applied to the Forsmark site. SKB TR-10-56, Svensk Kärnbränslehantering AB.

Brydsten L, Strömgren M, 2013. Landscape development in the Forsmark area from the past into the future (8500 BC – 40 000 AD). SKB R-13-27, Svensk Kärnbränslehantering AB.

Bultmark F, 2017. Korrosion av armeringsjärn i betongtankar i 1-2BTF. SKBdoc 1577565 ver 1.0, Svensk Kärnbränslehantering AB.

Bäckblom G, Munier R, 2002. Effects of earthquakes on the deep repository for spent fuel in Sweden based on case studies and preliminary model results. SKB TR-02-24, Svensk Kärnbränslehantering AB.

Bödvarsson R, Lund B, Roberts R, Slunga R, 2006. Earthquake activity in Sweden. Study in connection with a proposed nuclear waste repository in Forsmark or Oskarshamn. SKB R-06-67, Svensk Kärnbränslehantering AB.

Börgesson L, Åkesson M, Kristensson O, Malmberg D, Birgersson M, Hernelind J, 2015. Modelling of critical H-M processes in the engineered barriers of SFR. SKB TR-14-27, Svensk Kärnbränslehantering AB.

Chambers A V, Gould L J, Jackson C P, Pilkington N J, Tearle W M, Tweed C-J, 2002. The development of methodologies for characterising the uncertainties in time-dependent chemical parameters: impact of organic complexants. Report AEAT/ERRA-0377, AEA Technology.

Chapin F S, Matson P A, Mooney H A, 2002. Principles of terrestrial ecosystem ecology. New York: Springer.

Cohen-Corticchiato D, Zwinger T, 2021. Modeling permafrost evolution at Olkiluoto for the next 120 000 years. Posiva Working Report 2021-14, Posiva Oy, Finland.

Collins G S, Melosh H J, Marcus R A, 2005. Earth impact effects program: a web-based computer program for calculating the regional environmental consequences of a meteorid impact on Earth. Meteoritics & Planetary Science 40, 817–840.

Crawford J, 2017. Organic complexation in the geosphere for SR PSU. SKBdoc 1577134 ver 1.0, Svensk Kärnbränslehantering AB.

Cronstrand P, 2007. Modelling the long-time stability of the engineered barriers of SFR with respect to climate changes. SKB R-07-51, Svensk Kärnbränslehantering AB.

Cronstrand P, 2014. Evolution of pH in SFR 1. SKB R-14-01, Svensk Kärnbränslehantering AB.

Cronstrand P, 2016. Long-term performance of the bentonite barrier in the SFR silo. SKB TR-15-08, Svensk Kärnbränslehantering AB.

Curtis P, Markström I, Petersson J, Triumf C-A, Isaksson H, Mattsson H, 2011. Site investigation SFR. Bedrock geology. SKB R-10-49, Svensk Kärnbränslehantering AB.

Dario M, Molera M, Allard B, 2004. Effect of organic ligands on the sorption of europium on TiO_2 and cement at high pH. SKB TR-04-04, Svensk Kärnbränslehantering AB.

Duro L, Grivé M, Domènech C, Roman-Ross G, Bruno J, 2012a. Assessment of the evolution of the redox conditions in SFR 1. SKB TR-12-12, Svensk Kärnbränslehantering AB.

Duro L, Grivé M, Gaona X, Bruno J, Andersson T, Borén H, Dario M, Allard B, Hagberg J, Källström K, 2012b. Study the effect of the fibre mass UP2 degradation products on radionuclide mobilisation. SKB R-12-15, Svensk Kärnbränslehantering AB.

Earon R, Rasul H, Öhman J, 2022. Utredning angående flacka strukturer med underlag från KFR117, KFR118, KFR119, KFR120 och KFR121. SKBdoc 1966551 ver 1.0, Svensk Kärnbränslehantering AB. (In Swedish.)

Ek B-M, Thunholm B, Östergren I, Falk R, Mjönes L, 2007. Naturlig radioaktivitet, uran och andra metaller i dricksvatten. SGU rapport 2007:13, Geological Survey of Sweden. (In Swedish.)

Ekström P-A, 2017. Konvergens av probabilistiska beräkningar. SKBdoc 1581608 ver 1.0, Svensk Kärnbränslehantering AB. (In Swedish.)

Elfwing M, von Schenck H, Åstrand P-G, 2018. Uppdaterad analys av strålsäkerheten efter förslutning för 1BMA i SFR1. SKBdoc 1686798 ver 1.0, Svensk Kärnbränslehantering AB. (In Swedish.)

Eliasson P, 1992. ”Genom helvetets port, men…” – skogsdikning som mål och medel. Aktuellt om historia 3–4, 46–60. (In Swedish.)

Engkvist I, Albinsson Y, Johansson Engkvist W, 1996. The long-term stability of cement – Leaching tests. SKB TR 96-09, Svensk Kärnbränslehantering AB.

Ferry J G, 1993. Fermentation of acetate. In Ferry J G (ed). Methanogenesis: ecology, physiology, biochemistry and genetics. New York: Chapman & Hall, 304–334.

Follin S, Levén J, Hartley L, Jackson P, Joyce S, Roberts D, Swift B, 2007. Hydrogeological characterisation and modelling of deformation zones and fracture domains, Forsmark modelling stage 2.2. SKB R-07-48, Svensk Kärnbränslehantering AB.

French H M, 2007. The periglacial environment. 3rd ed. Chichester: Wiley.

Gangopadhyay A, Talwani P, 2003. Symptomatic features of intraplate earthquakes. Seismological Research Letters 74, 863–883.

Gaona X, Tasi A, Szabo P, 2021. Impact of the degradation products of the UP2 resin on the uptake of radionuclides by cement. Progress update on the first year of the project. Karlsruhe Institute of Technology. SKBdoc 1925094 ver 2.0, Svensk Kärnbränslehantering AB.

Garnier-Laplace J, Della-Vedova C, Andersson P, Copplestone D, Cailes C, Beresford N A, Howard B J, Howe P, Whitehouse P, 2010. A multi-criteria weight of evidence approach for deriving ecological benchmarks for radioactive substances. Journal of Radiological Protection 30, 215–233.

Gaucher E, Tournassat C, Nowak C, 2005. Modelling the geochemical evolution of the multi-barrier system of the silo of the SFR repository. Final report. SKB R-05-80, Svensk Kärnbränslehantering AB.

Georgiev G, 2013. A seismic evaluation of SFR. Analysis of the Silo structure for earthquake load. SKB R-13-52, Svensk Kärnbränslehantering AB.

Gimeno M J, Auqué L F, Gómez J B, Acero P, 2009. Water–rock interaction modelling and uncertainties of mixing modelling. Site descriptive modelling SDM-Site Laxemar. SKB R-08-110, Svensk Kärnbränslehantering AB.

Gimeno M J, Auqué L F, Gómez J B, Acero P, 2011. Site investigation SFR. Water–rock interaction and mixing modelling in the SFR. SKB P-11-25, Svensk Kärnbränslehantering AB.

Glaus M A, Van Loon L R, 2004. A generic procedure for the assessment of the effect of concrete admixtures on the retention behaviour of cement for radionuclides: Concept and case studies. PSI Bericht 04-02, Paul Scherrer Institute, Switzerland.

Glaus M A, Van Loon L R, 2008. Degradation of cellulose under alkaline conditions: new insights from a 12 year degradation study. Environmental Science & Technology 42, 2906–2911.

Glaus M A, Van Loon L R, Achatz S, Chodura A, Fischer K, 1999. Degradation of cellulosic materials under the alkaline conditions of a cementitious repository for low and intermediate level radioactive waste. Part I: Identification of degradation products. Analytica Chimica Acta 398, 111–122.

Gorbunova O A, Barinov A S, 2012. Microbiological evaluation of the condition of cement compounds with radioactive wastes after long-term storage in near-surface repositories. Radiochemistry 54, 198–204.

Gosling S, Müller Schmied H, Betts R, Chang J, Ciais P, Dankers R, Döll P, Eisner S, Flörke M, Gerten D, Grillakis M, Hanasaki N, Hagemann S, Huang M, Huang Z, Jerez S, Kim H, Koutroulis A, Leng G, Liu X, Masaki Y, Montavez P, Morfopoulos C, Oki T, Papadimitriou L, Pokhrel Y, Portmann F T, Orth R, Ostberg S, Satoh Y, Seneviratne S, Sommer P, Stacke T, Tang Q, Tsanis I, Wada Y, Zhou T, Büchner M, Schewe J, Zhao F, 2019. ISIMIP2a simulation data from water (global) sector (V. 1.1). GFZ Data Services. doi:10.5880/PIK.2019.003

Grbić-Galić S, Churchman-Eisel N, Mraković I, 1990. Microbial transformation of styrene by anaerobic consortia. Journal of Applied Bacteriology 69, 247–260.

Green M, 2019. Fågelövervakning i Forsmark 2018. SKB P-19-02, Svensk Kärnbränslehantering AB. (In Swedish.)

Greenfield B F, Harrison W N, Robertson G P, Somers P J, Spindler M W, 1993. Mechanistic studies of the alkaline degradation of cellulose in cement. Nirex Report NSS/R272, Nirex Ltd., UK.

Greenfield B F, Hurdus M H, Pilkington N J, Spindler M W, Williams S J, 1994. The degradation of cellulose in the near field of a radioactive waste repository. In Barkatt A, Van Konynenburg R A (eds). Scientific basis for nuclear waste management XVII: symposium held in Boston, Massachusetts, USA, 29 November – 3 December. Pittsburgh, PA: Materials Research Society. (Materials Research Society Symposium Proceedings 333), 705–710.

Grolander S, 2013. Biosphere parameters used in radionuclide transport modelling and dose calculations in SR-PSU. SKB R-13-18, Svensk Kärnbränslehantering AB.

Hamrén U, Collinder P, 2010. Vattenverksamhet i Forsmark. Ekologisk fältinventering och naturvärdesklassificering samt beskrivning av skogsproduktionsmark. SKB R-10-16, Svensk Kärnbränslehantering AB. (In Swedish.)

Hartikainen J, Kouhia R, Wallroth T, 2010. Permafrost simulations at Forsmark using a numerical 2D thermo-hydro-chemical model. SKB TR-09-17, Svensk Kärnbränslehantering AB.

Hedström S, 2019a. Steel corrosion in SFR by waste type and vault without solubility or transport limitations. SKBdoc 1858222 ver 1.0, Svensk Kärnbränslehantering AB.

Hedström S, 2019b. Komplexbildande flyttillsatsmedel i kringgjutningsbetong i kokiller till SFR. SKBdoc 1870598 ver 1.0, Svensk Kärnbränslehantering AB. (In Swedish.)

Hedström S, 2020. Utvärdering av komplexbildande tri- och tetraminer i rostskyddsfärg. SKBdoc 1892917 ver 1.0, Svensk Kärnbränslehantering AB. (In Swedish.)

Hejll A, Hassanzadeh M, Hed G, 2012. Sprickor i BMA:s betongbarriär – Inspektion och orsak. Rapport AE-NCC 12-004, Rev 1.0, Vattenfall AB. SKBdoc 1430853 ver 1.0, Svensk Kärnbränslehantering AB. (In Swedish.)

Herting G, Odnevall I, 2021. Corrosion of aluminium and zinc in concrete at simulated conditions of the repository of low active waste in Sweden. Corrosion and Materials Degradation 2, 150–162.

Hjerpe T, Marcos N, Ikonen A, Åstrand P-G, Reijonen H, 2021. Safety case for the operating licence application – FEP database description. Posiva Working Report 2020-19, Posiva Oy, Finland.

Holmén J G, Stigsson M, 2001. Modelling of future hydrogeological conditions at SFR. SKB R-01-02, Svensk Kärnbränslehantering AB.

Honda A, Masuda K, Nakanishi H, Fujita H, Negishi K, 2008. Modeling of pH elevation due to the reaction of saline groundwater with hydrated ordinary portland cement phases. MRS Online Proceedings Library 1124. doi:10.1557/PROC-1124-Q10-12

Hummel W, Anderegg G, Rao L, Puigdomenech I, Tochiyama O, 2005. Chemical thermodynamics. vol 9. Chemical thermodynamics of compounds and complexes of U, Np, Pu, Am, Tc, Se, Ni and Zr with selected organic ligands. Paris: OECD/NEA.

Hyenstrand Å, 1994. Kulturminnen och kulturmiljövård. In Selinge K-G (ed). Sveriges Nationalatlas. Kulturminnen och kulturmiljövård. Stockholm: SNA. (In Swedish.)

Höglund L O, 2001. Project SAFE. Modelling of long-term concrete degradation processes in the Swedish SFR repository. SKB R-01-08, Svensk Kärnbränslehantering AB.

Höglund L O, 2014. The impact of concrete degradation on the BMA barrier functions. SKB R-13-40, Svensk Kärnbränslehantering AB.

Höglund L O, 2017. Svar på frågor från SSM rörande kemisk modellering av betongdegradering. SKBdoc 1593574 ver 2.0, Svensk Kärnbränslehantering AB. (In Swedish.)

Höglund L O, 2018. pH-utveckling i bergssal BRT. SKBdoc 1608409 ver 2.0, Svensk Kärnbränslehantering AB. (In Swedish.)

Höglund L O, 2019. pH evolution in 2BMA – Assumptions, data and modelling results. Kemakta Konsult AB. SKBdoc 1698794 ver 1.0, Svensk Kärnbränslehantering AB.

Höglund L O, Bengtsson A, 1991. Some chemical and physical processes related to the long-term performance of the SFR repository. SKB SFR 91-06, Svensk Kärnbränslehantering AB.

IAEA, 2006. Fundamental safety principles. Vienna: International Atomic Energy Agency. (IAEA Safety Standards Series SF-1)

IAEA, 2009. Classification of radioactive waste, general safety guide. Vienna: International Atomic Energy Agency. (IAEA Safety Standards Series GSG-1)

IAEA, 2011. Disposal of radioactive waste. Vienna: International Atomic Energy Agency. (IAEA Safety Standards Series SSR-5)

IAEA, 2012. The safety case and safety assessment for the disposal of radioactive waste. Vienna: International Atomic Energy Agency. (IAEA Safety Standards Series SSG-23)

IAEA, 2018. IAEA safety glossary: terminology used in nuclear safety and radiation protection. 2018 edition. Vienna: International Atomic Energy Agency.

ICRP, 1991. 1990 Recommendations of the International Commission on Radiological Protection. Oxford: Pergamon Press. (ICRP Publication 60; Annals of the ICRP 21 (1-3))

ICRP, 2003. A framework for assessing the impact of ionising radiation on non-human species. Oxford: Pergamon. (ICRP Publication 91; Annals of the ICRP 33 (3))

ICRP, 2006. Assessing dose of the representative person for the purpose of radiation protection of the public and the optimisation of radiological protection – broadening the process. Amsterdam: Elsevier. (ICRP Publication 101; Annals of the ICRP 36 (3))

ICRP, 2007. The 2007 Recommendations of the International Commission on Radiological Protection. Amsterdam: Elsevier. (ICRP Publication 103; Annals of the ICRP 37 (2-4))

ICRP, 2008. Environmental protection: the concept and use of reference animals and plants. Amsterdam: Elsevier. (ICRP Publication 108; Annals of the ICRP 38 (4-6))

Idiart A, Olmeda J, Laviña M, 2019. Modelling of concrete degradation – influence of concrete mix design. Report for the safety evaluation SE-SFL. SKB R-19-14, Svensk Kärnbränslehantering AB.

Idiart A, Laviña M, Grandia F, Pont A, 2020. Reactive transport modelling of montmorillonite dissolution. Report for the safety evaluation SE-SFL. SKB R-19-15, Svensk Kärnbränslehantering AB.

Ingmar T, Moreborg K, 1976. The leaching and original content of calcium carbonate in northern Uppland, Sweden. Geologiska Föreningen i Stockholm Förhandlingar 98, 120–132.

IPCC, 2013. Climate change 2013: the physical science basis: summary for policymakers. Contribution of working group I to the fifth assessment report of the intergovernmental panel on climate change. Available at: http://www.ipcc.ch

IPCC, 2021. Climate change 2021: the physical science basis. Contribution of working group I to the sixth assessment report of the intergovernmental panel on climate change [Masson-Delmotte V, Zhai P, Pirani A, Connors S L, Péan C, Berger S, Caud N, Chen Y, Goldfarb L, Gomis M I, Huang M, Leitzell K, Lonnoy E, Matthews J B R, Maycock T K, Waterfield T, Yelekçi O, Yu R, Zhou B (eds)]. Cambridge University Press. In press. doi:10.1017/9781009157896

ISO 14001:2015. Environmental management – Requirements. Geneva: International Organization for Standardization.

ISO 45001:2018. Occupational health and safety – Requirements. Geneva: International Organization for Standardization.

ISO 9001:2015. Quality management systems – Requirements. Geneva: International Organization for Standardization.

Jaeschke B, Smith K, Nordén S, Alfonso B, 2013. Assessment of risk to non-human biota from a repository for the disposal of spent nuclear fuel at Forsmark. Supplementary information. SKB TR-13-23, Svensk Kärnbränslehantering AB.

Jenni A, Mäder U, Lerouge C, Gaboreau S, Schwyn B, 2014. In situ interaction between different concretes and Opalinus clay. Physics and Chemistry of the Earth 70–71, 71–83.

Johannesson L-E, Dueck A, Andersson L, Jensen V, 2015. Investigations of hydraulic and mechanical processes of the barriers embedding the silo in SFR. Laboratory tests. SKB TR-15-05, Svensk Kärnbränslehantering AB.

Johansson M, Christensen T R, Åkerman J, Callaghan T V, 2006. What determines the current presence or absence of permafrost in the Torneträsk region, a sub-Arctic landscape in Northern Sweden? Ambio 35, 190–197.

Karlsson A, Eriksson C, Borell Lövstedt C, Liungman O, Engqvist A, 2010. High-resolution hydrodynamic modelling of the marine environment at Forsmark between 6500 BC and 9000 AD. SKB R-10-09, Svensk Kärnbränslehantering AB.

Keith-Roach M J, 2008. The speciation, stability, solubility and biodegradation of organic co-contaminant radionuclide complexes: a review. Science of the Total Environment 396, 1–11.

Keith-Roach M, Höglund L-O, 2018. Review of the long-term risks associated with the use of superplasticizers. Posiva Working Report 2017-52, Posiva Oy, Finland.

Keith-Roach M, Shahkarami P, 2021. Organic materials with the potential for complexation in SFR, the final repository for short-lived radioactive waste. Investigation of new acceptance criteria. SKB R-21-03, Svensk Kärnbränslehantering AB.

Keith-Roach M, Lindgren M, Källström K, 2014. Assessment of complexing agent concentrations in SFR. SKB R-14-03, Svensk Kärnbränslehantering AB.

Keith-Roach M, Lindgren M, Källström K, 2021. Assessment of complexing agent concentrations for the post-closure safety assessment in PSAR SFR. SKB R-20-04, Svensk Kärnbränslehantering AB.

Kyzioł-Komosińska J, Rosik-Dulewska C, Franus M, Antoszczyszyn-Szpicka P, Czupioł J, KrzyżewskaI I, 2015. Sorption capacities of natural and synthetic zeolites for Cu(II) ions. Polish Journal of Environmental Studies 24, 1111–1123.

Laaksoharju M, Smellie J, Tullborg E-L, Gimeno M, Hallbäck L, Molinero J, Waber N, 2008. Bedrock hydrogeochemistry Forsmark. Site descriptive modelling, SDM-Site Forsmark. SKB R-08-47, Svensk Kärnbränslehantering AB.

Lagerblad B, Trägårdh J, 1994. Conceptual model for concrete long time degradation in a deep nuclear waste repository. SKB TR 95-21, Svensk Kärnbränslehantering AB.

Lagerblad B, Golubeva M, Cirera Rui, J, 2016. Lämplighet för krossberg från Forsmark och SFR att användas som betongballast. SKB P-16-13, Svensk Kärnbränslehantering AB. (In Swedish.)

Lagerblad B, Rogers P, Vogt C, Mårtensson P, 2017. Utveckling av konstruktionsbetong till kassunerna i 2BMA. SKB R-17-21, Svensk Kärnbränslehantering AB. (In Swedish.)

Larsson C-M, 2008. An overview of the ERICA integrated approach to the assessment and management of environmental risks from ionising contaminants. Journal of Environmental Radioactivity 99, 1364–1370.

Lindborg T (ed), 2010. Landscape Forsmark – data, methodology and results for SR-Site. SKB TR-10-05, Svensk Kärnbränslehantering AB.

Lord N S, Lunt D, Thorne M, 2019. Modelling changes in climate over the next 1 million years. SKB TR-19-09, Svensk Kärnbränslehantering AB.

Löfgren A (ed), 2010. The terrestrial ecosystems at Forsmark and Laxemar-Simpevarp. SR-Site Biosphere. SKB TR-10-01, Svensk Kärnbränslehantering AB.

Löfgren M, 2014. Recommendation of rock matrix effective diffusivities for SR-PSU. Based on formation factor logging in situ by electrical methods in KFR102B and KFR105. SKB R-13-39, Svensk Kärnbränslehantering AB.

Lönnqvist M, 2019. SFR extension: estimates of tunnel stability and transmissivity of fractures intersecting the repository host rock. Clay Technology AB. SKBdoc 1858314 ver 1.0, Svensk Kärnbränslehantering AB.

Lönnqvist M, 2022. SFR Extension – Influence of degradation of rock mass strength. SKBdoc 1964794 ver 1.0, Svensk Kärnbränslehantering AB.

Machell G, Richards G N, 1960. Mechanism of saccharinic acid formation. Part I. Competing in the alkaline degradation of 4-O-methyl-D-glucose, maltose, amylose and cellulose. Journal of the Chemical Society, 1960, 1924–1931.

Maier A, 2021. Radiation chemical gas production from bitumen and ion-exchange resins – a literature study. SKBdoc 1939037 ver 1.0, Svensk Kärnbränslehantering AB.

Marty N C M, Tournassat C, Burnol A, Giffaut E, Gaucher E C, 2009. Influence of reaction kinetics and mesh refinement on the numerical modelling of concrete/clay interactions. Journal of Hydrology 364, 58–72.

Mas Ivars D, Veiga Ríos M, Shiu W, Johansson F, Fredriksson A, 2014. Long term stability of rock caverns BMA and BLA of SFR, Forsmark. SKB R-13-53, Svensk Kärnbränslehantering AB.

Means J L, Alexander C A, 1981. The environmental biogeochemistry of chelating agents and recommendations for the disposal of chelated radioactive wastes. Nuclear and Chemical Waste Management 2, 183–196.

Moreno L, Neretnieks I, 2013. Impact of gas generation on radionuclide release – comparison between results for new and old data. SKB P-13-40, Svensk Kärnbränslehantering AB.

Moreno L, Skagius K, Södergren S, Wiborgh M, 2001. Project SAFE. Gas related processes in SFR. SKB R-01-11, Svensk Kärnbränslehantering AB.

Mäder U, Jenni A, Lerouge C, Gaboreau S, Miyoshi S, Kimura Y, Cloet V, Fukaya M, Claret F, Otake T, Shibata M, Lotenbach B, 2017. 5-year chemico-physical evolution of concrete-claystone interfaces. Mont Terri rock laboratory (Switzerland). Swiss Journal of Geosciences 110, 307–327.

Mårtensson P, 2014. He-läcksökning av sprickor i betongkonstruktionen i 1BMA. SKBdoc 1452199 ver 1.0, Svensk Kärnbränslehantering AB. (In Swedish.)

Mårtensson P, 2017. Hållfasthetsegenskaper hos betongkonstruktionerna i 1–2BMA under de första 20 000 åren efter förslutning. SKBdoc 1577237 ver 1.0, Svensk Kärnbränslehantering AB. (In Swedish.)

Mårtensson P, Vogt C, 2019. Concrete caissons for 2BMA. Large scale test of design and material. SKB TR-18-12, Svensk Kärnbränslehantering AB.

Mårtensson P, Vogt C, 2020. Concrete caissons for 2BMA. Large scale test of design, material and construction method. SKB TR-20-09, Svensk Kärnbränslehantering AB.

Mårtensson P, Luterkort D, Nyblad B, Wimelius H, Pettersson A, Aghili B, Andolfsson T, 2022. SFR förslutningsplan. SKBdoc 1358612 ver 4.0, Svensk Kärnbränslehantering AB. (In Swedish.)

NDA, 2017. The impact of the use of polycarboxylate ether superplasticisers for the packaging of low heat generating wastes on GDF post-closure safety. NDA Report no. NDA/RWM/135, Nuclear Decommissioning Authority, UK.

NEA, 2000. Features, events and processes (FEPs) for geologic disposal of radioactive waste. An international database. Paris: OECD Publishing.

NEA, 2006. Electronic version 2.1 of the NEA FEP database developed on behalf of the Nuclear Energy Agency by Safety Assessment Management Ltd.

NEA, 2012. Methods for safety assessment of geological disposal facilities for radioactive wastes: outcomes of the NEA MeSA Initiative. Paris: OECD/NEA.

NEA, 2019. International features, events and processes (IFEP) list for the deep geological. Version 3.0. Disposal of Radioactive Waste NEA/RWM/R(2019)1, Nuclear Energy Agency.

Neuzil C E, 2012. Hydromechanical effects on continental glaciation on groundwater systems. Geofluids 12, 22–37.

Nilsson A-C, Tullborg E-L, Smellie J, Gimeno M J, Gómez J B, Auqué L F, Sandström B, Pedersen K, 2011. SFR site investigation. Bedrock hydrogeochemistry. SKB R-11-06, Svensk Kärnbränslehantering AB.

Nummi O, Kyllönen J, Eurajoki T, 2012. Long-term safety of the maintenance and decommissioning waste of the encapsulation plant. Posiva 2012-37, Posiva Oy, Finland.

NWMO, 2011. OPG's deep geological repository for low & intermediate level waste. Postclosure safety assessment: features, events and processes. NWMO DGR-TR-2011-29, Nuclear Waste Management Organization, Canada.

Näslund J-O, Brandefelt J, Claesson Liljedahl L, 2013. Climate considerations in long-term safety assessments for nuclear waste repositories. Ambio 42, 393–401.

Näslund J-O, Mårtensson P, Lindgren M, Åstrand P-G, 2017a. Information om klimat och effekter på SFR till följd av frysning av betong. SKBdoc 1572377 ver 1.0, Svensk Kärnbränslehantering AB. (In Swedish.)

Näslund J-O, Mårtensson P, Andersson E, 2017b. Svar till SSM på begäran om komplettering av ansökan om utökad verksamhet vid SFR – effekter av tidig permafrostpåverkan. SKBdoc 1564242 ver 1.0, Svensk Kärnbränslehantering AB. (In Swedish.)

Odén M, Follin S, Öhman J, Vidstrand P, 2014. SR-PSU Bedrock hydrogeology. Groundwater flow modelling methodology, setup and results. SKB R-13-25, Svensk Kärnbränslehantering AB.

Olsson D, 2017. Silo – utredning kring gas och svällning. SKBdoc 1535026 ver 1.0, Svensk Kärnbränslehantering AB. (In Swedish.)

Omori T, Jigami Y, Minoda Y, 1974. Microbial oxidation of alpha-methylstyrene and beta-methylstyrene. Agricultural and Biological Chemistry 38, 409–415.

Omori T, Jigami Y, Minoda Y, 1975. Isolation, identification, and substrate assimilation specificity of some aromatic hydrocarbon utilizing bacteria. Agricultural and Biological Chemistry 39, 1775–1779.

Pavasars I, 1999. Characterisation of organic substances in waste materials under alkaline conditions. PhD thesis. Linköping University, Sweden.

Pedersen K, 2001. Project SAFE. Microbial features, events and processes in the Swedish final repository for low- and intermediate-level radioactive waste. SKB R-01-05, Svensk Kärnbränslehantering AB.

Pedersen K, Nilsson E, Arlinger J, Hallbeck L, O'Neill A, 2004. Distribution, diversity and activity of microorganisms in the hyper-alkaline spring waters of Maqarin in Jordan. Extremophiles 8, 151–164.

Pellikka H, Särkkä J, Johansson M, Pettersson H, 2020. Probability distributions for mean sea level and storm contribution up to 2100 AD at Forsmark, Sweden. SKB TR-19-23, Svensk Kärnbränslehantering AB.

Petrone J, Sohlenius G, Ising J, 2020. Baseline Forsmark – Depth and stratigraphy of regolith. SKB R-17-07, Svensk Kärnbränslehantering AB.

Pettersson M, Elert M, 2001. Characterisation of bituminised waste in SFR 1. SKB R-01-26, Svensk Kärnbränslehantering AB.

Pusch R, 1985. Buffertar av bentonitbaserade material i siloförvaret. Funktion och utförande. SKB SFR 85-08, Svensk Kärnbränslehantering AB. (In Swedish.)

Pusch R, Hökmark H, 1987. Megaparameterstudie av gastransport genom SFR-buffertar. SKB SFR 87-06, Svensk Kärnbränslehantering AB.

Rajec P, Macášek F, Misaelides P, 1999. Sorption of heavy metals and radionuclides on zeolites and clays. In Misaelides P, Macášek F, Pinnavaia T J, Colella C (eds). Natural microporous materials in environmental technology. Dordrecht: Kluwer Academic, 353–363.

Rébufa C, Traboulsi A, Labed V, Dupuy N, Sergent M, 2015. Experimental design approach for identification of the factors influencing the γ-radiolysis of ion exchange resins. Radiation Physics and Chemistry 106, 223–234.

Regeringen, 2021. Ansökan om tillstånd enligt lagen (1984:3) om kärnteknisk verksamhet att inneha, bygga ut och fortsatta driva slutförvaret för låg- och medelaktivt avfall (SFR). M2019/01879. Regeringen. (In Swedish.)

Román-Ross G, Trinchero P, Maia F, Molinero J, 2014. Hydrogeochemical modelling and evolution of the groundwater types and processes in geosphere of SFR, SR-PSU. SKB R-13-30, Svensk Kärnbränslehantering AB.

Rout S P, Radford J, Laws A P, Sweeney F, Elmekawy A, Gillie L J, Humphreys P N, 2014. Biodegradation of the alkaline cellulose degradation products generated during radioactive waste disposal. PLoS One 9, e107433. doi:10.1371/journal.pone.0107433

Rozalén M L, Huertas F J, Brady P V, Cama J, García-Palma S, Linares J, 2008. Experimental study of the effect of pH on the kinetics of montmorillonite dissolution at 25 °C. Geochimica et Cosmochimica Acta 72, 4224–4253.

Rozalén M L, Huertas F J, Brady P V, 2009. Experimental study of the effect of pH and temperature on the kinetics of montmorillonite dissolution. Geochimica et Cosmochimica Acta 73, 3752–3766.

Saetre P, Ekström P-A, 2016. Drainage of runoff water from 157_2 into 157_1 via a stream – Biosphere complementary information for SR-PSU. SKBdoc 1554499 var 1.0, Svensk Kärnbränslehantering AB.

Saetre P, Ekström P-A, 2017. Kompletterande beräkningar om biosfärsobjekt. SKBdoc 1571087 ver 1.0, Svensk Kärnbränslehantering AB. (In Swedish.)

Saetre P, Nordén S, Keesmann S, Ekström P-A, 2013a. The biosphere model for radionuclide transport and dose assessment in SR-PSU. SKB R-13-46, Svensk Kärnbränslehantering AB.

Saetre P, Valentin J, Lagerås P, Avila R, Kautsky U, 2013b. Land use and food intake of future inhabitants: outlining a representative individual of the most exposed group for dose assessment. Ambio 42, 488–496.

Sandström B, Tullborg E-L, 2011. Site investigation SFR. Fracture mineralogy and geochemistry of borehole sections sampled for groundwater chemistry and Eh. Results from boreholes KFR01, KFR08, KFR10, KFR19, KFR7A and KFR105. SKB P-11-01, Svensk Kärnbränslehantering AB.

Sandström B, Tullborg E-L, Sidborn M, 2014. Iron hydroxide occurrences and redox capacity in bedrock fractures in the vicinity of SFR. SKB R-12-11, Svensk Kärnbränslehantering AB.

Sassner M, Liakka J, Mayotte J-M, 2022. Effects of a warmer climate on near-surface water balances of biosphere objects examined in the post-closure safety assessments for SFR. Simulations with MIKE SHE SR-PSU 5000 AD model. SKB P-22-05, Svensk Kärnbränslehantering AB.

Sato T, Oda C, 2015. Kinetics of smectite dissolution at high pH conditions for long-term safety assessment of radioactive waste disposal: effect of Gibbs free energy and secondary minerals. In Proceedings of International Conference on Clay Science and Technology (EUROCLAY 2015), Edinburgh, UK, 6 July 2015.

Sato T, Kuroda M, Yokoyama S, Tsutsui, M, Fukushi K, Tanaka T, Nakayama S, 2004. Dissolution mechanism and kinetics of smectite under alkaline conditions. In Proceedings of International Workshop on Bentonite–Cement Interaction in Repository Environments, Tokyo, 14–16 April 2004. A3–38.

Satoh H, Ishii T, Owada H, 2013. Dissolution of compacted montmorillonite at hyperalkaline pH and 70 °C: *in situ* VSI and *ex situ* AFM measurements. Clay Minerals 48, 285–294.

Sercombe J, Gwinner B, Tiffreau C, Simondi-Teisseire B, Adenot F, 2006. Modelling of bituminised radioactive waste leaching. Part I: Constitutive equations. Journal of Nuclear Materials 349, 96–106.

SFS 1984:3. Lag om kärnteknisk verksamhet (Nuclear activities act). Stockholm: Ministry of the Environment. (In Swedish.)

SFS 1998:808. Miljöbalk (Environmental code). Stockholm: Ministry of the Environment. (In Swedish.)

SFS 2018:396. Strålskyddslag (Radiation protection act). Stockholm: Ministry of the Environment. (In Swedish.)

Shirai K, Hisatsuka K, 1979. Production of beta-phenethyl alcohol from styrene by *Pseudomonas* 305-STR-1-4. Agricultural and Biological Chemistry 43, 1399–1406.

Sielicki M, Focht D D, Martin J P, 1978. Microbial transformations of styrene and [^{14}C] styrene in soil and enrichment cultures. Applied and Environmental Microbiology 35, 124–128.

Sitch S, Smith B, Prentice I C, Arneth A, Bondeau A, Cramer W, Kaplan J O, Levis S, Lucht W, Sykes M T, Thonicke K, Venevsky S, 2003. Evaluation of ecosystem dynamics, plant geography and terrestrial carbon cycling in the LPJ dynamic global vegetation model. Global Change Biology 9, 161–185.

Sjökvist E, Asp M, Axén Mårtensson J, Berggreen-Clausen S, Berglöv G, Björck E, Johnell A, Nylén L, Ohlsson A, Persson H, 2015. Framtidsklimat i Uppsala län – enligt RCP-scenarier. SMHI Klimatologi Nr 20. Available at: https://www.smhi.se/polopoly_fs/1.165054!/Klimatologi_20 %20 Framtidsklimat%20i%20Uppsala%20l%C3 %A4n%20-%20enligt%20RCP-scenarier.pdf (In Swedish.)

SKB, 2001. SFR 1. Slutförvar för radioaktivt driftavfall. Slutlig säkerhetsrapport, version 1.0, Svensk Kärnbränslehantering AB. (In Swedish.)

SKB, 2014. Miljökonsekvensbeskrivning. Utbyggnad och fortsatt drift av SFR. Svensk Kärnbränslehantering AB. (In Swedish.)

SKB, 2017a. Svar till SSM på begäran om komplettering av ansökan om utbyggnad av SFR avseende geokemi. SKBdoc 1581237 ver 1.0, Svensk kärnbränslehantering AB. (In Swedish.)

SKB, 2017b. Svar till SSM på begäran om komplettering av ansökan om utökad verksamhet vid SFR – effekter av tidig permafrostpåverkan. SKBdoc 1564242, Svensk Kärnbränslehantering AB. (In Swedish.)

SKB P-13-01. SKB 2013. Plats för slutförvaring av kortlivat rivningsavfall. Svensk Kärnbränslehantering AB. (In Swedish.)

SKB R-01-13. SKB 2001. Project SAFE. Scenario and system analysis. Svensk Kärnbränslehantering AB.

SKB R-01-14. SKB 2001. Project SAFE. Compilation of data for radionuclide transport analysis. Svensk Kärnbränslehantering AB.

SKB R-07-34. SKB 2007. Forsmark site investigation. Programme for long-term observations of geosphere and biosphere after completed site investigations. Svensk Kärnbränslehantering AB.

SKB R-08-12. SKB 2008. Project SFR 1 SAR-08. Update of priority of FEPs from Project SAFE. Svensk Kärnbränslehantering AB.

SKB R-08-130. SKB 2008. Safety analysis SFR 1. Long-term safety. Svensk Kärnbränslehantering AB.

SKB R-13-43. SKB 2013. Components, features, processes and interactions in the biosphere. Svensk Kärnbränslehantering AB.

SKB R-14-02. SKB 2015. Handling of biosphere FEPs and recommendations for model development in SR-PSU. Svensk Kärnbränslehantering AB.

SKB R-18-07. SKB 2019. Låg- och medelaktivt avfall i SFR. Referensinventarium för avfall 2016. Svensk Kärnbränslehantering AB. (In Swedish.)

SKB TR-08-05. SKB 2008. Site description of Forsmark at completion of the site investigation phase. SDM-Site Forsmark. Svensk Kärnbränslehantering AB.

SKB TR-10-09. SKB 2010. Biosphere analyses for the safety assessment SR-Site – synthesis and summary of results. Svensk Kärnbränslehantering AB.

SKB TR-10-45. SKB 2010. FEP report for the safety assessment SR-Site. Svensk Kärnbränslehantering AB.

SKB TR-10-48. SKB 2010. Geosphere process report for the safety assessment SR-Site. Svensk Kärnbränslehantering AB.

SKB TR-10-49. SKB 2010. Climate and climate-related issues for the safety assessment SR-Site. Svensk Kärnbränslehantering AB.

SKB TR-10-52. SKB 2010. Data report for the safety assessment SR-Site. Svensk Kärnbränslehantering AB.

SKB TR-11-01. SKB 2011. Long-term safety for the final repository for spent nuclear fuel at Forsmark. Main report of the SR-Site project. Svensk Kärnbränslehantering AB.

SKB TR-11-04. SKB 2013. Site description of the SFR area at Forsmark at completion of the site investigation phase. SDM-PSU Forsmark. Svensk Kärnbränslehantering AB.

SKB TR-13-05. SKB 2014. Climate and climate-related issues for the safety assessment SR-PSU. Svensk Kärnbränslehantering AB.

SKB TR-14-01. SKB 2015. Safety analysis for SFR. Long-term safety. Main report for the safety assessment SR-PSU. Revised edition. Svensk Kärnbränslehantering AB.

SKB TR-14-02. SKB 2014. Initial state report for the safety assessment SR-PSU. Svensk Kärnbränslehantering AB.

SKB TR-14-03. SKB 2014. Waste form and packaging process report for the safety assessment SR-PSU. Svensk Kärnbränslehantering AB.

SKB TR-14-04. SKB 2014. Engineered barrier process report for the safety assessment SR-PSU. Svensk Kärnbränslehantering AB.

SKB TR-14-06. SKB 2014. Biosphere synthesis report for the safety assessment SR-PSU. Svensk Kärnbränslehantering AB.

SKB TR-14-08. SKB 2014. Handling of future human actions in the safety assessment SR-PSU. Svensk Kärnbränslehantering AB.

SKB TR-14-09. SKB 2015. Radionuclide transport and dose calculations for the safety assessment SR-PSU. Revised edition. Svensk Kärnbränslehantering AB.

SKB TR-14-12. SKB 2014. Input data report for the safety assessment SR-PSU. Updated 2017-04. Svensk Kärnbränslehantering AB.

SKB TR-19-05. SKB 2019. Biosphere synthesis for the safety evaluation SE-SFL. Svensk Kärnbränslehantering AB.

SKB TR-19-06. SKB 2019. Radionuclide transport and dose calculations for the safety evaluation SE-SFL. Svensk Kärnbränslehantering AB.

SKB TR-19-24. SKB 2019. RD&D Programme 2019. Programme for research, development and demonstration of methods for the management and disposal of nuclear waste. Svensk Kärnbränslehantering AB.

SKB TR-22-11. SKB 2022. RD&D Programme 2022. Programme for research, development and demonstration of methods for the management and disposal of nuclear waste. Svensk Kärnbränslehantering AB.

SKI, 1992. Project seismic safety. Characterization of seismic ground motions for probabilistic safety analyses of nuclear facilities in Sweden. Summary report. SKI Technical Report 92:3, Swedish Nuclear Power Inspectorate.

SKI/SSI, 2008. SKI's and SSI's review of SKB's safety report SR-Can. SKI Report 2008:23, Swedish Nuclear Power Inspectorate, SSI Report 2008:04 E, Swedish Radiation Protection Institute.

Small J, Nykyri M, Helin M, Hovi U, Sarlin T, Itävaara M, 2008. Experimental and modelling investigations of the biogeochemistry of gas production from low and intermediate level radioactive waste. Applied Geochemistry 23, 1383–1418.

Sohlenius G, Schoning K, Baumgartner A, 2013a. Development, carbon balance and agricultural use of peatlands – overview and examples from Uppland, Sweden. SKB TR-13-20, Svensk Kärnbränslehantering AB.

Sohlenius G, Strömgren M, Hartz F, 2013b. Depth and stratigraphy of regolith at Forsmark. SR-PSU Biosphere. SKB R-13-22, Svensk Kärnbränslehantering AB.

Sorokin D Y, Abbas B, Geleijnse M, Pimenov N V, Sukhacheva MV, van Loosdrecht M C M, 2015. Methanogenesis at extremely haloalkaline conditions in the soda lakes of Kulunda Steppe (Altai, Russia). FEMS Microbiology Ecology 91. doi:10.1093/femsec/fiv016

SS-EN 1992-1-1:2005. Eurocode 2: Design of concrete structures – Part 1-1: General rules and rules for buildings. Stockholm: Swedish Standards Institute.

SSM, 2009. Granskning av SFR-1 SAR-08. SSM dnr 2008/981-30, Swedish Radiation Safety Authority. (In Swedish.)

SSM, 2017. SSM's external experts' review of SKB's safety assessment SR-PSU – dose assessment, K_d-values, and safety analysis methodology. Rapport 2017:33, Swedish Radiation Safety Authority.

SSM, 2018. Strålsäkerhet efter slutförvarets förslutning. Beredning inför regeringens prövning Slutförvaring av använt kärnbränsle. Rapport 2018:07, Swedish Radiation Safety Authority. (In Swedish.)

SSM, 2019. Granskningsrapport – Utbyggnad och fortsatt drift av SFR. Rapport 2019:18, Swedish Radiation Safety Authority. (In Swedish.)

SSM, 2020. Granskningsrapport av SKB:s uppdaterade redovisning av tidpunkt för återtag av feldeponerat avfall i SFR. SSM2013-2073-99, Swedish Radiation Safety Authority. (In Swedish.)

SSM, 2021. Granskning av SKB:s säkerhetsvärdering av slutförvarskoncept för långlivat låg- och medelaktivt avfall. SSM2019-10359-17, Swedish Radiation Safety Authority. (In Swedish.)

SSMFS 2008:1. Strålsäkerhetsmyndighetens föreskrifter och allmänna råd om säkerhet i kärntekniska anläggningar (Regulations concerning safety in nuclear facilities). Stockholm: Swedish Radiation Safety Authority. (In Swedish.)

SSMFS 2018:19. Föreskrifter om ändring i Strålsäkerhetsmyndighetens föreskrifter (SSMFS 2008:37) om skydd av människors hälsa och miljön vid slutligt omhändertagande av använt kärnbränsle och kärnavfall. Stockholm: Swedish Radiation Safety Authority. (In Swedish.)

SSMFS 2008:21. Strålsäkerhetsmyndighetens föreskrifter och allmänna råd om säkerhet vid slutförvaring av kärnämne och kärnavfall (Regulations concerning safety in connection with the disposal of nuclear material and nuclear waste). Stockholm: Swedish Radiation Safety Authority. (In Swedish.)

SSMFS 2008:23. Strålsäkerhetsmyndighetens föreskrifter om skydd av människors hälsa och miljön vid utsläpp av radioaktiva ämnen från vissa kärntekniska anläggningar. Stockholm: Swedish Radiation Safety Authority. (In Swedish.)

SSMFS 2008:37. Strålsäkerhetsmyndighetens föreskrifter och allmänna råd om skydd av människors hälsa och miljön vid slutligt omhänder-tagande av använt kärnbränsle och kärnavfall (Regulations on the protection of human health and the environment in connection with the final management of spent nuclear fuel and nuclear waste). Stockholm: Swedish Radiation Safety Authority. (In Swedish.)

SSMFS 2008:38. Strålsäkerhetsmyndighetens föreskrifter om arkivering vid kärntekniska anläggningar. Stockholm: Swedish Radiation Safety Authority. (In Swedish.)

Stephens M B, Fox A, La Pointe P, Simeonov A, Isaksson H, Hermansson J, Öhman J, 2007. Geology Forsmark. Site descriptive modelling Forsmark stage 2.2. SKB R-07-45, Svensk Kärnbränslehantering AB.

Strömgren M, Brydsten L, 2013. Digital elevation model of Forsmark. Site-descriptive modelling. SR-PSU Biosphere. SKB R-12-03, Svensk Kärnbränslehantering AB.

Stumpf T, Tits J, Walther C, Wieland E, Fanghänel T, 2004. Uptake of trivalent actinides (curium(III)) by hardened cement paste: a time-resolved laser fluorescence spectroscopy study. Journal of Colloid and Interface Science 276, 118–124.

Sundberg J, Back P-E, Ländell M, Sundberg A, 2009. Modelling of temperature in deep boreholes and evaluation of geothermal heat flow at Forsmark and Laxemar. SKB TR-09-14, Svensk Kärnbränslehantering AB.

Svensson T, Bastviken D, Löfgren A, 2021. Cl distribution in different terrestrial habitats along hill slope gradients in Forsmark. SKB R-21-04, Svensk Kärnbränslehantering AB.

Swanton S, Alexander W R, Berry J A, 2010. Review of the behaviour of colloids in the near field of a cementitious repository. Report to NDA RWMD. Serco/TAS/000475/01, Serco, UK.

Taborowski T, Pedersen K, 2019. Methanogens in SFR. SKB R-18-08, Svensk Kärnbränslehantering AB.

Tasi A, 2018. Solubility, redox and sorption behavior of plutonium in the presence of α-D-isosaccharinic acid and cement under reducing, alkaline conditions. PhD thesis, Karlsruhe Institute of Technology, Germany.

Tasi A G, Gaona X, Fellhauer D, Böttle M, Rothe J, Dardenne K, Schild D, Grivé M, Colàs E, Bruno J, Källström K, Altmaier M, Geckeis H, 2018. Redox behavior and solubility of plutonium under alkaline, reducing conditions. Radiochimica Acta 106, 259–279.

Tasi A, Gaona X, Rabung Th, Fellhauer D, Rothe J, Dardenne K, Lützenkirchen J, Grivé M, Colàs E, Bruno J, Källstrom K, Altmaier A, Geckeis H, 2021. Plutonium retention in the isosaccharinate–cement system. Applied Geochemistry 126, 104862. doi:10.1016/j.apgeochem.2020.104862

Terada K, Tani A, Harada S, Satoh H, Hayashi D, 2019. Monte Carlo analysis of montmorillonite particle structures and modeling of dissolution rate reduction. Materials Research Express 6, 035514. doi:10.1088/2053-1591/aaf829

Thomson G, Herben M, Lloyd P, Rose D, Smith C, Barraclough I, 2008. Implementation of project safe in Amber. Verification study for SFR1 SAR-08. SKB R-08-13, Svensk Kärnbränslehantering AB.

Tits J, Fujita T, Harfouche M, Dähn R, Tsukamoto M, Wieland E, 2014. Radionuclide uptake by calcium silicate hydrates: case studies with Th(IV) and U(VI). PSI Bericht Nr. 14-03. Paul Scherrer Institute, Switzerland.

Traboulsi A, Labed V, Dauvois V, Dupuy N, Rébufa C, 2013. Gamma radiation effect on gas production in anion exchange resins. Nuclear Instruments and Methods in Physics Research B 312, 7–14.

Tröjbom M, Grolander S, 2010. Chemical conditions in present and future ecosystems in Forsmark. Implications for selected radionuclides in the safety assessment SR-Site. SKB R-10-27, Svensk Kärnbränslehantering AB.

Ueta S, Satoh H, Kato H, Ueda A, Tsukamoto K, 2016. Interlayer dissolution of montmorillonite observed by internal refraction interferometry. Journal of Nuclear Science and Technology 53, 184–191.

UNSCEAR, 2011. Sources and effects of ionizing radiation. United Nations Scientific Committee on the Effects of Atomic Radiation (UNSCEAR). UNSCEAR 2008 Report to the General Assembly with Scientific Annexes – Volume II Scientific Annexes C, D and E. New York: United Nations.

Van Loon L R, Glaus M A, 1998. Experimental and theoretical studies on alkaline degradation of cellulose and its impact on the sorption of radionuclides. Nagra Technical Report NTB 97-04, Nagra, Switzerland. Also published as PSI Bericht 98-07, Paul Scherrer Institute, Switzerland.

Van Loon L R, Hummel W, 1995. The radiolytic and chemical degradation of organic ion exchange resins under alkaline conditions: effect on radionuclide speciation. Nagra NTB 95-08, Nagra, Schweitz.

Van Loon L R, Hummel W, 1999a. Radiolytic and chemical degradation of strong acidic ion-exchange resins: study of the ligands formed. Nuclear Technology 128, 359–371.

Van Loon L R, Hummel W, 1999b. The degradation of strong basic anion exchange resins and mixed-bed ion exchange resins: Effect of degradation products on radionuclide speciation. Nuclear Technology 128, 388–401.

Van Loon L R, Glaus M A, Stallone S, Laube A, 1997. Sorption of isosaccharinic acid, a cellulose degradation product, on cement. Environmental Science & Technology 31, 1243–1245.

Vestøl O, Ågren J, Steffen H, Kierulf H, Tarasov L, 2019. NKG2016LU: a new land uplift model for Fennoscandia and the Baltic Region. Journal of Geodesy 93, 1759–1779.

Vidstrand P, 2015. A depth sensitivity test of the scaling laws for Darcy fluxes during SR-Site's glacial scenarios. SKBdoc 1462415 ver 1.0, Svensk Kärnbränlsehantering AB.

Vidstrand P, Näslund J-O, Hartikainen J, Svensson U, 2007. Hydrogeological flux scenarios at Forsmark. Generic numerical flow simulations and compilation of climatic information for use in the safety analysis SFR1 SAR-08. SKB R-07-63, Svensk Kärnbränslehantering AB.

Vidstrand P, Follin S, Selroos J-O, Näslund J-O, Rhén I, 2013. Modeling of groundwater flow at depth in crystalline rock beneath a moving ice-sheet margin, exemplified by the Fennoscandian Shield, Sweden. Hydrogeology Journal 21, 239−255.

Vidstrand P, Follin S, Selroos J-O, Näslund J-O, 2014a. Groundwater flow modelling of periods with periglacial and glacial conditions for the safety assessment of the proposed high-level nuclear waste repository site at Forsmark, Sweden. Hydrogeology Journal 22, 1251–1267.

Vidstrand P, Follin S, Öhman J, 2014b. SR-PSU Hydrogeological modelling. TD13 – Periglacial climate conditions. SKB P-14-06, Svensk Kärnbränslehantering AB.

von Schenck H, Bultmark F, 2014. Effekt av bitumensvällning i silo och BMA. SKB R-13-12, Svensk Kärnbränslehantering AB. (In Swedish.)

Väisäsvaara J, 2009. Site investigation SFR. Difference flow logging in borehole KFR105. SKB P-09-09, Svensk Kärnbränslehantering AB.

Waber H N, Gimmi, T, Smellie J A T, 2009. Porewater in the rock matrix. Site descriptive modelling SDM-Site Forsmark. SKB R-08-105, Svensk Kärnbränslehantering AB.

Walke R, Limer L, Shaw G, 2017. In-depth review of key issues regarding biosphere models for specific radionuclides in SR-PSU. In SSM's external experts' review of SKB's safety assessment SR-PSU – dose assessment, K_d-values and safety analysis methodology. Main review phase. Report 2017:33, Swedish Radiation Safety Authority, Part 2.

Werner K, Hamrén U, Collinder P, 2010. Vattenverksamhet i Forsmark (del I). Bortledande av grundvatten från slutförvarsanläggningen för använt kärnbränsle. SKB R-10-14, Svensk Kärnbränslehantering AB. (In Swedish.)

Werner K, Sassner M, Johansson E, 2013. Hydrology and near-surface hydrogeology at Forsmark – synthesis for the SR-PSU project. SR-PSU Biosphere. SKB R-13-19, Svensk Kärnbränslehantering AB.

Werner K, Norville J, Öhman J, 2014. Meteorological, hydrological and hydrogeological monitoring data from Forsmark – compilation and analysis for the SR-PSU project. SR-PSU Biosphere. SKB R-13-20, Svensk Kärnbränslehantering AB.

Westman P, Wastegård S, Schoning K, Gustafsson B, Omstedt A, 1999. Salinity change in the Baltic Sea during the last 8 500 years: evidence, causes and models. SKB TR-99-38, Svensk Kärnbränslehantering AB.

Wieland E, 2014. Sorption data base for the cementitious near field of L/ILW and ILW repositories for provisional safety analyses for SGT-E2. NAGRA Technical Report 14-08, Nagra, Switzerland.

Wilmot R, Robinson P, 2004. The issue of risk dilution in risk assessments. management of uncertainty in safety cases and the role of risk. Proceedings of OECD/NEA Workshop, Stockholm, 2–4 February 2004. Paris: OECD/NEA.

Wold S, 2015. Are colloids released from different materials in SFR to the saturating groundwater? KTH. SKBdoc 1466123 ver 1.0, Svensk Kärnbränslehantering AB.

Yokoyama S, Shimbashi M, Minato D, Watanabe Y, Jenni A, Mäder U, 2021. Alteration of bentonite reacted with cementitious materials for 5 and 10 years in the Mont Terri rock laboratory (CI experiment). Minerals 11, 251. doi:10.3390/min11030251

Yu C, Drake H, Dideriksen K, Tillberg M, Song Z, Morup S, Åström M, 2020. A combined X-ray absorption and Mössbauer spectroscopy study on Fe valence and secondary mineralogy in granitoid fracture networks: implications for geological disposal of spent nuclear fuels. Environmental Science & Technology 54, 2832–2842.

Yumoto I, 2007. Alkaliphiles. In Gerday C, Glansdorff N (eds). Physiology and biochemistry of extremophiles. Washington DC: ASM Press.

Zänker H, Hennig C, 2014. Colloid-borne forms of tetravalent actinides: a brief review. Journal of Contaminant Hydrology 157, 87–105.

Åstrand P-G, Rasmusson M, Wessely O, 2022. Near-field radionuclide transport models for the post-closure safety assessment in PSAR SFR. SKB R-21-02, Svensk Kärnbränslehantering AB.

Öhman J, Odén M, 2017. TD15 Complementary simulation cases in support of SR-PSU. SKBdoc 1578373 ver 1.0, Svensk Kärnbränslehantering AB.

Öhman J, Odén M, 2018. SR-PSU (PSAR) Bedrock hydrogeology. TD18 – Temperate climate conditions. SKB P-18-02, Svensk Kärnbränslehantering AB.

Öhman J, Vidstrand P, 2014. SR-PSU Bedrock hydrogeology. TD12 – Water-supply wells in rock. SKB P-14-05, Svensk Kärnbränslehantering AB.

Öhman J, Bockgård N, Follin S, 2012. Bedrock hydrogeology. Site investigation SFR. SKB R-11-03, Svensk Kärnbränslehantering AB.

Öhman J, Follin S, Odén M, 2014. SR-PSU Hydrogeological modelling. TD11 – Temperate climate conditions. SKB P-14-04, Svensk Kärnbränslehantering AB.

Appendix A

Terms and abbreviations

The present report contains terms and abbreviations that either are rarely used outside SKB or can be regarded as specialised terminology within one or several of the scientific and modelling disciplines involved in the reported work. To facilitate the readability of the report, selected terms and abbreviations are explained in Table A-1.

Table A-1. Explanations of terms and abbreviations used in this report.

Term or abbreviation	Description
1–2BMA	Vaults for intermediate-level waste in SFR.
1–2BTF	Vaults for concrete tanks in SFR1.
1–5BLA	Vaults for low-level waste in SFR.
1BRT	Vault for reactor pressure vessels in SFR3.
1STT	Silo roof tunnel.
1TT	Transverse tunnel in SFR1.
2BST	Waste vault tunnel in SFR3.
2TT	Transverse tunnel in SFR3.
3D	Three-dimensional.
Abiotic	Non-living physical or chemical component or process.
Absorbed dose rate	Amount of energy deposited in matter by ionizing radiation per unit mass and per unit time.
AD	Anno Domini.
Annual dose	Assessment endpoint calculated as the annual effective dose to an adult, where the annual effective dose is defined as the effective dose from external exposure in a year, plus the committed effective dose from intakes of radionuclides in that year.
Annual effective dose	The effective dose from external exposure in a year, plus the committed effective dose from intakes of radionuclides in that year.
Assessment team	The group of persons responsible for performing the safety assessment. The team judge the material delivered by the data supplier and recommend data for use in the assessment.
Barrier	In the safety assessment context, a barrier is a physical feature, engineered or natural, which in one or several ways contributes to the containment and retention or prevention of dispersion of radioactive substances, either directly or indirectly by protecting other barriers.
Barrier function	In the safety assessment context, a barrier function is a role by means of which the barrier contributes to post-closure safety.
Base case	The *base case* constitutes the basis for the radionuclide transport and dose calculations. The *present-day climate calculation case* is selected as the *base case* for the analysis of the main scenario. Models built and assumptions made for the other calculation cases are only described if they deviate from the *base case* and results from these cases are compared with those for the *base case*.
Basin	In the terminology used in this safety assessment for the drainage area of a biosphere object (cf. below) minus the drainage area of any upstream object. When the basin is below sea level, the basin is identical to the biosphere object.
BAT	Best available technique. The most effective measure available to limit the release of radioactive substances and the harmful effects of releases on human health and the environment, and which does not entail unreasonable costs.
BC	Before Christ.
Bedrock	In the safety assessment context, the solid rock beneath the regolith also including the groundwater in the rock.
Best estimate	A single value for a parameter, describing a property or a process, used in deterministic calculations. Best estimates are typically derived from site and/or literature data and often correspond to mean values of the underpinning datasets.
Biosphere object	A part of the landscape that will potentially receive radionuclides released from a repository, directly or indirectly via other biosphere objects.
Biosphere system	In the safety assessment context, refers to the part of the repository system that is above the geosphere, with all its abiotic and biotic processes and features, as well as humans and human behaviour. Synonymous with Surface system.
BioTEx	The Biosphere Transport and Exposure model. Used to calculate concentrations and subsequent transport of radionuclides in different environmental media in a biosphere object and potential doses to human and dose rates to non-human biota.

Term or abbreviation	Description
Biotic	Living ecosystem component or process involving living organisms.
BST	Waste vault tunnel.
BT	Construction tunnel (one of two access tunnels).
BWR	Boiling water reactor.
Calculation case	Used for the quantitative assessment of the scenarios selected in the safety assessment, typically by calculating doses.
Cautious	Indicates an expected overestimate of annual effective dose that follows from assumptions made, or models and parameter values selected, within the reasonably expected range of possibilities.
Central block	The volume of bedrock that is bounded to the northeast and southwest by two broad belts, the Northern boundary belt and the Southern boundary belt, of concentrated ductile and brittle deformation. The Central block is less affected by deformation than the bounding belts.
Climate domain	A climatically determined environment with a specific set of characteristic processes of importance for post-closure safety.
Climate variant	A climate development used in describing the range of possible future climate developments that may influence post-closure safety.
Clab	Central interim storage facility for spent nuclear fuel in Simpevarp, Sweden.
Clink	Facility comprising the central interim storage (currently Clab) and the planned encapsulation plant.
Collective dose	In the safety assessment context, equal to the collective effective dose, which is the sum of all the individual effective doses to members of a population. The special name of the unit of the collective effective dose is the man sievert (man Sv).
Conditioning	Those operations that produce a waste package suitable for handling, transport, storage and/or disposal.
Connecting tunnel	General term used for tunnels outside waste vaults, for example BST.
Conceptual model	A qualitative description of a physical system, including important processes and components and interactions between these components.
Crushed rock	Mechanically crushed rock material with varying grain size distribution and hydraulic properties. The selected grain size distribution is dependent on the required properties. See also macadam.
CSH	Calcium silicate hydrates.
CT	Central tunnel in SFR.
Data uncertainty	Uncertainties concerning all quantitative input data, that is parameter values, used in the assessment.
DEM	Digital elevation model. Describes the topography and bathymetry of the modelled area.
Discharge locations/points	Locations/areas where groundwater reaches the surface ecosystem. In the safety assessment context, this term refers to discharge of groundwater that has passed though the repository volume in the geosphere and hence could bring radionuclides to the surface. Synonymous with Discharge points.
DM	Drained-mire farmers. Refers to self-sustained agriculture in which wetlands are drained and cultivated (both crop and fodder production). It is one of four potentially exposed groups (PEGs) in this safety assessment.
Effective dose	Effective dose is a measure of dose designed to reflect the amount of radiation detriment likely to result from the dose. It is defined as a weighted summation of the tissue or organ equivalent doses, that is the summation of the absorbed dose in each tissue or organ multiplied by appropriate radiation weighting factor, each multiplied by the appropriate tissue weighting factor.
ERICA	Environmental Risk from Ionising Contaminants – Assessment and management. EU-project that provided screening values to assess environmental risk.
Eustasy	Change in sea level due to, for example, changes in the volume and spatial distribution of sea water in the world's oceans.
Exposure	The act or condition of being subject to irradiation (not to be used as a synonym for dose, which is a measure of the effects of exposure).
External exposure	Exposure to radiation from a source outside the body.
F-PSAR	First Preliminary Safety Analysis Report.
FEPs	Features, events and processes.
FHA	Future human actions.
Geosphere	The bedrock, including groundwater, surrounding the repository, bounded above by the surface system.
GP	Garden-plot households. Refers to a type of household that is self-sustained with respect to vegetables and root crops produced through small-scale horticulture. It is one of four potentially exposed groups (PEGs) in this safety assessment.

Term or abbreviation	Description
Harmful effects	Cancer (fatal and non-fatal) as well as hereditary effects in humans caused by ionising radiation, in accordance with paragraphs 47–51 in ICRP Publication 60 (ICRP 1991).
HG	Hunter-gatherers. Refers to a community that uses the undisturbed surface ecosystems as living space and to obtain food. It is one of four potentially exposed groups (PEGs) in this safety assessment.
IAEA	International Atomic Energy Agency.
ICRP	International Commission on Radiological Protection.
Infilling	Infilling describes the combined process of sedimentation and organogenic deposition, which turns lakes into wetlands.
Initial state	The expected state of the repository and its environs at closure of the repository.
Insolation	The amount of solar radiation received per unit area at the top of the Earth's atmosphere.
Interaction matrix	A tool used to identify processes, and interactions between processes, that have to be considered in quantitative analyses in the safety assessment.
Intermediate-level waste	Radioactive waste that requires final disposal in a geological repository and shielding during handling. Cooling of the waste is not required.
Internal exposure	Exposure to radiation from a source within the body.
IO	Infield-outland farmers. Refers to a self-sustained agriculture in which infield farming of crops is dependent on nutrients from wetlands for haymaking (outland). It is one of four potentially exposed groups (PEGs) in this safety assessment.
IPCC	Intergovernmental Panel on Climate Change.
ISA	Isosaccharinate, a complexing agent that is a cellulose degradation product.
ISO	International Organization for Standardization.
Isostasy	Vertical movement of the Earth's crust, which in Forsmark is dominated by isostatic rebound following the latest glaciation.
KBS-3	Method developed by SKB for final disposal of spent nuclear fuel.
Layout 2020	Layout for SFR3 from 2020, used in the post-closure safety assessment (PSAR SFR).
Layout 2021	Final layout for SFR3 used in the PSAR SFR application.
Long-lived radionuclide	In the safety assessment context, radionuclides with a half-life exceeding 31 years.
Long-lived waste	In the safety assessment context, radioactive waste that contain significant levels of radionuclides with a half-life greater than 31 years.
Low-level waste	Radioactive waste that requires final disposal in a geological repository. Shielding during handling and cooling are not required.
m.b.s.l.	Metres below sea level.
Macadam	Crushed rock sieved in fractions 2–65 mm. Macadam has no or very little fine material (grain size < 2 mm). The fraction is given as intervals, for example "Macadam 16-32" is crushed rock comprising the fraction 16–32 mm.
Mathematical model	A quantitative description of a physical system, where important processes and components, and interactions between components, are represented by parameters and equations.
Modelling uncertainty	Uncertainties arising from a necessarily imperfect understanding of the nature of processes involved in repository evolution which leads to imperfect conceptual models. The mathematical representation of conceptual models and imprecision in the numerical solution of mathematical models are other sources of uncertainty which fall into this category.
NBT	Lower construction tunnel.
NEA	OECD Nuclear Energy Agency.
Near-field	Typically used for the model domain representing the repository, which may contain part of the nearby bedrock to obtain boundary conditions.
NHB	Non-human biota.
NPP	Nuclear power plant.
NSP	Lower silo plug.
NTA	Nitrilotriacetic acid, a complexing agent.
Optimisation	In radiological protection, optimisation means to strive to reduce the radiation doses as low as reasonably achievable while taking economic and societal factors into account.
Packaging	The outer container, such as a mould, drum or ISO-container, protecting the waste form (synonymous with Waste packaging).
PEG	Potentially exposed group. Groups of individuals potentially subjected to the highest exposure during any time of the assessment period.
Pessimistic	Indicates an expected overestimate of annual effective dose that follows from assumptions made, or models and parameter values selected, beyond the reasonably expected range of possibilities.
PFL-f	Discrete inflow detected by the Posiva Flow Logging method.

Term or abbreviation	Description
Potentially exposed group	Groups of individuals potentially subjected to the highest exposure during any time of the assessment period.
Probabilistic analysis	Mathematical analysis of stochastic (random) events or processes and their consequences. Since the input is described in stochastic terms, the output is also stochastic (for example in the form of probabilities or distributions).
Protective capability	The capability to protect human health and the environment from the harmful effects of ionising radiation.
PSAR	Preliminary Safety Analysis Report.
PSU	Programme SFR extension.
PVC	Polyvinyl chloride.
PWR	Pressurised water reactor.
Radiotoxicity	The product of the activity of a radionuclide and it's corresponding dose coefficient for intake.
RCP4.5	Emission scenario from IPCC in which radiative forcing is stabilised at approximately 4.5 W m^{-2} at 2100 AD.
RCP6.0	Emission scenario from IPCC in which radiative forcing is stabilised at approximately 6.0 W m^{-2} at 2100 AD.
RD&D	Research, development and demonstration.
RDM	Regolith depth and stratigraphy model. A three-dimensional model of regolith extension.
Reference design	A design of the repository that is valid from a defined point in time until further notice. Here used as prerequisite in the post-closure safety assessment.
Reference evolution	The probable post-closure evolution of the repository and its environs, including uncertainties in the evolution that may affect the protective capability of the repository.
Regolith	All matter overlying the bedrock. This includes both minerogenic and organogenic (i.e. derived from organic substances) deposits.
Relative sea level	The vertical position of the sea relative to land, as measured in the reference height system RH 2000. The relative sea level is determined by the net effect of eustasy and isostasy.
Repository	The disposed waste packages, the engineered barriers and other repository structures.
Repository system	The repository, the bedrock and the biosphere surrounding the repository. Synonymous with repository and its environs.
Risk	Refers in the post-closure safety assessment to the radiological risk, defined as the product of the probability of receiving a radiation dose and the harmful effects of that radiation dose.
Risk dilution	In the context of the radionuclide transport, dose and risk calculations, risk dilution in a broad sense refers to a situation in which an increase in the uncertainty of the values of important input parameters, or in the assumptions with respect to the timing of an event, leads to a decrease in the calculated annual dose and associated annual radiological risk.
RLDM	Regolith-lake development model. Used to project the future regolith depth and stratigraphy in the model area. Consists of a marine module describing sediment dynamics caused by wave action and a lake module that describes infilling of lakes.
RNT	Radionuclide transport.
RPV	Reactor pressure vessel.
SAFE	Post-closure safety assessment for SFR1 reported to the regulatory authorities in 2001.
Safety analysis	In the context of the present safety assessment, the distinction is generally not viewed as important and therefore safety analysis and safety assessment are used interchangeably. However, if the distinction is important, safety analysis should be used as a documented process for the study of safety and safety assessment should be used as a documented process for the evaluation of safety.
Safety assessment	The safety assessment is the systematic process periodically carried out throughout the lifetime of the repository to ensure that all the relevant safety requirements are met and entails evaluating the performance of the repository system and quantifying its potential radiological impact on human health and the environment. The safety assessment corresponds to the term *safety analysis* in the Swedish Radiation Safety Authority's regulations.
Safety function	A role through which a repository component contributes to post-closure safety
Safety function indicator	A measurable or calculable property of a repository component that indicates the extent to which a safety function is fulfilled.
SAR	Safety Analysis Report.
SAR-08	Post-closure safety assessment for SFR1 reported to the regulatory authorities in 2008.
SBA	Shallow bedrock aquifer. Sections with an elevated frequency of gently dipping to horizontal fractures in the uppermost c. 150 m of bedrock between the geologically modelled steeply dipping deformation zones.

Term or abbreviation	Description
Scenario	A description of a potential evolution of the repository and its environs, given an initial state and specified external conditions and their development and how the protective capability of the repository is affected.
Scenario uncertainty	Uncertainties with respect to external conditions and internal processes in terms of type, degree and time sequence, resulting in an uncertainty in the future states of the repository system
SDM	Site descriptive model. A synthesis of qualitative and quantitative information on the present-day conditions in the bedrock and surface system at the repository site, based on both direct observations and modelling studies. Includes geological, rock mechanical, thermal, hydrogeological, hydrogeochemical and surface system properties of the repository site.
SDM-PSU	Site descriptive model for the SFR area.
SDM-Site	Site descriptive model for the Forsmark site for the spent nuclear fuel repository.
SE-SFL	The evaluation of post-closure safety for a proposed repository concept for SFL.
SFL	Final repository for long-lived radioactive waste.
SFR	Final repository for short-lived radioactive waste at Forsmark.
SFR1	The existing part of SFR.
SFR3	The extension part of SFR.
SGU	Geological Survey of Sweden.
Shoreline displacement	The movement of the shoreline, that is the variation in time of the spatial location of the shoreline.
Shoreline migration	The movement of the shoreline, that is the variation in time of the spatial location of the shoreline.
Shoreline regression	Migration of the coastline away from the land as the relative sea level decreases, which in turn increases the extent of the land area.
Short-lived radionuclide	In the safety assessment context, radionuclides with a half-life shorter than 31 years.
Short-lived waste	In the safety assessment context, radioactive waste that does not contain significant levels of radionuclides with a half-life greater than 31 years.
Silo	Cylindrical vault for intermediate-level waste (part of SFR1).
SKB	Swedish Nuclear Fuel and Waste Management Company.
SKBdoc	Internal document management system at SKB.
SKI	Swedish Nuclear Power Inspectorate. SKI and SSI were merged into SSM in July 2008.
Sorption coefficient	Element-specific sorption coefficient, defined as the ratio between the elemental concentrations in the solid and liquid phases.
SR-Can	Preliminary post-closure safety assessment for the planned spent nuclear fuel repository, published in 2006.
SR-PSU	Post-closure safety assessment that was a reference to the F-PSAR for the extended SFR, reported to the regulatory authority in 2014.
SRF	Sorption Reduction Factor (due to complexing agents).
SRF group	Group of radionuclides with analogous complexation properties and thus same SRF values.
SR-Site	Post-closure safety assessment for a spent nuclear fuel repository in Forsmark, reported to the regulatory authority in 2011.
SSI	Swedish Radiation Protection Authority. SSI and SKI were merged into SSM in July 2008.
SSM	Swedish Radiation Safety Authority.
SSMFS	Regulations of the Swedish Radiation Safety Authority.
STP	Silo roof plug.
Sub-catchment	In the safety assessment context, defined as the drainage area of a biosphere object minus the drainage area of the inlets to the object. For objects without a stream inlet the sub-catchment is identical to the basin.
Surface ecosystem	The surface ecosystem refers to the part of the environment above the bedrock, with all its abiotic and biotic processes and features.
Surface system	In the safety assessment context, refers to the part of the repository system that is above the geosphere, with all its abiotic and biotic processes and features, as well as humans and human behaviour. Synonymous with Biosphere system.
System component	A physical component of the repository system; a sub-system.
System uncertainty	Uncertainties concerning comprehensiveness issues, i.e. the question of whether all aspects important for the safety evaluation have been identified and whether the assessment is capturing the identified aspects in a qualitatively correct manner.
Transition material	Component in earth dam plug e.g. 30/70 mixture bentonite and crushed rock. The role of the transition material is to hinder bentonite transport from the hydraulically tight section, to take up the load from bentonite swelling and transfer it to the backfill material.
WAC	Waste acceptance criteria.

Term or abbreviation	Description
Waste domain	Part of waste vaults where waste is placed (inside the engineered barriers).
Waste form	Waste in its physical and chemical form after treatment and/or conditioning.
Waste package	The waste (form) and its packaging.
Waste packaging	The outer container, such as a mould, drum or ISO-container, protecting the waste form (synonymous with Packaging).
Waste stream	The pathway of a specific waste, from its origin through to its disposal in a defined waste type.
Waste type	SKB's systematic classification of wastes according to a developed code system.
Waste type description	Safety report for a waste type. The waste type description contains, among other things, information about the waste, waste packaging, treatment of the waste and where the waste is to be disposed.
Waste vault	Part of repository where waste is disposed.
ÖSP	Upper silo plug.

Appendix B

Handling of requirements from SSMFS 2008:21

This appendix describes how the Swedish Radiation Safety Authority's regulations and general advice concerning safety in connection with the disposal of nuclear material and nuclear waste (SSMFS 2008:21) has been handled in the current assessment. References are given to the parts of the assessment where the requirement in question have been addressed. The text of SSMFS 2008:21 is reproduced and SKB's handling of the requirements (Section B1) and general advice (Section B2) is inserted with blue font. It should be noted that only the Swedish version of the regulations have legal status and that the translation lacks legal force.

B1 SSMFS 2008:21

The Swedish Radiation Safety Authority's regulations concerning safety in connection with the disposal of nuclear material and nuclear waste issued on 19 December 2008.

On the basis of Sections 20a and 21 of the Nuclear Activities Ordinance (1984:14), the Swedish Radiation Safety Authority hereby issues the following regulations.

Application

Section 1 These regulations apply to facilities for the disposal of nuclear material and nuclear waste (repositories).

The regulations do not apply to facilities for landfill disposal of low-level nuclear waste under Section 16 of the Nuclear Activities Ordinance (1984:14).

The regulations contain supplementary provisions to the Swedish Radiation Safety Authority's regulations (SSMFS 2008:1) concerning safety in nuclear facilities and the Swedish Radiation Safety Authority's regulations (SSMFS 2018:1) on basic requirements on activities involving ionising radiation requiring permit.

Section 1a Terms and concepts that are used in this regulation have the same meaning as in the Act on Nuclear Activities (1984:3), the Environmental Code, and the Swedish Radiation Safety Authority's regulations (SSMFS 2018:1) on basic requirements on activities involving ionising radiation requiring permit.

Barriers and their Functions

Section 2 Safety after the closure of a repository shall be maintained through a system of passive barriers.

Handling in the PSAR: The compliance with the requirement is demonstrated in Section 11.1.2.

Section 3 The function of each barrier shall be to, in one or several ways, contribute to the containment and prevention or retention of dispersion of radioactive substances, either directly or indirectly by protecting other barriers in the barrier system.

Handling in the PSAR: The compliance with the requirement is demonstrated in Section 11.1.2.

Section 4 A deficiency in any of the repository's barrier functions that is detected during the construction or operational surveillance of the repository, and that can lead to a deterioration in safety after closure in addition to that anticipated in the safety analysis report[49], shall be reported to the Swedish Radiation Safety Authority without unnecessary delay.[50] The same applies if such a deficiency is suspected to occur or if it is suspected that such a deficiency may possibly occur in the future.

Handling in the PSAR: This requirement relates to reporting to SSM during the construction and operational phases, which is not discussed in the post-closure safety assessment.

Design and Construction

Section 5 The barrier system shall be able to withstand such features, events and processes that can affect the post-closure performance of the barriers.

Handling in the PSAR: The compliance with the requirement is demonstrated in Section 11.1.2 and the confidence in the compliance is discussed in 11.2.

Section 6 The barrier system shall be designed and constructed taking into account the best available technique[51]

Handling in the PSAR: The compliance with the requirement is demonstrated in Section 11.1.2.

Section 7 The barrier system shall comprise several barriers so that, as far as possible, the necessary safety is maintained despite a single deficiency in a barrier.

Handling in the PSAR: The compliance with the requirement is demonstrated in Section 11.1.2 and the confidence in the compliance is discussed in 11.2.

Section 8 The impact on safety of measures adopted to facilitate the monitoring or retrieval of disposed nuclear material or nuclear waste from the repository, or to make access to the repository difficult, shall be analysed and reported to the Swedish Radiation Safety Authority.

Handling in the PSAR: This relates to the design of the repository and is not discussed in this report.

Safety analysis

Section 9 In addition to the provisions contained in Chapter 4, Section 1 of the Swedish Radiation Safety Authority's regulations (SSMFS 2008:1) concerning safety in nuclear facilities, the safety analyses shall also comprise features, events and processes that can lead to the dispersion of radioactive substances after closure, and such analyses shall be made before repository construction, before repository operation and before repository closure.

Handling in the PSAR: The systematic management of the FEPs that can lead to the dispersion of radioactive substances after closure is reported in Chapter 3. The effect of these FEPs on the dispersion of radioactive substances disposed in SFR is analysed in the reference evolution (Chapter 6), scenario analysis (Chapters 7–9), and risk evaluation (Chapter 10). The post-closure safety assessment in the PSAR is a part of the application for approval of construction by SSM.

Section 10 A safety analysis shall comprise the requisite duration of barrier functions, though a minimum of ten thousand years.

Handling in the PSAR: The timescales of relevance are discussed in Section 2.4.2. The safety assessment covers the period up to 100 000 years after closure of SFR.

---

[49] Cf. Chapter 4, Section 2 of the Swedish Radiation Safety Authority's regulations (SSMFS 2008:1) concerning safety in nuclear facilities.

[50] Cf. Chapter 2, Section 3 of the Swedish Radiation Safety Authority's regulations (SSMFS 2008:1) concerning safety in nuclear facilities.

[51] Cf. Chapter 2, Section 3 of the Swedish Environmental Code.

Safety analysis reports

Section 11 The safety analysis report for a repository shall, in addition to what is required by Chapter 4, Section 2 of the Swedish Radiation Safety Authority's regulations (SSMFS 2008:1) concerning safety in nuclear facilities, contain the information shown in Appendix B1 of these regulations and which concerns the period of time following closure.

Handling in the PSAR: See Appendix B1 below.

Prior to repository closure, the safety analysis report shall be renewed and subjected to a safety review in accordance with Chapter 4, Section 3 of the Swedish Radiation Safety Authority's regulations (SSMFS 2008:1) concerning safety in nuclear facilities and shall be reviewed and approved by the Swedish Radiation Safety Authority.

Exemptions

Section 12 If there are particular grounds, the Swedish Radiation Safety Authority may grant exemptions from these regulations if this can be done without circumventing the aim of the regulations and on the condition that safety can be maintained.

Appendix 1

The following shall be reported with regard to analysis methods:

– how one or several methods have been used to describe the passive system of barriers in the repository, its performance and evolution over time; the method or methods shall contribute to providing a clear understanding of the features, events and processes that can affect the performance of the barriers and the links between these features, events and processes

  Handling in the PSAR: The system of passive barriers in the repository and its initial state is described in Chapter 4. The method for describing the performance of the barrier system is based on the FEP handling described in Chapter 3 and safety functions and safety function indicators that relate to the different barriers, as described in Chapter 5. Influence tables and process influence diagrams as well as interaction matrices are described in the **FEP report** as a means to ensure that links between FEPs are adequately accounted for. In the process reports a structed approach is used for describing processes and how they are influenced by relevant variables. In the reference evolution (Chapter 6) the evolution of the barrier system over time is described. In the scenario analysis (Chapters 7–9) a number of scenarios comprising relevant evolutions of combinations of external and internal conditions are used to analyse repository performance.

– how one or several methods have been used to identify and describe relevant scenarios for sequences of events and conditions that can affect the future evolution of the repository; the scenarios shall include a main scenario that takes into account the most probable changes in the repository and its environment

  Handling in the PSAR: The method for selection of the scenarios is described in Section 2.6.8. The main scenario takes into account the most probable changes in the repository and its environment (Sections 7.1–7.2). The selection of the main scenario, less probable scenarios and residual scenarios is described in Sections 7.2, 8.2 and 9.2, respectively.

– the applicability of models, parameter values and other assumptions used for the description and quantification of repository performance as far as reasonably achievable

  Handling in the PSAR: In the **Model tools report**, the suitability of the models for their purpose is discussed. In the **Data report**, applicable data are selected based on a structured approach.

– how uncertainties in the description of the barrier system's functions, scenarios, calculation models and calculation parameters as well as variations in barrier properties have been dealt with in the safety analysis, including the reporting of a sensitivity analysis showing how the uncertainties affect the description of the evolution of barrier performance and the analysis of the impact on human health and the environment

  Handling in the PSAR: General aspects of the handling of uncertainties in the post-closure safety assessment are described in Section 2.5. The approach to handling of uncertainties in each step of the safety assessment methodology is described in Section 2.6. The role of handling of uncertainties in lending confidence in the compliance with regulatory requirements regarding barrier system robustness as well as human health and the environment is discussed in Section 11.2.4.

The following shall be reported with respect to the analysis of post-closure conditions:

– The safety analysis in accordance with Section 9 comprising descriptions of the evolution in the biosphere, geosphere and repository for selected scenarios; the environmental impact of the repository for selected scenarios, including the main scenario, thereby considering defects in engineered barriers and other identified uncertainties

  Handling in the PSAR: The evolution of the biosphere, geosphere and repository is described for the selected scenarios (Chapters 7–9) based on the descriptions given in the reference evolution (Chapter 6). The environmental (radiological) impact of the repository is reported for relevant scenarios including the main scenario (Chapters 7–10, **Biosphere synthesis report**). In the scenario analysis defects in engineered barriers and other identified uncertainties are considered by including scenarios that relate to uncertainties in the initial state, external conditions, and internal processes (Section 7.2, 8.2 and 9.2).

B2 Excerpts from the Swedish Radiation Safety Authority's general advice on the application of the regulations (SSMFS 2008:21) concerning safety in connection with the disposal of nuclear material and nuclear waste

On Section 9 and Appendix

The safety of a repository after closure is analysed quantitatively, primarily by estimating the possible dispersion of radioactive substances and how it is distributed over time for a relevant selection of potential future sequences of events (scenarios). The purpose of the safety analysis is to show, inter alia, that the risks from these scenarios are acceptable in relation to the requirements on the protection of human health and the environment imposed by the Swedish Radiation Safety Authority (SSMFS 2008:37). The safety analysis should also aim to provide a basic understanding of repository performance during different time periods and to identify requirements regarding the performance and design of different repository components.

A ***scenario*** in the safety analysis comprises a description of how a given combination of external and internal conditions affects repository performance.

Two groups of such conditions are:

– external conditions in the form of features, events and processes which occur outside repository barriers; these include climate changes and their consequential impact on the repository environment, such as permafrost, glaciation, land subsidence, land uplift as well as the impact of human activities, and

– internal conditions in the form of features, events and processes which occur inside the repository; examples of such conditions are properties including defects, nuclear material, nuclear waste and engineered barriers and related processes, as well as properties of the surrounding geological formation and related processes.

Based on an analysis of the probability of occurrence of different types of scenarios in different time periods, scenarios with a significant impact on repository performance should be divided into different categories:

– main scenario
– less probable scenarios
– other scenarios or residual scenarios.

The ***main scenario*** should be based on the probable evolution of external conditions and realistic, or where justified, conservative assumptions with respect to the internal conditions. It should comprise future external events which have a significant probability of occurrence or which cannot be shown to have a low probability of occurrence during the period of time covered in the safety analysis. Furthermore, it should as far as possible be based on credible assumptions with respect to internal conditions, including substantiated assumptions concerning the occurrence of manufacturing defects and other imperfections, and which allow for an analysis of the repository barrier performance (for example, it is insufficient to always base the analysis on leaktight waste containers over an extended period of time, even if this can be shown to be the most probable case). The main scenario should be used as the starting point when analysing the impact of uncertainties (see below), which means that the analysis of the main scenario also includes a number of calculation cases.

Less probable scenarios should be prepared for the evaluation of scenario uncertainty (see also below). This includes variations of the main scenario with alternative sequences of events and periods of time as well as scenarios that take into account the impact of future human activities, such as damage inflicted on barriers. (Detriment to humans intruding into the repository is illustrated by residual scenarios; see below.) An analysis of less probable scenarios should include analyses of uncertainties that are not evaluated within the framework of the main scenario.

Residual scenarios should include sequences of events and conditions that are selected and studied independently of probabilities in order to, inter alia, illustrate the significance of individual barriers and barrier functions. The residual scenarios should also include cases to illustrate detriment to humans intruding into the repository as well as cases to illustrate the consequences of an unclosed repository that is not monitored.

Handling in the PSAR: The analysis includes a main scenario, less probable scenarios and residual scenarios in line with the recommendations. The methodology for selection of scenarios is presented in Section 2.6.8 and the selected scenarios are presented in Chapters 7–9.

Lack of knowledge and other uncertainties in the calculation presumptions (assumptions, models, data) are in this context denoted as ***uncertainties***. These uncertainties can be classified as follows:

– Scenario uncertainty: uncertainty with respect to external and internal conditions in terms of type, degree and time sequence
– System uncertainty: uncertainty as to the completeness of the description of the system of features, events and processes used in the analysis of both individual barrier performance and the performance of the repository as a whole
– Model uncertainty: uncertainty in the calculation models used in the analysis
– Parameter uncertainty: uncertainty in the parameter values (input data) used in the calculations
– Spatial variation in the parameters used to describe the barrier performance of the rock (primarily with respect to hydraulic, mechanical and chemical conditions)

There are often no clear boundaries between the different types of uncertainties. The most important requirement is that the uncertainties are to be described and handled in a consistent and structured manner.

The evaluation of uncertainties is an important part of the safety analysis. This means that uncertainties should be discussed and examined in depth when selecting calculation cases, calculation models and parameter values, as well as in the assessment of calculation results.

Handling in the PSAR: General aspects of handling of uncertainties in the post-closure safety assessment are described in Section 2.5. This includes a description of the classification of uncertainties adopted in the safety assessment, which is in line with the recommendations. The approach to handling of uncertainties in each step in the safety assessment methodology is described in Section 2.6. The role of handling of uncertainties in lending confidence in the compliance with regulatory requirements regarding barrier system robustness and human health and the environment is discussed in Section 11.2.4.

The assumptions and calculation models used should be carefully selected with respect to the principle that the application and selection should be justified by means of a discussion of alternatives and with reference to science. In cases where there is doubt as to the applicability of a model, several models should be used to illustrate the impact of the uncertainty involved in the choice of model.

Handling in the PSAR: This matter is addressed in the **Process reports** and the **Biosphere synthesis report** and, for external influences, in the **Climate report**. A structured account of important selected model tools is given in the **Model tools report**.

Both deterministic and probabilistic methods should be used so that they complement each other and, consequently, provide as comprehensive a picture of the risks as possible.

Handling in the PSAR: Probabilistic models are used in different parts of the safety assessment. For instance, the radionuclide inventory is estimated using probabilistic methods (Section 4.3.7) and the radionuclide transport and dose calculations are performed both deterministically and probabilistically for most calculation cases (Section 7.3.1).

The ***probabilities*** of the scenarios and calculation cases actually occurring should be estimated as far as possible in order to calculate risk. Such estimates cannot be exact. Consequently, the estimates should be substantiated through the use of several methods, for example assessments by several independent experts. This can for instance be done through estimates of when different events can be expected to have occurred.

Handling in the PSAR: The probabilities of the less probable scenarios are discussed in the descriptions of the scenarios in Chapter 8 and the risk calculation procedure is described in Section 10.2.

A number of ***design basis cases*** should be identified based on scenarios that can be shown to be especially important from the standpoint of risk. Together with other information, such as regarding manufacturing method and controllability, these cases should be used to substantiate the design basis, such as requirements on barrier properties.

Handling in the PSAR: The handling of this recommendation is discussed in Section 11.3.2 as part of the feedback to subsequent steps in the repository programme.

Particularly in the case of disposal of nuclear material, for example spent nuclear fuel, it should be demonstrated that criticality cannot occur in the initial configuration of the nuclear material. With respect to the redistribution of the nuclear material through physical and chemical processes, which can lead to criticality, it should be demonstrated that such redistribution is very improbable.

Handling in the PSAR: The recommendation is not applicable in the present safety assessment.

The result of calculations in the safety analysis should contain such information and should be presented in such a way that an overall judgement of safety compliance with the requirements can be made.

Handling in the PSAR: Compliance with requirements relating to safety and the protection of human health and the environment is demonstrated in Section 11.1 and the confidence in the compliance is discussed with reference to the information gathered in the safety assessment (Section 11.2).

The validity of assumptions used, such as models and parameter values, should be supported, for example by citing references to scientific literature, special investigations and research results, laboratory experiments on different scales, field experiments and studies of natural phenomena (natural analogues).

Handling in the PSAR: Justification of models, on the bases mentioned, is discussed in the **Process reports** and the **Biosphere synthesis report,** and for external influences, in the **Climate report**. A structured account of all important model tools is given in the **Model tools report**. Parameter values are justified in the **Data report**.

Scientific background material, such as from expert assessments, should be documented in a traceable manner by conscientiously referring to scientific literature and other material.

Handling in the PSAR: All scientific background material to the safety analysis report, which consists of first-order references, is referred to in a traceable manner. These references are found in SKB's document management system (SKBdoc) or in publicly available publications (for example books or scientific articles).

On Section 10

The time period for which safety needs to be maintained and demonstrated should be a starting point for the safety analysis. One way of discussing and justifying the establishment of the relevant time period is to start from a comparison of the hazard of the radioactive inventory of the repository with the hazard of radioactive substances occurring in nature. However, it should also be possible to take into consideration the difficulties of conducting meaningful analyses for extremely long periods of time, beyond one million years, in some other way than by demonstrating how the hazard of the radioactive substances in the repository declines over time.

In the case of a repository intended for long-lived waste, the safety analysis may need to include scenarios taking greater expected climate changes into account, primarily in the form of future glaciations. For example, the next complete glacial cycle, currently estimated to be in the order of 100 000 years, should be particularly taken into account.

Handling in the PSAR: The timescale is discussed in Section 2.4.2.

In the case of periods up to 1 000 years after closure, in accordance with the provisions of SSMFS 2008:37, the dose and risk calculated for current conditions in the biosphere constitute the basis for assessing repository safety and the repository's protective capabilities.

Furthermore, in the case of more extended periods of time, the assessment can be made using dose as one of several safety indicators. This should be taken into account in connection with calculations as well as presentation of analysis results. Examples of these supplementary safety indicators include the concentrations of radioactive substances from the repository which can build up in soils and near-surface groundwater as well as the calculated flow of radioactive substances to the biosphere.

Handling in the PSAR: For the period up to 1 000 years after closure, the current conditions in the biosphere are the basis for the radionuclide transport and dose calculations (Chapters 7–9). In addition to the dose calculations, supplementary safety indicators are used for time periods beyond 1 000 years after closure (Section 10.7).

Appendix C

Handling of requirements from SSMFS 2008:37

This appendix describes how the Swedish Radiation Safety Authority's Regulations concerning the protection of human health and the environment in connection with the final management of spent nuclear fuel and nuclear waste (SSMFS 2008:37) has been handled in the current assessment. References are given to the parts of the assessment where the requirement in question have been addressed. The text of SSMFS 2008:37 is reproduced and SKB's handling of the requirements (Section C1) and general advice (Section C2) is inserted with blue font. It should be noted that only the Swedish version of the regulations have legal status and that the translation lacks legal force. The translation is based on SSMFS 2008:37 and the amendments given in SSMFS 2018:19.

C1 SSMFS 2008:37

The Swedish Radiation Safety Authority's Regulations concerning the Protection of Human Health and the Environment in connection with the Final Management of Spent Nuclear Fuel and Nuclear Waste issued on 19 December 2008.

On the basis of Sections 7 and 8 of the Radiation Protection Ordinance (1988:293), the Swedish Radiation Safety Authority hereby issues the following regulations.

Application and definitions

Section 1 These regulations apply to the final management of spent nuclear fuel and nuclear waste. The regulations do not apply to landfills for low-level nuclear waste in accordance with Section 19 of the Nuclear Activities Ordinance (1984:14).

Section 2 Terms and concepts that are used in this regulation have the same meaning as in Radiation Protection Act (1988:220), the Act on Nuclear Activities (1984:3), and the Environmental Code. In these regulations the following terms and concepts are used with the meanings specified here.

intrusion:	human intrusion into a repository which can affect its protective capability
harmful effects:	cancer (fatal and non-fatal) as well as hereditary effects in humans caused by ionising radiation, in accordance with paragraphs 47–51 in Publication 60, 1990, of the International Commission on Radiological Protection (ICRP)
protective capability:	the capability to protect human health and the environment from the harmful effects of ionising radiation
final management:	handling, treatment, transport, interim storage prior to, and in connection with, disposal as well as the disposal itself
risk:	the product of the probability of receiving a radiation dose and the harmful effects of the radiation dose

Holistic approach, etc.

Section 3 Human health and the environment shall be protected from detrimental effects of ionising radiation during the period of time when the various stages of the final management of spent nuclear fuel and nuclear waste are being implemented as well as in the future. The final management may not cause impacts on human health and the environment outside Sweden's borders that are more severe than those accepted inside Sweden.

Section 4 Optimisation must be performed and the best available technique shall be taken into consideration in the final management of spent nuclear fuel and nuclear waste. The collective dose, as a result of the expected outflow of radioactive substances over a period of 1,000 years after closure of a repository for spent nuclear fuel or nuclear waste shall be estimated as the sum, over 10,000 years, of the annual collective dose. The estimate shall be reported in accordance with Sections 10 to 12.

Handling in the PSAR: Optimisation and BAT is discussed in Section 11.1.2. The collective doses due to C-14 releases for the global population, and due to all released radionuclides for the regional population around the Baltic Sea, have been calculated as required in the regulation (Section 11.2.3, **Radionuclide transport report**, Chapter 9).

Protection of human health

Section 5 A repository for spent nuclear fuel or nuclear waste shall be designed so that the annual risk of harmful effects after closure does not exceed 10^{-6} for a representative individual in the group exposed to the greatest risk.[52]

The probability of harmful effects as a result of a radiation dose shall be calculated using the probability coefficients provided in Publication 60, 1990 of the International Commission on Radiological Protection.

Handling in the PSAR: The fulfilment of the risk criterion is demonstrated in Section 11.1.1 with reference to the risk calculations in Chapter 10. In Section 11.2 the confidence in the compliance demonstration is discussed.

Environmental protection

Section 6 The final management of spent nuclear fuel and nuclear waste shall be implemented so that biodiversity and the sustainable use of biological resources are protected against the harmful effects of ionising radiation.

Section 7 Biological effects of ionising radiation in the habitats and ecosystems concerned shall be described. The report shall be based on available knowledge on the ecosystems concerned and shall take particular account of the existence of genetically distinctive populations such as isolated populations, endemic species and species threatened with extinction and in general any organisms worth protecting.

Handling in the PSAR: The fulfilment of the requirements regarding environmental protection is demonstrated in Section 11.1.1 with reference to Section 10.8 and the **Biosphere synthesis report**.

Intrusion and access

Section 8 A repository shall be primarily designed with respect to its protective capability. If measures are adopted to facilitate access or to make intrusion more difficult, the effects on the protective capability of the repository shall be reported.

Section 9 The consequences of intrusion into a repository shall be reported for the different time periods specified in Sections 11 to 12.

The protective capability of the repository after intrusion shall be described.

Handling in the PSAR: Intrusion is discussed in Section 9.11 and further elaborated in the **FHA report**.

Time periods

Section 10 An assessment of a repository's protective capability shall be reported for two time periods of the orders of magnitude specified in Sections 11 to 12. The description shall include a case based on the assumption that the biospheric conditions prevailing at the time when an application for a licence to construct the repository is submitted will not change. Uncertainties in the assumptions made shall be described and taken into account when assessing the protective capability.

[52] Facilities in operation are subject to the Swedish Radiation Safety Authority's regulations (SSMFS 2008:23) on protection of human health and the environment in connection with discharges of radioactive substances from certain nuclear facilities as well as the the Swedish Radiation Safety Authority's regulations (SSMFS 2018:1) on basic requirements on activities involving ionising radiation requiring permit.

The first thousand years following closure of a repository

Section 11 For the first thousand years following repository closure, the assessment of the repository's protective capability shall be based on quantitative analyses of the impact on human health and the environment.

Period after the first thousand years following closure of a repository

Section 12 For the period after the first thousand years following repository closure, the assessment of the repository's protective capability shall be based on various possible sequences for the development of the repository's properties, its environment and the biosphere.

Handling in the PSAR: The reference evolution (Chapter 6) is divided into two time periods. The initial period of submerged conditions, which has a duration of at least 1 000 years (Section 6.2), and the period thereafter which addresses the evolution of the repository system during periods of present-day climate (Section 6.3), a warm climate variant (Section 6.4), and a cold climate variant (Section 6.5). The present-day climate variant assumes that the biosphere conditions currently prevailing will not change during the analysis period. The protective capability of the repository is analysed with a risk and scenario analysis that is based on various possible sequences for the development of the repository's properties, its environment and the biosphere (Chapters 7–10). Relevant uncertainties are considered, for instance by accounting for the three climate variants. Conclusions regarding the protection of human health and the environment are presented in Chapter 11.

Exemptions

Section 13 If there are particular grounds, the Swedish Radiation Safety Authority may grant exemptions from these regulations if this can be done without circumventing the aim of the regulations.

C2 The Swedish Radiation Safety Authority's general advice on the application of the regulations (SSMFS 2008:37) concerning the protection of human health and the environment in connection with the final management of spent nuclear fuel and nuclear waste

Section 1: Application

This advice is applicable to final geological disposal of spent nuclear fuel and nuclear waste. The advice covers measures undertaken with a view to developing, siting, constructing, operating and closing a repository, which can have an impact on the protective capability of the repository and the environmental consequences after closure.

The advice is also applicable to measures that are to be undertaken with spent nuclear fuel and nuclear waste before disposal and which can have an impact on the protective capability of a repository and its environmental consequences. This includes activities at installations other than the repository, such as the conditioning of waste that takes place by casting waste in concrete and by encapsulation of spent nuclear fuel, as well as transports between installations and steering of waste to different repositories, including shallow land burials for low-level nuclear waste that are licenced in accordance with Section 16 of the Nuclear Activities Ordinance (1984:14). However, as is the case with the regulations, the advice is not applicable to the installation for land burial.

Section 2: Definitions

Terms and concepts used in the Radiation Protection Act (2018:396), the Act on Nuclear Activities (1984:3), the Environmental Code and the Swedish Radiation Safety Authority's regulations (SSMFS 2008:37) on protection of human health and the environment in connection with final management of spent nuclear fuel and nuclear waste have the same meanings in this advice. The following definitions are also used:

scenario:	a description of the potential evolution of the repository given an initial state and specified conditions in the environment and their development
exposure pathway:	the migration of the radioactive substances from a repository to a place where human beings are present, or where an organism covered by the environmental protection regulations is present. This includes dispersion in the geological barrier, transport with water and air flows, migration in ecosystems and uptake in human beings or organisms in the environment.
risk analysis:	an analysis with the aim of clarifying the protective capability of a repository and its consequences with regard to the environmental impact and the risk for human beings

Sections 4, 8 and 9: Holistic approach, etc.; intrusion and access

Optimisation and Best Available Technique

The regulations require optimisation to be performed and the best available technique to be taken into account. Optimisation and best available technique should be applied in parallel with a view to improving the protective capability of the repository.

Measures for optimisation of a repository should be evaluated on the basis of calculated risks.

Application of best available technique in connection with disposal means that the siting, design, construction and operation of the repository and appurtenant system components should be carried out so as to prevent, limit and delay releases from both engineered and geological barriers as far as is reasonably possible. When striking balances between different measures, an overall assessment should be made of their impact on the protective capability of the repository.

In cases where considerable uncertainty is attached to the calculated risks, for instance in analyses of the repository a long time after closure, or analyses made at an early stage of the development work with the repository system, greater weight should be placed on best available technique.

In the event of any conflicts between application of optimisation and best available technique, priority should be given to best available technique.

Experiences from recurrent risk analyses and the successive development work with the repository should be used when applying optimisation and best available technique.

Handling in the PSAR: Optimisation and BAT is discussed in Section 11.1.2.

Collective dose

The regulations require an account of the collective dose from releases taking place during the first thousand years after closure. As far as concerns disposal, the collective dose should also be used in comparisons between alternative repository concepts and sites. The collective dose need not be reported if the repository concept entails a complete containment of the spent nuclear fuel or nuclear waste in engineered barriers during the first thousand years after closure.

Handling in the PSAR: The collective doses due to C-14 releases for the global population, and due to all released radionuclides for the regional population around the Baltic Sea, have been calculated as required in the regulation (Section 11.2.3, **Radionuclide transport report**, Chapter 9).

Occupational radiation protection

An account should be given of measures undertaken for radiation protection of workers that may have a negative impact on the protective capability of the repository or make it more difficult to assess.

Handling in the PSAR: No such measures have been identified.

Future human action and the preservation of information

When applying best available technique, consideration should also be given to the possibility to reduce the probability and consequences of inadvertent future human impact on the repository, for instance inadvertent intrusion. Increased repository depth and avoidance of sites with extractable mineral assets may, for instance, be considered to reduce the probability of unintentional human intrusion.

Handling in the PSAR: The site selection was approved as a part of the government's licensing of SFR. Underlying SKB's license application in 2014 was a document that discusses the site selection (SKB P-13-01), including aspects related to inadvertent future human action.

Preservation of knowledge about the repository could reduce the risk of future human impact. A strategy for preservation of information should be produced so that measures can be undertaken before closure of the repository. Examples of information that should be taken into consideration include information about the location of the repository, its content of radioactive substances and its design.

Handling in the PSAR: The strategy for preservation of information is not a part of the safety assessment. SKB is obliged to follow the provisions of the Swedish Radiation Safety Authority's regulations (SSMFS 2008:38) on archiving at nuclear facilities that requires long-term preservation of information regarding the location of the repository, its content of radioactive substances and its design.

Sections 5–7: Protection of human health and the environment

Risk for the individual from the general public

The relationship between dose and risk

Under the regulations, the recommendations of the International Commission on Radiological Protection (ICRP) are to be used when calculating the harmful effects of a radiation dose. According to ICRP Publication 60, 1990, the factor for conversion of effective dose to risk is 7.3 per cent per sievert.

The regulations' criterion for individual risk

Under the regulations, the risk for harmful effects for a representative individual in the group exposed to the greatest risk (the most exposed group) shall not exceed 10^{-6} per year. Since the most exposed group cannot be described in an unambiguous way, the group should be regarded as a way of quantifying the protective capability of the repository.

One way of defining the most exposed group is to include the individuals who receive a risk in the interval from the highest risk down to one-tenth of this risk. If a larger number of individuals can be considered to be included in such a group, the arithmetic average of individual risks in the group should be used for demonstrating compliance with the criterion for individual risk contained in the regulations. One example of this kind of exposure situation is a release of radioactive substances into a large lake that can be used as a source of drinking water and for fishing.

If the exposed group only consists of a few individuals, the criterion of the regulations for individual risk can be considered as being complied with if the highest calculated individual risk does not exceed 10^{-5} per year. An example of a situation of this kind might be if consumption of drinking water from a drilled well is the dominant exposure pathway. In such a calculation example, the choice of individuals with the highest risk load should be justified by information about the spread in calculated individual risks with respect to assumed living habits and places of stay.

Handling in the PSAR: Four groups of exposed populations are used in the assessment. Different exposure pathways are mapped to the exposed groups which are used as bounding cases to identify most exposed group (Section 7.3.6). Risk evaluation for the most exposed group is described in Chapter 10.

Averaging risk over a lifetime

The individual risk should be calculated as an annual average on the basis of an estimate of the lifetime risk for all relevant exposure pathways for every individual. The lifetime risk can be calculated as the accumulated lifetime dose multiplied by the conversion factor of 7.3 per cent per sievert.

Handling in the PSAR: The averaging of risk over a lifetime is discussed in the **Biosphere synthesis report**, Section 2.3.5.

Averaging risk between generations

Deterministic and probabilistic calculations can both be used to illustrate how risk posed by the repository develops over time. However, a probabilistic analysis can in certain cases give an insufficient picture of how an individual detrimental event, for instance, a major earthquake, would affect the risk for a particular generation. The probabilistic calculations should in such cases be supplemented as specified in Appendix 1.

Handling in the PSAR: The issue of risk dilution and how it has been handled is discussed in Section 10.6.

Selection of scenarios

An assessment of the protective capability of a repository and the environmental consequences should be based on a set of scenarios that together illustrate the most important courses of development of the repository, its surroundings and the biosphere.

Dealing with climate evolution

Taking into consideration the great uncertainties associated with the assumptions concerning climate evolution in a remote future and to facilitate interpretation of the risk to be calculated, the risk analysis should be simplified to include a few possible climate evolutions.

A realistic set of biosphere conditions should be associated with each climate evolution. The different climate evolutions should be selected so that they together illustrate the most important and reasonably foreseeable sequences of future climate states and their impact on the protective capability of the repository and their environmental consequences. The choice of the climate evolutions that serve as the basis for the analysis should be based on a combination of sensitivity analyses and expert judgements. Additional guidance is provided in the section containing advice on Sections 10 to 12.

The risk posed by the repository should be calculated for each assumed climate evolution by summing the risk contributions from a number of scenarios that together illustrate how the more or less probable courses of development in the repository and the surrounding rock affect the repository's protective capability and environmental consequences. The calculated risk should be reported and evaluated separately for each climate evolution in relation to the criterion of the regulations for individual risk. Hence, it should be shown that the repository complies with the risk criterion for each of the alternative climate evolutions. If a lower probability than one (1) is stated for a particular climate evolution, this should be justified, for instance by expert judgements.

Handling in the PSAR: In the main scenario, three climate variants are considered, the present-day climate variant, the warm climate variant, and the cold climate variant (Chapter 7). These are based on the corresponding climate cases defined in Section 2.6.3 and in the **Climate report**, Chapter 5. Another climate case describing glacial climate conditions is also considered in a less probable scenario (Section 8.3). Together these climate cases illustrate the most important and reasonably foreseeable sequences of future climate states. The selection of the climate cases and the likelihood of their occurrence is discussed in the **Climate report**. In the scenario analysis the impact of the climate cases on the protective capability of the repository is analysed (Chapter 7, Section 8.3). The handling of the three climate cases in the main scenario in relation to the less probable scenarios is discussed in Section 8.7.1. In Section 10.4, it is confirmed that the present-day climate parameterisation is limiting with respect to the risk criterion., i.e. it gives the highest maximum risk among the climate cases. Furthermore, a residual scenario analysing the impact of early permafrost has been included (Section 9.3).

Future human action

A number of future scenarios for inadvertent human impact on the repository should be presented. The scenarios should include a case of direct intrusion in connection with drilling in the repository and some examples of other activities that indirectly lead to a deterioration in the protective capability of the repository, for example by changing the hydrological conditions or groundwater chemistry in the repository or its surroundings. The selection of intrusion scenarios should be based on present living habits and technical prerequisites and take into consideration the repository's properties.

The consequences of the disturbance for the repository's protective capability should be illustrated by calculations of the doses for individuals in the most exposed group and be reported separately from the risk analysis for the undisturbed repository. The results should be used to illustrate conceivable countermeasures and to provide a basis for the application of best available technique (see the advice on optimisation and best available technique).

An account need not be given of the direct consequences for the individuals intruding into the repository.

Handling in the PSAR: Four stylised FHA residual scenarios have been identified (Section 9.11), including a case with direct intrusion and other cases that indirectly could potentially lead to a deterioration of the protective capability of the repository. The location of SFR is selected considering best available technique, for instance the location beneath the Baltic Sea protects from intrusion during the initial period when a large fraction of the initial activity decays. An account of direct consequences for the individual intruding into the repository is given in line with the general advice to SSMFS 2008: 21, noting that this is not needed according to the general advice to SSMFS 2008:37, as stated in previous paragraph.

Special scenarios

For repositories primarily based on containment of the spent nuclear fuel or nuclear waste, an analysis of a conceivable loss during the first thousand years after closure of one or more barrier functions of key importance for the protective capability should be presented separately from the risk analysis. The intention of this analysis should be to clarify how the different barriers contribute to the protective capability of the repository.

Handling in the PSAR: Several residual scenarios have been selected to show the impact of the loss of different barrier functions on the protective capability of the repository (Section 9.2).

Biosphere conditions and exposure pathways

The future biosphere conditions for calculations of consequences for human beings and the environment should be selected in agreement with the assumed climate state. Unless it is clearly inconsistent, however, today's biosphere conditions at the repository and its surroundings should be evaluated, i.e. agricultural land, forest, wetland (mire), lake, sea or other relevant ecosystems. Furthermore, consideration should be taken to land uplift (or subsidence) and other predictable changes.

The risk analysis can include a limited selection of exposure pathways, although the selection of these should be based on an analysis of the diversity of human use of environmental and natural resources which can occur in Sweden today. Consideration should also be taken to the possibility of individuals being exposed to combinations of exposure pathways within and between different ecosystems.

Handling in the PSAR: In the present-day climate calculation case of the main scenario the present biosphere conditions are applied for all ecosystems (Section 7.4.4). In the warm and cold climate calculation cases, the biosphere conditions are defined to be in agreement with the climate states (Section 7.5.3 and 7.6.3, respectively). An exposure pathway analysis has been performed and the identified exposure pathways have been included for one or more of the four groups identified to be used as bounding cases of most exposed group (Section 7.3.6).

Environmental protection

The description of exposure pathways as mentioned above should also include exposure pathways to certain organisms in the above-mentioned ecosystems that should be included in the risk analysis. The concentration of radioactive substances in soil, sediment and water should be accounted for where relevant for the respective ecosystem.

When a biological effect for the identified organisms can be presumed, an evaluation should be made of the consequence this may have for the affected ecosystems, with the view to facilitating an assessment of impact on biological diversity and sustainable use of the environment.

The analysis of consequences for organisms in "today's biosphere", carried out as above, should be used for the assessment of environmental consequences in a long-term perspective. For assumed climates, where the present biosphere conditions are clearly unrealistic, for example during a colder climate with permafrost, it is sufficient to conduct a general analysis based on knowledge currently available about applicable ecosystems. Additional advice is contained in Appendix 2.

Handling in the PSAR: The of exposure to non-human biota is handled in line with the recommendation and the results of the analysis are described in Section 10.8 with reference to the **Biosphere synthesis report**.

Reporting of uncertainties

Identification and assessment of uncertainties in (for instance) site-specific and generic data and models should take place in accordance with the instructions given in the general advice for the Swedish Radiation Safety Authority's regulations (SSMFS 2008:21) concerning safety in connection with the disposal of nuclear material and nuclear waste. The different categories of uncertainties specified there should be evaluated and reported on in a systematic way and evaluated on the basis of their importance for the result of the risk analysis. The report should also include a motivation of the methods selected for dealing with different types of uncertainties, for instance in connection with the selection of scenarios, models and data. All calculation steps with appurtenant uncertainties should be reported on.

Peer review and expert panel elicitation may be used in cases where the basic data is insufficient to strengthen the credibility of assessments of uncertainties in matters of great importance for assessing the protective capability of the repository.

Handling in the PSAR: The approach to handling of uncertainties is described in Chapter 2 and a discussion of the handling of uncertainties in relation to the demonstration of compliance is given in Section 11.2.4.

Sections 10–12: Time periods

Two time periods are defined in the regulations: the period up to one thousand years after closure and the subsequent period.

For longer time periods, the result of the risk analysis should be successively regarded more as an illustration of the protective capability of the repository given certain assumptions.

Limitation of the risk analysis in time

The following principles should provide guidance for the limitation of the risk analysis in time:

1. For a repository for spent nuclear fuel or other long-lived nuclear waste, the risk analysis should at least cover approximately one hundred thousand years or the period for a glaciation cycle to illustrate reasonably predictable external strains on the repository. The risk analysis should thereafter be extended in time for as long as it provides important information about the possibility of improving the protective capability of the repository, although for a maximum time period of up to one million years.

2. For repositories for nuclear waste other than those referred to in item 1, the risk analysis should at least cover the period of time until the expected maximum consequences in terms of risk and environmental impact have taken place, although for a maximum time period of up to one hundred thousand years. The arguments for the selected limitations of the risk analysis should be presented.

Handling in the PSAR: The timescale for the assessment is discussed in Section 2.4.2. An assessment time period of 100 000 years is selected.

Reporting on the first thousand years after closure

The period of time of one thousand years should be regarded as the approximate time period for which a risk analysis can be carried out with a high level of credibility with regard to many factors, such as climate and biosphere conditions. For this time period, available measurement data and other knowledge about the initial conditions should be used for a detailed analysis and description of the protective capability of the repository and the evolution of its surroundings.

The conditions and processes during the early evolution of the repository which can affect its long-term protective capability should be described in as much detail as possible. Examples of such conditions and processes include the resaturation of the repository, stabilisation of hydrogeological and geochemical conditions, thermal evolution and other transient events.

Biosphere conditions and known trends in the surroundings of the repository should also be described in detail, partly to be able to characterise "today's biosphere" (see advice for Section 5), and partly to be able to characterise the possible conditions applicable to a conceivable early release from the repository. Known trends here for instance refer to land uplift (or subsidence), any trends in climate evolution and appurtenant changes in use of land and water.

Handling in the PSAR: The reference evolution (Chapter 6) is divided into two time periods, the initial period of submerged conditions, which has a duration of at least 1 000 years (Section 6.2) and the time thereafter. The analysis of the protective capability (Chapters 7–10) is based on the information provided in the reference evolution.

Reporting on very long time periods

Up to one hundred thousand years

Reporting should be based on a quantitative risk analysis in accordance with the advice on Sections 5 to 7. Supplementary indicators of the repository's protective capability, such as barrier functions, radionuclide fluxes and concentrations in the environment, should be used to strengthen the confidence in the calculated risks.

The given period of time of one hundred thousand years is approximate and should be selected in such a way so that the effect of expected large climate changes, for instance a glaciation cycle, on the protective capability of the repository, and the consequences for the surroundings can be illustrated.

Handling in the PSAR: Supplementary indicators of the repository's protective capability are discussed in Section 10.7.

Beyond one hundred thousand years

The risk analysis should illustrate the long-term evolution of the repository's barrier functions and the impact of major external disturbances on the repository, such as earthquakes and glaciations. Taking into consideration the increasing uncertainties over time, the calculation of doses to people and the environment should be made in a simplified way with respect to climate development, biosphere conditions and exposure pathways. The climate evolution may be described as an idealised repetition of identical glaciation cycles.

A strict quantitative comparison of calculated risk with the criterion for individual risk contained in the regulations is not meaningful. The assessment of the protective capability of the repository should instead be based on reasoning on the calculated risk together with several supplementary indicators of the protective capability of the repository, such as barrier functions, radionuclide fluxes and concentrations in the environment. If the calculated risk exceeds the criterion of the regulations

for individual risk or if there are other indications of substantial disruptions to the protective capability of the repository, the underlying causes of this should be reported on as well as possible measures to improve the protective capability of the repository.

Handling in the PSAR: Based on Section 10 to 12 and related general advice, an assessment time period of 100 000 years has been used. The maximum radiological consequence takes place during this time period.

Summary of arguments for demonstrating compliance with the requirements of the regulations

The reporting should include an account of how the principles for optimisation and the best possible technique have been applied in the siting and design of the repository and appurtenant system components, and how quality assurance has been used in the work with the repository and appurtenant risk analyses.

Handling in the PSAR: Optimisation and BAT is discussed in Section 11.1.2 and quality assurance in Section 2.8.

The arguments for the protective capability of a repository should be evaluated and reported on in a systematic way. The reporting should include a logically structured argument for the protective capability of the repository with information on calculated risks, uncertainties in the calculations made and the credibility of the assumptions made. To provide a good understanding of the results of the risk analysis, it should be evident how individual scenarios contribute to the level of risk posed by the repository.

Handling in the PSAR: The arguments for the protective capability of the repository are given in a structured way in Chapter 11 with reference to the other parts of this report, including Chapter 2 that describes the systematic safety assessment methodology and Chapter 10 that includes a description of how individual scenarios contribute to the total annual risk.

Appendix 1. Advice on the averaging of risk between generations

For certain exposure situations, the annual risk, calculated as an average of all conceivable outcomes of a probabilistic risk assessment, provides an insufficient picture of how risk is allocated between future generations.

This particularly applies to events which:

– can be assessed as leading to doses during a limited period of time in relation to the time period covered by the risk analysis, and

– if they arise, can be assessed as giving rise to a conditional individual risk exceeding the criterion contained in the regulations for individual risk, and

– can be assessed as having such a high probability of occurring during the time period covered by the risk analysis that the product of this probability and the calculated conditional risk is of the same order of magnitude as, or exceeds, the criterion for individual risk contained in the regulations.

For exposure situations of this kind, a probabilistic calculation of risk should be supplemented by calculating the risk for the individuals who are assumed to live after the event has taken place and who are affected by its calculated maximum consequence. The calculation can for instance be made by illustrating the significance of an event occurring at different points in time (T1, T2 […],Tn), taking into consideration the probability of the event occurring during the respective time interval (T0 to T1, T0 to T2 […],T0 to Tn, where T0 corresponds to the time of closure of the repository). The results from these, or similar calculations, can in this way be expected to provide an illustration of the effects of the spreading of risk between future generations and should, together with other risk calculations, be reported on and evaluated in relation to the regulations' criterion for individual risk.

Handling in the PSAR: The issue of risk dilution and how it has been handled is discussed in Section 10.6.

Appendix 2. Advice on the evaluation of environmental protection

The organisms included in the analysis of environmental impact should be selected on the basis of their importance in the ecosystems, but also in line with their protection value according to other biological, economic or conservation criteria. Other biological criteria refer (among other things) to genetic distinctiveness and isolation (for example, presently known endemic species). Economic criteria refer to the importance of the organisms for establishment of different kinds of livelihood (for instance, hunting and fishing). Conservation criteria refer to possible protection by current legislation or local regulations. Other aspects, such as cultural history, for instance, should also be taken into consideration when identifying such organisms.

An assessment of effects of ionising radiation in selected organisms deriving from radioactive substances that may have spread from a repository can be made on the basis of the general guidance provided by Publication 91 from the International Commission on Radiological Protection (ICRP).1 The applicability of the knowledge and databases used for the analyses of dispersion and transfer of radioactive substances in ecosystems and for analysing the effects of radiation on different organisms should be assessed and reported on.

Handling in the PSAR: The evaluation of environmental protection is handled in line with the recommendation and the results of the analysis is described in Section 10.8 with reference to the **Biosphere synthesis report**.

Appendix D

FEPs in the SFR FEP catalogue

This appendix provides tables of the complete set of FEPs included in the SFR FEP catalogue (PSAR version). The 353 FEPs are divided into the following seven main categories: *initial state, internal processes, system variables, biosphere, external factors, methodology* and *site-specific factors*, presented in separate subsections below. For each FEP, the FEP ID, FEP name and a reference to the corresponding description in various reports, is given.

D1 Initial state

In Table D-1, the five *initial state* FEPs included in the FEP catalogue are listed.

Table D-1. Initial state FEPs in the FEP catalogue with references to the corresponding descriptions in the FEP report and this report.

FEP ID	FEP name	Section in the FEP report and this report (*in italics*)
ISGen01	Major mishaps/accidents/sabotage	5.2, *3.5.3*
ISGen02	Effects of phased operation	5.2, *3.5.3*
ISGen03	Incomplete closure	5.2, *3.5.3, 9.10*
ISGen04	Monitoring activities	5.2, *3.5.3*
ISGen05	Design deviations – Mishaps	5.2, *3.5.3, 8.2.3, 8.2.6, 8.5.2, 9.8*

D2 Internal processes

In Table D-2 to D-4, the 178 FEPs included in the main category *internal processes* in the FEP catalogue are listed. These are subdivided into the SFR system components *waste form* (22 FEPs, WM*nn*), *concrete and steel packaging* (16 FEPs, Pa*nn*), *silo barriers* (26 FEPs, SiBa*nn*), *BMA barriers* (19 FEPs, BMABa*nn*), *BRT barriers* (18 FEPs, BRTBa*nn*), *BTF barriers* (18 FEPs, BTFBa*nn*), *BLA barriers* (16 FEPs, BLABa*nn*), *plugs and other closure components* (21 FEPs, Pg*nn*) and *geosphere* (22 FEPs, Ge*nn*).

Table D-2. Waste form and Concrete and steel packaging FEPs in the FEP catalogue with references to the corresponding descriptions in the Waste process report.

FEP ID	FEP name	Section in Waste process report
WM01	Radioactive decay	3.1.1
WM02	Radiation attenuation/heat generation	3.1.2
WM03	Radiolytic decomposition of organic material	3.1.3
WM04	Water radiolysis	3.1.4
WM05	Heat transport	3.2.1
WM06	Phase changes/freezing	3.2.2
WM07	Water uptake and transport during unsaturated conditions	3.3.1
WM08	Water transport under saturated conditions	3.3.2
WM09	Fracturing	3.4.1
WM10	Advective transport of dissolved species	3.5.1
WM11	Diffusive transport of dissolved species	3.5.2
WM12	Sorption/uptake	3.5.3
WM13	Colloid formation and transport	3.5.4
WM14	Dissolution, precipitation and recrystallisation	3.5.5
WM15	Degradation of organic materials	3.5.6
WM16	Water uptake/swelling	3.5.7
WM17	Microbial processes	3.5.8
WM18	Metal corrosion	3.5.9
WM19	Gas formation and transport	3.5.10
WM20	Speciation of radionuclides	3.6.1
WM21	Transport of radionuclides in the water phase	3.6.2
WM22	Transport of radionuclides in the gas phase	3.6.3
Pa01	Heat transport	4.1.1
Pa02	Phase changes/freezing	4.1.2
Pa03	Water uptake and transport during unsaturated conditions	4.2.1
Pa04	Water transport under saturated conditions	4.2.2
Pa05	Fracturing/deformation	4.3.1
Pa06	Advective transport of dissolved species	4.4.1
Pa07	Diffusive transport of dissolved species	4.4.2
Pa08	Sorption/uptake	4.4.3
Pa09	Colloid transport and filtering	4.4.4
Pa10	Dissolution, precipitation and recrystallisation	4.4.5
Pa11	Microbial processes	4.4.6
Pa12	Metal corrosion	4.4.7
Pa13	Gas formation and transport	4.4.8
Pa14	Speciation of radionuclides	4.5.1
Pa15	Transport of radionuclides in the water phase	4.5.2
Pa16	Transport of radionuclides in the gas phase	4.5.3

Table D-3. Engineered barrier FEPs in the FEP catalogue with references to the corresponding descriptions in the Barrier process report.

FEP ID	FEP name	Section in the Barrier process report
SiBa01	Heat transport	7.1.1
SiBa02	Phase changes/freezing	7.1.2
SiBa03	Water uptake and transport during unsaturated conditions	7.2.1
SiBa04	Water transport under saturated conditions	7.2.2
SiBa05	Gas transport/dissolution	7.2.3
SiBa06	Piping/erosion	7.2.4
SiBa07	Mechanical processes	7.3.1
SiBa08	Advection and dispersion	7.4.1
SiBa09	Diffusion	7.4.2

FEP ID	FEP name	Section in the Barrier process report
SiBa10	Sorption (including ion exchange of major ions)	7.4.3
SiBa11	Alteration of impurities	7.4.4
SiBa12	Colloid transport and filtering	7.4.5
SiBa13	Concrete degradation	7.4.7
SiBa14	Dissolution/precipitation	7.4.6
SiBa15	Aqueous speciation and reactions	7.4.8
SiBa16	Osmosis	7.4.9
SiBa17	Montmorillonite transformation	7.4.10
SiBa18	Iron-bentonite interaction	7.4.11
SiBa19	Montmorillonite colloid release	7.4.12
SiBa20	Microbial processes	7.4.13
SiBa21	Cementation in bentonite	7.4.14
SiBa22	Metal corrosion	7.4.15
SiBa23	Gas formation	7.4.16
SiBa24	Speciation of radionuclides	7.5.1
SiBa25	Transport of radionuclides in the water phase	7.5.2
SiBa26	Transport of radionuclides in the gas phase	7.5.3
BMABa01	Heat transport	5.1.1
BMABa02	Phase changes/freezing	5.1.2
BMABa03	Water uptake and transport during unsaturated conditions	5.2.1
BMABa04	Water transport under saturated conditions	5.2.2
BMABa05	Gas transport/dissolution	5.2.3
BMABa06	Mechanical processes	5.3.1
BMABa07	Advection and dispersion	5.4.1
BMABa08	Diffusion	5.4.2
BMABa09	Sorption on concrete/shotcrete	5.4.3
BMABa10	Sorption on crushed rock backfill	5.4.4
BMABa11	Colloid stability, transport and filtering	5.4.5
BMABa12	Concrete degradation	5.4.6
BMABa13	Aqueous speciation and reactions	5.4.7
BMABa14	Microbial processes	5.4.8
BMABa15	Metal corrosion	5.4.9
BMABa16	Gas formation	5.4.10
BMABa17	Speciation of radionuclides	5.5.1
BMABa18	Transport of radionuclides in the water phase	5.5.2
BMABa19	Transport of radionuclides in the gas phase	5.5.3
BRTBa01	Heat transport	9.1.1
BRTBa02	Phase changes/freezing	9.1.2
BRTBa03	Water uptake and transport during unsaturated conditions	9.2.1
BRTBa04	Water transport under saturated conditions	9.2.2
BRTBa05	Gas transport/dissolution	9.2.3
BRTBa06	Mechanical processes	9.3.1
BRTBa07	Advection and dispersion	9.4.1
BRTBa08	Diffusion	9.4.2
BRTBa09	Sorption	9.4.3
BRTBa10	Colloid stability, transport and filtering	9.4.4
BRTBa11	Concrete degradation	9.4.5
BRTBa12	Aqueous speciation and reactions	9.4.6
BRTBa13	Microbial processes	9.4.7
BRTBa14	Metal corrosion	9.4.8
BRTBa15	Gas formation	9.4.9
BRTBa16	Speciation of radionuclides	9.5.1
BRTBa17	Transport of radionuclides in the water phase	9.5.2
BRTBa18	Transport of radionuclides in the gas phase	9.5.3
BTFBa01	Heat transport	6.1.1
BTFBa02	Phase changes/freezing	6.1.2

FEP ID	FEP name	Section in the Barrier process report
BTFBa03	Water uptake and transport during unsaturated conditions	6.2.1
BTFBa04	Water transport under saturated conditions	6.2.2
BTFBa05	Gas transport/dissolution	6.2.3
BTFBa06	Mechanical processes	6.3.1
BTFBa07	Advection and dispersion	6.4.1
BTFBa08	Diffusion	6.4.2
BTFBa09	Sorption	6.4.3
BTFBa10	Colloid stability, transport and filtering	6.4.4
BTFBa11	Concrete degradation	6.4.5
BTFBa12	Aqueous speciation and reactions	6.4.6
BTFBa13	Microbial processes	6.4.7
BTFBa14	Metal corrosion	6.4.8
BTFBa15	Gas formation	6.4.9
BTFBa16	Speciation of radionuclides	6.5.1
BTFBa17	Transport of radionuclides in the water phase	6.5.2
BTFBa18	Transport of radionuclides in the gas phase	6.5.3
BLABa01	Heat transport	8.1.1
BLABa02	Phase changes/freezing	8.1.2
BLABa03	Water uptake and transport during unsaturated conditions	8.2.1
BLABa04	Water transport under saturated conditions	8.2.2
BLABa05	Gas transport/dissolution	8.2.3
BLABa06	Mechanical processes	8.3.1
BLABa07	Advection and dispersion	8.4.1
BLABa08	Diffusion	8.4.2
BLABa09	Sorption	8.4.3
BLABa10	Colloid stability, transport and filtering	8.4.4
BLABa11	Aqueous speciation and reactions	8.4.5
BLABa12	Microbial processes	8.4.6
BLABa13	Degradation of rock bolts, reinforcement and concrete	8.4.7
BLABa14	Speciation of radionuclides	8.5.1
BLABa15	Transport of radionuclides in the water phase	8.5.2
BLABa16	Transport of radionuclides in the gas phase	8.5.3
Pg01	Heat transport	10.1.1
Pg02	Phase changes/freezing	10.1.2
Pg03	Water uptake and transport during unsaturated conditions	10.2.1
Pg04	Water transport under saturated conditions	10.2.2
Pg05	Gas transport/dissolution	10.2.3
Pg06	Piping/erosion	10.2.4
Pg07	Mechanical processes	10.3.1
Pg08	Advection and dispersion	10.4.1
Pg09	Diffusion	10.4.2
Pg10	Sorption (including ion exchange of major ions)	10.4.3
Pg11	Alteration of impurities in bentonite	10.4.4
Pg12	Dissolution, precipitation, recrystallisation and clogging in backfill	10.4.5
Pg13	Aqueous speciation and reactions	10.4.6
Pg14	Osmosis	10.4.7
Pg15	Montmorillonite transformation	10.4.8
Pg16	Montmorillonite colloid release	10.4.9
Pg17	Microbial processes	10.4.10
Pg18	Degradation of rock bolts, reinforcements and concrete	10.4.11
Pg19	Speciation of radionuclides	10.5.1
Pg20	Transport of radionuclides in the water phase	10.5.2
Pg21	Transport of radionuclides in the gas phase	10.5.3

Table D-4. Geosphere FEPs in the FEP catalogue with references to the corresponding descriptions in the Geosphere process report.

FEP ID	FEP name	Section in the Geosphere process report
Ge01	Heat transport	2.1
Ge02	Freezing	2.2
Ge03	Groundwater flow	3.2
Ge04	Gas flow/dissolution	3.3
Ge05	Deformation of intact rock	4.2
Ge06	Displacements along existing fractures	4.3
Ge07	Fracturing	4.4
Ge09	Erosion and sedimentation in fractures	4.5
Ge10	Advective transport/mixing of dissolved species	5.2
Ge11	Diffusive transport in the rock mass	5.3
Ge12	Speciation and sorption	5.4
Ge13	Reactions groundwater/rock matrix	5.5
Ge14	Dissolution/precipitation of fracture-filling minerals	5.6
Ge15	Microbial processes	5.7
Ge16	Degradation of grout	5.8
Ge17	Colloidal processes	5.9
Ge19	Methane hydrate formation	5.10
Ge20	Salt exclusion	5.11
Ge21	Earth currents	5.12
Ge22	Speciation of radionuclides	6.1
Ge23	Transport of radionuclides in the water phase	6.2
Ge24	Transport of radionuclides in the gas phase	6.3

D3 System variables

In Table D-5 to D-7, the 71 FEPs included in the main category *system variables* in the FEP catalogue are listed. In the same way as for *internal processes*, these are subdivided into the SFR system components *waste form* (9 FEPs), *concrete and steel packaging* (7 FEPs), *silo barriers* (7 FEPs), *BMA barriers* (7 FEPs), *BRT barriers* (7 FEPs), *BTF barriers* (7 FEPs), *BLA barriers* (7 FEPs), *plugs and other closure components* (7 FEPs) and *geosphere* (13 FEPs).

Table D-5. System variable FEPs for the system components Waste form and Concrete and steel packaging in the FEP catalogue with references to the corresponding descriptions in the Waste process report and references to the initial state variable values in the Initial state report.

FEP ID	FEP name	Section in the Waste process report	Section in the Initial state report
VarWM01	Geometry	2.1.2	12.1.1
VarWM02	Radiation intensity	2.1.2	12.1.2
VarWM03	Temperature	2.1.2	12.1.3
VarWM04	Hydrological variables	2.1.2	12.1.4
VarWM05	Mechanical stresses	2.1.2	12.1.5
VarWM06	Radionuclide inventory	2.1.2	12.1.6
VarWM07	Material composition	2.1.2	12.1.7
VarWM08	Water composition	2.1.2	12.1.8
VarWM09	Gas variables	2.1.2	12.1.9
VarPa01	Geometry	2.2.2	12.2.1
VarPa02	Temperature	2.2.2	12.2.2
VarPa03	Hydrological variables	2.2.2	12.2.3
VarPa04	Mechanical stresses	2.2.2	12.2.4
VarPa05	Material composition	2.2.2	12.2.5
VarPa06	Water composition	2.2.2	12.2.6
VarPa07	Gas variables	2.2.2	12.2.7

Table D-6. System variable FEPs for the engineered barriers in the FEP catalogue with references to the corresponding descriptions in the Barrier process report and references to the initial state variable values in the Initial state report.

FEP ID	FEP name	Section in the Barrier process report	Section in the Initial state report
VarSi01	Geometry	4.2.4	12.3.1
VarSi02	Temperature	4.2.4	12.3.2
VarSi03	Hydrological variables	4.2.4	12.3.3
VarSi04	Mechanical stresses	4.2.4	12.3.4
VarSi05	Material composition	4.2.4	12.3.5
VarSi06	Water composition	4.2.4	12.3.6
VarSi07	Gas variables	4.2.4	12.3.7
VarBMA01	Geometry	4.2.4	12.4.1
VarBMA02	Temperature	4.2.4	12.4.2
VarBMA03	Hydrological variables	4.2.4	12.4.3
VarBMA04	Mechanical stresses	4.2.4	12.4.4
VarBMA05	Material composition	4.2.4	12.4.5
VarBMA06	Water composition	4.2.4	12.4.6
VarBMA07	Gas variables	4.2.4	12.4.7
VarBRT01	Geometry	4.2.4	12.5.1
VarBRT02	Temperature	4.2.4	12.5.2
VarBRT03	Hydrological variables	4.2.4	12.5.3
VarBRT04	Mechanical stresses	4.2.4	12.5.4
VarBRT05	Material composition	4.2.4	12.5.5
VarBRT06	Water composition	4.2.4	12.5.6
VarBRT07	Gas variables	4.2.4	12.5.7
VarBTF01	Geometry	4.2.4	12.6.1
VarBTF02	Temperature	4.2.4	12.6.2
VarBTF03	Hydrological variables	4.2.4	12.6.3
VarBTF04	Mechanical stresses	4.2.4	12.6.4
VarBTF05	Material composition	4.2.4	12.6.5
VarBTF06	Water composition	4.2.4	12.6.6
VarBTF07	Gas variables	4.2.4	12.6.7
VarBLA01	Geometry	4.2.4	12.7.1
VarBLA02	Temperature	4.2.4	12.7.2
VarBLA03	Hydrological variables	4.2.4	12.7.3
VarBLA04	Mechanical stresses	4.2.4	12.7.4
VarBLA05	Material composition	4.2.4	12.7.5
VarBLA06	Water composition	4.2.4	12.7.6
VarBLA07	Gas variables	4.2.4	12.7.7
VarPg01	Geometry	4.2.4	12.8.1
VarPg02	Temperature	4.2.4	12.8.2
VarPg03	Hydrological variables	4.2.4	12.8.3
VarPg04	Mechanical stresses	4.2.4	12.8.4
VarPg05	Material composition	4.2.4	12.8.5
VarPg06	Water composition	4.2.4	12.8.6
VarPg07	Gas variables	4.2.4	12.8.7

Table D-7. System variable FEPs for the geosphere in the FEP catalogue with references to the corresponding descriptions in the Geosphere process report and references to the initial state variable values.

FEP ID	FEP name	Section in the Geosphere process report	Reference to the initial state variable values
VarGe01	Temperature	1.4.2	SKB TR-11-04
VarGe02	Groundwater flow	1.4.2	SKB TR-11-04
VarGe03	Groundwater pressure	1.4.2	SKB TR-11-04
VarGe04	Gas phase flow	1.4.2	SKB TR-11-04
VarGe05	Repository geometry	1.4.2	SKB TR-11-04
VarGe06	Fracture and pore geometry	1.4.2	SKB TR-11-04
VarGe07	Rock stresses	1.4.2	SKB TR-11-04
VarGe08	Matrix minerals	1.4.2	SKB TR-11-04
VarGe09	Fracture minerals	1.4.2	SKB TR-11-04
VarGe10	Groundwater composition	1.4.2	SKB TR-11-04
VarGe11	Gas composition	1.4.2	SKB TR-11-04
VarGe12	Structural and stray materials	1.4.2	SKB TR-11-04
VarGe13	Saturation	1.4.2	SKB TR-11-04

D4 Biosphere

In Table D-8, the 68 *biosphere* FEPs included in the FEP catalogue are listed. These are identified as 50 *biosphere processes*, 12 *biosphere subsystem components* (divided into 10 *physical components* and 2 *boundary components)*, and 6 *biosphere variables* (features).

Table D-8. Biosphere FEPs in the FEP catalogue with references to the corresponding descriptions in SKB (R-13-43, R-14-02).

FEP ID	FEP name	Section in SKB (R-13-43)	Section in SKB (R-14-02)
Bio01	Bioturbation	6.1.1	2.4.1
Bio02	Consumption	6.1.2	2.4.2
Bio03	Death	6.1.3	2.4.3
Bio04	Decomposition	6.1.4	2.4.4
Bio05	Excretion	6.1.5	2.4.5
Bio06	Food supply	6.1.6	2.4.6
Bio07	Growth	6.1.7	2.4.7
Bio08	Habitat supply	6.1.8	2.4.8
Bio09	Intrusion	6.1.9	2.4.9
Bio10	Material supply	6.1.10	2.4.10
Bio11	Movement	6.1.11	Excluded[1)]
Bio12	Particle release/trapping	6.1.12	2.4.11
Bio13	Primary production	6.1.13	2.4.12
Bio14	Stimulation/inhibition	6.1.14	2.4.13
Bio15	Uptake	6.1.15	2.4.14
Bio16	Anthropogenic release	6.2.1	2.4.15
Bio17	Material use	6.2.2	2.4.16
Bio18	Species introduction/extermination	6.2.3	2.4.17
Bio19	Water use	6.2.4	2.4.18
Bio20	Change of pressure	6.3.1	Excluded[1)]
Bio21	Consolidation	6.3.2	2.4.19
Bio22	Element supply	6.3.3	2.4.20
Bio23	Loading	6.3.4	Excluded[1)]

FEP ID	FEP name	Section in SKB (R-13-43)	Section in SKB (R-14-02)
Bio24	Phase transitions	6.3.5	2.4.21
Bio25	Physical properties change	6.3.6	2.4.22
Bio26	Reactions	6.3.7	2.4.23
Bio27	Sorption/desorption	6.3.8	2.4.24
Bio28	Water supply	6.3.9	2.4.25
Bio29	Weathering	6.3.10	2.4.26
Bio30	Wind stress	6.3.11	2.4.27
Bio31	Acceleration	6.4.1	2.4.28
Bio32	Convection	6.4.2	2.4.29
Bio33	Covering	6.4.3	2.4.30
Bio34	Deposition	6.4.4	2.4.31
Bio35	Export	6.4.5	2.4.32
Bio36	Import	6.4.6	2.4.33
Bio37	Interception	6.4.7	2.4.34
Bio38	Relocation	6.4.8	2.4.35
Bio39	Resuspension	6.4.9	2.4.36
Bio40	Saturation	6.4.10	2.4.37
Bio41	Radioactive decay	6.5.1	2.4.38
Bio42	Exposure	6.5.2	2.4.39
Bio43	Heat storage	6.5.3	2.4.40
Bio44	Irradiation	6.5.4	Excluded[2)]
Bio45	Light-related processes	6.5.5	2.4.41
Bio46	Radiolysis	6.5.6	Excluded[2)]
Bio47	Radionuclide release	6.5.7	2.4.42
Bio48	Change in rock surface location	6.6.1	2.4.43
Bio49	Sea level change	6.6.2	2.4.44
Bio50	Thresholding	6.6.3	2.4.45
CompBio01	Geosphere (Boundary condition)	4.11.1	2.2.11
CompBio02	Regolith	4.1	2.2.1
CompBio03	Water in regolith	4.2	2.2.2
CompBio04	Surface water	4.3	2.2.3
CompBio05	Gas and local atmosphere	4.4	2.2.4
CompBio06	Primary producers	4.5	2.2.5
CompBio07	Decomposers	4.6	2.2.6
CompBio08	Filter feeders	4.7	2.2.7
CompBio09	Herbivores	4.8	2.2.8
CompBio10	Carnivores	4.9	2.2.9
CompBio11	Humans	4.10	2.2.10
CompBio12	External conditions (Boundary condition)	4.11.2	2.2.11
VarBio01	Geometry	5.1	
VarBio02	Material composition	5.2	
VarBio03	Radionuclide inventory	5.3	
VarBio04	Stage of succession	5.4	
VarBio05	Temperature	5.5	
VarBio06	Water composition	5.6	

[1)] Process excluded since it is not important for a low- and intermediate level waste repository located in the Forsmark area (see SKB R-13-43, Section 7.2).

[2)] Process excluded since the expected radionuclide activities are too low to affect regolith and water in regolith by irradiation (see SKB R-13-43, Section 7.2).

D5 External factors

In Table D-9 to D-12, the 27 FEPs included in the main category *external factor* in the FEP catalogue are listed. These are divided into the subcategories *climatic processes and effects* (7 FEPs), *large-scale geological processes and effects* (2 FEPs), *future human actions* (17 FEPs) and *other* (1 FEP).

Table D-9. Climate FEPs in the FEP catalogue with references to the corresponding descriptions in the Climate report.

FEP ID	FEP name	Section in the Climate report
Cli02	Climate forcing	3.1, 3.4
Cli03	Climate evolution	3.2, 3.3, 3.4
Cli05	Development of permafrost	2.1
Cli06	Ice-sheet dynamics and hydrology	2.3
Cli08	Glacial isostatic adjustment	2.2
Cli09	Shore-level changes	2.2, 3.5
Cli10	Denudation	2.4

Table D-10. Large-scale geological FEPs in the FEP catalogue with references to the corresponding descriptions in the SR-Site Geosphere process report (SKB TR-10-48).

FEP ID	FEP name	Section in SKB (TR-10-48)
LSGe01	Mechanical evolution of the Shield	4.1.2
LSGe02	Earthquakes	4.1.3

Table D-11. FHA FEPs in the FEP catalogue with references to the corresponding descriptions in the FHA report.

FEP ID	FEP name	Section in the FHA report
FHA01	State of knowledge	4.4.1
FHA02	Societal development	4.4.2
FHA03	Technical development	4.4.3
FHA04	Heat storage	4.4.4
FHA05	Heat pump system	4.4.5
FHA06	Geothermal energy	4.4.6
FHA07	Heating/cooling plant	4.4.7
FHA08	Drilled well	4.4.8
FHA09	Water management	4.4.9
FHA10	Altered land use	4.4.10
FHA11	Drilling	4.4.11
FHA12	Underground constructions	4.4.12
FHA13	Quarry	4.4.13
FHA14	Landfill	4.4.14
FHA15	Bombing or blasting, explosions and crashes	4.4.15
FHA16	Hazardous waste facility	4.4.16
FHA17	Contamination with chemical substances	4.4.17

Table D-12. Other FEPs in the FEP catalogue with references to the corresponding descriptions in this report.

FEP ID	FEP name	Reference
Oth01	Meteorite impact	3.5.7 in this report

D6 Methodology

In Table D-13, the two *methodology* FEPs included in the FEP catalogue are listed.

Table D-13. Methodology FEPs in the FEP catalogue with references to the corresponding descriptions in this report.

FEP ID	FEP name	Reference
Meth01	Assessment basis	2.2–2.4 in this report
Meth02	Assessment methodology	Chapter 2 in this report

D7 Site-specific factors

In Table D-14, the two *site-specific factor* FEPs included in the FEP catalogue are listed.

Table D-14. Site-specific factor FEPs in the FEP catalogue with references to the corresponding descriptions in various report.

FEP ID	FEP name	Reference
SiteFact02	Construction of nearby rock facilities	SKB TR-11-01, Section 10.2.5
SiteFact03	Nearby nuclear power plant	**Data report**, Section 5.1 **Waste process report**, Section 3.5.9 **Geosphere process report**, Section 5.12 **FHA report**, Section 5.5

Appendix E

Reference inventory

E1 Radionuclide inventory

The reference inventory at 2075, the estimated year of repository closure, is presented in Table E-1 and an estimate of the 95-procentile for activity per radionuclide and repository area is given in Table E-2. The uncertainties are handled in a probabilistic manner and include measurement uncertainties, uncertainties in correlation factors and uncertainties in other methods used to calculate the best estimate of the radionuclide inventory (see more details in the **Initial state report** and SKB R-18-07).

Table E-1. Calculated reference radionuclide inventory (Bq) for each waste vault in SFR at closure in 2075 (Initial state report).

Activity reference case (2075-12-31)/Bq

Radionuclide	Silo	1BMA	2BMA	1BRT	1BTF	2BTF	1BLA	2–5BLA
H-3	1.35E + 10	3.34E + 08	2.99E + 12	1.04E + 09	1.66E + 08	4.88E + 07	3.34E + 06	1.82E + 11
Be-10	1.30E + 06	1.95E + 05	4.15E + 04	2.83E + 02	1.28E + 04	2.52E + 04	8.18E + 02	2.11E + 03
C-14 (inorg)	1.52E + 12	1.51E + 12	6.57E + 11	1.33E + 08	2.50E + 11	4.25E + 11	8.47E + 09	9.39E + 08
C-14 (org)	5.47E + 11	1.97E + 11	2.06E + 10	5.72E + 07	1.28E + 10	8.05E + 09	1.52E + 08	2.25E + 08
C-14 (ind)	0.00E + 00	0.00E + 00	1.99E + 10	1.33E + 10	0.00E + 00	0.00E + 00	0.00E + 00	1.23E + 09
Cl-36	5.32E + 08	2.28E + 08	2.64E + 08	7.38E + 06	9.64E + 06	9.27E + 06	1.86E + 07	4.86E + 07
Ca-41	0.00E + 00	0.00E + 00	1.98E + 10	0.00E + 00	0.00E + 00	0.00E + 00	0.00E + 00	4.14E + 09
Fe-55	2.69E + 12	1.43E + 07	2.16E + 11	1.45E + 10	1.11E + 09	3.16E + 05	2.47E + 05	5.12E + 08
Co-60	1.47E + 13	1.95E + 10	4.10E + 12	1.89E + 11	8.51E + 10	1.78E + 09	3.35E + 08	3.17E + 10
Ni-59	8.38E + 12	1.14E + 12	1.53E + 12	1.78E + 11	1.47E + 10	2.47E + 10	3.11E + 09	1.28E + 10
Ni-63	7.00E + 14	7.73E + 13	1.50E + 14	1.52E + 13	9.83E + 11	1.47E + 12	2.25E + 11	1.19E + 12
Se-79	1.54E + 09	1.98E + 08	6.37E + 07	0.00E + 00	2.84E + 07	1.96E + 07	5.77E + 05	6.17E + 06
Sr-90	1.98E + 12	1.56E + 11	5.49E + 11	2.24E + 10	2.13E + 10	2.71E + 10	3.29E + 08	2.21E + 10
Zr-93	4.94E + 09	3.25E + 08	1.74E + 09	2.44E + 08	2.14E + 07	4.20E + 07	1.36E + 06	3.06E + 07
Nb-93m	1.03E + 13	9.30E + 09	1.64E + 13	1.07E + 12	2.93E + 09	1.36E + 09	7.78E + 07	1.27E + 11
Nb-94	1.08E + 11	4.08E + 09	1.08E + 11	9.27E + 09	2.14E + 08	4.19E + 08	3.64E + 07	1.08E + 09
Mo-93	1.47E + 10	6.43E + 08	5.62E + 09	3.10E + 09	8.50E + 07	1.37E + 08	9.22E + 06	1.40E + 08
Tc-99	2.05E + 10	3.25E + 09	3.49E + 09	4.82E + 08	3.10E + 08	3.52E + 08	6.95E + 07	1.05E + 09
Pd-107	3.98E + 08	4.95E + 07	2.57E + 09	0.00E + 00	7.10E + 06	4.91E + 06	1.44E + 05	2.23E + 06
Ag-108m	2.60E + 11	1.70E + 10	6.60E + 10	4.81E + 09	1.19E + 09	2.22E + 09	2.39E + 08	1.55E + 09
Cd-113m	1.73E + 10	4.85E + 08	1.17E + 09	0.00E + 00	4.42E + 08	3.34E + 07	2.86E + 06	3.15E + 07
In-115	0.00E + 00	0.00E + 00	3.10E + 05	0.00E + 00	0.00E + 00	0.00E + 00	0.00E + 00	0.00E + 00
Sn-126	2.67E + 08	2.47E + 07	2.80E + 07	8.17E + 05	3.55E + 06	2.45E + 06	7.22E + 04	1.01E + 07
Sb-125	2.70E + 11	1.66E + 06	1.65E + 10	2.15E + 07	1.21E + 08	4.13E + 04	1.22E + 04	4.41E + 06
I-129	5.16E + 08	7.60E + 07	8.18E + 07	0.00E + 00	7.44E + 06	4.35E + 06	2.43E + 05	2.81E + 06
Cs-134	1.59E + 11	9.18E + 03	2.55E + 10	0.00E + 00	1.60E + 06	1.31E + 01	1.14E + 02	1.42E + 06
Cs-135	2.95E + 09	6.52E + 08	7.49E + 08	0.00E + 00	1.94E + 07	5.77E + 06	2.00E + 06	1.84E + 08
Cs-137	1.02E + 14	6.77E + 12	5.74E + 12	0.00E + 00	2.36E + 12	5.89E + 11	2.79E + 10	4.85E + 11
Ba-133	9.18E + 08	1.61E + 07	1.38E + 08	5.62E + 04	1.11E + 07	2.31E + 06	1.81E + 05	1.23E + 07
Pm-147	2.66E + 11	1.10E + 06	4.21E + 10	1.37E + 06	2.20E + 08	1.91E + 03	9.92E + 03	3.78E + 06
Sm-151	7.21E + 11	7.57E + 10	6.93E + 10	3.57E + 08	1.46E + 10	7.22E + 09	2.48E + 08	6.05E + 09
Eu-152	1.86E + 09	4.82E + 07	1.47E + 11	4.84E + 05	6.21E + 07	3.25E + 06	9.16E + 07	1.72E + 10
Eu-154	8.18E + 11	7.81E + 09	7.17E + 10	8.09E + 07	1.96E + 10	3.48E + 08	6.56E + 07	3.58E + 08
Eu-155	9.63E + 10	8.47E + 07	1.24E + 10	2.10E + 06	1.11E + 09	1.09E + 06	8.43E + 05	1.88E + 07
Ho-166m	8.40E + 09	1.24E + 09	6.41E + 08	8.50E + 06	8.32E + 07	1.60E + 08	5.24E + 06	9.58E + 07
U-232	4.56E + 05	5.24E + 04	9.89E + 05	7.18E + 03	5.71E + 03	4.87E + 03	1.60E + 02	2.51E + 04
U-234	3.77E + 07	4.66E + 06	7.47E + 07	1.87E + 06	3.80E + 05	3.86E + 05	1.17E + 04	3.55E + 07
U-235	6.92E + 06	9.83E + 05	6.92E + 06	3.80E + 04	1.84E + 07	1.01E + 05	2.18E + 08	6.34E + 08
U-236	1.22E + 07	1.73E + 06	2.28E + 07	4.30E + 05	1.77E + 05	2.70E + 05	3.05E + 03	4.99E + 05
U-238	1.88E + 07	2.12E + 06	1.80E + 07	4.89E + 05	3.46E + 05	5.03E + 05	7.16E + 08	1.48E + 08
Np-237	6.44E + 07	7.91E + 06	3.40E + 07	5.24E + 05	4.64E + 05	1.48E + 06	1.03E + 04	4.65E + 05
Pu-238	4.07E + 10	2.82E + 09	1.23E + 11	2.86E + 09	5.11E + 08	2.54E + 08	1.48E + 07	2.10E + 09
Pu-239	1.70E + 10	2.65E + 09	5.92E + 10	4.75E + 08	2.02E + 08	2.01E + 08	6.62E + 06	3.83E + 08
Pu-240	1.37E + 10	1.63E + 09	1.16E + 10	6.58E + 08	1.65E + 08	1.65E + 08	4.70E + 06	4.01E + 08
Pu-241	2.39E + 11	7.50E + 09	5.64E + 11	8.23E + 09	2.29E + 09	8.09E + 08	3.91E + 07	9.23E + 09
Pu-242	7.48E + 07	8.91E + 06	2.14E + 08	3.38E + 06	8.92E + 05	8.08E + 05	2.53E + 04	2.34E + 06
Am-241	1.06E + 11	1.68E + 10	2.32E + 11	2.29E + 09	1.78E + 09	1.22E + 09	6.24E + 07	2.82E + 09
Am-242m	2.61E + 08	2.94E + 07	6.12E + 08	1.36E + 07	2.44E + 06	2.19E + 06	7.45E + 04	6.50E + 06
Am-243	1.20E + 09	2.09E + 08	2.36E + 09	4.71E + 07	1.31E + 07	1.38E + 07	1.61E + 06	2.56E + 07
Cm-243	1.62E + 08	1.08E + 07	3.77E + 08	6.15E + 06	1.26E + 06	8.12E + 05	3.67E + 04	4.87E + 06
Cm-244	1.26E + 10	5.83E + 08	2.69E + 10	6.38E + 08	7.28E + 07	2.06E + 07	2.55E + 06	4.06E + 08
Cm-245	1.78E + 07	2.47E + 06	2.78E + 07	7.55E + 05	1.13E + 05	1.06E + 05	4.97E + 03	2.82E + 05
Cm-246	4.86E + 06	5.64E + 05	8.30E + 06	2.49E + 05	3.36E + 04	3.43E + 04	1.23E + 03	8.32E + 04

Table E-2. Estimated radionuclide inventory including uncertainties (Bq) (95th percentile) for each waste vault in SFR at closure in 2075 (Initial state report).

Activity 95-percentile (2075-12-31)/Bq								
Radionuclide	**Silo**	**1BMA**	**2BMA**	**1BRT**	**1BTF**	**2BTF**	**1BLA**	**2–5BLA**
H-3	2.92E + 10	5.73E + 08	3.48E + 12	1.70E + 09	4.55E + 08	9.76E + 07	8.22E + 06	2.79E + 11
Be-10	2.44E + 06	2.81E + 05	9.28E + 04	6.64E + 02	3.31E + 04	4.74E + 04	1.96E + 03	4.08E + 03
C-14 (inorg)	2.58E + 12	3.38E + 12	1.80E + 12	2.42E + 08	4.03E + 11	6.70E + 11	2.20E + 10	1.37E + 09
C-14 (org)	1.07E + 12	3.80E + 11	4.28E + 10	1.03E + 08	2.20E + 10	1.36E + 10	3.88E + 08	3.79E + 08
C-14 (ind)	0.00E + 00	0.00E + 00	2.13E + 10	1.55E + 10	0.00E + 00	0.00E + 00	0.00E + 00	2.03E + 09
Cl-36	5.85E + 08	2.43E + 08	2.87E + 08	8.27E + 06	1.04E + 07	1.32E + 07	2.02E + 07	7.68E + 07
Ca-41	0.00E + 00	0.00E + 00	2.17E + 10	0.00E + 00	0.00E + 00	0.00E + 00	0.00E + 00	6.84E + 09
Fe-55	4.48E + 12	2.20E + 07	3.92E + 11	1.65E + 10	2.10E + 09	3.89E + 05	4.69E + 05	6.28E + 08
Co-60	1.57E + 13	2.15E + 10	4.39E + 12	2.07E + 11	1.01E + 11	1.84E + 09	4.40E + 08	3.84E + 10
Ni-59	9.30E + 12	1.36E + 12	1.59E + 12	1.94E + 11	1.71E + 10	2.93E + 10	4.87E + 09	1.58E + 10
Ni-63	7.76E + 14	9.23E + 13	1.56E + 14	1.66E + 13	1.13E + 12	1.63E + 12	3.64E + 11	1.49E + 12
Se-79	2.08E + 09	2.07E + 08	8.27E + 07	0.00E + 00	3.66E + 07	2.24E + 07	8.32E + 05	1.03E + 07
Sr-90	2.21E + 12	1.81E + 11	6.33E + 11	2.51E + 10	2.55E + 10	3.02E + 10	4.17E + 08	3.42E + 10
Zr-93	6.91E + 09	4.66E + 08	1.86E + 09	2.80E + 08	5.76E + 07	8.07E + 07	3.21E + 06	3.87E + 07
Nb-93m	1.17E + 13	1.28E + 10	1.72E + 13	1.19E + 12	6.78E + 09	2.06E + 09	1.74E + 08	1.58E + 11
Nb-94	1.21E + 11	4.82E + 09	1.13E + 11	1.04E + 10	3.01E + 08	4.94E + 08	4.68E + 07	1.30E + 09
Mo-93	1.58E + 10	7.12E + 08	5.86E + 09	3.44E + 09	1.03E + 08	1.60E + 08	1.18E + 07	1.80E + 08
Tc-99	2.29E + 10	3.91E + 09	3.95E + 09	5.34E + 08	3.78E + 08	4.14E + 08	1.04E + 08	1.59E + 09
Pd-107	7.95E + 08	7.49E + 07	3.19E + 09	0.00E + 00	1.97E + 07	1.08E + 07	3.97E + 05	3.10E + 06
Ag-108m	3.71E + 11	2.42E + 10	7.14E + 10	5.68E + 09	3.12E + 09	4.25E + 09	4.06E + 08	2.12E + 09
Cd-113m	3.95E + 10	8.62E + 08	2.80E + 09	0.00E + 00	1.29E + 09	7.50E + 07	8.49E + 06	5.07E + 07
In-115	0.00E + 00	0.00E + 00	3.93E + 05	0.00E + 00	0.00E + 00	0.00E + 00	0.00E + 00	0.00E + 00
Sn-126	4.54E + 08	3.88E + 07	3.79E + 07	9.13E + 05	9.80E + 06	5.59E + 06	2.01E + 05	1.41E + 07
Sb-125	5.50E + 11	3.22E + 06	4.10E + 10	2.44E + 07	2.87E + 08	5.83E + 04	3.51E + 04	5.38E + 06
I-129	5.66E + 08	8.71E + 07	9.26E + 07	0.00E + 00	1.07E + 07	6.18E + 06	3.37E + 05	4.13E + 06
Cs-134	2.17E + 11	1.12E + 04	3.71E + 10	0.00E + 00	1.78E + 06	1.60E + 01	1.97E + 02	1.81E + 06
Cs-135	3.64E + 09	8.47E + 08	8.55E + 08	0.00E + 00	2.53E + 07	8.27E + 06	3.21E + 06	3.01E + 08
Cs-137	1.32E + 14	7.05E + 12	6.57E + 12	0.00E + 00	2.85E + 12	6.19E + 11	3.46E + 10	7.73E + 11
Ba-133	9.96E + 08	1.76E + 07	1.52E + 08	9.34E + 04	1.36E + 07	2.50E + 06	2.51E + 05	1.80E + 07
Pm-147	3.48E + 11	1.39E + 06	5.84E + 10	1.55E + 06	3.39E + 08	2.25E + 03	1.53E + 04	4.83E + 06
Sm-151	9.69E + 11	7.93E + 10	7.88E + 10	3.99E + 08	1.88E + 10	8.25E + 09	3.47E + 08	1.00E + 10
Eu-152	2.38E + 09	5.31E + 07	1.63E + 11	5.45E + 05	7.54E + 07	3.63E + 06	1.07E + 08	2.63E + 10
Eu-154	9.97E + 11	9.07E + 09	8.10E + 10	9.13E + 07	2.57E + 10	3.87E + 08	9.39E + 07	4.68E + 08
Eu-155	1.14E + 11	1.05E + 08	1.55E + 10	2.39E + 06	1.55E + 09	1.21E + 06	1.27E + 06	2.44E + 07
Ho-166m	9.15E + 09	1.27E + 09	7.04E + 08	1.47E + 07	9.84E + 07	1.71E + 08	6.53E + 06	1.61E + 08
U-232	5.19E + 05	6.28E + 04	2.02E + 06	8.04E + 03	6.53E + 03	5.67E + 03	1.84E + 02	4.06E + 04
U-234	4.67E + 07	6.80E + 06	1.11E + 08	2.10E + 06	4.51E + 05	4.89E + 05	1.36E + 04	7.80E + 07
U-235	7.58E + 06	1.07E + 06	1.19E + 07	4.25E + 04	2.03E + 07	1.11E + 05	2.43E + 08	8.10E + 08
U-236	1.45E + 07	2.27E + 06	4.21E + 07	4.82E + 05	2.05E + 05	3.08E + 05	3.55E + 03	7.99E + 05
U-238	2.10E + 07	2.61E + 06	2.55E + 07	5.48E + 05	4.20E + 05	6.02E + 05	9.60E + 08	1.89E + 08
Np-237	7.04E + 07	8.82E + 06	6.04E + 07	5.84E + 05	5.28E + 05	1.62E + 06	1.37E + 04	6.51E + 05
Pu-238	4.40E + 10	3.22E + 09	1.81E + 11	3.21E + 09	5.47E + 08	2.85E + 08	1.69E + 07	2.77E + 09
Pu-239	1.86E + 10	3.06E + 09	1.02E + 11	5.32E + 08	2.24E + 08	2.26E + 08	7.71E + 06	5.18E + 08
Pu-240	1.68E + 10	2.37E + 09	1.22E + 10	7.36E + 08	1.91E + 08	2.02E + 08	5.41E + 06	5.41E + 08
Pu-241	3.15E + 11	1.09E + 10	1.01E + 12	9.26E + 09	2.94E + 09	9.93E + 08	4.67E + 07	1.15E + 10
Pu-242	9.21E + 07	1.30E + 07	4.06E + 08	3.78E + 06	1.02E + 06	1.00E + 06	2.93E + 04	3.16E + 06
Am-241	1.34E + 11	2.37E + 10	4.54E + 11	2.49E + 09	1.97E + 09	1.50E + 09	7.13E + 07	3.77E + 09
Am-242m	3.21E + 08	4.17E + 07	1.09E + 09	1.53E + 07	2.83E + 06	2.69E + 06	8.78E + 04	8.57E + 06
Am-243	1.46E + 09	2.76E + 08	4.19E + 09	5.28E + 07	1.49E + 07	1.62E + 07	2.27E + 06	3.37E + 07
Cm-243	2.06E + 08	1.56E + 07	7.00E + 08	6.91E + 06	1.54E + 06	1.01E + 06	4.37E + 04	6.29E + 06
Cm-244	1.82E + 10	9.52E + 08	3.82E + 10	7.15E + 08	9.96E + 07	3.03E + 07	3.11E + 06	5.04E + 08
Cm-245	2.30E + 07	3.71E + 06	4.64E + 07	8.48E + 05	1.30E + 05	1.29E + 05	5.98E + 03	3.65E + 05
Cm-246	5.96E + 06	8.34E + 05	1.35E + 07	2.82E + 05	3.92E + 04	4.20E + 04	1.46E + 03	1.06E + 05

E2 Material quantities

A summary of the material quantities in the waste packages in the different waste vaults is given in Table E-3. Material quantities are specified for materials that are frequently occurring or are known to have an impact on safety. Other materials are accounted for within the categories *other organic* or *other inorganic* where the specific material composition is considered to be of negligible importance to the safety. Complexing agents and other substances that can have an impact on safety in relatively small amounts are not specified among the materials but are accounted for in Keith-Roach et al. (2021).

Table E-3. Best estimates of material quantities, corrosion surface areas, voids and pore volume in waste packages along with disposal and outer volumes for the waste vaults in SFR (Initial state report).

	Waste vault								
	Silo	**1BMA**	**2BMA**	**1BRT**	**1BTF**	**2BTF**	**1BLA**	**2–5BLA**	**SFR**
Waste material/tonnes									
Aluminium	6.0	0.5	15	0	4.9	0	55	173	254
Zinc	0	0.5	0.2	0	0.009	0	8.5	3.4	13
Ashes	0	0.03	30	0	337	0	0	358	725
Cellulose	6.5	22	9.2	0	0.09	0	302	276	616
Filter aid	552	213	40	0	132	383	0	0	1321
Evaporation concentrate	0	206	193	0	0	0	0.8	0	399
Ion-exchange resin	4737	2252	350	0	1584	2747	93	0	11764
Iron/Steel	523	265	7530	6051	55	59	2147	26920	43550
Sludge	53	85	105	0	2.3	0	13	2.4	260
Plastic/Rubber	26	153	48	0	0.8	0.2	698	424	1350
Other inorganics	242	198	127	0	9.9	19	783	4887	6265
Other organics	62	1.4	15	0	1.4	2.2	260	817	1158
Sand/Soil	0	0	108	0	0	0	0	6127	6235
Concrete	0	0	2587	0	68	0	107	14066	16827
Matrix material/tonnes									
Concrete	2963	2658	12662	7122	1412	216	242	0	27276
Bitumen	1107	1333	411	0	0	0	94	0	2946
Cement	8888	2271	326	0	135	0	56	0	11676
Iron/Steel	1.2	42	13	0	0.1	0	0	0	56
Packaging material/tonnes									
Zinc	9.7	3.6	2.0	0	0	0	10	12	38
Cellulose	0	0	0	0	0	0	34	25	59
Iron/Steel	2508	1564	4991	2541	609	909	1391	6511	21024
Plastic/Rubber	2.2	3.7	0.3	0.04	22	43	0	0	71
Other inorganics	0	0	0	0	230	450	0	0	680
Other organics	0	0	0	0	0	0	8.7	6.2	15
Concrete	6469	5745	937	0	4066	7553	7.2	4.2	24780
Corrosion surface waste/m^2									
Aluminium	884	104	5034	0	491	0	5127	25397	37038
Zinc	0	262	49	0	11	0	407	275	1004
Iron/Steel	26609	12723	344784	14769	13522	3024	99393	2395164	2909 988
Corrosion surface matrix/m^2									
Iron/Steel	55	1441	375	0	5	0	0	0	1877
Corrosion surface packaging/m^2									
Zink	33117	13292	7304	0	0	0	56426	67962	178101
Iron/Steel	124166	90311	116898	51047	42284	44939	90552	386250	946446
Volume/m^3									
Void	587	896	2665	1334	422	657	9956	41780	58296
Pore volume	2418	1143	948	297	661	870	385	3911	10633
Disposal volume	15930	10611	16105	7896	5806	7680	13880	76441	154350
Outer volume	15640	10229	16018	7641	5218	7578	13652	75271	151246

Appendix F

Approach to estimate dose from barrier failure in the silo following an earthquake

In the PSAR, an alternative approach to the calculation applied in the risk summation (Equation 10-3) is used to estimate the dose resulting from barrier failure in the silo following an earthquake. Details of the calculations applied in this alternative approach are given here. In these calculations, the cumulative probability for a disruptive earthquake for a time interval is combined with the consequences from an earthquake occurring at any time in that interval. That is, in the alternative approach maximum consequences across generations are averaged regardless of when the consequences occur in time.

After the earthquake event, the concrete barriers in the silo are assumed to have failed and groundwater flow increases. As the barriers in the silo are assumed to fail completely due to the earthquake, barrier failure can only occur once. Consequently, the probability for such an earthquake is conditioned on the cumulative probability that the earthquake has not occurred in the period prior to the considered point in time:

$$p_{fail}(T_n) \;=\; p_{EQ}^{per} \cdot \left(Cuml_{p_{Nonfail}}(T_{n-1}) \right) \;=\; p_{EQ}^{per} \cdot \left(1 - p_{EQ}^{per}\right)^{n-1} \qquad \text{(Equation F-1)}$$

where

$p_{fail}(T_n)$ is the probability of failure of the silo barriers in time interval *n*,

T_n is the n:th time interval of length T_{per},

p_{EQ}^{per} is the probability of an earthquake in the Forsmark area that has the strength to break the silo within a time period of length T_{per} (load spectrum with probability of 10^{-6} a^{-1}, Section 8.6.1),

$Cuml_{p_{Nonfail}}(T_{n-1})$ is the cumulative probability of an earthquake not having occurred during the n-1 number of time intervals prior to T_n.

The cumulative probability of an earthquake having occurred during the *n* number of time intervals to T_n is:

$$\begin{aligned} Cuml_{p_{fail}}(T_n) \;&=\; \sum_{i=1}^{n} p_{fail}(T_i) \qquad \text{(Equation F-2)} \\ &=\; p_{EQ}^{per} \cdot \left(1 + \left(1 - p_{EQ}^{per}\right) + \left(1 - p_{EQ}^{per}\right)^2 + \cdots + \left(1 - p_{EQ}^{per}\right)^{n-1}\right) \\ &= 1 - \left(1 - p_{EQ}^{per}\right)^n \end{aligned}$$

For an event with a low annual likelihood combined with a short enough time interval, the probability of occurrence for one interval, p_{EQ}^{per}, can be estimated by the annual probability p_{EQ}^{an} times the length of the period T_{per}. This approximation is carried out by removing the small higher order terms in the Taylor series expansion of the exponent term:

$$\begin{aligned} p_{EQ}^{per} &= \int_0^{T_{per}} p_{EQ}^{an} \cdot e^{-t \cdot p_{EQ}^{an}} dt \qquad \text{(Equation F-3)} \\ &= 1 - e^{-\,p_{EQ}^{an} \cdot T_{per}} \\ &= 1 - \sum_{n=0}^{\infty} \frac{\left(-\,p_{EQ}^{an} \cdot T_{per}\right)^n}{n!} \\ &= 1 - 1 + p_{EQ}^{an} \cdot T_{per} - \frac{\left(p_{EQ}^{an} \cdot T_{per}\right)^2}{2} + \frac{\left(p_{EQ}^{an} \cdot T_{per}\right)^3}{6} - \cdots \\ &\approx\; p_{EQ}^{an} \cdot T_{per} \end{aligned}$$

The expected dose contribution from an earthquake in the interval $\{T_1, T_n\}$ is the weighted arithmetic mean of the maximum doses from each of the earthquakes occurring in the interval:

$$\overline{Dose}_n\{T_1, T_n\} = \frac{\sum_{i=1}^{n}\left(p_{fail}(T_i)\cdot \max_t Dose(T_i,t)\right)}{\sum_{i=1}^{n} p_{fail}(T_i)} \quad \text{(Equation F-4)}$$

where

$\max_t Dose(T_i, t)$ is the maximum annual dose (at any time t) from an earthquake occurring in time period T_i.

Thus, the expected value for the maximum annual dose from a silo that fails due to an earthquake in the time period between T_1 and T_n equals the probability of an earthquake in that time interval, times the average annual dose from an earthquake, occurring in the period between time intervals T_1 and T_n:

$$ExpDose_{fail}\{T_1, T_n\} = Cuml_{p_{fail}}(T_n)\cdot \overline{Dose}_n\{T_1, T_n\} = \sum_{i=1}^{n}\left(p_{fail}(T_i)\cdot \max_t Dose(T_i, t)\right) \quad \text{(Equation F-5)}$$

The annual dose calculated with this method represents a type of *mean-of-peak* estimate, that accounts for an increase in the probability of an earthquake having occurred with time since closure. The estimate can be directly contrasted against the annual dose level corresponding to the regulatory risk criterion, keeping in mind that it accounts for the annual dose from the silo given that its barrier functions were to fail. A risk dilution ratio can also be derived by dividing the estimate by the *peak-of-means* from the *earthquake calculation case*.

Appendix G

Map of the Forsmark area

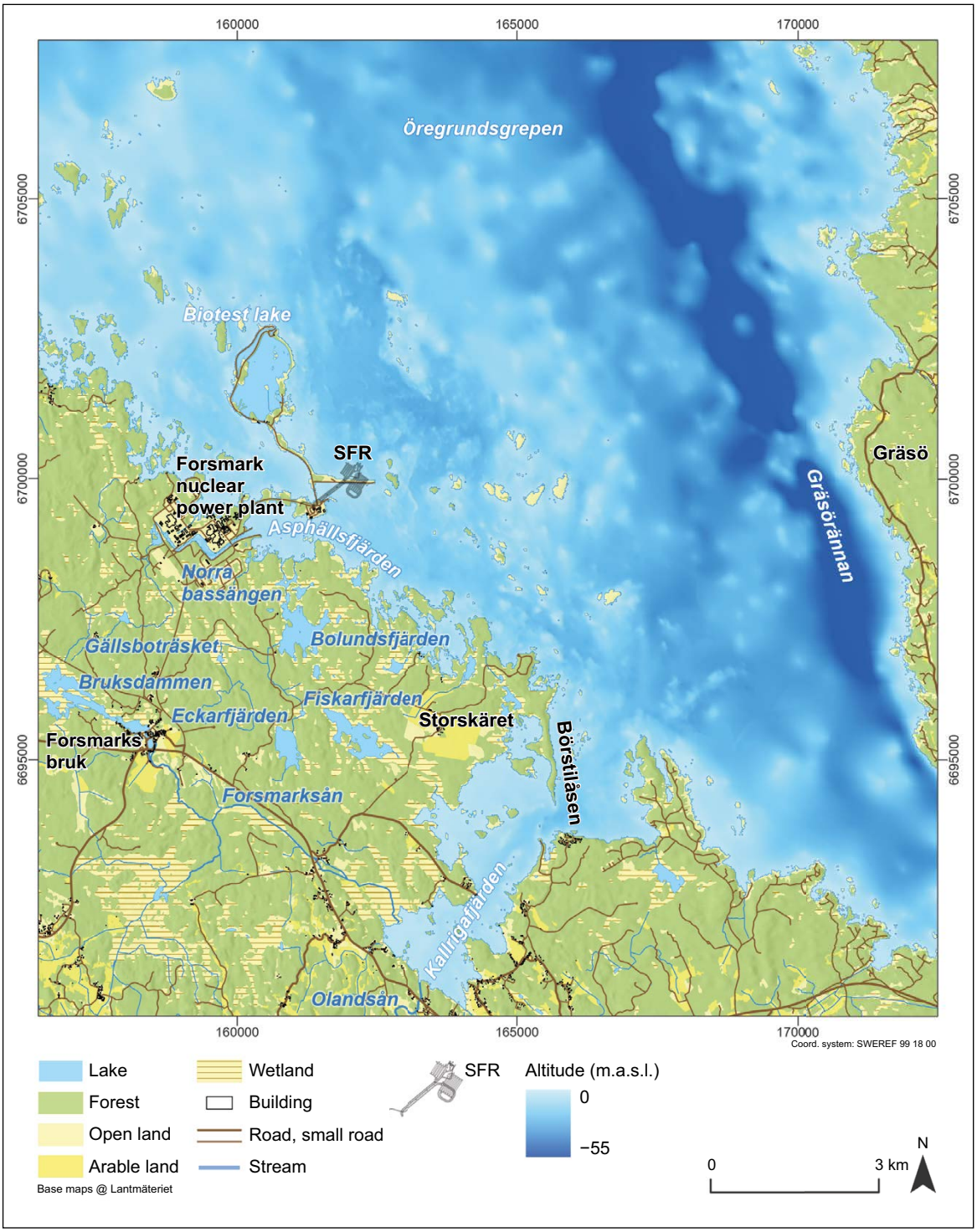

Figure G-1. *Overview map of the Forsmark area in the vicinity of SFR. The geographical position of the Forsmark nuclear power plant, the esker Börstilsåsen and the farmland Storskäret, as well as lakes, streams and marine areas mentioned in the report are shown in the map.*

Appendix H

Post-closure safety assessment flowchart

H1 Introduction

The post-closure safety assessment involves a large number of activities performed in support of the different methodological steps (Section 2.6). These activities contribute to determining the reference evolution based on the initial state, as well as the selection of data, scenarios and calculation cases in support of the evaluation of post-closure safety. In the SR-PSU, a compilation of input data and references to input data used in many activities in the post-closure safety assessment was given in the so-called input data report (SKB TR-14-12). The report used an assessment model flowchart to map datasets transferred between activities. In the PSAR, activities and input data are documented in a database, replacing the input data report in SR-PSU. Furthermore, to provide an overview of the various activities, as well as the connection between them in the form of datasets transferred from one activity to the other, an html-based interactive flowchart is produced (Brandefelt et al. 2023).

This appendix provides an overview of the contents of the flowchart for the PSAR. The flowchart consists of activities and dataflows. The activities are divided into five categories; climate, biosphere, geosphere, near-field and annual risk. The activities included in each category are listed in Table H-1 together with a short description of each activity. Each activity is identified by an ID consisting of a letter and a number, with the letter indicating the category. Each dataflow consists of one or more datasets. The datasets are assigned unique identifications in the database. The activities are displayed in Figure H-1 with arrows representing dataflows.

The flowchart includes activities that support the assessment of annual risk and protection of the environment. Thus, the flowchart shows only activities that contribute to evaluating the main and less probable scenarios, while activities that describe assumptions and data selection for residual scenarios are not shown.

Table H-1. Activities included in the post-closure safety assessment flowchart. The activities are coloured according to category: climate (C; brown), biosphere (B; green), geosphere (G; pink), near-field (N; blue) and annual risk (R; white).

ID	ACTIVITY NAME	Description
N1	Initial state	Expected state of the near-field materials at closure.
N2	Layout and dimensions of components	Layout and dimensions of components in SFR.
N3	Reference evolution of waste and repository chemical conditions	Probable future evolution of waste, repository chemical conditions and sorption properties.
N4	Reference evolution of engineered barriers	Probable future evolution of engineered barriers.
N5	Reference evolution of near-field hydrology	Probable future evolution of near-field hydrology.
N6	Transport of radionuclides	Calculation of radionuclide transport in the near-field, including selection of data.
G1	Initial state	Present-day conditions of the geosphere based on the site-descriptive model.
G2	Reference thermal and mechanical evolution	Probable future evolution of thermal and mechanical conditions in the geosphere.
G3	Reference hydrogeological evolution	Probable future evolution of hydrogeology.
G4	Reference geochemical evolution	Probable future evolution of geochemistry.
G5	Non-flow-related transport properties	Data for non-flow-related transport properties.
G6	Transport of radionuclides	Calculation of radionuclide transport in the geosphere, including selection of data.
B1	Initial state	Present-day conditions of the surface systems based on the site-descriptive model.
B2	Reference development of surface systems	Probable future evolution of regolith and topography, near-surface hydrology, chemical conditions, ecosystems, land use and human influence on the landscape.
B3	Biosphere object identification	Identification of areas in the landscape that will potentially receive radionuclides released from the repository.
B4	Properties for potentially exposed groups and non-human biota	Data for potentially exposed groups and non-human biota.
B5	Sorption and uptake properties	Element-specific sorption coefficients (Kd), concentration ratios (CR) and transfer coefficients (TC).
B6	Transport of and exposure to radionuclides	Calculation of radionuclide transport in the biosphere system and evaluation of potential exposure to humans and non-human biota, including selection of data.
C1	Initial state	Present-day climate and shoreline displacement.
C2	Past and future evolution of climate and climate related issues	Reconstructed past and range of potential future evolution in climate drivers and climate, shoreline displacement, permafrost development, ice-sheet development and surface denudation.
C3	Climate cases	Possible future evolutions of climate and climate-related issues.
	Initial state and reference evolution of repository and its environs	Collection of activities for initial state and reference evolution of the near-field (N1–N5), geosphere (G1–G4) and surface systems (B1–B2).
R1	Selection of scenarios	Selection of scenarios, calculation cases and probabilities for less probable scenarios.
R2	Risk calculation	Calculation of total annual radiological risk accounting for contributions from the main and less probable scenarios.

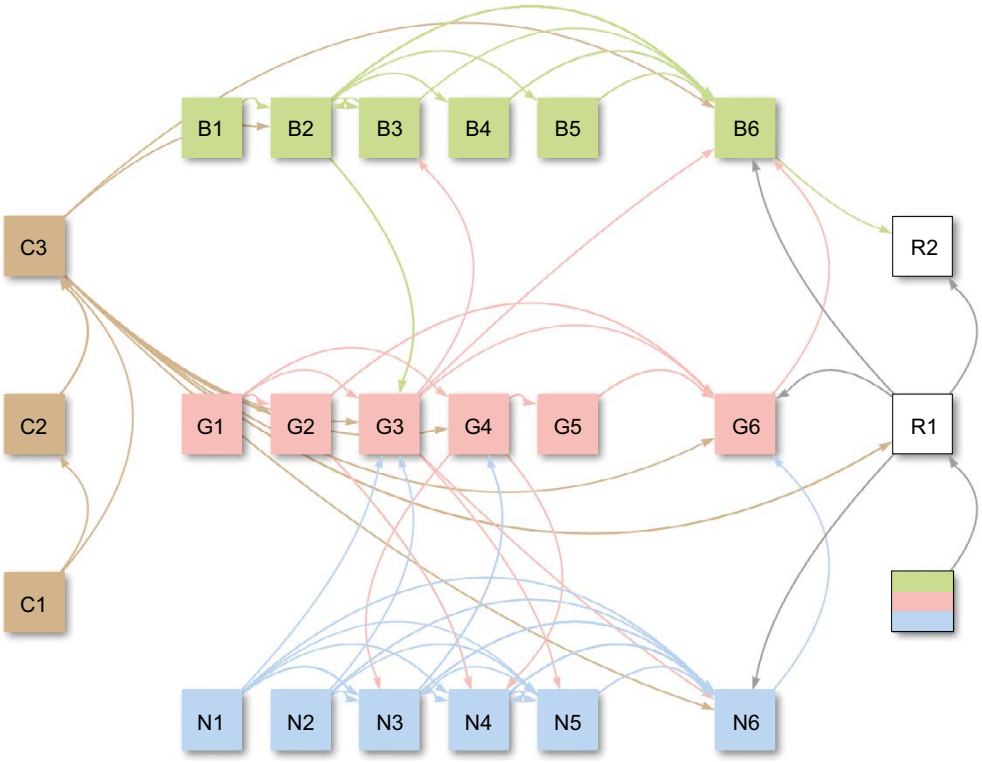

N1	Initial state	B1	Initial state
N2	Layout and dimensions of components	B2	Reference development of surface systems
N3	Reference evolution of waste and repository chemical conditions	B3	Biosphere object identification
N4	Reference evolution of engineered barriers	B4	Properties for potentially exposed groups and non-human biota
N5	Reference evolution of near-field hydrology	B5	Sorption and uptake properties
N6	Transport of radionuclides	B6	Transport of and exposure to radionuclides
G1	Initial state	C1	Initial state
G2	Reference thermal and mechanical evolution	C2	Past and future evolution of climate and climate related issues
G3	Reference hydrogeological evolution	C3	Climate cases
G4	Reference geochemical evolution		Initial state and reference evolution of repository and its environs
G5	Non-flow-related transport properties	R1	Selection of scenarios
G6	Transport of radionuclides	R2	Risk calculation

Figure H-1. *Activities included in the post-closure safety assessment flowchart. Activities (squares) and dataflows between the activities (lines with arrows) are displayed in the upper part of the figure. The activities are coloured according to category: climate (brown), biosphere (green), geosphere (pink), near-field (blue) and annual risk (white).*

H2 Information provided in the flowchart

For each activity (square in Figure H-1) in the flowchart, the html-based interactive application provides a panel with the following information:

- Activity name, ID and description
- Input datasets:
  - Name and ID of activity that the dataset originates from
    - Description of each dataset transferred from that activity, including references to the source and usage of the data
    - For datasets used in radionuclide transport and dose calculation: information on location of data files
- Output datasets:
  - Name and ID of the activity/activities that use the dataset
    - Description of each dataset transferred to the activity, including references to the source and usage of the data
    - For datasets used in radionuclide transport and dose calculations: information on location of data files
- References to publications that describe the activity as well as to publications that provide input datasets or use output datasets.

For illustrative purposes, the panel with the information listed above is shown in Figure H-2 for one of the activities together with the flowchart.

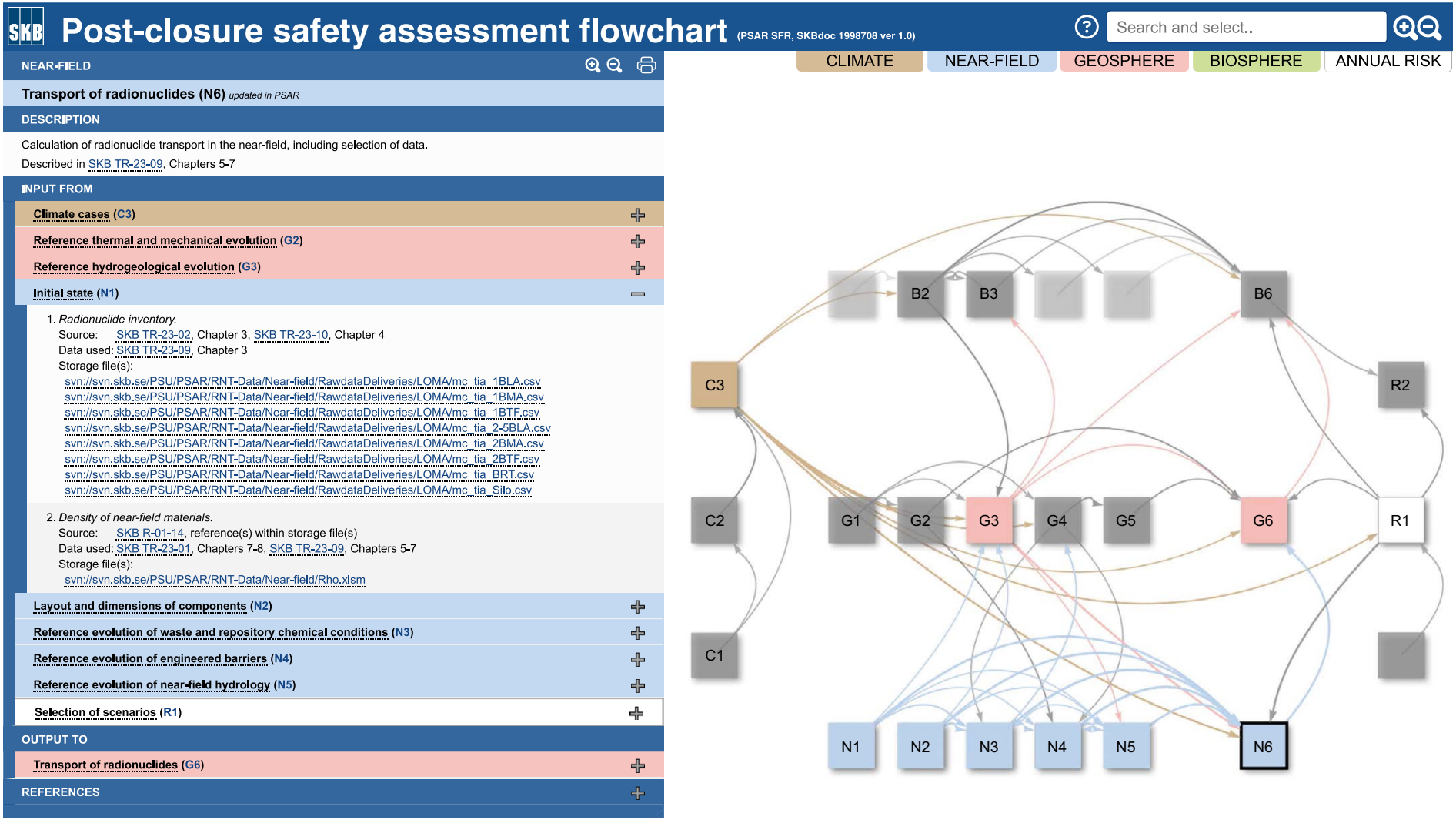

Figure H-2. *Example of the information provided in the html-based interactive application for one of the activities, N6 Transport of radionuclides in the near-field. Note that activities that are directly connected to the selected activity (N6 in the figure) are coloured, whereas activities that are connected to those activities are shown in dark grey. All other activities are shown in light grey.*

Arkitektkopia AB, Bromma, 2023

SKB is responsible for managing spent nuclear fuel and radioactive waste produced by the Swedish nuclear power plants such that man and the environment are protected in the near and distant future.

skb.se